

**Dissertation zur Erlangung des Doktorgrades
der Fakultät für Chemie und Pharmazie
der Ludwig-Maximilians-Universität München**

**Towards the Total Synthesis of Oldhamine A
A Symmetry-Based Approach towards New Ion Channel
Blockers
Self-Assembly of Highly Symmetric Molecules**

v o n

Michael Pangerl

aus

Gräfelfing, Deutschland

2013

Erklärung:

Diese Dissertation wurde im Sinne von §7 der Promotionsordnung vom 28. November 2011 von Herrn Prof. Dr. Dirk Trauner betreut.

Eidesstattliche Versicherung:

Diese Dissertation wurde eigenständig und ohne unerlaubte Hilfe erarbeitet.

München, 18.06.2013

Michael Pangerl

Dissertation eingereicht am: 06.05.2013

Erstgutachter: Prof. Dr. Trauner

Zweitgutachter: Prof. Dr. Heuschmann

Mündliche Prüfung am: 05.06.2013

*„Der unermesslich reichen, stets sich erneuernden Natur gegenüber wird der Mensch,
soweit er auch in der wissenschaftlichen Erkenntnis fortgeschritten sein mag,
immer das sich wundernde Kind bleiben
und muss sich stets auf neue Überraschungen gefasst machen.“*
(Max Planck)

Meinem Schatz, der Dani

ABSTRACT

This thesis describes the synthetic work on the natural product (–)-*ent*-oldhamine A (CHAPTER I), the establishment of a compound library with molecules featuring fivefold symmetry for a symmetry-based approach towards new ion channel blockers (CHAPTER II) and studies towards the self-assembly of highly symmetric polyhedra (CHAPTER III).

The first and main chapter focuses on the synthesis design and the synthetic studies towards the norterpene alkaloid (–)-*ent*-oldhamine A. Due to its intriguing structure incorporating a highly unusual cyclopentadienyl anion that forms an internal salt with a tertiary ammonium ion and with the intention to perform full evaluation of its biological activities, this molecule was a logical target for total synthesis. The establishment of two key building blocks, first, of a highly functionalized pyrrolizidine featuring four of the five stereogenic centers of the natural product and, second, a bicyclic lactone is described. The synthesis of the pyrrolizidine portion was carried out asymmetrically in a series of elegant and highly robust reaction steps, which allowed a performance on multigram scales. For the synthesis of the bicyclic lactone building block, several methodologies were investigated and finally, a palladium-catalyzed [3+2] cycloaddition gave rise to the desired carbon framework in a straightforward fashion.

Searching for new opportunities to control ion channels and thus neuronal activities, a new approach towards the design of potential drugs was explored that is described in the second chapter. It was intended to employ fivefold symmetric molecules as channel antagonists to match the inherent fivefold symmetry of pentameric ion channels and thus enable pentavalent binding. Hence, a series of compounds with fivefold symmetry was synthesized and subjected to biological screening to determine their potential in neuronal control. Indeed, some of these molecules were found to be very biologically active and pentameric ion channels are in fact their targets.

Studies on the self-assembly of highly symmetric icosahedral structures are described in the third chapter. It was planned that fivefold symmetric small molecules having adequate coordinating groups would act as ligands on threefold symmetric transition metal complexes and thus assemble to highly symmetric polyhedra with dodecahedral structures. In the course of extensive experimental studies, new compounds could be characterized and several new crystal structures of interesting transition metal complexes were elucidated.

INHALT

Diese Dissertation beschreibt synthetische Studien am Naturstoff (-)-*ent*-Oldhamine A (CHAPTER I), die Erstellung einer Verbindungsbibliothek von fünffachsymmetrischen Verbindungen für einen symmetriebasierten Zugang zu Ionenkanalblockern (CHAPTER II) und Studien zum *self-assembly* hochsymmetrischer Polyeder (CHAPTER III).

Das erste Kapitel konzentriert sich auf das Synthesedesign sowie auf synthetische Arbeiten am Norterpenoidalkaloid (-)-*ent*-Oldhamine A. Aufgrund seiner faszinierenden Struktur, die ein äußerst ungewöhnliches Zyklopentadienylanion aufweist, welches ein internes Salz mit einem tertiären Ammoniumion bildet, als auch der Absicht die vollständige biologische Aktivität dieses Moleküls zu evaluieren stellt dieser Naturstoff ein deduziertes Ziel für eine Totalsynthese dar. Konkret wird die Entwicklung von zwei Schlüsselbausteinen beschrieben. Zum Einen ist dies ein hochfunktionalisiertes Pyrrolizidin, das bereits vier der fünf stereogenen Zentren des besagten Naturstoffs aufweist und zum Anderen ein bizyklisches Lakton. Die Synthese des Pyrrolizidinbausteins wurde asymmetrisch in einer Reihe von eleganten und robusten Reaktionsschritten durchgeführt, die eine Umsetzung im Multigrammmaßstab erlaubten. Im Hinblick auf die Synthese des Laktonbausteins wurden verschiedene Synthesestrategien eruiert, wobei schließlich eine palladiumkatalysierte [3+2] Zyклоaddition elegant zur Bildung des erwünschten Kohlenstoffgerüsts führte.

Auf der Suche nach neuen Wegen zur Kontrolle von Ionenkanälen und damit neuronaler Aktivität wurde ein neuer Denkansatz zur Entwicklung potentieller Wirkstoffe untersucht, der im zweiten Kapitel beschrieben ist. Hierzu wurde die Anwendung fünffachsymmetrischer Moleküle angedacht, die der inhärenten Symmetrie pentamerer Ionenkanäle entsprechen und damit pentavalent an diese binden können. Dementsprechend wurde eine Reihe von Molekülen mit Fünffachsymmetrie synthetisiert und einem biologischem Screening unterworfen. Es stellte sich heraus, dass einige dieser Moleküle eine außerordentlich potente biologische Aktivität zeigen und dass tatsächlich pentamere Ionenkanäle deren Ziele sind.

Studien zum *self-assembly* hochsymmetrischer, ikosaedrischer Strukturen sind im dritten Kapitel beschrieben. Fünffachsymmetrische kleine Moleküle mit geeigneten funktionellen Gruppen sollten als Liganden an dreifachsymmetrischen Übergangsmetallkomplexen agieren und sich durch Selbstorganisation zu hochsymmetrischen Strukturen mit dodekaedrischer Geometrie zusammenfügen. Im Zuge dieser Studien konnten einige interessante neue Verbindungen und Kristallstrukturen charakterisiert werden.

SUMMARY

CHAPTER I: TOWARDS THE TOTAL SYNTHESIS OF OLDHAMINE A

Daphniphyllum alkaloids are a structurally diverse group of natural products found in *Daphniphyllum*, a genus of dioecious evergreen trees and shrubs native to the Southeast of Asia. Presently, more than two hundred *Daphniphyllum* alkaloids have been isolated from this genus.^[9] Some of them have been shown to exhibit considerable biological activities and alkaloidal extracts of their parent plants had applications in traditional folk medicine for the treatment of a variety of diseases.^{[4]-[7]}

One representative of this class of natural products is (+)-oldhamine A (**I.226**), a norterpene alkaloid featuring a highly unusual cyclopentadienyl anion in its fused-hexacyclic carbon skeleton (Figure A).^[63]

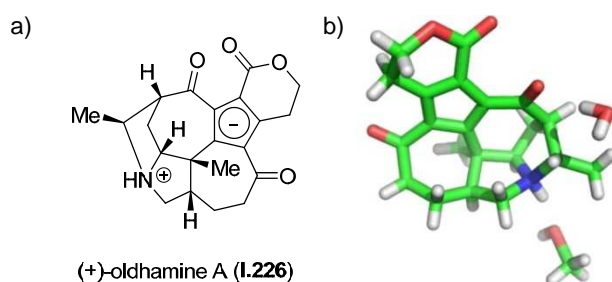
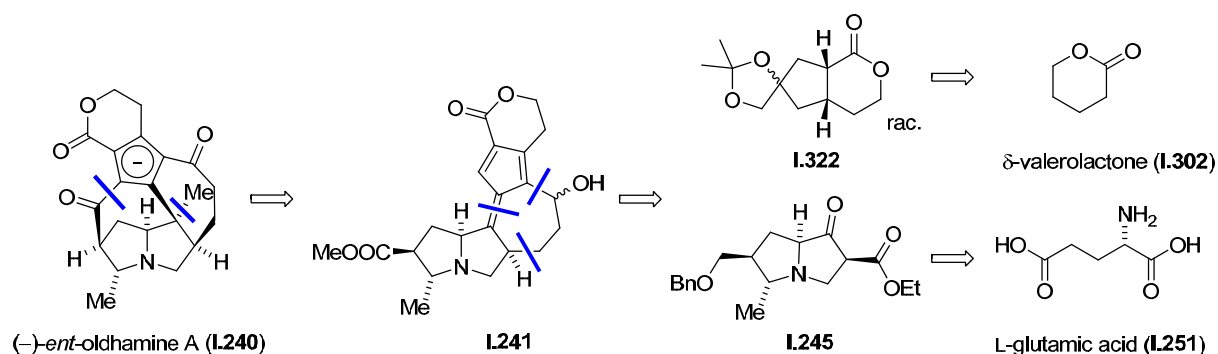


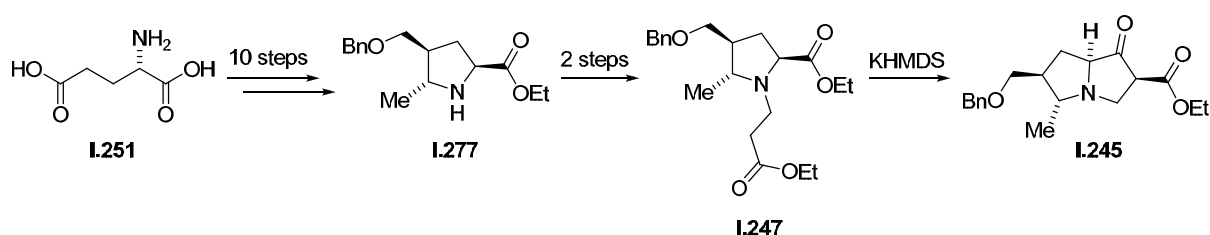
Figure A: (+)-Oldhamine A (**I.226**): a) Chemical structure; b) crystal structure.

The unique structure of **I.226** and the intent to perform a full biological and pharmaceutical characterization necessitated a launch of a total synthesis of this intriguing natural product. Possible synthetic precursors are depicted in Scheme A.



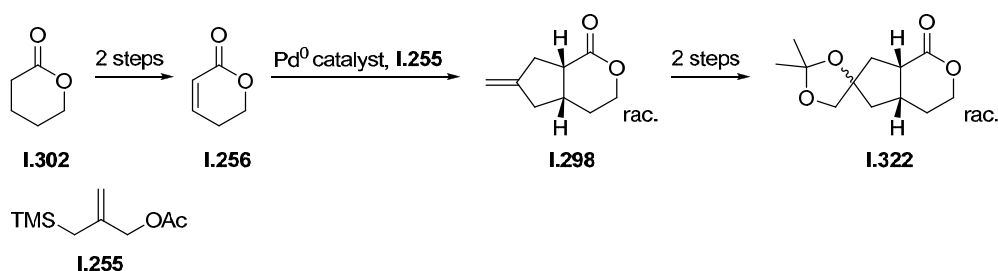
Scheme A: (-)-ent-Oldhamine A (**I.240**) and its possible precursors in the total synthesis program.

In terms of the retrosynthetic analysis, which for economic reasons targeted the unnatural enantiomer (–)-*ent*-oldhamine A (**I.240**), it was planned to construct the quaternary stereogenic center in **I.240** by a stereoselective addition of methyl cuprate to the fulvene system in **I.241**. The resulting anion could easily attack the vicinal methyl ester, thereby giving the natural product in an elegant and convenient fashion. Fulvene **I.241** can be dissected by conjugate addition, subsequent enolate addition and a McMurry reaction to the bicyclic precursors **I.322** and **I.245**. Lactone **I.322** can be traced back to δ -valerolactone (**I.302**), while pyrrolizidine **I.245** was planned to be made from L-glutamic acid (**I.251**). The synthesis in the “forward direction” is shown in Schemes B and C.



Scheme B: Synthetic route towards pyrrolizidine **I.245**.

Transferring this strategy, the synthesis started with **I.251**, which was converted into **I.277** over ten steps. Formation of two new stereogenic centers was directed by the stereochemical information of natural L-glutamic acid (**I.251**). A conjugate addition of the sterically hindered secondary amine **I.277** to ethyl propiolate and subsequent reduction furnished tertiary amine **I.247**. Finally, a Dieckmann cyclization gave rise to pyrrolizidine **I.245**, which features four of the five stereogenic centers present in the natural product.



Scheme C: Synthetic route towards lactone **I.322**.

Concerning lactone **I.322**, the synthesis started from δ -valerolactone (**I.302**), which was unsaturated in two steps (\rightarrow **I.256**) and then coupled in a [3+2] cycloaddition with acetate **I.255** using a methodology, which has been developed by Trost and coworkers.^[72] Resulting intermediate **I.298** was dihydroxylated and protected to give key building block **I.322**.

CHAPTER II: A SYMMETRY-BASED APPROACH TOWARDS NEW ION CHANNEL BLOCKERS

Pentameric ion channels play a huge role in neuronal transduction. In order to investigate new opportunities for the design of potential ion channel blockers, a new approach towards their design was explored. It was planned to apply fivefold symmetric molecules to match the inherent fivefold symmetry of pentameric ion channels and thus enable pentavalent binding. The GABA_A receptor, for example, is a ligand-gated pentameric ion channel that controls neuronal activity by regulating the influx of chloride ions.^{[108],[109]} According to the symmetry approach, blocking the GABA_A channel requires a pentasymmetric small molecule (Figure B).

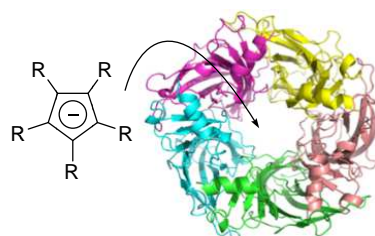


Figure B: A generic fivefold symmetric small molecule next to the GABA_A receptor.

Model studies with pentasymmetric compounds revealed potential binding sites in the targeted ion channels. In the case of the MscL channel (PDB code: 2OAR),^[100] for example, functionalized pillar[5]arenes seemed to be suitable fivefold symmetric frameworks to allow interaction with the protein (Figure C).

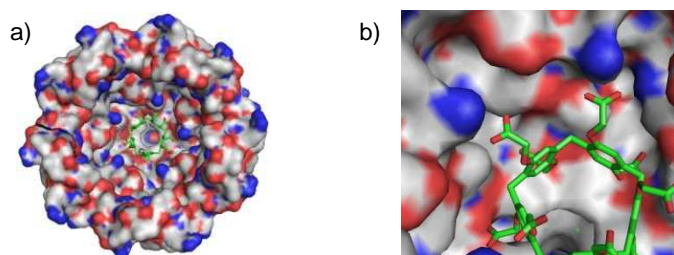


Figure C: A pillar[5]arene with carboxylic acid substituents inside the MscL channel: a) Full view; b) close view.

Accordingly, a series of compounds with fivefold symmetry was synthesized and subjected to biological screening to determine their potential in neuronal control. Compounds were selected by their functional groups and solubility in water (Figure D).

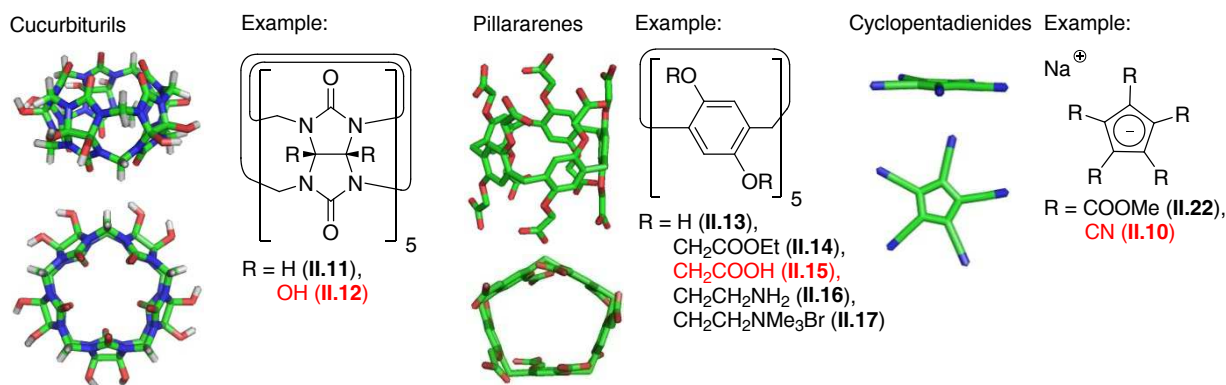


Figure D: Chemical structure and shape on the basis of selected crystal structures of fivefold symmetric small molecules prepared for the symmetry approach.

Pleasingly, it was found that some of these molecules are highly biologically active and indeed pentameric ion channels are their targets. More specifically, it was sodium pentacyanocyclopentadienide **II.10**, which was found to be a potent open channel blocker of the GABA_A receptor ($IC_{50} = 1.3 \mu\text{M}$). In cooperation with Prof. Dr. Erwin Sigel and Novartis AG, the detailed mode of action is currently being studied and its potential application as an insecticide is investigated.

CHAPTER III: SELF-ASSEMBLY OF HIGHLY SYMMETRIC MOLECULES

Fivefold symmetric molecules appear to be suitable building blocks for highly symmetric organometallic complexes.^{[144]-[149]} Based on model studies, it was speculated that the pentacyanocyclopentadienide anion could act as a ligand on facially substituted threefold symmetric transition metal complexes and thus, due to the distances and angles „encoded“ in these building blocks, self-assemble into highly symmetric polyhedra (Figure E).

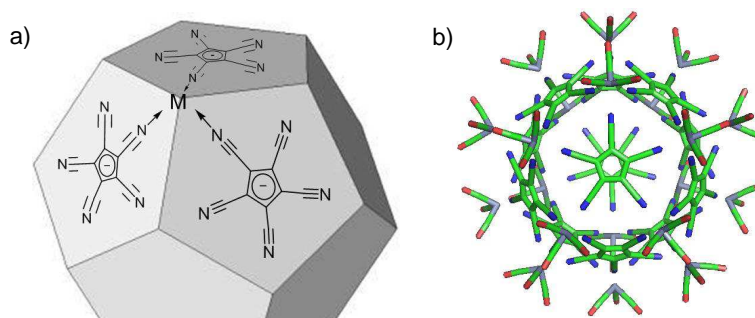
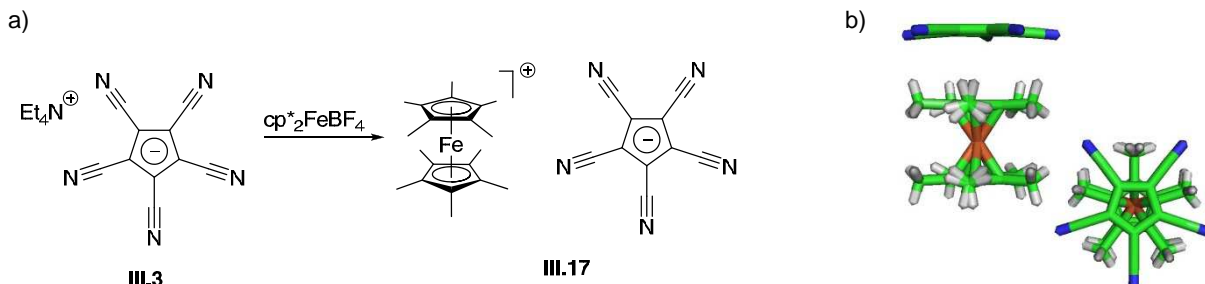


Figure E: Self-assembly of a molecular dodecahedron: a) Schematic illustration of a single vertex; b) model of a dodecahedral arrangement of $[\text{Cr}(\text{CO})_3]_{20}[\text{C}_{10}\text{N}_5]_{12}^{12-}$.

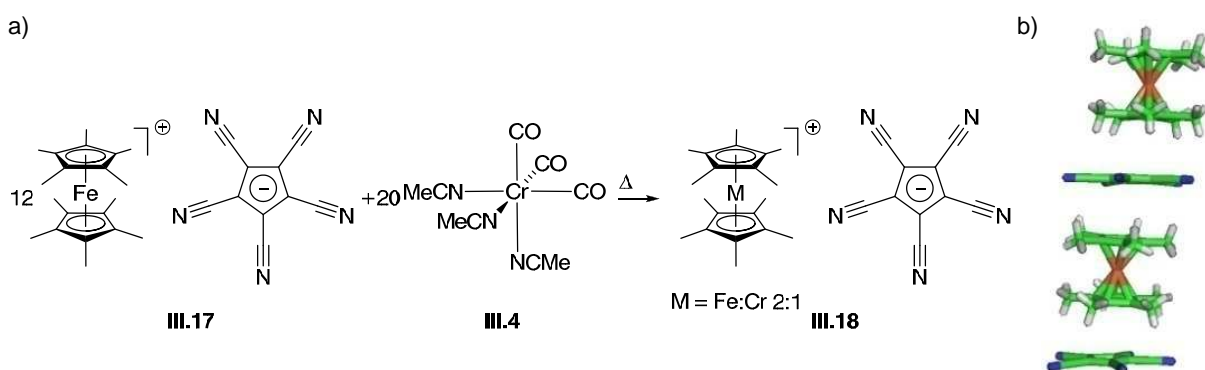
In order to „neutralize“ the 12 negative charges that would accumulate in a dodecahedron formed of a neutral transition metal complex and the anionic ligand, tight ion pair salts of pentacyanocyclopentadienide with fivefold symmetric counter ion were synthesized (Scheme D).



Scheme D: Decamethylferrocenium pentacyanocyclopentadienide (**III.3**): a) Synthesis; b) crystal structure.

This counter ion was found in the decamethylferrocenium cation, which could be introduced by a simple salt metathesis with **III.3**. X-ray analysis of a single crystal confirmed the structure of **III.17** and showed an orthogonal arrangement of discrete ion pairs.

A number of facially substituted threefold symmetric transition metal complexes was prepared and reacted with pentacyanocyclopentadienide salts. Upon extensive experimental efforts, several new compounds and crystal structures could be characterized. When, for example, $[\text{Cr}(\text{MeCN})_3(\text{CO})_3]$ (**III.4**) was treated with **III.17**, formation of an interesting metallocene complex with an intriguing structure was observed (Scheme E).



Scheme E: Metallocene $(\text{C}_5\text{Me}_5)_2\text{Cr}_{0.33}\text{Fe}_{0.67}\text{C}_{10}\text{N}_5$ (**III.18**): a) Synthesis; b) crystal structure.

Discrete ion pairs arrange towards each other in a shifted but linear fashion, thus generating linear metallocenium pentacyanocyclopentadienide rods. This fascinating structure represents a new and highly unusual fivefold symmetric metallocenium salt.

ACKNOWLEDGEMENTS

In the three and a half years in which this work was carried out, I had the opportunity to learn, to develop and to gain invaluable experiences, which will be part of me for the rest of my life. This happened under the great guidance of Prof. Dr. Dirk Trauner, who I would like to thank first and foremost. He is a great mentor and a brilliant visionary and lateral thinker. Thank you Dirk for supporting me throughout this dissertation with your constant input of ideas and encouragement!

My lab mates Dr. Vilius Franckevicius, Simon Geiger, Dr. Dominik Hager, Dr. Maria Matveenko, Dimitri Mazunin, Martin Olbrich, Marco Stein, Giulio Volpin and Nina Vrieling were absolutely phenomenal and I thank them for providing helpful discussions, invaluable hands-on expertise and occasional “blue lab” dinners. It has been a pleasure to work with you!

Of course, I would also like to thank all members of the Trauner research group for the great working atmosphere and for their constant assistance. I especially want to express my gratitude to Dr. Laura Salonen for her help with modeling studies, to Dr. Elena Herrero-Gómez for her support with the DFT calculations and to Pascal Ellerbrock, Dr. Nicolas Guimond, Martin Olbrich, Dr. Laura Salonen and Giulio Volpin for taking the time to carefully proofread this thesis. Furthermore, I am grateful for support provided by the Trauner group staff Petra Böhrer, Tobias Kauer, Carrie Louis, Dr. Martin Sumser and Heike Traub.

I am also very thankful to my practical students Ignaz Höhle, Wolfgang Pfister, Patrick Jüstel and Julian Rotter for their assistance in the lab.

Parts of this work were carried out in cooperation with the group of Prof. Dr. Erwin Sigel. I thank Valentina Carta, Roland Baur and Prof. Erwin Sigel of the Institute of Biochemistry and Molecular Medicine at the University of Bern for being excellent collaboration partners.

Thanks, Philippe Bretan, for helping me calculate “the dodecahedral angle”.

I want to express my gratitude to my parents Marga and Ernst and my brothers Thomas and Simon, with whom I share both the most valuable and the most hilarious moments of my life. Thank you for your love, your constant support and encouragement and for being there, whenever I needed you.

Besides all the people in my “chemical world”, I would also like to thank my girlfriend Daniela for being part of my life. Words cannot express my appreciation for you.

TABLE OF ABBREVIATIONS

[18]crown-6	1,4,7,10,13,16-hexaoxacyclooctadecane
5-HT	5-hydroxytryptophane
Å	Ångström (10^{-10} m)
Ac	acetyl
ACh	acetylcholine
$[\alpha]_D^t$	specific optical rotation at temperature t and 589 nm (sodium D line)
AIBN	azobisisobutyronitrile
AP	action potential
aq.	aqueous
ATP	adenosine triphosphate
ATR	attenuated total reflection
BC	before Christ
BHT	butylated hydroxytoluene, 2,6-di- <i>tert</i> -butyl-4-methylphenol
BINAP	2,2'-bis(diphenylphosphino)-1,1'-binaphthyl
br	broad
Bn	benzyl
Boc	<i>tert</i> -butoxycarbonyl
bp	boiling point
Bu	butyl
Bz	benzoyl
c	concentration
CAM	cerium ammonium molybdate
CCDC	Cambridge Crystallographic Data Centre
concd.	concentrated
cy	cyclohexyl
d	days
d	deutero
DA	Diels-Alder reaction
DBU	1,8-Diazabicyclo[5.4.0]undec-7-ene
DCE	dichloroethane
DFT	density functional theory
DIBAL-H	diisobutylaluminium hydride
diglyme	bis(2-methoxyethyl)ether
DIPEA	<i>N,N</i> -diisopropylethylamine
DIPHOS	1,2-Bis(diphenylphosphino)ethane
DLS	dynamic light scattering
DMAP	4-dimethylaminopyridine
DMSO	dimethyl sulfoxide
DME	dimethoxyethane
DMF	<i>N,N</i> -dimethylformamide
DMP	Dess-Martin periodinane
DMPU	<i>N,N'</i> -dimethylpropyleneurea

<i>dr</i>	diastereomeric ratio
DTBMP	2,6-di- <i>t</i> -butyl-4-methylpyridine
δ	chemical shift
<i>E</i>	opposite, <i>trans</i>
EC	effective concentration
EDCI	1-ethyl-3-(3-dimethylaminopropyl)carbodiimide
EEG	electroencephalogram
<i>e.g.</i>	<i>exempli gratia</i>
EI	electron ionization
ELIC	pentameric ligand gated ion channel from <i>Erwinia Chrysanthemi</i>
<i>ent</i>	unnatural enantiomer of natural product
eq	equivalent(s)
<i>er</i>	enantiomeric ratio
ESI	electrospray ionization
Et	ethyl
g	gram(s)
GABA	γ -aminobutyric acid
GC	gas chromatography
GluCl	<i>Caenorhabditis elegans</i> glutamate-gated chloride channel α
h	hour(s)
Hex	hexanes
HMPA	hexamethylphosphoramide
HPLC	high performance liquid chromatography
HRMS	high resolution mass spectrometry
HV	high vacuum
Hz	hertz
<i>i</i>	<i>iso</i>
<i>i.a.</i>	<i>inter alia</i>
IBX	2-iodoxybenzoic acid
IC	inhibitory concentration
iGluR	ionotropic glutamate receptor
IR	infrared
<i>J</i>	coupling constant
KHMDS	potassium hexamethyldisilazide
K _v	voltage gated potassium channel
L	liter(s)
LAH	lithium aluminium hydride
LDA	lithium diisopropylamide
LED	light-emitting diode
LiHMDS	lithium hexamethyldisilazide
λ	wavelength
m	meter(s)
M	molar
M1, 2, 3, 4	transmembrane domain 1, 2, 3, 4
Me	methyl
XIV	

Mes	mesitylene
min	minute(s)
mol	mole(s)
MOM	methoxymethyl ether
mp	melting point
Ms	mesylate
MS	mass spectrometry
MscL	mechanosensitive channel of large conductance
MTSET	[2-(trimethylammonium)ethylmethanthiosulfonate bromide
m/z	proportion mass/charge
<i>n</i>	normal
Na _v	voltage gated sodium channel
NBD	norbornadiene
NMO	<i>N</i> -methylmorpholine <i>N</i> -oxide
NMR	nuclear magnetic resonance
Nu	nucleophile
<i>p</i>	para
PDB	Protein Data Bank
PCC	pyridinium chlorochromate
pccp	pentacyanocyclopentadienide
PDC	pyridinium dichromate
PE	petroleum ether, hexanes
pent	pentyl
Ph	phenyl
Piv	pivaloyl
PKR	Pauson-Khand reaction
PMP	<i>para</i> -methoxyphenyl
ppm	parts per million
PPTS	pyridinium <i>p</i> -toluenesulfonate
py	pyridine
Pr	propyl
quant.	quantitative
RCM	ring closing metathesis
RDL	resistance to dieldrin
<i>R_f</i>	retardation factor
RP	reversed phase
r.t.	room temperature
s	second(s)
sat.	saturated
S _N 1	unimolecular nucleophilic substitution
S _N 2	bimolecular nucleophilic substitution
t	temperature
<i>t</i>	<i>tert</i>
TACN	1,4,7-triazacyclononane
TBAF	tetrabutylammonium fluoride

TBS	<i>tert</i> -butyldimethylsilyl
TEM	transmission electron microscopy
Tf	trifluoromethanesulfonyl
TFA	trifluoroacetic acid
THF	tetrahydrofuran
TIPS	triisopropylsilyl
TLC	thin layer chromatography
TMAO	Trimethylamine <i>N</i> -oxide
TMEDA	tetramethylethylenediamine
TMP	2,2,6,6-tetramethylpiperidine
TMS	trimethylsilyl
Ts	<i>p</i> -toluenesulfonyl
UV	ultra-violet
Z	together, <i>cis</i>

TABLE OF CONTENTS

ABSTRACT	V
INHALT	VI
SUMMARY	VII
ACKNOWLEDGEMENTS	XII
TABLE OF ABBREVIATIONS	XIII
TABLE OF CONTENTS	XVII
CHAPTER I: TOWARDS THE TOTAL SYNTHESIS OF OLDHAMINE A	1
1.1 Project Background and Aims	1
1.1.1 <i>Daphniphyllum</i> Alkaloids	1
1.1.2 Synthetic Approaches towards the <i>Daphniphyllum</i> Alkaloids.....	6
1.1.3 Isolation and Structure of (+)-Oldhamine A	33
1.1.4 Retrosynthetic Analysis of (–)- <i>ent</i> -Oldhamine A	36
1.2 Results and Discussion	41
1.2.1 Studies on C4- and C5-functionalized L-glutamic Acid Derivatives.....	41
1.2.2 Intramolecular Conjugate Addition Approach towards the Synthesis of the Pyrrolizidine Portion of (–)- <i>ent</i> -Oldhamine A	45
1.2.3 Dieckmann Cyclization Approach to Construct the Pyrrolizidine Ring System of (–)- <i>ent</i> -Oldhamine A	49
1.2.4 Studies on the Construction of the Bicyclic Lactone Portion of (–)- <i>ent</i> -Oldhamine A by a Pauson-Khand Reaction	53
1.2.5 Studies on the Construction of the Bicyclic Lactone Portion of (–)- <i>ent</i> -Oldhamine A via a Copper-Catalyzed Cyclization Reaction	57
1.2.6 Studies on the Construction of the Bicyclic Lactone Portion of (–)- <i>ent</i> -Oldhamine A via a [3+2] Cycloaddition.....	60
1.2.7 Summary, Conclusions and Outlook.....	67
1.3 Experimental Section	71

CHAPTER II: A SYMMETRY-BASED APPROACH TOWARDS NEW ION CHANNEL BLOCKERS	116
2.1 Introduction.....	116
2.1.1 Project Background and Aims	116
2.2 Results and Discussion	122
2.2.1 Model Studies of Fivefold Symmetric Compounds with Pentameric Proteins	122
2.2.2 Synthesis of Pentasymmetric Potential Ion Channel Blockers.....	125
2.2.3 Outline on Biological Studies	140
2.2.4 Summary, Conclusions and Outlook	144
2.3 Experimental Section.....	146
CHAPTER III: SELF-ASSEMBLY OF HIGHLY SYMMETRIC MOLECULES.....	168
3.1 Introduction.....	168
3.1.1 Appearance of the Platonic Solids in Daily Life and in Science.....	168
3.1.2 Project Background and Aims	173
3.2 Results and Discussion	175
3.2.1 Synthetic Studies on the Self-Assembly of a Molecular Dodecahedron.....	175
3.2.2 Summary, Conclusions and Outlook	188
3.3 Experimental Section.....	190
APPENDICES	203
Appendix 1: NMR Spectra of Chapter I.....	203
Appendix 2: Crystallographic Data of Chapter I.....	244
Appendix 3: NMR Spectra and IR Spectra of Chapter II.....	246
Appendix 4: Crystallographic Data of Chapter II	269
Appendix 5: NMR and IR Spectra of Chapter III, Magnetic Properties of III.17 ...	277
Appendix 6: Crystallographic Data of Chapter III.....	282
Appendix 7: Computational Details	294
Appendix 8: Screening Tables.....	300
REFERENCES.....	308

CHAPTER I: TOWARDS THE TOTAL SYNTHESIS OF OLDHAMINE A

1.1 Project Background and Aims

1.1.1 *Daphniphyllum* Alkaloids

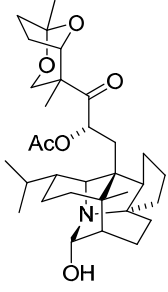
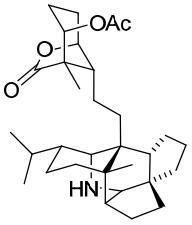
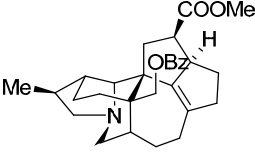
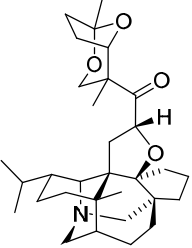
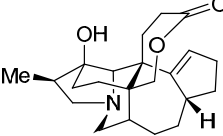
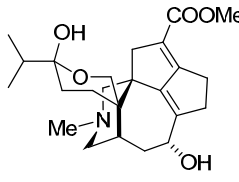
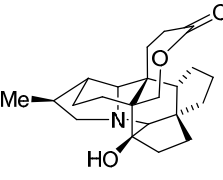
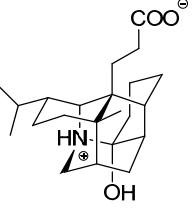
Nature has always been a great source of inspiration for chemists. She manages to solve complex problems in efficient and elegant ways, making the accomplishment look simple. One impressive example is how small molecules with low molecular weight are used in many different ways to perform highly specific tasks.

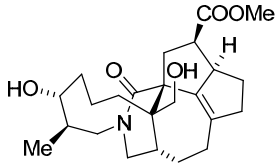
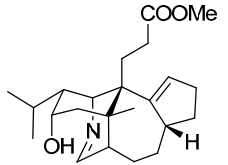
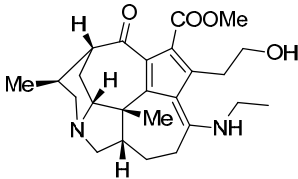
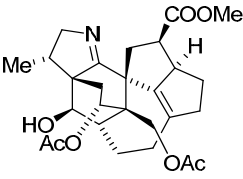
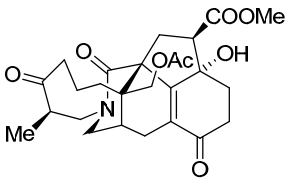
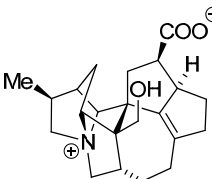
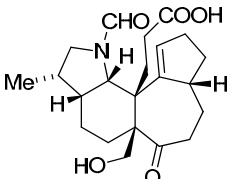
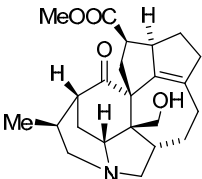
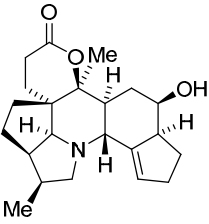
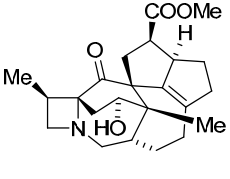
Thus, it is not surprising that studying natural products has been demonstrated to be the most important source of discovery of pharmaceutical drugs.^[1] Their development has heavily contributed to the elongation of life expectancy to an average of 80 years in 2012 in industrialized countries and is thus of great significance for mankind.^[2]

A rich source of a large number of natural products with diverse structures is the genus *Daphniphyllum*, which comprise the dioecious evergreen trees and shrubs of the family *Daphniphyllaceae*. These vegetals are native to the east and Southeast of Asia and predominantly to Japan.^[3] Crude extracts from these trees have been used in traditional folk medicine for many purposes such as the treatment of asthma.^[4] Some natural products isolated from these plants were also shown to have considerable cytotoxic effects,^[5] antioxidation properties,^[6] and some also enhance neurotropic factor biosynthesis.^[7] However, the overall biological functions and pharmacology of the *Daphniphyllum* alkaloids are poorly studied to date due to their limited natural supply.

Since the isolation of the first alkaloid from *Daphniphyllum* was reported in 1909,^[8] these natural products have attracted considerable attention by research groups worldwide resulting in the identification of more than 230 *Daphniphyllum* alkaloids to date. Hence, a series of manifold complex polycyclic structures has been elucidated, which have been classified according to their carbon skeletons.^[9] Up to now, 22 different structural types have been characterized. This number is likely to further increase given that new compounds from this genus are continuously discovered. In 2012 alone, three new structures were disclosed.^[10] In order to illustrate the diversity of these compounds, a complete collection of carbon skeletons present in *Daphniphyllum* alkaloids is shown in Figure I.1. The structures are ordered and

classified by their carbon backbone.^[9] However, members of each skeletal class can heavily differ by their oxidation states and degree of functionalization.

<p>Daphniphylline-type</p>  <p>Leaves of <i>Daphniphyllum oldhamii</i>, 2008.^[11]</p> <p>Potent effects against platelet aggregation.</p> <p>(+)-daphnioldhanin H (I.1)</p>	<p>Secodaphniphylline-type</p>  <p>Roots of <i>Daphniphyllum oldhamii</i>, 2007.^[6]</p> <p>Antioxidant activities against hydrogen peroxide-induced impairment in PC12 cells.</p> <p>(-)-daphnioldhanin D (I.2)</p>
<p>Yuzurimine-type</p>  <p>Whole plant of <i>Daphniphyllum angustifolium</i> HUTCH, 2011.^[12]</p> <p>Weak inhibition of tumor growth against HL-60, MCF-7 and A549 cell lines.</p> <p>(-)-daphangustifoline B (I.3)</p>	<p>Daphnilactone A-type</p>  <p>Leaves of <i>Daphniphyllum teijsmannii</i>, 2011.^[13]</p> <p>Unusual 2,8-dioxabicyclo [3.2.1] octane moiety.</p> <p>(-)-daphtenidine A (I.4)</p>
<p>Daphnilactone B-type</p>  <p>Leaves of <i>Daphniphyllum humile</i>, 2006.^[14]</p> <p>Features a seven-membered lactone moiety.</p> <p>(-)-daphnezomine H (I.5)</p>	<p>Yuzurine-type</p>  <p>Fruits of <i>Daphniphyllum longeracemosum</i>, 2010.^[15]</p> <p>Spiro <i>Daphniphyllum</i> alkaloid.</p> <p>(-)-daphlongamine I (I.6)</p>
<p>Bukittingine-type</p>  <p>Twigs of <i>Daphniphyllum calycinum</i>, 2008.^[16]</p> <p>Features a [5-6-6-5-5-7] hexacyclic core.</p> <p>(-)-caldaphnidine N (I.7)</p>	<p>Daphnezomine A-type</p>  <p>Leaves of <i>Daphniphyllum humile</i>, 1999.^[17]</p> <p>Contains an aza-adamantane core.</p> <p>(-)-daphnezomine A (I.8)</p>

<p>Daphnezomine F-type</p>  <p>(-)-daphlongeranine C (I.9)</p> <p>Fruits of <i>Daphniphyllum longeracemosum</i>, 2011.^[18]</p> <p>Contains 1-azabicyclo[5.2.2]undecane ring system.</p>	<p>Daphnezomine L-type</p>  <p>(-)-caldaphnidine L (I.10)</p> <p>Twigs of <i>Daphniphyllum calycinum</i>, 2008.^[16]</p> <p>Unusual 2,3,4,5-tetrahydropyridine moiety.</p>
<p>Daphnicyclidin-type</p>  <p>(-)-angustifolimine (I.11)</p> <p>Whole plant of <i>Daphniphyllum angustifolium</i> HUTCH, 2011.^[19]</p> <p>Diamino <i>Daphniphyllum</i> alkaloid.</p>	<p>Daphmanidin A-type</p>  <p>(-)-daphtenidine C (I.12)</p> <p>Leaves of <i>Daphniphyllum teijsmannii</i>, 2011.^[13]</p> <p>Shows moderate cytotoxicity against murine lymphoma L1210 cells.</p>
<p>Daphmanidin C-type</p>  <p>(-)-daphmanidin D (I.13)</p> <p>Leaves of <i>Daphniphyllum teijsmannii</i>, 2005.^[20]</p> <p>Together with daphmanidin C the sole member of this group to date.</p>	<p>Daphniglaucin A-type</p>  <p>(-)-daphangustifoline A (I.14)</p> <p>Whole plant of <i>Daphniphyllum angustifolium</i> HUTCH, 2011.^[12]</p> <p>Effects against platelet aggregation.</p>
<p>Daphniglaucin C-type</p>  <p>(-)-daphnimacropodumine B (I.15)</p> <p>Fruits of <i>Daphniphyllum macropodum</i>, 2007.^[21]</p> <p>Features a [5-6-7-5] tetracyclic core.</p>	<p>Calyciphylline A-type</p>  <p>(-)-daphniglaucin D (I.16)</p> <p>Leaves of <i>Daphniphyllum glaucenses</i>, 2004.^[22]</p> <p>Highly fused hexacyclic core.</p>
<p>Calyciphylline B-type</p>  <p>(-)-oldhamiphylline A (I.17)</p> <p>Leaves of <i>Daphniphyllum oldhamii</i>, 2004.^[23]</p> <p>Features nine stereogenic centers.</p>	<p>Calyciphylline C-type</p>  <p>(-)-calydaphninone (I.18)</p> <p>Fruits of <i>Daphniphyllum macropodum</i>, 2007.^[24]</p> <p>Features an unusual azetidinium ring.</p>

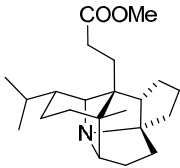
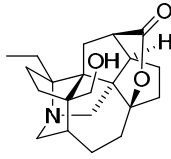
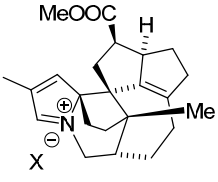
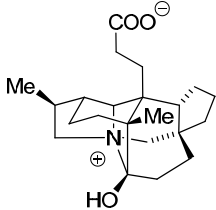
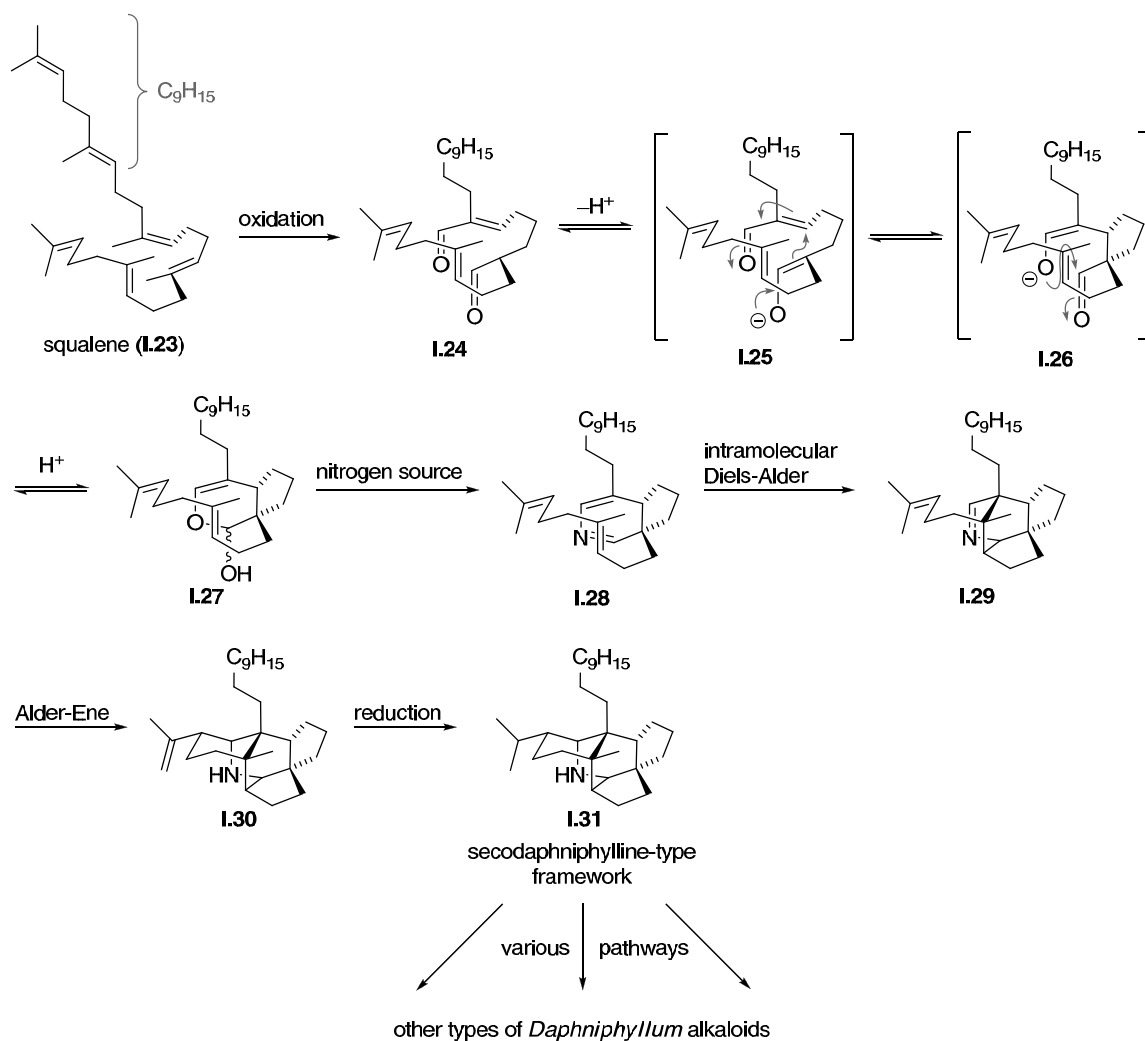
<p>Calyciphylline D-type</p>  <p>Leaves of <i>Daphniphyllum calycinum</i>, 2007.^[25]</p> <p>Features a [6-5-5-5] tetracyclic core.</p> <p>(-)-calyciphylline F (I.19)</p>	<p>Paxdaphnine A-type</p>  <p>Fruits of <i>Daphniphyllum longeracemosum</i>, 2008.^[26]</p> <p>Heptacyclic ring system.</p> <p>(+)-daphlongamine A (I.20)</p>
<p>Calyciphylline G</p>  <p>Stem of <i>Daphniphyllum calycinum</i>, 2007.^[27]</p> <p>Contains a 2-<i>H</i> pyrrolium ring.</p> <p>(+)-calyciphylline G (I.21)</p>	<p>Angustimine</p>  <p>Whole plant of <i>Daphniphyllum angustifolium</i> HUTCH, 2011.^[19]</p> <p>Sole representative of this group.</p> <p>(-)-angustimine (I.22)</p>

Figure I.1: A selection of *Daphniphyllum* alkaloids, illustrating all their different skeletal types together with source and year of the first isolation.

This diversification among all the *Daphniphyllum* alkaloids is remarkable since they are proposed to biosynthetically arise from a common precursor: By performing feeding experiments, it was shown that the *Daphniphyllum* alkaloids are all derived from squalene (**I.23**, Scheme I.1).^[28] Since the number of carbon atoms in the framework can vary due to biosynthetic modifications, the *Daphniphyllum* alkaloids can not generally be classified by means of a compound class. However, being commonly derived from **I.23**, they are often referred to as norterpenoid alkaloids,^[9] although it would be more descriptive to call them triterpenoid and nortriterpenoid alkaloids.

A detailed mechanism for the formation of the secodaphnan framework from squalene was originally proposed by Heathcock and coworkers (Scheme I.1).^[29] They were able to support their concept by a biomimetic total synthesis of (\pm)-*proto*-daphniphylline, utilizing the proposed pentacyclization pathway (*vide infra*, Section 1.1.2, Scheme I.7).^[30] Even though participation of **I.23** in the biosynthesis of the *Daphniphyllum* alkaloids was already suggested before,^[28, 31] it was the success of this work which attracted large interest for the elucidation of detailed biosynthetic mechanisms and pathways towards other skeletal types of the *Daphniphyllum* alkaloids.^{[9],[32]}



Scheme 1.1: Proposed biosynthetic pathway to secodaphniphylline-type alkaloids from squalene (I.23) without showing enzymatic activities.

In the first step, squalene (I.23) could oxidatively be transformed into dialdehyde I.24 with loss of one double bond to form a desymmetrized species containing an enone and an aldehyde. This was proposed to occur *via* imine formation with an amine provided by either an enzyme^[32a] or pyridoxamine, followed by prototropic rearrangement.^[33] The corresponding enolate I.25 could then undergo an intramolecular conjugate addition, followed by cyclization of I.26 to afford hemiketal I.27. Formal condensation with one equivalent of ammonia (presumably provided by pyridoxamine) could give rise to 2-azadiene I.28, which would then be set up to form tetrahydropyridine I.29 *via* an intramolecular Diels-Alder reaction. This intermediate could undergo an Alder-Ene reaction to provide pentacycle I.30, which, upon reduction, would furnish the framework of the secodaphniphylline-type alkaloids (I.31).^[9]

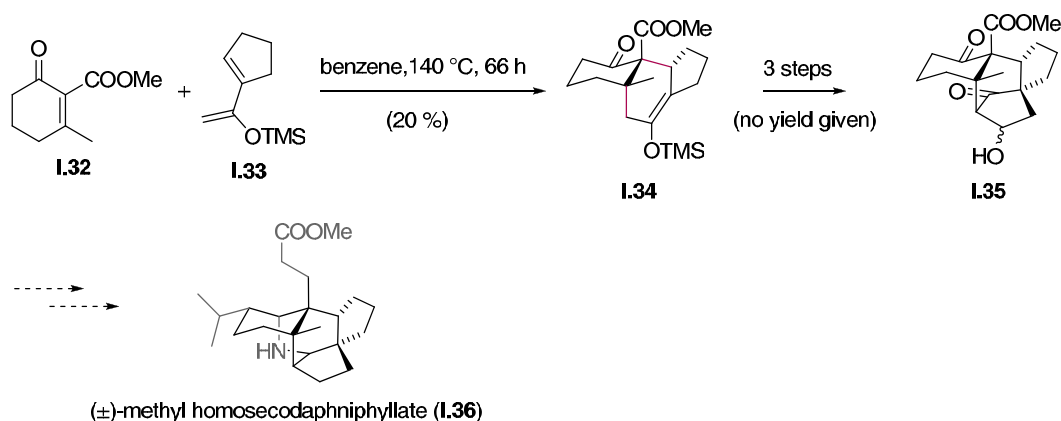
Their structural complexity and beauty has attracted the attention of synthetic chemists and a number of approaches to several of the *Daphniphyllum alkaloids* have been reported so far.

The construction of their polycyclic frameworks is the key task in their strategies. Many of these syntheses stand out for their use of elegant domino reactions, building key frameworks in a single step. A complete description of these follows in the next section.

1.1.2 Synthetic Approaches towards the *Daphniphyllum* Alkaloids

1.1.2.1 Turner's approach towards (±)-methyl homosecodaphniphyllate

The first attempt to construct the complex core of homosecodaphniphylline-type alkaloids was performed in 1983 by the group of Turner, who aimed for a Diels-Alder approach using acceptor-substituted dienophiles in an effort towards (±)-methyl homosecodaphniphyllate (**I.36**, Scheme I.2).^[34]

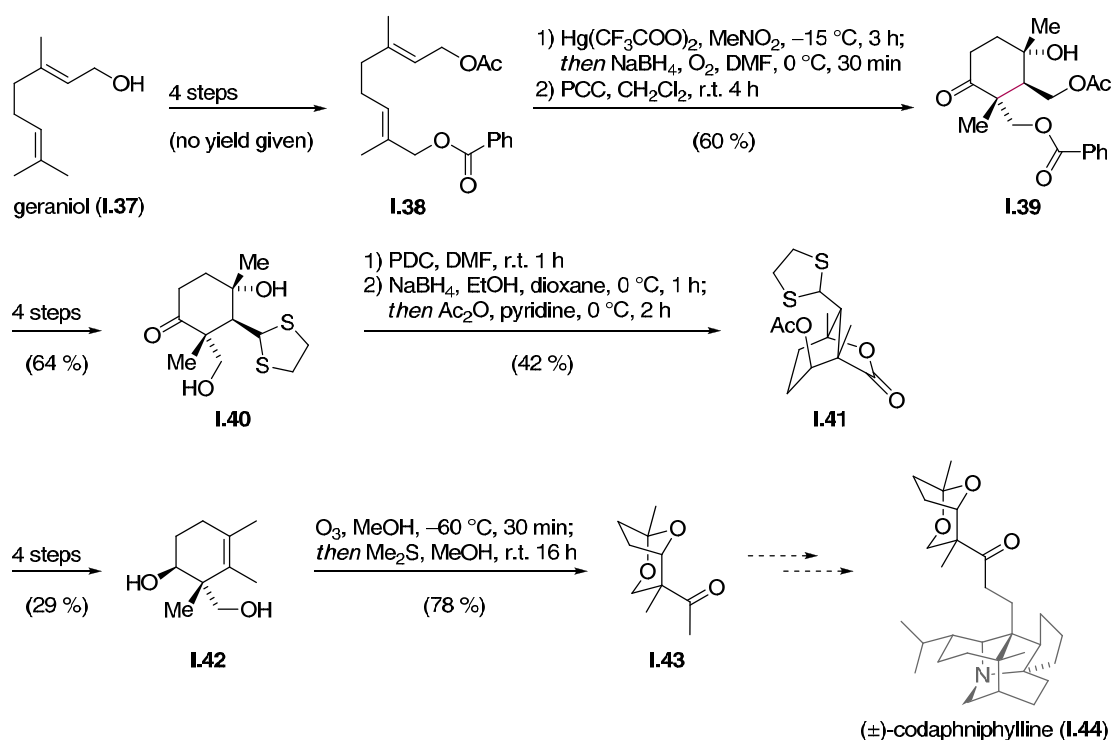


Scheme I.2: First synthetic approach towards *Daphniphyllum* alkaloids - construction of the tricyclic core of (±)-methyl homosecodaphniphyllate (**I.36**).

Starting from diene **I.32** and enone **I.33**, a regioselective suprafacial endo-addition under thermal conditions gave tricycle **I.34** in a moderate 20 % yield. **I.34** could then be converted in three steps into tetracycle **I.35**, which already features the core skeleton of (±)-methyl homosecodaphniphyllate (**I.36**).

1.1.2.2 Yamamura's approach towards (±)-codaphniphylline

The group of Yamamura reported in 1986 a synthesis of the northern part of (±)-codaphniphylline (**I.44**, Scheme I.3),^[35] a daphniphylline-type alkaloid which they had previously isolated and characterized.^[36] Their synthesis was of great use to confirm the proposed structure.

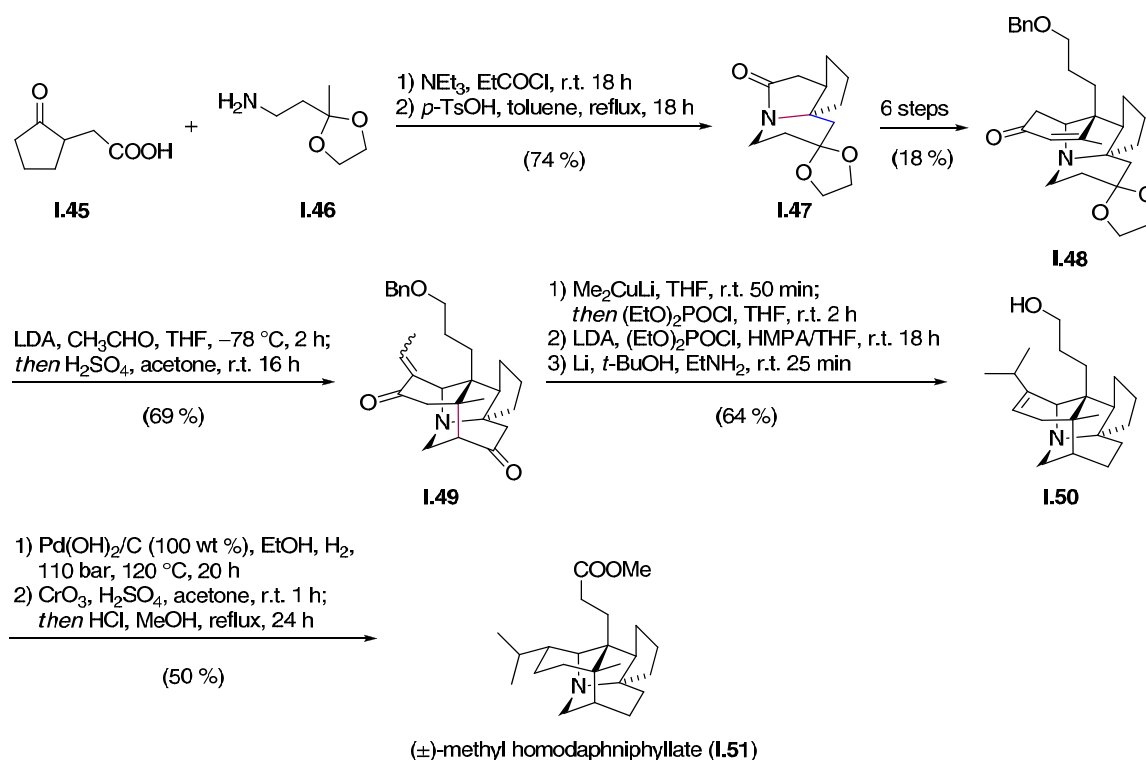


Scheme I.3: A synthetic approach towards the northern part of (±)-codaphniphylline (**I.44**) to confirm the structure of **I.44**.

Geraniol (**I.37**) was converted in four steps into acetate **I.38**, which was then subjected to mercury-promoted cyclization, reductive demercuration and subsequent oxidation to yield ketone **I.39**. This intermediate was processed in four steps into thioacetal **I.40**, which upon oxidation and spontaneous lactone formation was chemoselectively reduced and acetylated to furnish bicycle **I.41**. Compound **I.41** was converted over four steps into alkene **I.42**, which was subjected to ozonolysis followed by reductive workup to result in spontaneous formation of desired ketal **I.43**, which features the northern part of (±)-codaphniphylline (**I.44**).

1.1.2.3 Heathcock's first generation synthesis of (±)-methyl homodaphniphyllate

The total synthesis of (±)-methyl homodaphniphyllate (**I.51**, Scheme I.4) in 1986 represents the first completed total synthesis of a *Daphniphyllum* alkaloid. It was executed by the group of Heathcock, who dominated this field in the following years by presenting a series of elegant total syntheses of several *Daphniphyllum* alkaloids with different skeletal types. The first generation synthesis of **I.51** was carried out in 14 linear steps and provided the natural product in an overall yield of 2 %.^[37]



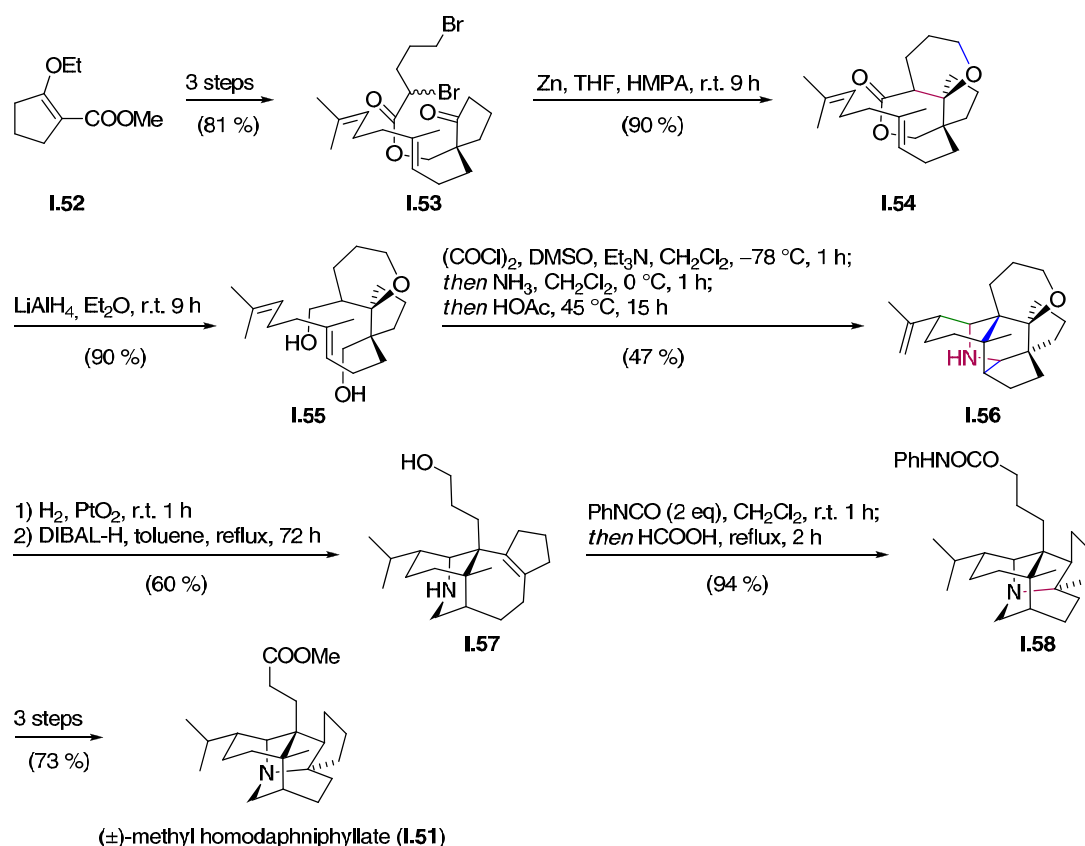
Scheme I.4: Total synthesis of (±)-methyl homodaphniphyllate (**I.51**).

Amide formation of ketone **I.45** with acetal **I.46** followed by acid-catalyzed iminium ion formation and intramolecular nucleophilic trapping by means of a Mannich-type reaction gave rise to tetracycle **I.47**. This molecule was then converted in six steps into enone **I.48**. An *E/Z* unselective aldol condensation with acetaldehyde followed by acid-mediated hydrolysis of the ketal triggered an intramolecular conjugate addition to furnish **I.49**, which exhibits the cyclic core of the natural product. Conjugate addition of methyl cuprate and trapping the resulting enolate with diethyl phosphochloridate gave an enol phosphate, which was transformed into a double enol phosphate using LDA and diethyl phosphochloridate. The resulting intermediate was then reduced with lithium in *tert*-butanol and ethyl amine to give the deoxygenated and *O*-deprotected alkene **I.50**. The following reduction was achieved using highly optimized

conditions employing Pearlman's catalyst with high pressure of hydrogen and at high temperature, under which a 1:1 mixture of diastereomers with respect to the isopropyl group was obtained. This mixture of diastereomers was subjected to Jones oxidation and Fischer esterification and could then be separated to give (\pm)-methyl homosecodaphniphyllate (**I.51**).

1.1.2.4 Heathcock's second generation synthesis of (\pm)-methyl homodaphniphyllate

In 1989, Heathcock *et al.* reported the second generation synthesis of (\pm)-methyl homodaphniphyllate (**I.51**, Scheme I.5), employing a bio-inspired sequence, which featured a condensation/Diels-Alder/Alder-Ene cascade reaction previously developed in their own laboratories (*vide supra*, Section 1.1.1, Scheme I.1).^{[38],[39]} By implementing this elegant domino reaction sequence, the number of linear steps was reduced to 12 and the overall yield was significantly improved to 13 %.^{[40],[41]}



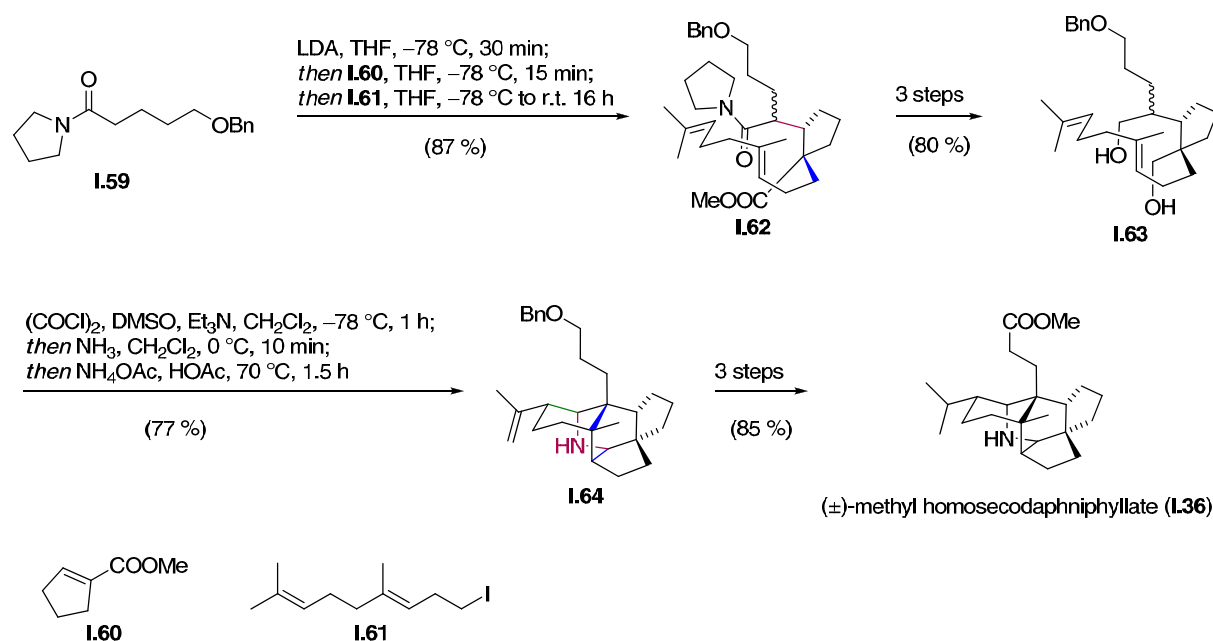
Scheme I.5: Second generation synthesis of (\pm)-methyl homodaphniphyllate (**I.51**).

The synthesis started with ester **I.52**, which was converted in three steps into dibromide **I.53**. This intermediate then participated in a Reformatsky reaction to give tricyclic lactone **I.54**.

Upon LAH reduction, diol **I.55** was obtained, which was subsequently oxidized using Swern conditions. Reacting the corresponding dialdehyde *in situ* with a stream of gaseous ammonia resulted in the formation of a 2-azadiene, which upon treatment with acid underwent an intramolecular Diels-Alder/Alder-Ene cascade reaction to yield amine **I.56**. Reduction of the methylene group was then performed using hydrogen in the presence of Adam's catalyst and the resulting intermediate was treated with DIBAL-H. This triggered a ring opening *via* a retro aza-Prins reaction and the reduction of the resulting iminium ion to provide alcohol **I.57**. Double addition of phenyl isocyanate followed by acid-mediated cyclization led to formation of carbamate **I.58**, which could be transformed to (\pm)-methyl homodaphniphyllate in three steps. Trapping the secondary amine with phenyl isocyanate was necessary to prevent protonation of the amine in the subsequent ring closing step.

1.1.2.5 Heathcock's first generation synthesis of (\pm)-methyl homosecodaphniphyllate

The total synthesis of (\pm)-methyl homosecodaphniphyllate (**I.36**) was reported by the Heathcock group in 1988 (Scheme I.6). This synthesis was carried out in only nine linear steps, making use of the bio-inspired condensation/Diels-Alder/Alder-Ene cascade reaction (*vide supra*, section 1.1.1, Scheme I.1) to obtain the natural product in an overall yield of 48 %. This biomimetic approach opened a short, elegant and convenient pathway towards the secodaphniphylline-type alkaloids.^[39]

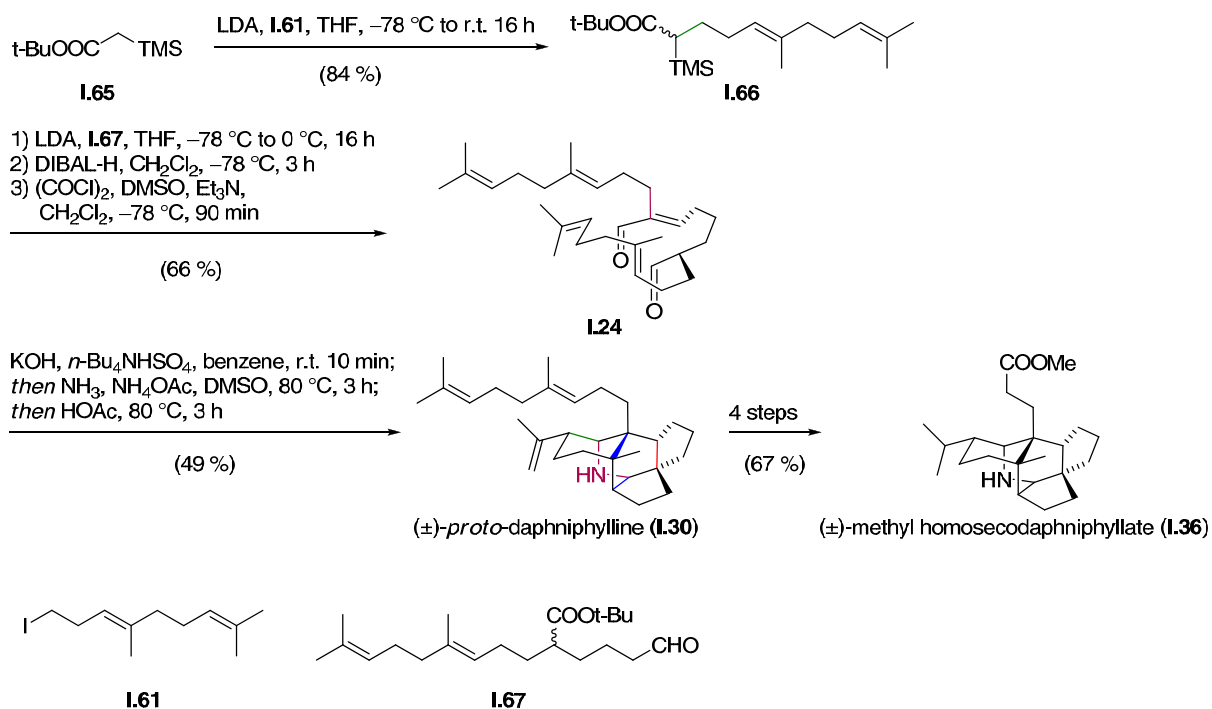


Scheme I.6: First generation synthesis of (\pm)-methyl homosecodaphniphyllate (**I.36**).

Amide **I.59** was turned into the corresponding lithium enolate, which underwent a conjugate addition into ester **I.60** before being trapped with homogeranyl iodide (**I.61**). The resulting intermediate **I.62** was then converted in three steps into diol **I.63**. Swern oxidation followed by reaction of the resulting dialdehyde with ammonia gave a 2-azadiene, which underwent an acid-catalyzed Diels-Alder/Alder-Ene cascade reaction to give pentacycle **I.64**. Having the desired carbon framework in hands, (\pm)-methyl homosecodaphniphyllate (**I.36**) could be obtained after three further steps.

1.1.2.6 Heathcock's second generation synthesis of (\pm)-methyl homosecodaphniphyllate

A second generation synthesis of (\pm)-methyl homosecodaphniphyllate (**I.36**, Scheme I.7) was described by Heathcock *et al.* in 1990. This synthesis includes a biomimetic transformation of a squalene-derived bisaldehyde **I.24** into (\pm)-*proto*-daphniphylline (**I.30**) *via* the proposed biosynthetic pathway for the formation of the secodaphniphylline-type alkaloids (*i.a.* Michael addition/condensation/Diels-Alder/Alder-Ene cascade, *vide supra*, Section 1.1.1, Scheme I.1). Even though obtaining the natural product in nine linear steps in an overall yield of 18 % appears less efficient than the first generation synthesis, employing the proposed biological intermediate, bisaldehyde **I.24** and constructing all rings in one single step using simple reaction conditions is of great significance. This makes for one of the most elegant total syntheses reported so far.^[30, 32a]

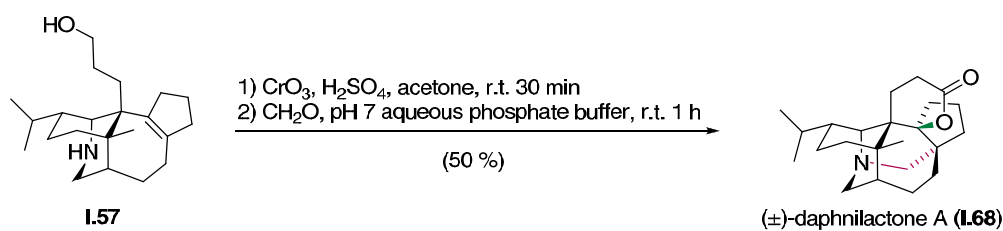


Scheme 1.7: Biomimetic total syntheses of **(±)-proto-daphniphylline (I.30)** and **(±)-methyl homosecodaphniphyllate (I.36)**.

Tert-butyl (trimethylsilyl)acetate (**I.65**) was alkylated with homogeranyl iodide (**I.61**) to give ester **I.66**. Peterson-type olefination with aldehyde **I.67** followed by double reduction and double Swern oxidation yielded bisaldehyde **I.24**. After treatment of **I.24** with **KOH** to trigger a Michael addition, the reaction mixture was exposed to gaseous ammonia to form a 2-azadiene, which, upon heating in acetic acid, underwent an intramolecular Diels-Alder/Alder-Ene cascade reaction to furnish **(±)-proto-daphniphylline (I.30)**. Compound **I.30** could then be converted into **(±)-methyl homosecodaphniphyllate (I.36)** in four steps.

1.1.2.7 Heathcock's total synthesis of **(±)-daphnilactone A**

In 1989, Heathcock and coworkers succeeded in synthesizing **(±)-daphnilactone A (I.68)**, Scheme I.8). The synthesis proceeded over eleven linear steps and produced the natural product in 9 % overall yield. Alcohol **I.57**, which was accessible *via* the condensation/Diels-Alder/Alder-Ene cascade reaction, was a common intermediate in both the total synthesis of **(±)-methyl homodaphniphyllate (I.51)**, Scheme I.5) and the total synthesis of **I.68**.^{[38],[41]}

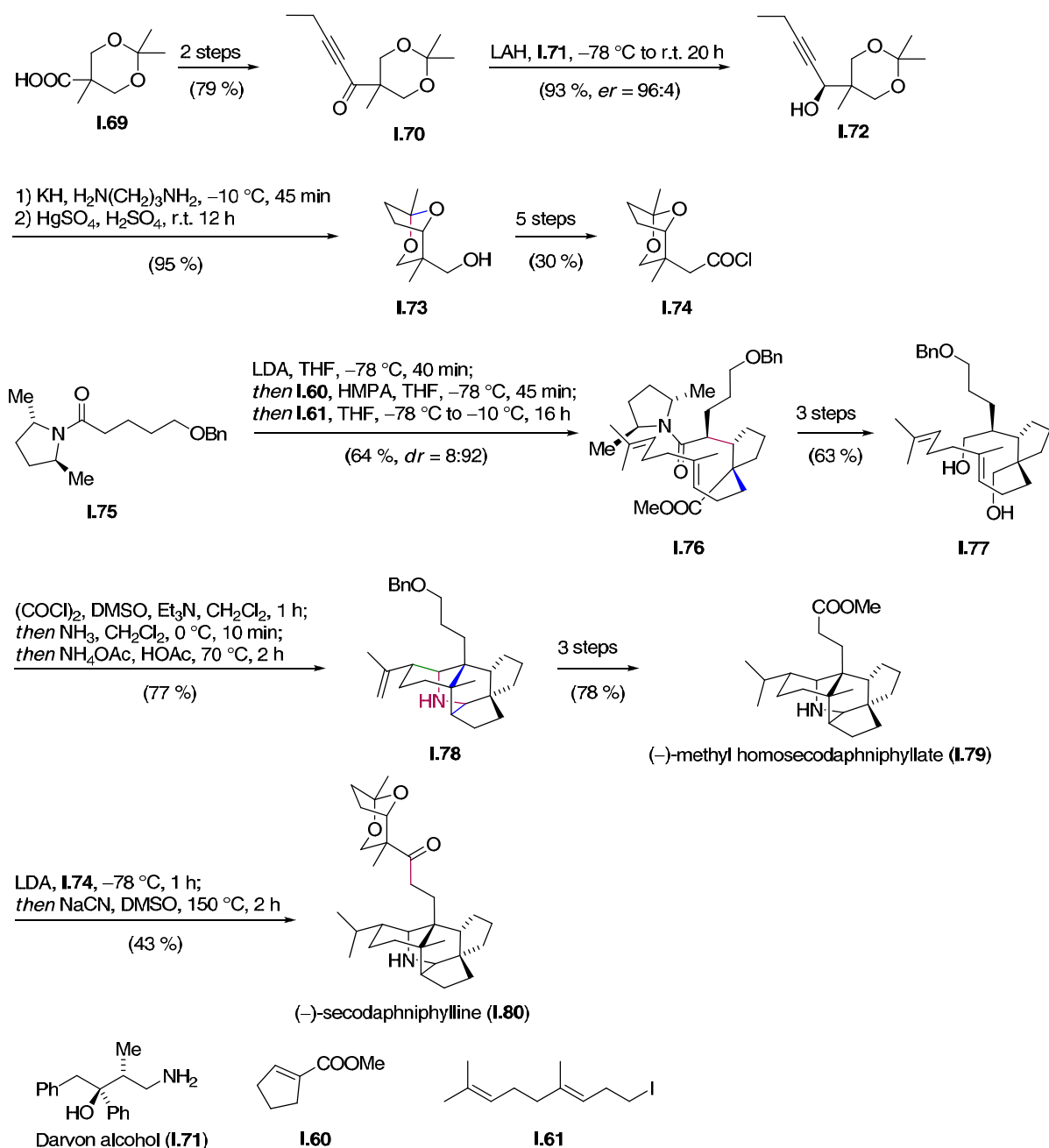


Scheme 1.8: Total synthesis of (±)-daphnilactone A (**I.68**).

Alcohol **I.57** was first subjected to Jones oxidation. The resulting carboxylic acid then participated in an oxa-Prins-Mannich-type reaction employing a formalin solution in an aqueous phosphate buffer. This reaction sequence furnished (±)-daphnilactone A (**I.68**) in 50 % yield.

1.1.2.8 Heathcock's asymmetric total syntheses of (–)-methyl homosecodaphniphyllate and (–)-secodaphniphylline

Another important achievement realized by the Heathcock group was the first asymmetric total synthesis of a *Daphniphyllum* alkaloid. In 1990, they introduced an asymmetric third generation synthesis of (–)-methyl homosecodaphniphyllate (**I.79**, Scheme I.9) and the total synthesis of (–)-secodaphniphylline (**I.80**, Scheme I.9). The northern part was constructed by means of a stereoselective carbonyl reduction using a chiral reducing agent. The synthesis of the southern part was accomplished using the previously established strategy employed for the racemic total synthesis of (±)-methyl homosecodaphniphyllate (**I.36**, *vide supra*, Scheme I.6), but starting from an L-alanine-derived chiral amide **I.75**. Thus, the total synthesis of **I.80** proceeds over 9 linear steps and affords the natural product in 10 % overall yield.^[42]



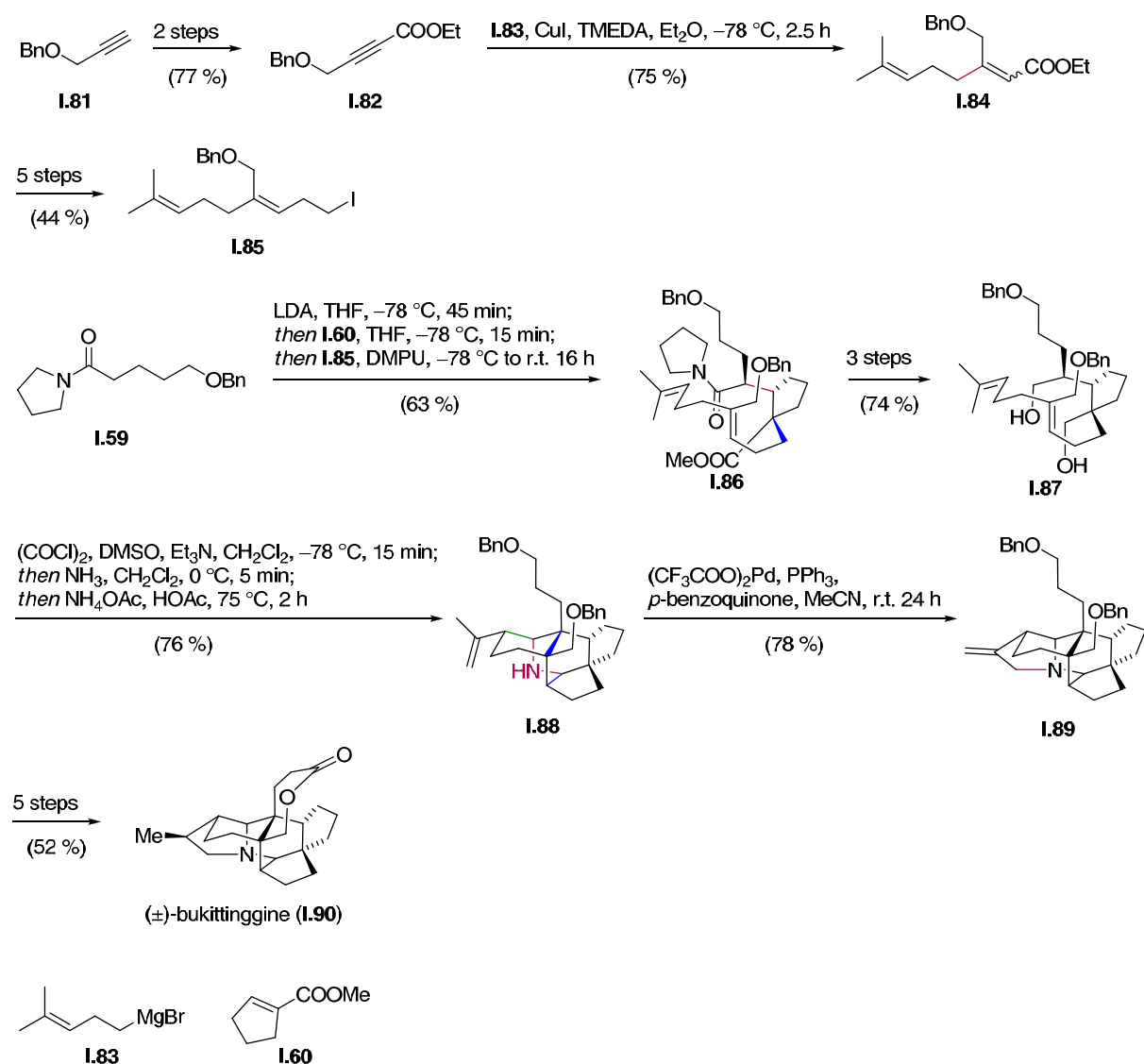
Scheme 1.9: Asymmetric total syntheses of (-)-methyl homosecodaphniphyllate (**1.79**) and (-)-secodaphniphylline (**1.80**).

After converting carboxylic acid **1.69** into ketone **1.70**, an asymmetric reduction using a chiral aluminum complex with Darvon alcohol (**1.71**) afforded the enantiomerically enriched alkyne **1.72**. Alkyne zipper reaction followed by alkoxymercuration and ketal hydrolysis resulted in spontaneous cyclization to desired ketal **1.73**, which was converted in five steps into acid chloride **1.74**.

Chiral amide **I.75** was subjected to a previously described Michael addition/alkylation sequence (*vide supra*, Scheme I.9) combining **I.60** and **I.61** to give intermediate **I.76**. Upon conversion into diol **I.77** and oxidation to the dialdehyde, the Michael addition/condensation/Diels-Alder/Alder-Ene reaction sequence (*vide supra*, Section 1.1.1, Scheme I.1) gave rise to enantiomerically pure benzyl ether **I.78**. This intermediate was converted into (–)-methyl homosecodaphniphyllate (**I.79**) in three steps. Mixed Claisen condensation with acid chloride **I.74** followed by Krapcho decarboxylation finally afforded (–)-secodaphniphylline (**I.80**).

1.1.2.9 Heathcock's total synthesis of (±)-bukittinggine

The total synthesis of (±)-bukittinggine (**I.90**, Scheme I.10), which is the eponymous representative of its skeletal type within the *Daphniphyllum alkaloids*, was reported by the Heathcock group in 1992. The established condensation/Diels-Alder/Alder-Ene cascade reaction (*vide supra*, Section 1.1.1, Scheme I.1) was again key transformation in the synthesis. A palladium-catalyzed cyclization led to formation of the hexacyclic framework of **I.90**, thus providing the natural product in 14 % overall yield over 11 steps.^[43]

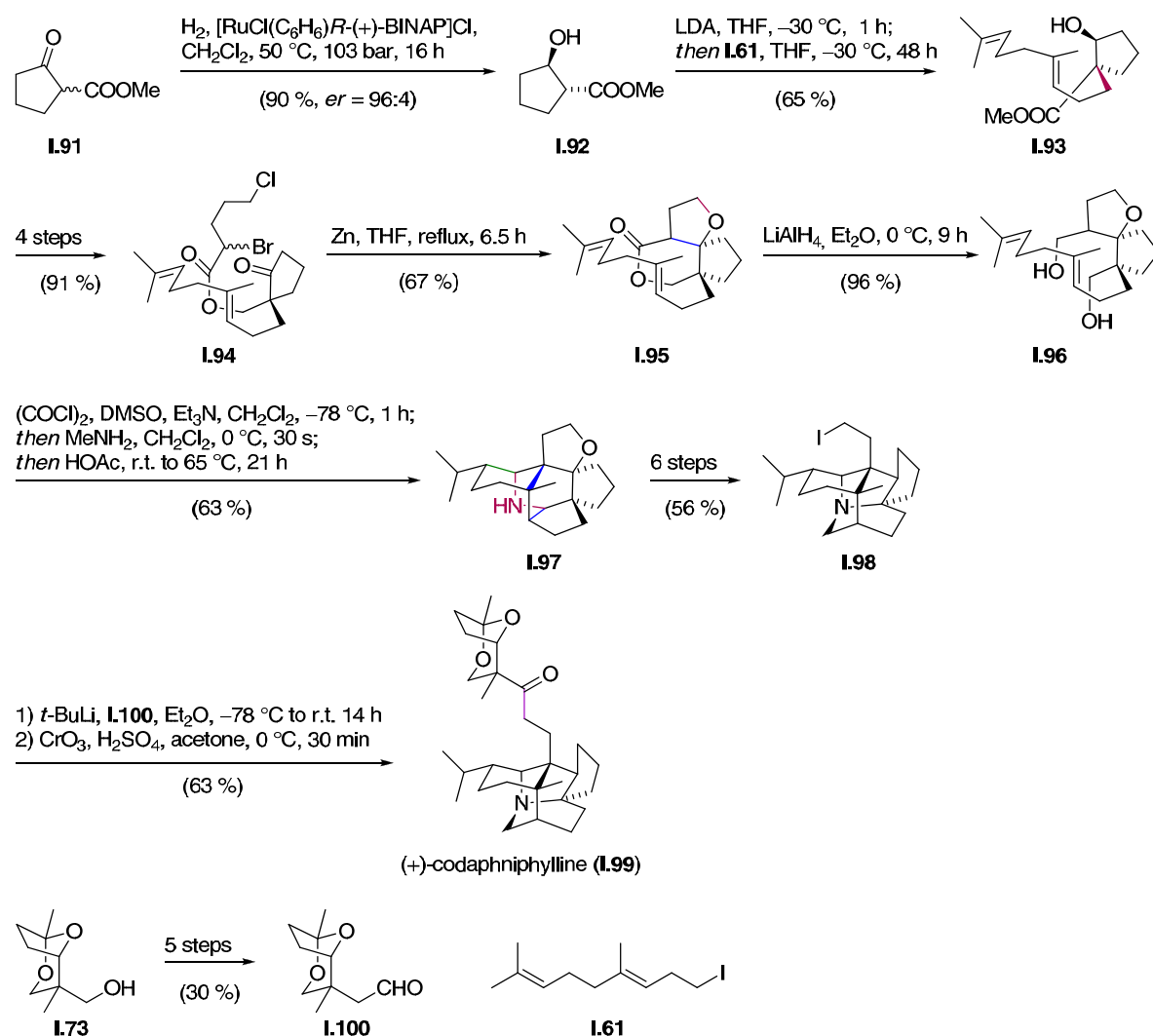


Scheme I.10: Total synthesis of (±)-bukittinggine (I.90).

Starting from benzyl ether **I.81**, ester **I.82** was obtained in two steps and was then converted into alkene **I.84** via a cuprate conjugate addition employing **I.83**. Iodide **I.85** was obtained in 5 steps from **I.84**. This building block was then employed as electrophile in the previously developed Michael addition/alkylation sequence (*vide supra*, Scheme I.9). Upon treatment of amide **I.59** with LDA followed by addition of ester **I.60** and **I.85**, benzyl ether **I.86** was obtained. It was converted into diol **I.87** in three steps. Serial treatment of **I.87** under Swern conditions, gaseous ammonia and warm acetic acid resulted in the desired cascade reaction to form pentacycle **I.88**. The key C-N bond was formed via intramolecular aminopalladation to give hexacycle **I.89**, which could be converted in five steps into (±)-bukittinggine (**I.90**).

1.1.2.10 Heathcock's asymmetric total synthesis of (+)-codaphniphylline

In 1995, Heathcock and coworkers developed an asymmetric total synthesis of (+)-codaphniphylline (**I.99**, Scheme I.11). The synthesis started from previously reported enantiomerically enriched compound **I.92**, which was accessible by Noyori asymmetric reduction and featured the well-established condensation/Diels-Alder/Alder-Ene cascade reaction (*vide supra*, Section 1.1.1, Scheme I.1) to form the polycyclic secodaphniphylline carbon skeleton. This core structure could then be converted into the daphniphylline skeleton of **I.99** using a previously developed strategy (*vide supra*, Scheme I.5). Overall, this asymmetric synthesis proceeded over 17 steps and furnished the natural product in 9 % yield.^[44]

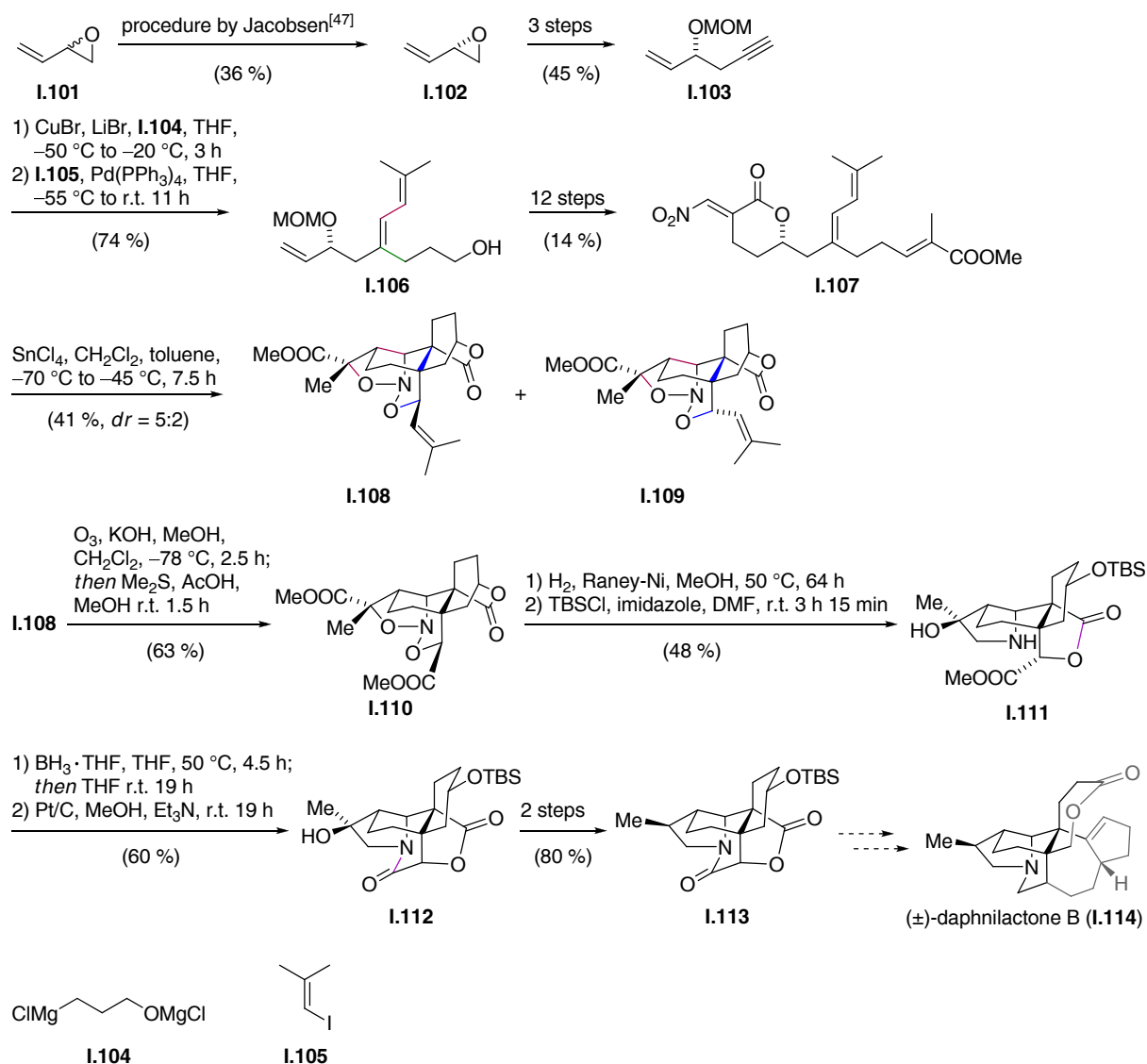


Scheme I.11: Total synthesis of (+)-codaphniphylline (**I.99**).

A Noyori asymmetric reduction of ketoester **I.91** provided starting alcohol **I.92** in good yield and enantiomeric purity. Alkylation of this compound with homogeranyl iodide (**I.61**) gave ester **I.93**, which was converted in four steps into halide **I.94**. A Reformatsky reaction utilizing inactivated zinc dust in the presence of zinc chloride resulted in formation of lactone **I.95**, which was then reduced to the corresponding diol **I.96**. Swern oxidation gave a dialdehyde, which was reacted *in situ* with methylamine to undergo the previously developed Diels-Alder/Alder-Ene cascade reaction (*vide supra*, Section 1.1.1, Scheme I.1). This sequence provided a tertiary cation which underwent an intramolecular hydride transfer to give an iminium ion. This species was hydrolyzed upon aqueous workup to provide directly the saturated pentacycle **I.97**. From this intermediate, iodide **I.98** was obtained in six further steps. Chiral alcohol **I.73**, a building block which had been prepared during the asymmetric synthesis of (–)-secodaphniphylline (**I.80**, *vide supra*, Scheme I.9) was converted in five steps into aldehyde **I.100**. Lithiation of **I.98** and subsequent treatment with aldehyde **I.100** gave a mixture of alcohols, which was directly subjected to Jones oxidation to furnish (+)-codaphniphylline (**I.99**).

1.1.2.11 Denmark's approach towards (±)-daphnilactone B

In the course of their study on tandem double-intramolecular [4+2]/[3+2] cycloadditions of nitroalkenes,^[45] the group of Denmark successfully built in 2009 the south-western part of the daphnilactone B-type alkaloids. The key transformation involved a tetracyclic nitroso acetal **I.110**, which resembles the core structure of (±)-daphnilactone B (**I.114**, Scheme I.12) and encouraged to devise a strategy for the total synthesis.^[46]



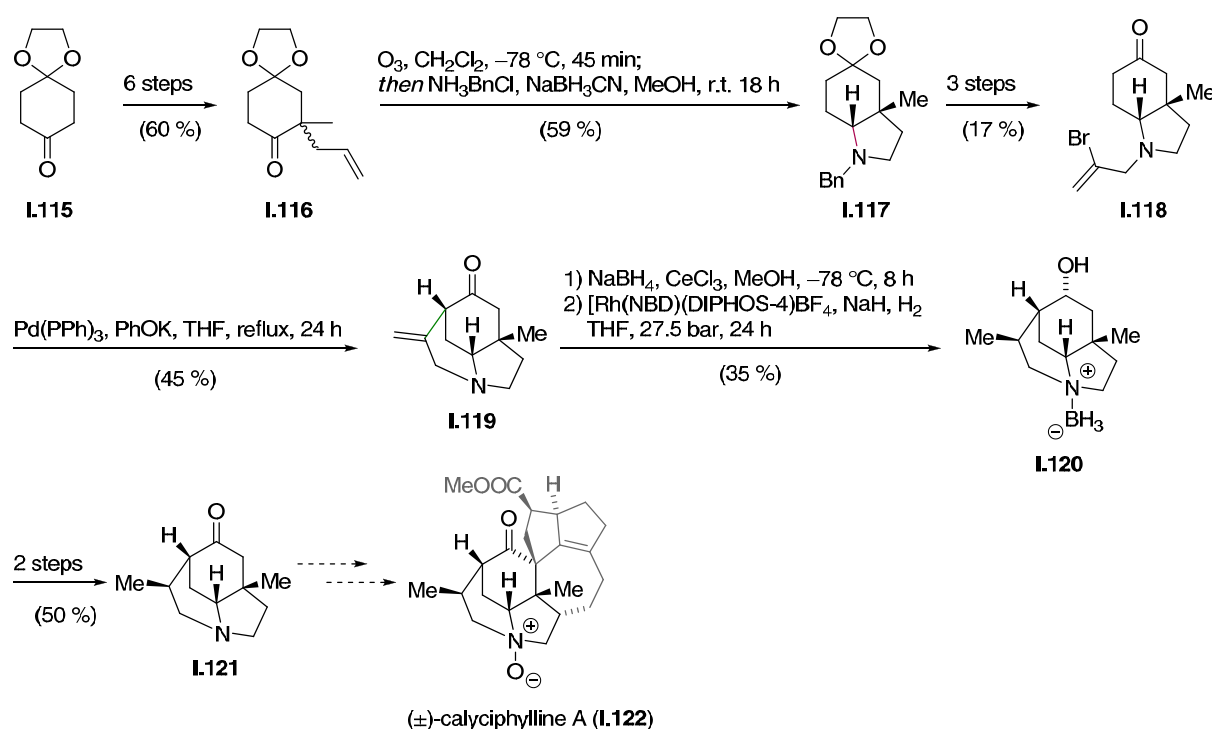
Scheme 1.12: Tandem double-intramolecular [4+2]/[3+2] cycloaddition approach towards daphnilactone B-type alkaloids.

Enantiomerically enriched epoxide **I.102** was available from the racemate **I.101** using Jacobsen's hydrolytic kinetic resolution protocol,^[47] and was converted into **I.103** in three steps. A carbocupration using **I.104** followed by a palladium-catalyzed cross coupling with iodide **I.105** afforded alcohol **I.106**. Compound **I.107**, which was obtained in 12 steps from **I.106** was then treated with SnCl₄. This gave rise to an intramolecular *exo*-hetero Diels-Alder reaction between the electron rich trisubstituted olefin and the heterodiene contained in the nitroolefin moiety. Subsequent intramolecular [3+2] cycloaddition between the resulting nitronate and the electron poor double bond formed nitroso acetal **I.108** together with diastereoisomer **I.109**. Isomer **I.108** was separated and subjected to ozonolysis in the presence of sodium methoxide followed by reductive workup to obtain methyl ester **I.110**.

Raney-nickel mediated hydrogenation and subsequent TBS protection gave lactone **I.111**. After formation of an amine-borane complex, cyclization could be achieved using triethylamine in the presence of platinum on charcoal to yield lactam **I.112**. Reduced pentacycle **I.113** could then be obtained in two further steps. This completed the western carbon framework of (\pm)-daphnilactone B (**I.114**).

1.1.2.12 Bonjoch's approach towards (\pm)-calyciphylline A

The group of Bonjoch reported in 2005 their work on methyloctahydroindoles on a way to calyciphylline A-type alkaloids such as (\pm)-calyciphylline A (**I.122**, Scheme I.13). The key step was a palladium-catalyzed intramolecular coupling of an amino-tethered vinyl bromide with the α -position of a ketone.^[48]



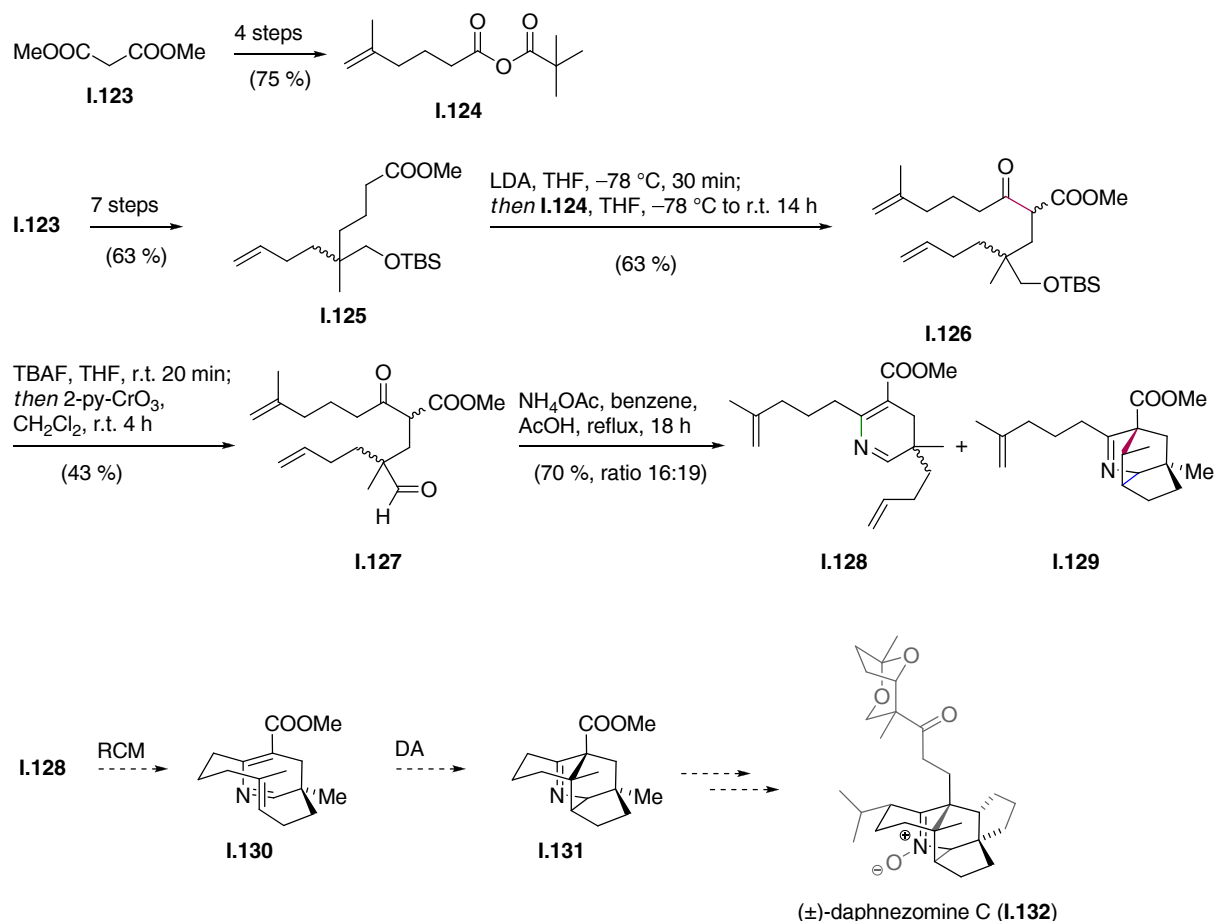
Scheme I.13. Construction of the south-western part of (\pm)-calyciphylline A (**I.122**).

Ketone **I.115** was alkylated in a six-step sequence to form alkene **I.116**, which was subjected to a tandem ozonolysis/double reductive amination sequence to provide amine **I.117**. This intermediate was converted in three steps into bromide **I.118** and was then engaged in a palladium-catalyzed cyclization to give tricycle **I.119**. In order to achieve reduction of the alkene with the correct diastereoselectivity, a Luche reduction employing sodium borohydride

was performed. The resulting amine-borane complex could be reduced in a diastereoselective manner using hydrogen in the presence of a chiral rhodium catalyst. Saturated tricycle **I.120** was converted in two steps into ketone **I.121**, which features the carbon skeleton of the southwestern part of (\pm)-calyciphylline A (**I.122**).

1.1.2.13 Tanabe's approach towards the construction of the ring system of (\pm)-daphnezomine C

In 2007, Tanabe and coworkers reported their studies on ring closing metathesis for the formation of the 11-membered ring system of the secodaphniphylline-type alkaloid (\pm)-daphnezomine C (**I.132**, Scheme I.14).^[49]



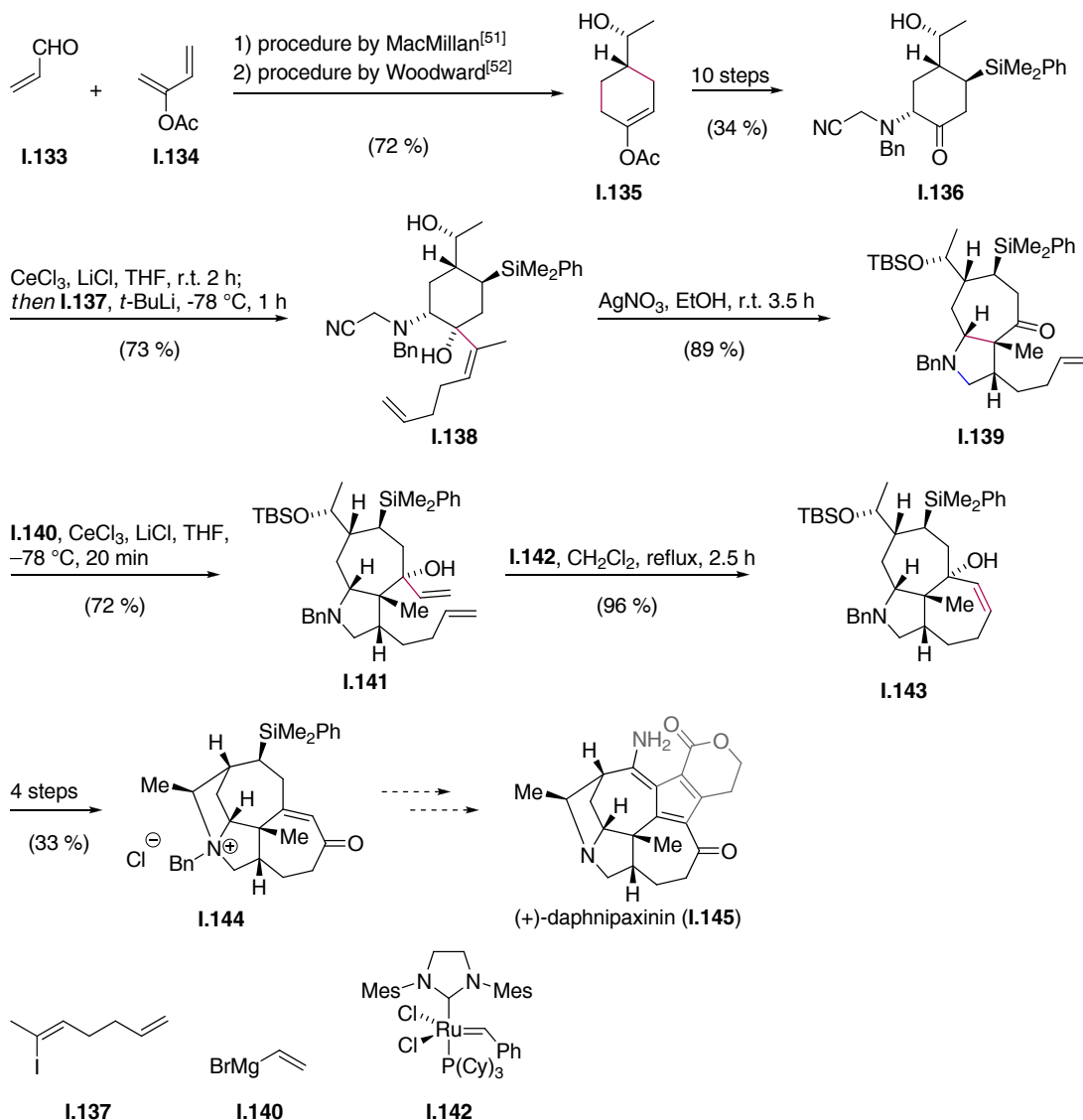
Scheme I.14: Studies on a RCM approach towards (\pm)-daphnezomine C (**I.132**).

Dimethylmalonate (**I.123**) was the common starting material for both the mixed anhydride **I.124** and the TBS ether **I.125**. Addition of the lithium enolate of **I.125** to **I.124** led to formation of ester **I.126**. Upon *O*-deprotection and oxidation, aldehyde **I.127** was obtained,

which was heated in the presence of ammonium acetate and acetic acid to give a mixture of dihydropyridine **I.128** and undesired Diels-Alder product **I.129**. In order to convert **I.128** to macrocyclic compound **I.130**, **I.129** was subjected to several ring closing metathesis conditions. However, no conditions could be found to achieve this transformation. The initial plan was to subsequently undergo a Diels-Alder reaction to form tetracycle **I.131**, which would have already featured the southern section of **I.132**. Thus, the group concluded that molecules of the type **I.128** were too rigid and therefore inappropriate for a RCM approach towards (\pm)-daphnezomine C (**I.132**).

1.1.2.14 Overman's approach towards (+)-daphnipaxinin

An asymmetric approach towards the skeleton of the daphnicyclidin-type alkaloids was described in 2009 by Overman *et al.* The key transformation was an aza-Cope-Mannich reaction, which was utilized to construct the [7-5] bicyclic ring system, also setting the correct stereochemistry at the important quaternary stereogenic center at the ring junction. The third cycle was formed *via* a ring closing metathesis, thus completing the south-western part of (+)-daphnipaxinin (**I.145**, Scheme I.15).^[50]

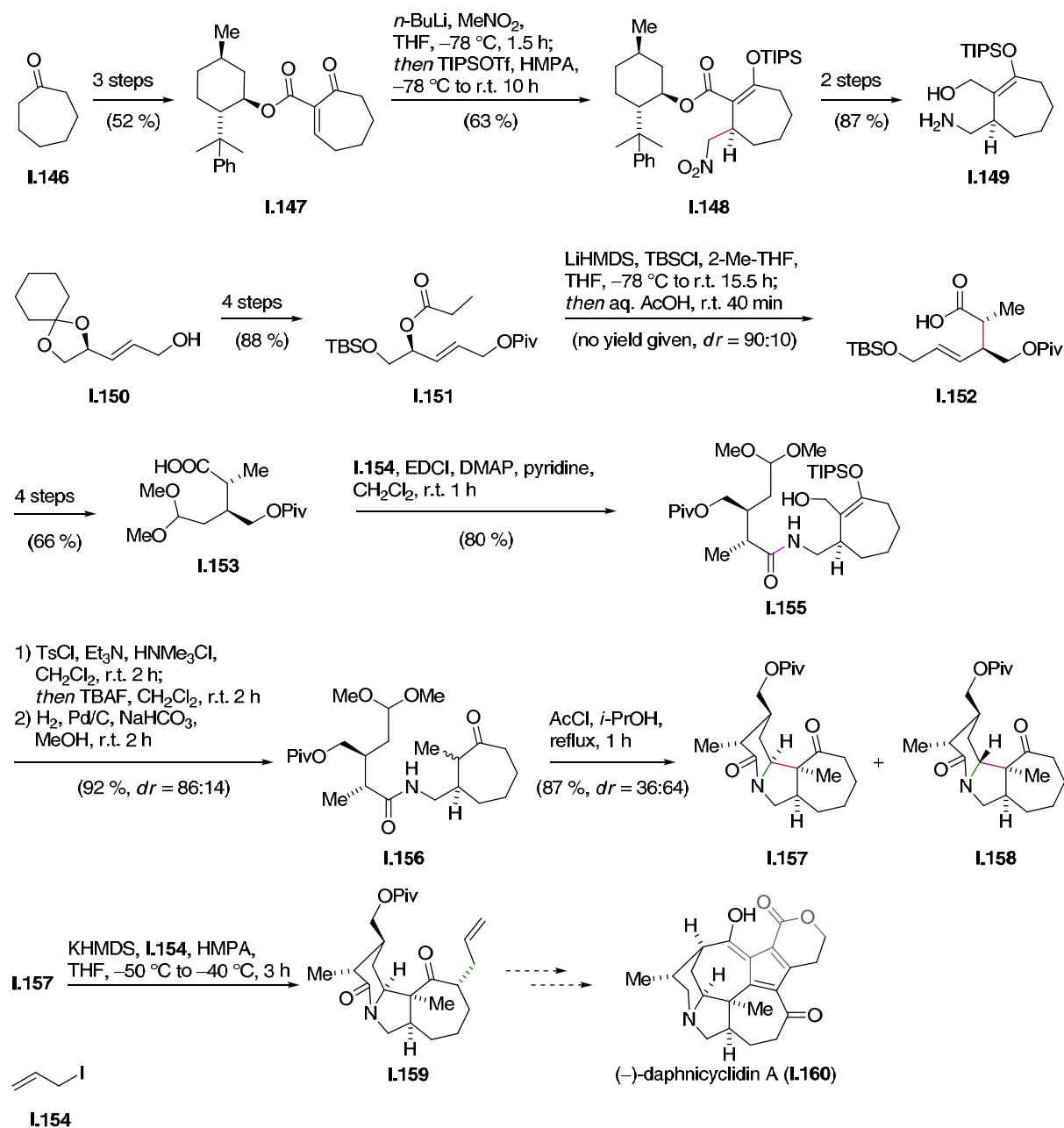


Scheme 1.15: Synthesis of the south-western part of (+)-daphnipaxinin (**I.145**).

An organocatalytic asymmetric Diels-Alder reaction of diene **I.134** with dienophile **I.133** gave a chiral aldehyde,^[51] which was methylated using nickel-catalysis to give alcohol **I.135**.^[52] This compound was converted in ten steps into ketone **I.136**, which was subjected to stereoselective addition of lithiated **I.137** to give alkene **I.138**. Treatment with silver nitrate led to *in situ* generation of an iminium ion, which underwent a sequence of aza-Cope rearrangement followed by Mannich reaction to form bicycle **I.139**. Addition of vinylmagnesium bromide (**I.140**) provided allylic alcohol **I.141**, which underwent ring closing metathesis in the presence of Grubbs second generation catalyst **I.142**. The resulting tricyclic amine **I.143** was converted in four steps into ammonium salt **I.144**, which already features the south-western rings of (+)-daphnipaxinin (**I.145**).

1.1.2.15 Iwabuchi's approach towards (-)-*ent*-daphnicyclidin A

Another approach towards the daphnicyclidin alkaloids was reported by Iwabuchi and coworkers in 2009 when they presented their strategy to construct the tricyclic southern core of (-)-*ent*-daphnicyclidin A (**I.160**, Scheme I.16). The synthesis features a highly stereoselective conjugate addition of nitromethane, an Ireland-Claisen rearrangement and a tandem acyliminium Mannich-type reaction.^[53]

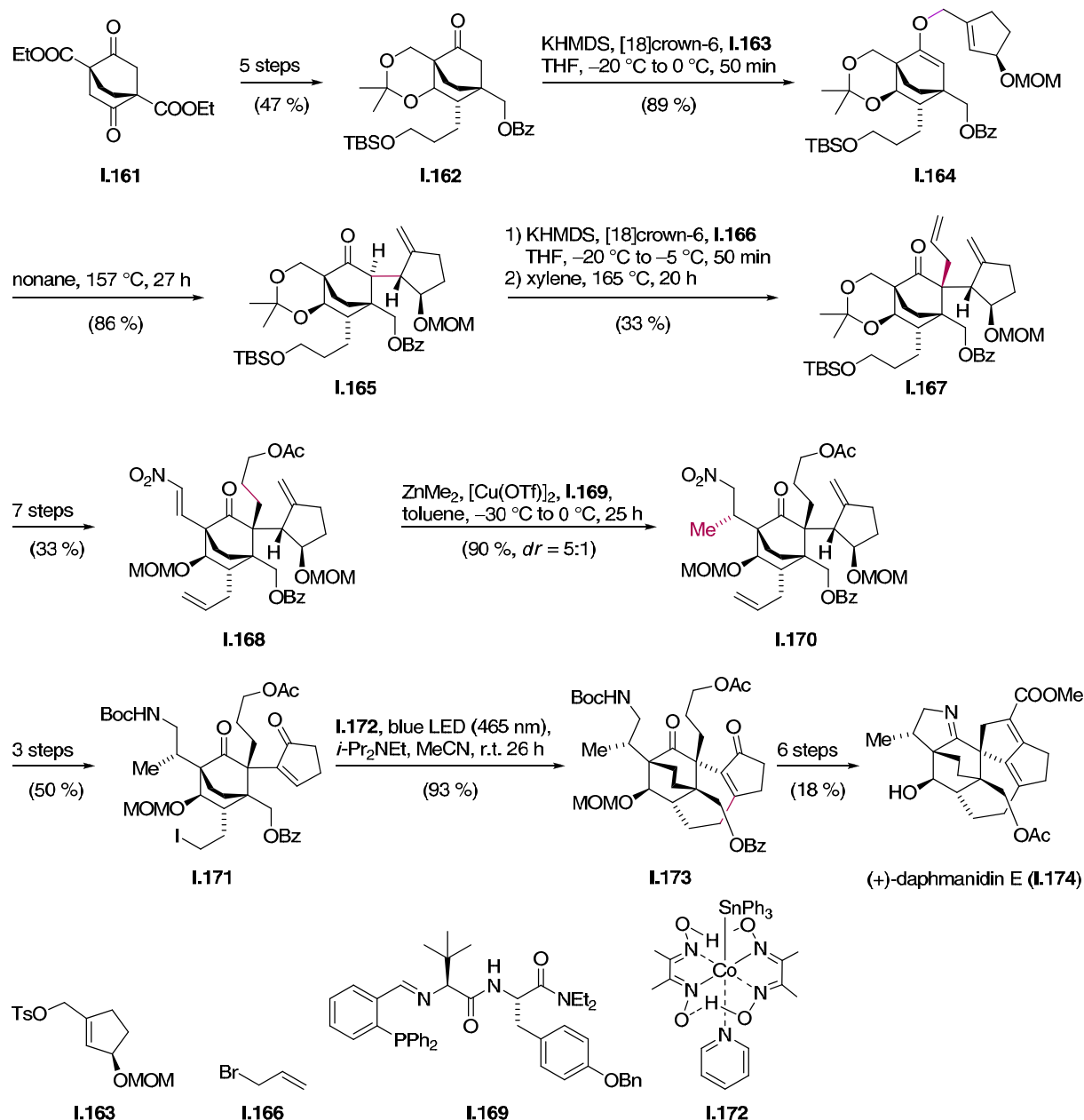


Scheme I.16: Synthesis of the southern part of (-)-*ent*-daphnicyclidin A (**I.160**).

After conversion of cycloheptanone (**I.146**) into 8-phenyl(-)-menthyl ester **I.147**, a diastereoselective alkylation using the lithium salt of nitromethane followed by the trapping of the resulting enolate with TIPSOTf gave nitrocompound **I.148**. This intermediate was then converted into amine **I.149** in two further steps. Acetal **I.150**, which was available from D-mannitol, was the precursor of ester **I.151**. Compound **I.151** was turned into the corresponding TBS-enol ether, and, upon treatment with acid, it underwent an Ireland-Claisen rearrangement to give acid **I.152**. Ketal **I.153** was obtained after four further steps and was then coupled with **I.154** to give amide **I.155**. This intermediate was sequentially treated with TsCl in the presence of a base and TBAF to achieve a one-pot elimination and deprotection. Following hydrogenation gave ketone **I.156**, which was carried on as a mixture of diastereomers with respect to the newly generated stereogenic center. *In situ* generation of HCl resulted in acetal cleavage and subsequent formation of an acyliminium ion, which directly underwent a Mannich-type reaction to give **I.157** and **I.158**. The minor isomer **I.157** was allylated to yield tricyclic amine **I.159**, which was planned to be used as building block to complete the total synthesis of (-)-*ent*-daphnicyclidin A (**I.160**).

1.1.2.16 Carreira's asymmetric total synthesis of (+)-daphmanidin E

In 2011, the group of Carreira reported an asymmetric total synthesis of the daphmanidin A-type alkaloid (+)-daphmanidin E (**I.174**, Scheme I.17). Key transformations were a series of two subsequent Claisen rearrangements to install a quaternary stereogenic center in a hindered position and a cobalt-catalyzed alkyl-Heck cyclization. Overall, the synthesis proceeded over 27 linear steps and provided the natural product in 0.3 % yield.^[54]



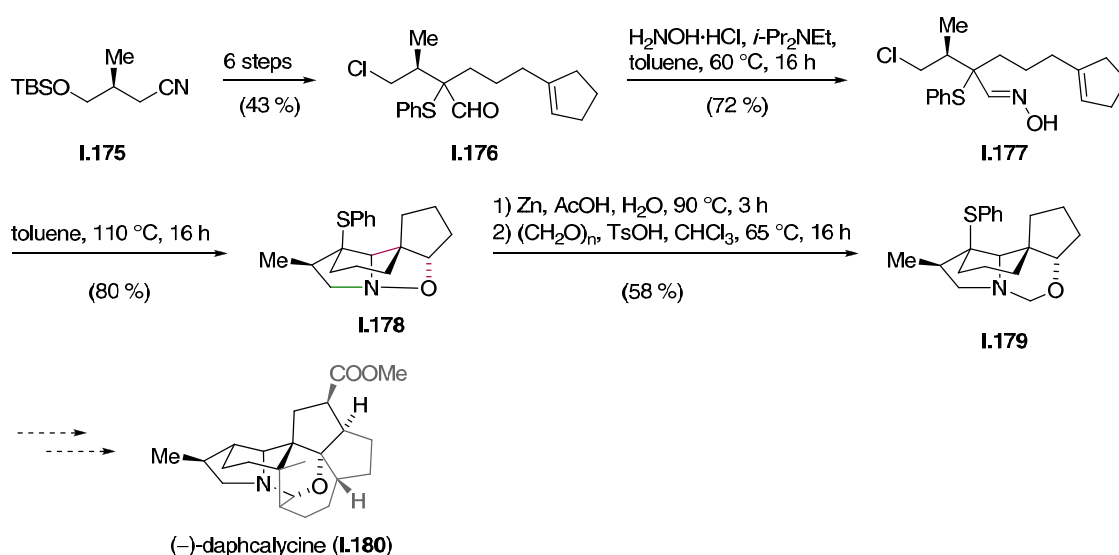
Scheme I.17: Total synthesis of (+)-daphmanidin E (**I.174**).

Enantiomerically enriched bicyclo[2.2.2]octadienone **I.161** was accessible from diethyl succinate and could be resolved by either enzymatic resolution of the racemate or by chromatographic separation of the corresponding diastereomeric hydrazones. **I.161** was converted in five steps into acetal **I.162**, which was *O*-alkylated with cyclic alkene **I.163** to form enol ether **I.164**. Upon heating, this compound underwent a Claisen rearrangement to provide ketone **I.165**. A similar sequence of *O*-allylation/Claisen rearrangement using **I.166** was repeated to give alkene **I.167**, thus selectively establishing the desired quaternary stereocenter. Nitroolefin **I.168**, which was generated from **I.167** in seven steps, was

diastereoselectively methylated using dimethylzinc in the presence of copper(I) and chiral ligand **I.169** to give nitroalkane **I.170**. Compound **I.170** was converted in three steps into iodide **I.171**, which underwent alkyl-Heck-type cyclization in the presence of cobalt catalyst **I.172** and blue light in excellent yield. The resulting tetracyclic ketone **I.173** could be converted into (+)-daphmanidin E (**I.174**) in six steps.

1.1.2.17 Coldham's approach towards (-)-daphcalycine

The yuzurimine-type alkaloid (-)-daphcalycine (**I.180**) was the target of an approach described by Coldham and coworkers in 2011 (Scheme I.18). In the context of their studies on intramolecular 1,3-dipolar cycloadditions, the group was able to construct the main core of this natural product.^[55]

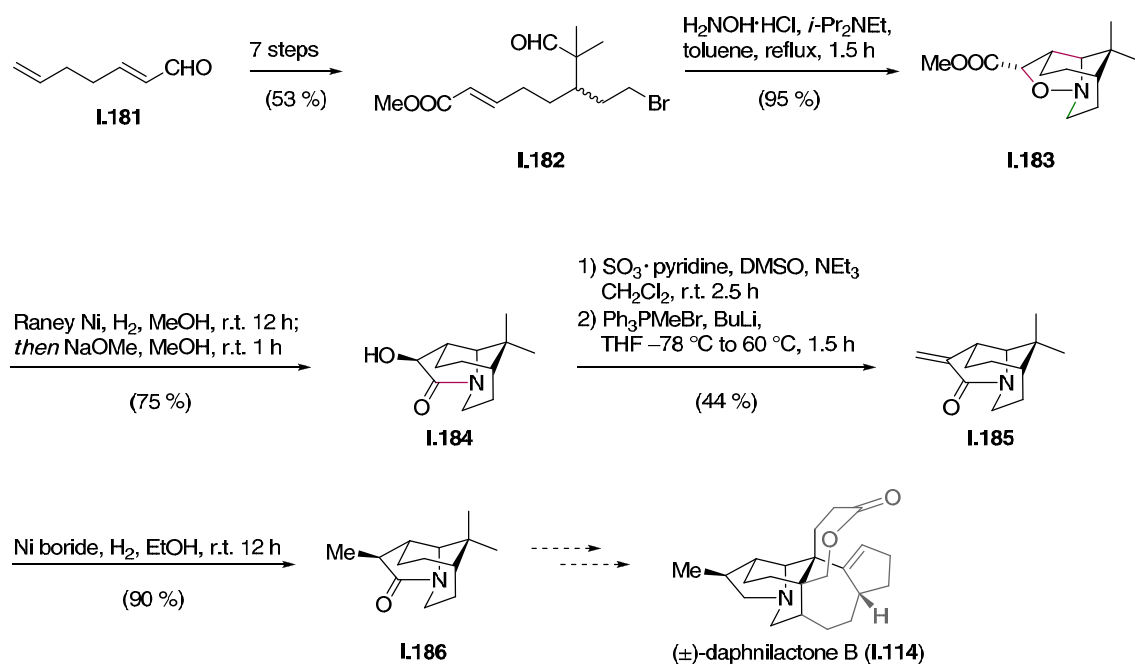


Scheme I.18: Approach towards the synthesis of (-)-daphcalycine (**I.180**).

Known nitrile **I.175** was converted in six steps into aldehyde **I.176**, which was reacted with hydroxylamine to give oxime **I.177**. A tandem intramolecular *N*-alkylation/intramolecular 1,3-dipolar cycloaddition then furnished isoxazolidine **I.178**. Reductive cleavage of the *N*-*O*-bond, followed by formation of the *N*-*O*-acetal gave tetracycle **I.179**, which features the carbon framework of the western part of (-)-daphcalycine (**I.180**).

1.1.2.18 Coldham's approach towards (\pm)-daphnilactone B

In 2011, Coldham and coworkers also described an approach towards the daphnilactone B-type alkaloids by synthesizing the carbon skeleton of their eponymous representative (\pm)-daphnilactone B (**I.114**). The key transformation was again a tandem *N*-alkylation/1,3-dipolar cycloaddition reaction cascade (Scheme I.19).^[56]



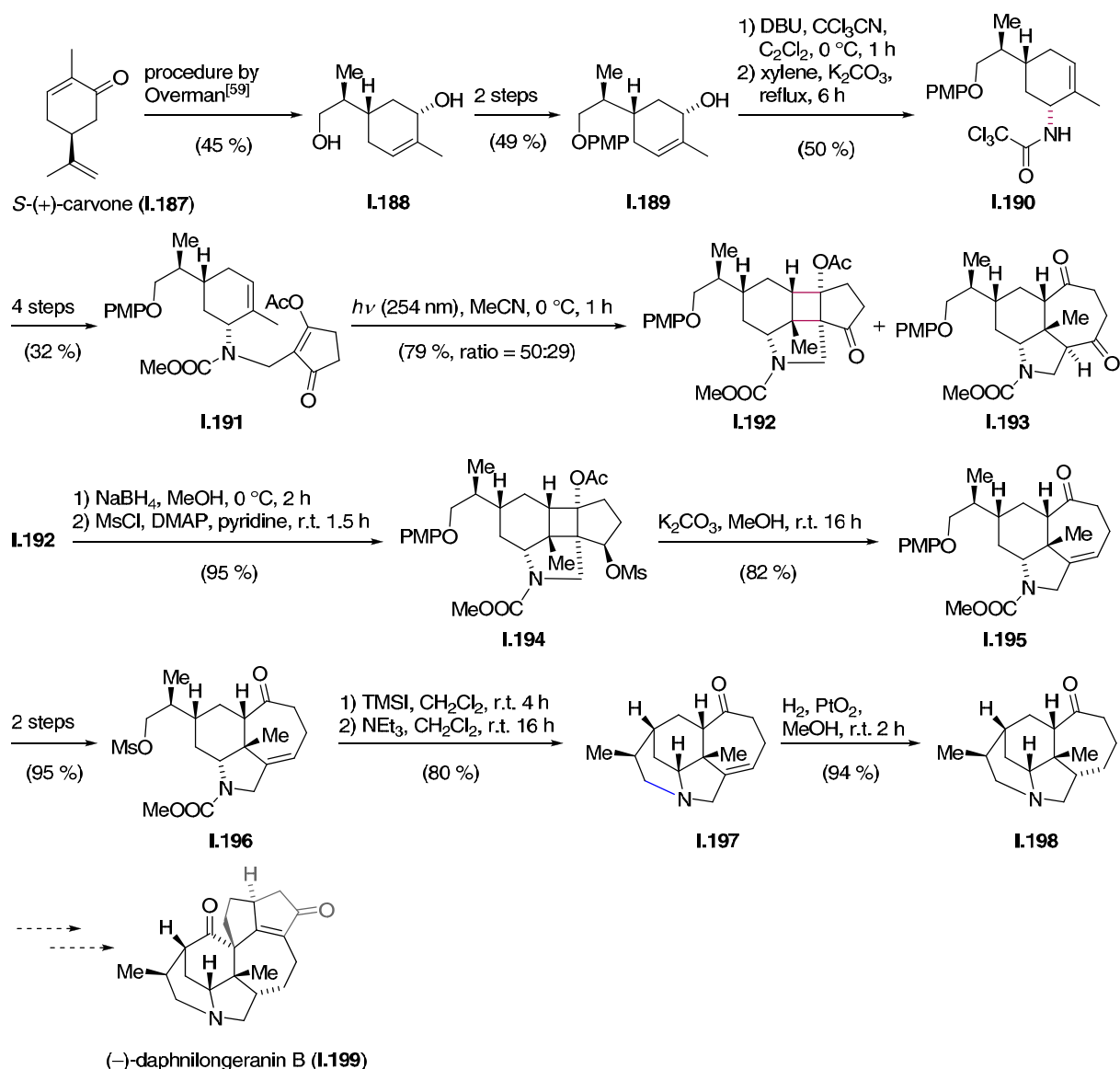
Scheme I.19: Approach towards the synthesis of (\pm)-daphnilactone B (**I.114**).

Aldehyde **I.181** was converted in seven steps into bromide **I.182**. Reacting **I.182** with hydroxylamine gave an oxime, which immediately underwent an *N*-alkylation cyclization reaction followed by intramolecular 1,3-dipolar cycloaddition to form isoxazolidine **I.183**. Cleavage of the *N*-*O*-bond using H_2 in the presence of Raney nickel followed by treatment with base resulted in the formation of lactam **I.184**. Parikh-Döring oxidation followed by a Wittig reaction yielded alkene **I.185**, which was reduced with hydrogen in the presence of nickel boride to selectively obtain tricycle **I.186**, representing the scaffold of (\pm)-daphnilactone B (**I.114**).

1.1.2.19 Wang's approach towards (–)-daphnilongeranin B

In the course of their studies on the construction of the tricyclic core of calyciphylline A-type alkaloids using a Grob fragmentation,^[57] the group of Wang reported in 2012 the synthesis of

the tetracyclic core of (-)-daphnilongeranin B (**I.199**, Scheme I.20).^[58] The nitrogen atom was incorporated utilizing an Overman rearrangement. The key strategy employed to establish the [5-6-7] tricyclic core was a [2+2] photochemical cycloaddition followed by a Grob fragmentation.



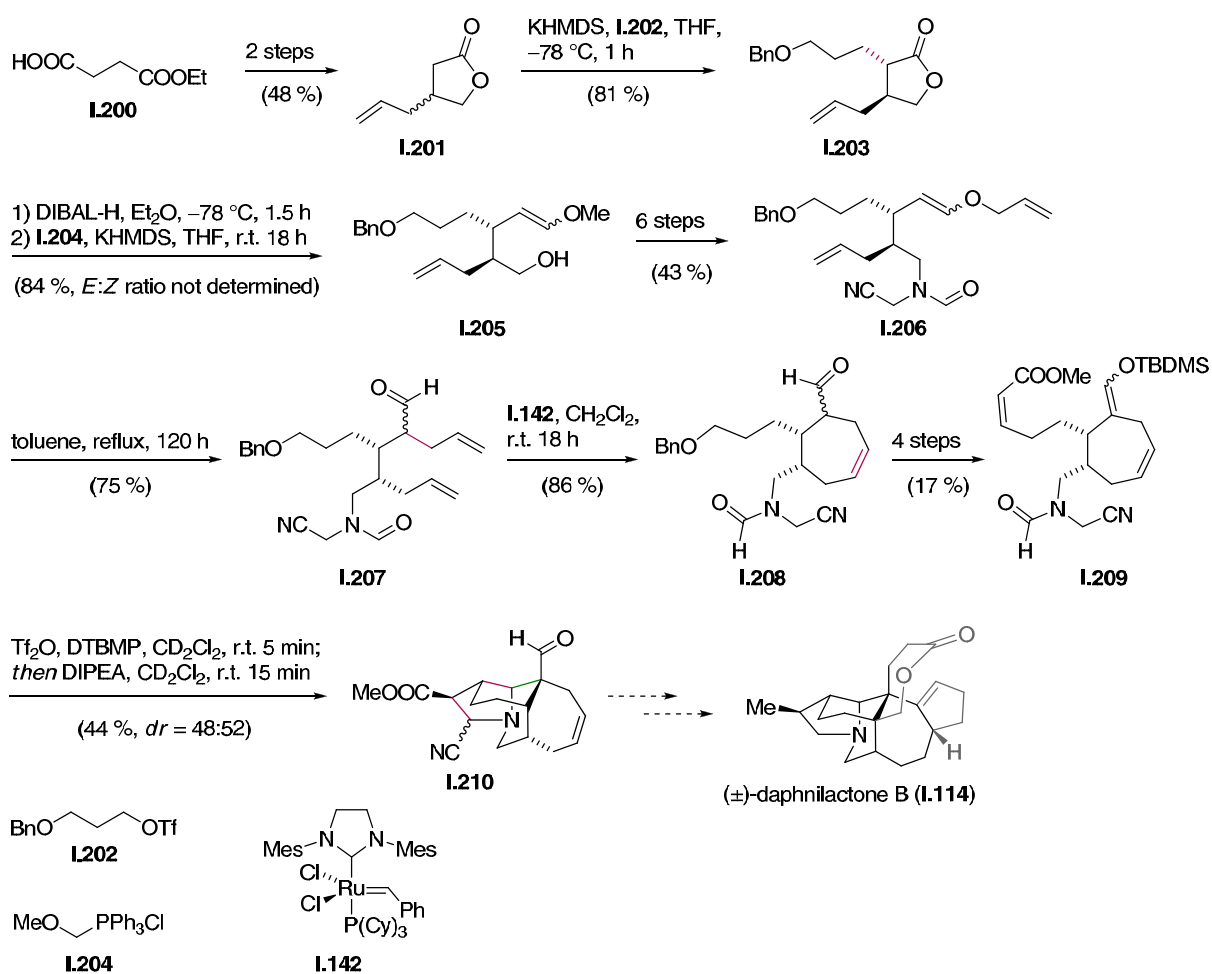
Scheme I.20: Approach towards the synthesis of (-)-daphnilongeranin B (**I.199**).

Diol **I.188**, which was available as a single enantiomer from *S*-(+)-carvone (**I.187**),^[59] was converted in two steps into PMP-ether **I.189**. Formation of a trichloroacetimidate and subsequent Overman rearrangement provided carbamate **I.190**, which could be transformed into enone **I.191** in 4 steps. Irradiation with UV-light triggered a [2+2] cycloaddition to give **I.192** together with side product **I.193**. The latter was speculated to be formed *via* a retroaldol-type pathway to release ring strain. Diastereoselective reduction and mesylation of **I.192**

gave **I.194**, which was treated with potassium carbonate in methanol to initiate a Grob fragmentation. Resulting tricycle **I.195** was converted in two steps into mesylate **I.196** and was then treated with TMSI followed by triethylamine to give tetracyclic amine **I.197**. Compound **I.197** could be reduced diastereoselectively, resulting in the formation of ketone **I.198**, which represents the south-western part of (–)-daphnilongerinin B (**I.199**).

1.1.2.20 Lévesque's approach towards (±)-daphnilactone B

In 2011, the group of Lévesque reported another approach towards the hexacyclic core of (±)-daphnilactone B (**I.114**). Key sequence was a Vilsmeier-Haack cyclization followed by an intramolecular azomethine ylide cycloaddition cascade, constructing three rings in one single step (Scheme I.21).^[60]

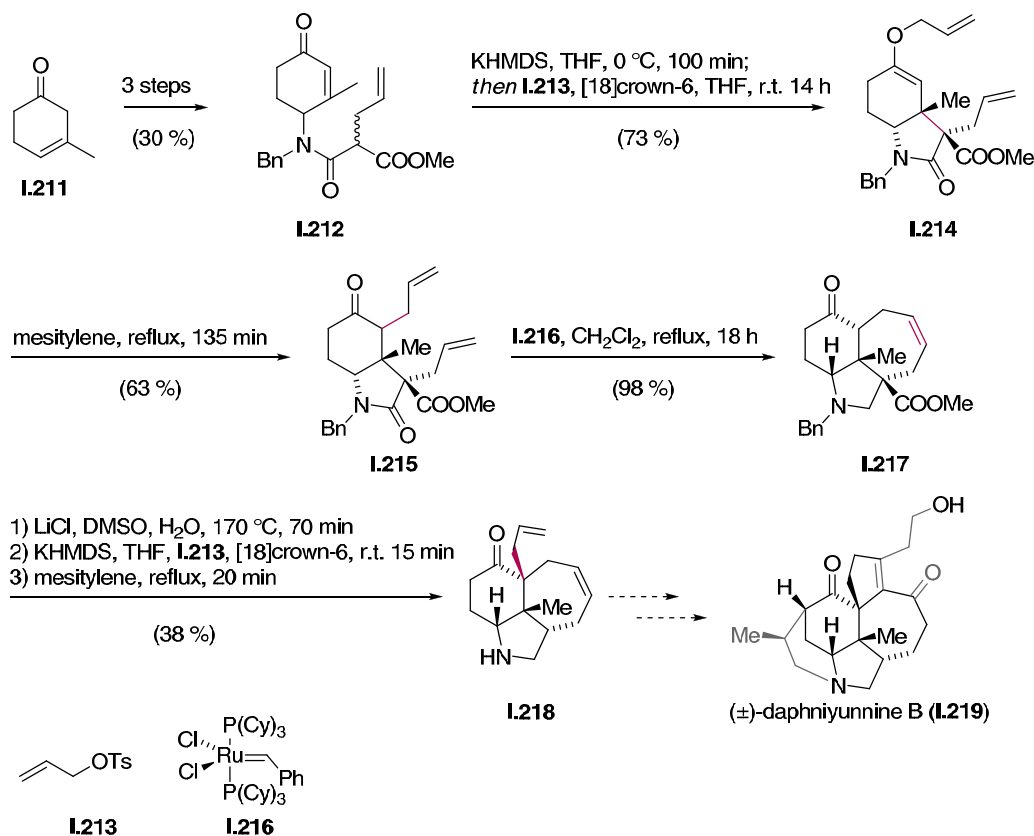


Scheme I.21: Approach for the synthesis of (±)-daphnilactone B (**I.114**).

Succinic acid monoethyl ester **I.200** was converted in two steps into lactone **I.201**, which was alkylated using KHMDS and triflate **I.202** to produce benzyl ether **I.203**. Upon reduction to the corresponding lactol, an unselective Kluge-Wittig reaction using **I.204** gave methyl enol ether **I.205** as a mixture of *E/Z*-isomers. Upon conversion to allyl enol ether **I.206**, this intermediate underwent a thermal Claisen rearrangement to give aldehyde **I.207**, which was subjected to RCM using Grubbs second generation catalyst. The resulting cycloheptene **I.208** could be transformed over four steps into enone **I.209**, which underwent a Vilsmeier-Haack cyclization upon treatment with triflic anhydride. The resulting iminium ion was treated with DIPEA to generate an azomethine ylide, which was intramolecularly trapped by the electron poor double bond by means of a [3+2] cycloaddition. The thus generated tetracycle **I.210** represents the south-western part of (\pm)-daphnilactone B (**I.114**).

1.1.2.21 Dixon's approach towards (\pm)-daphniyunnine B

The group of Dixon reported in 2011 a strategy to synthesize the core of calyciphylline A-type alkaloids. Employing a ring closing metathesis to create the [5-6-7] tricyclic ring system and a Claisen rearrangement to install the quaternary stereogenic center gave rise to the southern core of (\pm)-daphniyunnine B (**I.219**, Scheme I.22).^[61]

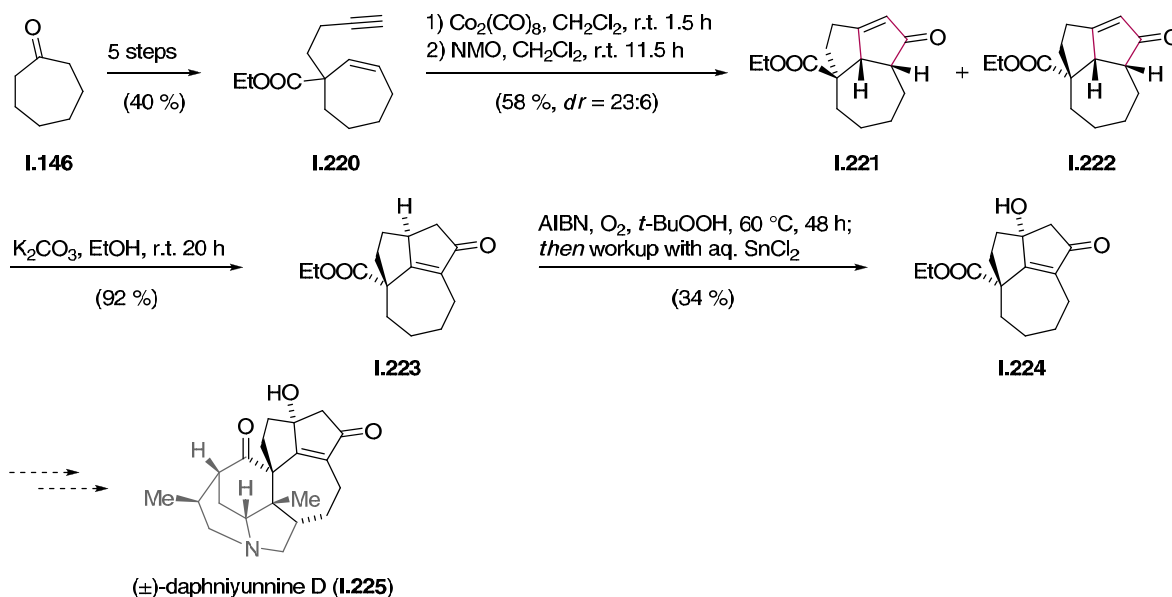


Scheme I.22: Approach towards the synthesis of (\pm)-daphniyunnine B (**I.219**).

Ketone **I.211** was converted into enone **I.212** in three steps. An intramolecular conjugate addition of the *in situ* generated potassium enolate and subsequent trapping with allyl tosylate **I.213** provided allyl enol ether **I.214**. Heating this compound resulted in a thermal Claisen rearrangement to give bisalkene **I.215**, which was subjected to RCM using Grubbs first generation catalyst **I.216** to yield tricycle **I.217**. After performing a Krapcho decarboxylation and *O*-allylation, subsequent heating provoked another Claisen rearrangement which provided tricyclic amine **I.218**. This intermediate features the [5-6-7] tricyclic core and the quaternary stereogenic center of (\pm)-daphniyunnine B (**I.219**).

1.1.2.22 Dixon's approach towards (\pm)-daphniyunnine D

In 2012, Dixon and coworkers described their approach to construct the north-eastern part of calyciphylline A-type alkaloids. The key step in this synthesis was an intramolecular Pauson-Khand reaction to obtain the tricyclic scaffold featured in (\pm)-daphniyunnine D (**I.225**, Scheme I.23).^[62]



Scheme I.23: Approach towards the synthesis of (±)-daphniyunnine D (I.225).

Cycloheptanone (I.146) was converted in five steps into alkyne I.220. Formation of the cobalt-alkyne complex followed by treatment with NMO to trigger a Pauson-Khand reaction provided a diastereomeric mixture of enones I.221 and I.222. This mixture was stirred with base to perform a double-bond migration, which gave ester I.223 as single a diastereomer. Stereoselective radical allylic oxidation followed by reductive workup finally provided tricyclic I.224 with the substitution pattern of (±)-daphniyunnine D (I.225).

Another fascinating molecule of this natural product family is the daphnicyclidin-type alkaloid (+)-oldhamine A (I.226, *vide infra*, Figure I.2), the isolation and structure of which will be discussed in the next section.

1.1.3 Isolation and Structure of (+)-Oldhamine A

(+)-Oldhamine A (I.226, Figure I.2) is a striking example of a daphnicyclidin-type *Daphniphyllum* alkaloid with an intriguing structure. This remarkable natural product has been isolated from the tree *Daphniphyllum oldhamii* and its structure was elucidated in 2008 by Hao and coworkers. The determination of the structure was supported by X-ray analysis of a single crystal.^[63]

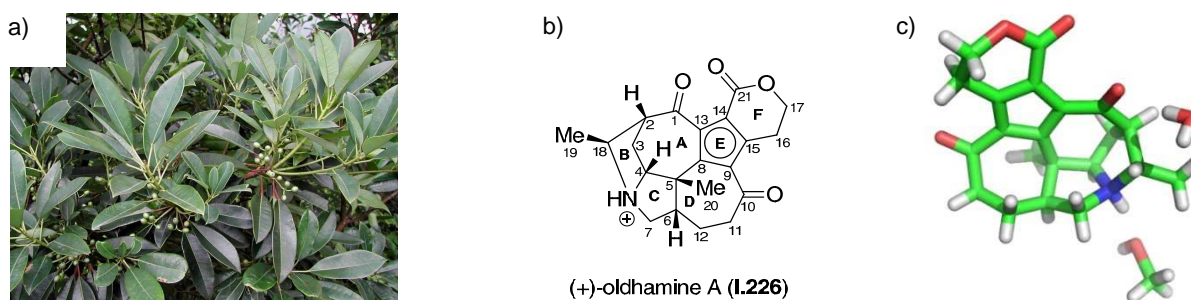
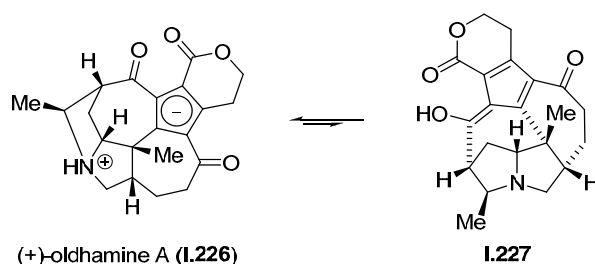


Figure I.2: (+)-Oldhamine A (**I.226**): a) Source of isolation, *Daphniphyllum oldhamii*;^[64] b) chemical structure; c) crystal structure of **I.226**·H₂O·MeOH (CCDC-code: 671960).^[63]

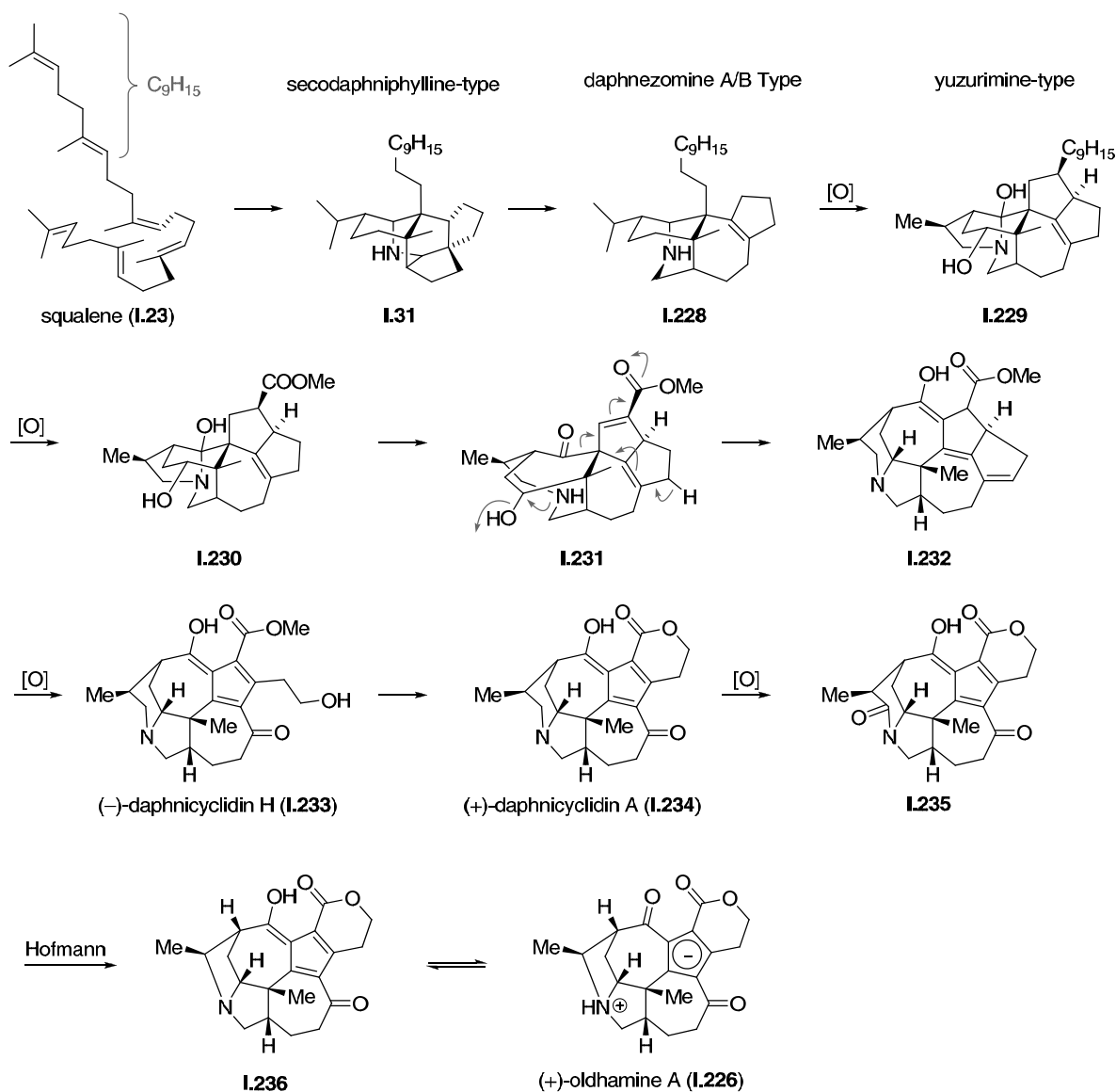
(+)-Oldhamine A (**I.226**) is a zwitterionic nortriterpenoid alkaloid which is composed of six fused rings (A-F) including five stereogenic centers, one of which is quaternary. A unique feature of **I.226** is the presence of a cyclopentadienyl anion forming an internal salt with a tertiary ammonium ion. A cyclopentadienyl anion which is not part of a polyaromatic system is an extremely rare structural motif in nature and has been found in only one other instance, that is to say in the *Daphniphyllum* alkaloid (–)-macropodumine B.^[65] The complex scaffold of **I.226** can be divided in the south-western rings B and C, representing a pyrrolizidine part that bears all the stereogenic centers and northern rings E and F, forming a bicyclic lactone portion.

By titrating **I.226** in an NMR tube with TFA or Na₂CO₃, respectively, it was shown that **I.226** is in equilibrium with its tautomer **I.227**, however strongly favoring the zwitterionic structure (Scheme I.24).



Scheme I.24: (+)-Oldhamine A (**I.226**) and its tautomer **I.227**.

A speculated biosynthetic pathway for the formation of **I.226** in nature is shown in Scheme I.25.



Scheme I.25: Biosynthesis of (+)-oldhamine A (I.226) as speculated by Hao.^[63]

As described in detail in the previous section, squalene (I.23) was proposed to form secodaphniphyllate-type structures like I.31 (*vide supra*, Section 1.1.1, Scheme I.1).^{[29],[33]} I.31 is assumed to be a precursor of I.228, representing the daphnezomine A/B-type skeleton.^[32c] Further biosynthetic modifications^[32c] were speculated to lead to yuzurimine-type alkaloids like I.229 and I.230.^[17] These were said to originate from the daphnicyclidin-type alkaloids. I.230 was proposed to be converted into I.231, which could rearrange to give I.232. Oxidative cleavage would lead to daphnicyclidin H (I.233), which could cyclize to give daphnicyclidin A (I.234).^[66] Hao and coworkers speculated that a sequence of oxidation and a subsequent unusual Hofmann rearrangement would lead to the formation of (+)-oldhamine A

(I.226).^[63] These proposed biosynthetic pathways are highly speculative and detailed studies are still to be carried out.

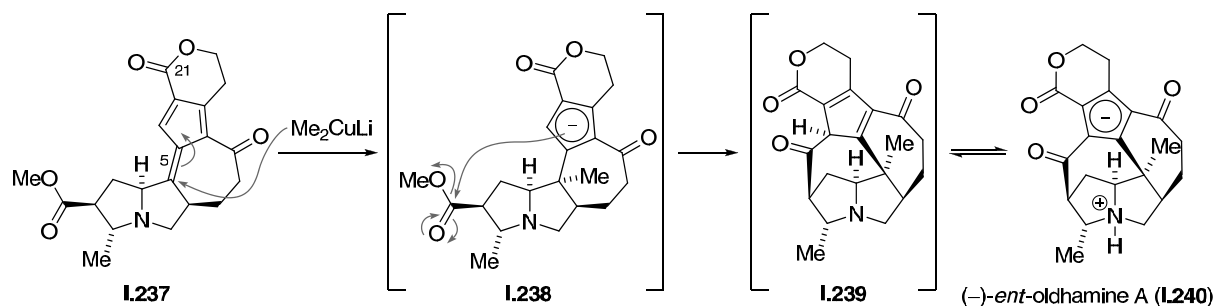
Although some preliminary studies on the pharmacology of **I.226** have been completed,^[63] the biological activity of **I.226** is yet to be determined. Thus, the reason why **I.226** is made by species of the genus *Daphniphyllum* and the role this natural product plays in nature still remains unknown.

Intrigued by its aesthetical appeal and in order to get access to sufficient amounts to fully evaluate its biological activity, a synthetic approach towards the synthesis of **I.226** was initiated in this work, the retrosynthetic analysis of which is described in the next section.

1.1.4 Retrosynthetic Analysis of (–)-*ent*-Oldhamine A

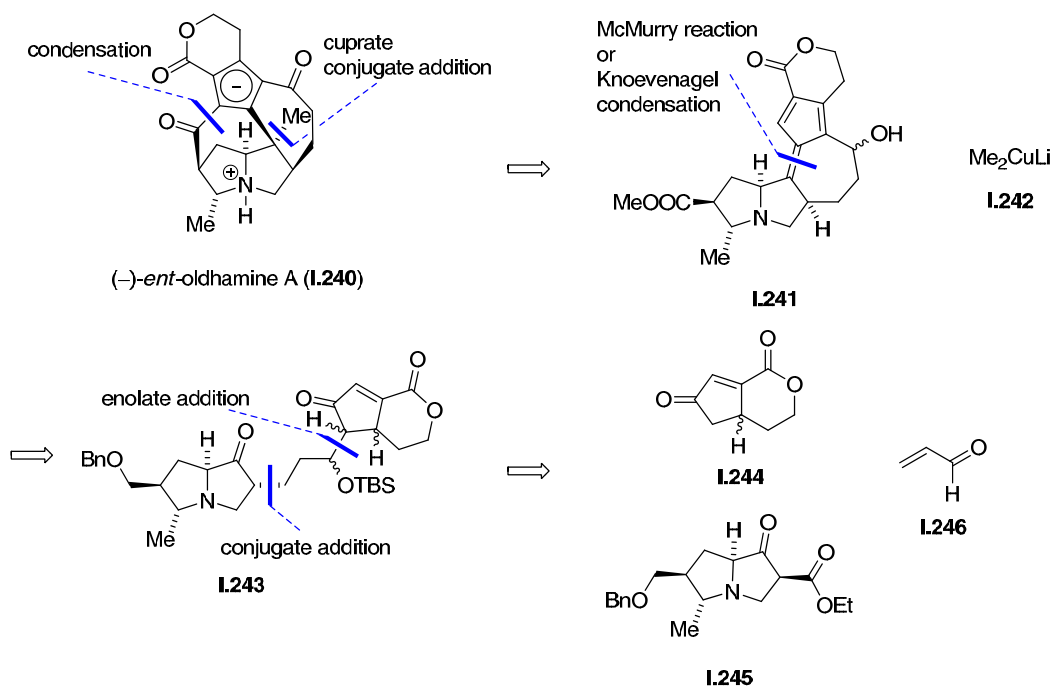
The retrosynthetic strategy aimed at an asymmetric and short yet flexible route to also allow for the efficient preparation of natural product analogues. This could potentially be achieved by constructing the B-C pyrrolizidine ring system and the E-F lactone ring system separately, and then assembling them using a short and robust reaction sequence. Starting from amino acids would allow the natural product to be synthesized separately in both enantiomeric series. This work, however, focused on the synthesis of unnatural (–)-*ent*-oldhamine A (**I.240**) as a model system, as it can be traced back to cheaper natural L-amino acids as starting materials.

A key element of the strategy was to devise a plan for the installation of the quaternary stereogenic center. It was initially intended to implement a cascade reaction triggered by the addition of an organometallic species like, for example, a cuprate into a fulvene (Scheme I.26). This cascade reaction process would allow for a swift and elegant access to the natural product.



Scheme 1.26: Planned tandem conjugate addition condensation sequence as key step to synthesize **(-)-ent-oldhamine A (I.240)**.

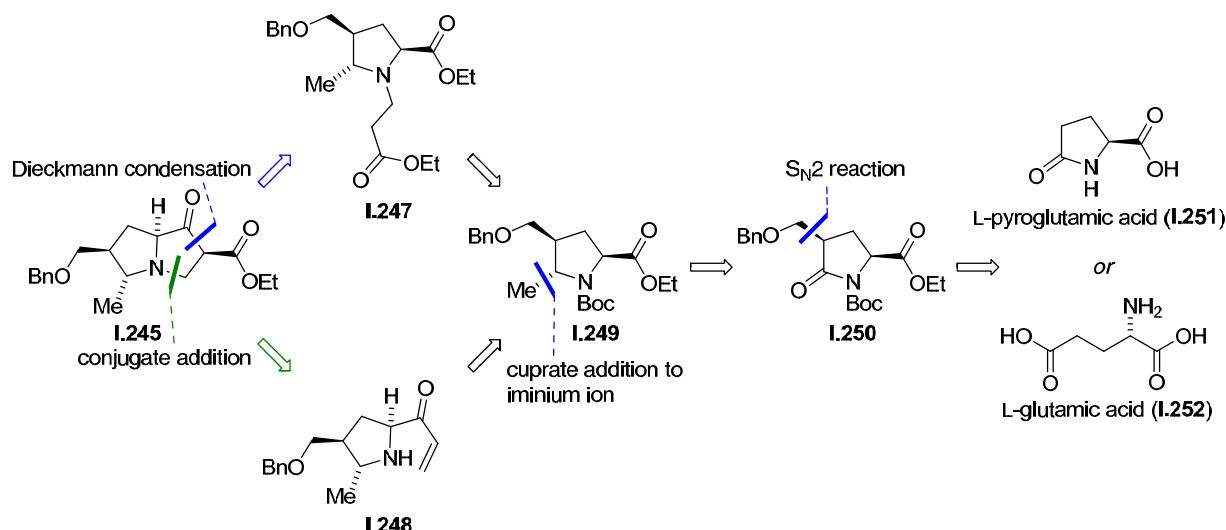
More specifically, it can be speculated that methyl cuprate (**I.242**) would attack fulvene **I.237** at the *C5*-position to form cyclopentadienyl anion **I.238**, which could then intercept the vicinal methyl ester in an intramolecular fashion to form the A-ring of **I.240**. Hexacycle **I.239** might spontaneously aromatize to form its tautomer **(-)-ent-oldhamine A (I.240)**. The addition of organometallic species into fulvenes at the desired position has recently been investigated.^[67] Even though several alternative reaction pathways such as 1,4-additions or even attacks on the ketone might compete with the proposed key reaction, careful optimization could lead to the required conditions to achieve the attack selectively at the desired position. The fulvene is activated by the lactone carbonyl group at *C*-21, for which reason the desired reaction represents a vinylogous conjugate addition onto the corresponding Michael system. This reaction would lead to a stabilized aromatic system and would as well result in a significant release of strain. The retrosynthetic analysis based on the key cyclization process is shown in Scheme I.27.



Scheme I.27: Retrosynthetic analysis of (-)-*ent*-oldhamine A (**I.240**).

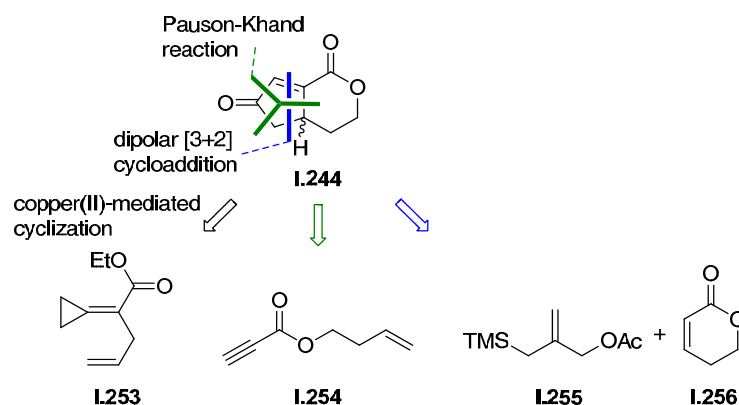
Cleaving **I.240** according to the projected key step leads to fulvene **I.241** and methyl cuprate **I.242**. Further dissection by means of a McMurry cyclization gives diketone **I.243**.^[68] Alternatively, the same bond can easily be formed *via* a Knoevenagel condensation between the pyrrolizidine ketone and the cyclopentadiene in the bicyclic lactone. **I.243** can be traced back to bicyclic lactone **I.244**, pyrrolizidine **I.245** and acrolein **I.246** by conjugate addition and Krapcho decarboxylation followed by enolate addition and appropriate protection. Stereogenic centers formed in the latter reactions are of no consequence for the formation of the natural product.

The envisaged synthesis of building blocks **I.245** and **I.244** should not only be short and straightforward, but also high yielding with the potential to produce gram quantities of the key precursors. Therefore, several strategies for the synthesis of **I.245** and **I.244** have been considered (Scheme I.28).



Scheme I.28: Strategies to synthesize pyrrolizidine **I.245**.

First, pyrrolizidine **I.245** was traced back to enone **I.248** by means of an intramolecular conjugate addition. Even though this 5-endo-trig cyclization is unfavoured according to the Baldwin rules, literature precedence was found for the corresponding cyclization reaction of analogous proline derivatives.^[69] On the other hand, **I.245** can be dissected by means of a Dieckmann cyclization, leading to tertiary amine **I.247**. Both intermediates **I.248** and **I.247** were planned to be made from benzyl ether **I.249**, which can be traced back to **I.250** by means of a 1,2-addition to the corresponding *N*-acyl iminium ion. The introduction of the stereogenic center in **I.250** via an S_N2 reaction is considered as an important challenge. A literature procedure for the synthesis of **I.250** from L-pyroglutamic acid (**I.251**) is known. However, it provides the desired product in poor yield.^[70] Thus, in order to efficiently and reliably produce large amounts of **I.250**, either improved conditions to acquire **I.250** from **I.251** have to be found or an alternative procedure to functionalize the C4-position has to be developed, e.g. starting from L-glutamic acid (**I.252**). For the synthesis of **I.244**, three different strategies were considered, which are depicted in Scheme I.29.



Scheme 1.29: Different possible strategies to synthesize lactone **1.244**.

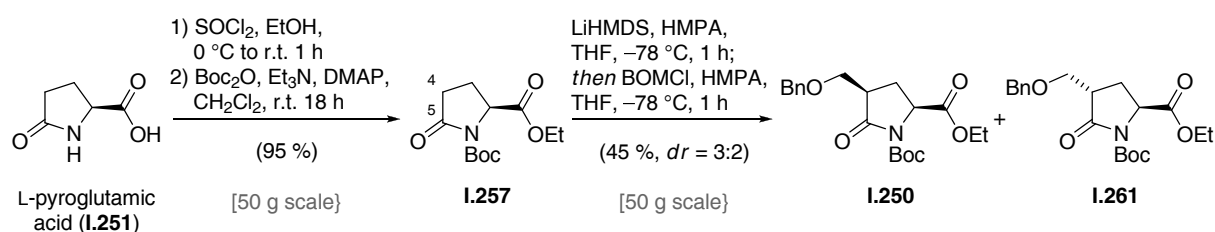
A first method to dissect lactone **1.244** by means of a Pauson-Khand reaction leads back to ester **1.254**. This reaction is well preceded, as exemplified by the construction of the skeletal core of *Daphniphyllum* alkaloids by Dixon,^[62] and was thus considered to provide swift access to the desired carbon framework. Besides, a literature procedure to deliver bicyclic lactones from cyclopropylidenes such as **1.253** using copper(II)salts was intended to be investigated as well.^[71] Finally, **1.244** can be traced back to acetate **1.255** and enone **1.256** via a palladium-catalyzed [3+2] dipolar cycloaddition. This reaction process has been introduced by Trost and coworkers^[72] and has proven useful in two past total syntheses.^[73]

All depicted reaction sequences to synthesize **1.245** and **1.244** have been investigated and the results of these studies are described in the next section.

1.2 Results and Discussion

1.2.1 Studies on C4- and C5-functionalized L-glutamic Acid Derivatives

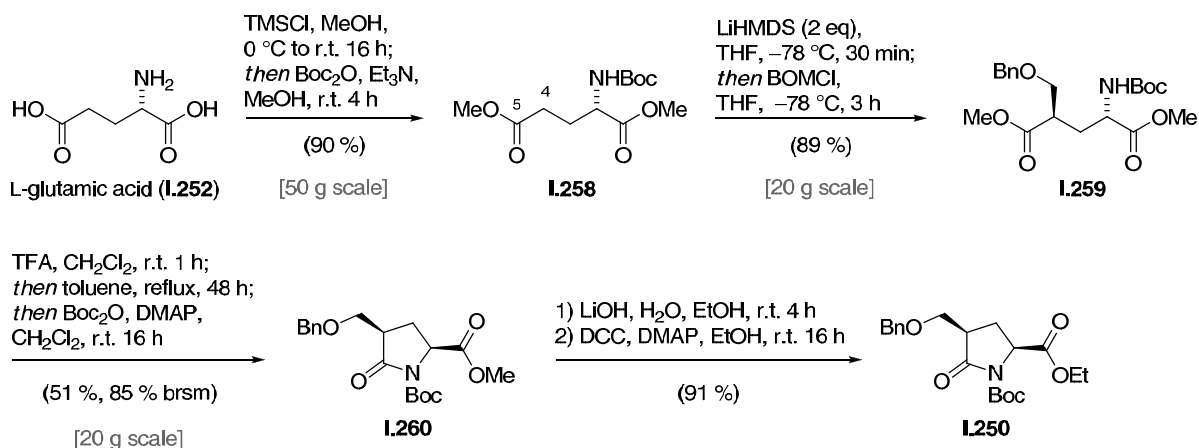
At first, a convenient route towards the asymmetric synthesis of **I.249** was to be elaborated starting from inexpensive amino acids. The main challenge of this approach was to effect stereoselective C-C bond formations at the C4- and the C5-position. For this purpose, L-pyroglutamic acid was initially chosen as a starting material (**I.251**, Scheme I.30).



Scheme I.30: Literature procedure for C4-functionalization of L-pyroglutamic acid derivative **I.257**.

L-pyroglutamic acid (**I.251**) was esterified and N-protected following established procedures.^{[74],[75]} In order to form the desired C-C bond at C₄, N-acyl carbamate **I.257** was treated with LiHMDS followed by benzyloxymethyl chloride.^[70] However, desired product **I.250** was only obtained in a moderate 27 % yield due to the formation of the C₄-diastereomer **I.261** (18 %) as well as other side products such as double-alkylation species. No conditions could be found to enhance the ratio of **I.250** to **I.261**. Improved workup and chromatographic purification protocols finally allowed to perform the reaction on a 50 g scale to afford sufficient quantities of the desired product. However, the low yield and the requirement to separate diastereomers by extensive column chromatography demanded for an alternative pathway.

More specifically, it was found that the desired C₄-functionalization can be cleanly achieved by employing L-glutamic acid (**I.252**)-derived linear starting materials (Scheme I.31). The general method for this transformation was already established^[76] and was found to be of great use in the synthesis of **I.250**.



Scheme I.31: Improved synthesis of **I.250** by C4-functionalization of L-glutamic acid derivative **I.258**.

After conversion of L-glutamic acid (**I.252**) into *N*-protected diester **I.258** following a known literature procedure,^[77] treatment with two equivalents of LiHMDS followed by alkylation with BOMCl cleanly afforded benzyl ether **I.259**. Since formation of the diastereomer at the C4-position was not observed, this reaction process was much more convenient than the corresponding functionalization of L-pyroglutamate derivative **I.257** (Scheme I.30). It could thus be easily performed on a 20 g scale. **I.259** was then *N*-deprotected with TFA and heated in toluene for two days to trigger cyclization. Upon reprotecting the secondary amine, **I.260** could be isolated in 51 % yield together with 45 % of protected starting material **I.259**, raising the yield to 85 % based on recovered **I.259**. In order to convert **I.260** into **I.250**, methyl ester **I.260** was saponified and converted into ethyl ester **I.250** using Steglich conditions. This protecting group swap was necessary to achieve subsequent functionalizations in high yields and to confirm the desired stereochemistry at C4 by comparison with the literature precedent.^[70] At this point, it is worth mentioning that the same C4 alkylation employing the corresponding diethyl ester **I.264** provides the desired product only in a poor 4 % yield, as shown in Scheme I.32. Overall, the five-step procedure starting from L-glutamic acid (**I.252**) provides **I.250** in a total yield of 62 %, whereas the three-step procedure starting from L-pyroglutamic acid (**I.251**) gives **I.250** in only 25 % yield.

The discrepancy in selectivity for the C4-alkylation of **I.257** in contrast to **I.258** is remarkable. The low selectivity in the functionalization of **I.257** was attributed to the flexibility of the five-membered ring system. In contrast, linear L-glutamic acid derivative **I.258** can adopt a closed transition state, thus allowing for a highly enhanced selectivity of the nucleophilic attack. A plausible transition state was proposed by Hanessian and coworkers and is shown in Figure I.3.^[76]

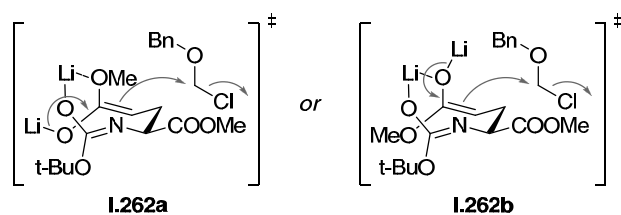
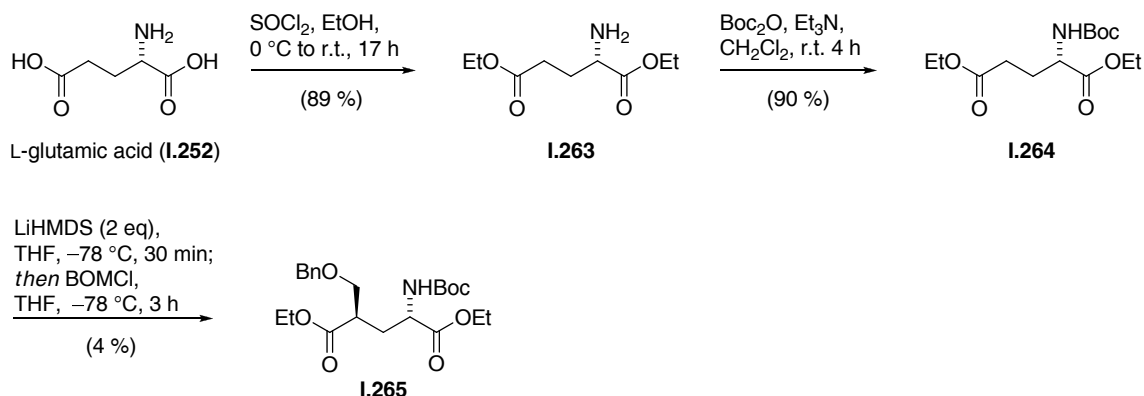


Figure 1.3: Proposed transition states for the formation of **I.250**.^[76]

The double anion formed *in situ* presumably adopts a closed transition state tethered by the corresponding counter ion. More specifically, a lithium ion was proposed to be coordinated by the carbamoyl anion of the Boc protecting group and either the methoxy oxygen of the ester moiety (transition state **I.262a**) or the ester enolate oxygen (transition state **I.262b**). In both cases, the electrophile would preferentially be attacked in an equatorial fashion, resulting in formation of **I.250**.^[76]

As mentioned before, it was intended to improve the step economy and avoid the final ester protecting group swap by employing the same reaction sequence with diester **I.265**. However, **I.264** failed to deliver advantageous quantities of the functionalized product **I.265** (Scheme I.32).

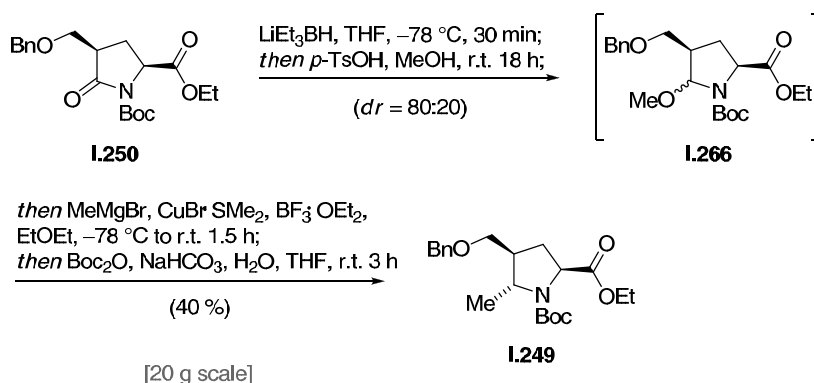


Scheme I.32: Attempted C4-functionalization of diethyl ester **I.264**.

The sequence started with esterification of L-glutamic acid (**I.252**)^[78] (\rightarrow **I.263**) and subsequent *N*-protection to afford diethyl ester **I.264**.^[79] Subjecting **I.264** to the same reaction conditions as for the synthesis of **I.259** resulted in formation of a complex mixture, from which **I.265** could be isolated in 4 % yield upon extensive chromatographic purification. NMR analysis of the crude reaction mixture showed formation of the undesired diastereomer at the C4-position as well as overalkylated species.^[80] It can be speculated that with the

change from the methyl ester to the more bulky ethyl ester, no closed transition state can be adopted and thus no stereoselective functionalization can be carried out. Thus, the five-step procedure as described in Scheme I.31 was the method of choice to synthesize **I.250**.

At this point, attention was focused on the introduction of the methyl group at the C5-position. A literature precedent suggested that this could be achieved by employing an organocuprate reagent to undergo a 1,2-addition to an *in situ* formed iminium ion (Scheme I.33).^[70]



Scheme I.33: Stereoselective C5-functionalization of **I.250** to synthesize **I.249**.

After superhydride-mediated reduction of the *N*-acyl lactam, treatment with *p*-TsOH in the presence of methanol resulted in the formation of hemiaminal ether **I.266** as a 4:1 mixture of diastereomers, which was directly used in the next step without further purification. Addition of methyl cuprate to the *in situ* generated *N*-acyl iminium ion (**I.267**, Figure I.4) and treatment of the resulting product with Boc_2O in the presence of aqueous sodium bicarbonate furnished carbamate **I.249** in an overall 40 % yield. Treatment with Boc_2O became necessary in order to reprotect the amino function, which was partially deprotected under the previous reaction conditions.

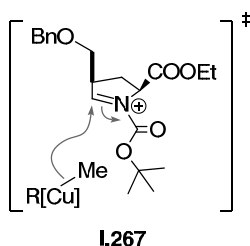


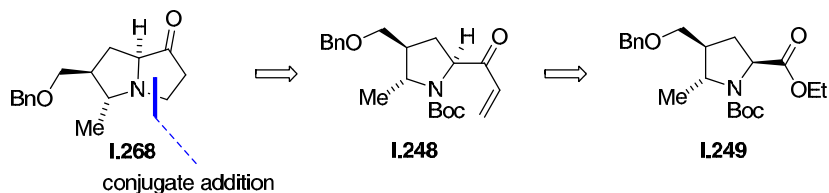
Figure I.4: Illustration of the cuprate addition to *N*-acyl iminium ion **I.267** generated from **I.266**.

The conversion of **I.266** into **I.249** proved to be highly selective. The benzyloxy side chain in **I.266** shields the si-face of the *N*-acyl iminium ion and therefore directs the cuprate attack to occur on the opposite side. NMR analysis of the crude reaction mixture showed no signals of the *C4*-epimer.

Having installed the key stereogenic centers at *C4* and *C5*, a strategy to construct the bicyclic pyrrolizidine part of (–)-*ent*-oldhamine A (**I.240**) was explored, the development of which is described in the next two sections.

1.2.2 Intramolecular Conjugate Addition Approach towards the Synthesis of the Pyrrolizidine Portion of (–)-*ent*-Oldhamine A

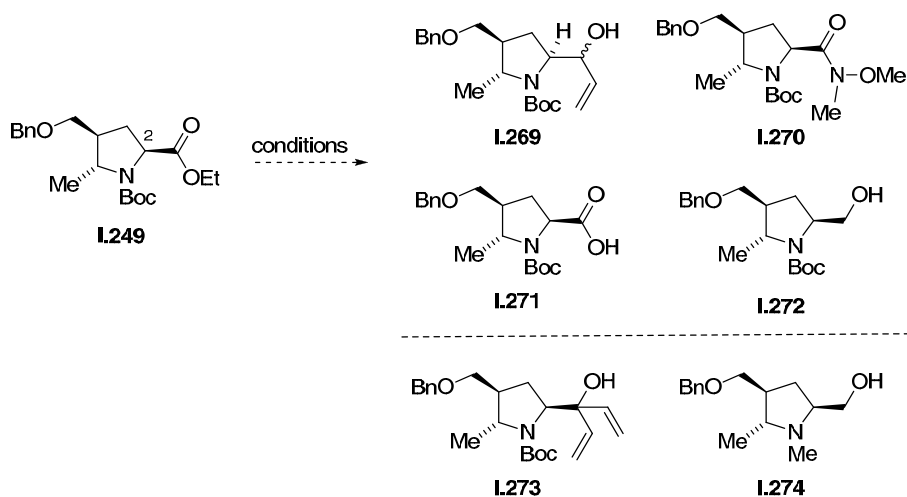
After the successful synthesis of **I.249**, its subsequent functionalization and, more specifically, pathways for the formation of the bicyclic pyrrolizidine ring system were then explored. In the first approach to construct the pyrrolizidine core of (–)-*ent*-oldhamine (**I.240**), it was planned to employ a known protocol to cyclize the pyrrolidines in an intramolecular fashion. In the course of their studies on the total synthesis of (–)-*ent*-absouline and (+)-laburnamine the group of Potier presented a simple construction of pyrrolizidine ring systems *via* a 5-endo-trig cyclization, albeit without *C4* and *C5* modifications.^[69] Based on the literature precedent, a similar approach to construct **I.268** was investigated (Scheme I.34), although this reaction process is unfavored according to the Baldwin rules.



Scheme I.34: Pyrrolizidine-formation *via* a 5-endo-trig cyclization.

Hence, enone **I.248** had to be prepared. It was planned to be achieved by simple modification of the ester side chain of **I.249**.

First, a redox-economical one-step procedure was investigated in order to synthesize allyl alcohol **I.269** via an *in situ* formed aluminum complex at the aldehyde oxidation state. However, the ester moiety in **I.249** proved to be relatively unreactive and standard transformations required unusually harsh conditions. Thus, a variety of reaction conditions were screened to elaborate the most convenient method (Table I.1).



Entry	Reagent	Solvent	Temperature	Time	Yield
1	DIBAL-H, CH ₂ =CH-MgCl	THF	-5 °C to reflux	18 h	(I.269) - ^[a]
2	HNMe(OMe)·HCl, <i>i</i> -PrMgCl	THF	0 °C to reflux	18 h	(I.270) - ^[b]
3	HNMe(OMe)·HCl, Me ₃ Al	THF	0 °C to reflux	18 h	(I.270) - ^[c]
4	LiOH	THF, H ₂ O	reflux	18 h	(I.271) 36 % ^[d]
5	LiOOH	THF, H ₂ O	reflux	18 h	(I.271) 39 % ^[d]
6	Me ₃ SnOH	THF	reflux	18 h	(I.271) - ^[b]
7	DIBAL-H	THF	50 °C	18 h	(I.272) 35 % ^[e]
8	NaAlH ₂ (OCH ₂ CH ₂ OCH ₃) ₂	THF	50 °C	18 h	(I.272) 33 % ^[e]
9	LiAlH ₄	THF	r.t. then 45 °C	18 h, then 3 h	(I.272) 20 % ^[e]
10	LiBH ₄	THF	r.t.	18 h	(I.272) 48 %

[a] double addition, formation of **I.273**; [b] no reaction observed, reisolation of starting material; [c] formation of a complex mixture of polar materials; [d] formation of the C2-epimer; [e] overreduction, formation of **I.274**.

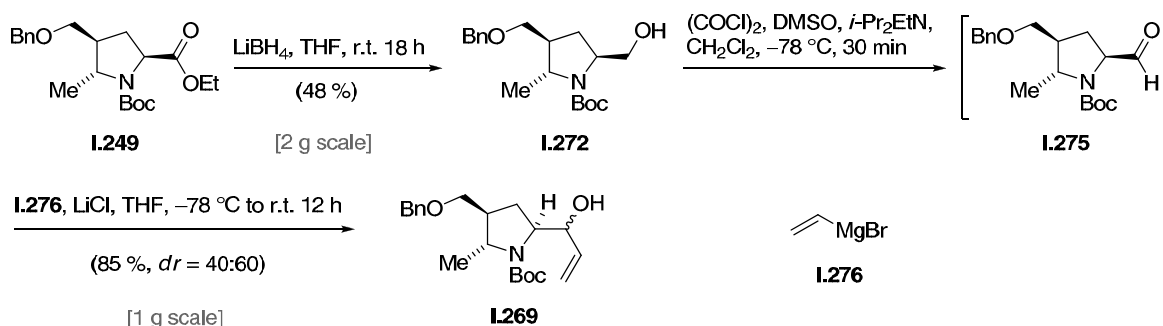
Table I.1: Selected conditions for the transformation of **I.249**.

It was found that reacting **I.249** with DIBAL-H followed by treatment with vinylmagnesium chloride to synthesize **I.269** in one step resulted in the double addition of the Grignard reagent to give **I.273** (Table I.1, Entry 1), indicating an unsuccessful initial reduction of the ester moiety. If **I.249** was subjected to a mixture of *N,O*-dimethylhydroxyamide hydrochloride salt

and isopropylmagnesium chloride to form Weinreb amide **I.270**, no reaction was observed and starting material was recovered (Table I.1, Entry 2). Using a mixture of the same reagent and trimethylaluminium resulted in the formation of a complex mixture of polar materials (Table I.1, Entry 3). Saponification using aqueous lithium hydroxide in refluxing THF provided the corresponding acid **I.271**, however, as a mixture of diastereomers at the C2-carbon (Table I.1, Entry 4). This epimerization was also observed when a mixture of lithium hydroxide and hydrogen peroxide was employed (Table I.1, Entry 5). The use of even milder conditions, specifically trimethyltin hydroxide, did not provide any desired product and the starting material could be recovered (Table I.1, Entry 6). Reduction of the ester to **I.272** using DIBAL-H occurred in THF only at elevated temperatures, however, accompanied with the formation of the *N*-methyl derivative **I.274** as a result of overreduction of the Boc-protecting group (Table I.1, Entry 7). Similar results were observed when Red-Al[®] (Table I.1, Entry 8) and LAH (Table I.1, Entry 9) were employed. Interestingly, the reduction could be carried out at room temperature when lithium borohydride was used, providing the alcohol **I.272** as single product albeit in a moderate 48 % yield (Table I.1, Entry 10).

The relatively low reactivity of **I.249** could potentially be related to the large protecting groups (representing ca. 50% of the molecular weight of **I.249**), which could shield the pyrrolidine core and thus lower the reactivity of the vicinal ester.

The lithium borohydride reduction was chosen as the method to prepare gram quantities of **I.272** and subsequently, a strategy for the required carbon chain elongation was elaborated (Scheme I.35).

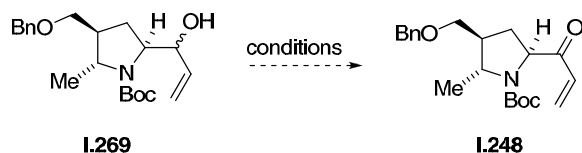


Scheme I.35: Synthesis of allylic alcohol **I.269**.

Upon reduction of **I.249** according to the previously established procedure, alcohol **I.272** was obtained and was subjected to Swern oxidation conditions. The resulting aldehyde **I.275** was

directly reacted with vinylmagnesium bromide (**I.276**) in the presence of lithium chloride to give allylic alcohol **I.269** as a 2:3 mixture of diastereomers.

The subsequently planned oxidation to corresponding enone **I.248** proved to be a challenging task due to the instability of the product under various reaction conditions. Hoping to find conditions under which the sensitive product could be isolated, several oxidation methods were applied. A selection of these attempts is summarized in Table I.2.



Entry	Oxidant	Additive	Solvent	Temperature	Time	Yield
1	DMP, NaHCO ₃	-	CH ₂ Cl ₂	r.t.	3 h	-[a]
2	(COCl) ₂ , DMSO, <i>then</i> <i>i</i> -Pr ₂ EtN	-	CH ₂ Cl ₂	-78 °C	0.5 h	-[a]
3	Pr ₄ NRuO ₄ , NMO	-	CH ₂ Cl ₂	r.t.	18 h	-[a]
4	MnO ₂	-	CH ₂ Cl ₂	reflux	2 h	-[b]
5	DMP, NaHCO ₃	BHT	CH ₂ Cl ₂	r.t.	3 h	-[a]
6	(COCl) ₂ , DMSO, <i>then</i> <i>i</i> -Pr ₂ EtN	BHT	CH ₂ Cl ₂	-78 °C	0.5 h	-[a]
7	Pr ₄ NRuO ₄ , NMO	BHT	CH ₂ Cl ₂	r.t.	18 h	-[a]
8	MnO ₂	BHT	CH ₂ Cl ₂	reflux	2 h	-[b]

[a] formation of a complex product mixture; [b] formation of insoluble material.

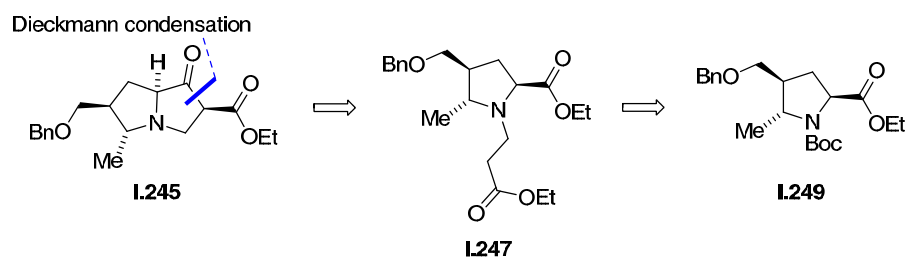
Table I.2. Selected conditions for the attempted allylic oxidation of **I.269**.

Treatment of the diastereomeric mixture of alcohols **I.269** with DMP in the presence of sodium bicarbonate resulted in the formation of a complex reaction mixture (Table I.2, Entry 1). The same result was observed when **I.269** was subjected to Swern conditions (Table I.2, Entry 2) or to Ley oxidation (Table I.2, Entry 3). Employing manganese dioxide to perform the desired allylic oxidation resulted in the formation of insoluble material and no organic product could be isolated from the reaction mixture. In order to improve these results, the same reactions were performed under exclusion of light and in the presence of a radical inhibitor such as BHT (Table I.2, Entries 5-8). Moreover, the diastereomeric mixture of alcohols **I.269** was separated by HPLC and the individual alcohols were separately subjected to the same reaction conditions. Again, complex reaction mixtures were obtained and formation of **I.248** could never be observed.

The instability of **I.248** represented a major obstruction in the development of a reliable and scalable route to pyrrolizidine **I.268**. Thus, the intramolecular conjugate addition strategy was abandoned and a different, more convenient pathway for the construction of the pyrrolizidine core was elaborated. These results are described in the next section.

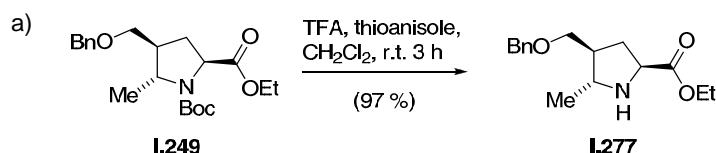
1.2.3 Dieckmann Cyclization Approach to Construct the Pyrrolizidine Ring System of (–)-*ent*-Oldhamine A

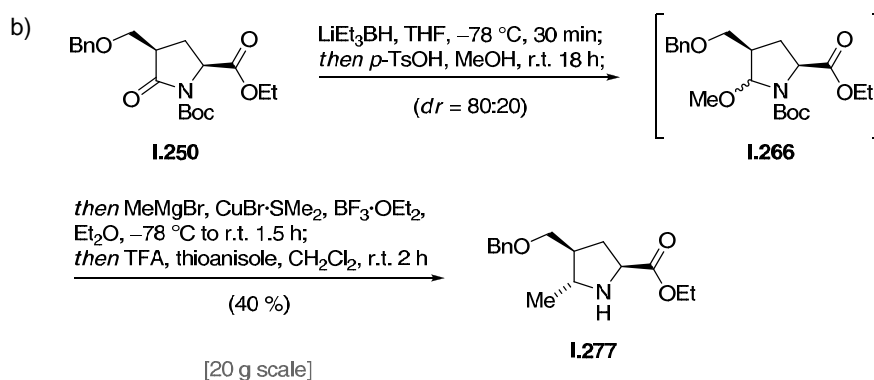
In order to establish a new strategy that would allow swift access to the desired pyrrolizidine framework, **I.245** was now retrosynthetically disconnected at the α -position of the carbonyl group (Scheme I.36).



Scheme I.36: Pyrrolizidine-formation *via* Dieckmann cyclization.

Thus, **I.245** can be traced back to aminoester **I.247** by means of a Dieckmann cyclization, which could be prepared from **I.249** *via* a straightforward functionalization of the nitrogen atom. More specifically, **I.249** had to be deprotected and subsequently *N*-alkylated. The required *N*-deprotection was found to be easily achieved under standard conditions (Scheme I.37).

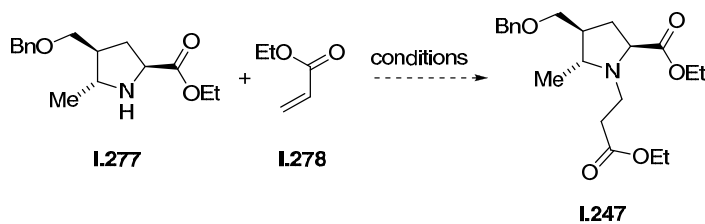




Scheme I.37: a) Standard *N*-deprotection; b) direct incorporation of the *N*-deprotection into the established procedure.

Secondary amine **I.277** was obtained upon treating carbamate **I.249** with TFA in the presence of thioanisole (Scheme I.37a). **I.277** could also be obtained more readily by incorporating the deprotection in the established procedure (Scheme I.37b). **I.250** was reduced and methylated using the same conditions as for the synthesis of **I.249** (*vide supra*, Section 1.2.1, Scheme I.33). Then, *N*-acyl iminium ion **I.257** was generated and intercepted by methyl cuprate. Subsequent treatment of the resulting product mixture with TFA in the presence of thioanisole completed the *N*-deprotection and afforded amine **I.277** in an overall 40 % yield.

As for the subsequent *N*-alkylation, it was first envisaged to obtain saturated tertiary amine **I.247** in one step *via* a Michael addition of **I.277** to ethyl acrylate (**I.278**). This venture proved to be challenging as the secondary amine underwent the desired reaction only under relatively harsh conditions (Table I.3). Addition of Lewis acids, which are known to catalyze conjugate additions of amines to acrylates did not lead to an improvement in yield, but to extended polymerization.^{[81],[82]} This observation was attributed to sterical hindrance at the aminofunction of **I.277**.



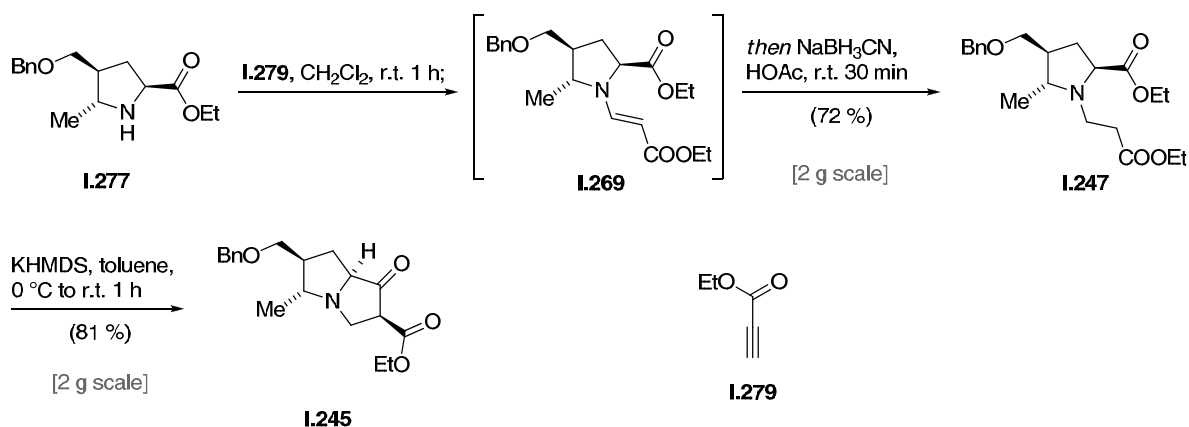
Entry	Solvent	Additive	Temperature	Time	Yield
1	- ^[a]	-	reflux	72 h	39 % ^[b]
2	- ^[a]	TiCl ₄	r.t.	24 h	- ^[b,c]
3	MeCN	Bi(OTf) ₃	r.t.	6 d	- ^[b,c]
4	CH ₂ Cl ₂	FeCl ₃	reflux	24 h	- ^[b,c]
5	- ^[a]	SMe ₂ Br ₂	r.t.	24 h	37 %

[a] The reaction was performed neat in an excess of **I.278**; [b] formation of polymeric material was observed; [c] traces of product mass could be observed by LCMS.

Table I.3: Selection of reaction conditions for the Michael addition of **I.277** to **I.278**.

In the first instance, amine **I.277** was heated to reflux for 72 h in neat ethyl acrylate (**I.278**) to afford a complex product mixture of polymerized material from which the desired product could be isolated in 39 % yield (Table I.3, Entry 1). When stirring a mixture of **I.277** and **I.278** in the presence of titanium tetrachloride, a complex mixture was obtained, in which only traces of the desired product could be detected (Table I.3, Entry 2). Similar results were obtained when bismuth triflate was present in an acetonitrile solution of **I.277** and **I.278** (Table I.3, Entry 3), or when refluxing a mixture of **I.277**, **I.278** and iron trichloride in dichloromethane (Table I.3, Entry 4). Employing SMe₂Br₂ as additive under solvent-free conditions provided the product in a moderate yield of 37 % (Table I.3, Entry 5).

Since the low reactivity of **I.277** was speculated to be due to the sterically hindered nature of the secondary amine, a smaller and more reactive electrophile was utilized. Thus, ethyl propiolate (**I.279**), which was previously shown to react with highly hindered amines such as TMP, was employed.^[83] Indeed, **I.279** smoothly underwent the desired conjugate addition with amine **I.277** (Scheme I.38). From this intermediate desired pyrrolizidine **I.245** could be prepared in only two steps.



Scheme 1.38: Synthesis of pyrrolizidine **I.245**.

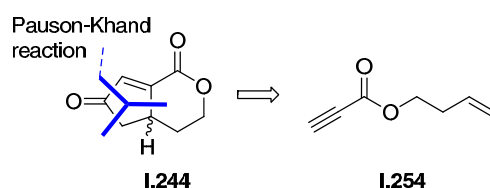
Michael addition of **I.277** onto ethyl propiolate (**I.279**) afforded enamine **I.269**. Subsequent reduction of the corresponding iminium ion, which was generated in glacial acid, provided amine **I.247**. Even though a two-step process was required to access saturated amine **I.247**, this procedure proved to be more convenient than the previously investigated usage of ethyl acrylate (**I.278**) and therefore became the method of choice to synthesize **I.247**. Having gram quantities of **I.247** in hands, the stage was set for the cyclization to form pyrrolizidine **I.245**. After screening several bases,^[84] KHMDS was found to be most efficient to effect the following Dieckmann cyclization and to provide pyrrolizidine **I.245** in good yield.

The elaborated synthesis of the properly functionalized pyrrolizidine proved to be reliable and can be carried out on a multigram scale. Building block **I.245** represents the B-C-ring system of (–)-*ent*-oldhamine A (**I.240**) and already features four of the five stereogenic centers of the natural product.

The synthesis of the E-F-ring system of (–)-*ent*-oldhamine A (**I.240**) was investigated subsequently and is described in the next sections.

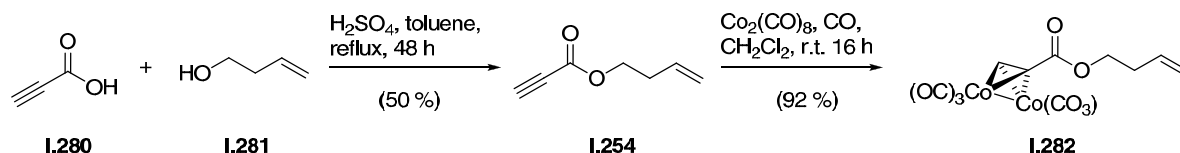
1.2.4 Studies on the Construction of the Bicyclic Lactone Portion of (-)-*ent*-Oldhamine A by a Pauson-Khand Reaction

For the construction of the bicyclic lactone framework of the E- and F-rings of (-)-*ent*-oldhamine A (**I.240**), a one-step procedure utilizing a Pauson-Khand reaction was first considered. The success of this method would allow a swift access to lactone **I.244** from a simple starting material, namely ester **I.254** (Scheme I.39).



Scheme I.39: Formation of bicyclic lactone **I.244** by means of a Pauson-Khand reaction.

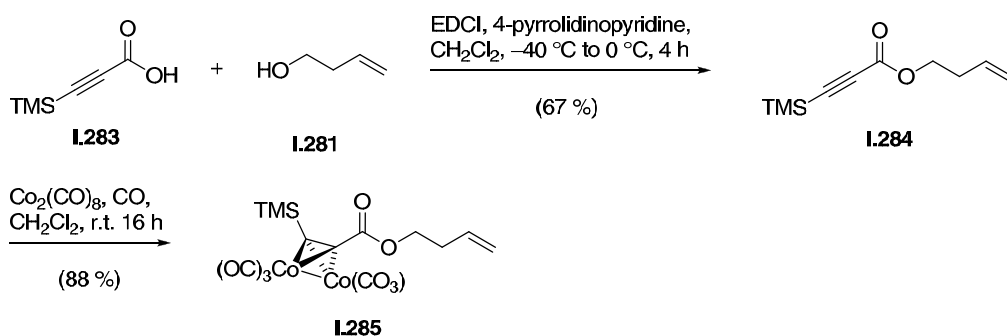
Synthesis of ester **I.254** proved to be straightforward and also the subsequent formation of a cobalt-alkyne complex required for the Pauson-Khand reaction was achieved using standard conditions (Scheme I.40).



Scheme I.40: Synthesis of cobalt-alkyne complex **I.282** as a precursor for the Pauson-Khand reaction.

A Fischer esterification of propiolic acid (**I.280**) and alcohol **I.281** provided ester **I.254** in moderate yield. Formation of cobalt-alkyne complex **I.282** was then achieved by treatment of propiolate **I.254** with dicobalt octacarbonyl.

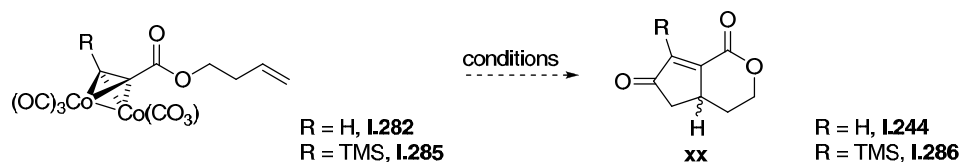
As a second precursor for the Pauson-Khand reaction, TMS-propiolate **I.284** was prepared (Scheme I.41).



Scheme I.41: Synthesis of alternative PKR-precursor **I.285**.

3-(Trimethylsilyl)propionic acid (**I.283**) was esterified using **I.281** in the presence of EDCI and 4-pyrrolidinopyridine, which had to be conducted at low temperatures to avoid side reactions. Conversion into **I.285** was achieved employing the same conditions as in the synthesis of **I.282** (Scheme I.40).

Subsequently, **I.282** and **I.285** were subjected to a number of conditions which had previously been developed for Pauson-Khand reactions, a selection of which is summarized in Table I.4.^[85] In general, the reaction mixtures were stirred until complete consumption of the starting material and the crude mixture was analyzed by TLC, GCMS, LCMS and NMR.



Entry	Additive	Solvent	Temperature	Atmosphere	Yield (1.244)	Yield (1.286)
1	-	DME	reflux	CO	-[a]	-[a]
2	-	DME/CF ₃ CH ₂ OH 1:1	reflux	Ar	-[a]	-[a]
3	-	DME/CF ₃ CH ₂ OH 1:1	reflux	CO	-[a]	-[a]
4	-	CF ₃ CH ₂ OH	reflux	Ar	-[a]	-[a]
5	-	CF ₃ CH ₂ OH	reflux	CO	-[a]	-[a]
6	cy-NH ₂	DME	reflux	Ar	-[a]	-[a]
7	cy-NH ₂	DME	reflux	CO	-[a]	-[a]
8	cy-NH ₂	DME/CF ₃ CH ₂ OH 1:1	reflux	Ar	-[a]	-[a]
9	cy-NH ₂	DME/CF ₃ CH ₂ OH 1:1	reflux	CO	-[a]	-[a]
10	NMO	CH ₂ Cl ₂	0 °C to r.t.	Ar	-[a]	-[a]
11	NMO	CH ₂ Cl ₂	0 °C to r.t.	air	-[a]	-[a]
12	NMO	CH ₂ Cl ₂	0 °C to r.t.	CO	-[a]	-[a]
13	NMO	DME	0 °C to r.t.	Ar	-[a]	-[a]
14	NMO·H ₂ O	CH ₂ Cl ₂	0 °C to r.t.	Ar	-[a]	-[a]
15	NMO·H ₂ O	CH ₂ Cl ₂	0 °C to r.t.	air	-[a]	-[a]
16	NMO·H ₂ O	CH ₂ Cl ₂	0 °C to r.t.	CO	-[a]	-[a]
17	NMO·H ₂ O	DME	0 °C to r.t.	Ar	-[a]	-[a]
18	TMANO	CH ₂ Cl ₂	0 °C to r.t.	Ar	-[a]	-[a]
19	TMANO	CH ₂ Cl ₂	0 °C to r.t.	Ar	-[a]	-[a]
20	TMANO	CH ₂ Cl ₂	0 °C to r.t.	CO	-[a]	-[a]
21	TMANO	DME	0 °C to r.t.	Ar	-[a]	-[a]

[a] formation of a complex mixture of polar materials.

Table I.4: Selected conditions for the transformation of **1.282** and **1.285**.

At first, **1.282** and **1.285** were subjected to thermal PKR-conditions.^[85f] When **1.282** and **1.285**, respectively, were heated to reflux in DME under a CO atmosphere, a complex mixture of polar materials was slowly formed (Table I.4, Entry 1). The same result was obtained when **1.282** or **1.285**, respectively, were heated to reflux in a 1:1 mixture of DME and CF₃CH₂OH under either an argon atmosphere (Table I.4, Entry 2) or a CO atmosphere (Table I.4,

Entry 3). The same outcome was also observed in pure $\text{CF}_3\text{CH}_2\text{OH}$ under either an argon atmosphere (Table I.4, Entry 4) or a CO atmosphere (Table I.4, Entry 5).

After these first trials, the same reaction was performed using cyclohexylamine as additive. These conditions have been shown to drastically accelerate the rate of PKR in some instances.^[85c, 85d] Again, formation of a complex mixture of polar materials was observed if **I.282** and **I.285**, respectively, were heated in the presence of cyclohexylamine in DME under an argon (Table I.4, Entry 6) or a CO atmosphere (Table I.4, Entry 7). Changing to a DME/ $\text{CF}_3\text{CH}_2\text{OH}$ solvent system did not improve the results regardless to the atmosphere under which the reaction was run (Table I.4, Entry 8 and 9).

Addition of oxidants to transform a carbonyl ligand into CO_2 and therefore facilitate its loss was also investigated.^[85a, 85b] When **I.282** and **I.285**, respectively, were stirred in CH_2Cl_2 in the presence of NMO under an argon (Table I.4, Entry 10), an air (Table I.4, Entry 11) or a CO atmosphere (Table I.4, Entry 12), a complex mixture of polar materials was formed. The same results were obtained if NMO monohydrate (Table I.4, Entries 14-16) or TMAO (Table I.4, Entries 18-20) were used instead. Stirring **I.282** and **I.285**, respectively, in DME under an argon atmosphere did not improve the results for either NMO (Table I.4, Entry 13), NMO monohydrate (Table I.4, Entry 17) or TMAO (Table I.4, Entry 21).

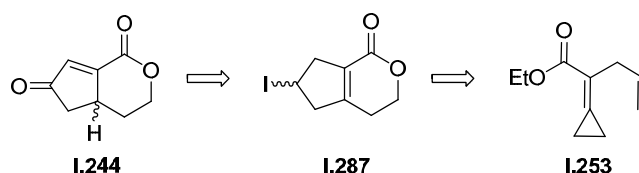
A possible explanation for the low reactivity of **I.282** and **I.285** is the high stability of cobalt complexes with propiolic acid derivatives, as already observed by Pauson.^[86] Side reactions are presumably faster than the desired reaction, thus leading to the formation of a complex mixture of reaction products.

Although there are many more conditions that could have been applied in the Pauson-Khand reaction, like the use of different metals and additives, an alternative method for the construction of the desired carbon framework had been found in the meantime (*vide infra*, Section 1.2.6). Therefore, no more reaction conditions were screened in the scope of this work.

A different approach featuring a copper-catalyzed cyclization reaction is described in the next section.

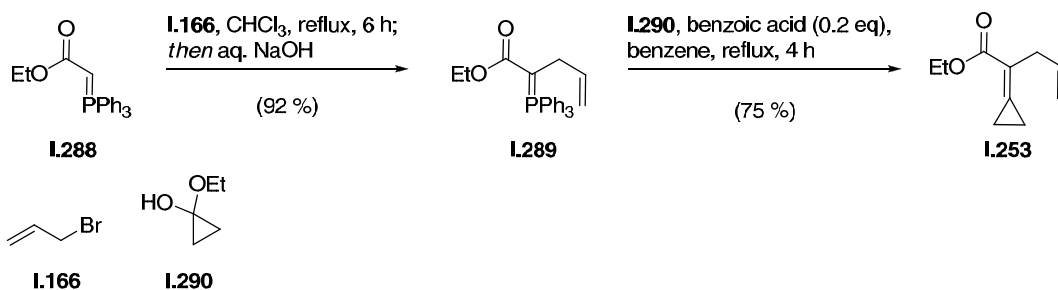
1.2.5 Studies on the Construction of the Bicyclic Lactone Portion of (-)-*ent*-Oldhamine A via a Copper-Catalyzed Cyclization Reaction

In this approach, **I.244** was planned to be synthesized *via* a literature-known procedure to construct the bicyclic lactone framework (Scheme I.42).



Scheme I.42: Dissection of **I.244** by means of a Kornblum oxidation and an established copper(II)-mediated cyclization.^[71]

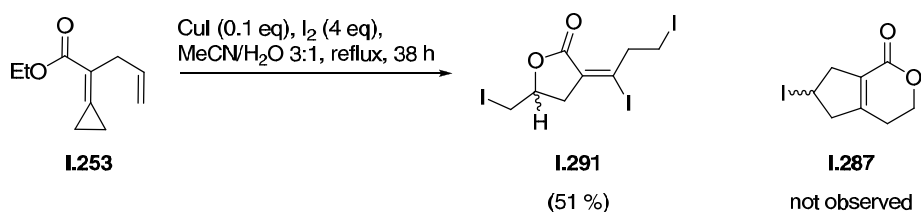
Bicyclic lactone **I.244** can be traced back to literature-known iodide **I.287** by means of a Kornblum oxidation. A synthesis of this intermediate from **I.253** was presented by Huang and coworkers in the course of their study on the use of copper(II) halides to mediate cyclization reactions of cyclopropylidene esters.^[71] The synthesis of cyclopropylidene ester **I.253** was straightforward and could be achieved following literature procedures (Scheme I.43).



Scheme I.43: Synthesis of cyclopropylidene **I.253**.

Commercially available ylen **I.288** was allylated using **I.166** in refluxing chloroform followed by treatment with aq. NaOH to deliver allyl phosphonate **I.289**.^[87] A Wittig reaction employing **I.290** in the presence of a catalytic amount of benzoic acid then furnished cyclopropylidene ester **I.253**.^[88]

With **I.253** in hands, the reported copper(II)-mediated cyclization process was investigated.^[71] Unfortunately, when employing the reaction conditions described in literature, the desired product could never be observed. Instead, triiodide **I.291** was isolated (Scheme I.44).



Scheme I.44: Attempted synthesis of iodide **I.287**.

When cyclopropylidene ester **I.253** was treated with catalytic amounts of copper(I) iodide and an excess of iodine and heated in a 3:1 mixture of acetonitrile and water, instead of the desired product **I.287**, triiodide **I.291** was obtained in 51 % yield. This was the only product that could be characterized and despite extensive efforts to analyze side products of this reaction process, formation of desired bicycle **I.287** was not observed. The structure of **I.291** could be confirmed by means of single crystal X-ray analysis (Figure I.5).

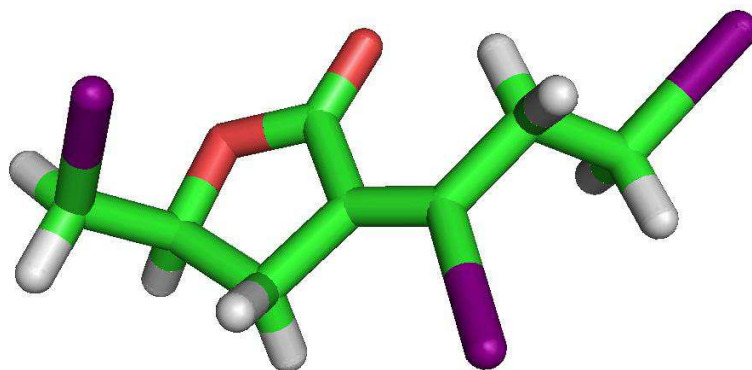
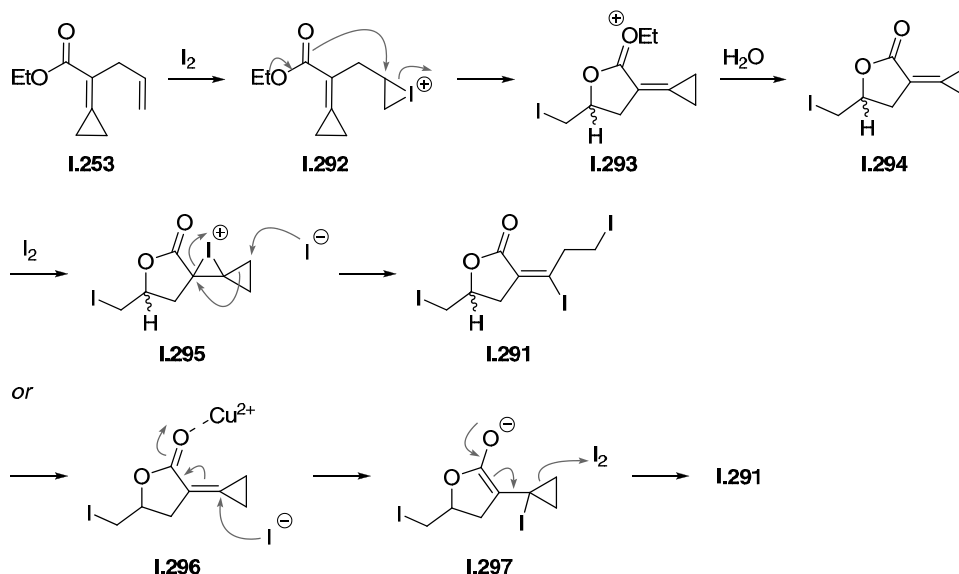


Figure I.5: Crystal structure of triiodide **I.291**.

The formation of **I.291** was speculated to occur *via* iodolactonization and subsequent opening of the cyclopropane (Scheme I.45).



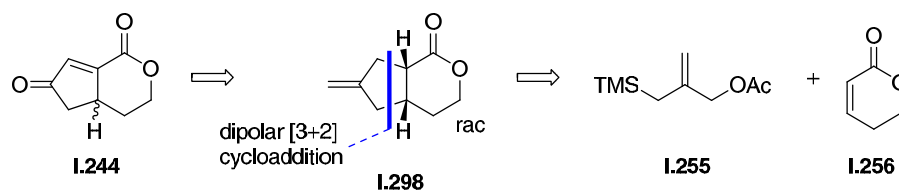
Scheme 1.45: Speculated reaction mechanism for the formation of iodide **I.291**.

Upon initial formation of iodonium ion **I.292**, the molecule could undergo a iodolactonization to form intermediate **I.293**, which can be assumed to be hydrolyzed under the reaction conditions. The resulting iodolactone **I.294** can be speculated to react with a second equivalent of iodine to form the spiro iodonium ion **I.295**, which could undergo ring opening to form triiodide **I.291**. An alternative mechanism for the iodolysis of the three-membered ring could proceed *via* a copper-mediated conjugate addition of previously formed iodide (\rightarrow **I.296**) to give enolate **I.297** and subsequent attack on iodine.

Since the desired bicyclic lactone was not obtained with the copper catalysis approach, another route for the formation of **I.244** had to be explored, the details of which are described in the next section.

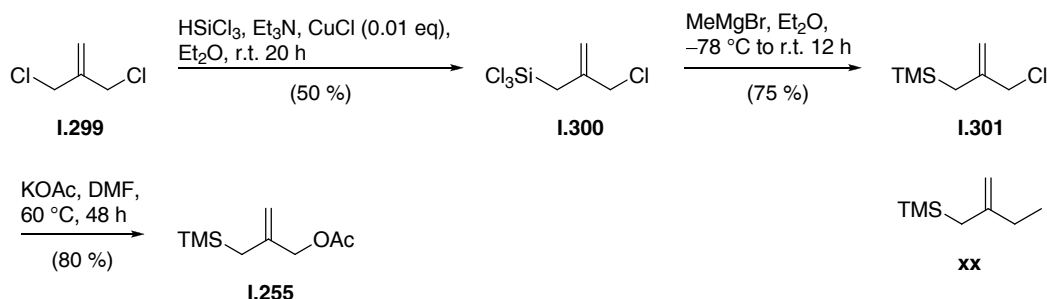
1.2.6 Studies on the Construction of the Bicyclic Lactone Portion of (-)-*ent*-Oldhamine A via a [3+2] Cycloaddition

The third approach for the construction of the E-F-ring system utilized a palladium-catalyzed [3+2] cycloaddition reaction (Scheme I.46), which was discovered by Trost and coworkers.^[72]



Scheme I.46: Dissection of **I.244** via [3+2] cycloaddition.

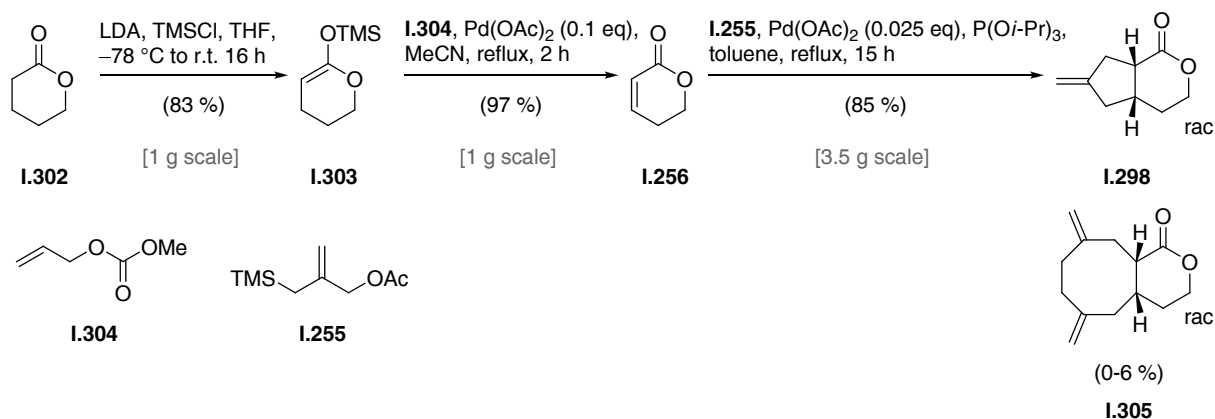
Lactone **I.244** could be the result of an oxidation sequence from **I.298**. By means of the envisaged palladium-catalyzed [3+2] cycloaddition reaction, **I.298** can be traced back to acetate **I.255** and lactone **I.256**, both of which are readily available starting materials. Acetate **I.255** was prepared first following an established procedure (Scheme I.47).^[89]



Scheme I.47: Synthesis of acetate **I.255**.

Dichloride **I.299** was monosilylated using trichlorosilane in the presence of triethylamine and catalytic amounts of copper(I) to provide silylchloride **I.300**. After conversion to the corresponding trimethyl silane **I.301**, the mixture was heated in the presence of potassium acetate to furnish acetate **I.255**.

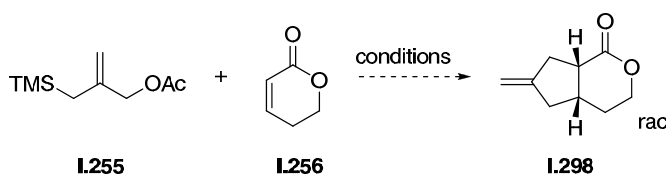
With large amounts of acetate **I.255** in hands, the synthesis of **I.298** was initiated. The reaction sequence started with a literature-known unsaturation of δ -valerolactone using a Saegusa oxidation.^{[90],[91]} The subsequent [3+2] cycloaddition proved to be suitable for the synthesis of **I.298** and could be carried out on large scale (Scheme I.48).



Scheme 1.48: Synthesis of bicyclic lactone **I.298**.

δ -Valerolactone (**I.302**) was converted into silyl enol ether **I.303** by treatment with LDA and TMS chloride. Subsequent treatment with catalytic amounts of palladium acetate in the presence of methyl allyl carbonate (**I.304**) smoothly provided unsaturated lactone **I.256**. Bicyclic lactone **I.298** could then be obtained by heating a mixture of **I.255** and **I.256** in the presence of palladium acetate and triisopropyl phosphite. In some instances, formation of small amounts of bisalkene **I.305** was observed as a byproduct. However, since **I.305** could easily be separated by column chromatography, this was of no consequence for the successful synthesis of gram-quantities of **I.298**.

In the course of the studies on this reaction, it was found that small amounts of water were essential to produce **I.298** in high yields. Yields dropped significantly when no water or too much water was present in the reaction mixture (Table I.5).

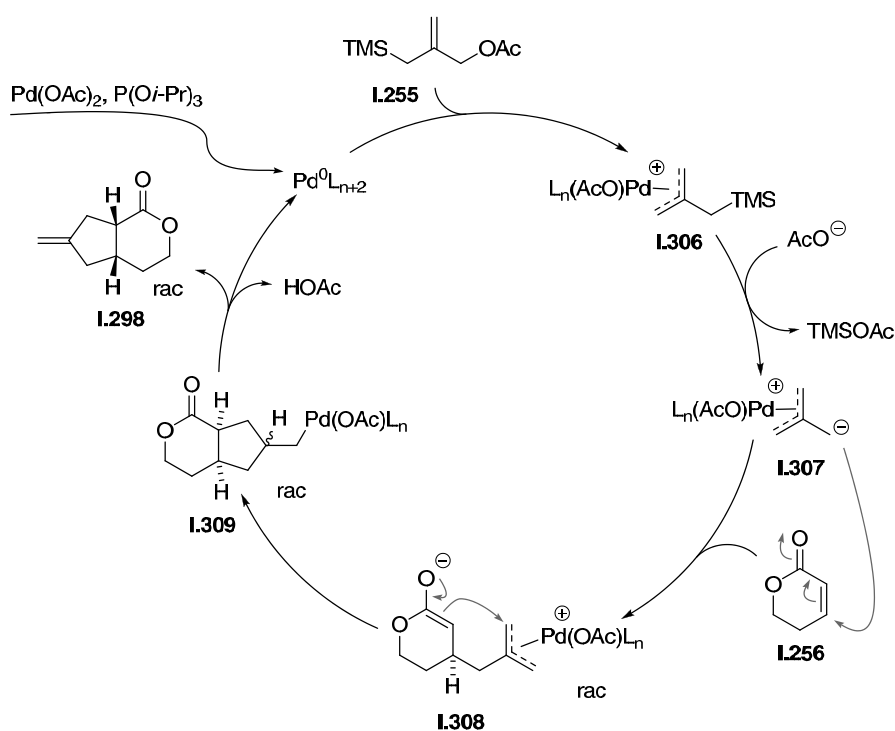


Entry	Conditions	Solvent	Temperature	Time	water-additive	yield
1	Pd(OAc) ₂ (2.5 mol %), P(O <i>i</i> -Pr) ₃	toluene	reflux	15 h	-	.. ^[a]
2	Pd(OAc) ₂ (2.5 mol %), P(O <i>i</i> -Pr) ₃	toluene	reflux	15 h	1.00 eq	39 %
3	Pd(OAc) ₂ (2.5 mol %), P(O <i>i</i> -Pr) ₃	toluene	reflux	15 h	0.100 eq	61 %
4	Pd(OAc) ₂ (2.5 mol %), P(O <i>i</i> -Pr) ₃	toluene	reflux	15 h	traces ^[b]	85 %

[a] reisolation of starting material, traces of product observed by LCMS; [b] utilization of analytical grade solvent, which has been exposed to air moisture prior to use.

Table I.5: Selection of reaction conditions employed in the optimization of the [3+2] cycloaddition.

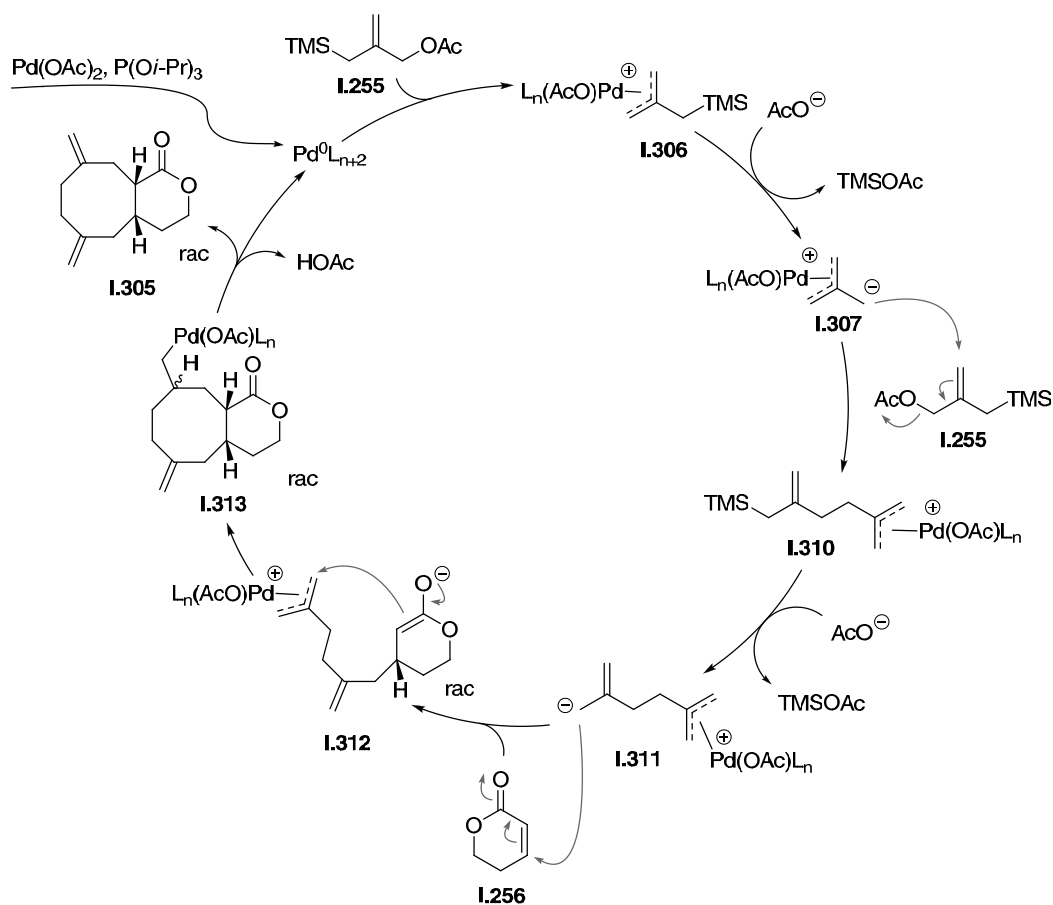
If water-free conditions were applied, only traces of product could be observed in the resulting reaction mixture and starting material was recovered (Table I.5, Entry 1). If, however, the same reaction was carried out in the presence of one equivalent of water, a yield of 39 % was obtained (Table I.5, Entry 2), When a defined amount of 0.100 eq of water was added, the reaction provided a 62 % yield of **I.298** (Table I.5, Entry 3). The best yield was obtained when trace amounts of water were present in the reaction mixture. It was thus found that employing analytical grade toluene that had been exposed to air moisture prior to the reaction was ideal and led to a 85 % yield of **I.298** (Table I.5, Entry 4). The reaction process has already been studied in detail and a proposed mechanism is depicted in Scheme I.49.^[92]



Scheme I.49: Proposed reaction mechanism for the formation of **I.298**.

First, palladium acetate in the presence of triisopropyl phosphite and catalytic amounts of water forms a palladium(0) complex, which oxidatively inserts into acetate **I.255** to form palladium π -allyl complex **I.306**. This compound can be attacked by the previously formed acetate to give **I.307**, which can then undergo a conjugate addition onto enone **I.256**. The thereby generated enolate **I.308** intramolecularly attacks the π -allyl palladium complex, thus providing organopalladium compound **I.309**. Upon β -hydride elimination and reductive elimination of acetic acid, the catalyst is generated and **I.298** is liberated.

The formation of byproduct **I.305** is indeed intriguing and can be rationalized *via* a mechanism such as described in Scheme I.50.

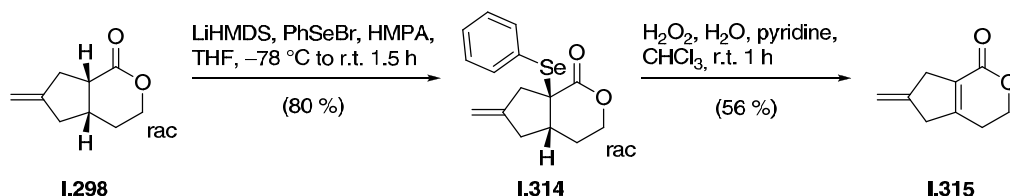


Scheme I.50: Proposed mechanism for the formation of side product **I.305**.

It can be speculated that intermediate **I.307**, which is formed analogously to the previously described mechanism *via* **I.306**, first undergoes an $S_{N2'}$ reaction with acetate **I.255** instead of the usual conjugate addition to enone **I.256**. The resulting intermediate **I.310** then presumably follows the known reaction mechanism where allylic anion **I.311** is formed as a result of the attack of the acetate anion. Then, zwitterion **I.311** could undergo a conjugate addition onto enone **I.256** to form intermediate **I.312**. Intramolecular trapping of the resulting enolate would result in formation of organo-palladium compound **I.313**, which upon β -hydride elimination would provide **I.305**.

Having the bicyclic lactone **I.298**, which represents a key building block in the synthesis of both enantiomers of oldhamine A (**I.226** and **I.240**), in hands, preliminary studies on its subsequent oxidation were carried out.

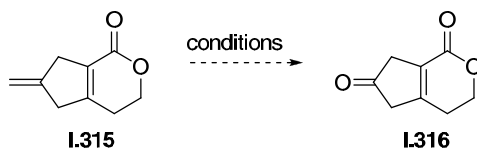
The first strategy to convert **I.298** into **I.244** involved the formation of the lactone alpha-beta unsaturation, followed by oxidative cleavage of the *exo*-methylene group. This order of ketone formation and unsaturation was considered to be crucial to avoid problems concerning the regioselectivity of the olefin formation step. Thus, unsaturated bicyclic lactone was synthesized first, which could be achieved by means of a Grieco elimination (Scheme I.51).



Scheme I.51: Synthesis of unsaturated lactone **I.315**.

Lactone **I.298** was converted into selenide **I.314** using LiHMDS and phenyl selenyl bromide in the presence of HMPA. Upon treatment with aqueous hydrogen peroxide, **I.314** underwent Grieco elimination to form unsaturated lactone **I.315**.

The subsequently planned oxidative cleavage of the *exo*-methylene group proved to be difficult. Various well-known one-step procedures failed to provide desired ketone **I.316** (Table I.6).



Entry	Conditions	Solvent	Temperature	Time	yield
1	O ₃ , then Me ₂ S	CH ₂ Cl ₂	-78 °C, then r.t.	5 min, then 18 h	-[a]
2	OsO ₄ , NaIO ₄	CH ₂ Cl ₂	r.t.	16 h	-[a]
3	<i>m</i> -CPBA, then HIO ₄	CH ₂ Cl ₂	r.t. then reflux	16 h, then 16 h	-[b]

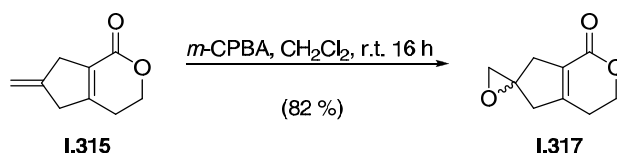
[a] Formation of a complex mixture of polar compounds; [b] isolation of epoxide **I.317** in 49 % yield.

Table I.6: Conditions for the attempted oxidative cleavage of **I.315**.

When **I.315** was treated with ozone followed by a reductive workup, formation of a complex mixture of polar compounds was observed (Table I.6, Entry 1). A similar result was obtained when performing a Lemieux-Johnson oxidation with osmium tetroxide and sodium periodate (Table I.6, Entry 2). If **I.315** was treated with *meta*-chloroperbenzoic acid and then with

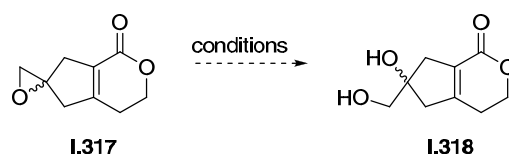
periodic acid, no oxidative cleavage could be accomplished and epoxide **I.317** was isolated (Table I.6, Entry 3).

Since all typical one-step procedures failed to deliver **I.316**, alternative procedures to oxidize the *exo*-methylene double bond were tested. First, **I.315** was subjected to a Prileschajew reaction to obtain epoxide **I.317** (Scheme I.52).



Scheme I.52: Synthesis of epoxide **I.317**.

Epoxide **I.317**, which was obtained from **I.315** after treatment with *m*-CPBA, was then subjected to several standard conditions for epoxide opening. However, despite extensive efforts, a selection of which is shown in Table I.7, no conditions for the synthesis of glycol **I.318** could be found.



Entry	Reagent	Solvent	Temperature	Time	yield
1	H ₂ SO ₄ , H ₂ O	THF	r.t. to reflux	18 h	-[a]
2	HClO ₄ , H ₂ O	THF	r.t.	16 h	-[b]
3	KOH	DMSO, H ₂ O	50 °C	16 h	-[b]
4	BF ₃ ·OEt ₂ , <i>then</i> H ₂ O	THF	r.t. to reflux	16 h	-[a]

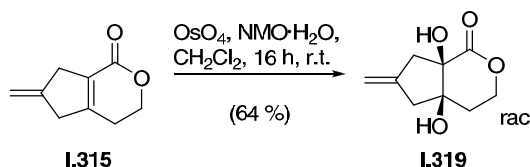
[a] Reisolation of starting material; [b] formation of a complex mixture of polar compounds.

Table I.7: Selection of conditions for the attempted epoxide opening.

When **I.317** was subjected to oleum in wet THF and heated to reflux for 18 h, no reaction was observed and starting material was reisolated (Table I.7, Entry 1). Upon treatment with an aq. 60 % solution of perchloric acid, a complex mixture of polar compounds was formed (Table I.7, Entry 2). A similar result was obtained, when a DMSO solution of **I.317** was treated with aqueous potassium hydroxide and heated to 50 °C for 16 h (Table I.7, Entry 3). Subsequently, Lewis acid-mediated ring opening was investigated. However, **I.317** proved to

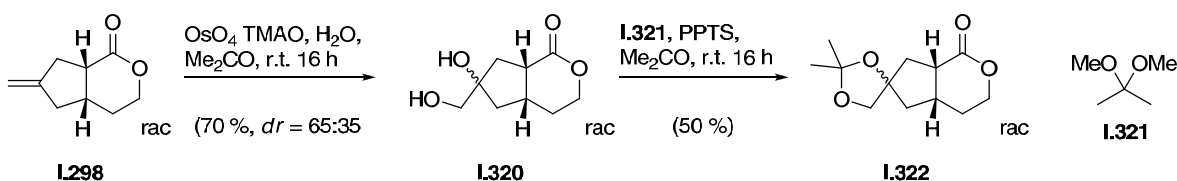
be unreactive under these conditions and starting material was recovered. If, for example, **I.317** was heated in the presence of boron trifluoride diethyl etherate in THF, no reaction was observed (Table I.7, Entry 4).

Attempts to directly access diol **I.318** *via* Upjohn dihydroxylation on **I.315** resulted in the formation of an undesired product (Scheme I.53).



Scheme I.53: Osmium tetroxide-mediated dihydroxylation of **I.315**.

Upon treatment with osmium tetroxide in the presence of NMO and water, **I.315** underwent an unusual dihydroxylation and **I.319** was formed. Instead of the electron rich and more accessible double bond, the enone in **I.315** was found to react preferentially. In order to further investigate this dihydroxylation approach and to potentially find a pathway to avoid the observed regioselectivity issues, the diol moiety was already introduced in **I.298** (Scheme I.54).



Scheme I.54: Synthesis of dioxolane **I.322**.

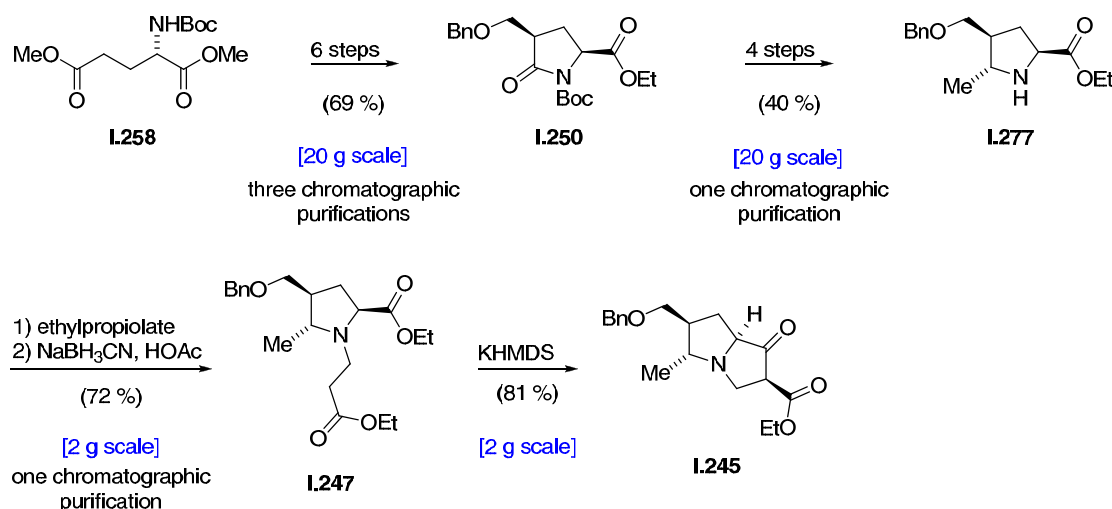
Upon osmium tetroxide-mediated dihydroxylation, diol **I.320** was obtained, which was directly protected using **I.321** to provide dioxolane **I.322**.^[93] The further functionalization of **I.322** remains to be studied in more details.

The achievements towards the total synthesis of (–)-*ent*-oldhamine A (**I.240**) are summarized in the next section.

1.2.7 Summary, Conclusions and Outlook

In summary, a reliable large-scale preparation of the two key building blocks towards the total synthesis of (–)-*ent*-oldhamine A (**I.240**) was established in this work. The literature-known synthesis of key precursor **I.250** has successfully been optimized and can now be carried out routinely on a 50 g scale. Also, an alternative pathway for the synthesis of **I.250** has been elaborated, which delivers this key precursor in a much more convenient fashion with 69 % yield over six steps from literature-known L-glutamic acid derivative **I.258**.

Two methods to prepare highly functionalized pyrrolizidine **I.245** have been investigated. While a conjugate addition approach failed to deliver the desired product, a reliable and scalable process to access **I.245** was established utilizing a Dieckmann cyclization. Intermediate **I.277** could be prepared in a short and convenient fashion on a multigram scale, which can be carried out with only one chromatographic purification step in a 40 % yield from **I.250**. Pyrrolizidine **I.245** was accessible in three further steps and was successfully prepared on a two gram scale. Thus, the construction of the southern B-C-ring system bearing four of the five stereogenic centers of **I.240** has been completed (Scheme I.55).

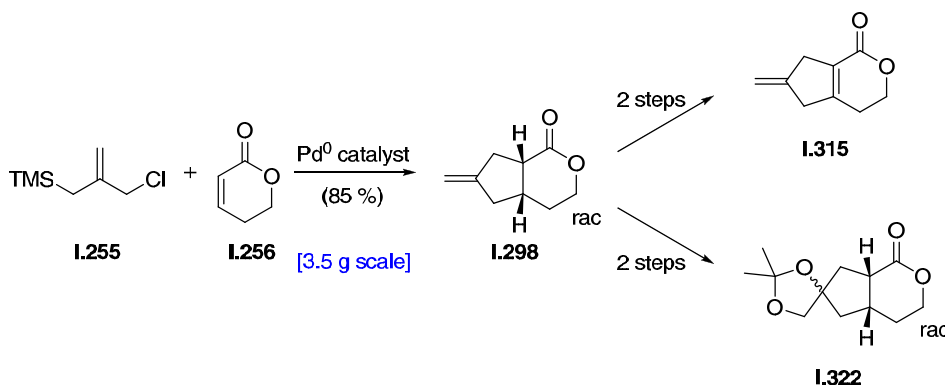


Scheme I.55: Summarized overview on the developed synthesis of **I.245** from literature-known compound **I.258**.

After investigation of three methodologies, the palladium-mediated [3+2] cycloaddition turned out to be a powerful method to construct the southern E-F-ring system of **I.240**. The key reaction was optimized and was successfully carried out on a multigram scale. Overall, the elaborated synthesis opens a short and convenient pathway for the construction of the

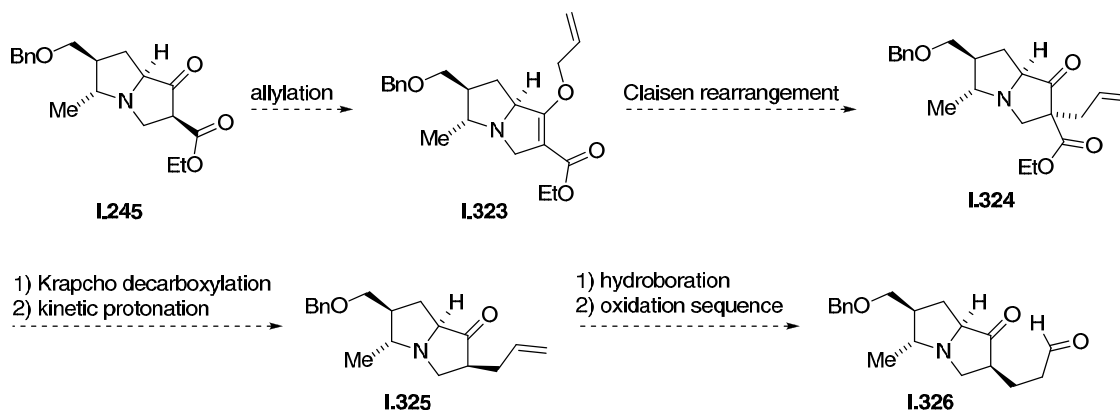
bicyclic lactone portion in **I.240**, which can be carried out in a single step from literature-known starting materials **I.255** and **I.256** and provides **I.298** in a 85 % yield.

Furthermore, first experiments to further functionalize **I.298** have been carried out. Pleasingly, it was found that **I.298** can easily be converted into **I.315** employing a Grieco elimination. Additionally it was found that **I.298** can be oxidized by means of an Upjohn oxidation furnishing dioxolane **I.322** (Scheme I.56).



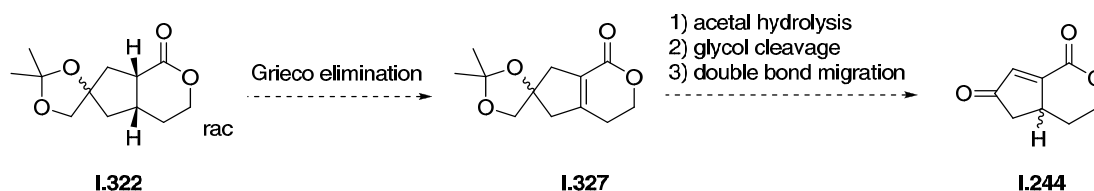
Scheme I.56: Successful synthesis of bicyclic lactones from literature-known compounds **I.255** and **I.256**.

Future work will have to focus on functionalization of the β -ketoester moiety in **I.245** to incorporate the C_3 -carbon chain into the molecule. This could, for example, be achieved by an *O*-allylation/Claisen rearrangement sequence *via* **I.323** and **I.324**, followed by Krapcho decarboxylation. At this stage, an opportunity is provided to adjust the stereochemistry at the allyl side-chain by a deprotonation-protonation sequence under kinetic conditions to obtain **I.325**. A hydroboration and double-oxidation sequence should provide aldehyde **I.326** (Scheme I.57).



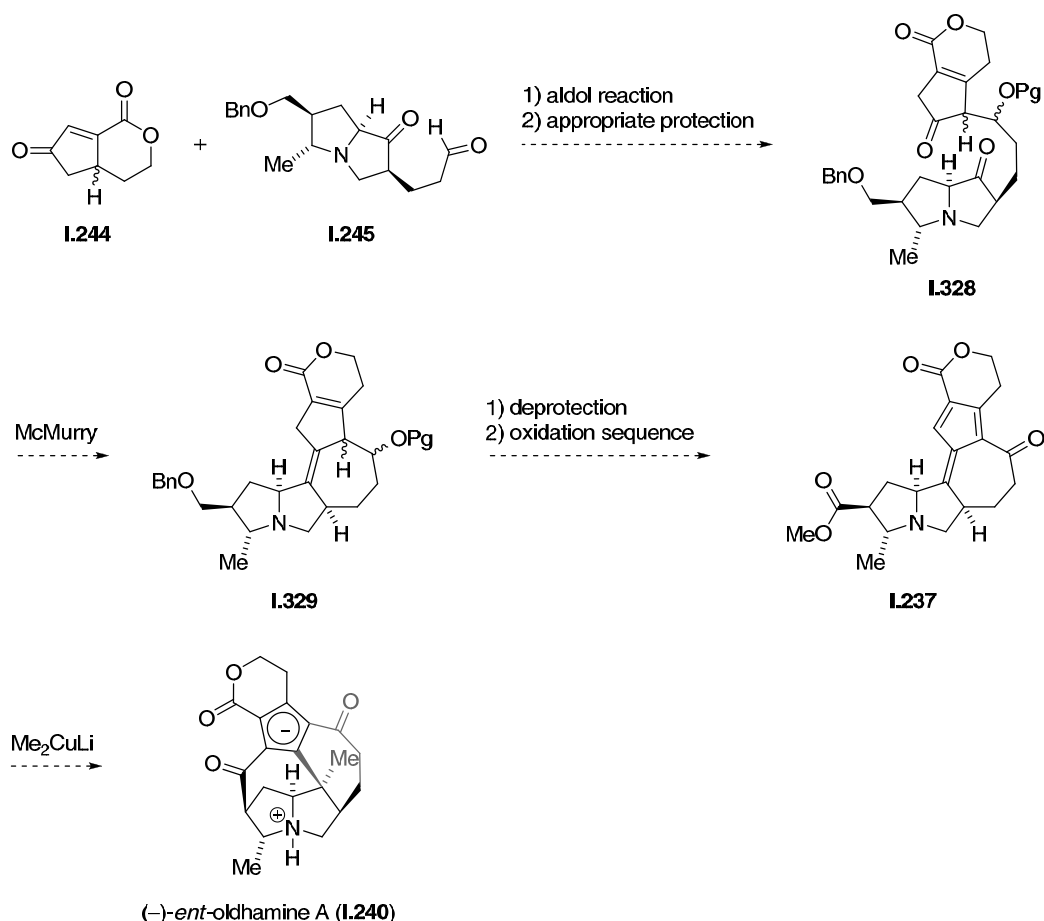
Scheme I.57: Envisioned synthetic route to install the C_3 -carbon chain at **I.245**.

Bicyclic lactone **I.322** will be converted into unsaturated derivative **I.327** followed by a deprotection, oxidative cleavage and double bond migration sequence to provide **I.244** (Scheme I.58).



Scheme I.58: Envisioned sequence for the synthesis of **I.244**.

Possible strategies to convert **I.245** and **I.244** into the natural product have been lined out in the retrosynthetic analysis (*vide supra*, Section 1.1.4), the execution of which will require further experimental studies. One possible pathway for the endgame is shown in Scheme I.59.



Scheme I.59: Possible strategy to complete the total synthesis of **I.240**.

Compounds **I.244** and **I.245** could be coupled by means of an aldol-type reaction followed by appropriate protection to give **I.328**. One possible pathway to close the seven-membered ring

would be a McMurry coupling to provide **I.329**. Upon global deprotection and sequential oxidation of both alcohols and the cyclopentene to the corresponding fulvene **I.237**, the stage is set for the key step (*vide supra*, Section 1.1.4), which would directly provide **I.240** in a single step from **I.237**.

1.3 Experimental Section

General experimental details:

Unless specified otherwise, all reactions were performed with magnetic stirring under an atmosphere of argon and in oven-dried glassware. Isolated products were dried on a high vacuum line at a pressure of 10^{-2} mbar using an *ATB-Loher* oil pump by *Flender*. Diethyl ether and THF were distilled prior to use from sodium and benzophenone. Triethylamine, diisopropylamine and diisopropylethylamine were distilled over calcium hydride. Toluene, benzene dichloromethane (CH_2Cl_2), chloroform (CHCl_3), ethanol (EtOH), methanol (MeOH), acetonitrile (MeCN) and acetone (Me_2CO) were purchased from *Acros Organics* as 'extra dry' reagents under inert gas atmosphere and over molecular sieves. All other reagents were purchased from commercial sources and used without further purification. Petroleum ether is referred to as hexanes and relates to fractions of isohexanes, which boil between 40 °C and 60 °C. Reactions were monitored by TLC using *E. Merck* 0.25 mm silica gel 60 F₂₅₄ glass plates. TLC plates were visualized by exposure to UV light (254 nm) and subsequent treatment with an aqueous solution of CAM, an aqueous solution of potassium permanganate, an acidic solution of vanillin, a solution of ninhydrin or a mixture of silica and finely grounded iodine followed by heating the plate with a heat gun. If appropriate, reactions were additionally monitored by Proton nuclear magnetic resonance (¹H-NMR) using a *Varian 200* spectrometer or LCMS using an *Agilent Technologies 1260 infinity* machine equipped with an *Agilent ZORBAX Eclipse Plus C18* reversed phase analytical 4.6 mm x 150 mm column. Flash column chromatography was performed as described by *Still et al.* employing silica gel (60 Å, 40-63 µm, *Merck*) at a pressure of approx. 1.3-1.5 bar generated by a gentle nitrogen flow.^[94] Reversed phase (RP) column chromatography was performed on *Waters* silica gel (Preparative C18, 125 Å, 55-105 µm) with the same techniques as described above. Analytical RP TLC was performed using pre-coated glass plates (silica gel C18 RP-18W/UV254) from *Macherey-Nagel*. Yields refer to isolated and spectroscopically pure compounds.

Instrumentalization:

Infrared (IR) spectra were recorded on a *Perkin Elmer Spectrum BX II* (FTIR System), equipped with an attenuated total reflection (ATR) measuring unit. IR data is reported in frequency of absorption (cm^{-1}).

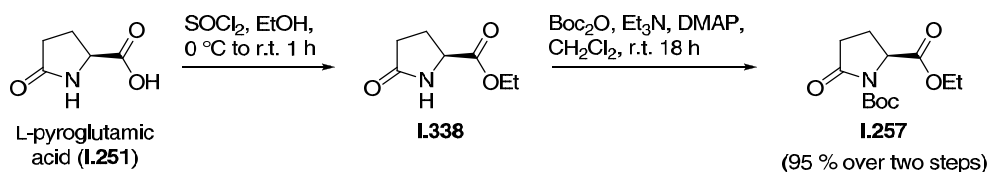
Proton nuclear magnetic resonance ($^1\text{H-NMR}$) spectra were recorded on a *Varian 300*, *Varian 400*, *Inova 400* or *Varian 600* spectrometer. Chemical shifts (δ scale) are expressed in parts per million (ppm) and are calibrated using residual protic solvent as an internal reference (CDCl_3 : $\delta = 7.26$ ppm, $(\text{D}_3\text{C})_2\text{CO}$: $\delta = 2.05$ ppm, $(\text{CD}_3)_2\text{SO}$: $\delta = 2.50$ ppm, CD_2Cl_2 : $\delta = 5.32$ ppm).^[95] Unless noted otherwise, data was recorded at 27 °C. Data for $^1\text{H-NMR}$ spectra are reported as follows: chemical shift (δ ppm) (multiplicity, coupling constants (Hz), integration). Couplings are expressed as: s = singlet, d = doublet, t = triplet, q = quartet, m = multiplet, br = broad, app = apparent or combinations thereof. Carbon nuclear magnetic resonance ($^{13}\text{C-NMR}$) spectra were recorded on the same spectrometers at 75, 100 and 150 MHz, respectively. Carbon chemical shifts (δ scale) are also expressed in parts per million (ppm) and are referenced to the central carbon resonances of the solvents (CDCl_3 : $\delta = 77.16$ ppm, $(\text{D}_3\text{C})_2\text{CO}$: $\delta = 29.84$ ppm, $(\text{CD}_3)_2\text{SO}$: $\delta = 39.52$ ppm, CD_2Cl_2 : $\delta = 53.84$ ppm).^[95]

Mass spectroscopy (MS) experiments were performed on a *Thermo Finnigan MAT 95* (electron ionization, EI) or on a *Thermo Finnigan LTQ FT* (electrospray ionization, ESI) instrument.

Optical rotation was measured in a *Polarimeter P8100-T* of the company *KRÜSS*. $[\alpha]_D$ values are quoted in units of $\text{deg } 10^{-1} \text{ cm}^2 \text{ g}^{-1}$; concentration c takes units of g/100 mL.

Melting points were measured on an *EZ-Melt* automated melting point apparatus made by *Stanford Research Systems* and are uncorrected.

(*S*)-dimethyl 2-(*tert*-butoxycarbonylamino) pentanedioate (**I.338**)^[74] and (*S*)-1-*tert*-butyl 2-ethyl 5-oxopyrrolidine-1,2-dicarboxylate (**I.257**)^[75]



To a suspension of (*S*)-pyroglutamic acid (**I.251**, 50.0 g, 387 mmol, 1.00 eq) in dry ethanol (700 mL, 12.1 mol, 31.1 eq) was added SOCl_2 (28.1 mL, 387 mmol, 1.00 eq) dropwise over the course of 30 min at 0 °C. The resulting mixture was stirred for 10 min at 0 °C and was then allowed to warm to room temperature to be stirred for 1 h at this temperature. Then, water (200 mL) and solid NaHCO_3 (120 g) were added in small portions. The resulting solid was filtered off and the filtrate was concentrated until the bulk of EtOH was removed. The remaining aqueous solution was extracted with CH_2Cl_2 (3 x 500 mL). The combined extracts were washed with brine (200 mL), dried over MgSO_4 , filtered and concentrated to a white solid, which was used without further purification. An analytical sample was purified by recrystallization from ethanol to give **I.338** as a colorless crystalline solid.

TLC (EtOAc:Hex 2:1): $R_f = 0.17$.

mp: 48 °C.

$[\alpha]_D^{21} = -44.8$ ($c = 1.0$, MeOH).

$^1\text{H NMR}$ (300 MHz, CDCl_3): $\delta = 6.38$ (s, br, 1H), 4.27-4.16 (m, 3H), 2.52-2.32 (m, 3H), 2.28-2.17 (m, 1H), 1.28 (t, $J = 7.1$ Hz, 3H).

$^{13}\text{C NMR}$ (75 MHz, CDCl_3): $\delta = 177.8$, 171.9, 61.7, 55.4, 25.2, 24.8, 14.1.

IR (neat): $\tilde{\nu}_{\text{max}} = 1693$, 1199, 1156.

HRMS (EI^+): m/z calcd. for $\text{C}_7\text{H}_{11}\text{NO}_3^+$: 157.0739 $[\text{M}]^+$;
 found: 157.0735 $[\text{M}]^+$.

To a solution of the crude material obtained as described above (58.0 g, 449 mmol, 1.00 eq) in CH_2Cl_2 (1.00 L) was added DMAP (5.49 g, 44.9 mmol, 0.100 eq), BOC_2O (196 g, 898 mmol, 2.00 eq) and Et_3N (187 mL, 1.35 mol, 3.00 eq). After gas evolution had ceased (3 h), the

mixture was stirred for 15 h at room temperature. Then, a 10 % aq. citric acid solution (300 mL) was added and the mixture was stirred until gas evolution had ceased (1 h). The organic layer was separated, washed with a 10 % aq. citric acid solution (2 x 300 mL) and brine (500 mL), dried over MgSO_4 and concentrated. Purification by silica flash column chromatography (EtOAc:Hex 1:2 \rightarrow 1:1) afforded crude **I.257** as a yellow solid. This material was recrystallized from ethanol (40.0 mL) and washed with hexanes (100 mL) to afford **I.257** as colorless crystals (110 g, 95 % over two steps).

TLC (EtOAc:Hex 2:1): $R_f = 0.46$.

mp: 53 °C.

$[\alpha]_D^{21}$: -40.1 ($c = 1.0$, MeOH).

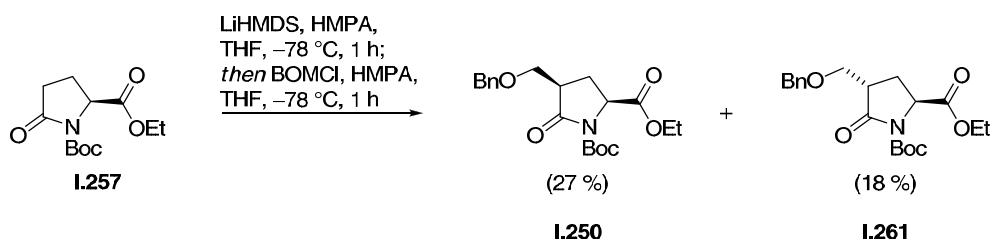
^1H NMR (300 MHz, CDCl_3): $\delta = 4.59$ (dd, $J = 9.2, 3.0$ Hz, 1H), 4.23 (q, $J = 7.1$ Hz, 2H), 2.72-2.55 (m, 1H), 2.55-2.41 (m, 1H), 2.39-2.34 (m, 1H), 2.08-1.96 (m, 1H), 1.49 (s, 9H), 1.29 (t, $J = 7.1$ Hz, 3H).

^{13}C NMR (75 MHz, CDCl_3): 173.2, 171.3, 149.3, 83.5, 61.6, 58.9, 31.1, 27.9 (3C), 21.5, 14.2.

IR (neat): $\tilde{\nu}_{\text{max}} = 1772, 1247, 1025$.

HRMS (ESI^+): m/z calcd. for $\text{C}_{12}\text{H}_{20}\text{NO}_5^+$: 258.1341 $[\text{M}+\text{H}]^+$;
found: 258.1358 $[\text{M}+\text{H}]^+$.

(2*S*,4*R*)-1-*tert*-butyl 2-ethyl 4-(benzyloxymethyl)-5-oxopyrrolidine-1,2-dicarboxylate (I.250) from **I.257** and **(2*S*,4*S*)-1-*tert*-butyl 2-ethyl 4-(benzyloxymethyl)-5-oxopyrrolidine-1,2-dicarboxylate (I.261)**:^[70]



To a solution of HMDS (56.3 mL, 256 mmol, 1.30 eq) in THF (88.0 mL) was added a solution of *n*-BuLi (2.50 M in hexanes, 95.6 mL, 241 mmol, 1.20 eq) dropwise at 0 °C. After complete addition, the mixture was allowed to warm to room temperature and stirred for another 30 min at this temperature.

The resulting LiHMDS solution was cooled to $-78\text{ }^{\circ}\text{C}$ and to this solution was added dropwise a solution of **I.257** (51.7 g, 201 mmol, 1.00 eq) in THF (200 mL) over the course of 20 min. Then, HMPA (45.4 mL, 261 mmol, 1.30 eq) was added over the course of 5 min and the mixture was stirred for 1 h at $-78\text{ }^{\circ}\text{C}$. The resulting mixture was cannulated to a cooled solution of benzyloxymethyl chloride (55.7 mL, 402 mmol, 2.00 eq) in THF (100 mL) at $-78\text{ }^{\circ}\text{C}$ over the course of 25 min and stirred for 1 h at this temperature. The reaction was quenched with a 1:1 mixture of water and a sat. aq. NH_4Cl solution (35.0 mL) and after warming to room temperature, the bulk of the solvent was removed *in vacuo*. The residue was diluted with diethyl ether (1000 mL) and successively washed with a sat. aq. NaHCO_3 solution (800 mL) and brine (800 mL). The organic layer was separated, dried over MgSO_4 , filtered and concentrated *in vacuo*. The resulting residue was purified by column chromatography (silica, EtOAc:Hex 1:10 \rightarrow 1:2) to give **I.250** as a colorless oil (20.8 g, 27 %) and **I.261** as a colorless oil (13.6 g, 18 %).

I.250 was isolated by concentrating later fractions of the chromatographic purification step.

TLC (EtOAc:Hex 1:2): $R_f = 0.34$.

$[\alpha]_D^{18}$: -47.6 ($c = 1.0$, MeOH).

$^1\text{H NMR}$ (300 MHz, CHCl_3): $\delta = 7.40\text{-}7.26$ (m, 5H), 4.65-4.42 (m, 3H), 4.23-4.10 (m, 2H), 3.76 (dd, $J = 9.4, 4.2$ Hz, 1H), 3.66 (dd, $J = 9.4, 7.3$ Hz, 1H), 2.99-2.79 (m, 1H), 2.67-2.43 (m, 1H), 2.16-1.96 (m, 1H), 1.49 (s, 9H), 1.24 (t, $J = 7.1$ Hz, 3H).

$^{13}\text{C NMR}$ (75 MHz, CHCl_3): $\delta = 173.0, 171.3, 149.3, 137.8, 128.6, 128.4$ (2C), 127.7 (2C), 83.6, 73.3, 69.1, 61.5, 57.6, 43.6, 27.9 (3C), 25.0, 14.1.

IR (neat): $\tilde{\nu}_{\text{max}} = 2981, 1791, 1748, 1719, 1369, 1318, 1153$.

HRMS (ESI^+):
m/z calcd. for $\text{C}_{20}\text{H}_{27}\text{NNaO}_6^+$: 400,1736 $[\text{M}+\text{Na}]^+$;
found: 400.1731 $[\text{M}+\text{Na}]^+$.

I.261 was isolated by concentrating earlier fractions of the chromatographic purification step.

TLC (EtOAc:Hex 1:2): $R_f = 0.38$.

$[\alpha]_D^{18}$: -34.9 ($c = 1.0$, MeOH).

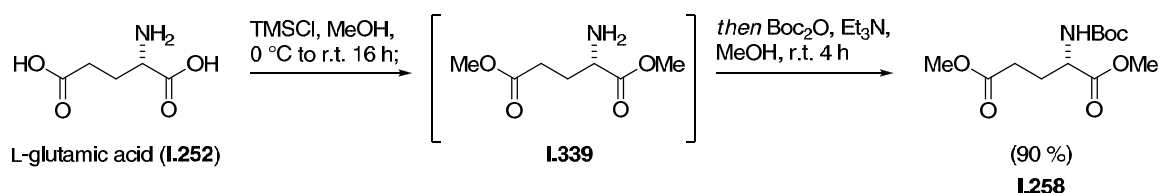
$^1\text{H NMR}$ (600 MHz, CHCl_3): $\delta = 7.36\text{--}7.25$ (m, 5H), 4.58–4.44 (m, 3H), 4.25–4.15 (m, 2H), 3.71 (ddd, $J = 13.1, 9.5, 4.6$ Hz, 2H), 2.87 (dddd, $J = 10.5, 9.1, 5.5, 3.7$ Hz, 1H), 2.35 (ddd, $J = 13.3, 10.5, 9.9$, 1H), 2.20–2.12 (m, 1H), 1.48 (s, 9H), 1.26 (t, $J = 7.1$ Hz, 3H).

$^{13}\text{C NMR}$ (150 MHz, CHCl_3): $\delta = 173.0, 171.4, 149.3, 137.8, 128.4, 127.7$ (2C), 127.6 (2C), 83.5, 73.4, 68.4, 61.6, 57.4, 42.8, 27.9 (3C), 25.6, 14.2.

IR (film): $\tilde{\nu}_{\text{max}} = 2980, 1791, 1748, 1719, 1369, 1154$.

HRMS (ESI⁺): m/z calcd. for $\text{C}_{20}\text{H}_{27}\text{NNaO}_6^+$: 400.1736 [M+Na]⁺;
found: 400.1729 [M+Na]⁺.

(S)-dimethyl 2-(tert-butoxycarbonylamino)pentanedioate (I.258):^[77]



To a solution of L-glutamic acid (14.7 g, 100 mmol, 1.00 eq) in methanol (250 mL) was added TMSCl (51.1 mL, 400 mmol, 4.00 eq) at $0\text{ }^\circ\text{C}$. After complete addition, the mixture was allowed to warm to room temperature and stirred overnight at this temperature.

To the resulting solution containing **I.339** was added NEt_3 (90.0 mL, 650 mmol, 6.50 eq) and Boc_2O (23.5 g, 110 mmol, 1.10 eq) to be stirred at room temperature until no more gas evolution was observed (4 h). The solvent was removed under reduced pressure, the resulting crude product was redissolved in diethyl ether (400 mL) and cooled to $0\text{ }^\circ\text{C}$. The thereby formed solid was filtered off, washed with diethyl ether (200 mL) and discarded. The combined filtrates were concentrated and purified by column chromatography (silica, $\text{EtOAc}:\text{Hex}$ 4:1 \rightarrow 2:1) to give **I.258** as a colorless oil (24.6 g, 90 %).

TLC ($\text{EtOAc}:\text{Hex}$ 1:2): $R_f = 0.29$.

$[\alpha]_D^{19}$: -25.5 ($c = 1.0$, MeOH).

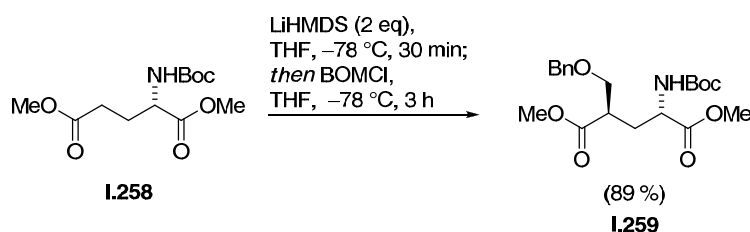
$^1\text{H NMR}$ (300 MHz, CHCl_3): $\delta = 5.14$ (s, br, 1H), 4.39–4.22 (m, 1H), 3.73 (s, 3H), 3.66 (s, 3H), 2.47–2.33 (m, 2H), 2.23–2.08 (m, 1H), 2.02–1.89 (m, 1H), 1.42 (s, 9H).

^{13}C NMR (75 MHz, CHCl_3): $\delta = 173.1, 172.6, 155.3, 80.0, 52.8, 52.4, 51.7, 30.0, 28.3$ (3C), 27.7.

IR (neat): $\tilde{\nu}_{\text{max}} = 2956, 1737, 1712, 1514, 1366, 1159$.

HRMS (ESI⁺): m/z calcd. for $\text{C}_{12}\text{H}_{21}\text{NO}_6$ ⁺: 275.1369 [M]⁺;
found: 275.1375 [M]⁺.

(2*R*,4*S*)-dimethyl 2-(benzyloxymethyl)-4-(*tert*-butoxycarbonylamino)pentanedioate
(**I.259**):



To a solution of HMDS (36.4 mL, 171 mmol, 2.31 eq) in THF (30.4 mL) was added a solution of *n*-BuLi (2.50 M in hexanes, 62.2 mL, 156 mmol, 2.10 eq) dropwise at 0 °C. After complete addition, the mixture was allowed to warm to room temperature and stirred for another 30 min at this temperature.

The resulting LiHMDS solution was cooled to $-78\text{ }^\circ\text{C}$ and to this solution was added dropwise a solution of **I.258** (20.4 g, 74.1 mmol, 1.00 eq) in THF (200 mL) over the course of 20 min. After being stirred for 30 min at this temperature, a solution of BOMCl (20.5 mL, 148 mmol, 2.00 eq) in THF (200 mL) was added dropwise over the course of 20 min to be stirred for additional 3 h at $-78\text{ }^\circ\text{C}$. The reaction mixture was quenched with an aq. 1.00 M HCl solution (100 mL) and the bulk of solvent was removed *in vacuo*. The residue was redissolved in diethyl ether (500 mL) and washed with a sat. aq. NaHCO_3 solution (500 mL) and brine (300 mL), dried over MgSO_4 , filtered and concentrated. The crude product was purified by column chromatography (silica, EtOAc:Hex 1:10 \rightarrow 1:2) to give **I.259** as a colorless oil (26.1 g, 89 %).

TLC (EtOAc:Hex 1:3): $R_f = 0.38$.

$[\alpha]_D^{19}$: -39.6 ($c = 1.0$, MeOH).

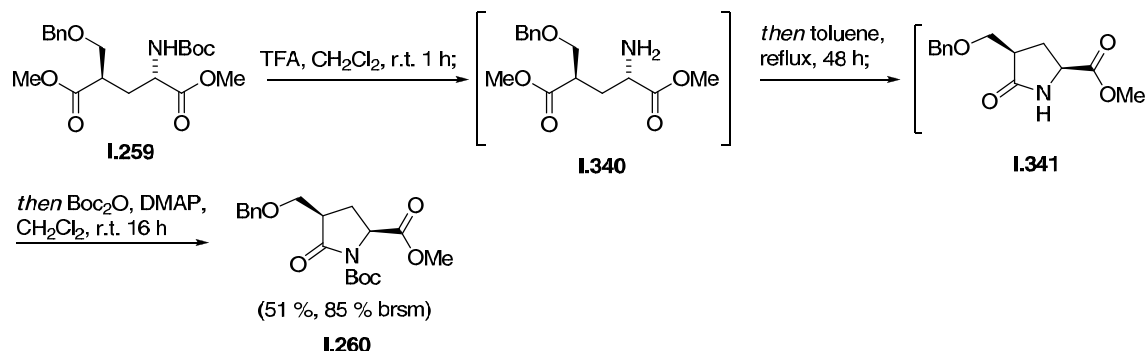
$^1\text{H NMR}$ (300 MHz, CDCl_3 , mixture of rotation isomers): $\delta = 7.39\text{-}7.23$ (m, 5H), 5.13 (s, br, 0.5H) 4.72-4.67 (s, 2H) 4.55-4.50 (m 1H) 4.35 (s, br, 0.5H) 3.76-3.63 (m, 6.5H) 2.88-2.75 (m, 0.5H) 2.52-2.29 (m, 1H), 2.24-1.92 (m, 3H), 1.46 (s, 4.5H), 1.45 (s, 4.5H).

$^{13}\text{C NMR}$ (75 MHz, CDCl_3 , mixture of rotation isomers): $\delta = 174.1, 173.2, 172.7, 172.6, 155.4, 155.4, 141.0, 137.9, 128.5$ (2C), 128.2 (2C), 127.9, 127.8, 127.7 (2C), 127.6 (2C), 127.5, 127.0, 80.1, 80.0, 73.1, 70.1, 65.3, 52.4, 52.3, 52.1, 52.0, 51.8, 42.6, 31.1, 30.1, 28.3, 28.2 (3C), 27.8 (3C).

IR (neat): $\tilde{\nu}_{\text{max}} = 3370, 2978, 1731, 1712, 1512, 1366, 1160$.

HRMS (ESI $^+$): m/z calcd. for $\text{C}_{20}\text{H}_{29}\text{NNaO}_7^+$: 418.1842 [M+Na] $^+$;
found: 418.1835 [M+Na] $^+$.

(2*R*,4*R*)-1-*tert*-butyl 2-methyl 4-(benzyloxymethyl)-5-oxopyrrolidine-1,2-dicarboxylate (I.260):



A mixture of **I.259** (17.9 g, 45.4 mmol, 1.00 eq), CH_2Cl_2 (50.0 mL) and trifluoroacetic acid (46.0 mL) was stirred for 1 h at room temperature. After removal of the solvent *in vacuo*, the residue was diluted with a sat. aq. Na_2CO_3 solution (30.0 mL) and a sat. aq. NaHCO_3 solution (270 mL) and subsequently extracted with diethyl ether (5 x 350 mL). The combined extracts were washed with brine (500 mL), dried over MgSO_4 and concentrated.

The resulting residue containing **I.340** was dissolved in toluene (150 mL) and heated to reflux for 48 h. The mixture was allowed to cool to room temperature and concentrated to give a brown oil.

To a solution of this residual oil containing **I.341** and **I.340** in CH_2Cl_2 (60.0 mL) was added DMAP (6.65 g, 54.4 mmol, 1.20 eq), Boc_2O (10.9 g, 49.9 mmol, 1.10 eq) and triethylamine (6.94 mL, 49.9 mmol, 1.10 eq) to be stirred for 16 h at room temperature. The reaction

mixture was diluted with diethyl ether (350 mL), washed with an aq. 1.00 M HCl solution (350 mL), a sat. aq. NaHCO₃ solution (350 mL) and brine (250 mL), dried over MgSO₄ and concentrated. The crude product was purified by column chromatography (EtOAc:Hex 1:5 → 1:2) to give **I.260** as a colorless oil (8.46 g, 51 %) along with recovered starting material **I.259** (7.71 g, 45 %).

TLC (EtOAc:Hex 1:3): $R_f = 0.25$.

$[\alpha]_D^{18}$: -42.2 ($c = 1.0$, MeOH).

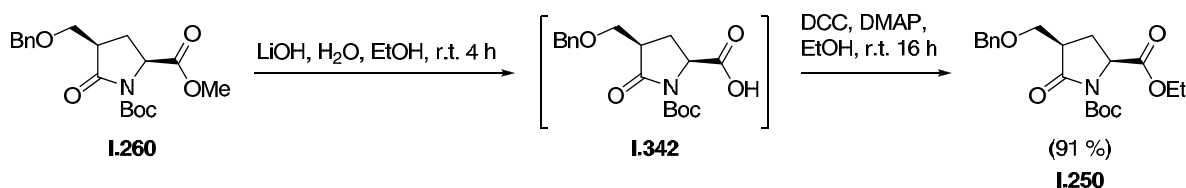
¹H NMR (400 MHz, CDCl₃): $\delta = 7.44$ -7.09 (m, 5H), 4.56-4.48 (td, $J = 9.1, 6.2$ Hz, 1H), 4.48-4.41 (d, $J = 3.44$ Hz, 2H), 3.79-3.56 (m, 5H) 2.90-2.77 (m, 1H), 2.54-2.44 (dt, $J = 13.6, 9.5$ Hz, 1H) 2.10, 1.99 (dt, $J = 13.4, 6.7$ Hz, 1H), 1.46 (s, 9H).

¹³C NMR (75 MHz, CDCl₃): $\delta = 173.0$ 171.7, 149.2, 137.8, 128.4 (2C), 127.7 (2C), 127.6, 83.6, 73.3, 69.0, 57.5, 52.3, 43.6, 27.8 (3C), 25.0.

IR (neat): $\tilde{\nu}_{\max} = 1727, 1181$.

HRMS (ESI⁺): m/z calcd. for C₁₉H₂₅NNaO₆⁺: 386.1580 [M+Na]⁺;
found: 386.1575 [M+Na]⁺.

(2S,4R)-1-tert-butyl 2-ethyl 4-(benzyloxymethyl)-5-oxopyrrolidine-1,2-dicarboxylate (I.250) from **I.260**:



To a solution of **I.260** (150 mg, 413 μ mol, 1.00 eq) in ethanol (2.50 mL) was added a 1.50 M aq. lithium hydroxide solution (0.550 mL, 0.826 μ mol, 2.00 eq). The mixture was stirred for 4 h at room temperature and was then concentrated *in vacuo*. The residue was diluted with an aq. 1.00 M HCl solution (25.0 mL) and extracted with CH₂Cl₂ (3 x 25.0 mL). The combined extracts were dried over MgSO₄, filtered and concentrated.

The resulting residue containing **I.342** was redissolved in CH₂Cl₂ (2.50 mL) and to the solution was added DCC (93.7 mg, 454 μ mol, 1.10 eq), DMAP (55.5 mg, 454 μ mol, 1.10 eq)

and ethanol (0.200 mL, 3.39 mmol, 8.20 eq) to be stirred for 16 h at room temperature. Then, the mixture was filtered and the filter cake was washed with diethyl ether (3 x 5.00 mL). The combined filtrates were washed with brine (15.0 mL), dried over MgSO₄, filtered and concentrated. Purification by column chromatography (silica, EtOAc:Hex 1:5 → 1:1) gave **I.250** as a colorless oil (141 mg, 91 %).

TLC (EtOAc:Hex 1:2): $R_f = 0.34$.

$[\alpha]_D^{18}$: -47.6 ($c = 1.0$, MeOH).

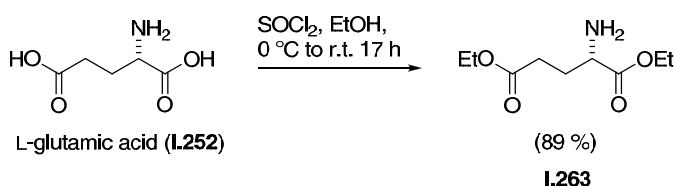
¹H NMR (300 MHz, CHCl₃): $\delta = 7.40$ -7.26 (m, 5H), 4.65-4.42 (m, 3H), 4.23-4.10 (m, 2H), 3.76 (dd, $J = 9.4, 4.2$ Hz, 1H), 3.66 (dd, $J = 9.4, 7.3$ Hz, 1H), 2.99-2.79 (m, 1H), 2.67-2.43 (m, 1H), 2.16-1.96 (m, 1H), 1.49 (s, 9H), 1.24 (t, $J = 7.1$ Hz, 3H).

¹³C NMR (75 MHz, CHCl₃): $\delta = 173.0, 171.3, 149.3, 137.8, 128.4$ (2C), 127.7 (2C), 83.6, 73.3, 69.1, 61.5, 57.6, 43.6, 27.9 (3C), 25.0, 14.1.

IR (neat): $\tilde{\nu}_{\max} = 2981, 1791, 1748, 1719, 1369, 1318, 1153$.

HRMS (ESI⁺): m/z calcd. for C₂₀H₂₇NNaO₆⁺: 400.1736 [M+Na]⁺;
found: 400.1731 [M+Na]⁺.

(S)-diethyl 2-aminopentanedioate (I.263):^[78]



To a suspension of L-glutamic acid (**I.252**, 40.0 g, 272 mmol, 1.00 eq) in ethanol (400 mL, 6.80 mol, 25.0 eq) was added dropwise thionyl chloride (43.4 mL, 600 mmol, 2.20 eq) at 0 °C. After being stirred for 1 h at 0 °C, the mixture was allowed to warm to room temperature and stirred for 16 h at this temperature. Then, the bulk of solvent was removed *in vacuo* and to the remaining solution was added water (50.0 mL) and Na₂CO₃ (60.0 g, 571 mmol, 2.10 eq) in small portions. The resulting mixture was diluted with a sat. aq. NaHCO₃ solution (750 mL) and extracted with dichloromethane (5 x 750 mL). The combined extracts were dried over MgSO₄ and concentrated to yield **I.263** as a colorless oil (49.0 g,

89 %). The resulting crude product was pure enough to be used in the next step without further purification.

TLC (EtOAc:Hex 3:1): $R_f = 0.29$.

$[\alpha]_D^{19}$: +10.2 ($c = 1.0$, CHCl_3).

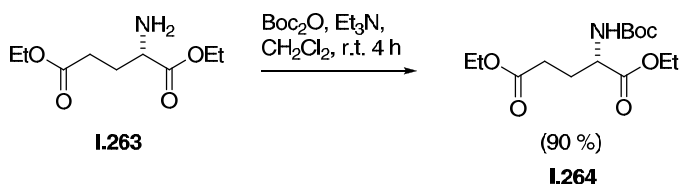
$^1\text{H NMR}$ (600 MHz, CDCl_3): $\delta = 4.06$ (q, $J = 7.1$ Hz, 2H), 4.02 (q, $J = 7.1$ Hz, 2H), 3.41 (dd, $J = 8.3, 5.3$ Hz, 1H), 2.41 (t, $J = 7.5$ Hz, 2H) 2.10-1.97 (m, 1H), 1.75-1.69 (m, 1H), 1.36 (s, br, 2H), 1.27-1.18 (m, 6H).

$^{13}\text{C NMR}$ (75 MHz, CDCl_3): $\delta = 175.5, 173.0, 60.8, 60.3, 53.7, 30.6, 30.0, 14.1$ (2C).

IR (neat): $\tilde{\nu}_{\text{max}} = 1727, 1181$.

HRMS (ESI⁺): m/z calcd. for $\text{C}_9\text{H}_{17}\text{NO}_4^+$: 203.1158 [M]⁺;
found: 203.1148 [M]⁺.

(S)-diethyl 2-(tert-butoxycarbonylamino)pentanedioate (I.264):^[79]



To a mixture of **I.263** (53.6 g, 264 mmol, 1.00 eq), Boc_2O (63.3 g, 290 mmol, 1.10 eq) and CH_2Cl_2 (1000 mL) was added Et_3N (110 mL, 791 mmol, 3.00 eq) and then DMAP (3.22 g, 26.4 mmol, 0.100 eq). The flask was equipped with a bubbler and the mixture was stirred for 16 h at room temperature. Then, a 10 % aq. citric acid solution (800 mL) was slowly added and the mixture was stirred until gas evolution had ceased (1 h). The organic layer was separated, washed with brine (900 mL), dried over MgSO_4 and concentrated. Purification by column chromatography (silica, EtOAc:Hex 4:1 \rightarrow 2:1) gave **I.264** as a colorless solid (72.0 g, 90 %).

TLC (EtOAc:Hex 3:1): $R_f = 0.32$.

$[\alpha]_D^{19}$: +11.0 ($c = 1.0$, CHCl_3).

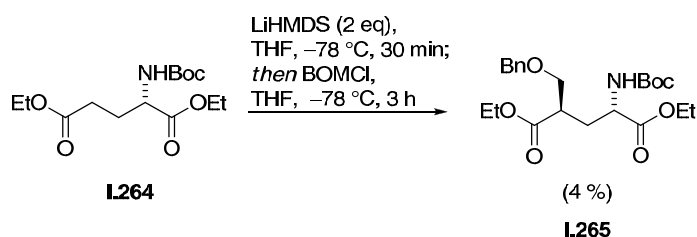
^1H NMR (300 MHz, CDCl_3): δ = 5.10 (s, br, 1H), 4.41-4.26 (m, 1H), 4.17 (q, J = 7.1 Hz, 2H), 4.11 (q, J = 7.1 Hz, 2H), 2.44-2.29 (m, 2H), 2.20-2.09 (m, 1H), 2.03-1.89 (m, 1H), 1.42 (s, 9H), 1.28-1.21 (m, 6H).

^{13}C NMR (75 MHz, CDCl_3): δ = 172.7, 172.2, 155.3, 79.8, 61.4, 60.6, 52.9, 30.3, 28.5, 28.2 (3C), 14.1, 14.0.

IR (film): $\tilde{\nu}_{\text{max}}$ = 1726, 1249, 1159.

HRMS (ESI⁺): m/z calcd. for $\text{C}_{14}\text{H}_{25}\text{NO}_6$ ⁺: 303.1682 [M]⁺;
found: 303.1671 [M]⁺.

(2*R*,4*S*)-diethyl 2-(benzyloxymethyl)-4-(*tert*-butoxycarbonylamino)pentanedioate (I.265):



To a solution of HMDS (66.0 mL, 311 mmol, 2.31 eq) in THF (90.0 mL) was added a solution of *n*-BuLi (2.25 M in hexanes, 126 mL, 282 mmol, 2.10 eq) dropwise at 0 °C. After complete addition, the mixture was allowed to warm to room temperature to be stirred for another 30 min at this temperature.

Then, the resulting LiHMDS solution was cooled to -78 °C and to this solution was added dropwise a solution of **I.264** (40.8 g, 134 mmol, 1.00 eq) in THF (525 mL) at -78 °C. After being stirred for 30 min, a solution of BOMCl (15.5 mL, 79.0 mmol, 2.00 eq) in THF (525 mL) was added dropwise to be stirred for additional 3 h at this temperature. The reaction mixture was quenched at -78 °C with an 1.00 M aq. HCl solution (185 mL) and the bulk of solvent was removed *in vacuo*. The residue was redissolved in diethyl ether (850 mL) and washed with a sat. aq. NaHCO_3 solution (800 mL) and brine (400 mL), dried over MgSO_4 , filtered and concentrated. The crude product was purified by repeated column chromatography (silica, EtOAc:Hex 1:20 \rightarrow 1:6; then EtOAc:Hex 1:100 \rightarrow 1:12) to give **I.265** as a colorless oil (2.11 g, 4 %).

TLC (EtOAc:Hex 1:3): R_f = 0.55.

$[\alpha]_D^{19}$: +1.2 ($c = 1.0$, MeOH).

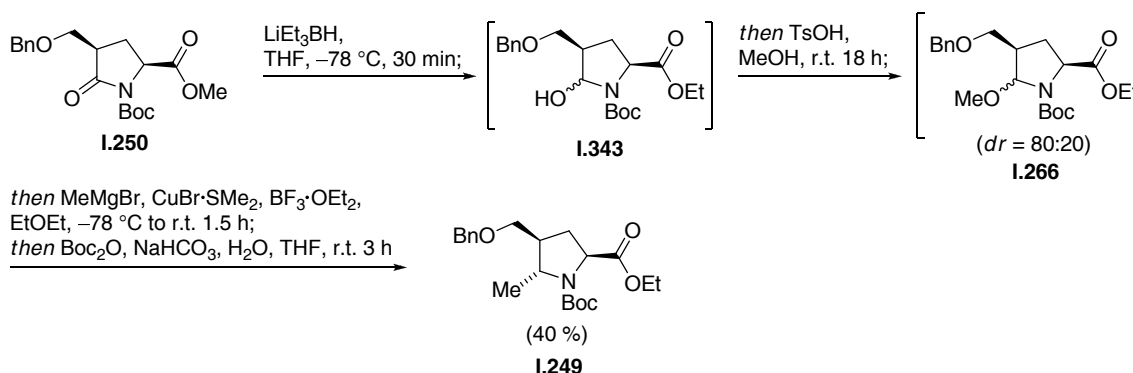
$^1\text{H NMR}$ (300 MHz, CDCl_3): $\delta = 7.37$ - 7.26 (m, 5H) 5.04 (s, br, 1H), 4.51 (s, 2H), 4.39-4.22 (m, 1H), 4.22-4.11 (m, 4H), 3.75-3.57 (m, 2H), 2.82-2.70 (m, 1H), 2.16-2.96 (m, 2H), 1.42 (s, 9H), 1.30-1.22 (m, 6H).

$^{13}\text{C NMR}$ (75 MHz, CDCl_3): $\delta = 173.6$, 172.3, 155.4, 137.9, 128.3 (2C), 127.6, 127.5 (2C), 79.9, 73.1, 70.2, 61.4, 60.8, 52.2, 42.8, 31.0, 28.3 (3C), 14.1, 14.1.

IR (neat): $\tilde{\nu}_{\text{max}} = 1708$.

HRMS (ESI⁺): m/z calcd. for $\text{C}_{22}\text{H}_{33}\text{NNaO}_7^+$: 446.2155 [M+Na]⁺;
found: 446.2153 [M+Na]⁺.

(2*S*,4*R*)-1-*tert*-butyl 2-ethyl 4-(benzyloxymethyl)-5-methoxypyrrolidine-1,2-dicarboxylate (**I.266**) and (2*S*,4*S*,5*R*)-1-*tert*-butyl 2-ethyl 4-(benzyloxymethyl)-5-methylpyrrolidine-1,2-dicarboxylate (**I.249**) from **I.250**:^[70]



To a solution of **I.250** (18.3 g, 48.4 mmol, 1.00 eq) in THF (250 mL) was added dropwise a solution of lithium triethylborohydride (1.00 M in THF, 58.0 mL, 58.0 mmol, 1.00 eq) at $-78\text{ }^\circ\text{C}$ over the course of 10 min. After being stirred for 30 min at this temperature, the reaction was quenched with a sat. aq. NaHCO_3 solution (20.0 mL) and allowed to warm to $0\text{ }^\circ\text{C}$. To the mixture was added H_2O_2 (25.0 mL) in one portion and stirred at $0\text{ }^\circ\text{C}$ for 30 min. The solvent was removed *in vacuo* and the residue was redissolved in ethyl acetate (540 mL) and water (270 mL). The organic layer was separated, dried over MgSO_4 , filtered and concentrated to a colorless oil.

To a solution of this residual oil containing **I.343** (~18.0 g) in methanol (255 mL) was added *p*-toluenesulfonic acid monohydrate (1.84 g, 9.67 mmol, 0.200 eq) to be stirred for 18 h at

room temperature. The reaction was quenched with a sat. aq. NaHCO₃ solution (22.0 mL), the solvent was removed *in vacuo* and the residue was redissolved in a mixture of diethyl ether (540 mL) and water (270 mL). The organic layer was separated, washed with brine (180 mL), dried over MgSO₄, filtered and concentrated to give a colorless oil. By NMR, **I.266** was found to be a 4:1 mixture of diastereomers.

TLC (EtOAc:Hex 1:3): $R_f = 0.23$ (both diastereomers).

¹H NMR (400 MHz, CHCl₃, crude mixture of diastereomers): $\delta = 7.39-7.20$ (m, 5H), 5.31-5.05 (m, 1H), 4.55-4.45 (m, 2H), 4.27-4.08 (m, 3H), 3.71-3.54 (m, 1H), 3.46-3.38 (m, 4H), 2.61-2.26 (m, 2H), 1.87-1.73 (m, 1H), 1.48-1.42 (m, 9H), 1.28-1.22 (m, 3H).

¹³C NMR (100 MHz, CHCl₃, crude mixture of diastereomers): $\delta = 172.6, 172.2, 154.2, 153.9, 138.3, 138.2, 128.5, 128.4, 128.3$ (2C), 127.7 (2C), 127.5 (2C), 126.9 (2C), 87.9, 87.8, 80.9, 80.5, 73.3, 73.2, 68.7, 68.5, 65.8, 65.3, 60.9, 60.9, 58.9, 58.2, 55.7, 55.3, 44.7, 44.0, 31.3, 30.0, 28.3 (3C), 28.1 (3C), 14.2, 14.1.

IR (neat): 1750, 1451.

HRMS (ESI⁺): m/z calcd. for C₂₁H₃₁NNaO₆⁺: 416.2049 [M+Na]⁺;
found: 416.2045 [M+Na]⁺.

To a suspension of copper(I)bromide-dimethyl sulfide complex (46.3 g, 225 mmol, 4.65 eq) in diethyl ether (400 mL) was added a solution of MeMgBr (3.00 M in diethyl ether, 75.0 mL, 225 mmol, 4.65 eq) dropwise over the course of 15 min at -40 °C and stirred for 1 h at this temperature. Then, the resulting yellow suspension was cooled to -78 °C and boron trifluoride diethyl etherate (27.8 mL, 225 mmol, 4.65 eq) was added dropwise over the course of 15 min. After being stirred for 30 min at -78 °C, a solution of crude **I.266** (~19.0 g) in diethyl ether (60.0 mL) was added over the course of 10 min. The flask was rinsed with additional diethyl ether (15.0 mL) and the reaction mixture was stirred for 15 min at -78 °C. Then, the mixture was allowed to warm to room temperature and stirred for 1 h at this temperature. The reaction was quenched by dropwise addition of a 1:1 mixture of a sat. aq. NH₄Cl solution and a 28 % aq. NH₃ solution (260 mL). The resulting mixture was stirred for 30 min at room temperature and was then diluted with diethyl ether (250 mL). The organic layer was separated, washed with water (300 mL) and brine (250 mL), dried over MgSO₄ and concentrated *in vacuo* to give a residue which was redissolved in THF (120 mL).

To the mixture was successively added a sat. aq. NaHCO₃ solution (21.0 mL), Boc₂O (10.6 g, 48.4 mmol, 1.00 eq) and DMAP (60.0 mg, 0.480 mmol, 0.010 eq) and the mixture was stirred for 4 h at room temperature. The bulk of the solvent was removed and the residue was diluted in a mixture of EtOEt (540 mL) and water (270 mL). The organic layer was separated, washed with brine (250 mL), dried over MgSO₄, filtered and concentrated *in vacuo*. The resulting residue was purified by column chromatography (Silica, EtOAc:Hex 1:9 → 1:4) to give **I.249** as a colorless oil (7.31 g, 40 %).

TLC (EtOAc:Hex 1:2): $R_f = 0.22$.

$[\alpha]_D^{19} = -42.0$ ($c = 1.0$, MeOH).

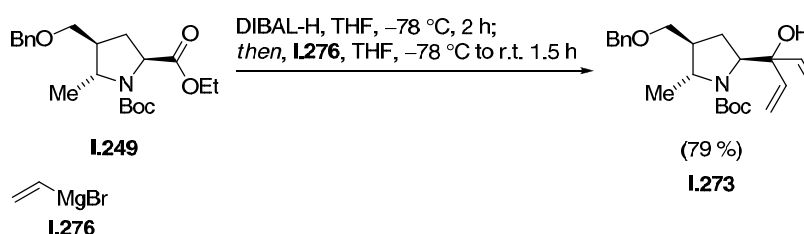
¹H NMR (400 MHz, DMSO, 100 °C): 7.38-7.17 (m, 5H), 4.43 (d, $J = 2.3$ Hz, 2H), 4.17 (dd, $J = 9.8, 4.1$ Hz, 1H), 4.05 (q, $J = 7.1$ Hz, 2H), 3.73-3.68 (m, 1H), 3.49 (dd, $J = 9.5, 7.3$ Hz, 1H), 3.35 (dd, $J = 9.5, 7.3$ Hz, 1H), 2.44-2.37 (m, 1H), 2.13-2.08 (m, 1H), 1.71 (dt, $J = 13.5, 4.1$ Hz, 1H), 1.35 (s, 9H), 1.20 (d, $J = 6.2$ Hz, 3H), 1.15 (t, $J = 7.1$, 3H).

¹³C NMR (100 MHz, DMSO, 100 °C): $\delta = 172.9, 153.5, 139.0, 128.5$ (2C), 127.7 (2C), 127.6, 79.3, 72.7, 71.6, 60.6, 59.2, 57.0, 45.5, 30.5, 28.5 (3C), 20.3, 14.3.

IR (neat): $\tilde{\nu}_{\max} = 2976, 1745, 1698, 1454, 1388, 1367, 1185$.

HRMS (ESI⁺): m/z calcd. for C₂₁H₃₂NO₅⁺: 378.2280 [M+H]⁺;
found: 378.2274 [M+H]⁺.

(2*R*,3*S*,5*S*)-*tert*-butyl 3-(benzyloxymethyl)-5-(3-hydroxypenta-1,4-dien-3-yl)-2-methylpyrrolidine-1-carboxylate (**I.273**):



To a solution of **I.249** (100 mg, 0.256 mmol, 1.00 eq) in THF (1.00 mL) was added dropwise a DIBAL-H solution (1.00 M solution in hexanes, 0.290 mL, 0.291 mmol, 1.10 eq) at -78 °C. After being stirred for 2 h at this temperature, a solution of vinylmagnesium bromide (1.00 M in THF, 0.530 mL, 0.530 mmol, 2.00 eq) was added dropwise and the resulting mixture was

stirred for 1 h at $-78\text{ }^{\circ}\text{C}$. Then, the reaction mixture was allowed to warm to room temperature, stirred for 1.5 h at this temperature and was subsequently quenched by dropwise addition of a sat. aq. NH_4Cl solution (0.500 mL). The solvent was removed *in vacuo* and the resulting crude solid was redissolved in a 2:1 mixture of EtOAc:water (12.0 mL). The organic layer was separated, washed with brine (4.00 mL), dried over MgSO_4 , filtered and concentrated. Purification by column chromatography (silica, EtOAc:Hex 1:2) afforded **I.273** as a colorless oil (81.0 mg, 79 %).

TLC (EtOAc:Hex 1:2): $R_f = 0.18$.

$[\alpha]_D^{19} = -51.3$ ($c = 1.0$, MeOH).

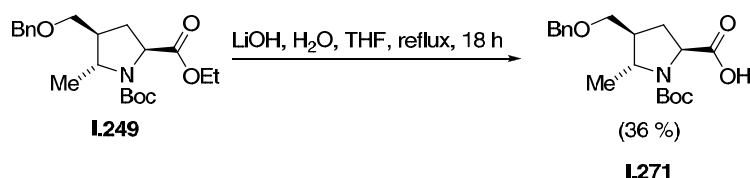
$^1\text{H NMR}$ (600 MHz, CDCl_3): 7.37-7.29 (m, 5H), 5.90 (dd, $J = 17.1, 10.6$ Hz, 2H), 5.41 (dd, $J = 17.1, 1.8$ Hz, 2H), 5.15 (dd, $J = 10.6, 1.8$ Hz, 2H), 4.52-4.49 (m, 2H), 3.94 (dd, $J = 9.6, 7.6$ Hz, 1H), 3.57-3.51 (m, 1H), 3.47-3.42 (m, 1H), 3.39-3.34 (dd, $J = 9.3, 6.5$ Hz, 1H), 2.12 (dt, $J = 13.4, 7.6$ Hz, 1H), 1.93-1.88 (m, 1H), 1.58-1.53 (m, 1H), 1.43 (s, 9H), 1.25 (d, $J = 6.0$ Hz, 3H).

$^{13}\text{C NMR}$ (150 MHz, DMSO): $\delta = 140.3, 138.1$ (2C), 136.5, 128.4 (2C), 127.7, 127.5 (2C), 115.9 (2C), 114.7, 80.6, 77.8, 73.2, 71.5, 67.5, 58.5, 44.3, 31.7, 28.3 (3C), 20.7.

IR (neat): $\tilde{\nu}_{\text{max}} = 1716, 1366, 1152$.

HRMS (ESI⁺): m/z calcd. for $\text{C}_{23}\text{H}_{33}\text{NNaO}_4^+$: 410.2307 $[\text{M}+\text{Na}]^+$;
found: 410.2301 $[\text{M}+\text{Na}]^+$.

(2S,4S,5R)-4-(benzyloxymethyl)-1-(tert-butoxycarbonyl)-5-methylpyrrolidine-2-carboxylic acid (I.271):



To a solution of **I.249** (11.0 mg, 29.1 μmol , 1.00 eq) in THF (0.200 mL) was added a 2.50 M aq. LiOH solution (0.200 mL, 0.468 mmol, 12.0 eq) and the resulting mixture was heated to reflux for 18 h. The mixture was allowed to cool to room temperature and upon removal of the solvent *in vacuo*, the residue was diluted with a mixture of a sat. aq. NH_4Cl solution

(4.00 mL), a 2.00 M aq. HCl solution (5.00 mL) and Et₂O (10.0 mL). The organic layer was separated, washed with brine (4.00 mL), dried over MgSO₄ and concentrated. The crude product was purified by column chromatography (silica, EtOAc:Hex 1:1 → 2:1) to give **I.271** as a colorless oil (3.70 mg, 36 %).

TLC (EtOAc:Hex 2:1): $R_f = 0.09$.

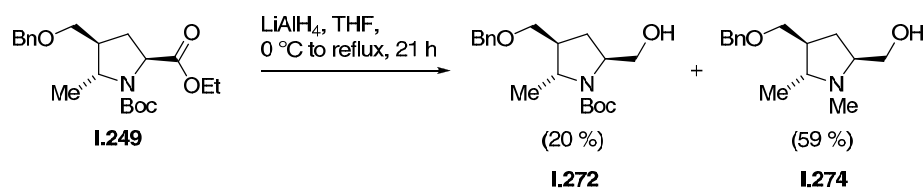
¹H NMR (400 MHz, CDCl₃, mixture of rotation isomers): 7.35-7.25 (m, 5H), 4.50-4.45 (m, 2H), 4.37-4.23 (m, 1H), 3.98-3.79 (m, 1H), 3.51-3.34 (m, 2H), 2.54-1.97 (m, 3H), 1.49-1.37 (m, 9H), 1.27-1.21 (m, 3H).

¹³C NMR (100 MHz, DMSO, mixture of rotation isomers): $\delta = 177.9, 174.3, 156.7, 153.2, 138.1, 137.9, 128.4$ (2C), 128.4 (2C), 127.7 (2C), 127.6 (2C), $127.5, 127.4, 81.8, 80.4, 73.2, 73.1, 71.6, 71.3, 58.9, 58.7, 57.4, 57.0, 45.4, 45.0, 31.0, 29.7, 28.4$ (3C), 28.2 (3C), $20.1, 19.7$.

IR (neat): $\tilde{\nu}_{\max} = 1741, 1550$.

HRMS (ESI): m/z calcd. for C₁₉H₂₆NO₅⁻: 348.1816 [M-H]⁻;
found: 348.1812 [M-H]⁻.

(*2R,3S,5S*)-tert-butyl 3-(benzyloxymethyl)-5-(hydroxymethyl)-2-methylpyrrolidine-1-carboxylate (**I.272**) and ((*2S,4S,5R*)-4-(benzyloxymethyl)-1,5-dimethylpyrrolidin-2-yl)methanol (**I.274**):



To a suspension of LiAlH₄ (8.63 mg, 0.227 mmol, 1.10 eq) in THF (0.500 mL) was added dropwise a solution of **I.249** (78.0 mg, 0.207 mmol, 1.00 eq) in THF (0.500 mL) at 0 °C. The resulting mixture was allowed to warm to room temperature to be stirred for 18 h at this temperature. Then, THF (6.00 mL) was added and the reaction mixture was heated to reflux for 3 h. The mixture was allowed to cool to room temperature and the solvent was removed *in vacuo*. The mixture was redissolved in a sat. aq. Rochelle salt solution (20.0 mL) and extracted with EtOAc (3 x 20.0 mL). The combined extracts were washed with brine (15.0 mL), dried over MgSO₄ and concentrated. The crude product mixture was purified with

column chromatography (silica, EtOAc:Hex 1:4 → 1:3) to afford **I.272** as a colorless oil (14.0 mg, 20 %) and **I.274** as a colorless oil (30.2 mg, 59 %).

I.274 was isolated by concentrating earlier fractions of the chromatographic purification step.

TLC (EtOAc:Hex 1:2): $R_f = 0.22$.

$[\alpha]_D^{19} = -21.2$ ($c = 1.0$, MeOH).

^1H NMR (400 MHz, DMSO): $\delta = 7.39\text{--}7.19$ (m, 5H), 4.44 (s, 2H), 3.69 (s, br, 1H), 3.50–3.32 (m, 5H), 3.23–3.18 (m, 1H), 2.14–2.05 (m, 1H), 1.99–1.89 (m, 1H), 1.58 (dt, $J = 12.7, 8.2$ Hz, 1H), 1.25 (s, 9H), 1.14 (d, $J = 6.2$ Hz, 3H).

^{13}C NMR (100 MHz, DMSO): $\delta = 154.5, 139.1, 128.6$ (2C), 127.7 (2C), 127.7, 78.7, 72.8, 72.4, 63.7, 59.7, 57.0, 45.0, 30.2, 28.7 (3C), 21.5.

IR (neat): $\tilde{\nu}_{\text{max}} = 2971, 1686, 1662, 1390, 1172, 1089$.

HRMS (ESI ⁺):	m/z calcd. for C ₁₉ H ₃₀ NO ₄ ⁺ :	336.2175 [M+H] ⁺ ;
	found:	336.2194 [M+H] ⁺ .

I.272 was isolated by concentrating later fractions of the chromatographic purification step.

TLC (EtOAc:Hex 1:2): $R_f = 0.15$.

$[\alpha]_D^{19} = -9.1$ ($c = 1.0$ MeOH).

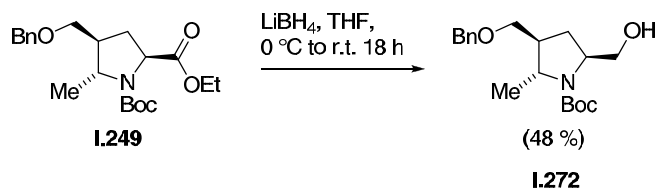
^1H NMR (600 MHz, CDCl₃): $\delta = 7.36\text{--}7.29$ (m, 5H), 4.53–4.49 (m, 2H), 4.45 (t, $J = 8.4$ Hz, 1H), 4.13 (dd, $J = 8.9, 3.6$ Hz, 1H), 4.06–4.02 (m, 1H), 3.75–3.71 (m, 1H), 3.50–3.42 (m, 1H), 2.29–2.22 (m, 1H), 2.20–2.14 (m, 1H), 1.47 (s, 3H), 1.38 (dd, $J = 22.4, 10.5$ Hz, 1H), 1.30 (d, $J = 6.6$ Hz, 3H), 1.26 (s, br, 1H).

^{13}C NMR (150 MHz, CDCl₃): $\delta = 138.0, 128.4$ (2C), 127.7, 127.6 (2C), 73.3, 71.7, 67.6, 58.1, 57.7, 49.5, 35.8, 26.5, 21.6.

IR (neat): $\tilde{\nu}_{\text{max}} = 2869, 1371, 1149$.

HRMS (EI ⁺):	m/z calcd. for C ₁₅ H ₂₃ NO ₂ ⁺ :	249.1729 [M] ⁺ ;
	found:	249.1726 [M] ⁺ .

(2*R*,3*S*,5*S*)-*tert*-butyl 3-(benzyloxymethyl)-5-(hydroxymethyl)-2-methylpyrrolidine-1-carboxylate (**I.272**):



To a solution of **I.249** (117 mg, 0.310 mmol, 1.00 eq) in THF (1.50 mL) was added a solution of LiBH_4 (2.00 M solution in THF, 0.170 mL, 0.341 mmol, 1.10 eq) over the course of 5 min at 0 °C. Then, the mixture was allowed to warm to room temperature, stirred for 18 h at this temperature and concentrated. The resulting solid was redissolved in water (20.0 mL) and extracted with EtOEt (3 x 20.0 mL). The combined extracts were washed with brine (15.0 mL), dried over MgSO_4 and concentrated. Upon purification by column chromatography (silica, EtOAc:Hex 1:3), **I.272** was obtained as a colorless oil (50.1 mg, 48 %).

TLC (EtOAc:Hex 1:2): $R_f = 0.22$.

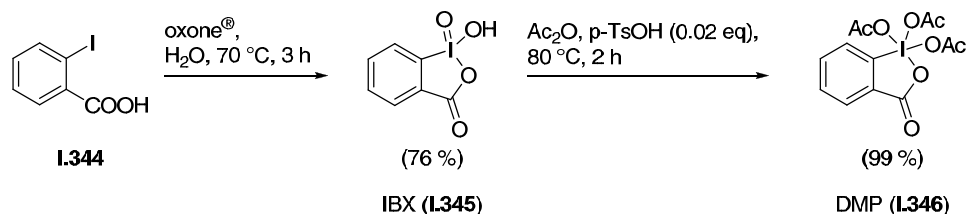
$[\alpha]_D^{19} = -21.2$ ($c = 1.0$, MeOH).

$^1\text{H NMR}$ (400 MHz, DMSO): $\delta = 7.39\text{--}7.19$ (m, 5H), 4.44 (s, 2H), 3.69 (s, br, 1H), 3.50–3.32 (m, 5H), 3.23–3.18 (m, 1H), 2.14–2.05 (m, 1H), 1.99–1.89 (m, 1H), 1.58 (dt, $J = 12.7, 8.2$ Hz, 1H), 1.25 (s, 9H), 1.14 (d, $J = 6.2$ Hz, 3H).

$^{13}\text{C NMR}$ (100 MHz, DMSO): $\delta = 154.5, 139.1, 128.6$ (2C), 127.7 (2C), 127.7, 78.7, 72.8, 72.4, 63.7, 59.7, 57.0, 45.0, 30.2, 28.7 (3C), 21.5.

IR (neat): $\tilde{\nu}_{\text{max}} = 2971, 1686, 1662, 1390, 1172, 1089$.

HRMS (ESI⁺): m/z calcd. for $\text{C}_{19}\text{H}_{30}\text{NO}_4^+$: 336,2175 [M+H]⁺;
found: 336,2194 [M+H]⁺.

1-Hydroxy-3H-benz[d][1,2]iodoxole-1,3-dione (I.345) and **1,1,1-tris(acetoxy)-1,1-dihydro-1,2-benziodoxol-3(1H)-one (I.346)**.^[96]

In a 4.00 L three-necked flask equipped with a mechanical stirrer and a thermometer, a mixture of iodobenzoic acid (**I.344**, 200 g, 0.810 mol, 1.00 eq), water (2.60 L) and oxone[®] (704 g, 1.15 mol, 1.42 eq) was stirred at 70 °C without sealing the third joint. After 3 h, the mixture was allowed to cool to room temperature and was then cooled to 0 °C for 2 h. The resulting precipitate was filtered off, washed with cold water (2.00 L), acetone (2.00 L), hexanes (0.500 L) and diethyl ether (0.500 L) and dried to give **I.345** as a colorless solid (172 g, 76 %) which was used without further purification.

mp: 230 °C.

¹H NMR (400 MHz): δ = 8.15 (d, J = 7.8 Hz, 1H), 8.01 (d, J = 7.8 Hz, 1H), 7.98 (t, J = 7.8 Hz, 1H), 7.84 (t, J = 7.8 Hz, 1H).

¹³C NMR (75 MHz, DMSO): δ = 168.4, 147.4, 133.8, 132.3, 131.3, 131.0, 125.9.

IR (neat): 1640.

To a suspension of IBX (**I.345**) prepared as described above (120 g, 429 mmol, 1.00 eq) in Ac₂O (450 mL) was added *p*-TsOH monohydrate (1.63 g, 8.57 mmol, 0.020 eq) and the resulting mixture was heated to 80 °C for 2 h. The mixture was allowed to cool to room temperature and was then cooled to 0 °C for 2 h. The resulting solid was filtered off, washed with diethyl ether (3.00 L) and hexanes (2.00 L) and dried. DMP (**I.346**) was afforded as a colorless solid (180 g, 99 %) and was pure enough to be used without further purification.

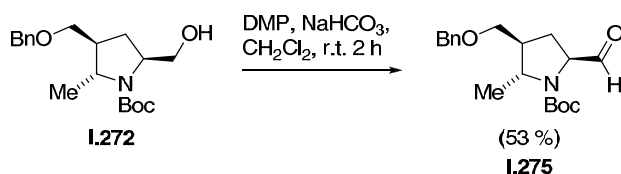
mp: ca. 100 °C (explosive decomposition).

¹H NMR (400 MHz, CDCl₃): δ = 8.33–8.24 (m, 2H), 8.11–8.04 (m, 1H), 7.90 (td, J = 0.9, 7.4 Hz, 1H), 2.32 (s, 3H), 1.99 (s, 6H).

¹³C NMR (75 MHz, CDCl₃): δ = 175.8, 174.1, 166.2, 142.3, 135.9, 133.9, 131.9, 126.6, 126.0, 20.5, 20.4.

IR (neat): $\tilde{\nu}_{\max}$ = 1700, 1671.

(2*R*,3*S*,5*S*)-*tert*-butyl 3-(benzyloxymethyl)-5-formyl-2-methylpyrrolidine-1-carboxylate (**I.272**) using DMP (**I.346**):



To a suspension of DMP (**I.346**) prepared as described above (45.5 mg, 107 μmol , 1.20 eq) and sodium bicarbonate (11.3 mg, 134 μmol , 1.50 eq) in CH_2Cl_2 (1.00 mL) was added a solution of **I.272** (30.0 mg, 89.4 μmol , 1.00 eq) in CH_2Cl_2 (1.00 mL) dropwise at room temperature. The mixture was stirred for 2 h at room temperature, then diluted with a mixture of diethyl ether (15.0 mL) and 1.30 M NaOH (7.50 mL) and stirring was continued for another 15 min. The organic layer was then separated, washed with a 1.30 M NaOH solution (15.0 mL) and water (15.0 mL), dried over MgSO_4 , filtered and concentrated to give **I.275** as a colorless oil (15.8 mg, 53 %).

TLC (EtOAc:Hex 1:2): R_f = 0.61.

$[\alpha]_D^{18} = -27.2$ ($c = 1.0$, MeOH).

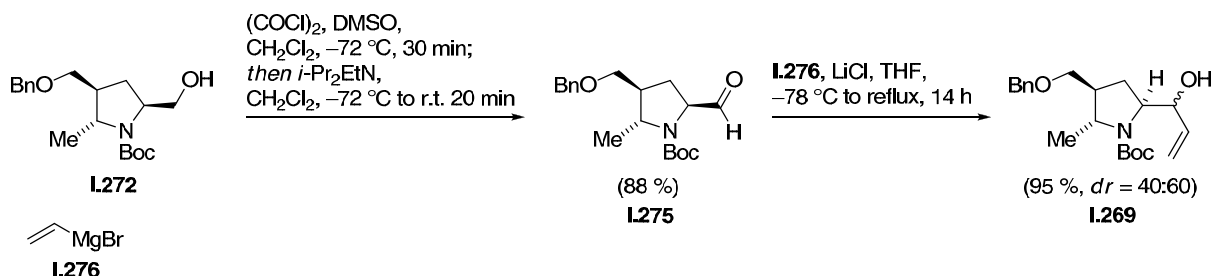
^1H NMR (400 MHz, DMSO, 100 $^\circ\text{C}$): $\delta = 9.41$ (d, $J = 2.46$ Hz, 1H), 7.34-7.22 (m, 5H), 4.46 (s, 2H), 4.17-4.08 (m, 1H), 3.74-3.67 (m, 1H), 3.42-3.35 (m, 2H), 2.08-1.99 (m, 2H), 1.91-1.82 (m, 1H), 1.37 (s, 9H), 1.21 (d, $J = 6.3$ Hz, 3H).

^{13}C NMR (100 MHz, DMSO, 100 $^\circ\text{C}$): $\delta = 201.0, 159.5, 139.0, 128.6$ (2C), 127.7, 127.7 (2C), 79.7, 72.8, 71.7, 65.4, 57.0, 45.2, 28.5 (3C), 27.9, 20.9.

IR (neat): $\tilde{\nu}_{\max}$ = 2974, 1735, 1684, 1388, 1364, 1171.

HRMS (ESI $^+$):
 m/z calcd. for $\text{C}_{19}\text{H}_{27}\text{NNaO}_4^+$: 356.1838 [M+Na] $^+$;
 found: 356.1831 [M+Na] $^+$.

(2*R*,3*S*,5*S*)-*tert*-butyl 3-(benzyloxymethyl)-5-formyl-2-methylpyrrolidine-1-carboxylate (**I.275**) and (2*R*,3*S*,5*S*)-*tert*-butyl 3-(benzyloxymethyl)-5-(1-hydroxyallyl)-2-methylpyrrolidine-1-carboxylate (**I.269**):



To a solution of oxalyl chloride (0.150 mL, 1.57 mmol, 1.20 eq) in CH_2Cl_2 (3.00 mL) was added a solution of DMSO (0.210 mL, 2.89 mmol, 2.50 eq) in CH_2Cl_2 (0.800 mL) at $-72\text{ }^\circ\text{C}$ over the course of 10 min. To the resulting mixture was added a solution of **I.272** (440 mg, 1.31 mmol, 1.00 eq) in CH_2Cl_2 (1.20 mL) over a period of 15 min to be stirred for 30 min at $-72\text{ }^\circ\text{C}$. Then, DIPEA (0.910 mL, 5.25 mmol, 4.00 eq) was added over 5 min and the mixture was allowed to warm to room temperature. The resulting mixture was diluted with 5.00 mL of CH_2Cl_2 and washed with a 5 % aq. HCl solution (3x 10.0 mL), water (3x 10.0 mL) and brine (10.0 mL). The solvent was removed *in vacuo* and the resulting yellow oil containing **I.275** was pure enough to be used without further purification (384 mg, 88 %).

TLC (EtOAc:Hex 1:2): $R_f = 0.61$.

$[\alpha]_D^{18} = -27.2$ ($c = 1.0$, MeOH).

^1H NMR (400 MHz, DMSO, $100\text{ }^\circ\text{C}$): $\delta = 9.41$ (d, $J = 2.46$ Hz, 1H), 7.34-7.22 (m, 5H), 4.46 (s, 2H), 4.17-4.08 (m, 1H), 3.74-3.67 (m, 1H), 3.42-3.35 (m, 2H), 2.08-1.99 (m, 2H), 1.91-1.82 (m, 1H), 1.37 (s, 9H), 1.21 (d, $J = 6.3$ Hz, 3H).

^{13}C NMR (100 MHz, DMSO, $100\text{ }^\circ\text{C}$): $\delta = 201.0$, 159.5, 139.0, 128.6 (2C), 127.7, 127.7 (2C), 97.7, 72.8, 71.7, 65.4, 57.0, 45.2, 28.5 (3C), 27.9, 20.9.

IR (neat): $\tilde{\nu}_{\text{max}} = 2974$, 1735, 1684, 1388, 1364, 1171.

HRMS (ESI⁺): m/z calcd. for $\text{C}_{19}\text{H}_{27}\text{NNaO}_4^+$: 356.1838 $[\text{M}+\text{Na}]^+$;
 found: 356.1831 $[\text{M}+\text{Na}]^+$.

To a solution of **I.275** (383 mg, 1.15 mmol, 1.00 eq) and LiCl (97.4 mg, 2.30 mmol, 2.00 eq) in THF (3.00 mL) was added dropwise a solution of vinylmagnesium bromide (1.00 M in THF, 2.30 mL, 2.30 mmol, 2.00 eq) at $-78\text{ }^{\circ}\text{C}$. The mixture was stirred for 15 min at this temperature and was then allowed to warm up to be stirred for 12 h at room temperature. Subsequently, the mixture was heated to reflux for 1.5 h and was then allowed to cool to room temperature. The reaction was quenched with a sat. aq. NH_4Cl solution (2.50 mL) and the bulk of the solvent was removed *in vacuo*. The residue was diluted with a sat. aq. NH_4Cl solution (50.0 mL) and water (50.0 mL) and was extracted with CH_2Cl_2 (3 x 75.0 mL). The combined extracts were washed with brine (100 mL), dried over MgSO_4 and concentrated. Purification by column chromatography (silica, EtOAc:Hex 1:4 \rightarrow 1:3) gave **I.269** as a 3:2 mixture of diastereomers (394 mg, 95 %). A 25.0 mg sample of the mixture was separated by reversed phase HPLC (*Varian Dynamax* 250x21.4 mm *Microsorb* 60-8 C18 column equipped with a *Dynamax HPLC guard column* operating on a *Varian PrepStar HPLC* system; $\text{H}_2\text{O}/\text{MeOH}$; 15.5 mL/min) to afford a minor diastereomer (8.10 mg) and a major diastereomer as colorless oils.

Minor diastereomer:

HPLC (gradient program: $t = 0\text{ min } 72\% \text{ MeOH}$, $t = 2\text{ min } 72\% \text{ MeOH}$, $t = 30\text{ min } 90\% \text{ MeOH}$, $t = 35\text{ min } 90\% \text{ MeOH}$): $R_t = 14.73\text{ min}$.

$[\alpha]_D^{16} = -89.0$ ($c = 1.0$, MeOH).

^1H NMR (400 MHz, DMSO, $100\text{ }^{\circ}\text{C}$, mixture of rotation isomers): $\delta = 7.39\text{-}7.19$ (m, 5H), 5.81-5.53 (m, 1H), 5.18-5.03 (m, 2H), 4.79-4.60 (m, 1H), 4.44-4.39 (m, 2H), 3.88-3.17 (m, 1H), 3.38-3.32 (m, 1H), 3.31-3.26 (m, 2H), 3.25-3.20 (m, 1H), 2.04-1.82 (m, 2H), 1.60-1.43 (m, 1H), 1.39-1.35 (m, 9H), 1.19-1.13 (m, 3H).

^{13}C NMR (100 MHz, DMSO, $100\text{ }^{\circ}\text{C}$, mixture of rotation isomers): $\delta = 154.7$, 154.6, 139.0, 138.9, 138.2, 138.1, 128.7 (2C), 128.6 (2C), 127.8 (2C), 127.8 (2C), 127.7, 127.7, 116.2, 114.6, 79.0, 78.6, 72.5, 72.4, 72.2, 71.9, 70.2, 70.1, 62.4, 61.2, 58.0, 57.1, 44.6, 44.0, 28.6 (3C), 28.5 (3C), 27.0, 26.9, 20.6, 20.5.

IR (neat): $\tilde{\nu}_{\text{max}} = 2973$, 1688, 1660, 1391, 1365, 1114.

HRMS (ESI^+): m/z calcd. for $\text{C}_{21}\text{H}_{31}\text{NNaO}_4^+$: 384.2151 $[\text{M}+\text{Na}]^+$;
found: 384.2146 $[\text{M}+\text{Na}]^+$.

Major diastereomer:

HPLC (gradient program: $t = 0$ min 72% MeOH, $t = 2$ min 72% MeOH, $t = 30$ min 90 % MeOH, $t = 35$ min 90 % MeOH): $R_f = 18.89$ min.

$[\alpha]_D^{16} = -77.8$ ($c = 1.0$, MeOH).

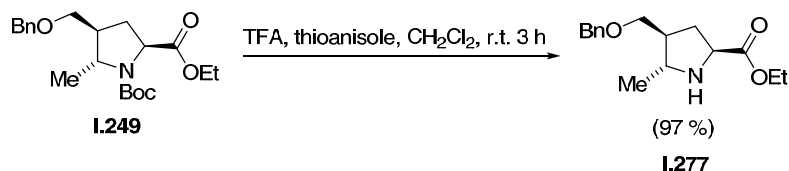
^1H NMR (400 MHz, DMSO, 100 °C): $\delta = 7.39$ -7.17 (m, 5H), 5.75 (ddd $J = 17.2$, 10.6, 5.0 Hz, 1H), 5.16 (dt, $J = 17.2$, 1.8 Hz, 1H), 5.02 (dt, $J = 10.6$, 1.8 Hz, 1H), 4.63-4.61 (m, 1H), 4.45 (s, 2H), 3.74-3.70 (m, 1H), 3.59-3.54 (m, 2H), 3.42 (dd, $J = 9.6$, 5.9 Hz, 1H), 2.98 (s, br, 1H), 1.97-1.91 (m, 2H), 1.67-1.61 (m, 1H), 1.40 (s, 9H), 1.19 (d, $J = 6.2$ Hz, 3H).

^{13}C NMR (100 MHz, DMSO, 100 °C): $\delta = 154.3$, 140.5, 139.3, 128.5 (2C), 127.7 (2C), 127.6, 114.4, 78.8, 72.8, 72.6, 70.4, 62.1, 58.1, 45.0, 28.7, 26.2, 20.5.

IR (neat): $\tilde{\nu}_{\text{max}} = 2972$, 1665, 1392, 1365, 1113.

HRMS (ESI⁺): m/z calcd. for $\text{C}_{21}\text{H}_{31}\text{NNaO}_4^+$: 384.2151 [M+Na]⁺;
found: 384.2146 [M+Na]⁺.

(2S,4S,5R)-ethyl 4-(benzyloxymethyl)-5-methylpyrrolidine-2-carboxylate (I.277) from **I.249**:



To a solution of **I.249** (2.50 g, 6.62 mmol, 1.00 eq) and thioanisole (0.800 mL, 6.62 mmol, 1.00 eq) in CH_2Cl_2 (10.0 mL) was added trifluoroacetic acid (9.84 mL, 132 mmol, 20.0 eq) *via* syringe and stirred for 3 h at room temperature. The resulting slight orange solution was quenched by dropwise addition of a sat. aq. Na_2CO_3 solution (30.0 mL) and then poured into a sat. aq. NaHCO_3 solution (270 mL). The mixture was extracted with CH_2Cl_2 (5 x 150 mL) and the combined extracts were washed with brine (300 mL), dried over MgSO_4 , filtered and concentrated. The colorless crude product was purified *via* column chromatography (silica, $\text{CHCl}_3/\text{MeOH}/\text{NEt}_3$ 100:1:1 \rightarrow 100:2:1) to give **I.277** as a colorless oil (1.78 g, 97 %).

TLC ($\text{CHCl}_3/\text{MeOH}$ 100:5): $R_f = 0.2$.

$[\alpha]_D^{19} = -12.1$ ($c = 1.0$, MeOH).

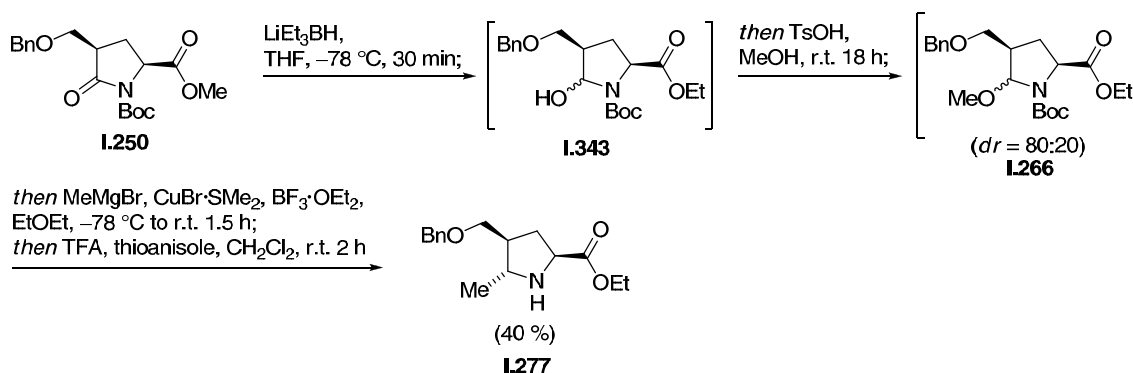
$^1\text{H NMR}$ (600 MHz, CDCl_3): $\delta = 7.36\text{--}7.27$ (m, 5H), 4.51–4.47 (m, 2H), 4.15 (q, $J = 7.2$ Hz, 2H), 3.89–3.81 (m, 1H), 3.46 (dd, $J = 9.2, 5.9$ Hz, 1H), 3.36 (dd, $J = 9.2, 6.8$ Hz, 1H), 3.15–3.03 (m, 1H), 2.46–2.40 (m, 1H), 2.20 (s, br, 1H), 1.98–1.94 (m, 1H), 1.76–1.69 (m, 1H), 1.25 (t, $J = 6.8$ Hz, 3H), 1.17 (d, $J = 6.2$ Hz, 3H).

$^{13}\text{C NMR}$ (150 MHz, CDCl_3): $\delta = 175.5, 138.4, 128.3$ (2C), 127.5, 127.4 (2C), 73.1, 72.1, 60.9, 58.4, 56.7, 46.6, 34.1, 20.8, 14.2.

IR (neat): $\tilde{\nu}_{\text{max}} = 2960, 2859, 1728, 1367, 1204$.

HRMS (ESI⁺): m/z calcd. for $\text{C}_{16}\text{H}_{23}\text{NO}_3^+$: 277.1678 [M]⁺;
found: 277.1685 [M]⁺.

(2*S*,4*S*,5*R*)-ethyl 4-(benzyloxymethyl)-5-methylpyrrolidine-2-carboxylate (**L.277**) from **L.250**:



To a solution of **L.250** (18.3 g, 48.4 mmol, 1.00 eq) in THF (250 mL) was added dropwise a solution of lithiumtriethylborohydride (1.00 M in THF, 58.0 mL, 58.0 mmol, 1.00 eq) at $-78\text{ }^\circ\text{C}$ over the course of 10 min. After being stirred for 30 min, the reaction was quenched with a sat. aq. NaHCO_3 solution (20.0 mL) and allowed to warm to $0\text{ }^\circ\text{C}$. To the mixture was added H_2O_2 (25.0 mL) in one portion and stirred at $0\text{ }^\circ\text{C}$ for 30 min. The solvent was removed *in vacuo* and the residue was redissolved in a 2:1 mixture of ethyl acetate and water (810 mL). The organic layer was separated, dried over MgSO_4 , filtered and concentrated to a colorless oil.

To a solution of this residual oil containing **L.343** (~18.0 g) in methanol (255 mL) was added *p*-toluenesulfonic acid monohydrate (1.84 g, 9.67 mmol, 0.200 eq) to be stirred for 18 h at

room temperature. The reaction was quenched with a sat. aq. NaHCO₃ solution (22.0 mL), the solvent was removed *in vacuo* and the residue was redissolved in a mixture of diethyl ether (540 mL) and water (270 mL). The organic layer was separated, washed with brine (180 mL), dried over MgSO₄, filtered and concentrated to give a colorless oil containing **I.266**.

To a suspension of copper(I)bromide-dimethyl sulfide complex (46.3 g, 225 mmol, 4.65 eq) in diethyl ether (400 mL) was added dropwise a solution of MeMgBr (3.00 M in diethyl ether, 75.0 mL, 225 mmol, 4.65 eq) over the course of 15 min at -40 °C and stirred for 1 h at this temperature. Then, the resulting yellow suspension was cooled to -78 °C and boron trifluoride diethyl etherate (27.8 mL, 225 mmol, 4.65 eq) was added dropwise over the course of 15 min. After being stirred for 30 min at -78 °C, a solution of the residual colorless oil from the previous reaction (~19.0 g) in diethyl ether (60.0 mL) was added over the course of 10 min. The flask was rinsed with additional diethyl ether (15.0 mL) and the reaction mixture was stirred for 15 min at -78 °C. Then, the mixture was allowed to warm to room temperature and stirred for 1 h at this temperature. The reaction was quenched by a dropwise addition of a 1:1 mixture of a sat. aq. NH₄Cl solution and a 28 % aq. NH₃ solution (260 mL). The resulting mixture was stirred for 30 min at room temperature and was then diluted with diethyl ether (250 mL). The organic layer was separated, washed with water (300 mL) and brine (250 mL), dried over MgSO₄ and concentrated *in vacuo* to give a residue that was redissolved in a mixture of CH₂Cl₂ (50.0 mL) and trifluoroacetic acid (50.0 mL).

To the mixture was added thioanisole (5.69 mL, 48.4 mmol, 1.00 eq) to be stirred for 2 h at room temperature. The reaction mixture was quenched by dropwise addition of a sat. aq. Na₂CO₃ solution (100 mL) and was then poured into a sat. aq. NaHCO₃ solution (800 mL). The mixture was extracted with CH₂Cl₂ (5 x 250 mL), the combined extracts were concentrated and after purification with column chromatography (silica, CHCl₃:MeOH:NEt₃ 100:1:1), **I.277** was obtained as a colorless oil (5.43 g, 40 %).

TLC (CHCl₃:MeOH 100:5): $R_f = 0.2$.

$[\alpha]_D^{19} = -12.1$ ($c = 1.0$, MeOH).

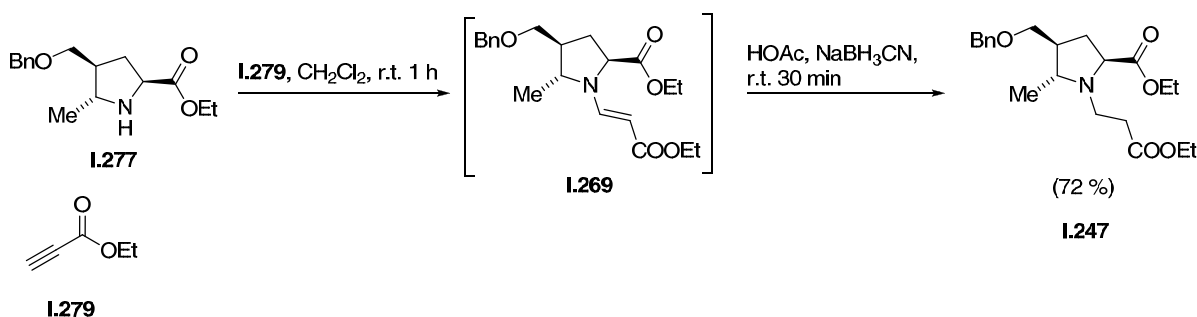
¹H NMR (600 MHz, CDCl₃): $\delta = 7.36-7.27$ (m, 5H), 4.51-4.47 (m, 2H), 4.15 (q, $J = 7.2$ Hz, 2H), 3.89-3.81 (m, 1H), 3.46 (dd, $J = 9.2, 5.9$ Hz, 1H), 3.36 (dd, $J = 9.2, 6.8$ Hz, 1H), 3.15-3.03 (m, 1H), 2.46-2.40 (m, 1H), 2.20 (s, br, 1H), 1.98-1.94 (m, 1H), 1.76-1.69 (m, 1H), 1.25 (t, $J = 6.8$ Hz, 3H), 1.17 (d, $J = 6.2$ Hz, 3H).

^{13}C NMR (150 MHz, CDCl_3): $\delta = 175.5, 138.4, 128.3$ (2C), 127.5, 127.4 (2C), 73.1, 72.1, 60.9, 58.4, 56.7, 46.6, 34.1, 20.8, 14.2.

IR (neat): $\tilde{\nu}_{\text{max}} = 2960, 2859, 1728, 1367, 1204$.

HRMS (ESI⁺): m/z calcd. for $\text{C}_{16}\text{H}_{23}\text{NO}_3^+$: 277.1678 [M]⁺;
found: 277.1685 [M]⁺.

(2*S*,4*S*,5*R*)-ethyl 4-(benzyloxymethyl)-1-(3-ethoxy-3-oxopropyl)-5-methylpyrrolidine-2-carboxylate (**I.247**):



To a solution of **I.277** (2.20 g, 7.93 mmol, 1.00 eq) in CH_2Cl_2 (8.50 mL) was added ethyl propiolate (**I.279**, 0.89 mL, 8.73 mmol, 1.10 eq) over the course of 1 min. After being stirred for 1 h at room temperature, all volatile substances were removed *in vacuo* to give crude **I.269**. An analytical sample was purified by column chromatography (silica, EtOAc:Hex 1:10 \rightarrow 1:5) to afford **I.269** as a colorless oil.

TLC (EtOAc:Hex 1:5): $R_f = 0.21$.

$[\alpha]_D^{20} = -66.4$ ($c = 1.0$, MeOH).

^1H NMR (400 MHz, CDCl_3): $\delta = 7.56$ (d, $J = 13.4$ Hz, 1H), 7.37-7.27 (m, 5H), 4.54-4.39 (m, 3H), 4.20-4.05 (m, 5H), 3.69-3.56 (m, 1H), 3.50 (dd, $J = 9.5, 6.7$ Hz, 1H), 3.40 (dd, $J = 9.5, 6.6$ Hz, 1H), 2.60-2.43 (m, 1H), 2.13-2.02 (m, 1H), 1.95-1.78 (m, 1H), 1.31 (d, $J = 6.3$ Hz, 3H), 1.26-1.19 (m, 6H).

^{13}C NMR (150 MHz, CDCl_3): $\delta = 172.1, 169.2, 145.7, 138.0, 128.4$ (2C), 127.7, 127.5 (2C), 87.3, 77.2, 73.2, 70.8, 61.4, 60.1, 59.0, 45.7, 31.5, 18.8, 14.6, 14.1.

IR (neat): $\tilde{\nu}_{\text{max}} = 1728, 1680$.

HRMS (ESI⁺): m/z calcd. for C₂₁H₃₀NO₅⁺: 376.2124 [M+H]⁺;
found: 376.2118 [M+H]⁺.

The crude material obtained as described above was redissolved in glacial acid (5.00 mL, 87.3 mmol, 11.0 eq). To this solution was added sodium cyanoborohydride (1.00 g, 15.9 mmol, 2.00 eq) and stirred for 30 min at room temperature. The reaction was quenched by dropwise addition of a 10 % aq. HCl solution (15.0 mL). After being stirred for 15 min, a sat. aq. Na₂CO₃ solution (30.0 mL) was added dropwise and the resulting mixture was poured into a sat. aq. NaHCO₃ solution (270 mL). The mixture was extracted with CH₂Cl₂ (3 x 150 mL), the combined extracts were washed with brine (300 mL), dried over MgSO₄, filtered and concentrated to a colorless crude product which was purified by column chromatography (EtOAc:Hex 1:11 → 1:9) to give **I.247** as a colorless oil (2.16 g, 72 %).

TLC (EtOAc:Hex 1:5): $R_f = 0.28$.

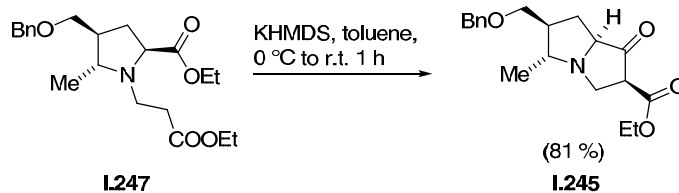
$[\alpha]_D^{19} = -63.8$ ($c = 1.0$, MeOH).

¹H NMR (400 MHz, CDCl₃): $\delta = 7.35$ -7.19 (m, 5H), 4.53-4.45 (m, 2H), 4.13-4.04 (m, 4H), 3.83-3.69 (m, 1H), 3.50 (dd, $J = 9.0, 6.7$ Hz, 1H), 3.40 (dd, $J = 8.9, 7.7$ Hz, 1H), 3.08-2.91 (m, 2H), 2.78-2.67 (m, 1H), 2.54-2.42 (m, 2H), 2.36-2.24 (m, 1H), 2.08-1.97 (m, 1H), 1.67-1.57 (m, 1H), 1.24-1.19 (m, 6H), 1.08 (d, $J = 5.9$ Hz, 3H).

¹³C NMR (150 MHz, CDCl₃): $\delta = 174.3, 172.3, 138.5, 128.3$ (2C), 127.5 (2C), 127.4, 73.3, 73.1, 62.2, 60.3, 60.1, 59.9, 45.3, 43.4, 34.2, 31.1, 18.1, 14.3, 14.2.

IR (neat): $\tilde{\nu}_{\max} = 2977, 2854, 1729, 1369, 1179$.

HRMS (ESI⁺): m/z calcd. for C₂₁H₃₂NO₅⁺: 378.2280 [M+H]⁺;
found: 378.2273 [M+H]⁺.

(2*S*,5*R*,6*S*,7*aS*)-ethyl 6-(benzyloxymethyl)-5-methyl-1-oxohexahydro-1*H*-pyrrolizine-2-carboxylate (I.245):

To a mixture of **I.247** (1.67 g, 4.40 mmol, 1.00 eq) and toluene (18.0 mL) was added a solution of KHMDS (0.500 M in toluene, 2.00 mL, 8.80 mmol, 2.00 eq) at 0 °C. The mixture was stirred for 0.5 h at 0 °C and was then allowed to warm to room temperature to be stirred for 0.5 h at this temperature. The reaction was quenched with a sat. aq. NH₄Cl solution (20.0 mL), diluted with a sat. aq. NH₄Cl solution (500 mL) and extracted with CH₂Cl₂ (5 x 150 mL). The aqueous phase was diluted with a sat. aq. Na₂CO₃ solution (100 mL) and extracted with CH₂Cl₂ (3 x 150 mL). A second time, the aqueous phase was diluted with a sat. aq. Na₂CO₃ solution (100 mL) and extracted with CH₂Cl₂ (2 x 150 mL). The combined extracts were concentrated and purified by reversed phase column chromatography (H₂O:MeOH 5:1 → 2:1) to give **I.245** as a colorless solid.

TLC (CHCl₃:MeOH 100:10): *R_f* = 0.33.

$[\alpha]_D^{19} = -36.2$ (*c* = 1.0 MeOH).

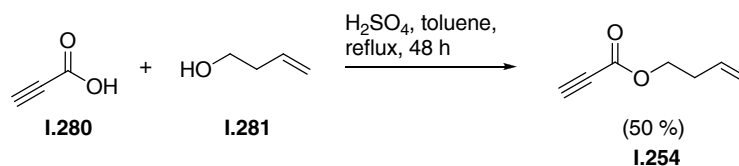
¹H NMR (400 MHz, *d*₆-acetone): δ = 7.35-7.24 (m, 5H), 4.51-4.47 (m, 2H), 4.16-4.09 (m, 2H), 3.67-3.29 (m, 5H), 2.71-2.47 (m, 1H), 2.33-2.20 (m, 1H), 2.10-2.07 (m, 1H), 2.04-1.94 (m, 1H), 1.72-1.58 (m, 1H), 1.22 (t, *J* = 7.1 Hz, 3H), 1.16 (d, *J* = 5.9 Hz, 3H).

¹³C NMR (100 MHz, *d*₆-acetone): δ = 214.9, 168.4, 138.9, 128.2 (2C), 127.3 (2C), 127.3, 72.6, 71.5, 71.1, 61.2, 60.7, 48.7, 47.1, 30.1, 29.2, 18.2, 13.6.

IR (neat): $\tilde{\nu}_{\text{max}}$ = 2978, 1677, 1580, 1452, 1260, 1171, 1071.

HRMS (ESI⁺):

	m/z calcd. for C ₁₉ H ₂₅ NO ₄ ⁺ :	332.1862 [M] ⁺ ;
	found:	332.1856 [M] ⁺ .

But-3-enyl propiolate (I.254):

In a 100 mL round bottom flask equipped with a Dean-Stark apparatus, a mixture of propiolic acid (**I.280**, 5.00 mL, 80.7 mmol, 1.10 eq), 3-buten-1-ol (**I.281**, 6.28 mL, 73.3 mmol, 1.00 eq), sulfuric acid (0.300 mL, 5.00 mmol, 0.050 eq) and toluene (50.0 mL) was heated to reflux for 48 h. Then, the reaction mixture was allowed to cool to room temperature and diluted with a sat. aq. NaHCO₃ solution (150 mL). The organic layer was separated, washed with brine (50.0 mL), dried over MgSO₄ and concentrated. The resulting crude product was purified by fractional distillation to give **I.254** as a colorless oil (4.60 g, 50 %).

TLC (EtOAc:Hex 1:10): $R_f = 0.20$.

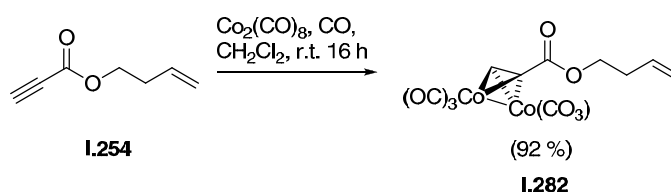
bp: 50 °C/5 mbar.

¹H NMR (300 MHz, CDCl₃): $\delta = 5.86\text{-}5.71$ (m, 1H), 5.19-5.05 (m, 2H), 4.25 (t, $J = 6.8$ Hz, 2H), 2.90 (s, 1H), 2.44 (qt, $J = 6.8, 1.4$ Hz, 2H).

¹³C NMR (75 MHz, CDCl₃): $\delta = 152.6, 133.2, 117.8, 74.7, 74.6, 65.2, 32.7$.

IR (neat): $\tilde{\nu}_{\max} = 1721, 998$.

HRMS (EI ⁺):	m/z calcd. for C ₇ H ₈ O ₂ ⁺ :	124.0524 [M] ⁺ ;
	found:	124.0528 [M] ⁺ .

But-3-enyl propiolate dicobalt hexacarbonyl complex (I.282):

To a solution of dicobalt octacarbonyl (5.00 g, 14.6 mmol, 1.10 eq) in CH₂Cl₂ (50.0 mL) was added dropwise **I.254** (1.70 ml, 13.3 mmol, 1.00 eq) at room temperature. The mixture was stirred for 14 h under a CO atmosphere. The resulting brownish mixture was filtered through

a short plug of celite, the solvent was removed under reduced pressure and the residue was purified by column chromatography (silica, EtOAc:Hex 1:100, then EtOAc:Hex 10:100) to afford **I.282** as a red oil (4.71 g, 92 %).

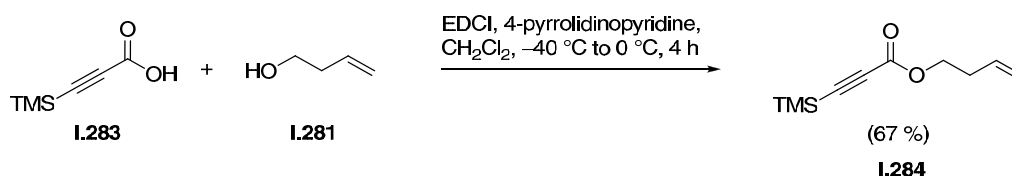
TLC (EtOAc:Hex 1:10): $R_f = 0.22$.

^1H NMR (600 MHz, CDCl_3): $\delta = 6.20$ (s, br, 1H), 5.79 (s, br, 1H), 5.09 (s, br, 2H), 4.29 (s, br, 2H), 2.43 (s, br, 2H).

^{13}C NMR (150 MHz, CDCl_3): $\delta = 198.1$ (br, 6C), 169.8, 133.7, 117.4, 73.4, 73.4, 65.0, 33.1.

IR (neat): $\tilde{\nu}_{\text{max}} = 2050, 2026$.

But-3-enyl 3-(trimethylsilyl)propiolate (**I.284**):



To a solution of 3-(trimethylsilyl)propionic acid (**I.283**, 3.00 g, 21.1 mmol, 1.10 eq) and EDCI (4.04 g, 21.1 mmol, 1.10 eq) in dichloromethane (25.0 mL) was added a solution of 3-butene-1-ol (**I.281**, 1.64 mL, 19.2 mmol, 1.00 eq) and 4-pyrrolidinopyridine (0.284 g, 1.90 mmol, 0.100 eq) in dichloromethane (20.0 mL) at $-40\text{ }^\circ\text{C}$. The mixture was allowed to warm to $-20\text{ }^\circ\text{C}$ to be stirred for 2 h at this temperature. The mixture was then allowed to slowly warm to $0\text{ }^\circ\text{C}$ over the course of 1 h to be stirred for 3 h at this temperature. The reaction mixture was then diluted with an aq. 2.00 M HCl solution (250 mL) and diethyl ether (250 mL). The organic layer was separated, washed with a sat. aq. NaHCO_3 solution (250 mL) and brine (250 mL), dried over MgSO_4 , filtered and concentrated. Purification by column chromatography (silica, EtOEt:pentane 3:97) and careful concentration at room temperature afforded a solution of **I.284** (2.79 g, 67 %) in pentanes, the concentration of which was determined by NMR. An analytical sample was further concentrated to give solvent-free **I.284** as a colorless oil.

TLC (EtOAc:Hex 1:10): $R_f = 0.49$.

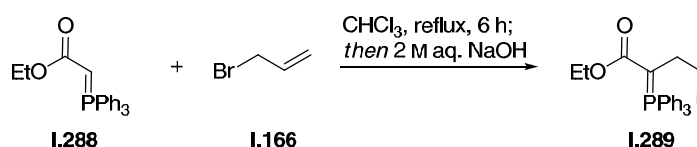
^1H NMR (300 MHz, CDCl_3): $\delta = 5.90$ -5.71 (m, 1H), 5.19-5.09 (m, 2H), 4.23 (t, $J = 6.9$ Hz, 2H), 2.45 (app qt, $J = 6.9$ Hz, 2H), 0.26 (s, 9H).

^{13}C NMR (75 MHz, CDCl_3): $\delta = 153.0, 133.3, 117.7, 94.5, 94.0, 65.0, 32.7, 0.9$ (3C).

IR (neat): $\tilde{\nu}_{\text{max}} = 1710, 1249, 841$.

HRMS (EI^+): m/z calcd. for $\text{C}_{10}\text{H}_{16}\text{O}_2\text{Si}^+$: 196.0920 [M] $^+$;
found: 196.0903 [M] $^+$.

1-Ethoxycarbonylbut-3-enylidene(triphenyl)phosphorane (I.289):^[87]



A solution of ethoxycarbonylmethylene(triphenyl)phosphorane (**I.288**, 5.00 g, 14.4 mmol, 1.00 eq) and allyl bromide (**I.166**, 3.10 mL, 35.9 mmol, 2.50 eq) in chloroform (29.0 mL) was heated to reflux for 6 h. The mixture was allowed to cool to room temperature and the solvent was removed *in vacuo* to provide a foam. To the residue was added water (150 mL) and the turbid mixture was washed with benzene (3 x 35.0 mL). Then, to the aqueous mixture was added a crystal of phenolphthalein, benzene (75.0 mL) and as much of an aq. 2 M NaOH solution until pH 8.2 was indicated (ca. 8.00 mL). The organic layer was separated and the aqueous layer was further extracted with benzene (3 x 40.0 mL). The combined extracts were washed with brine (100 mL), dried over MgSO_4 and concentrated to provide **I.289** as a yellow solid, which was used without further purification.

TLC (EtOAc:Hex 3:1): $R_f = 0.18$.

^1H NMR (400 MHz, CDCl_3 , 4:3 mixture of rotation isomers, major isomer quoted): $\delta = 7.72\text{--}7.43$ (m, 15H), 5.91–5.71 (m, 1H), 4.67–4.50 (m, 2H), 3.71 (q, $J = 7.1$ Hz, 2H), 2.71 (ddt, $J = 18.4, 6.2, 1.3$ Hz, 2H), 0.44 (t, $J = 7.1$ Hz, 3H).

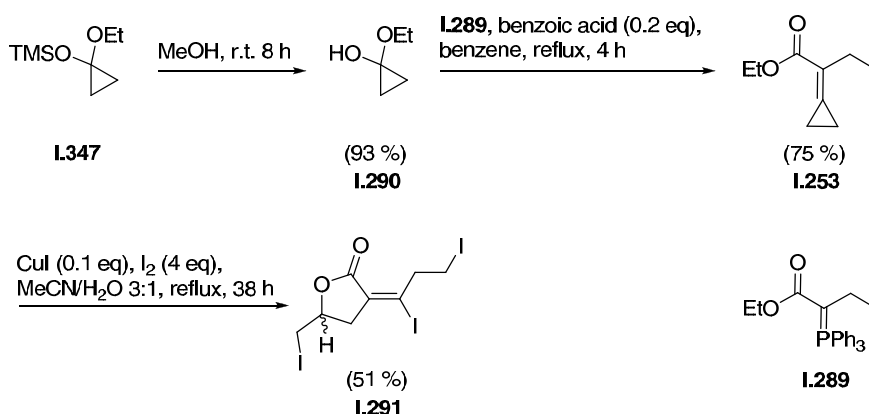
^{13}C NMR (100 MHz, CDCl_3 , 4:3 mixture of rotation isomers): $\delta = 170.1, 169.9, 141.6, 141.1, 133.7$ (d, $J = 9.7$ Hz, 6C), 132.9 (d, $J = 10.0$ Hz, 6C), 131.9 (d, $J = 2.8$ Hz, 3C), 131.5 (d, $J = 2.9$ Hz, 3C), 128.5 (d, $J = 12.1$ Hz, 6C), 128.3 (d, $J = 90.6$ Hz, 6C), 128.3 (d, $J = 12.0$ Hz, 3C), 127.9 (d, $J = 136.2$ Hz, 3C), 111.6, 111.5, 57.9, 57.2, 37.0 (d, $J = 119.8$ Hz), 36.4 (d, $J = 120.8$ Hz), 31.5 (d, $J = 12.7$ Hz), 30.7 (d, $J = 11.8$ Hz), 14.3, 14.0.

^{31}P NMR (160 MHz, CDCl_3 , 4:3 mixture of rotation isomers): $\delta = 22.8, 22.4$.

IR (neat): $\tilde{\nu}_{\max}$ = 3382, 2978, 1740, 1238.

HRMS (EI⁺): m/z calcd. for C₂₅H₂₆O₂P⁺: 389.1670 [M+H]⁺;
found: 389.1661 [M+H]⁺.

1-Ethoxycyclopropanol (I.290), ethyl 2-cyclopropylidenepent-4-enoate (**I.253**),^{[87],[188]} and
(E)-3-(1,3-diiodopropylidene)-5-(iodomethyl)dihydrofuran-2(3H)-one (I.291):



A solution of 1-ethoxy-1-trimethylsilyloxycyclopropane (**I.347**, 10.0 mL, 50.0 mmol, 1.00 eq) in methanol (75.0 mL) was stirred for 8 h at room temperature. The excess of solvent was removed at the rotary evaporator to leave a colorless oil, which was purified by distillation to give 1-ethoxycyclopropanol (**I.290**, 4.74 g, 93 %).

TLC (EtOAc:Hex 1:10): R_f = 0.18.

bp: 39 °C/9 mbar.

¹H NMR (300 MHz, CDCl₃): δ = 3.75 (q, J = 7.1 Hz, 2H), 3.15 (s, br, 1H), 1.20 (t, J = 7.1 Hz, 3H), 0.94-0.90 (m, 4H).

¹³C NMR (100 MHz, CDCl₃): δ = 85.5, 50.5, 15.3, 14.2 (2C).

IR (neat): $\tilde{\nu}_{\max}$ = 2973, 1622, 1597, 1436, 1098.

HRMS (EI⁺): m/z calcd. for C₅H₁₀O₂⁺: 102.0681 [M]⁺;
found: 102.0665 [M]⁺.

A solution of freshly prepared 1-ethoxycyclopropanol (**I.290**, 1.58 g, ca. 1.80 mL, 15.5 mmol, 1.00 eq) and benzoic acid (0.380 g, 3.10 mmol, 0.200 eq) in benzene (60.0 mL) was heated to reflux. To this mixture was added a solution of **I.289** (6.00 g, 15.5 mmol, 1.00 eq) in benzene

(75.0 mL) over the course of 3 h with a syringe pump. After complete addition, the reaction mixture was refluxed for an additional 30 min and was then allowed to cool to room temperature. The solvent was removed *in vacuo* and the residue was diluted with diethyl ether (10.0 mL). Upon addition of pentane (80.0 mL), triphenylphosphin oxide precipitated. The mixture was filtered, concentrated and filtered through a plug of silica (EtOEt:pentane 1:10) to afford **I.253** as a colorless oil (6.24 g, 75 %). The sensitive product was directly used in the next reaction without further purification.

TLC (EtOAc:Hex 1:10): $R_f = 0.31$.

IR (neat): 2982, 1715.

HRMS (EI⁺): m/z calcd. for C₁₀H₁₄O₂⁺: 166.0994 [M]⁺;
found: 166.0999 [M]⁺.

A mixture of **I.253** (1.19 g, 7.13 mmol, 1.00 eq), CuI (136 mg, 0.713 mmol, 0.100 eq), I₂ (7.24 g, 28.5 mmol, 4.00 eq), acetonitrile (115 mL) and water (28.5 mL) was heated to reflux for 38 h. The mixture was diluted with a sat. aq. Na₂S₂O₃ solution (275 mL) and extracted with diethyl ether (3 x 275 mL). The combined extracts were washed with brine (350 mL), dried over MgSO₄ and concentrated. Purification by column chromatography (silica, EtOEt:pentane 1:10 → 1:5, immediate concentration of fractions) gave **I.291** (956 mg, 52 %) as a colorless solid. Since **I.291** tends to rapidly decompose when exposed to air and slowly under exposure to light (as evidenced by formation of yellow and brownish colored material), samples were stored at -20 °C in darkness and were strictly kept under an argon atmosphere. Crystals suitable for single crystal X-ray crystallography were grown by slow evaporation of a diethyl ether solution of **I.291** under a gentle stream of argon.

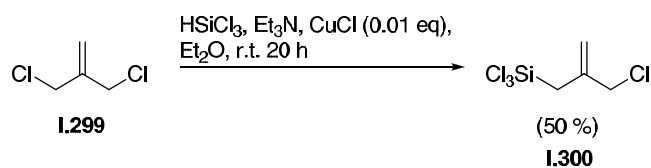
TLC (EtOAc:Hex 1:2): $R_f = 0.49$.

¹H NMR (600 MHz, CDCl₃): $\delta = 4.55$ (dddd, $J = 8.1, 7.1, 5.1, 3.9$ Hz, 1H), 3.89-3.80 (m, 2H), 3.41 (dd, $J = 10.5, 3.9$ Hz, 1H), 3.34-3.27 (m, 3H), 3.09 (ddt, $J = 18.0, 5.1, 1.5$ Hz, 1H), 2.69 (ddt, $J = 18.0, 8.1, 1.5$ Hz, 1H).

¹³C NMR (150 MHz, CDCl₃): $\delta = 162.7, 133.5, 125.0, 73.3, 44.1, 42.2, 8.3, 2.8$.

IR (neat): $\tilde{\nu}_{\max} = 1691, 1632, 1203$.

HRMS (EI⁺): m/z calcd. for C₈H₉I₂O₂⁺: 390.8692 [M-I]⁺;
found: 390.8691 [M-I]⁺.

Trichloro(2-(chloromethyl)allyl)silane (I.300):^[89]

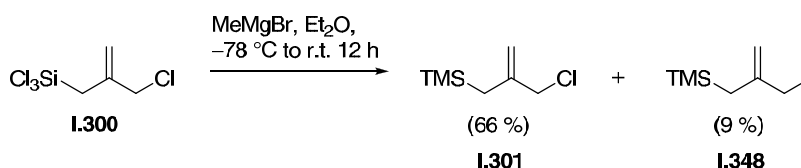
A 1 L three-necked flask equipped with bubbler, rubber stopper and mechanic stirrer was charged with triethylamine (34.7 mL, 0.250 mol, 1.25 eq), copper(I) chloride (0.198 mg, 2.00 mmol, 0.010 eq) and diethyl ether (390 mL). Under gentle stirring, to the green colored suspension was added dropwise a solution of 3-chloro-2-chloromethyl-1-propene (**I.299**, 23.1 mL, 0.200 mol, 1.00 eq) and trichlorosilane (25.3 mL, 0.250 mol, 1.25 eq) in diethyl ether (65.0 mL) over a period of 4 h at room temperature. After complete addition, the resulting mixture was stirred for 16 h at room temperature and then filtered under an argon atmosphere. The solvent was removed at atmospheric pressure and the residue was purified by fractional distillation (15 cm Vigreux column) to afford **I.300** as a colorless oil (22.7 g, 50 %). Since the product tends to rapidly decompose under exposure to air moisture (as evidenced by decomposition to a colorless, insoluble solid), it was strictly kept under an atmosphere of argon during all purification steps and was used in the next reaction immediately after purification.

bp: 92 °C/30 mbar.

¹H NMR (300 MHz, CDCl₃): δ = 5.36 (s, 1H), 5.17 (s, 1H), 4.15 (d, *J* = 1.0 Hz, 2H), 2.56 (d, *J* = 1.0 Hz, 2H).

¹³C NMR (75 MHz, CDCl₃): δ = 136.3, 118.7, 48.8, 29.6.

IR (neat): $\tilde{\nu}_{\max}$ = 3091, 2961, 1834, 1641.

(2-(Chloromethyl)allyl)trimethylsilane (I.301):^[89]

To a solution of **I.300** (21.5 g, 96.0 mmol, 1.00 eq) in diethyl ether (430 mL) was added dropwise a solution of methylmagnesium bromide (3.00 M in diethyl ether, 112 mL,

336 mmol, 3.50 eq) at $-78\text{ }^{\circ}\text{C}$. The resulting mixture was stirred for 1 h at $-78\text{ }^{\circ}\text{C}$ and was then allowed to slowly warm to room temperature to be stirred for 12 h at this temperature. The reaction mixture was poured into an ice cold sat. aq. NH_4Cl solution (300 mL) and the organic layer was separated. The aqueous phase was further extracted with diethyl ether (2 x 120 mL) and the combined extracts were washed with brine (180 mL), dried over MgSO_4 , filtered and concentrated at the rotary evaporator at $0\text{ }^{\circ}\text{C}$. The resulting crude product was purified by fractional distillation (15 cm Vigreux column) to afford a mixture of **I.301** and **I.348** (11.9 g, 75 %) as a colorless oil. The ratio of **I.301** and **I.348** was determined by NMR to be 87:13 and the mixture was used in the next reaction without further purification.

bp: $40\text{ }^{\circ}\text{C}/31\text{ mbar}$.

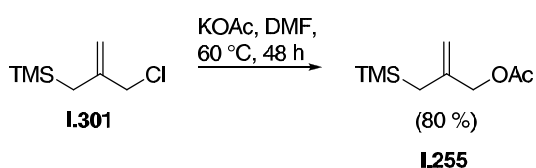
$^1\text{H NMR}$ (300 MHz, CDCl_3): $\delta = 5.36$ (s, 1H), 5.17 (s, 1H), 4.15 (d, $J = 1.0\text{ Hz}$, 2H), 2.56 (d, $J = 1.0\text{ Hz}$, 2H).

$^{13}\text{C NMR}$ (75 MHz, CDCl_3): $\delta = 143.1, 112.3, 50.0, 23.7, 1.5$ (3C).

IR (neat): $\tilde{\nu}_{\text{max}} = 3082, 2955, 1632$.

HRMS (EI^+): m/z calcd. for $\text{C}_7\text{H}_{15}\text{ClSi}^+$: 162.0632 $[\text{M}]^+$;
found: 162.0623 $[\text{M}]^+$.

2-((Trimethylsilyl)methyl)allyl acetate (**I.255**):^[89]



A mixture of **I.301** (11.5 g, 70.5 mmol, 1.00 eq), potassium acetate (27.7 g, 282 mmol, 4.00 eq) and DMF (100 mL) was heated to $60\text{ }^{\circ}\text{C}$ for 48 h. The resulting mixture was allowed to cool to room temperature, diluted with water (250 mL) and extracted with diethyl ether (2 x 150 mL). The combined extracts were washed with water (2 x 200 mL) and brine (150 mL), dried over MgSO_4 , filtered and concentrated. The residue was purified by fractional distillation to afford acetate **I.255** as a colorless oil (10.5 g, 80 %).

bp: $80\text{ }^{\circ}\text{C}/15\text{ mbar}$.

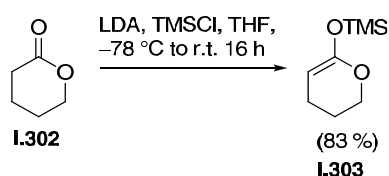
^1H NMR (300 MHz, CDCl_3): δ = 4.92-4.89 (m, 1H), 4.77-4.73 (m, 1H), 4.48-4.43 (m, 2H), 2.12 (s, 3H), 1.58-1.55 (m, 2H), 0.06 (s, 9H).

^{13}C NMR (75 MHz, CDCl_3): δ = 170.7, 141.7, 109.6, 67.9, 23.6, 20.9, 1.5 (3C).

IR (neat): $\tilde{\nu}_{\text{max}}$ = 3081, 2954, 1741, 1644.

HRMS (EI^+): m/z calcd. for $\text{C}_9\text{H}_{18}\text{O}_2\text{Si}^+$: 186.1076 $[\text{M}]^+$;
found: 186.1066 $[\text{M}]^+$.

(3,4-Dihydro-2H-pyran-6-yloxy)trimethylsilane (I.303):^[90]



A solution of *n*-BuLi (2.40 M in THF, 4.94 mL, 11.9 mmol, 1.00 eq) was added to a solution of diisopropylamine (1.68 mL, 11.9 mmol, 1.00 eq) in THF (5.30 mL) at 0 °C and the mixture was stirred for 30 min at this temperature.

The resulting solution of LDA was cooled to -78 °C and δ -valerolactone (**I.302**, 1.00 mL, 10.8 mmol, 1.00 eq) was added dropwise at this temperature. After being stirred for 1 h, TMSCl (1.82 mL, 14.2 mmol, 1.32 eq) was added dropwise at -78 °C and subsequently the mixture was allowed to warm to room temperature. After being stirred for 16 h at this temperature, the resulting suspension was filtered, the filter cake was washed with CH_2Cl_2 (25.0 mL) and the combined filtrates were concentrated. The residual oil was purified by fractional distillation to give silyl enol ether **I.303** as a colorless oil (1.54 g, 83 %). Since the material was sensitive to air moisture, it was directly used in the next reaction.

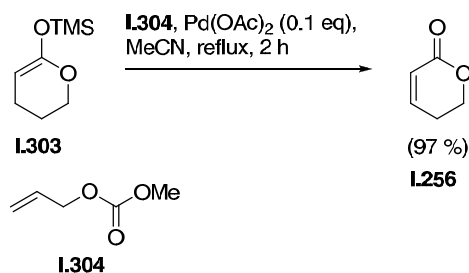
bp: 43 °C/6 mbar.

^1H NMR (300 MHz, CDCl_3): δ = 4.07 (dd, J = 5.7, 4.6 Hz, 2H), 3.87-3.79 (m, 1H), 2.06 (td, J = 6.4, 3.7 Hz, 2H), 1.81-1.74 (m, 2H), 0.23 (s, 9H).

^{13}C NMR (75 MHz, CDCl_3): δ = 154.5, 74.0, 67.2, 22.4, 19.9, 0.0 (3C).

IR (neat): $\tilde{\nu}_{\text{max}}$ = 2955, 1736, 1685.

MS (EI ⁺):	m/z calcd. for C ₈ H ₁₆ O ₂ Si ⁺ :	172.09 [M] ⁺ ;
	found:	172.19 [M] ⁺ .

5,6-Dihydro-2H-pyran-2-one (I.256):^[91a]

A mixture of silyl enol ether **I.303** (500 mg, 2.90 mmol, 1.00 eq), methylallyl carbonate (**I.304**, 0.660 mL, 5.80 mmol, 2.00 eq), palladium acetate (65.2 mg, 0.290 mmol, 0.100 eq) and acetonitrile (3.00 mL) was heated to reflux for 2 h. While heating, gas formation and formation of metallic palladium was observed. The resulting mixture was filtered through a short plug of florisil, which was washed with diethyl ether (10.0 mL). The filtrate was concentrated and purified by column chromatography (silica, EtOEt:pentane 1:10 → 1:1) to furnish **I.256** as a colorless oil (277 mg, 97 %).

TLC (EtOEt:pentane 1:2): $R_f = 0.15$.

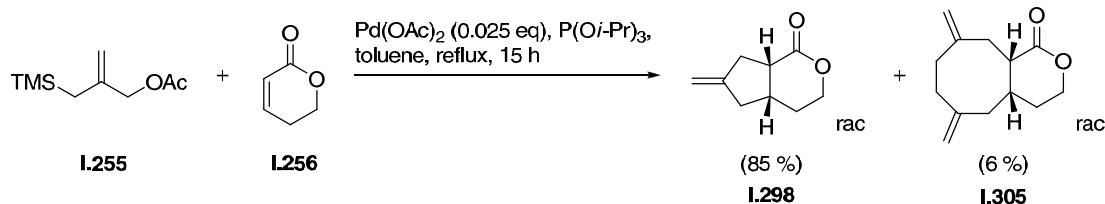
¹H NMR (300 MHz, CDCl₃): δ = 6.94 (dtt, $J = 9.8, 4.2, 0.6$ Hz, 1H), 6.01 (dt, $J = 9.8, 1.9$ Hz, 1H), 4.41 (dt, $J = 6.1, 0.6$ Hz, 2H), 2.48-2.42 (m, 2H).

¹³C NMR (75 MHz, CDCl₃): δ = 163.7, 145.8, 121.6, 66.5, 20.0.

IR (neat): $\tilde{\nu}_{\max} = 2951, 1715$.

HRMS (EI ⁺):	m/z calcd. for C ₅ H ₆ O ₂ ⁺ :	98.0368 [M] ⁺ ;
	found:	98.0355 [M] ⁺ .

**6-Methylenehexahydrocyclopenta[c]pyran-1(3*H*)-one (I.298) and
6,9-dimethylenedecahydro-1*H*-cycloocta[c]pyran-1-one (I.305):**



To a solution of 5,6-dihydro-2*H*-pyran-2-one (**I.256**, 3.19 mL, 37.0 mmol, 1.00 eq), 2-[(acetoxymethyl)allyl]trimethylsilane (**I.255**, 1.80 mL, 55.5 mmol, 1.50 eq) and palladium acetate (208 mg, 0.930 mmol, 0.025 eq) in toluene (375 mL; non dried, analytical grade solvent was used in this reaction since catalytic amounts of water were found to be essential for the reaction to proceed in good yields) was added triisopropyl phosphite (1.69 mL, 7.41 mmol, 0.200 eq). The mixture was heated to reflux for 15 h, was subsequently allowed to cool to room temperature and was then concentrated. Purification by column chromatography (silica, EtOEt:pentane 1:20 \rightarrow 1:4) gave **I.298** as a colorless oil (4.79 g, 85 %) and **I.305** as a colorless oil (426 mg, 6 %).

I.298 was obtained by concentration of later fractions in the chromatographic purification.

TLC (EtOAc:Hex 1:3): $R_f = 0.18$.

¹H NMR (300 MHz, CDCl₃): $\delta = 4.91\text{--}4.82$ (m, 2H), 4.38–4.31 (m, 1H), 4.22 (dt, $J = 11.3$, 2.6 Hz, 1H), 3.08–2.91 (m, 1H), 2.85–2.55 (m, 4H), 2.13–1.95 (m, 2H), 1.67–1.55 (m, 1H).

¹³C NMR (75 MHz, CDCl₃): $\delta = 174.1$, 148.0, 107.1, 67.8, 42.5, 40.0, 36.1, 34.9, 28.1.

IR (neat): $\tilde{\nu}_{\text{max}} = 2918$, 1726.

HRMS (EI ⁺):	m/z calcd. for C ₉ H ₁₂ O ₂ ⁺ :	152.0837 [M] ⁺ ;
	found:	152.0836 [M] ⁺ .

Bisalkene **I.305** was obtained by concentration of earlier fractions in the chromatographic purification step.

TLC (EtOAc:Hex 1:3): $R_f = 0.30$.

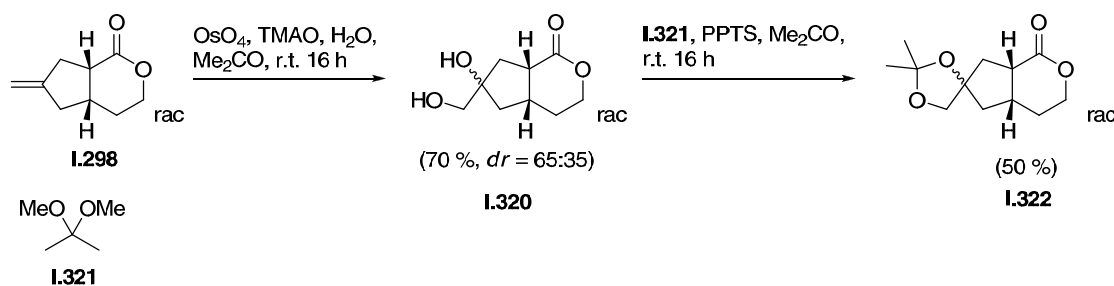
¹H NMR (300 MHz, CDCl₃): δ = 4.97-4.81 (m, 4H), 4.39 (dt, *J* = 11.1, 4.4 Hz, 1H), 4.27 (ddd, *J* = 11.1, 10.0, 3.5 Hz, 1H), 2.88-2.77 (m, 1H), 2.64-2.41 (m, 5H), 2.22-2.03 (m, 4H), 1.96-1.85 (m, 1H), 1.83-1.07 (m, 1H).

¹³C NMR (75 MHz, CDCl₃): δ = 174.2, 148.0, 147.9, 114.7, 114.6, 67.7, 44.8, 43.2, 37.7, 37.4, 37.2, 34.2, 31.1.

IR (neat): 2918, 1733.

HRMS (EI⁺): m/z calcd. for C₁₃H₁₈O₂⁺: 206.1307 [M]⁺;
found: 206.1303 [M]⁺.

6-Hydroxy-6-(hydroxymethyl)hexahydrocyclopenta[c]pyran-1(3*H*)-one (I.320) and 2',2'-dimethylhexahydro-1*H*-spiro[cyclopenta[c]pyran-6,4'-[1,3]dioxolan]-1-one (I.322):



To a solution of TMAO (92.7 mg, 1.23 mmol, 1.10 eq) in acetone (19.0 mL) and water (39.0 mL) was successively added osmium tetroxide (2.5 % solution in *tert*-butanol, 0.701 mL, 56.0 μmol, 0.050 eq) and **I.298** (170 mg, 1.11 mmol, 1.00 eq) at room temperature. After being stirred for 16 h at this temperature, the mixture was filtered through a short plug of florisil, which was washed with acetone (20.0 mL) and the combined filtrates were concentrated. Purification by column chromatography (silica, MeOH:CH₂Cl₂ 1:10) afforded **I.320** as an inseparable mixture of diastereomers as a colorless oil (146 mg, 70 %). **I.320** was directly used in the next reaction. (For storage, **I.320** was kept as a frozen 1.00 M solution in benzene at −25 °C, since **I.320** slowly decomposes if stored neat or at room temperature.)

TLC (CHCl₃:MeOH 100:10): *R_f* = 0.10 (both diastereomers).

¹H NMR (600 MHz, CD₂Cl₂, major diastereomer quoted): δ = 4.34 (dt, *J* = 11.2, 3.7 Hz, 1H), 4.21 (td, *J* = 11.2, 2.1 Hz, 1H), 3.63 (dd, *J* = 26.5, 10.8 Hz, 2H), 3.13 (td, *J* = 11.0, 8.6 Hz, 1H), 2.99-2.88 (m, 1H), 2.16-2.04 (m, 4H), 1.58-1.47 (m, 1H), 1.28 (dd, *J* = 13.3, 10.5 Hz, 1H).

^{13}C NMR (150 MHz, CD_2Cl_2 , major diastereomer quoted): $\delta = 175.3, 81.4, 68.9, 67.6, 43.6, 41.3, 39.1, 34.7, 29.4$.

IR (neat): $\tilde{\nu}_{\text{max}} = 3390, 2930, 1706$.

HRMS (EI^+): m/z calcd. for $\text{C}_9\text{H}_{14}\text{O}_4^+$: 186.0892 $[\text{M}]^+$;
found: 186.0901 $[\text{M}]^+$.

To a solution of **I.320** (20.0 mg, 107 μmol , 1.00 eq) and 2,2-dimethoxypropane (**I.321**, 31.8 μL , 257 μmol , 2.40 eq) in acetone (5.70 mL) was added pyridinium *p*-toluenesulfonate (2.70 mg, 10.7 μmol , 0.100 eq). The resulting solution was stirred for 16 hours at room temperature and was then diluted with diethyl ether (15.0 mL) and washed with water (2 x 7.00 mL). The organic layer was dried over MgSO_4 , filtered and concentrated. The residue was purified by column chromatography (silica, $\text{MeOH}:\text{CH}_2\text{Cl}_2$ 1:100 \rightarrow 1:50) to give **I.322** as an inseparable mixture of diastereomers as a colorless oil (12.1 mg, 50 % yield).

TLC ($\text{CHCl}_3:\text{MeOH}$ 100:7): $R_f = 0.41$ (both diastereomers).

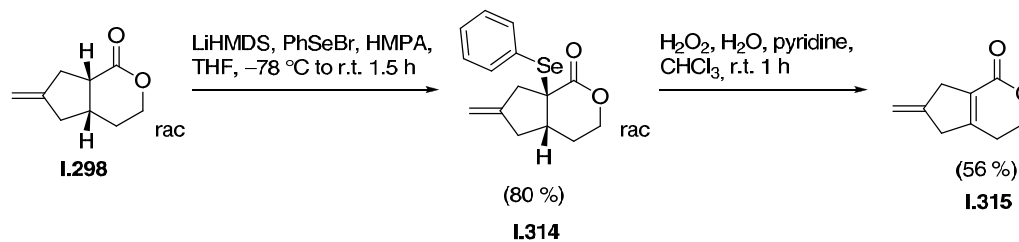
^1H NMR (400 MHz, CD_2Cl_2 , major diastereomer quoted): $\delta = 4.29$ (td, $J = 11.2, 3.8$ Hz, 1H), 4.22-4.14 (m, 1H), 3.90 (dd, $J = 26.7, 8.6$ Hz, 2H), 2.85-2.73 (m, 1H), 2.24-1.98 (m, 4H), 1.75-1.62 (m, 1H), 1.50-1.42 (m, 1H), 1.40-1.36 (m, 1H), 1.35-1.32 (m, 6H).

^{13}C NMR (100 MHz, CD_2Cl_2 , major diastereomer quoted): $\delta = 174.6, 109.4, 87.5, 71.3, 67.2, 44.5, 42.7, 41.2, 39.7, 34.2, 29.4, 26.5$.

IR (neat): $\tilde{\nu}_{\text{max}} = 2984, 1728$.

HRMS (EI^+): m/z calcd. for $\text{C}_{12}\text{H}_{18}\text{O}_4^+$: 226.1205 $[\text{M}]^+$;
found: 226.1192 $[\text{M}]^+$.

6-Methylene-7a-(phenylselenanyl)hexahydrocyclopenta[c]pyran-1(3H)-one (I.314) and
6-methylene-3,4,6,7-tetrahydrocyclopenta[c]pyran-1(5H)-one (I.315):



To a solution of **I.298** (2.07 g, 13.6 mmol, 1.00 eq) in THF (65.0 mL) was added dropwise a solution of KHMDS (0.500 M in toluene, 32.6 mL, 16.3 mmol, 1.20 eq) at $-78\text{ }^{\circ}\text{C}$ over the course of 10 min. The mixture was stirred for 15 min at $-78\text{ }^{\circ}\text{C}$ and was then treated with a solution of phenylselenenyl bromide (3.85 g, 16.3 mmol, 1.20 eq) and HMPA (2.60 mL, 15.0 mmol, 1.10 eq) in THF (60.0 mL), which was added over a period of 15 min. The resulting yellow colored reaction mixture was stirred at $-78\text{ }^{\circ}\text{C}$ for 15 min and was then allowed to warm up to be stirred for 1 h at room temperature. The reaction was then quenched with a sat. aq. NH_4Cl solution (3.00 mL) and the solvent was removed *in vacuo*. The resulting residue was diluted with diethyl ether (300 mL), washed with brine (200 mL), dried over MgSO_4 , concentrated and purified by rapid filtration through a plug of silica (silica, EtOAc:Hex 1:10 \rightarrow 1:4) to furnish **I.314** as a colorless oil (3.35 g, 80 %). Since the material slowly decomposed if exposed to air, it was directly used in the next reaction step.

TLC (EtOAc:Hex 1:3): $R_f = 0.22$.

$^1\text{H NMR}$ (300 MHz, CDCl_3): $\delta = 7.68\text{-}7.34$ (m, 5H), 4.98-4.90 (m, 2H), 4.37-4.22 (m, 2H), 3.10-3.02 (m, 1H), 2.86 (dddd, $J = 15.5, 8.6, 3.1, 1.6$ Hz, 1H), 2.71 (ddd, $J = 17.3, 2.9, 1.6$ Hz, 1H), 2.54 (ddt, $J = 11.3, 8.5, 6.4$ Hz, 1H), 2.22-2.13 (m, 1H), 2.05-1.97 (m, 1H), 1.62 (dtd, $J = 14.3, 11.3, 4.6$ Hz, 1H).

$^{13}\text{C NMR}$ (75 MHz, CDCl_3): $\delta = 172.4, 145.7, 137.5, 129.8$ (2C), 129.1 (2C), 127.6, 108.2, 67.4, 52.5, 44.2, 43.9, 39.7, 29.6.

IR (neat): $\tilde{\nu}_{\text{max}} = 3418, 2929, 1721, 1440$.

HRMS (EI^+): m/z calcd. for $\text{C}_{15}\text{H}_{16}\text{O}_2\text{Se}^+$: 308.0316 $[\text{M}]^+$;
found: 308.0308 $[\text{M}]^+$.

To a solution of **I.314** (1.10 g, 3.58 mmol, 1.00 eq) and pyridine (0.580 mL, 7.16 mmol, 2.00 eq) in chloroform (35.0 mL) was added dropwise a 30 % aq. H₂O₂ solution (2.90 mL, 28.6 mmol, 8.00 eq) at 0 °C. The mixture was stirred for 1 h at this temperature, was then diluted with dichloromethane (75.0 mL), washed with water (2 x 75.0 mL) and brine (75.0 mL), dried over MgSO₄ and concentrated. The crude product was purified by column chromatography (silica, EtOAc:Hex 1:10 → 1:6) to afford **I.315** (299 mg, 56 %) as a colorless oil. Since neat **I.315** tends to spontaneously polymerize at room temperature as evidenced by formation of a rubber-like solid, **I.315** was stored as a frozen 0.500 M solution in benzene at -25 °C.

TLC (EtOAc:Hex 1:5): $R_f = 0.12$.

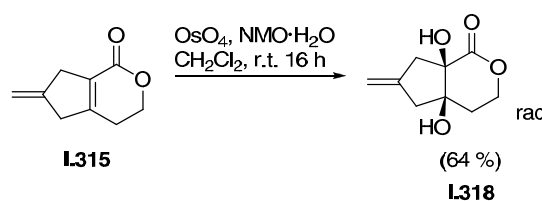
¹H NMR (300 MHz, CDCl₃): $\delta = 5.16$ -5.07 (m, 2H), 4.46 (t, $J = 6.35$ Hz, 2H), 3.41-3.33 (m, 4H), 2.53-2.46 (m, 2H).

¹³C NMR (75 MHz, CDCl₃): $\delta = 163.4, 157.8, 144.3, 128.8, 109.6, 66.6, 42.7, 36.7, 25.3$.

IR (neat): $\tilde{\nu}_{\max} = 2925, 1719, 1648$.

HRMS (EI⁺):
 m/z calcd. for C₉H₁₀O₂⁺: 150.0681 [M]⁺;
 found: 150.0672 [M]⁺.

4a,7a-Dihydroxy-6-methylenehexahydrocyclopenta[c]pyran-1(3H)-one (**I.318**):



To a solution of NMO-hydrate (5.48 mg, 46.7 μmol , 1.10 eq) in dichloromethane (1.10 mL), was added successively a solution of osmium tetroxide (2.5 % in *tert*-butanol, 22.0 μL , 1.70 μmol , 0.040 eq), and a solution of **I.315** (0.500 M in benzene, 85.0 μL , 42.5 μmol , 1.00 eq) and water (2.50 μL , 128 μmol , 3.00 eq). The reaction mixture was stirred vigorously for 16 h, concentrated and directly subjected to column chromatography without any previous workup (silica, CHCl₃:MeOH 100:1 → 100:5) to afford **I.318** (5.00 mg, 64 %) as a colorless oil.

TLC (CHCl₃:MeOH 100:6): $R_f = 0.11$.

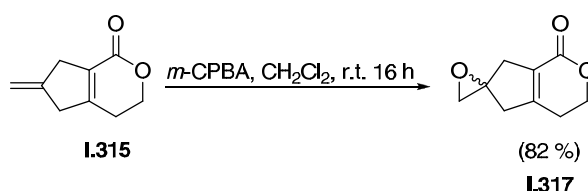
¹H NMR (300 MHz, CDCl₃): δ = 5.09-5.04 (m, 1H), 4.96-4.93 (m, 1H), 4.62 (td, *J* = 11.3, 3.4 Hz, 1H), 4.23 (ddd, *J* = 11.3, 5.0, 3.3 Hz, 1H), 3.61 (s, br, 1H), 3.14 (s, br, 1H), 2.86 (dq, *J* = 18.1, 2.5 Hz, 1H), 2.80-2.71 (m, 2H), 2.55 (dd, *J* = 16.0, 1.5 Hz, 1H), 2.17-2.11 (m, 1H), 2.02 (dt, *J* = 15.1, 3.4 Hz, 1H).

¹³C NMR (150 MHz, CDCl₃): δ = 175.4, 142.3, 110.6, 78.7, 77.7, 66.8, 45.5, 45.3, 32.6.

IR (neat): $\tilde{\nu}_{\text{max}}$ = 3426, 1718, 1069.

HRMS (EI⁺): m/z calcd. for C₉H₁₂O₄⁺: 184.0736 [M]⁺;
found: 184.0759 [M]⁺.

3,4,5,7-Tetrahydro-1*H*-spiro[cyclopenta[*c*]pyran-6,2'-oxiran]-1-one (**I.317**):



A solution of **I.315** (0.500 M in benzene, 85.0 μL, 42.5 μmol, 1.00 eq) was concentrated and immediately rediluted with chloroform (0.500 mL). To this solution was added sodium bicarbonate (4.28 mg, 51.0 μmol, 1.20 eq) and subsequently *m*-CPBA (8.80 mg, 51.0 μmol, 1.20 eq) at 0 °C and stirred for 1 h at this temperature. The mixture was allowed to warm up and stirred for 16 h at room temperature. Then, a sat. aq. Na₂S₂O₃ solution (0.100 mL) was added and the resulting mixture was stirred for 15 min at room temperature. The slurry was diluted with dichloromethane (5.00 mL) and a sat. aq. NaHCO₃ solution (5.00 mL). The organic layer was separated, treated with 100 mg of MgSO₄ and 100 mg of activated charcoal, cooled to 0 °C and filtered over a pad of celite. The pad was washed with dichloromethane (2 x 5.00 mL) and the combined filtrates were concentrated to give **I.317** as a colorless oil (6.10 mg, 86 %).

TLC (EtOAc:Hex 1:2): *R_f* = 0.40.

¹H NMR (200 MHz, CDCl₃): δ = 4.47 (t, *J* = 3.3 Hz, 2H), 3.09-2.92 (m, 4H), 2.77-2.63 (m, 2H), 2.55-2.46 (m, 2H).

¹³C NMR (150 MHz, CDCl₃): δ = 162.8, 156.4, 129.9, 66.6, 51.8, 42.6, 36.6, 29.7, 25.3.

IR (neat): $\tilde{\nu}_{\max} = 3052, 2986, 1747$.

HRMS (EI ⁺):	m/z calcd. for C ₉ H ₁₀ O ₃ ⁺ :	166.0630 [M] ⁺ ;
	found:	166.0628 [M] ⁺ .

CHAPTER II: A SYMMETRY-BASED APPROACH TOWARDS NEW ION CHANNEL BLOCKERS

2.1 Introduction

2.1.1 Project Background and Aims

Pentameric proteins play a huge role in nature, especially in neuronal transduction. Several of these belong to the family of ion channels, which mediate intracellular communication. In general, these channels can be controlled by a number of different stimuli, which trigger their opening and closing, *e.g.* by the binding of a ligand (ligand-gated ion channels), the difference in the membrane potential (voltage-gated ion channels), the action of light (light-gated ion channels), the influence of heat (temperature-gated ion channels) and the sensation of stretch, pressure or shear forces (mechanosensitive ion channels) or by several of these.^[97] A selection of pentameric proteins is depicted in Figure II.1.

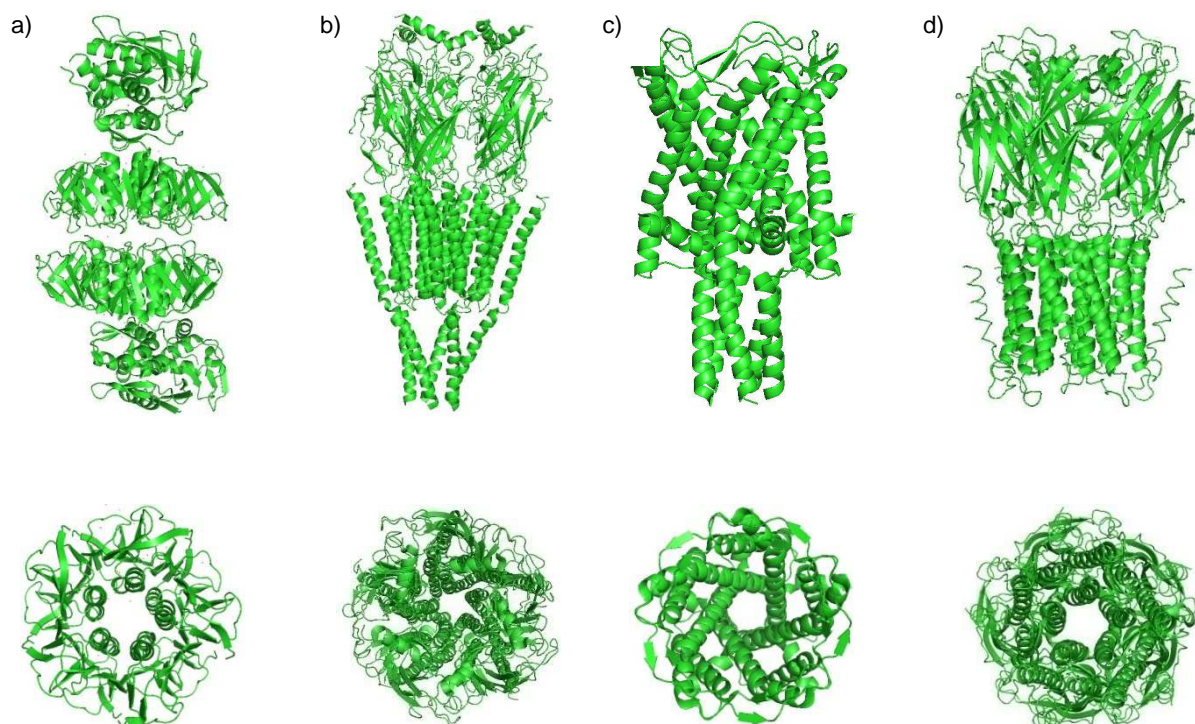


Figure II.1: Selection of pentamerically assembled proteins: a) Shiga toxin (PDB code: 1R4Q);^[98] b) nicotinic acetylcholine receptor (PDB code: 2BG9);^[99] c) MscL channel (PDB code: 2OAR);^[100] d) ELIC channel (PDB code: 2VL0).^[101]

Since the ion channel-mediated stream of ions is directly related to action potentials, the control of ion channels allows controlling neuronal activities and therefore intercellular communication. The action potential in context with exemplary ion channels is illustrated in Figure II.2.

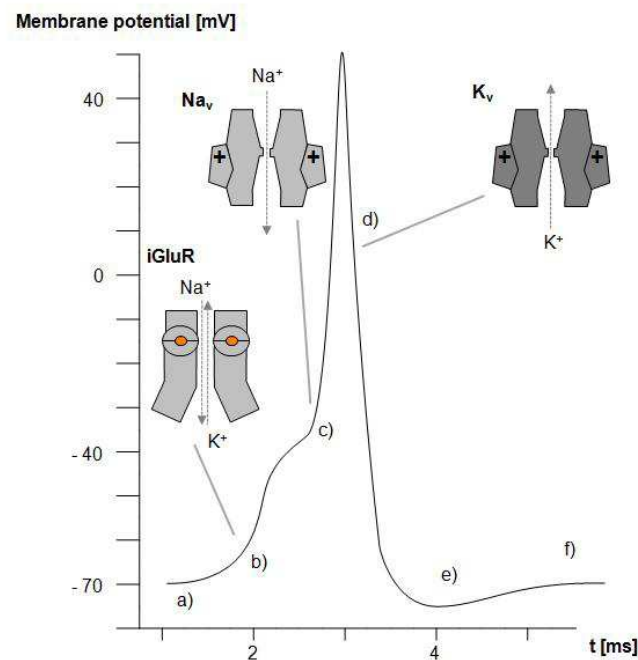


Figure II.2: The action potential: a) The transmembrane potential of a neuron at rest; b) a neurotransmitter binds to a ligand-gated ion channel, for example a glutamate receptor (iGluR), and evokes an excitatory postsynaptic potential; c) voltage-gated sodium channels (Na_v) respond and further depolarize the membrane, but quickly deactivate; d) voltage-gated potassium channels (K_v) follow suit and repolarize the membrane, even beyond its resting potential (\rightarrow e)); f) the hyperpolarization is removed through the concerted action of channels that are open at the resting potential and by ATP-driven ion pumps.^[102]

The initial depolarization of the cell membrane is caused by ligand-gated cationic ion channels, such as ionotropic glutamate receptors (*e.g.* iGluR) or nicotinic acetylcholine receptors. Pore opening is triggered by the binding of the respective neurotransmitter and results in an ion flux along the concentration gradient. This leads to a net influx of positive charge, which changes the membrane potential to a value of ca. -40 mV. At this point, voltage-gated sodium channels are being activated, resulting in a strong influx of sodium and thus a quick depolarization and even an overshoot to values of ca. $+50$ mV. Now, the sodium channels close and, upon a brief span, voltage-sensitive potassium channels activate to repolarize the membrane even beyond its resting potential. By the operation of ion pumps and several channels, the resting potential of ca. -70 mV is being restored.^[102]

Depending on whether they make the transmembrane potential less or more negative when being opened, ion channels can have both excitatory and inhibitory effects on neurons. In general, nonselective cation channels and sodium channels are depolarizing, whereas potassium channels hyper- or repolarize. Chloride channels, such as GABA_A or glycine receptors, are inhibitory on AP firing.^[103]

Having such specific tasks in the process of the action potential, it is not surprising that ion channel agonists, antagonists and blockers are of great pharmacological significance and a large number of these have important applications as drugs, *e.g.* in the field of anesthesia.^[104]

Ligand-gated ion channels are activated by the binding of a neurotransmitter such as GABA (II.1), acetylcholine (II.2), L-glutamic acid (II.3), glycine (II.4) or 5-HT (II.5), which is released from the presynaptic terminal (Figure II.3).^[105]

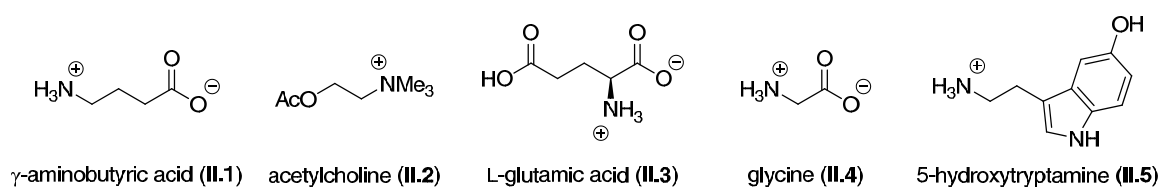


Figure II.3: Structures of the most important neurotransmitters acting on the ligand-gated ion channels.

As described in Figure II.2, the binding of such a neurotransmitter results in an ion flux through the postsynaptic membrane, thus generating a change in the membrane potential and triggering the action potential. Neurotransmitters are released from synaptic vesicles in the terminal rest of presynaptic axons and bind to receptor proteins, which are coupled to the respective ion channels on the recipient neuron (Figure II.4).^[106]

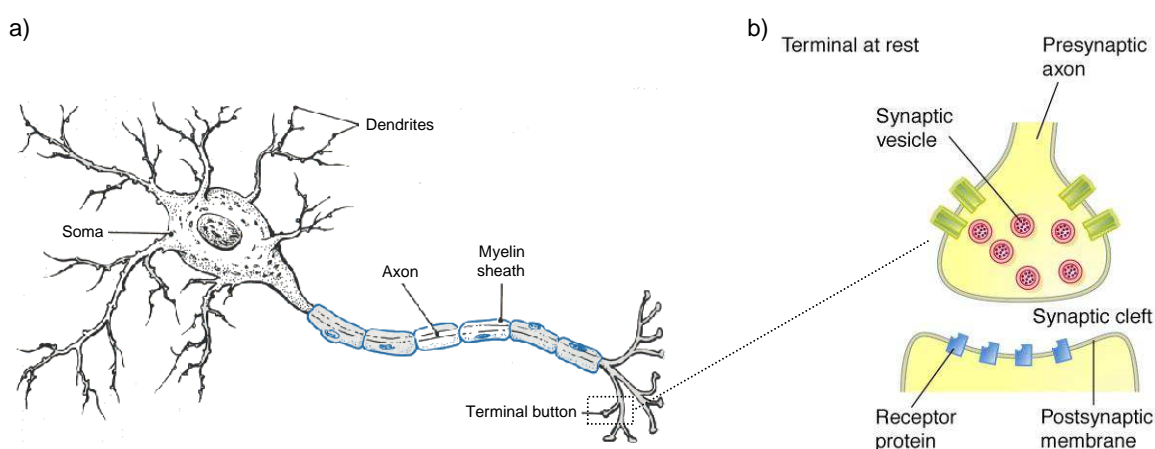


Figure II.4: The location of action of neurotransmitters: a) Artwork of a neuron;^[106] b) Artwork of the synaptic cleft.^[107]

Among the group of pentameric ligand-gated ion channels, which includes glycine, nicotinic acetylcholine, 5-HT₃ and the GABA_A receptors, the GABA_A receptor controls neuronal activity by regulating the influx of chloride ions. Thus, GABA_A counteracts the hyperpolarization of the membrane and hence action potential formation and therefore has an inhibitory function. More specifically, it plays a key role in inhibitory interneurons in the brain by regulating the spike timing and with that the activity pattern of neuronal circuits. GABAergic interneurons are considered to be essential for neuronal oscillations in the β and γ bands of the EEG, which have been associated with basic cognitive functions like object perception, selective attention, working memory and consciousness. These neurons have also been found to be crucial for the formation and the retrieval of cell assemblies required for encoding, consolidating and recalling information.^[108]

The GABA_A receptor consists of five subunits building a central pore. Each subunit comprises four transmembrane domains (M1-M4) with both the *N*- and *C*-terminus located extracellularly. The transmembrane domains M1 and M3 are oriented towards the adjacent subunits as well as to the lipid bilayer, M4 is buried in the membrane and M2 faces the lumen of the pore (Figure II.5).^[109]

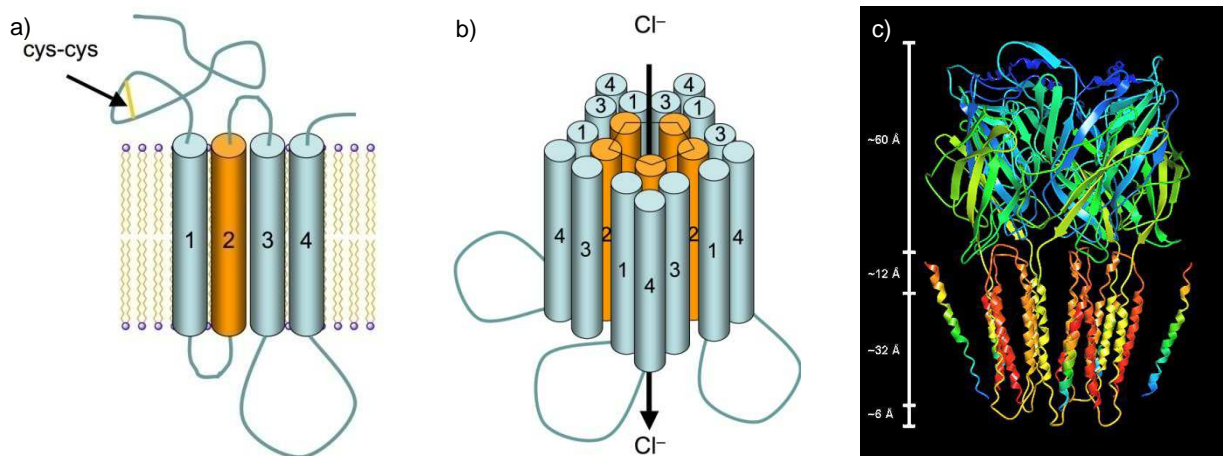


Figure II.5: Structure of the GABA_A receptor: a) Schematic structure of the transmembrane domains M1-M4 bearing a disulfide-bridge which is characteristic for the cys-loop superfamily,^[110] b) Schematic structure of pentamerically arranged transmembrane domains,^[110] c) Side view on a modeled structure of the $\alpha_1\beta_2\gamma_2$ GABA_A receptor.^[109]

There are several isoforms for each of the five subunits and all of them contain a conserved disulfide-bridge in the extracellular domain (Figure II.5 a)). The most abundant example is the $\alpha_1\beta_2\gamma_2$ (wild type) GABA_A receptor, which consists of two α_1 , two β_2 and one γ_2 subunit. Due to minor differences in these subunit isoforms, the heteromeric $\alpha_1\beta_2\gamma_2$ GABA_A receptor is not

exactly fivefold symmetric on a macroscopic scale. However, on a microscopic scale, *i.e.* in the channel lumen, all participating amino acids are identical, for which reason the channel can be considered pseudo-fivefold symmetric.

To date, no crystal structure of the GABA_A receptor has been reported in literature. However, Ulens and coworkers demonstrated that the ELIC channel is a suitable model to investigate GABA recognition and channel modulation by allosteric modulators.^[111] A crystal structure of GABA (**II.1**) bound to the ELIC channel is shown in Figure II.6.

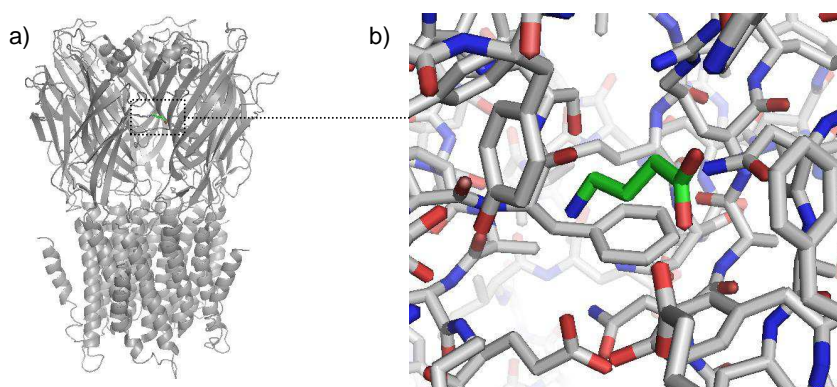


Figure II.6: Position of GABA in the ELIC channel (PDB code: 2YOE): a) Whole view on the crystal structure; b) zoom on the binding site.^[111]

A well-known open channel blocker of the GABA_A channel is picrotoxin (**II.6**, Figure II.7), which is a 1:1 mixture of the natural products picrotin (**II.7**) and picrotoxinin (**II.8**).^[112] **II.6** was first isolated from the South Asian climbing plant *Anamirta cocculus* in 1812 and is to date one of the most potent open channel blockers of the GABA_A receptor.^[113]

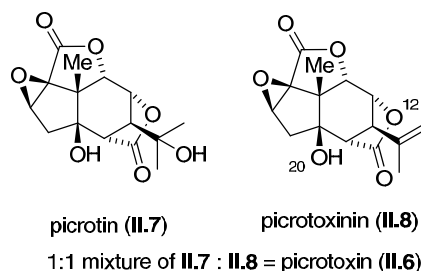


Figure II.7: Chemical structure of the open channel blocker picrotoxin (**II.6**).

The binding site of picrotoxin (**II.6**) in GABA_A has been discussed controversially and remains unclarified,^[114] although it could be shown that **II.6** interacts *via* a hydrogen bond to Thr 261.^[115] **II.6** is believed to bind either to an allosteric site or to the channel lumen.^[116] In addition, a crystal structure of picrotoxinin (**II.8**) bound to the GluCl channel, which, like

GABA_A belongs to the Cys-loop superfamily, was reported by Gouaux and coworkers in 2011 (Figure II.8) and shows **II.8** bound in the channel lumen.^[117]

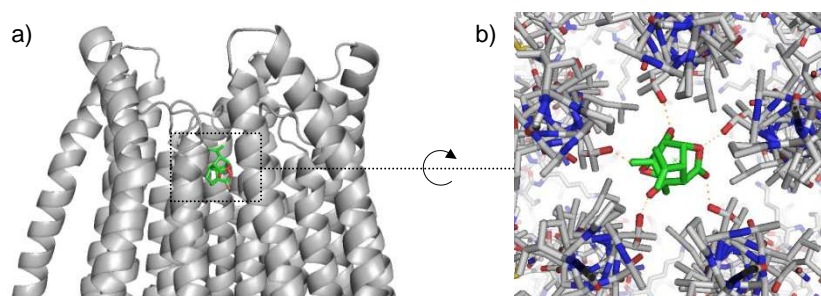


Figure II.8: Crystal structure of picrotoxinin (**II.8**) bound to the GluCl channel (PDB code: 3RI5): a) side view; b) top view.^[117]

Searching for opportunities to control ion channels and thus neuronal activities, a new symmetry-based approach towards the design of potential drugs was explored in this work. It was speculated that symmetric compounds matching the inherent fivefold symmetry of pentameric ion channels could potentially pentavalently interact with the protein and thus function as potent open channel blockers (Figure II.9).

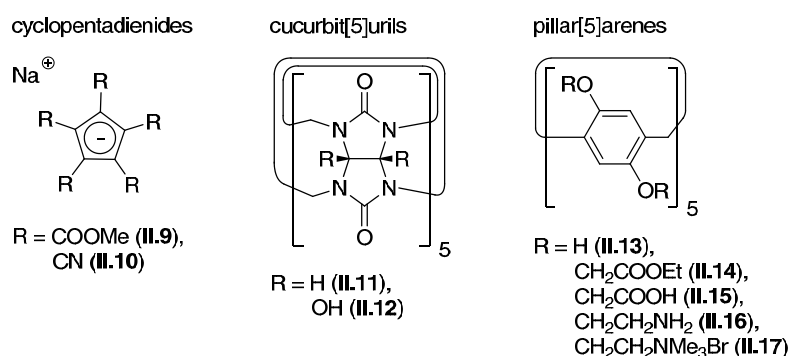


Figure II.9: Generic chemical structure of cyclopentadienides, cucurbit[5]urils and pillar[5]arenes.

Thus, pentasubstituted cyclopentadienides (**II.9**, **II.10**), functionalized cucurbit[5]urils (**II.11**, **II.12**) or substituted pillar[5]arenes (**II.13**, **II.14**, **II.15**, **II.16**, **II.17**) were chosen as attractive synthetic targets. Model studies with these compounds on pentameric proteins are described in the next section.

2.2 Results and Discussion

2.2.1 Model Studies of Fivefold Symmetric Compounds with Pentameric Proteins

Based on known crystal structures of pentameric proteins, preliminary model studies with the selected pentasymmetric compounds were carried out to assess if they could access the channel lumen, to give insights about proportions and to reveal potential interactions for pentavalent binding.^[118] Pentasymmetric molecules were manually placed inside the channel lumen and the binding mode was obtained after fixing the enzyme coordinates and minimizing the energy of the system using the MAB force field as implemented in the software MOLOC.^[118]

If, for example, a pillar[5]arene **II.15** bearing carboxylic acid substituents was optimized at the selectivity filter of the ELIC channel, the carboxylic acid groups seem to be able to interact with Glu231 through hydrogen bonding. However, due to the large diameter of the pillar[5]arene core ($d_{(\text{CH}_2-\text{CH}_2)} = 9.1 \text{ \AA}$), the substituents can hardly reach the site of action without sterical repulsions (Figure II.10).

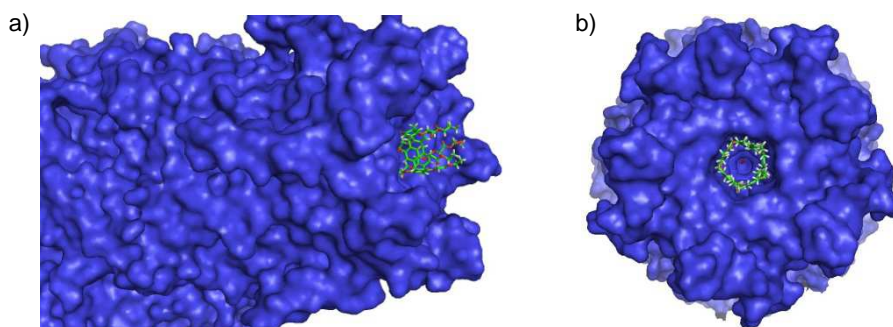


Figure II.10: Illustration of the surface of the ELIC channel (PDB code: 2VL0) with a pillar[5]arene at the selectivity filter: a) Side view showing the position of the fivefold symmetric molecule in the channel; b) top view, emphasizing the pentameric nature of the channel.

Cyclopentadienide **II.10**, on the other hand, seems to be able to bind deep in the selectivity filter without forming repulsive contacts (Figure II.11). Again, the potential interactions were found with Glu231 through hydrogen bonding.

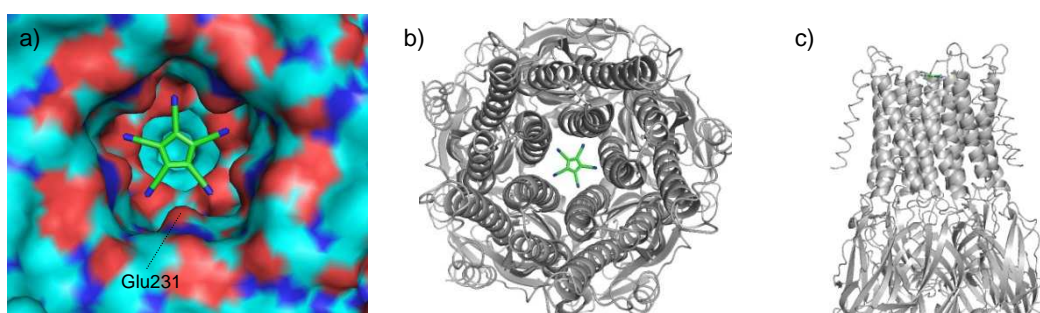


Figure II.11: Illustration of the ELIC channel (PDB code: 2VL0) with a cyclopentadienide binding at the selectivity filter: a) Illustration of the surface; b) top view; c) side view on the channel.

In order to compare the potential binding mode of **II.10** with that of picrotoxinin (**II.8**) on the GluCl channel, **II.10** was optimized at the extracellular domain thereof. Indeed, the compound seems to be able to bind at the binding site of picrotoxinin *via* hydrogen bonding. Although the diameter of **II.10** ($d_{(N-N)} = 7.2 \text{ \AA}$) is larger than the diameter of picrotoxinin (**II.8**, $d_{(O_{20}-O_{12})} = 4.6 \text{ \AA}$), no sterical repulsion was found (Figure II.12).

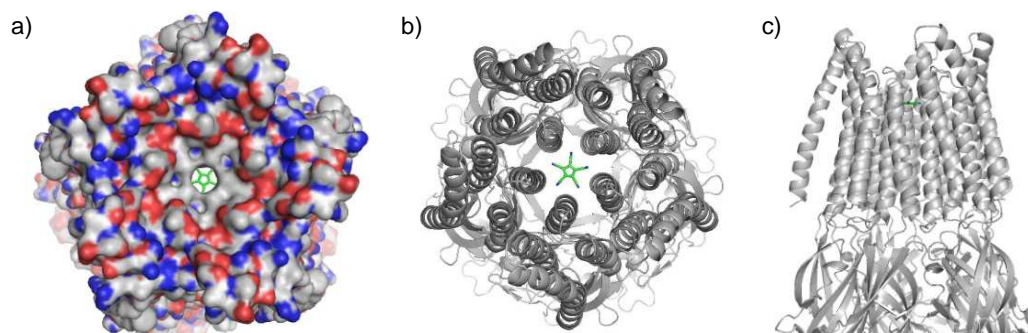


Figure II.12: The GluCl channel (PDB code: 3RHW) with a cyclopentadienide at the selectivity filter: a) Illustration of the surface; c) top view; d) side view on the channel.

Due to their greater size, pillar[5]arenes were anticipated to fit best in a channel with a large channel lumen, where enough space would be left to allow the substituents to rotate towards amino acid residues. When, accordingly, pillar[5]arene with carboxylic acid substituents **II.15** was positioned in the extracellular domain of the MscL channel, only limited sterical repulsion was observed. These studies also revealed potential interactions at Lys33 (Figure II.13).

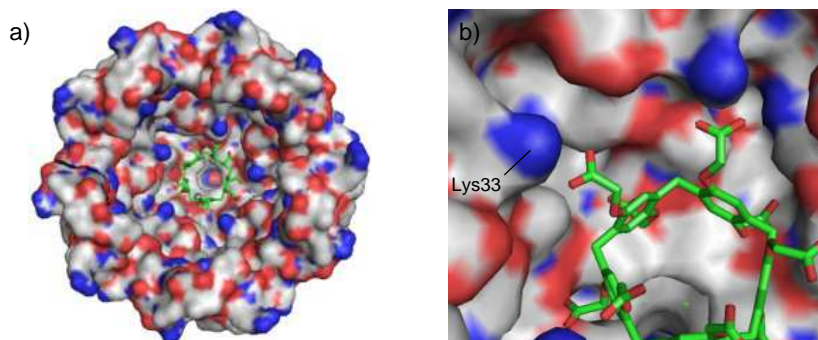


Figure II.13: Pillar[5]arene **II.15** with carboxylic acid substituents inside the MscL channel: a) Full view; b) zoom on carboxylic acid residues to illustrate potential interactions with the protein at Lys33.

Similar results were found when the pillar[5]arene was replaced by decahydroxycucurbit[5]uril (**II.12**). Again, the fivefold symmetric molecule could potentially interact with Lys33 (Figure II.14).

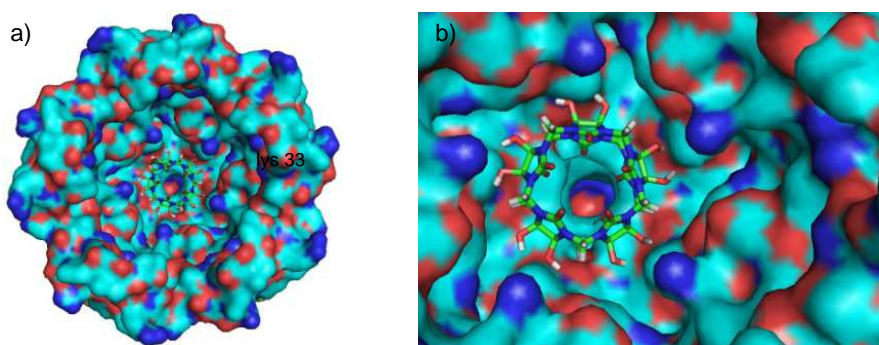


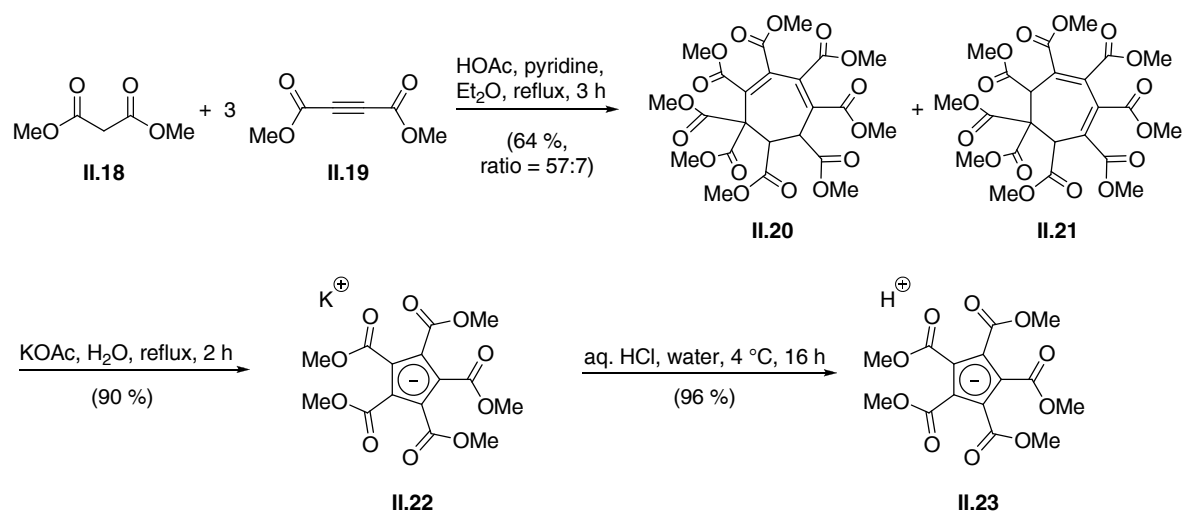
Figure II.14: Decahydroxycucurbit[5]uril inside the MscL channel: a) Full view; b) close view.

In summary, simple preliminary model studies were performed with molecules chosen according to a symmetry-based approach on a selection of pentameric proteins, which indeed revealed the possibility of pentavalent interactions. Thus, a synthesis program towards a series of fivefold symmetric compounds was launched to determine their potential in neuronal control, the details of which are described in the next section.

2.2.2 Synthesis of Pentasymmetric Potential Ion Channel Blockers

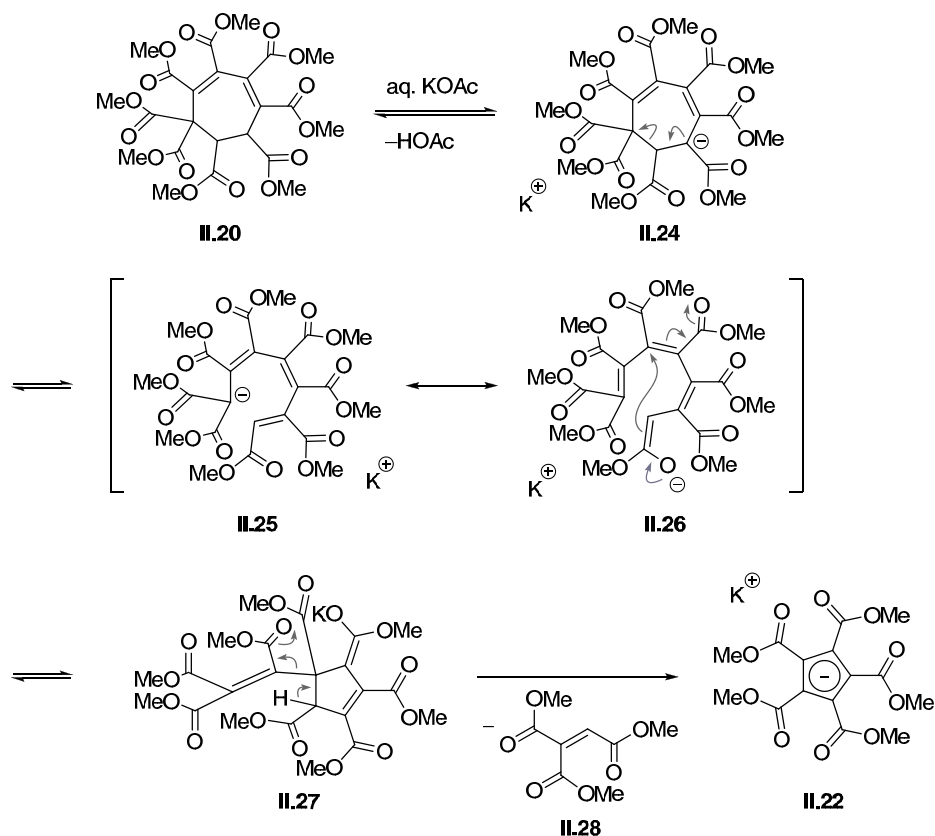
2.2.2.1 Synthesis of fivefold symmetric cyclopentadienides

A literature-known pentamethyl ester-substituted cyclopentadienide was the first target molecule among the fivefold symmetric compounds, the synthesis of which is depicted in Scheme II.1.^[119]



Scheme II.1: Synthesis of pentamethyl ester-substituted cyclopentadienides **II.22** and **II.23**.

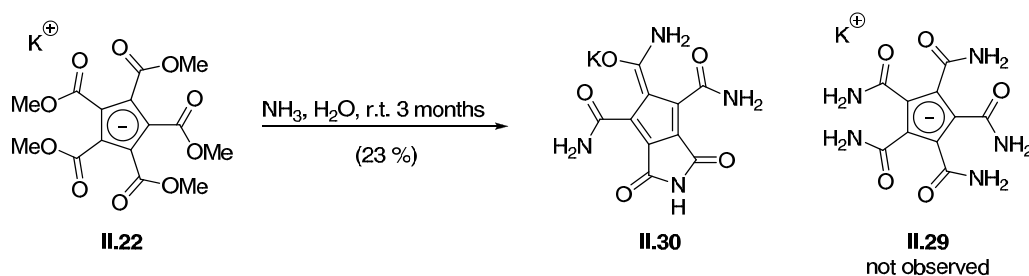
Upon heating a 1:3 mixture of dimethyl malonate (**II.18**) and dimethyl acetylene dicarboxylic acid (**II.19**) in the presence of pyridine, a triple-conjugate addition sequence followed by a fourth, intramolecular Michael addition furnished a 57:7 mixture of isomers **II.20** and **II.21**. This mixture was directly subjected to heating in the presence of potassium acetate, resulting in the formation of potassium salt **II.22**. This compound could be converted into the corresponding acid **II.23** by treatment with aqueous HCl. The formation of **II.22** is indeed intriguing and a proposed mechanism is shown in Scheme II.2.



Scheme II.2: Speculated mechanism for the formation of **II.22**.

Presumably, upon deprotonation of **II.20**, intermediate **II.24** undergoes a retro-Michael addition resulting in linear intermediate **II.25**. This anionic species could undergo intramolecular conjugate addition as shown in mesomeric structure **II.26**. The resulting five-membered ring **II.27** could eliminate **II.28** to form the aromatic product. Since deprotonation of **II.21** would also result in formation of intermediate **II.24**, this speculated mechanism would explain why using a mixture of isomers **II.20** and **II.21** gives the same yield of **II.22** as if pure **II.20** was employed.

When the conversion of pentaester **II.22** to its corresponding pentaamide **II.29** was attempted,^[120] the formation of an unexpected product was observed (Scheme II.3).



Scheme II.3: Attempted synthesis of pentaamide **II.29**.

A solution of **II.22** in aqueous ammonia was allowed to stand at room temperature for three months, upon which time a crystalline solid was obtained, identified as bicycle **II.30**. Interestingly, it was found that the mother liquor contained an inseparable, complex mixture of compounds and **II.29** could not be detected. The structure of **II.30** was confirmed by X-ray crystallography (Figure II.15).

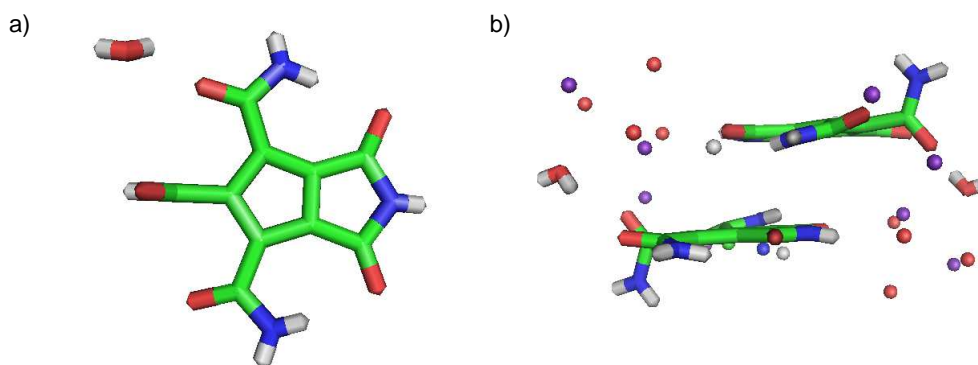
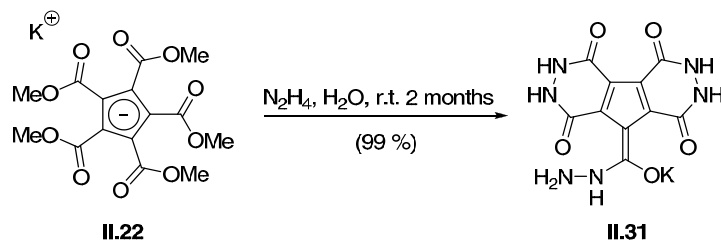


Figure II.15: a) Top view on the carbon framework of **II.30**; b) view along the *ab*-axis (potassium counter ions and water molecules are shown).

Compound **II.30** crystallized in the triclinic crystal system in the space group $P(-1)$. The unit cell contains two equivalents of **II.30** and two molecules of water, enabling an octahedral coordination of the potassium counter ion. The amide moieties in ortho position to the imid are rotated in a fashion that is almost parallel to the ring plane, whereas the terminal amide function is oriented orthogonally.

Although **II.30** has D_{2h} symmetry as opposed to **II.29** with D_{5h} symmetry, this compound was still considered a potential ion channel blocker according to the symmetry approach. More specifically, it can be speculated that the carbonyls could adopt a pseudo fivefold symmetric orientation, thus enabling pentavalent interaction with a protein regardless to its lower symmetry.

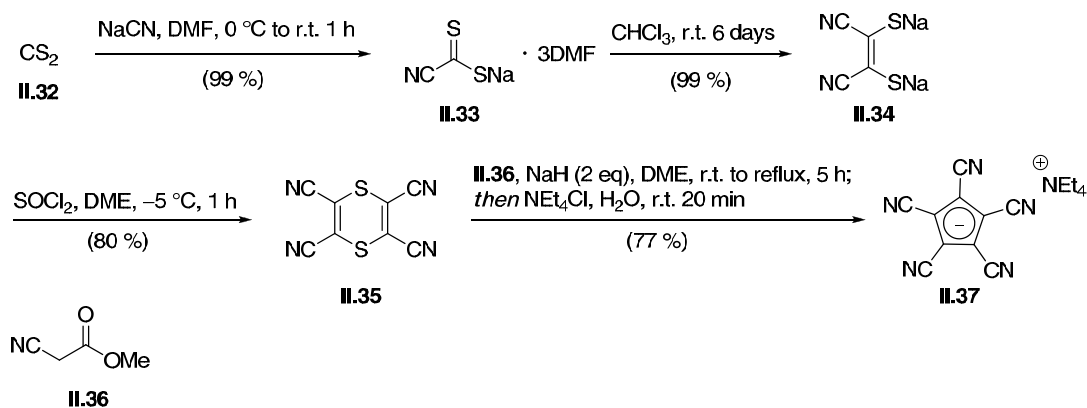
Envisaging to use **II.22** as precursor for more pseudo-fivefold symmetric compounds, it was interesting to investigate the reactivity of **II.22** with hydrazine and an analogous reaction to that reported for **II.30** using hydrazine hydrate as reagent was carried out next (Scheme II.4).



Scheme II.4: Reaction of **II.22** with hydrazine.

Indeed, the attempted reaction furnished a pseudo-fivefold symmetric compound and hydrazine adduct **II.31** was formed in almost quantitative yield.

Subsequently, the synthesis of nitrile-substituted cyclopentadienide (pccp) salts was targeted through a combination of literature-known procedures (Scheme II.5).



Scheme II.5: Synthesis of Et₄N pccp **II.37**.

Reacting sodium cyanide and carbon disulfide (**II.32**) in DMF resulted in the formation of solvate salt **II.33**,^[121] which upon standing at room temperature in chloroform for six days underwent spontaneous desulfurization to afford disulfide **II.34**.^[122] Compound **II.34** was oxidatively dimerized to give **II.35** using thionyl chloride.^[123] Treatment with deprotonated methylcyano acetate **II.36** finally delivered pentasymmetric nitrile **II.37**.^[124] By this four-step process, the use of highly reactive reagents such as chlorine gas as reported in other procedures could be avoided.^[125]

Oxidative dimerization of **II.35** required some optimization since the product proved to be sensitive towards byproducts of the reaction process such as SO₂ and HCl, as evidenced by formation of a complex product mixture. These problems could be encountered by a modified workup- and purification procedure. Specifically, it was found that upon addition of an aqueous NaHCO₃ solution, the product can be precipitated from the reaction mixture and can

be further purified by simple recrystallization. In the course of the optimization, an unprecedented solvate of **II.35** could be obtained upon recrystallization of **II.35** from toluene (Figure II.16).

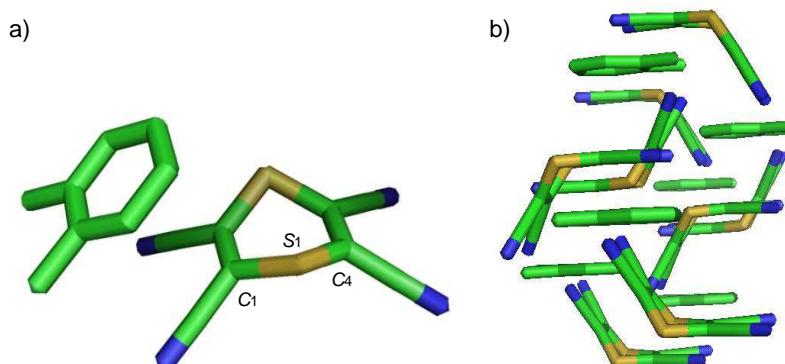
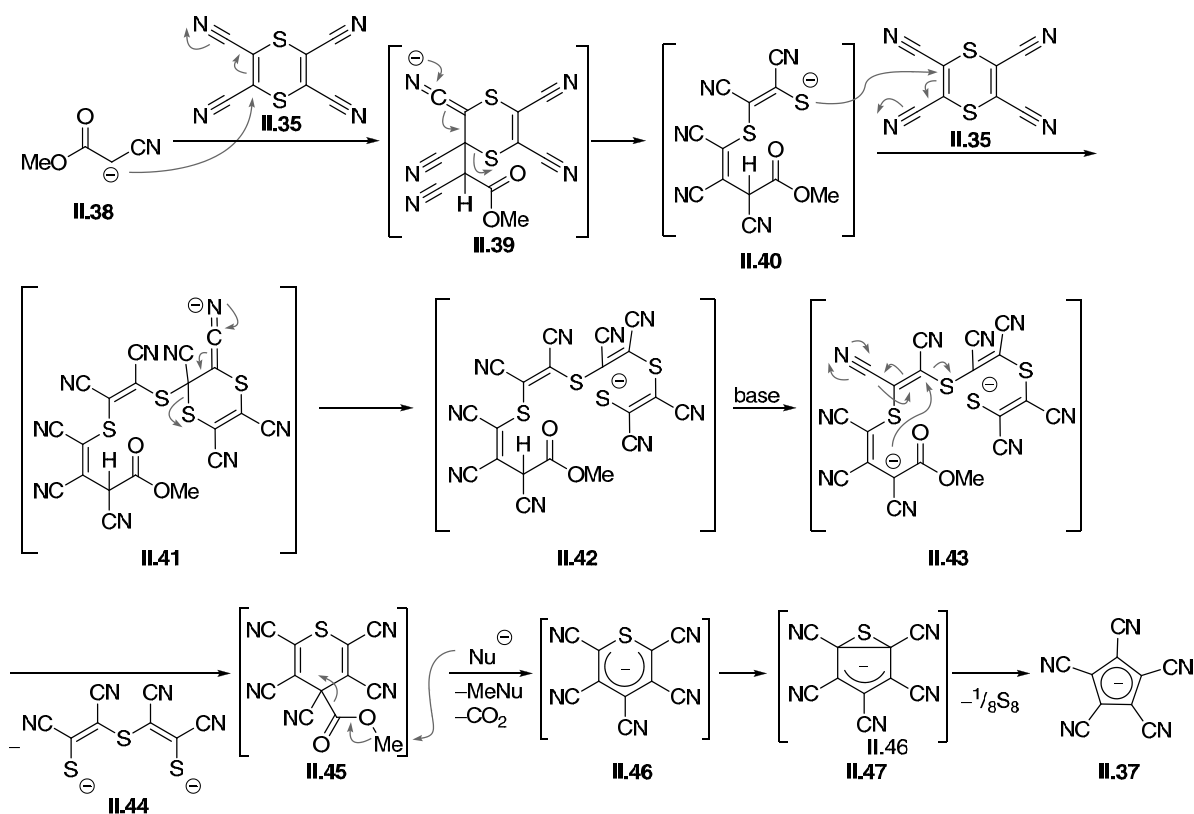


Figure II.16: Crystal structure of **II.35**·0.5toluene: a) Single pair of **II.35** and toluene; b) unit cell, view along the ac-axis (orientation of methyl group statistically disordered, hydrogens removed for clarity).

II.35 exists in a bent conformation ($\angle_{C1-S1-C4} = 97.1^\circ$) and is coordinated to 0.5 equivalents of toluene at the distance of 3.4 Å, indicating π -stacking interaction between toluene and the dicyanoethylene moiety. The orientation of the methyl group in toluene is statistically disordered.

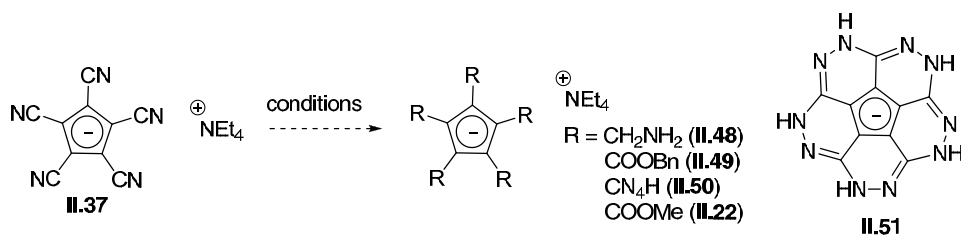
The conversion of **II.35** into **II.37** is intriguing and a speculated mechanism is depicted in Scheme II.5. The proposed mechanism is based on observations during previous studies which reported disulfide **II.43** as a byproduct of this reaction (Scheme II.6).^[124] However, further mechanistic studies should be carried out in order to ultimately confirm the proposed mechanism.



Scheme II.6. Speculated mechanism for the formation of II.37.

Upon an initial nucleophilic attack of anion **II.38** to **II.35**, intermediate **II.39** could undergo ring opening to give sulfide **II.40**. Compound **II.40** was speculated by Simmons *et al.* to intercept a second equivalent of **II.35** to form **II.41** and subsequently, upon ring opening, **II.42**.^[124] Deprotonation with a second equivalent of base (\rightarrow **II.43**) would result in an intramolecular conjugate addition, which, upon loss of one equivalent of **II.44**, would result in the formation of six-membered heterocycle **II.45**. The methyl ester could be lost by a Krapcho-type mechanism, thus resulting in the formation of **II.46**. Intermediates of the type of **II.46** were proposed by Simmons *et al.* to undergo thermal disrotatory ring closure (\rightarrow **II.47**), followed by thiirane ring opening and desulfurization to yield **II.37**.^[124]

In order to gain access to a larger variety of fivefold symmetric compounds, derivatization of **II.37** was investigated next. Unfortunately, **II.37** turned out to be extremely unreactive, an observation which was attributed to the fact that **II.37**, although bearing five electron-withdrawing groups, is still relatively electron rich and also aromatically stabilized. The results of the attempted functionalizations are summarized in Table II.1.



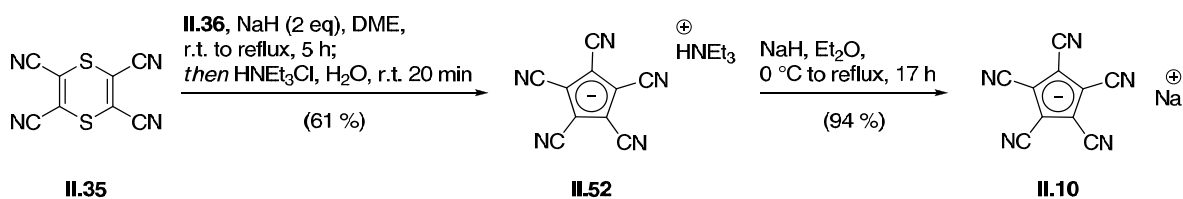
Entry	Reagent	Solvent	Temperature	Time	Yield
1	NaBH ₄ , CoCl ₂	THF	reflux	24 h	(II.48) -[a]
2	Silica, BnOH	CHCl ₃	reflux	24 h	(II.49) -[a]
3	LiAlH ₄	THF	reflux	18 h	(II.48) -[b]
4	NaN ₃ , HCl	H ₂ O	reflux	24 h	(II.50) -[b]
5	MeMgBr	THF	reflux	24 h	(II.22) -[b]
6	N ₂ H ₄	H ₂ O	reflux	24 h	(II.51) -[a]

[a] no reaction observed, reisolated starting material; [b] formation of a complex mixture of polar materials.

Table II.1: Selected conditions for the attempted functionalization of **II.37**.

When **II.37** was heated in THF with sodium borohydride in the presence of cobalt(II) chloride to obtain amine **II.48**, no reaction was observed and starting material was recovered (Table II.1, Entry 1). The same result was obtained in an attempt to synthesize **II.49**, when **II.37** was heated in chloroform in the presence of silica and benzyl alcohol (Table II.1, Entry 2). When a mixture of **II.37** and LAH was heated to reflux in THF, a complex mixture of polar material was obtained (Table II.1, Entry 3). An attempted cycloaddition with *in situ* generated hydrazoic acid to give **II.50** resulted in a mixture of black, insoluble material (Table II.1, Entry 4). A similar observation was made when **II.37** was reacted with methylmagnesium bromide in refluxing THF to obtain **II.22** (Table II.1, Entry 5). When a mixture of **II.37** and hydrazine hydrate was heated to reflux for 24 h, again, no formation of **II.51** was observed and starting material was recovered (Table II.1, Entry 6)

Even though functionalization of **II.37** remained unsuccessful, sufficient amounts of **II.37** could be produced to carry out initial biological tests (*vide infra*, Section 2.2.3). However, **II.37** was found to be only poorly soluble in water, thus limiting its potential application in physiological media. In order to encounter this problem, pccp salts with different counter ions such as sodium were prepared (Scheme II.7).



Scheme II.7. Synthesis of Na pccp (**II.10**).

Compound **II.52** could be synthesized in analogy to **II.37** by treatment with deprotonated methyl cyanoacetate (**II.38**) in the presence of a second equivalent of sodium hydride. Sodium salt **II.10** was then prepared by simple treatment of triethylammonium salt **II.52** with sodium hydride, a procedure similar to that sketched by the group of Wright.^[126] Subsequent purification by reversed-phase column chromatography was found to be the optimal method to provide pure and crystalline material, which was submitted to biological testing (*vide infra*, Section 2.2.3). The crystal structure of **II.10** is shown in Figure II.17.

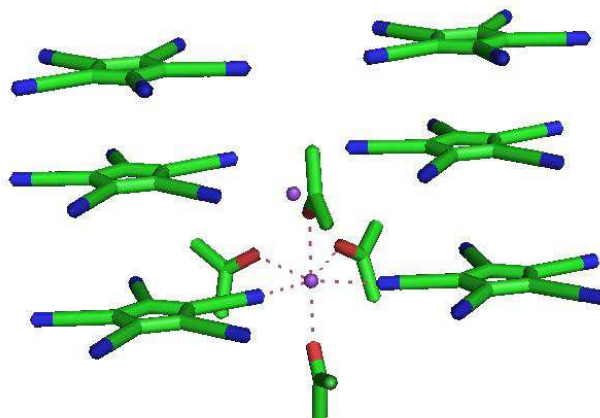


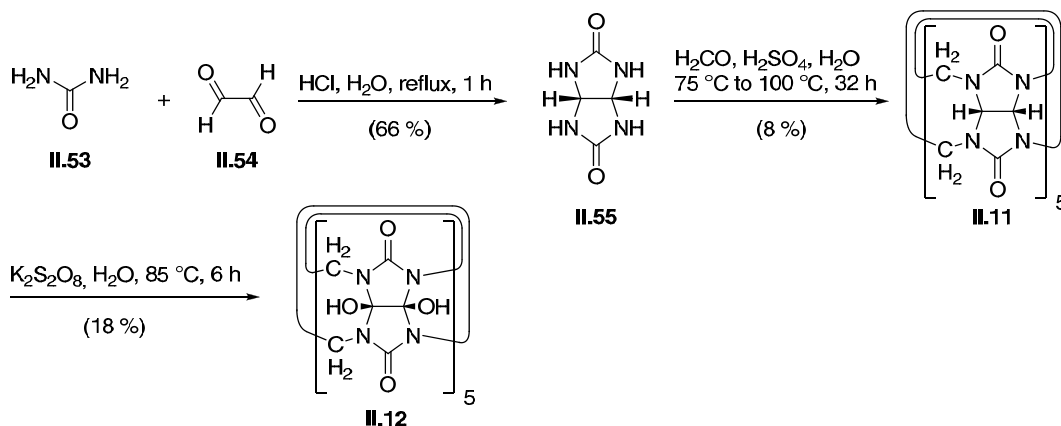
Figure II.17. Crystal structure of **II.10**·2acetone (a cutout of the unit cell is shown and hydrogens are removed for clarity).

Compound **II.10** crystallized as an acetone solvate with the formula **II.10**·2acetone in the monoclinic crystal system in the space group $C2/m$. Sodium ions are coordinated by acetone carbonyls and pccp nitriles in an octahedral fashion. Pccp anions stack in a staggered conformation.

Having produced a number of fivefold symmetric cyclopentadienides, the synthesis of cucurbit[5]urils was investigated subsequently and the results of these studies are presented in the next section.

2.2.2.2 Synthesis of cucurbit[5]urils

Starting from a known protocol to synthesize glycoluril, subsequent synthesis of cucurbit[5]urils was achieved by modified literature procedures (Scheme II.8).



Scheme II.8: Synthesis of decahydroxycucurbit[5]uril (II.12).

Heating a mixture of urea (II.53) and glyoxal (II.54) in aqueous HCl resulted in formation of glycoluril (II.55).^[127] Treatment of II.55 with formaldehyde in the presence of aqueous sulfuric acid provided a mixture of cucurbit[n]urils of different ring sizes. Upon fractional crystallization, the complex mixture could be separated and II.11 was isolated in 8 % yield.^[128] Conversion of II.11 into decahydroxycucurbit[5]uril (II.12) was achieved by treatment with potassium peroxodisulfate.^[129] It was found that the reaction produced a complex mixture of isomers, the separation of which could be accomplished by reversed-phase HPLC purification. The structures of II.11 and II.12 were confirmed by X-ray crystallography (Figures II.18 and II.19), with the crystal structure of II.11 identical to a reported structure of II.11 (CCDC-code: 883370).^[130]

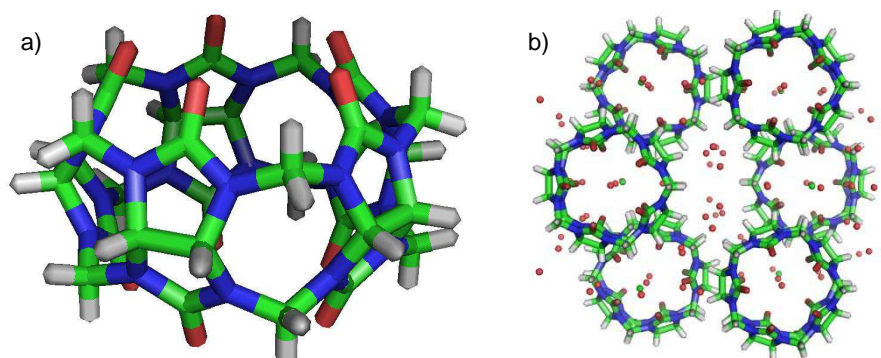


Figure II.18: Crystal structure of II.11: a) Depiction of a single molecule of II.11 without solvent; b) view along the c-axis in the unit cell, water and HCl molecules are shown.

Compound **II.11** crystallized in the monoclinic space group $C2/m$. The unit cell includes six units of **II.11**·4H₂O·HCl. It should be noted that water and HCl molecules are present in the molecular cavity of **II.11**, thus indicating a possible solvent exchange as guest in the cavity of **II.11**.^[131]

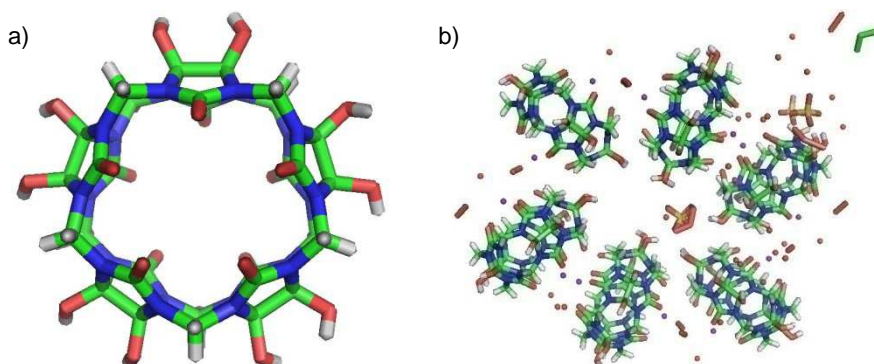
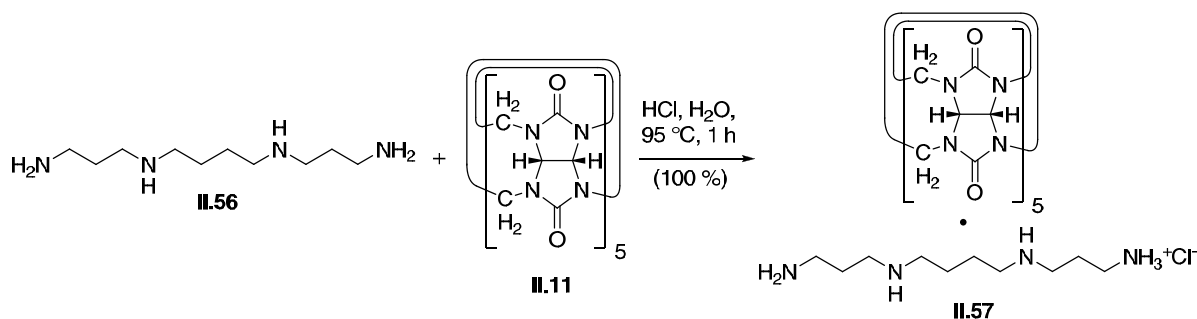


Figure II.19: Preliminary illustration of the crystal structure of **II.12**: a) Depiction of a single molecule without solvent; b) view along the a-axis in the unit cell, potassium ions, sulfate ions and water molecules are shown.

Preliminary data showed that **II.12** co-crystallized with K₂SO₄ as a water solvate in the triclinic space group $P(-1)$. Potassium ions are coordinated on each side in a pentagonal fashion by the cucurbit[5]uril carbonyl groups. Further refinement of the structure is currently in progress.

Whereas **II.12** showed excellent solubility in water (> 100 mM), **II.11** was only poorly soluble, thus restricting its use for biological applications. In order to render **II.11** more water-soluble, a complex of **II.11** with sperminium chloride was prepared in one step (Scheme II.9).^[132]



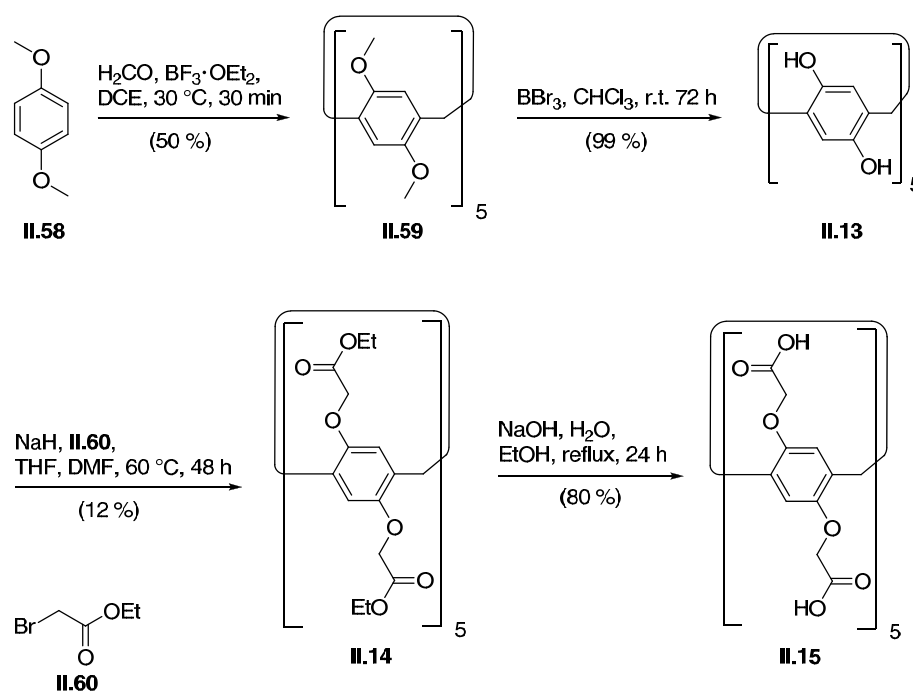
Scheme II.9: Synthesis of water-soluble cucurbit[5]uril complex **II.57**.

A stoichiometric mixture of spermine (**II.56**) and **II.11** was heated in the presence of aqueous HCl and upon removal of solvent, **II.57** was obtained in quantitative yield. The solubility of complex **II.57** in water was determined to be 1 mM.

The potential for functionalization of the cucurbit[5]urils is rather limited and only few examples for such transformations have been described in literature.^[129] Some further attempts have been carried out in the scope of this work (for detailed screening table, see Appendix 8), which, however, proved to be unsuccessful. In contrast, the pillar[5]arenes can easily be functionalized, thus rendering themselves ideal candidates in the symmetry approach. Their synthesis is described in the next section.

2.2.2.3 Synthesis of pillar[5]arenes

The synthesis of pillar[5]arene (**II.13**) was smoothly realized by following Nakamoto's improved procedure. Based on the reported compound, a water-soluble carboxylic acid-substituted pillar[5]arene (**II.15**) was synthesized (Scheme II.10).



Scheme II.10: Synthesis of carboxylic acid-substituted pillar[5]arene (**II.15**).

When 1,4-dimethoxybenzene (**II.58**) was treated with paraformaldehyde and boron trifluoride diethyl etherate as Lewis acid, a mixture of polymerized material and

decamethylpillar[5]arene (**II.59**) was obtained, from which **II.59** could be isolated by filtration and recrystallization.^[133] Upon *O*-deprotection, the resulting pillar[5]arene **II.13** was alkylated using ethyl bromoacetate (**II.60**) to afford ethyl ester-substituted pillar[5]arene (**II.14**) in a poor 12 % yield.^[134] Finally, saponification afforded carboxylic acid-substituted pillar[5]arene (**II.15**),^[134] which, upon recrystallization, gave crystals suitable for X-ray analysis. The preliminary crystal structure of **II.15** is shown in Figure II.20.

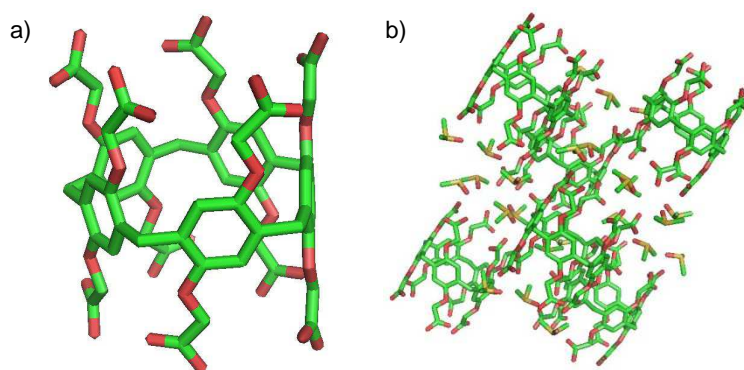
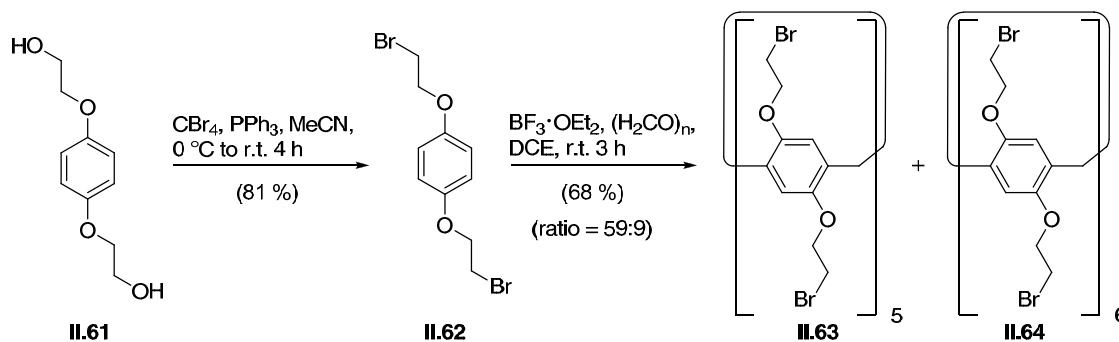


Figure II.20: Preliminary representation of the crystal structure of carboxylic acid-substituted pillar[5]arene **II.15**: a) Illustration of a single molecule (DMSO molecules and hydrogen atoms are removed for clarity); b) unit cell, view along the b-axis (DMSO molecules are shown, hydrogen atoms are removed for clarity).

Carboxylic acid-substituted pillar[5]arene (**II.15**) crystallized in the monoclinic space group *C2/c*. A unit cell contains four molecules of **II.15** and 12 molecules of DMSO. Further refinement of the structure is still in progress.

Further derivatives of **II.13** were accessible by cyclization of 1,4-bis(2-bromoethoxy)benzene (**II.62**). When this reaction was performed on large scale, bromoethoxy-substituted pillar[6]arene (**II.64**) could be isolated as a second reaction product (Scheme II.11).



Scheme II.11: Synthesis of bromoethoxy-substituted pillar[5]arene (**II.63**) and pillar[6]arene (**II.64**).

Subjecting 1,4-bis(2-hydroxyethyl)benzene (**II.61**) to an Appel reaction smoothly resulted in formation of dibromide **II.62**, which was converted into the corresponding pillar[n]arenes by treatment with paraformaldehyde in the presence of boron trifluoride diethyl etherate, analogous to the synthesis of **II.13**.^[135] Interestingly, a 59:9 mixture of the respective pillar[5]arene **II.63** and the pillar[6]arene **II.64** was obtained, the structures of which could be confirmed by X-ray analysis of single crystals (Figures II.21 and II.22).

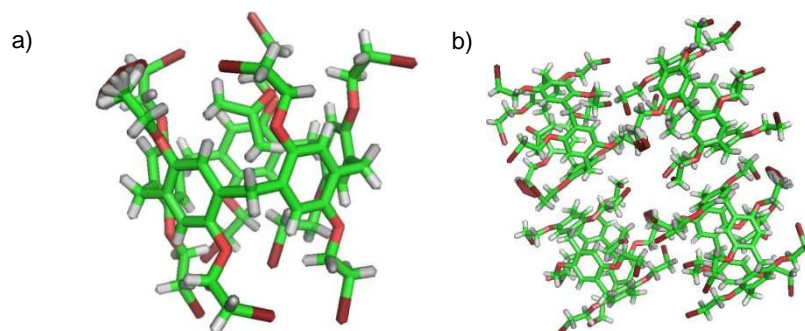


Figure II.21: Crystal structure of bromoethoxy-substituted pillar[5]arene (**II.63**): a) Illustration of a single molecule; b) unit cell, view along the b-axis.

Bromoethoxy-substituted pillar[5]arene **II.63** crystallized as an acetone solvate in the triclinic space group $P2_1/c$. The unit cell contains four equivalents of **II.63**·acetone with the solvent residing inside the cavity of **II.63**. The $-\text{CH}_2-$ moieties building the rims of the five-membered rings arrange in a planar fashion ($\angle_{\text{Ar}-\text{CH}_2-\text{Ar}} = 108^\circ$ for all $-\text{CH}_2-$ rims).

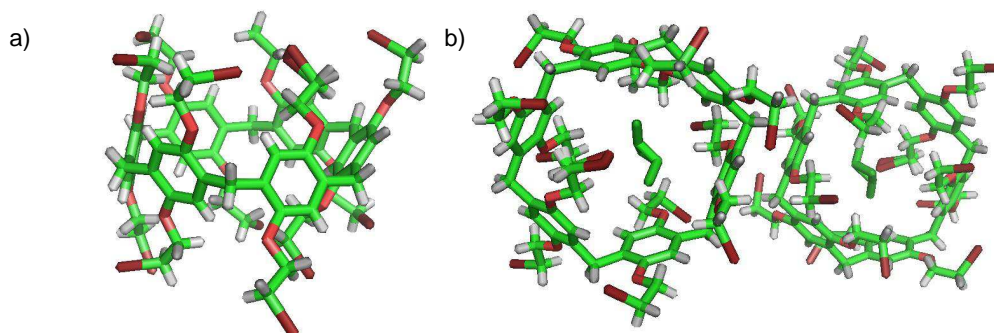
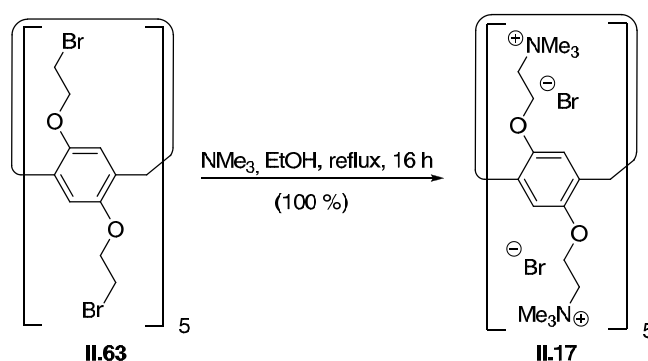


Figure II.22: Preliminary representation of the crystal structure of bromoethoxy-substituted pillar[6]arene (**II.64**): a) Illustration of a single molecule (solvent molecules are removed for clarity); b) unit cell, view along the a-axis, solvent molecules are not resolved.

Bromoethoxy-substituted pillar[6]arene (**II.64**) crystallized in the triclinic space group $P(-1)$. In contrast to the structures of pillar[5]arenes, the $-\text{CH}_2-$ rims are twisted and thus do not form the characteristic pillar-shaped structure. An explanation for this could be a significant

release of strain. In a hypothetical pillar-shaped structure in which the $-\text{CH}_2-$ rims arrange in a planar fashion, the bond angles of the methylene bridges would adopt values of 120° . However, in **II.64** the bond angles $\angle_{\text{Ar}-\text{CH}_2-\text{Ar}}$ adopt values of 111.0° , 113.8° , 114.7° , 115.1° , 115.9° and 116.5° , which are closer to the tetrahedral angle of 109° . According to a detailed literature search, this is the first example of a crystal structure of a pillar[6]arene to date. Further refinement of the structure is still in progress.

Bromoethoxy-substituted pillar[5]arene (**II.63**) was now converted into water-soluble compounds suitable for biological experiments. Starting from **II.63**, decatrimethylammonium salt **II.17** was prepared in one step (Scheme II.12).



Scheme II.12: Synthesis of trimethylammonium bromide-substituted pillar[5]arene (**II.17**).

Heating of **II.63** in the presence of an ethanolic trimethylamine solution afforded trimethylammonium bromide-substituted pillar[5]arene (**II.17**) in a quantitative yield.^[135] X-ray analysis of a single crystal confirmed the structure of **II.17** (Figure II.23).

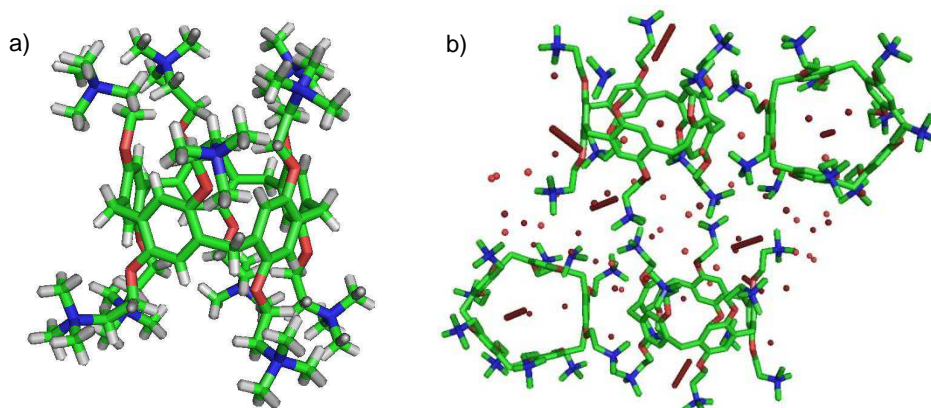
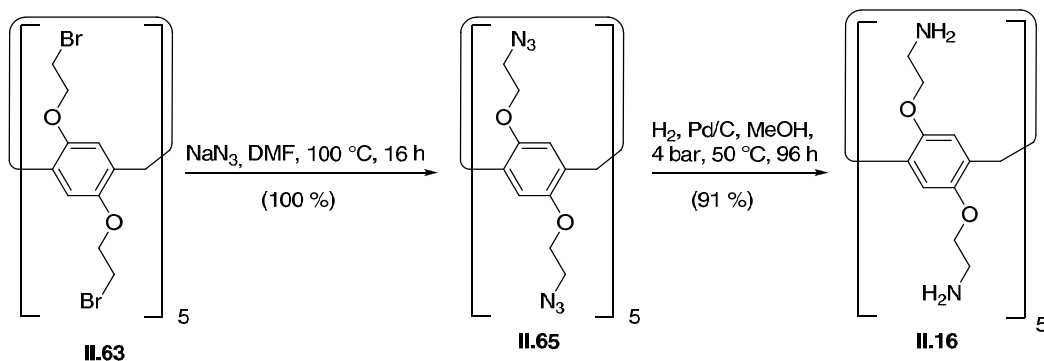


Figure II.23: Preliminary representation of the crystal structure of trimethylammonium bromide-substituted pillar[5]arene (**II.17**): a) Illustration of a single molecule (solvent molecules and counter ions are removed for clarity); b) unit cell, view along the ab -axis (water molecules and bromide counter ions are shown, hydrogens are removed for clarity).

Compound **II.17** crystallized as an aqueous solvate, in which the bromide counter ions as well as water molecules are highly disordered. The monoclinic cell with the space group $P2_1/c$ contains four molecules of **II.17**, which are oriented in an approximate 60° angle towards each other. Further refinement of the structure is still in progress.

Finally, conversion of **II.63** into an aminofunctionalized pillar[5]arene (**II.16**) was approached, which was achieved by following a modified literature procedure (Scheme II.13).



Scheme II.13: Synthesis of decaamine **II.16**.

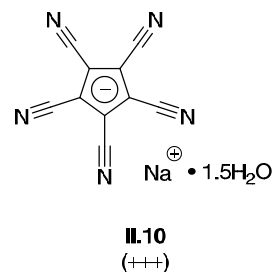
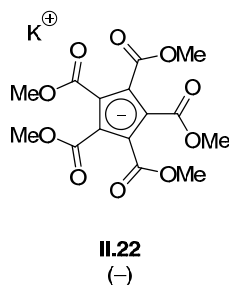
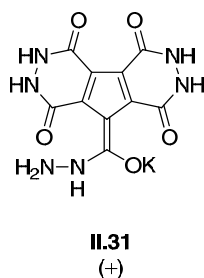
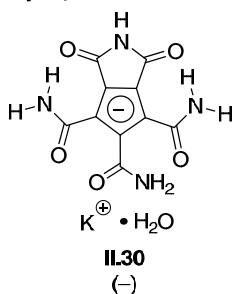
Decabromide **II.63** was converted into decaazide **II.65** by a simple $\text{S}_{\text{N}}2$ displacement in quantitative yield.^[136] The subsequent reduction to the corresponding amine **II.16** proved to be difficult and in initial attempts, complex mixtures of amino- and azide-functionalized pillar[5]arenes were obtained. After some optimization, it was found that the reaction works best if the hydrogenation catalyst is added portionwise over a period of four days.

With a set of fivefold symmetric compounds of different sizes featuring a number of diverse functional groups in hands, first biological studies were carried out, the preliminary results of which are described in the next section.

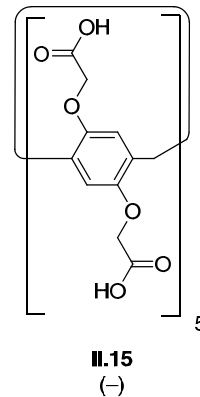
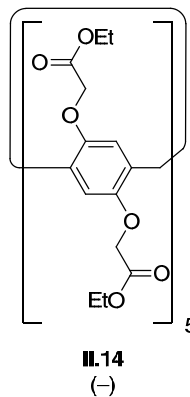
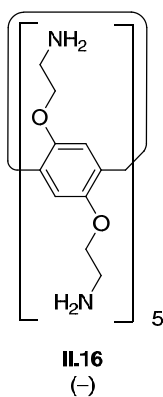
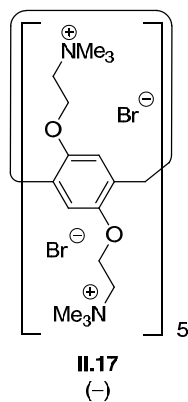
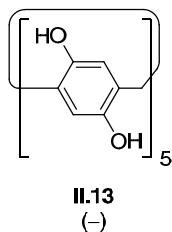
2.2.3 Outline on Biological Studies

Biological studies were carried out in collaboration. The results that are briefly summarized in this section were obtained by Valentina Carta and Roland Baur in the laboratory of Prof. Dr. Erwin Sigel at the Institute of Biochemistry and Molecular Medicine, University of Bern. Pharmacological activity of the herein reported fivefold symmetric molecules was investigated using the two-electrode voltage-clamp technique in *Xenopus* oocytes expressing GABA_A receptors. The results of the tested compounds are summarized in Figure II.24.

Cyclopentadienides:



Pillar[5]arenes:



Cucurbit[5]urils

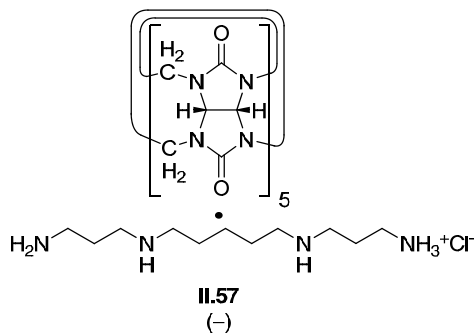
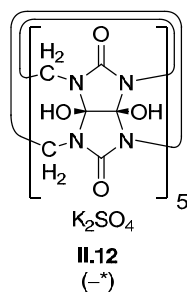
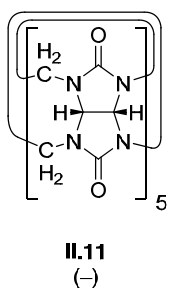


Figure II.24. Biological activity of fivefold symmetric compounds on the GABA_A receptor (+++ IC₅₀ < 10 μM; + IC₅₀ < 100 μM; - IC₅₀ > 100 μM; *compound seems to act as an allosteric modulator).

Among the cyclopentadienides, **II.30** and **II.22** were found to be inactive on the $\alpha_1\beta_2\gamma_2$ (wild type) GABA_A receptor, whereas **II.31** was shown to be a weak inhibitor ($IC_{50} < 100 \mu\text{M}$). **II.10**, on the other hand, was found to be highly active ($IC_{50} < 10\mu\text{M}$). Interestingly, it both stimulates and inhibits GABA_A currents. All pillar[5]arenes (**II.13**, **II.17**, **II.16**, **II.14**, **II.15**) and the cucurbit[5]urils **II.11** and **II.57** were found to be inactive. However, decahydroxycucurbit[5]uril (**II.12**) seemed to act as a low affinity positive allosteric modulator on the $\alpha_1\beta_2\gamma_2$ (wild type) GABA_A receptor, since **II.12** stimulated currents mediated by the channel. Further studies on this interesting observation are currently carried out by Valentina Carta in the Sigel laboratories.

Subsequently, the mode of action of **II.10** was studied in more detail. Current traces illustrating typical experiments on $\alpha_1\beta_2\gamma_2$ (wild type) GABA_A receptors that were expressed in *Xenopus* oocytes are shown at GABA concentrations eliciting about 1% or 10% of the maximal current amplitude (EC_{10} or EC_{10}) in Figures II.25 and II.26, respectively. The outward currents observed at very high concentrations of **II.10** are due to direct effects of **II.10** on membranes (not shown).

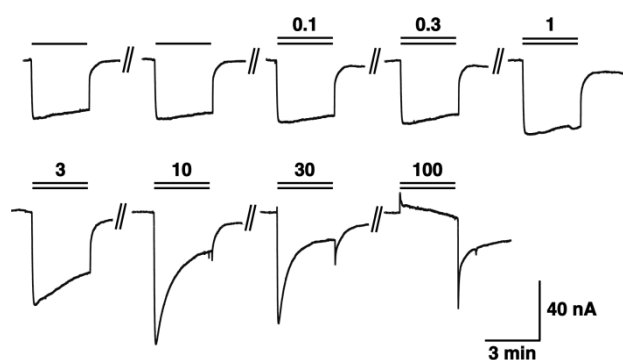


Figure II.25: TEVC recording of *Xenopus* oocytes expressing the $\alpha_1\beta_2\gamma_2$ (wild type) GABA_A receptor: Experiments were carried out at a GABA (**II.1**) concentration eliciting about 1% of the maximal current amplitude (EC_{10} ; $1\mu\text{M}$). Drug application was during 3 min. The lower bar indicates the application of **II.1**, the upper bar the application of Na pccp (**II.10**). The numbers indicate the concentration of **II.10** in μM .

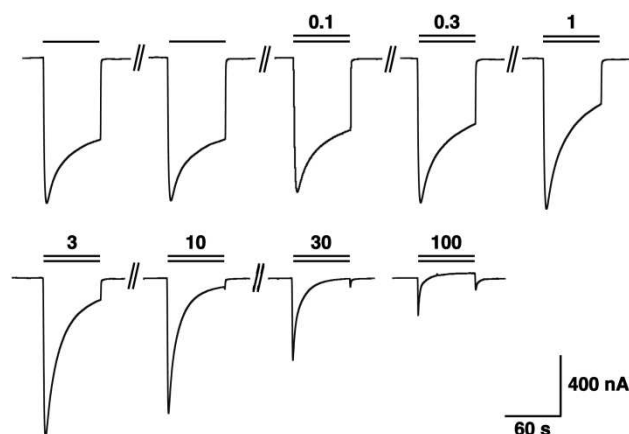


Figure II.26: TEVC recording of *Xenopus* oocytes expressing the $\alpha_1\beta_2\gamma_2$ (wild type) GABA_A receptor: Experiments were carried out at a GABA (II.1) concentration eliciting about 10% of the maximal current amplitude (EC₁₀; 7 μM). Drug application was during 1 min. The lower bar indicates the application of II.1, the upper bar the application of Na pccp (II.10). The numbers indicate the concentration of II.10 in μM.

At lower concentrations (1–10 μM), II.10 enhances currents elicited by low concentrations of GABA (II.1). The degree of stimulation is variable between individual oocytes. At concentrations > 1 μM, II.10 induces an open-channel block, characterized by an apparent desensitization of the current and an off-current (Figures II.25 and II.26, second row). As expected, this block becomes more prominent with increasing II.10 concentrations, whereas stimulation becomes less visible. Figure II.27 summarizes four experiments for each condition shown in Figures II.25 and II.26 (n = 4, SEM).

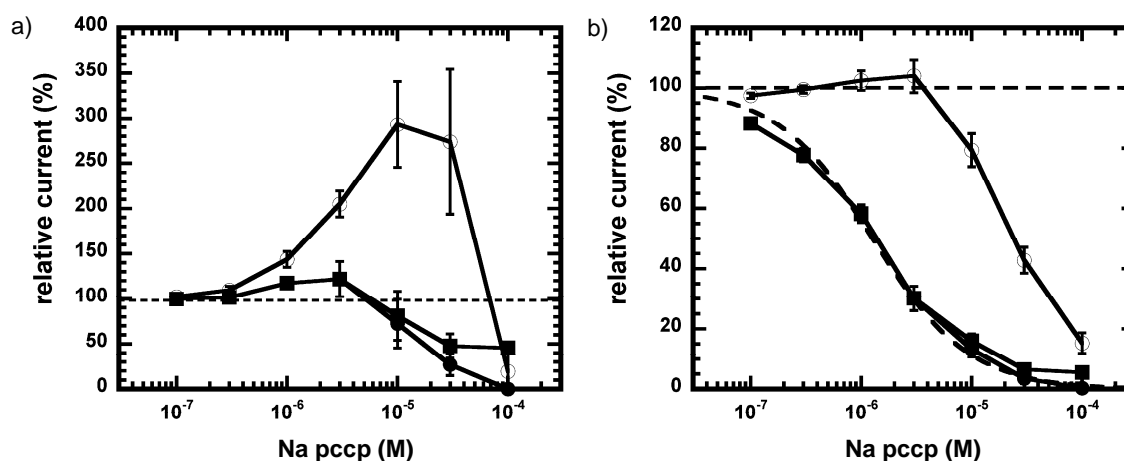


Figure II.27: Summary over four experiments as shown in Figure II.25 (a) and Figure II.26 (b): Open circles: Peak current amplitudes at the beginning of the drug application. Filled squares: Current amplitudes at the end of the drug application. Filled circles: Current amplitudes at the end of the drug application corrected for the effect of II.10 on membranes.

Subsequently, the concentration inhibition curve of **II.10** obtained for $\alpha_1\beta_2\gamma_2$ was compared with that of $\alpha_1\beta_1\gamma_2$ and $\alpha_1\beta_2\delta$ GABA_A receptors (Figure II.28).

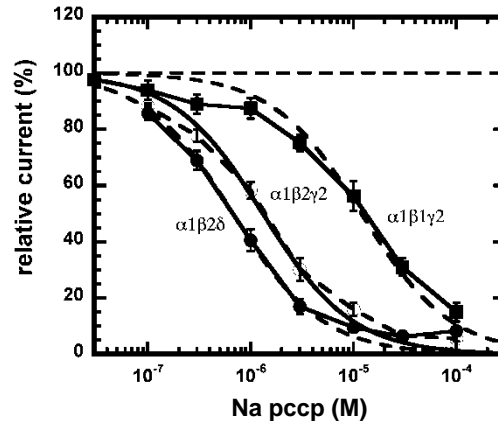


Figure II.28: Concentration-inhibition curve obtained from $\alpha_1\beta_2\gamma_2$, $\alpha_1\beta_1\gamma_2$ and $\alpha_1\beta_2\delta$ GABA_A receptors.

It was found that **II.10** acts on all investigated GABA_A receptor isoforms and did show some selectivity. **II.10** shows the most potent inhibition on the $\alpha_1\beta_2\delta$ isoform ($IC_{50} 0.7 \pm 0.3 \mu M$), whereas the effect on the $\alpha_1\beta_1\gamma_2$ isoform is less potent ($IC_{50} 13 \pm 5 \mu M$). The IC_{50} of **II.10** on $\alpha_1\beta_2\gamma_2$ (wild type) receptors was determined to be $1.4 \pm 0.5 \mu M$.

In *Drosophila*, the mutation RDL in the GABA_A receptor has been described to confer resistance to the insecticide dieldrin and partial resistance to picrotoxin (**II.6**). The RDL mutation Ala301Ser is located in the transmembrane region M2. It was interesting to compare *Drosophila* wild type and RDL mutant GABA_A receptor in the irrespective responses to picrotoxin (**II.6**) and Na pccp (**II.10**). Results of these experiments are shown in Figure II.29.

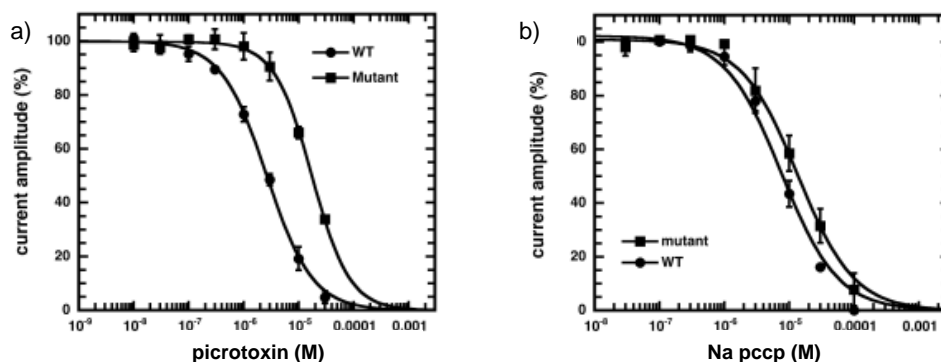


Figure II.29: Concentration-inhibition curves in *Drosophila* wild type GABA_A receptors and mutant receptors carrying the RDL resistance mutation: a) Picrotoxin (**II.6**); b) Na pccp (**II.10**).

While there is an about 7-fold shift in the IC_{50} in response to the mutation for **II.6**, there is a less than 2-fold shift for **II.10**. This suggests that **II.10** still will affect insects carrying this mutation.

In order to gain further insights into the detailed mode of action and the binding site of **II.10**, cysteine mutations in the M2 domain were introduced into amino acids, which are oriented towards the channel lumen and the behavior of **II.10** and **II.6** was monitored. In order to increase the effect by the mutation, the cysteine-reactive compound MTSET was used. Preliminary results indicate different binding modes for **II.10** compared to **II.6**. These experiments are presently being carried out by Valentina Carta in the laboratory of the Sigel group.

2.2.4 Summary, Conclusions and Outlook

Based on the idea of the symmetry approach, a library of fivefold symmetric compounds has been synthesized. The compound library includes water-soluble cyclopentadienide, cucurbit[5]uril and pillar[5]arene derivatives (Figure II.30). In preliminary studies, the compounds were tested for their biological activity on the $GABA_A$ receptor.

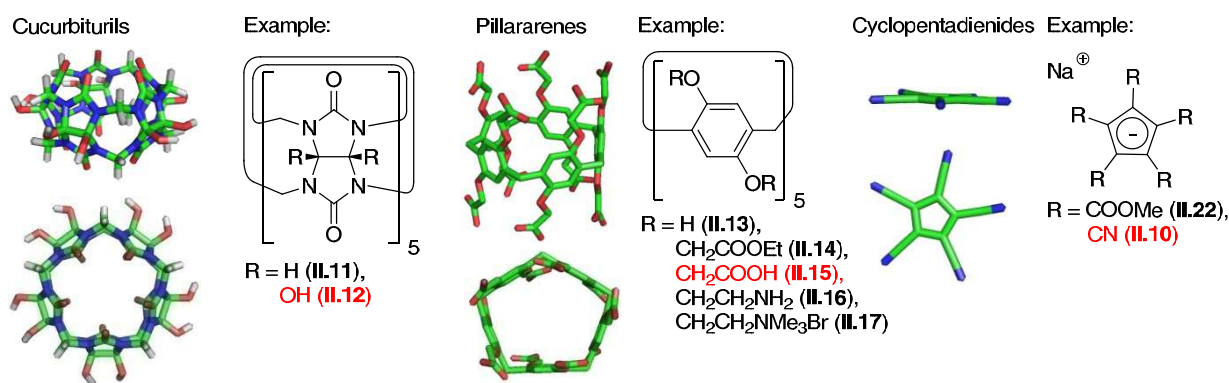


Figure II.30: Chemical structure and shape on the basis of selected crystal structures of fivefold symmetric small molecules prepared for the symmetry approach.

Pleasingly, it was found that some of the fivefold symmetric compounds are biologically active and indeed, pentameric ion channels are targets of these molecules. More specifically, it was **II.10** that was found to be highly biologically active on the $GABA_A$ receptor. At high concentrations, **II.10** acts as an open channel blocker of the $GABA_A$ receptor with an

efficiency of inhibition comparable to that of picrotoxin ($IC_{50} = 1.3 \mu M$). In cooperation with the group of Prof. Dr. Sigel at the Institute of Biochemistry and Molecular Medicine, University of Bern, its detailed mode of action and its potential application as an insecticide is currently being investigated.

Thus, the initial idea of the symmetry-based approach towards new ion channel blockers, which was affirmed by model studies, led to the development of a highly biologically active compound, which indeed targets a pentameric ion channel.

Future work will have to consist of the development of synthetic routes for the preparation of analogues of the cucurbit[5]urils and the pillar[5]arenes to access further frameworks and more functional groups. In the course of these studies, it would be reasonable to investigate the potential of the formation of five-membered rings of other macrocyclic compounds such as the bambus[n]urils (**II.66**)^[137] and the as[n]arenes (**II.67**)^[138] (Figure II.31).

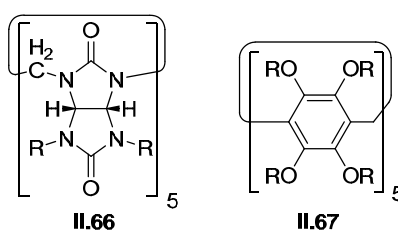


Figure II.31: Chemical structures of generic bambus[5]urils (**II.66**) and as[5]arenes (**II.67**) as potential future fivefold symmetric carbon frameworks for the symmetry approach.

Furthermore, the compounds will be tested on many more pentameric proteins in order to fully evaluate their biological profiles. These studies are currently carried out in various collaborations, the results of which will be presented in due course.

2.3 Experimental Section

General experimental details:

Unless specified otherwise, all reactions were performed with magnetic stirring under an atmosphere of argon and in oven-dried glassware. Isolated products were dried on a high vacuum line at a pressure of 10^{-2} mbar using an *ATB-Loher* oil pump by *Flender*. Diethyl ether and tetrahydrofuran (THF) were distilled prior to use from sodium and benzophenone. Dimethylformamide (DMF), 1,2-dimethoxyethane (DME), 1,2-dichloroethane (DCE), chloroform (CHCl_3), ethanol (EtOH), methanol (MeOH), acetonitrile (MeCN) and acetone (Me_2CO) were purchased from *Acros Organics* as 'extra dry' reagents under inert gas atmosphere and over molecular sieves. All other reagents were purchased from commercial sources and used without further purification. Petroleum ether is referred to as hexanes and relates to fractions of isohexanes, which boil between 40 °C and 80 °C. Reactions were monitored by TLC using *E. Merck* 0.25 mm silica gel 60 F₂₅₄ glass plates. TLC plates were visualized by exposure to UV light (254 nm) and subsequent treatment with an aqueous solution of CAM, an aqueous solution of potassium permanganate, an aqueous acidic solution of vanillin, a solution of ninhydrin or a mixture of silica and finely grounded iodine, followed by heating the plate with a heat gun. If appropriate, reactions were additionally monitored by proton nuclear magnetic resonance (¹H-NMR) using a *Varian 200* spectrometer or LCMS using an *Agilent Technologies 1260 infinity* machine equipped with an *Agilent ZORBAX Eclipse Plus C18* reversed phase analytical 4.6 mm x 150 mm column. Flash column chromatography was performed as described by *Still et al.* employing silica gel (60 Å, 40-63 µm, *Merck*) at a pressure of approx. 1.3-1.5 bar generated by a gentle nitrogen flow.^[94] Reversed phase (RP) column chromatography was performed on *Waters* silica gel (Preparative C18, 125Å, 55-105 µm) with the same techniques as described above. Analytical RP TLC was performed using pre-coated glass plates (silica gel C18 RP-18W/UV254) from *Macherey-Nagel*. Yields refer to isolated and spectroscopically pure compounds.

Instrumentalization:

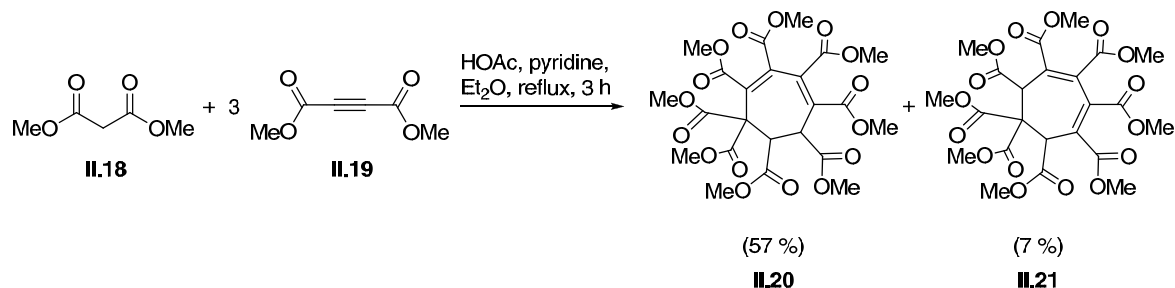
Infrared (IR) spectra were recorded on a *Perkin Elmer Spectrum BX II* (FTIR System), equipped with an attenuated total reflection (ATR) measuring unit. IR data is reported in frequency of absorption (cm^{-1}).

Proton nuclear magnetic resonance ($^1\text{H-NMR}$) spectra were recorded on a *Varian 300*, *Varian 400*, *Inova 400* or *Varian 600* spectrometer. Chemical shifts (δ scale) are expressed in parts per million (ppm) and are calibrated using residual protic solvent as an internal reference (CDCl_3 : $\delta = 7.26$ ppm, $(\text{D}_3\text{C})_2\text{CO}$: $\delta = 2.05$ ppm, $(\text{CD}_3)_2\text{SO}$: $\delta = 2.50$ ppm, $\text{CD}_3\text{OD} = 3.31$ ppm, $\text{D}_2\text{O} = 4.79$ ppm).^[95] Unless noted otherwise, data was recorded at 27 °C. Data for $^1\text{H-NMR}$ spectra are reported as follows: chemical shift (δ ppm) (multiplicity, coupling constants (Hz), integration). Couplings are expressed as: s = singlet, d = doublet, t = triplet, q = quartet, m = multiplet, br = broad, app = apparent or combinations thereof. Carbon nuclear magnetic resonance ($^{13}\text{C-NMR}$) spectra were recorded on the same spectrometers at 75, 100 and 150 MHz, respectively. Carbon chemical shifts (δ scale) are also expressed in parts per million (ppm) and are referenced to the central carbon resonances of the solvents (CDCl_3 : $\delta = 77.16$ ppm, $(\text{D}_3\text{C})_2\text{CO}$: $\delta = 29.84$ ppm, $(\text{CD}_3)_2\text{SO}$: $\delta = 39.52$ ppm, $\text{CD}_3\text{OD} = 49.00$ ppm).^[95]

Mass spectroscopy (MS) experiments were performed on a *Thermo Finnigan MAT 95* (electron ionization, EI), on a *Thermo Finnigan LTQ FT* (electrospray ionization, ESI) or on a *Jeol JMS-700* (fast atom bombardment, FAB) instrument.

Melting points were measured on an *EZ-Melt* automated melting point apparatus made by *Stanford Research Systems* and are uncorrected.

Octamethyl cyclohepta-2,4-dien-1,1,2,3,4,5,6,7-octacarboxylate (II.20) and Octamethyl cyclohepta-3,5-dien-1,1,2,3,4,5,6,7-octacarboxylate (II.21):^[119]



To a solution of dimethyl acetylenedicarboxylate (**II.19**, 33.1 mL, 270 mmol, 3.00 eq) and dimethyl malonate (**II.18**, 10.3 mL, 90.0 mmol, 1.00 eq) in diethyl ether (60.0 mL) was added dropwise a mixture of pyridine and acetic acid (1:1 mixture by weight, 2.50 mL) and an exothermic reaction started, evidenced by intense refluxing of the solvent. When the intensity of reflux had ceased, the dark red mixture was heated to reflux for 2 h and was then allowed to cool to room temperature. The resulting precipitate was filtered off, washed with diethyl ether (30.0 mL) and dried to give a 57:7 mixture of **II.20** and **II.21** as a slightly buff yellow solid (32.1 g, 64 %), which was used without further purification.

mp: 215-219 °C.

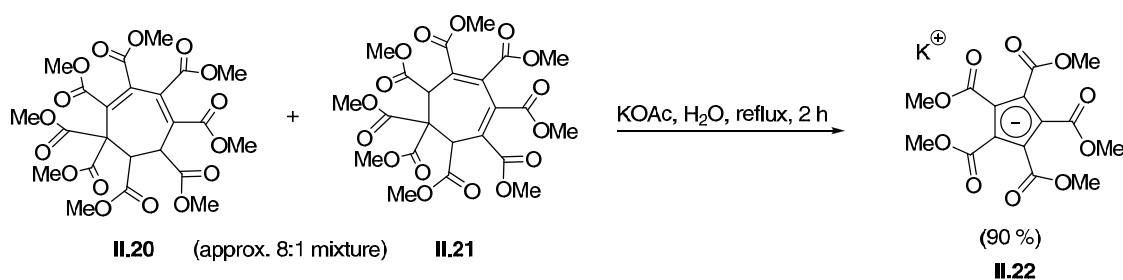
¹H NMR (300 MHz, CDCl₃, major isomer quoted): δ = 5.17 (d, *J* = 1.4 Hz, 1H), 3.90 (s, 6H), 3.76-3.74 (m, 7H), 3.73-3.71 (m, 12H).

¹³C NMR (75 MHz, CDCl₃, major isomer quoted): δ = 170.2, 169.3, 167.9 (2C), 166.0 (2C), 165.5, 164.5, 144.7, 140.5 (2C), 134.4, 63.8, 53.9, 53.3 (2C), 53.2 (2C), 52.8 (2C), 52.7, 47.8, 44.3.

IR (neat): $\tilde{\nu}_{\max}$ = 1726, 1238.

HRMS (ESI⁺): m/z calcd. for C₂₃H₂₆KO₁₆⁺: 597.0858 [M+K]⁺;
found: 597.0857 [M+K]⁺.

Potassium 1,2,3,4,5-pentacarbomethoxycyclopentadienide (II.22):^[119]



A mixture of **II.20** and **II.21** as obtained from the previous reaction (27.5 g, 49.2 mmol, 1.00 eq), water (140 mL) and potassium acetate (45.5 g, 464 mmol, 9.40 eq) was heated to reflux for 2 h with vigorous stirring. After hot filtration, the mixture was allowed to cool to room temperature and subsequently cooled to 4 °C over four days. The resulting precipitate was collected, washed with ice water (5.00 mL) and dried to afford **II.22** as a yellow solid (17.5 g, 90 %).

mp: 217-218 °C.

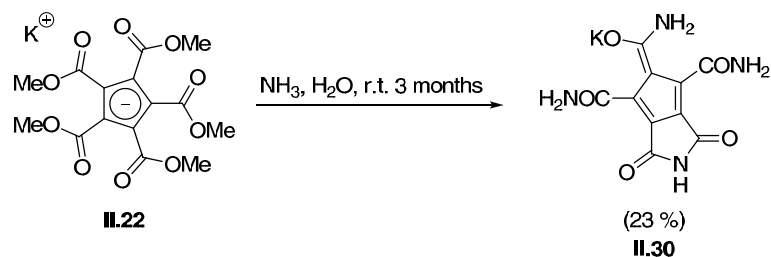
¹H NMR (400 MHz, D₂O): δ = 3.63 (s, 15H).

¹³C NMR (100 MHz, D₂O): δ = 169.0 (5C), 116.7 (5C), 52.3 (5C).

IR (neat): $\tilde{\nu}_{\text{max}}$ = 1678, 1456, 1172.

HRMS (ESI⁻): m/z calcd. for C₁₅H₁₅O₁₀⁻: 355.0671 [M-K]⁻;
found: 355.0663 [M-K]⁻.

Potassium amino(4,6-dicarbamoyl-1,3-dioxo-2,3-dihydrocyclopenta[c]pyrrol-5(1H)-ylidene)methanolate (II.30):



Potassium salt **II.22** (4.50 g, 11.4 mmol, 1.00 eq) was dissolved in a 30 % aq. ammonium hydroxide solution (75.0 mL) and was allowed to stand at room temperature for three months.

The product slowly crystallized, was then collected, washed with water and dried to afford **II.30** as large yellow crystals (820 mg, 23 %), which were suitable for X-ray crystallography.

mp: 310 °C (dec.).

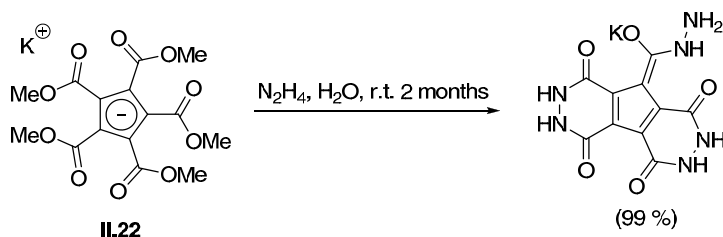
¹H NMR (400 MHz, *d*₆-DMSO): δ = 9.38 (s, br, 1H), 7.89 (s, br, 2H), 6.53 (s, br, 4H).

¹³C NMR (100 MHz, *d*₆-DMSO): δ = 171.0, 170.0 (2C), 165.8 (2C), 134.4, 119.1 (2C), 115.0 (2C).

IR (neat): $\tilde{\nu}_{\max}$ = 3463, 1650, 1426.

HRMS (ESI⁻): m/z calcd. for C₁₀H₇N₄O₅⁻: 263.0422 [M]⁻;
found: 263.0420 [M]⁻.

Potassium bis(1,4-dioxo-3,4-dihydro-1H-cyclopenta[d]pyridazin-5(2H)-ylidene)(hydrazinyl)methanolate (II.31):



A mixture of **II.22** (2.96 g, 7.50 mmol, 1.00 eq) and a 24 % aq. hydrazine hydrate solution (50.0 mL, 242 mmol, 32.0 eq) was allowed to stand at room temperature for 2 months. The resulting precipitate was filtered off, washed with hot water (2 x 25.0 mL) and dried to afford **II.31** as an amorphous powder (2.45 g, 99 %).

mp: ca. 340 °C (dec.).

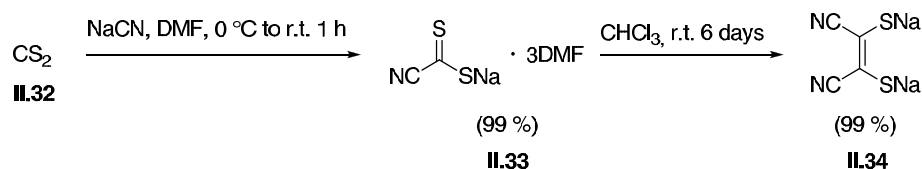
¹H NMR (400 MHz, *d*₆-DMSO): δ = 15.57 (s, 1H), 14.27 (s, 1H), 13.90 (s, 1H), 11.48 (s, 1H), 11.34 (s, 1H), 4.77 (s, br, 2H).

¹³C NMR (100 MHz, *d*₆-DMSO): δ = 165.7, 160.8, 160.1, 153.1 (2C), 123.1, 121.9, 115.2, 112.6, 105.2.

IR (neat): $\tilde{\nu}_{\max}$ = 2975, 1607, 1474, 1413.

HRMS (ESI⁻): m/z calcd. for C₁₀H₇N₆O₅⁻: 291.0483 [M]⁻;
 found: 291.0481 [M]⁻.

Sodium cyanodithioformiate·3DMF (II.33)^[121] and **disodium dimercaptomaleonitrile (II.34)**^[122]



A mixture of sodium cyanide (73.5 g, 1.50 mol, 1.00 eq) and DMF (440 mL, 5.68 mol, 3.80 eq) was cooled to 0 °C and CS₂ (**II.32**, 90.5 mL, 1.50 mmol, 1.00 eq) was added dropwise over a period of 15 min. After complete addition, the mixture was allowed to warm up to be stirred for 30 min at room temperature, upon which time crystallization occurred. The resulting red-brown slurry was diluted with isobutanol (185 mL), heated to 115 °C until the product had completely dissolved (10 min), filtered and allowed to cool to room temperature. The mixture was cooled to -10 °C, the resulting crystalline product was filtered off, washed with diethyl ether (500 mL) and dried. Sodium cyanodithioformiate·3DMF (**II.33**) was obtained as large red-brown needles (510 g, 99 %), which was used in the subsequent reaction without further purification.

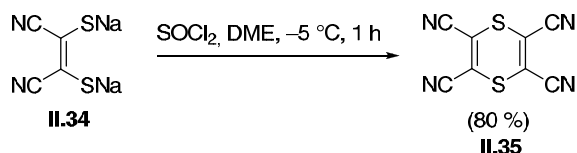
Sodium cyanodithioformiate·3DMF (**II.33**, 445 g, 1.30 mol) was suspended in chloroform (1.40 L) and stirred until a clear solution was obtained. Then, the mixture was allowed to stand at room temperature for six days. The resulting solid was filtered off, washed with chloroform (350 mL) and diethyl ether (1.30 L) and dried. Methanol (260 mL) was added and the mixture was heated until a suspension containing small, insoluble particles was obtained. After hot filtration, the filtrate was allowed to cool to room temperature and the product was precipitated by addition of diethyl ether (1.50 L) and vigorous stirring. Disodium dimercaptomaleonitrile (**II.34**) was obtained as a yellow powder, which was filtered off and dried (110 g, 92 %). An analytical sample was further purified by recrystallization from ethanol.

mp: ca. 300 (dec.).

¹³C NMR (100 MHz, *d*₆-DMSO): δ = 126.5 (2C), 124.1 (2C).

IR (neat): $\tilde{\nu}_{\max} = 3348, 2193, 1438, 1113$.

Tetracyano-1,4-dithiin (II.35):^[123]



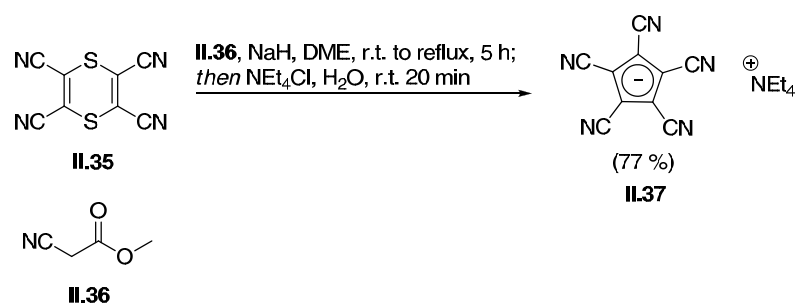
A suspension of **II.34** (64.0 g, 344 mmol, 1.00 eq) in DME (225 mL) was cooled to $-5\text{ }^\circ\text{C}$ (internal temperature) and a solution of thionyl chloride (24.9 mL, 344 mmol, 1.00 eq) in DME (30.0 mL) was added with a syringe pump over the course of 60 min. The resulting yellow suspension was allowed to warm to room temperature over a period of 60 min, filtered and the filter cake was washed with DME (3 x 60.0 mL). The combined filtrates were poured into a mixture of a sat. aq. NaHCO_3 solution (1.00 L) and ice water (2.00 L). The resulting precipitate was filtered off, washed with water (3 x 400 mL) and dried. (Note: If not all compounds employed in this reaction were carefully purified prior to use and if the temperature was not carefully controlled, instead of a buff yellow solid a dark brown or black solid may be obtained, from which only small quantities of **II.35** can be attained.) Recrystallization of the crude product from 1,2-dichloroethane provided **II.35** as a dark yellow crystalline solid (25.8 g, 80 %).

mp: $206\text{ }^\circ\text{C}$.

^{13}C NMR (100 MHz, *d*₆-DMSO): $\delta = 125.9$ (4C), 112.8 (4C).

IR (neat): $\tilde{\nu}_{\max} = 2229, 1519, 1158$.

A small sample was recrystallized from toluene to afford a toluene solvate of **II.35** as large, dark brown needles, which were suitable for X-ray crystallography.

Tetraethylammonium pccp (II.37):^[124]

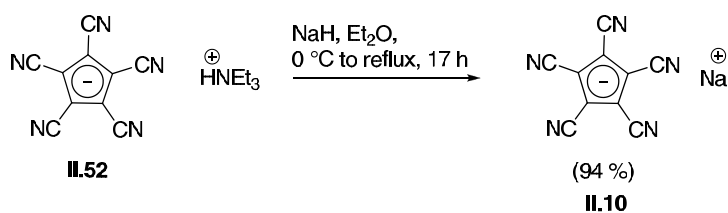
To a suspension of sodium hydride (3.12 g, 123 mmol, 2.00 eq) in DME (450 mL) was added methyl cyanoacetate (**II.36**, 5.50 mL, 61.7 mmol, 1.00 eq) at 0 °C. After gas evolution had ceased (1 h), **II.35** (13.4 g, 61.7 mmol, 1.00 eq) was added and the mixture was allowed to warm to room temperature. After being stirred for 2 h at this temperature, the mixture was heated to reflux for 3 h. The resulting red colored mixture was allowed to cool to room temperature and concentrated to dryness. Water (650 mL) was added and the mixture was filtered. To the filtrate was added tetraethylammonium chloride (10.2 g, 61.7 mmol, 1.00 eq) and the mixture was stirred for 20 min at room temperature. The resulting yellow precipitate was filtered off and dried. The solid was redissolved in concd. nitric acid (175 mL) at 0 °C and filtered. To the filtrate was added ice water (1350 mL) and the resulting precipitate was filtered off and dried to afford **II.37** as a slightly yellow powder (7.60 g, 77 %).

mp: 359-361 °C.

¹³C NMR (100 MHz, *d6*-DMSO): δ = 113.5 (5C), 102.2 (5C), 51.8 (t, J = 3.0 Hz, 4C), 7.5 (4C).

IR (neat): $\tilde{\nu}_{\max}$ = 2215, 1469.

HRMS (ESI⁻): m/z calcd. for C₁₀N₅⁻: 190.0154 [M-Et₄N]⁻;
found: 190.0157 [M-Et₄N]⁻.

Sodium pccp (II.10):

To a suspension of **II.52** (1.10 g, 3.80 mmol, 1.00 eq) in diethyl ether (60.0 mL) was added sodium hydride (106 mg, 4.18 mmol, 1.10 eq) at 0 °C. After gas evolution had ceased, the mixture was allowed to warm to room temperature and then heated to reflux for additional 17 h. The mixture was concentrated to dryness and purified by RP column chromatography (water:MeOH 99:1 → 90:10) to afford **II.10** as a yellow solid (761 mg, 94 %).

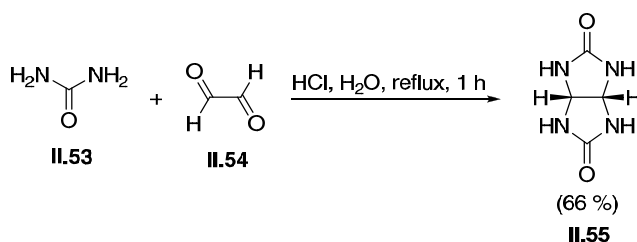
mp: 369-370 °C.

^{13}C NMR (100 MHz, *d*₆-DMSO): δ = 113.5 (5C), 102.2 (5C).

IR (neat): $\tilde{\nu}_{\text{max}}$ = 2226, 1656, 1482.

HRMS (ESI⁻): m/z calcd. for C₁₀N₅⁻: 190.0154 [M-Na]⁻;
found: 190.0159 [M-Na]⁻.

Crystals suitable for X-ray analysis were obtained by slowly evaporating the solvent of a solution of **II.10** in acetone, which afforded an acetone solvate of **II.10** as a colorless solid.

Glycoluril (II.55):^[127]

To a mixture of urea (**II.53**, 100 g, 1.67 mol, 2.60 eq) and water (200 mL) was added a 40 % aq. glyoxal solution (**II.54**, 73.5 mL, 640 mmol, 1.00 eq) and concd. aq. HCl (37 % in water, 8.90 mL, 64.0 mmol, 0.100 eq). The mixture was heated to 85 °C for 1 h, after which time a precipitate had formed. The mixture was then allowed to cool to room temperature. The precipitate was filtered off, washed with water (200 mL) and acetone (500 mL) and was dried *in vacuo* to give glycoluril (**II.55**) as a colorless solid (60.0 g, 66 %).

mp: ca. 310 °C (dec.).

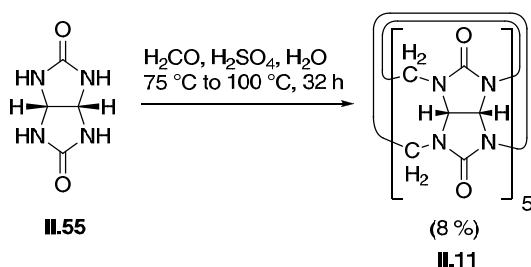
¹H NMR (300 MHz, *d*₆-DMSO): δ = 7.12 (s, 4H), .2 (s, 2H).

¹³C NMR (75 MHz, *d*₆-DMSO): δ = 161.7 (2C), 65.0 (2C).

IR (neat): $\tilde{\nu}_{\max}$ = 3158, 1681.

HRMS (ESI⁺): m/z calcd. for C₄H₆N₄O₂⁺: 142.0491 [M]⁺;
found: 142.0489 [M]⁺.

Cucurbit[5]uril (II.11).^[128]



A mixture of glycoluril (**II.55**, 56.8 g, 0.400 mol, 1.00 eq) and halfconcd. aq. sulfuric acid (9.00 M, 200 mL, 1.42 mol, 3.55 eq) was heated to 70 °C. At this temperature, a 40 % aq. formaldehyde solution (70.0 mL, 0.920 mol, 2.30 eq) was added over the course of 15 min. After being stirred at 75 °C for 24 h, the temperature was raised to 100 °C and the mixture was stirred for 12 h at this temperature. The resulting mixture was allowed to cool to room temperature and was diluted with water (0.500 L) and acetone (10.0 L). The resulting precipitate was filtered off, washed with acetone (1.00 L) and dried.

Then, water (2.00 L) was added and the resulting suspension was stirred vigorously for 15 min at room temperature. The mixture was filtered and to the filtrate was added acetone (8.00 L) to form a precipitate. The resulting solid was filtered off and diluted with a 1:1 mixture of water/methanol (2.00 L). The mixture was filtered and the filtrate was concentrated to form a precipitate, which was dried. The dried powder was dissolved in a 1 M aq. H₂SO₄ solution (65.0 mL) and upon slow cooling to 0 °C, cucurbit[5]uril (**II.11**) was furnished as a colorless, crystalline solid (5.33 g, 8 %).

mp: 286 (dec.).

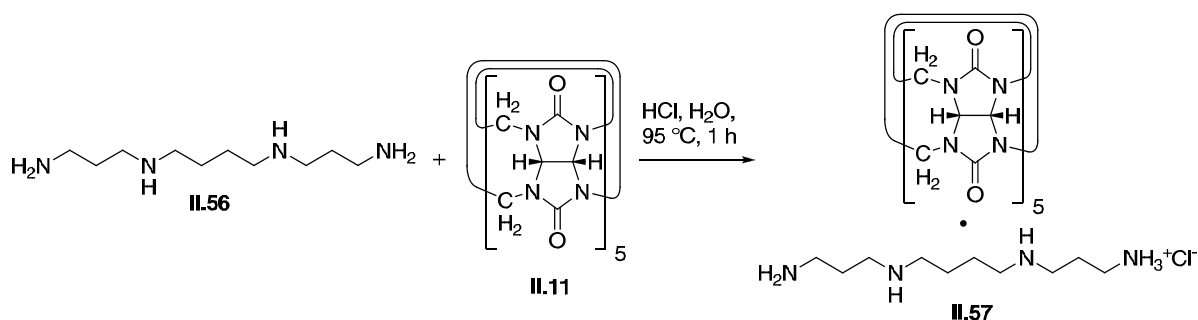
¹H NMR (600 MHz, *d*₆-DMSO): δ = 5.52-5.43 (m, 20H), 4.52 (d, *J* = 15.1 Hz, 10H).

^{13}C NMR (150 MHz, *d6*-DMSO): $\delta = 155.6$ (10C), 68.4 (10C), 49.7 (10C).

IR (neat): $\tilde{\nu}_{\text{max}} = 1733, 1470, 1182$.

HRMS (FAB⁺): m/z calcd. for $\text{C}_{30}\text{H}_{30}\text{N}_{20}\text{O}_{10}^+$: 848.2792 [M+NH₄]⁺;
found: 848.2750 [M+NH₄]⁺.

Sperminium chloride @ cucurbit[5]uril (**II.57**):^[132]



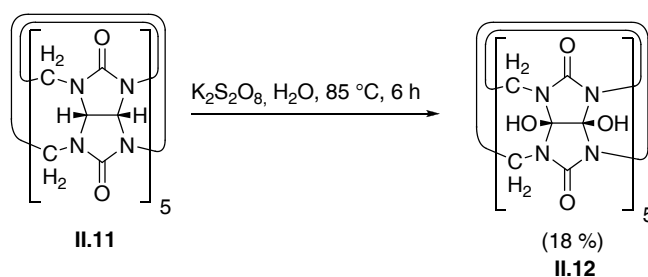
A mixture of spermine (**II.56**, 20.2 mg 0.100 mmol, 1.00 eq) and cucurbit[5]uril (**II.11**, 83.1 mg, 0.100 mmol, 1.00 eq) was suspended in a 16 % aq. HCl solution (3.75 mL, 18.8 mmol, 188 eq). The mixture was heated to 95 °C for 1 h and was then concentrated by evaporation of the solvent at 120 °C to afford **II.57** as a colorless powder.

mp: 278 (dec.).

^1H NMR (600 MHz, D₂O): $\delta = 5.65$ -5.46 (m, 20H), 4.37-4.25 (m, 10H), 3.35-2.99 (m, 16H), 2.09-2.03 (m, 5H), 1.71-1.65 (m, 5H).

^{13}C NMR (100 MHz, D₂O): $\delta = 156.4$ (10C), 69.0 (10C), 50.0 (10C), 46.9 (2C), 44.5 (2C), 36.5 (2C), 23.7 (2C), 22.7 (2C).

IR (neat): $\tilde{\nu}_{\text{max}} = 1730, 1474, 1184$.

Decahydroxycucurbit[5]uril (II.12):^[129]

A suspension of cucurbit[5]uril (**II.11**, 1.00 g, 1.20 mmol, 1.00 eq) and $\text{K}_2\text{S}_2\text{O}_8$ (4.69 g, 17.3 mmol, 14.4 eq) in water (60.0 mL) was degassed by irradiation with ultrasound while bubbling argon through the mixture for 20 min. Then, the mixture was heated to 85 °C for 6 h. Upon heating, a colorless solution was obtained, which became turbid after 90 min at the given temperature. The mixture was allowed to cool to room temperature, filtered and the filtrate was concentrated to a volume of 4.00 mL and cooled to 5 °C, by what K_2SO_4 precipitated. The remaining liquor was separated and concentrated to give a colorless solid, which was purified by HPLC (*Varian Dynamax 250x21.4 mm Microsorb 60-8 C18 column* equipped with a *Dynamax HPLC guard column* operating on a *Varian PrepStar HPLC system*; $\text{H}_2\text{O}/\text{MeCN}$; 60.0 mL/min) to afford **II.12** as a colorless solid (252 mg, 18 %).

HPLC (gradient program: $t = 0$ min 1 % MeCN, $t = 30$ min 30% MeCN, $t = 36$ min 30 % MeCN, $t = 40$ min 100 % MeCN): $R_t = 3.19$ min.

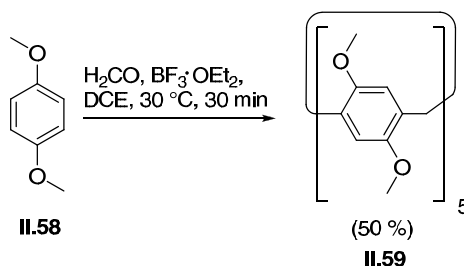
mp: 228 (dec.).

$^1\text{H NMR}$ (600 MHz, D_2O): $\delta = 5.32$ (d, $J = 15.9$ Hz, 10H), 4.45 (d, $J = 5.3$ Hz, 10H).

$^{13}\text{C NMR}$ (100 MHz, D_2O): $\delta = 153.8$ (10C), 93.7 (10C), 40.7 (10C).

IR (neat): $\tilde{\nu}_{\text{max}} = 1699, 1466, 1161$.

HRMS (ESI⁺):
 m/z calcd. for $\text{C}_{30}\text{H}_{30}\text{KN}_{20}\text{O}_{20}^+$: 1029.1582 [M+K]⁺;
 found: 1029.1581 [M+K]⁺.

Decamethoxypillar[5]arene (II.59):^[133]

To a solution of 1,4-dimethoxybenzene (**II.58**, 6.91 g, 50.0 mmol, 1.00 eq) in DCE (100 mL) was added paraformaldehyde (4.50 g, 150 mmol, 3.00 eq) in one portion. To this mixture was added dropwise boron trifluoride diethyl etherate (6.25 mL, 50.0 mmol, 1.00 eq) over the course of 10 min. The slightly green colored reaction mixture was heated to 30 °C for 30 min and was then allowed to cool to room temperature. The resulting black colored mixture was poured into methanol (500 mL) and the resulting precipitate was filtered off, washed with methanol (50.0 mL) and dried. The crude material was diluted with chloroform (150 mL) stirred for 15 min and filtered. The black filter cake was washed with hot chloroform (2 x 100 mL) and the combined filtrates were concentrated to a volume of 70.0 mL. Upon cooling to -25 °C, a precipitate formed, which was filtered off, washed with chloroform (10.0 mL) and acetone (100 mL) and dried. Concentrating the mother liquor and subsequent cooling to -25 °C afforded a second crop of product. **II.59** was obtained as a grey colored solid (combined yield: 3.77 g, 50 %).

TLC (CHCl₃:MeOH 100:1): $R_f = 0.43$.

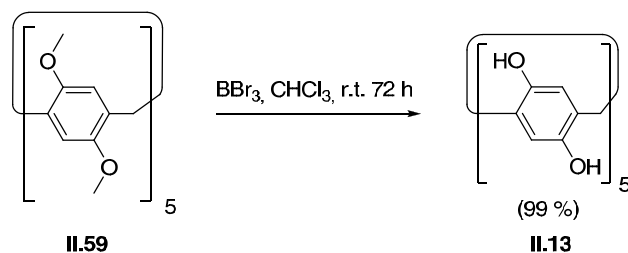
mp: 248-256 °C.

¹H NMR (300 MHz, CDCl₃): $\delta = 6.89$ (s, 10H), 3.76 (s, 10H), 3.74 (s, 30H).

¹³C NMR (75 MHz, CDCl₃): $\delta = 150.4$ (10C), 128.2 (10C), 113.3 (10C), 55.4 (10C), 29.3 (5C).

IR (neat): $\tilde{\nu}_{\text{max}} = 1497, 1209, 1046$.

HRMS (ESI ⁺):	m/z calcd. for C ₄₅ H ₅₄ NO ₁₀ ⁺ :	768.3748 [M+NH ₄] ⁺ ;
	found:	768.3743 [M+NH ₄] ⁺ .

Pillar[5]arene (II.13):^[133]

To a mixture of **II.59** (3.77 g, 5.02 mmol, 1.00 eq) and chloroform (280 mL) was added dropwise boron tribromide (9.77 mL, 103 mmol, 20.5 eq). The mixture was stirred for 72 h at room temperature and was then diluted with ice water (200 mL). The resulting precipitate was filtered off and washed with a 0.500 M aq. HCl solution (50.0 mL) and chloroform (50.0 mL). The crude material was dried and then recrystallized from acetone (200 mL) to give pillar[5]arene (**II.13**) as a grey colored solid (3.05 g, 99 %).

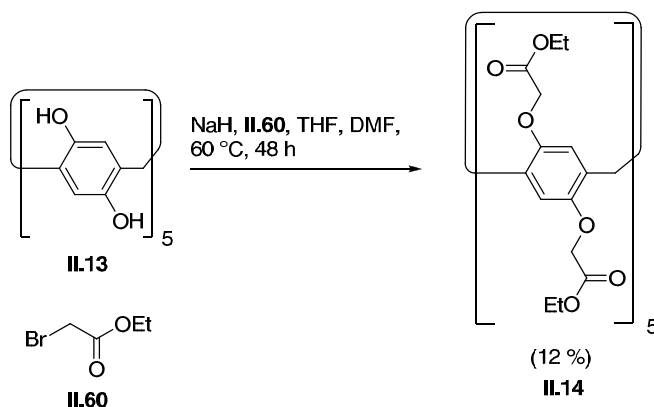
mp: ca. 385 °C (dec.).

¹H NMR (400 MHz, *d*₆-acetone): δ = 7.93 (s, 10H), 6.65 (s, 10H), 3.57 (s, 10H).

¹³C NMR (100 MHz, *d*₆-acetone): δ = 146.6 (10C), 127.1 (10C), 117.4 (10C), 29.7 (5C).

IR (neat): $\tilde{\nu}_{\text{max}}$ = 3214, 1691, 1430, 1197.

HRMS (ESI ⁺):	m/z calcd. for C ₃₅ H ₃₄ NO ₁₀ ⁺ :	628.2183 [M+NH ₄] ⁺ ;
	found:	628.2175 [M+NH ₄] ⁺ .

Ethoxycarbonylmethoxy-substituted pillar[5]arene (II.14**):**^[134]

To a suspension of **II.13** (2.42 g, 3.96 mmol, 1.00 eq) in THF (30.0 mL) and DMF (30.0 mL) was added sodium hydride (3.20 g, 127 mmol, 32.0 eq) and the mixture was stirred for 0.5 h at room temperature. Then, ethyl bromoacetate (**II.60**, 9.00 mL, 81.2 mmol, 20.5 eq) was added and the resulting mixture was heated to 60 °C for 48 h. After being allowed to cool to room temperature, the mixture was concentrated. The residue was diluted with CH₂Cl₂ (100 mL) and water (100 mL). The organic layer was separated, dried over MgSO₄ and purified by column chromatography (silica, DCM:acetone 100:0 → 95:5) to give **II.14** as a colorless solid (699 mg, 12 %).

TLC (CH₂Cl₂:acetone 95:5): $R_f = 0.35$.

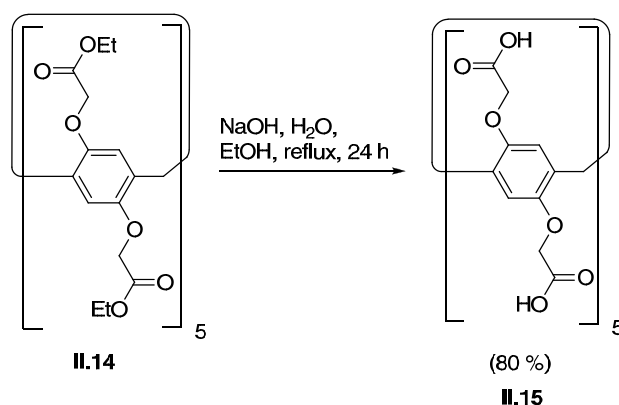
mp: 194 °C.

¹H NMR (400 MHz, CDCl₃): $\delta = 7.04$ (s, 10H), 4.55 (dd, $J = 15.8, 7.9$ Hz, 20H), 4.17-4.02 (m, 20H), 3.86 (s, 10H), 0.96 (t, $J = 7.1$ Hz, 30H).

¹³C NMR (100 MHz, CDCl₃): $\delta = 169.3$ (10C), 148.9 (10C), 128.7 (10C), 114.4 (10C), 65.7 (10C), 60.8 (10C), 29.2 (5C), 13.8 (10C).

IR (neat): $\tilde{\nu}_{\max} = 1760, 1191$.

HRMS (ESI⁺): m/z calcd. for C₇₅H₉₄NO₃₀⁺: 1488,5861 [M+NH₄]⁺;
found: 1488,5852 [M+NH₄]⁺.

Carboxylic acid-substituted pillar[5]arene (II.15):^[134]

A mixture of **II.14** (300 mg, 0.204 mmol, 1.00 eq), NaOH, (612 mg, 15.3 mmol, 75.0 eq), ethanol (30.0 mL) and water (30.0 mL) was heated to reflux for 24 h. Then, the reaction mixture was allowed to cool to room temperature and diluted with an aq. 2.00 M HCl solution (60.0 mL). The resulting precipitate was filtered off, washed with water (5 x 10.0 mL) and dried to afford **II.15** as a colorless solid (194 mg, 80 %).

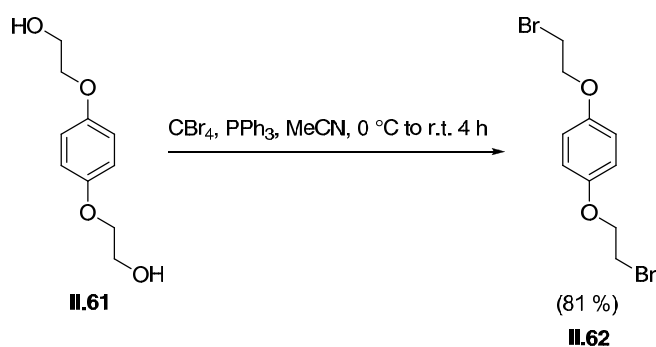
mp: 300 °C.

¹H NMR (400 MHz, *d*₆-DMSO): δ = 12.88 (s, br, 10H), 7.07 (s, 10H), 4.65 (d, *J* = 15.9 Hz, 10H), 4.37 (d, *J* = 15.9 Hz, 10H), 3.70 (s, 10H).

¹³C NMR (100 MHz, *d*₆-DMSO): δ = 170.9 (10C), 148.9 (10C), 128.5 (10C), 114.7 (10C), 65.5 (10C), 29.0 (5C).

IR (neat): $\tilde{\nu}_{\text{max}}$ = 1732, 1499, 1203.

HRMS (ESI⁺): m/z calcd. for C₅₅H₅₄NO₃₀⁺: 1208.2731 [M+NH₄]⁺;
found: 1208.2723 [M+NH₄]⁺.

1,4-bis(2-bromoethoxy)benzene (II.62):^[135]

To a mixture of 1,4-bis(2-hydroxyethyl)benzene (**II.61**, 10.0 g, 50.4 mmol, 1.00 eq) and triphenylphosphine (31.5 g, 120 mmol, 2.38 eq) in acetonitrile (300 mL) was added carbon tetrabromide (39.8 g, 120 mmol, 1.00 eq) over the course of 5 min in small portions at $0\text{ }^\circ\text{C}$. The reaction mixture was allowed to warm to room temperature and was stirred for another 4 h at this temperature. Then, 200 mL of ice water was added and the resulting precipitate was filtered off, washed with a mixture of methanol:water (3:2, 50.0 mL) and dried. The crude product was recrystallized by dilution in methanol (500 mL), heating to reflux for 15 min, hot filtration and cooling the filtrate to $-25\text{ }^\circ\text{C}$ for 16 h. **II.62** was obtained as colorless flakes (13.1 g, 81%).

TLC (CH_2Cl_2 :Hex 2:1): $R_f = 0.51$.

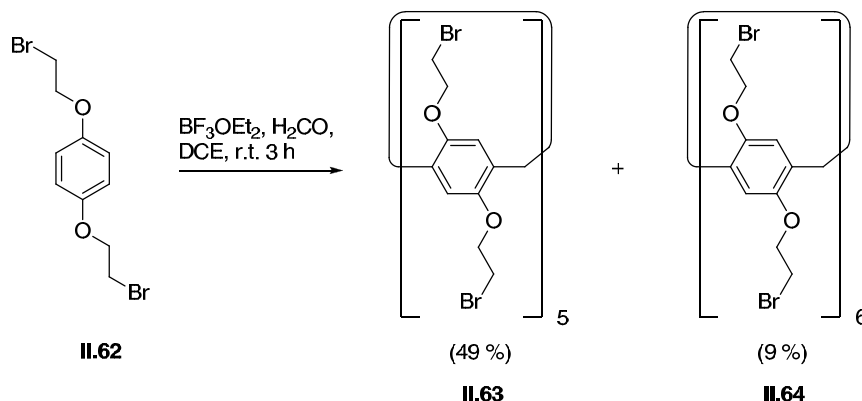
mp: $102\text{ }^\circ\text{C}$.

$^1\text{H NMR}$ (300 MHz, CDCl_3): $\delta = 6.86$ (s, 4H), 4.42 (t, $J = 6.3$ Hz, 4H), 3.61 (t, $J = 6.3$ Hz, 4H).

$^{13}\text{C NMR}$ (75 MHz, CDCl_3): $\delta = 152.8$ (2C), 116.1 (4C), 68.7 (2C), 29.2 (2C).

IR (neat): $\tilde{\nu}_{\text{max}} = 1505, 1216$.

HRMS (EI^+):
 m/z calcd. for $\text{C}_{10}\text{H}_{12}\text{Br}_2\text{O}_2^+$: 321.9204 $[\text{M}]^+$;
 found: 321.9201 $[\text{M}]^+$.

Bromoethoxy-substituted pillar[5]arene (II.63)^[135] and bromoethoxy-substituted pillar[6]arene (II.64)

To a solution of **II.62** (8.43 g, 26.0 mmol, 1.00 eq) in DCE (500 mL) was added paraformaldehyde (781 mg, 26.0 mmol, 1.00 eq) in one portion. To this mixture was added dropwise boron trifluoride diethyl etherate (3.25 mL, 26.0 mmol, 1.00 eq) over the course of 10 min. The slightly green colored reaction mixture was stirred for 3 h and was then concentrated to a grey powder. Purification by column chromatography (silica, CH₂Cl₂:Hex 1:1 → 2:1) gave **II.63** as a colorless solid (4.25 g, 49 %). Crystals suitable for X-ray crystallography were grown by slow evaporation of a chloroform solution containing **II.63**.

TLC (CH₂Cl₂:Hex 2:1): $R_f = 0.44$.

mp: 95 °C.

¹H NMR (300 MHz, CDCl₃): $\delta = 6.91$ (s, 10H), 4.22 (t, $J = 5.7$ Hz, 20H), 3.84 (s, 10H), 3.62 (t, $J = 5.7$ Hz, 20H).

¹³C NMR (75 MHz, CDCl₃): $\delta = 149.7$ (10C), 129.1 (10C), 116.1 (10C), 69.0 (10C), 30.6 (10C), 29.4 (5C).

IR (neat): $\tilde{\nu}_{\max} = 1494, 1201$.

HRMS (ESI⁻): m/z calcd. for C₅₅H₆₀Br₁₁O₁₀⁻: 1748.5204 [M+Br]⁻;
found: 1748.5956 [M+Br]⁻.

As a second product, **II.64** was obtained, which could be isolated by the concentration of later fractions in the chromatographic purification step. Crystals suitable for X-ray crystallography were obtained by slow evaporation of an acetone solution containing **II.64**.

TLC (CH₂Cl₂:Hex 2:1): $R_f = 0.22$.

mp: 110 °C.

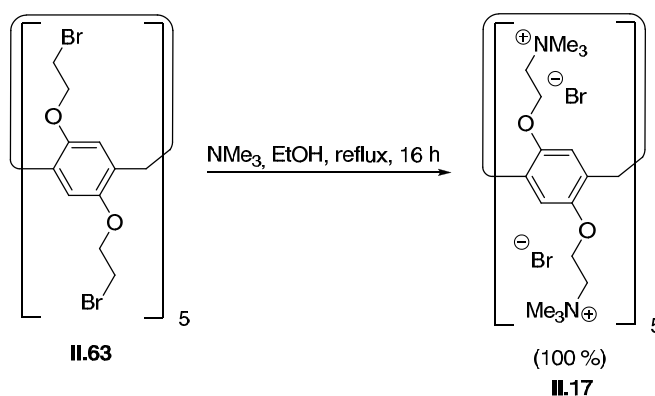
¹H NMR (300 MHz, CDCl₃): $\delta = 6.78$ (s, 12H), 4.16 (t, $J = 5.9$ Hz, 24H), 3.87 (s, 12H), 3.55 (t, $J = 5.9$ Hz, 24H).

¹³C NMR (75 MHz, CDCl₃): $\delta = 150.2$ (12C), 128.5 (12C), 115.8 (12C), 69.0 (12C), 30.6 (6C), 30.2 (12C).

IR (neat): $\tilde{\nu}_{\max} = 1496, 1404, 1208$.

HRMS (ESI⁻): m/z calcd. for C₆₆H₇₂Br₁₃O₁₂⁻: 2082.4408 [M+Br]⁻;
found: 2082.5112 [M+Br]⁻.

Trimethylammonium bromide-substituted pillar[5]arene (II.17).^[135]



To a solution of **II.63** (250 mg, 0.150 mmol, 1.00 eq) in ethanol (12.5 mL) was added a trimethylamine solution (33 % in ethanol, 1.61 mL, 5.95 mmol, 40.0 eq) and the mixture was heated to reflux for 16 h. Then, the resulting mixture was allowed to cool to room temperature, concentrated and diluted with water (5.00 mL). The resulting slurry was filtered and the filtrate was concentrated to give **II.17** as a colorless solid (339 g, 100 %).

mp: 100 °C.

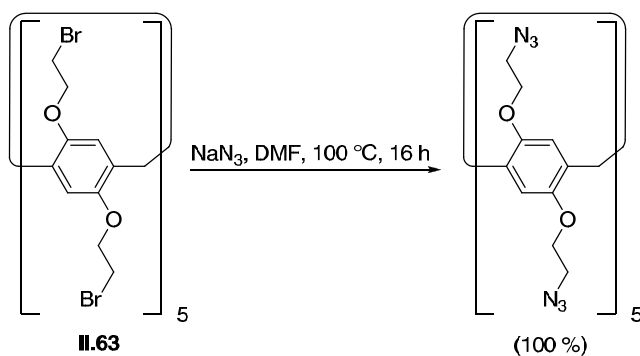
$^1\text{H NMR}$ (400 MHz, D_2O): $\delta = 6.81$ (s, 10H), 4.31 (s, 20H), 3.79 (s, 10H), 3.66 (s, 20H), 3.08 (s, br, 90H).

$^{13}\text{C NMR}$ (100 MHz, D_2O): $\delta = 149.3$ (10C), 129.8 (10C), 116.4 (10C), 64.8 (10C), 63.4 (10C), 53.9 (30C), 29.5 (5C).

IR (neat): $\tilde{\nu}_{\text{max}} = 3398, 1481, 1200$.

HRMS (ESI⁺): m/z calcd. for $\text{C}_{85}\text{H}_{150}\text{Br}_8\text{N}_{10}\text{O}_{10}^{2+}$: 1055.2466 $[\text{M}-2\text{Br}]^{2+}$;
found: 1055.2466 $[\text{M}-2\text{Br}]^{2+}$.

Azidoethoxy-substituted pillar[5]arene (II.65):^[136]



To a solution of **II.63** (1.00 g, 0.595 mmol, 1.00 eq) in DMF (50.0 mL) was added sodium azide (1.95 g, 30.0 mmol, 50.5 eq) in one portion and the mixture was heated to 100 °C for 16 h. Then, the resulting mixture was allowed to cool to room temperature and was poured into ice water (800 mL). The resulting precipitate was filtered off, washed with water (200 mL) and dried to give **II.65** as a colorless solid (775 mg, 100 %).

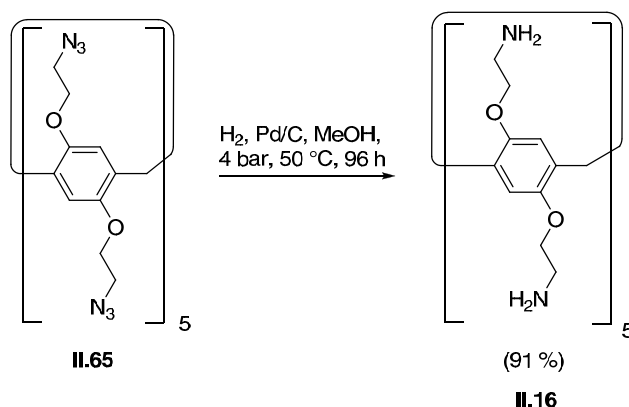
TLC (CH_2Cl_2 :Hex 2:1): $R_f = 0.15$.

$^1\text{H NMR}$ (300 MHz, CDCl_3): $\delta = 6.83$ (s, 10H), 4.00 (t, $J = 4.8$ Hz, 20H), 3.84 (s, 10H), 3.54 (t, $J = 4.8$ Hz, 20H).

$^{13}\text{C NMR}$ (75 MHz, CDCl_3): $\delta = 149.9$, (10C), 128.9 (10C), 115.7 (10C), 67.5 (10C), 50.9 (10C), 29.7 (5C).

IR (neat): $\tilde{\nu}_{\text{max}} = 2086, 1497, 1201$.

HRMS (ESI⁺): m/z calcd. for $\text{C}_{55}\text{H}_{62}\text{N}_{30}\text{O}_{11}^+$: 1318.5214 $[\text{M}+\text{H}_2\text{O}]^+$;
found: 1318.5432 $[\text{M}+\text{H}_2\text{O}]^+$.

Aminoethoxy-substituted pillar[5]arene (II.16):^[136]

A mixture of **II.65** (1.26 g, 0.968 mmol, 1.00 eq), Pd/C (10 % Pd, 100 mg, 0.968 mmol, 1.00 eq) and methanol (60.0 mL) was stirred at 50 °C in a pressure apparatus under hydrogen atmosphere at 4 bar for 24 h. Then, the mixture was allowed to cool to room temperature and the pressure was released to add another portion of Pd/C (10 % Pd, 100 mg, 0.968 mmol, 1.00 eq). The mixture was then again agitated at 50 °C under a 4 bar hydrogen atmosphere for 24 h. This procedure was repeated three times until a total reaction time of 96 h was reached and a total of 400 mg Pd/C had been added. The reaction mixture was allowed to cool to room temperature, filtered through a short pad of celite and concentrated to give **II.16** as a colorless solid (911 mg, 91 %).

mp: 100 °C.

¹H NMR (400 MHz, CD₃OD): δ = 6.74 (s, 10H), 4.79 (s, br, 20H), 3.84-3.68 (m, 30H), 2.91 (t, J = 5.2 Hz, 20H).

¹³C NMR (100 MHz, CD₃OD): δ = 149.9 (10C), 128.8 (10C), 115.0 (10C), 70.3 (10C), 40.8 (10C), 29.2 (5C).

IR (neat): $\tilde{\nu}_{\text{max}}$ = 1496, 1403, 1204.

HRMS (ESI ⁺):	m/z calcd. for C ₅₅ H ₈₁ N ₁₀ O ₁₀ ⁺ :	1041.6137 [M+H] ⁺ ;
	found:	1041.6129 [M+H] ⁺ .

CHAPTER III: SELF-ASSEMBLY OF HIGHLY SYMMETRIC MOLECULES

3.1 Introduction

3.1.1 Appearance of the Platonic Solids in Daily Life and in Science

Highly symmetric structures have fascinated mankind for thousands of years and their mathematical and geometrical description has been one of the earliest scientific tasks, which has attracted geniuses like Pythagoras, Plato, Euclid and Archimedes.

Especially the Platonic solids stand out due to their clarity and aesthetical appeal (Figure III.1). The Platonic solids are defined as convex polyhedra with faces of identical shape in the vertices of which the same number of faces and edges converge. Thus, they include the tetrahedron, the octahedron, the cube, the icosahedron and the dodecahedron.^[139]

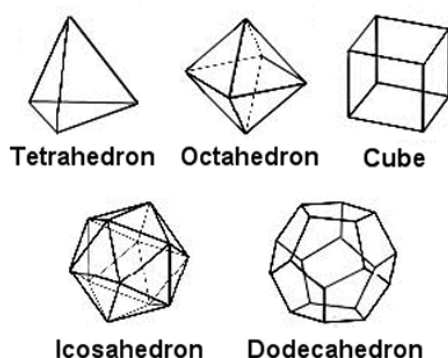


Figure III.1: The Platonic solids.^[139]

These highly symmetric polyhedra were not only subject of abstract scientific research, but also played a big role in other cultural areas such as arts and religion. The Pythagoreans, for example, idolized the Platonic solids as sacred ideas, in which the cosmos itself is displayed.^[139]

In Scotland, archaeologists found crenated stone objects with the geometry of the Platonic solids which they called “carved stone balls” (Figure III.2). They have been dated between 5000–2500 BC and their exact purpose is to date unknown.^[140]



Figure III.2: The carved stone balls in the Ashmolean Museum, Oxford.^[139]

The comprehensive understanding of geometry that is reflected in these ancient objects is astounding. The carved stone balls not only represent all five Platonic solids, but by the way they were created also picture the inscribed polar coordinate Platonic solid. For example, the cube which is depicted on Figure III.2 on the top left side shows meridians, the cutting points of which trace the octahedron which is inscribed into it.

The Platonic solids are, however, not a matter exclusively found in ancient arts, but are also featured in contemporary works. The dodecahedron was used as a stylistic device for surrealism in one of Salvador Dali's most popular compositions "The sacrament of the last supper". With its defined geometry based on pentagons, the Platonic solid underlined that the composition was designed using the golden ratio (Figure III.3).



Figure III.3: Salvador Dali: "The sacrament of the last supper" (1955).^[141]

The fascination for these geometric objects had also advanced into early science. Plato, for example, employed them for his elemental theory, in which he associated the classical elements to each Platonic solid (fire to the tetrahedron, earth to the cube, water to the icosahedron, air to the octahedron and ether to the dodecahedron).^[139] Johannes Kepler, on the other hand, attempted to explain the proportions of the natural world, or more specifically of the solar system, by associating spheres of inscribed platonic solids to the planetary orbits, which in context with his theory of the harmony of the world attracted huge interest (Figure III.4).^[142]

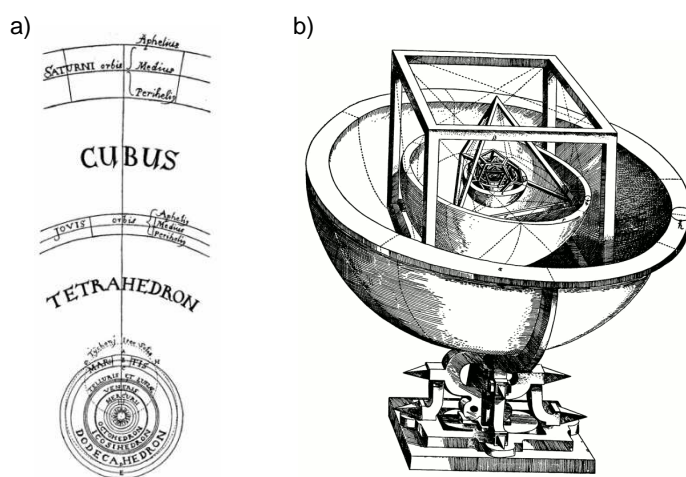


Figure III.4: Kepler's model of the solar system: a) schematic 2D drawing; b) picture of a 3D model.^[139]

The aforementioned geometries also play a huge role in Nature and are therefore topic of current research. Viruses, for example, build their capsids by self-assembly of smaller proteins to spherical structures with icosahedral geometry. An X-ray structure and an artwork of the cowpea mosaic virus are shown exemplarily in Figure III.5.^[143]

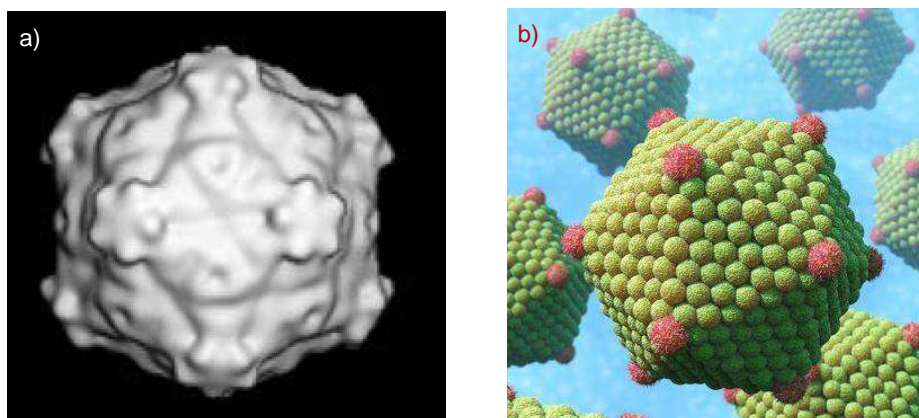


Figure III.5: Structure of the cowpea mosaic virus: a) Cryo-electron microscopy picture; b) artwork model.^[143]

Consequently, the self-organization of a disordered system of complementary small molecules that recognize each other through non-covalent interactions to form supramolecular structures without external guidance can be interpreted as a bio-inspired method. In fact, the self-assembly of such “programmed” molecules is a huge field of research, and the number of reported structures made by this approach progressively increases every year. This method allows to access supramolecular structures in a single step starting from simple precursors. The structure of these supramolecular frameworks can be “coded” in the design of these simple precursors with defined reactive groups such as metals and ligands.^[144]

The self-assembly approach to access metal-based molecules offers an alternative to the classical synthetic route. Predetermined building blocks with defined distances and angles between their reactive groups assemble in a highly convergent way under thermodynamic conditions and thus require fewer steps than the corresponding covalent synthesis. The kinetically labile coordinative bonds induce a self-healing process by forming an equilibrium between the constituents and the final product by a number of association and dissociation steps and therefore generate relatively defect-free structures, representing the thermodynamic minimum of this process.^[145] Nature has been using the same principals of non-covalent binding for the construction of various cell components, such as pentameric ion channels, microtubules, ribosomes, mitochondria and chromosomes, which mostly use hydrogen bonding to form specific structures.

The synthesis of highly symmetric chemical structures and especially of those with the geometry of the Platonic solids has been an important task in organometallic chemistry. Except for the challenge in synthesis design from a chemical point of view, interest lies also in the field of biology, *e.g.* for the translocation of drugs across membranes and material science, *e.g.* construction of devices on molecular level.^[146] These highly symmetric metal-organic structures have been termed metal-organic polyhedra.^[147]

The self-assembly of a dodecahedron or an icosahedron represents an especially intriguing and challenging task and only few examples of such metal-organic polyhedra have been reported to date. One such example was disclosed by the group of Stang and coworkers who succeeded in the synthesis of a metal-organic dodecahedron *via* an edge-directed approach (Figure III.6).^[148]

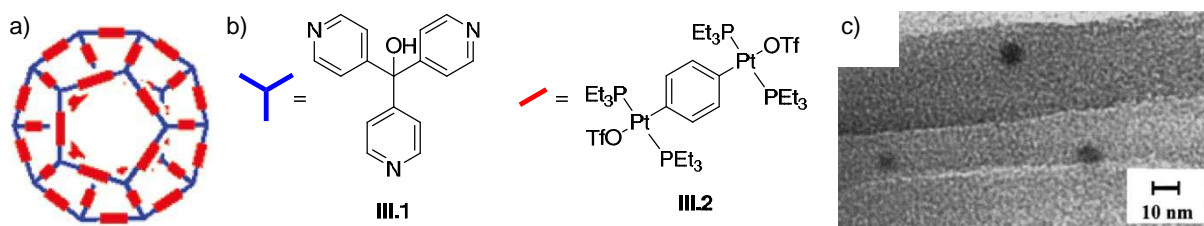


Figure III.6: Stang's edge-directed approach towards a dodecahedral metal-organic polyhedron: a) artwork model; b) chemical structure of the molecules representing the vertices (**III.1**) and edges (**III.2**); c) TEM image of the reaction product.^[148]

More specifically, reacting tri(4'-pyridyl)methanol (**III.1**) with linear bidentate unit **III.2** resulted in the formation of a metal-organic polyhedron with dodecahedral geometry. The reaction product was *i.a.* characterized by transition electron microscopy, confirming the size and thus the structure of the proposed reaction product.^[148]

Another example of a metal-based structure featuring the dodecahedron as geometrical unit was disclosed by the group of Wright, who reported a metal-organic framework structure of $[\text{Na}_{46}\text{pccp}_{48}][\text{Na}]_2[\text{MeNO}_2]_x[\text{Et}_2\text{O}]_y$ (Figure III.7).

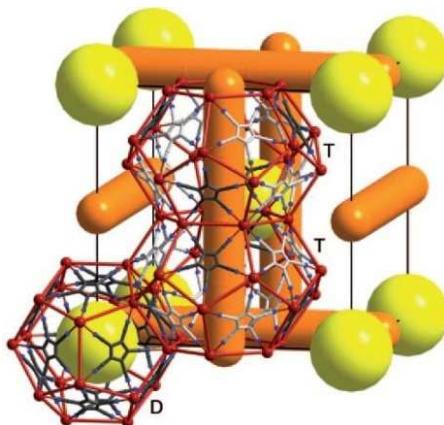


Figure III.7: Artwork model of the metal-organic framework structure of $[\text{Na}_{46}\text{pccp}_{48}][\text{Na}]_2[\text{MeNO}_2]_x[\text{Et}_2\text{O}]_y$ (CCDC-code: 822358).^[149]

Slow crystallization by diffusing diethyl ether into a MeNO_2 solution of Na pccp (**III.14**) resulted in the formation of crystals that contained a metal-organic framework, in which sodium was coordinated in a fashion that polyhedra with dodecahedral geometry were formed. Interestingly, the framework was found to be highly labile and rapidly lose solvent to interconvert to solvent-free Na pccp (**III.14**).^[149]

A striking example for an assembled icosahedron from UO_2^{2+} cations and carboxylic acid-substituted calix[5]arenes was described by deMendoza and coworkers in 2012. Slow

crystallization in the presence of a weak base such as pyridine resulted in the formation of the highly symmetric polyhedron (Figure III.8).^[150]

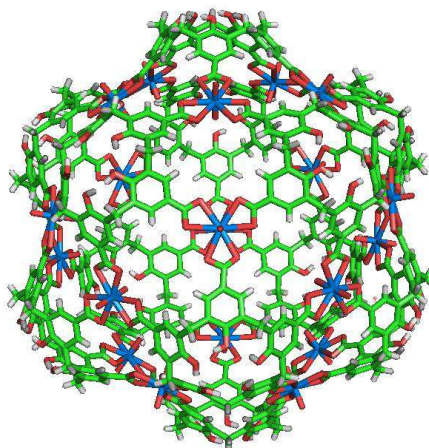


Figure III.8. Icosahedral assembly of calix[5]arenes and uranyl cations (CCDC-code: 856284).^[150]

The capsules consist of 12 calix[5]arenes building the vertices and 20 uranyl units forming the faces of the polyhedron. Furthermore, it was speculated that the uranyl oxygens positioned at the faces interact with guests encapsulated in the inside of the cages, thus allowing for interesting host-guest chemistry.

3.1.2 Project Background and Aims

Having appropriate fivefold symmetric building blocks in hands (*vide supra*, Chapter II, Section 2.2.2), it appeared consequent to investigate their coordination chemistry and their potential to compose highly symmetric polyhedral structures comprising the highest symmetry group I_h .^[151] Especially, structures of dodecahedral geometry were of high interest, since they are composed of 12 fused five-membered rings.

In order to design appropriate metal-containing building blocks to form the organo-metallic coordination polyhedron, the exact geometry within the dodecahedron had to be investigated. Important angles are illustrated in Figure III.9.

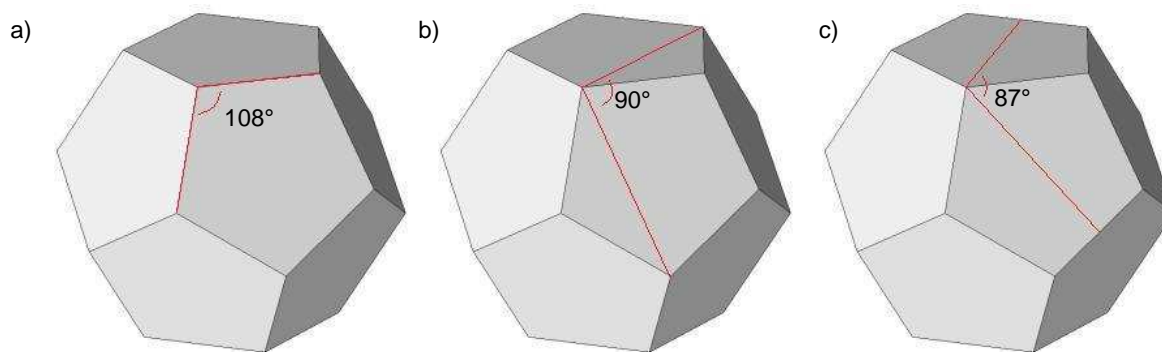


Figure III.9. Angles in a dodecahedron: a) 108°; b) 90°; c) 87°.

The angle merging the fivefold symmetric faces and the threefold symmetric vertices adopts a value of approximately 87°. Accordingly, metal units would have to consist of complexes capable to coordinate ligands in an 87° angle (Figure III.10). Inspired by modeling studies on silver pccp salts^[152] and the coordination framework of Na pccp reported by Wright and coworkers (*vide supra*, Section 3.1.1, Figure III.7),^[149] pccp salts were chosen as the molecules to form the faces of the dodecahedron. Thus, this approach represents a face-directed self-assembly of the highly symmetric structure.

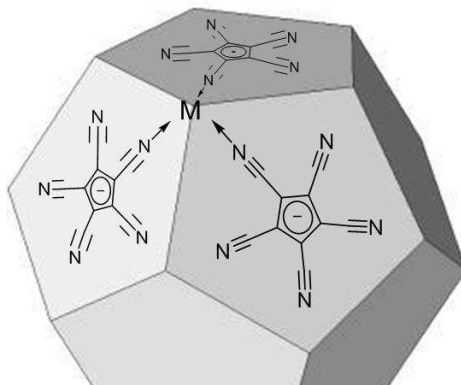


Figure III.10. Assembled dodecahedron following a face-directed approach.

Facially substituted octahedral structures seemed an obvious choice as threefold symmetric building blocks. One such example is $[(\text{CO})_3\text{Cr}(\text{NCMe})_3]$ (**III.4**), which had already been shown to form stable complexes with anionic ligands.^[153] Based on these building blocks, preliminary model studies were carried out using a PyMol code provided by Kateri DuBay in the Trauner group.^[154] Molecules with C_5 and C_3 symmetry were placed to the vertices and faces of a dodecahedron and its dual icosahedron in order to assess whether these are geometrically able to assemble into the highly symmetric polyhedra (Figure III.11).

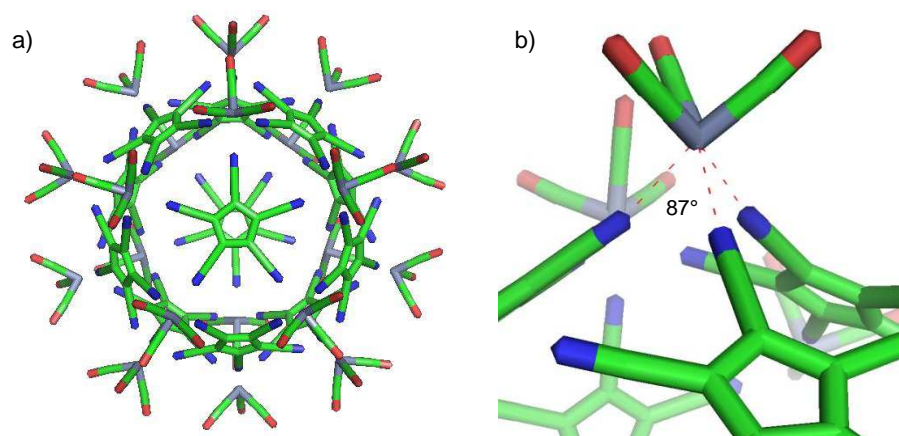


Figure III.11: Model of a dodecahedral arrangement of $[\text{Cr}(\text{CO})_3]_{20}[\text{pccp}]_{12}^{12-}$: a) Full view; b) zoom on a metal center, showing the 87° angle.

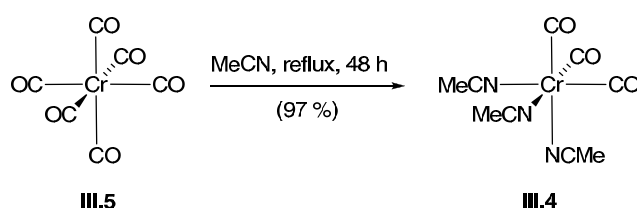
Pleasingly, the building blocks were found to be suitable to assemble a dodecahedral structure according to the face-directed approach. Distances and angles of the chosen building blocks seem to indeed “encode” the information required to assemble dodecahedral frameworks.

Hence, synthetic studies on the depicted self-assembly were started, the results of which are described in the next section.

3.2 Results and Discussion

3.2.1 Synthetic Studies on the Self-Assembly of a Molecular Dodecahedron

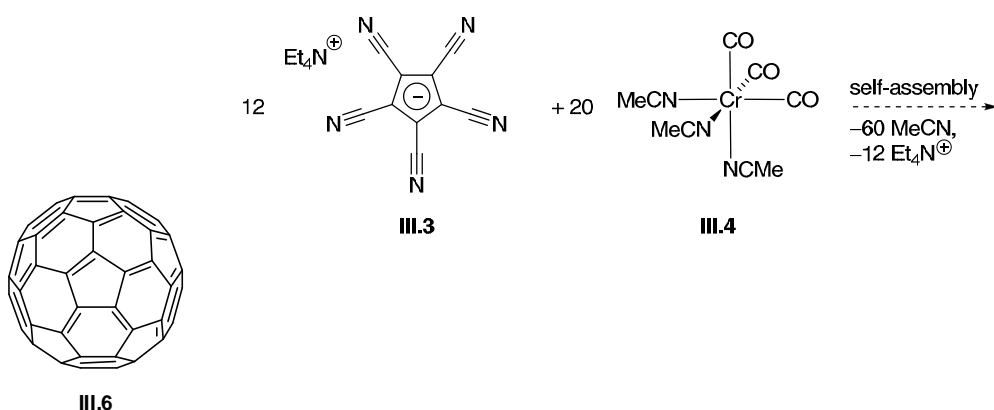
With fivefold symmetric building block $\text{Et}_4\text{N pccp}$ (**III.3**) already in hands (*vide supra*, Chapter II, Section 2.2.2, Scheme II.5), the synthesis of the transition metal building blocks was approached first. The synthesis of threefold symmetric chromium complex **III.4** was completed following a literature procedure (Scheme III.1).^[155]



Scheme III.1: Synthesis of tris(acetonitrile)tricarbonylchromium(0) (**III.4**).

Heating chromium hexacarbonyl (**III.5**) in acetonitrile resulted in the formation of facially substituted acetonitrile complex **III.4**. Compound **III.4** could be prepared on large scale, but had to be stored and weighed in a glove box due to its high sensitivity to air and its pyrophoric nature.

With the desired metal complex and the ligand in hands, first experiments towards a dodecahedral self-assembly were carried out. Acetonitrile was the solvent of choice for the reaction. Specifically, it was speculated to facilitate the formation of an equilibrium between the constituents and the product, thus enabling self-healing under thermodynamic conditions. Additional experiments were carried out in the presence of buckminster fullerene (**III.6**), which was envisioned to act as a template for the desired self-assembly. Furthermore, the metal complex was found to slowly decompose if heated in oxygen-containing solvents such as acetone. Products were characterized by IR spectroscopy, dynamic light scattering or single crystal X-ray crystallography, as appropriate. A selection of conditions employed for the assembly of **III.3** and **III.4** is summarized in Table III.1.



Entry	Additive	Solvent	Temperature	Time	Yield	Observation
1	-	MeCN	reflux	16 h	-	starting material
2	-	MeCN	r.t.	6 d	-	starting material
3	-	MeCN	reflux	6 d	-	complex mixture
4	-	THF	reflux	48 h	-	complex mixture
5	-	DMSO	100 °C	48 h	-	complex mixture
6	C ₆₀ (III.6)	<i>o</i> -C ₆ H ₄ Cl ₂	reflux	96 h	-	starting material

Table III.1: Selected conditions for the attempted self-assembly of **III.3** and **III.4**.

When a mixture of **III.3** and **III.4** was heated in acetonitrile for 16 h or was stirred at room temperature for six days, no reaction was observed and starting material was recovered (Table III.1, Entries 1 and 2). If the temperature was increased to reflux while being stirred for six days, a complex mixture of products was formed (Table III.1, Entry 3). Similar results were obtained when the reaction was carried out in THF or DMSO as solvent (Table III.1, Entries 4 and 5). When heating a mixture of **III.3**, **III.4** and buckminster fullerene (**III.6**) in 1,2-dichlorobenzene for four days and subsequently cooling the reaction mixture, starting material was recovered (Table III.1, Entry 6). In the course of purification efforts, an unprecedented solvate structure of **III.6** was obtained (Figure III.12). A full screening table of conditions employed for the self-assembly can be found in Appendix 8 (Table App.8a).

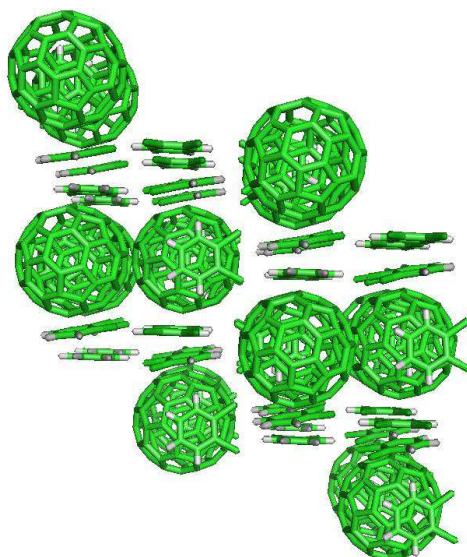
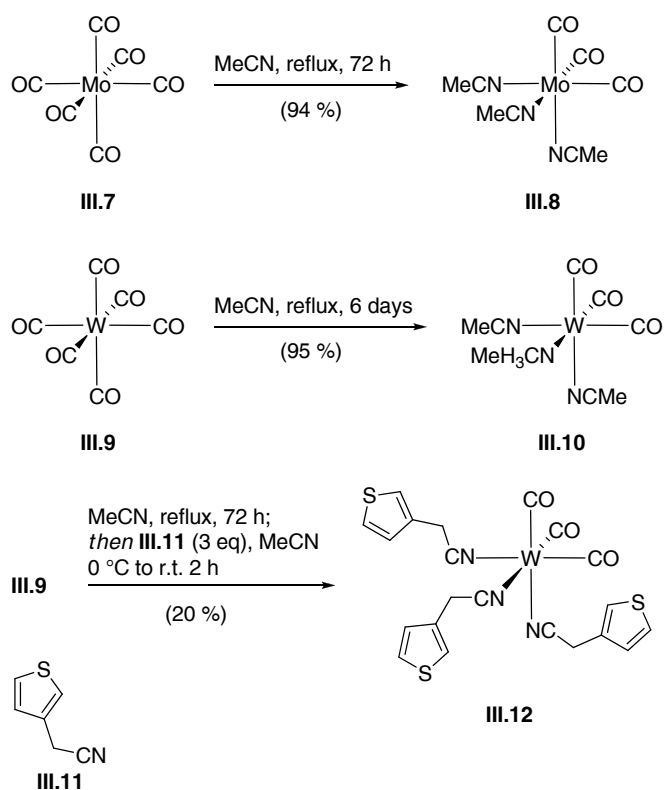


Figure III.12: View along the b-axis in the unit cell of **III.6**·3C₆H₄Cl₂ (based on preliminary data).

It was speculated that results could be improved, if chromium was replaced by other group 6 transition metals such as molybdenum and tungsten (Scheme III.2). A tungsten 3-thiopheneacetonitrile complex **III.12** had been shown to be a stable and versatile reagent and was thus of special interest as building block for the self-assembly.^[156]



Scheme III.2: Facially substituted octahedral group 6 transition metal complexes prepared for the dodecahedral self-assembly with **III.3**.

Analogous to the synthesis of **III.4**, **III.8** and **III.10** were prepared by heating the corresponding hexacarbonyl complexes **III.7** and **III.9** in acetonitrile.^[155] *In situ* generated **III.10** was further converted into **III.12** by addition of 3-thiopheneacetonitrile (**III.11**) to a previously heated acetonitrile solution of **III.9**.^[156]

These building blocks were subjected to the same reaction conditions as described for **III.4**, but no complexes with **III.3** as a ligand were ever observed and either starting material was recovered or complex mixtures were obtained (for detailed screening tables see Appendix 8, Tables App.8b, App.8c, App.8d). However, in the course of these studies and extensive purification efforts, crystalline material suitable for single crystal X-ray crystallography was obtained and thus the crystal structure of starting pccp salt **III.3** was elucidated for the first time (Figure III.13).

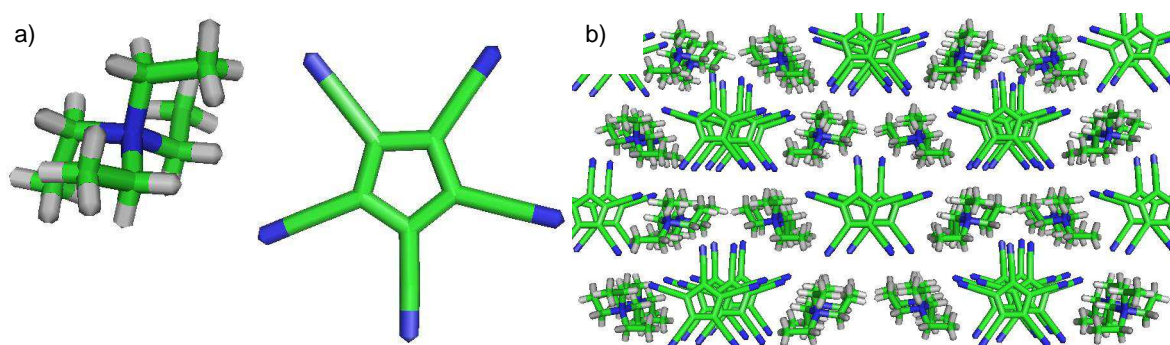


Figure III.13: Cc -structure of **III.3**: a) single ion pair; b) illustration of two unit cells, view along the c -axis.

Compound **III.3** crystallizes in a primitive monoclinic unit cell in the space group Cc and shows a very similar packing as HNet_3 pccp (**III.13**).^[126] The pccp anions form layers, which are stacking along the c -axis in a staggered fashion. In the course of extensive purification efforts, a second isomorph of **III.3** could also be obtained (Figure III.14).

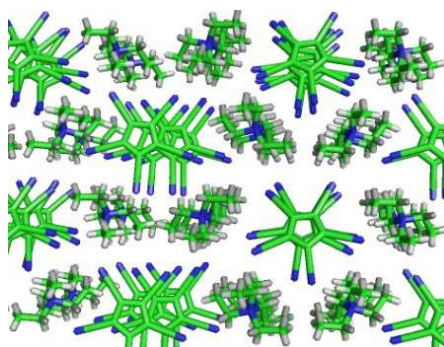


Figure III.14: View along the c -axis of the Pc -isomorph of **III.3**.

The second isomorph crystallizes in the space group Pc and shows a distinctly different packing, resulting from linearly stacked pccp units, which appear in addition to the staggered units as observed in the Cc structure.

At this point, further pccp salts as starting materials were explored. Being aware that the self-assembled dodecahedron would accumulate 12 negative charges and would thus experience considerable coulomb repulsion, counter ion effects were speculated to play a crucial role in the reaction. This assumption has also been supported by preliminary DFT calculations (*vide infra*, Appendix 7). When reaction partners for the self-assembly and the corresponding transition metal unit carrying pccp as ligand were optimized in the absence of solvent and counter ions, this substitution process was found to be endothermic. However, the accumulated charges can be neutralized by forming tight ion pair salts of pccp. In order to

retain the fivefold symmetry, a symmetry-matched counter ion would be required in the envisioned system such as the ferrocenium cation or the decamethylferrocenium cation. The resulting “neutral” dodecahedron is depicted in Figure III.15.

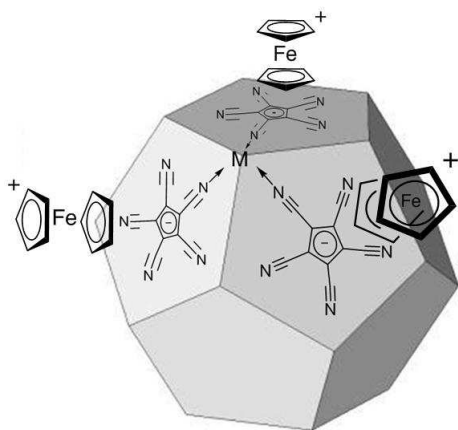
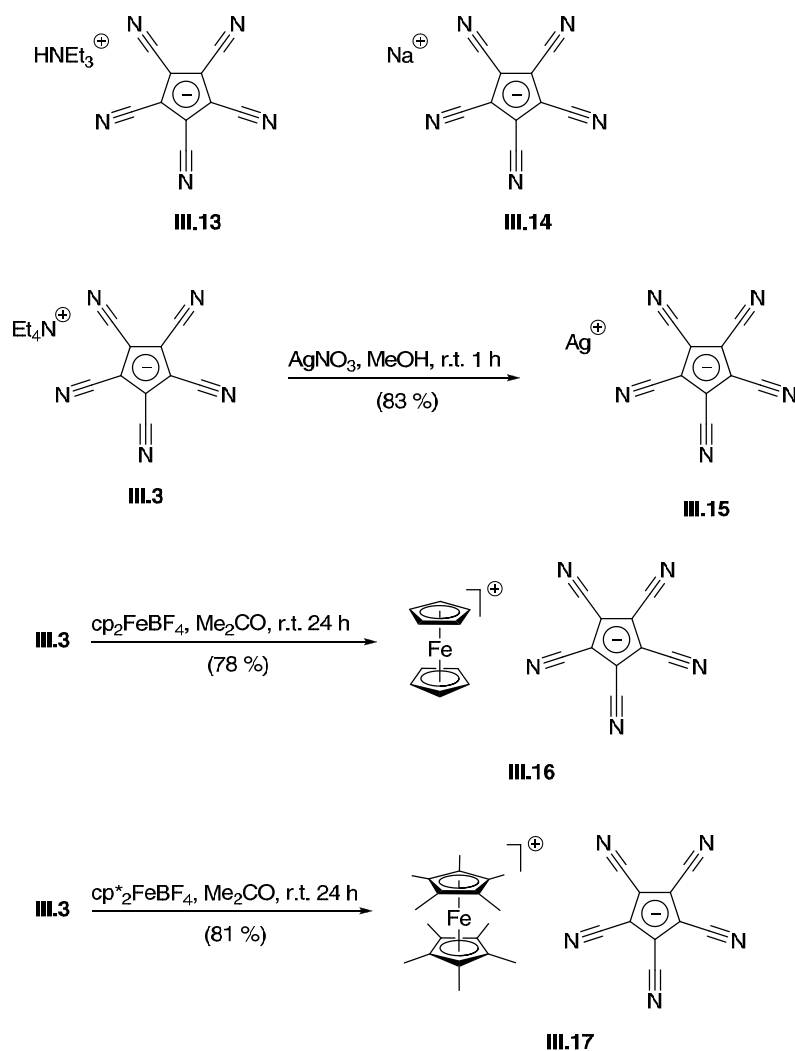


Figure III.15: Proposed self-assembled dodecahedron with symmetry-matched counter ion.

Ferrocenium salts were readily available from the corresponding ferrocenes. The ferrocenium pcp salts were prepared by simple salt metathesis. In order to evaluate the role of the counter ion for the self-assembly in more detail, in addition to these new pcp salts several more known pcp salts were prepared (Scheme III.3).



Scheme III.3: Structure and syntheses of pccp salts employed in the self-assembly approach.

In addition to **III.13** and **III.14**, the synthesis of which has already been described before (*vide supra*, Chapter II, Section 2.2.2), silver salt **III.15** was synthesized, following a literature-known procedure.^[152] Treatment of **III.3** with silver nitrate in methanol resulted in the precipitation of **III.15**. When **III.3** was stirred in the presence of ferrocenium tetrafluoroborate or decamethyl ferrocenium tetrafluoroborate, respectively, the corresponding ferrocenium pccp salts **III.16** and **III.17** formed smoothly and could be isolated in good yields. Interestingly, in preliminary NMR studies no ^{13}C signals of the pccp counter ion in salt **III.16** were observed. In contrast, the ^{13}C signals in a NMR solution of identical concentration were observed in the case of salt **III.17**. This finding was speculated to rely on a close proximity of pccp to the paramagnetic metal in solution, which might indicate **III.16** to exist as a tight ion pair. The crystal structure of **III.17** is shown in Figure III.16.

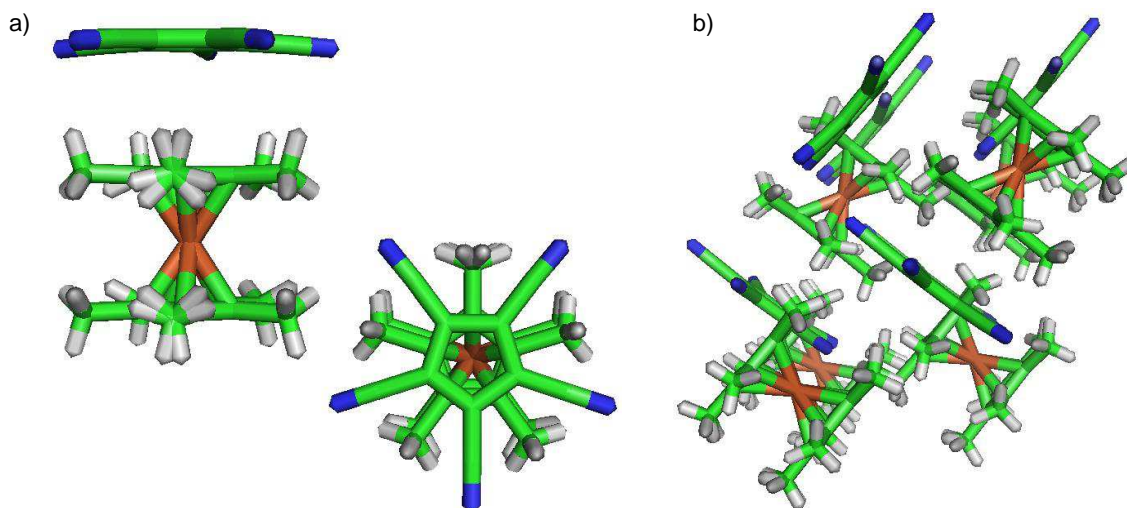
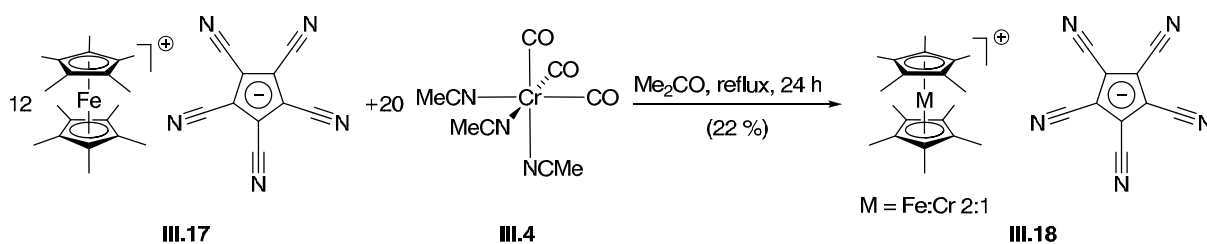


Figure III.16: Crystal structure of **III.17**: a) Close view on two ion pairs; b) view along the a-axis.

Compound **III.17** crystallizes in the orthorhombic space group $Cmc2_1$. Ferrocenium and pccp form a close ion pair ($d_{\text{pccp-cp}^*} = 3.3 \text{ \AA}$) with C_{5v} symmetry, which arranges in an orthogonal orientation towards vicinal pairs. Pccp resides directly over the adjacent ferrocene ring in a staggered configuration in respect to the substituents.

These new pccp salts were subjected to a large number of conditions to self-assemble with threefold symmetric transition metal complexes **III.4**, **III.8**, **III.10** and **III.12** (*vide supra*, Scheme III.2, for detailed screening tables see Appendix 8, Tables App.8a-App.8i). Unfortunately, no formation of transition metal complexes with pccp was observed. However, when **III.17** was reacted with **III.4**, formation of an interesting product was found (Scheme III.4).



Scheme III.4: Synthesis of the unusual metallocene $(C_5Me_5)_2Cr_{0.33}Fe_{0.67}C_{10}N_5$ (**III.18**).

When a mixture of **III.17** and **III.3** was heated in acetone for 24 h, formation of a yellow solid was observed, which was identified as decamethylferrocene. The resulting green solution was separated and subjected to fractional crystallization to afford a green crystalline

solid, which was identified as $(C_5Me_5)_2Cr_{0.33}Fe_{0.67}C_{10}N_5$ (**III.18**). The structure of **III.18** was confirmed by X-ray crystallography (Figure III.17).

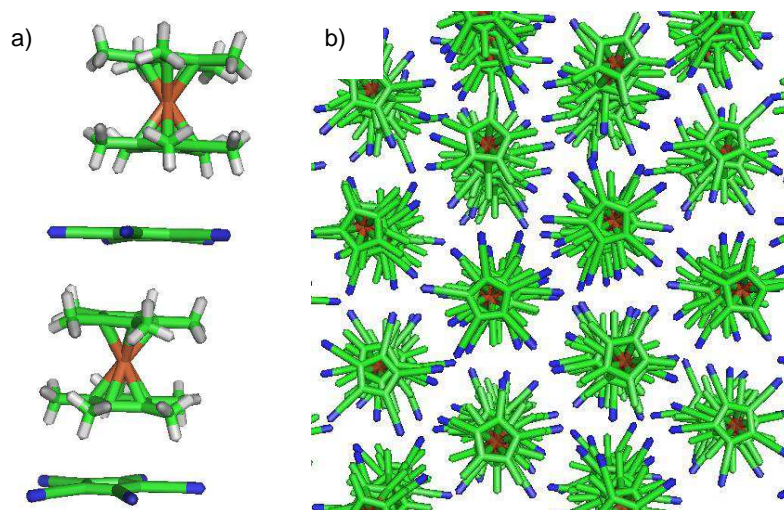
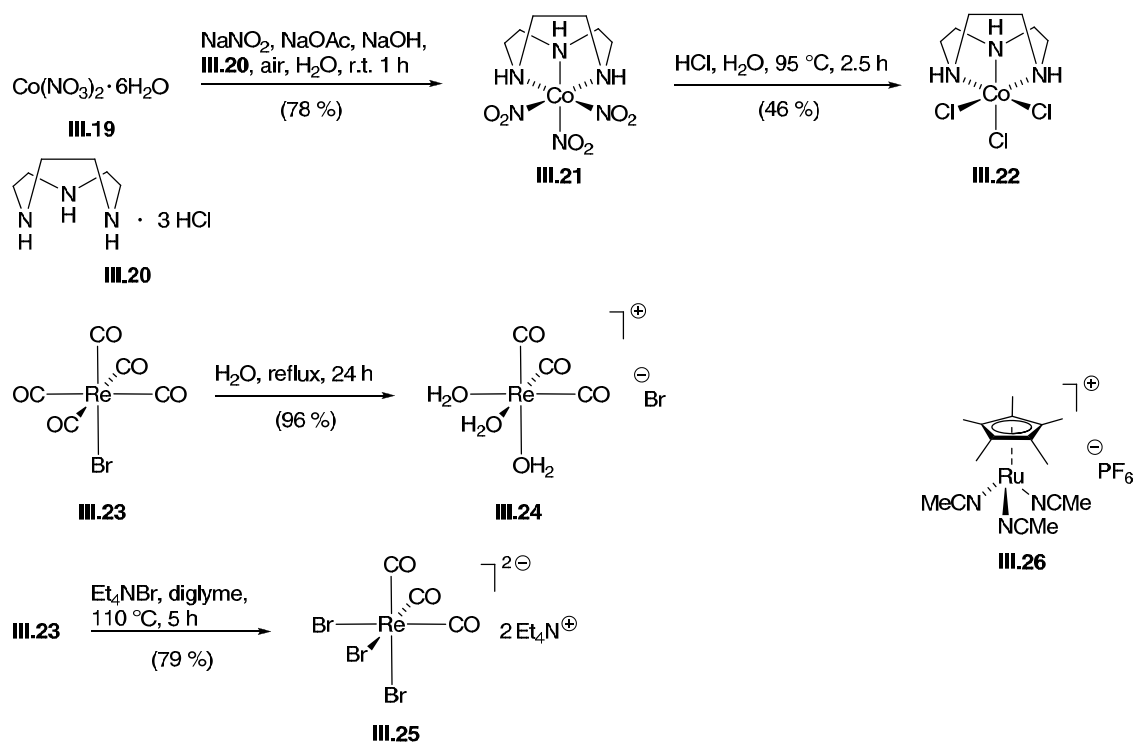


Figure III.17: Crystal structure of **III.18**: a) Close view on two ion pairs; b) view along the ac-axis, emphasizing the linear stacking, hydrogens removed for clarity.

The compound crystallizes in a monoclinic crystal system in the space group $P2_1/c$. Pccp and the metallocene form ion pairs with staggered conformation. Discrete ion pairs arrange towards each other in a shifted but linear fashion, thus generating infinite linear metallocene pccp rods appearing as coated “polydecker sandwiches”.

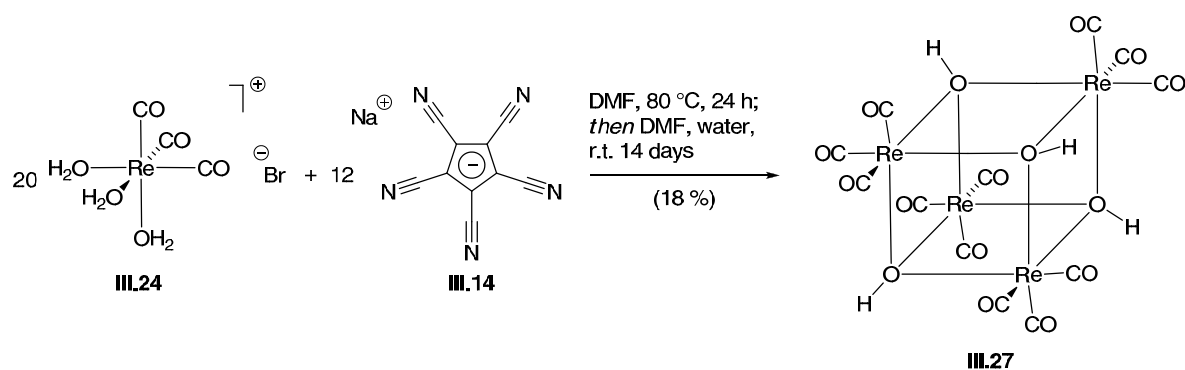
In subsequent attempts, further non-group 6 threefold symmetric transition metal complexes were investigated for the self-assembly (Scheme III.5). In order to be able to perform the self-assembly in water as solvent, which due to its high dielectric coefficient was speculated to facilitate the assembly of charged polyhedra, complexes were employed that were known to be air and water stable.



Scheme III.5: Synthesis of further threefold symmetric building blocks.

Cobalt(II)nitrate hexahydrate (**III.19**) was stirred in the presence of TACN trihydrochloride (**III.20**), sodium nitrate and a buffer of sodium acetate and sodium hydroxide while air was bubbled through the reaction mixture to afford cobalt TACN complex **III.21**.^[157] The nitrates were exchanged with chlorides by heating **III.21** in an aqueous HCl solution to provide **III.22**.^[157] Furthermore, rhenium aqua complex **III.24** was prepared by heating a rheniumpentacarbonyl bromide **III.23** in water.^[158] As a second threefold symmetric rhenium carbonyl complex, tribromide **III.25** was synthesized by heating a mixture of **III.23** and tetraethylammonium bromide in diglyme for 5 h.^[159] In addition, experiments were carried out with commercially available ruthenium complex **III.26**.

These new complexes were subjected to a multitude of conditions to trigger a self-assembly and to form the corresponding highly symmetric structures (for detailed screening table see Appendix 8, Tables App.8e-App.8i). Unfortunately, these attempts remained fruitless and no complexes of threefold symmetric transition metal building blocks with pccp as ligand were ever observed. However, in the course of these studies, formation of tetranuclear, tetrahedral rhenium complex **III.27** was found.^[160] An example of a reaction in which **III.27** was formed is shown in Scheme III.6.



Scheme III.6: Formation of tetranuclear rhenium complex **III.27**.

When a mixture of rhenium aqua complex **III.24** and sodium pccp (**III.14**) was heated in DMF to 80 °C for 24 h and was subsequently subjected to water-diffusion into the reaction mixture for 14 days, a colorless solid formed, which was identified by X-ray crystallography to be tetranuclear rhenium complex **III.27**. Compound **III.27** crystallized as a DMF/water solvate, which is depicted in Figure III.18.

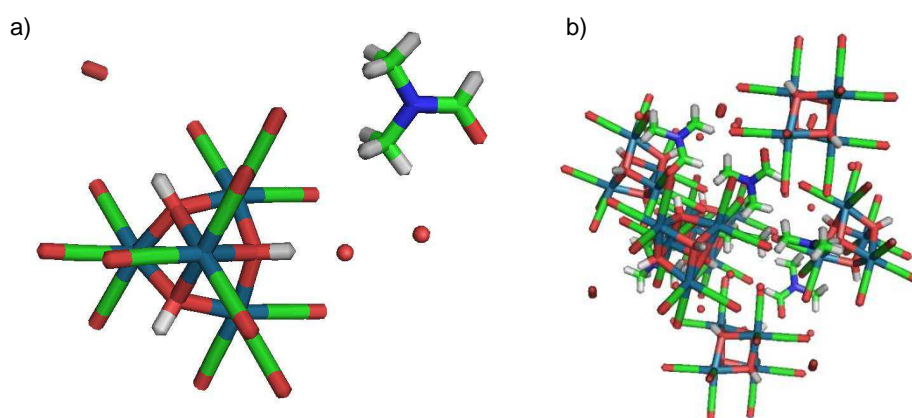


Figure III.18: Crystal structure of **III.27**·3H₂O·DMF: a) Single unit; b) view along the b-axis of the unit cell, water and acetone molecules are shown.

The compound crystallized in the triclinic crystal system in the space group $P3_221$, in which each unit cell includes three units of **III.27**·3H₂O·DMF. The X-ray structure revealed the tetranuclear rhenium core unit to possess T_d symmetry. In the course of further studies to access highly symmetric structures, a second X-ray structure containing **III.27** was obtained (Figure III.19).

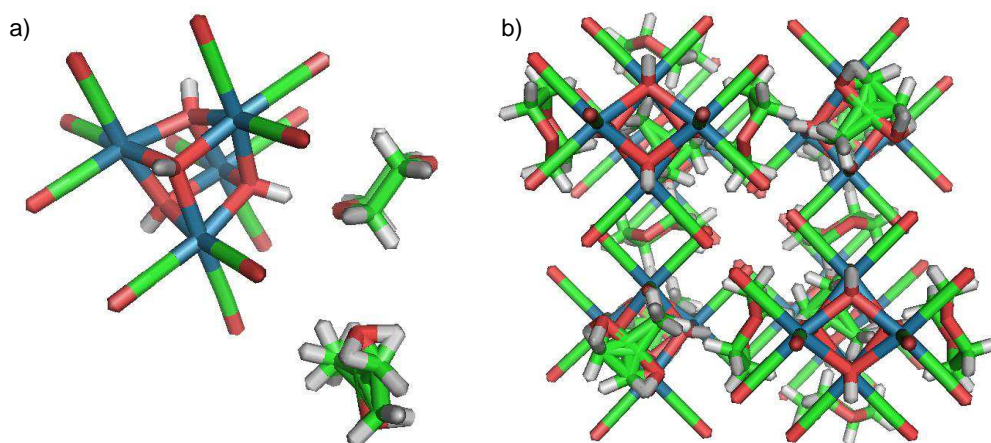
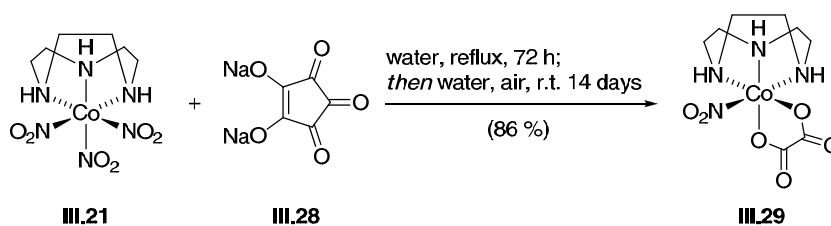


Figure III.19. Crystal structure of **III.27**·dioxane·acetone: a) Close view; b) view along the c-axis.

In this solvate structure, which crystallizes in the tetragonal crystal system in the space group $P4_22_12$, dioxane forms a hydrogen bond to the μ -OH moiety in **III.27** ($d_{(O-O)} = 2.6 \text{ \AA}$). The unit cell contains four units of **III.27**·dioxane·acetone.

Pcp has been described in the literature as weakly coordinating ion,^[161] which could possibly explain the fact that no metal pcp coordination was observed in the above mentioned attempts. Although some few metal pcp complexes have been described in literature,^[162] the formation of coordinative bonds with the pcp ligand seems to be limited to highly specific systems.

In order to further investigate the face-directed approach towards highly symmetric structures, some preliminary experiments with other fivefold symmetric ligand nodes such as sodium croconate (**III.28**) were carried out. However, these studies did not lead to formation of highly symmetric complexes. Interestingly, when **III.28** was reacted with cobalt TACN complex **III.21** and the mixture was exposed to air, yellow crystals of a new compound formed (Scheme III.7).



Scheme III.7. Synthesis of cobalt oxalate complex **III.29**.

A mixture of cobalt TACN complex **III.21**, sodium croconate **III.28** and water was heated to reflux for 72 h. Subsequently, the flask was opened and allowed to stand for 14 days at room temperature, upon which time oxalate complex **III.29** was isolated as small yellow crystals as a result of oxidation by oxygen (Figure III.20).

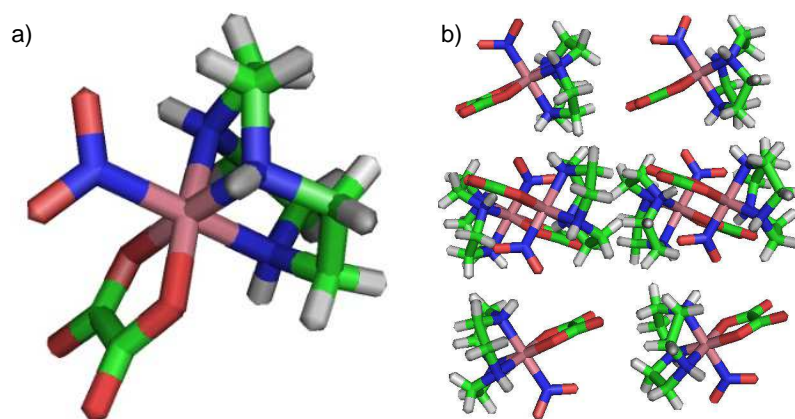


Figure III.20: X-ray structure of [Co(TACN)(NO₂)(C₂O₄)] complex (**III.29**).

The compound crystallizes in the orthorhombic crystal system in the space group *Pbca*. The unit cell contains four molecules of **III.29**, which form an intermolecular hydrogen bond between an *N-H* moiety within the TACN ligand and a nitrite oxygen ($d_{N-O} = 2.9 \text{ \AA}$).

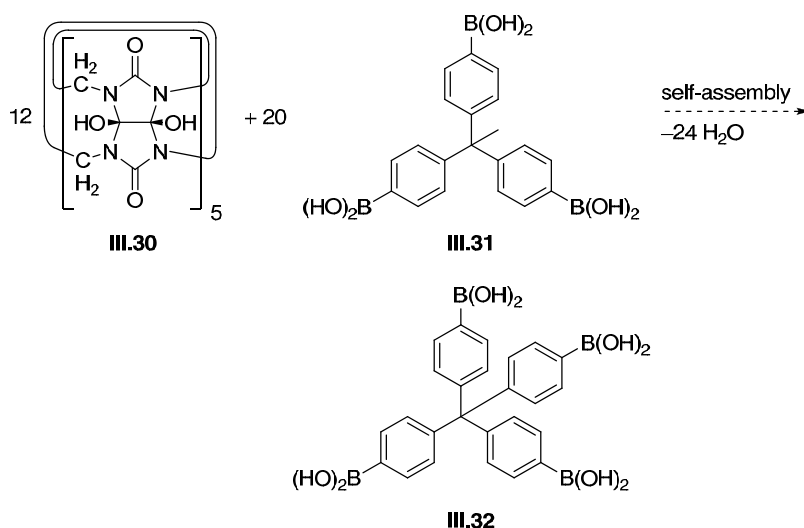
At this point, it was envisioned to synthesize further threefold symmetric and fivefold symmetric building blocks and to investigate alternative reaction pathways for the self-assembly. The results that were gathered in these studies are summarized in the next section.

3.2.2 Summary, Conclusions and Outlook

In summary, over 150 conditions for the self-assembly of threefold symmetric transition metal complexes with pccp as ligand were screened. The formation of highly symmetric polyhedra with dodecahedral geometry remained unsuccessful. After extensive experimental efforts, pccp does not seem to be an appropriate ligand for the metals that were chosen for the self-assembly.

In the course of these studies, the syntheses and crystal structures of new pccp salts with fivefold symmetric counter ions were discovered. In addition, two crystal structures of **III.3** could be elucidated for the first time. In some cases, formation of tetrahedral tetranuclear rhenium complex **III.27** was observed, which comprises the structure of the tetrahedron and thus the geometry of a Platonic solid.

Future work will have to consist of the development of new compounds with fivefold or threefold symmetry, respectively, which have the potential to self-assemble. For example, it can be speculated that decahydroxycucurbit[5]uril (**III.30**) can form a borate-ester with threefold symmetric boronic acid building blocks such as **III.31** and thus assemble to the desired dodecahedral framework (Scheme III.8).



Scheme III.8: Potential reaction partners **III.30** and **III.31** for a self-assembly. For modeling, known compound **III.32** (CCDC code: 204942) was used.

A model of a hypothetical dodecahedral assembly of **III.30** with **III.32** is depicted in Figure III.21.

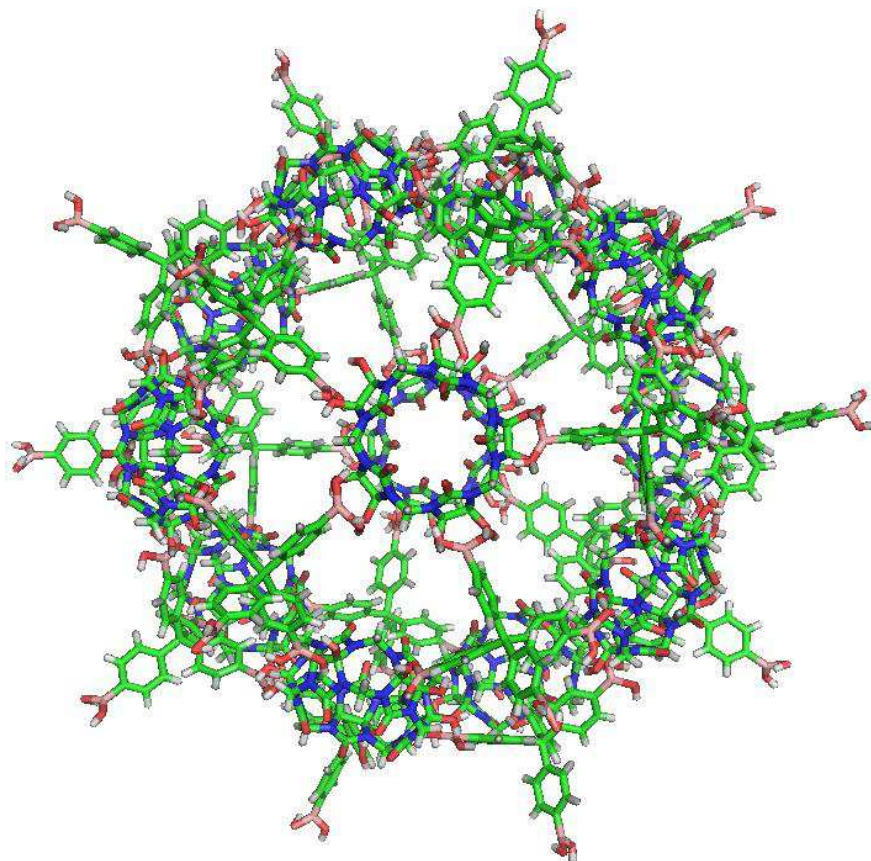


Figure III.21: Model of a dodecahedral arrangement of a threefold symmetric boronic acid-substituted building block **III.32** and decahydroxycucurbit[5]uril (**III.30**).

Overall, the synthetic approaches towards highly symmetric polyhedra gave valuable insights in the coordination chemistry of pccp and yielded a number of new crystal structures of known compounds as well as of unreported compounds. The hunt for the crystal structure of a polyhedron with dodecahedral geometry will continue in the Trauner laboratories.

3.3 Experimental Section

General experimental details:

Unless specified otherwise, all reactions were performed with magnetic stirring under an atmosphere of argon and in oven-dried glassware. Isolated products were dried on a high vacuum line at a pressure of 10^{-2} mbar using an *ATB-Loher* oil pump by *Flender*. Dimethylformamide (DMF), methanol (MeOH), acetonitrile (MeCN), acetone (Me₂CO) and bis(2-methoxyethyl) ether (diglyme) were purchased from *Acros Organics* as 'extra dry' reagents under inert gas atmosphere and over molecular sieves. All other reagents were purchased from commercial sources and used without further purification. Petroleum ether is referred to as hexanes and relates to fractions of isohexanes, which boil between 40 °C and 60 °C. If appropriate, reactions were monitored by TLC using *E. Merck* 0.25 mm silica gel 60 F₂₅₄ glass plates. TLC plates were visualized by exposure to UV light (254 nm) and subsequent treatment with an aqueous solution of CAM, an aqueous solution of potassium permanganate, an acidic solution of vanillin, a solution of ninhydrin or a mixture of silica and finely grounded iodine, followed by heating the plate with a heat gun. If appropriate, reactions were additionally monitored by Proton nuclear magnetic resonance (¹H-NMR) using a *Varian* 200 spectrometer or LCMS using an *Agilent Technologies 1260 infinity* machine equipped with an *Agilent ZORBAX Eclipse Plus C18* reversed phase analytical 4.6 mm x 150 mm column. Yields refer to isolated and spectroscopically pure compounds.

Instrumentalization:

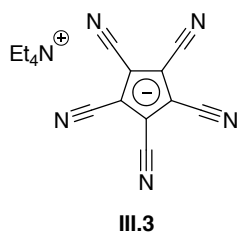
Infrared (IR) spectra were recorded on a *Perkin Elmer Spectrum BX II* (FTIR System), equipped with an attenuated total reflection (ATR) measuring unit. IR data is reported in frequency of absorption (cm^{-1}).

UV/VIS spectra were recorded on a *Cary 500 8.01* spectrophotometer made by *Varian*. Samples were measured neat without thermostating in a range of 200 nm to 2600 nm with a scan rate of 600 nm min^{-1} . UV/VIS data is reported in wavelength (nm).

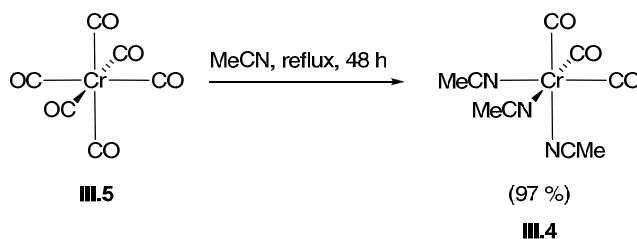
Proton nuclear magnetic resonance ($^1\text{H-NMR}$) spectra were recorded on a *Varian 300*, *Varian 400*, *Inova 400* or *Varian 600* spectrometer. Chemical shifts (δ scale) are expressed in parts per million (ppm) and are calibrated using residual protic solvent as an internal reference (CDCl_3 : $\delta = 7.26$ ppm, $(\text{D}_3\text{C})_2\text{CO}$: $\delta = 2.05$ ppm, $(\text{CD}_3)_2\text{SO}$: $\delta = 2.50$ ppm, $\text{D}_2\text{O} = 4.79$ ppm).^[95] Unless noted otherwise, data was recorded at 27°C . Data for $^1\text{H-NMR}$ spectra are reported as follows: chemical shift (δ ppm) (multiplicity, coupling constants (Hz), integration). Couplings are expressed as: s = singlet, d = doublet, t = triplet, q = quartet, m = multiplet, br = broad, app = apparent or combinations thereof. Carbon nuclear magnetic resonance ($^{13}\text{C-NMR}$) spectra were recorded on the same spectrometers at 75, 100 and 150 MHz, respectively. Carbon chemical shifts (δ scale) are also expressed in parts per million (ppm) and are referenced to the central carbon resonances of the solvents (CDCl_3 : $\delta = 77.16$ ppm, $(\text{D}_3\text{C})_2\text{CO}$: $\delta = 29.84$ ppm, $(\text{CD}_3)_2\text{SO}$: $\delta = 39.52$ ppm).^[95]

Mass spectroscopy (MS) experiments were performed on a *Thermo Finnigan MAT 95* (electron ionization, EI), on a *Thermo Finnigan LTQ FT* (electrospray ionization, ESI) or on a *Jeol JMS-700* (fast atom bombardment, FAB) instrument.

Melting points were measured on an *EZ-Melt* automated melting point apparatus made by *Stanford Research Systems* and are uncorrected.

Tetraethylammonium pccp (III.3):

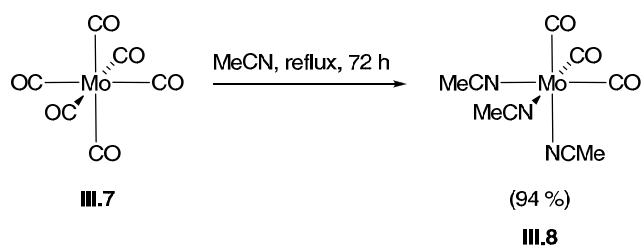
Tetraethylammonium pccp (**III.3**) was prepared according to the procedure described in Chapter II, Section 2.3, compound II.37.

Tris(acetonitrile)tricarbonylchromium(0) (III.4):^[155]

A mixture of cobalt hexacarbonyl (**III.5**, 20.0 g, 90.9 mmol, 1.00 eq) and acetonitrile (250 mL) was heated to gentle reflux for 24 h (95 °C oil bath temperature). In order to rinse sublimed cobalt hexacarbonyl back into the flask, the temperature was gradually increased after 24 h until strong reflux was reached and the mixture was stirred for 24 h at this temperature (140 °C oil bath temperature). Then, the mixture was allowed to cool to room temperature and the bulk of solvent was removed on the rotary evaporator. To the residue was added pentane (150 mL) and diethyl ether (100 mL), by what a monophasic solvent system was achieved, from which the product crystallized as a yellow powder. The solid was filtered under a stream of argon, washed with pentane (100 mL) and dried to yield **III.4** as a yellow solid (22.5 g, 95 %).

Since **III.4** decomposes violently (spontaneous ignition) if exposed to air, it was stored and weighed in a glove box.

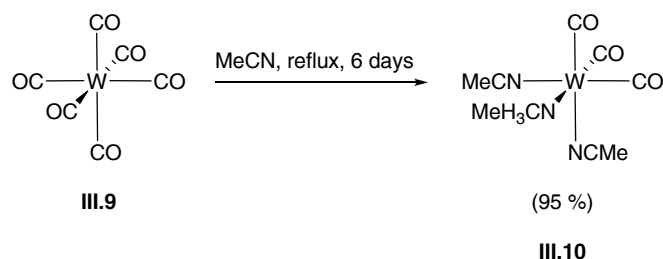
IR (neat): $\tilde{\nu}_{\max} = 2016, 1874, 1821, 1418, 1033$.

Tris(acetonitrile)tricarbonylmolybdenum(0) (III.8).^[155]

A flask containing molybdenum hexacarbonyl (**III.7**, 1.00 g, 3.79 mmol, 1.00 eq) was cooled to $-78\text{ }^{\circ}\text{C}$ and evacuated. Then, acetonitrile (30.0 mL) was added (freezes) and the flask was flushed with argon. The resulting mixture was allowed to warm to room temperature and then heated to gentle reflux for 24 h ($95\text{ }^{\circ}\text{C}$ oil bath temperature). In order to rinse sublimed molybdenum hexacarbonyl back into the flask, the temperature was gradually increased after 24 h until strong reflux was reached and the mixture was stirred for 48 h at this temperature ($140\text{ }^{\circ}\text{C}$ oil bath temperature). Then, the mixture was allowed to cool to room temperature and the bulk of solvent was removed on the rotary evaporator. To the residue was added pentane (18.0 mL) and diethyl ether (12.0 mL), by what a monophasic solvent system was achieved, from which the product crystallized as a dark yellow powder. The solid was filtered under a stream of argon, washed with pentane (15.0 mL) and dried to yield **III.8** as a dark yellow solid (1.08 g, 94 %).

Since **III.8** rapidly decomposes if exposed to air, it was stored and weighed in a glove box or freshly prepared solutions of **III.8** were directly used in subsequent reactions.

IR (neat): $\tilde{\nu}_{\text{max}} = 1920, 1796$.

Tris(acetonitrile)tricarbonyltungsten(0) (III.10).^[155]

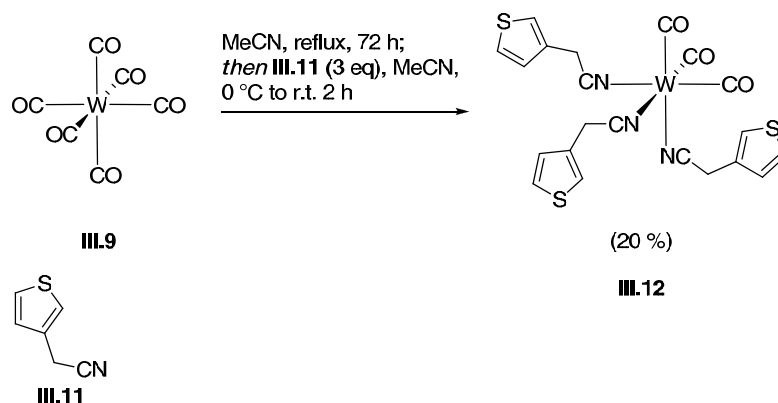
A flask containing tungsten hexacarbonyl (**III.9**, 1.00 g, 2.84 mmol, 1.00 eq) was cooled to $-78\text{ }^{\circ}\text{C}$ and evacuated. Then, acetonitrile (30.0 mL) was added (freezes) and the flask was flushed with argon. The resulting mixture was allowed to warm to room temperature and then

heated to gentle reflux for 24 h (95 °C oil bath temperature). In order to rinse sublimed molybdenum hexacarbonyl back into the flask, the temperature was gradually increased after 24 h until strong reflux was reached and the mixture was stirred for 48 h at this temperature (140 °C oil bath temperature). Then, the mixture was allowed to cool to room temperature and the bulk of solvent was removed on the rotary evaporator. To the residue was added pentane (18.0 mL) and diethyl ether (12.0 mL), by what a monophasic solvent system was achieved, from which the product crystallized as a dark yellow powder. The solid was filtered under a stream of argon, washed with pentane (15.0 mL) and dried to yield **III.10** as a brownish solid (1.05 g, 95 %).

Since **III.10** rapidly decomposes if exposed to air, it was stored and weighed in a glove box or freshly prepared solutions of **III.10** were directly used in subsequent reactions.

IR (neat): $\tilde{\nu}_{\max} = 1911, 1791$.

fac-[W(CO)₃(NCCH₂(3-C₄H₃S))₃] complex (**III.12**):^[156]



A dry 50.0 mL flask was charged with tungsten hexacarbonyl (**III.9**, 1.00 g, 2.84 mmol, 1.00 eq), cooled to -78 °C and evacuated. Acetonitrile (10.5 mL) was cannulated into the flask (freezes) and the flask was flushed with argon. The mixture was allowed to warm to room temperature and was subsequently heated to reflux for 72 h. The mixture was allowed to cool to room temperature and then cooled to 0 °C. A solution of thiophene-3-acetonitrile (**III.11**, 970 μ L, 8.53 mmol, 3.00 eq) in degassed acetonitrile (5.00 mL) was added and the mixture was allowed to warm up to be stirred for 2 h at room temperature. The mixture was filtered and the solvent was removed *in vacuo*. The resulting residue was washed with diethyl ether (25.0 mL) and dried to furnish **III.12** as a pale brown solid (388 mg, 20 %).

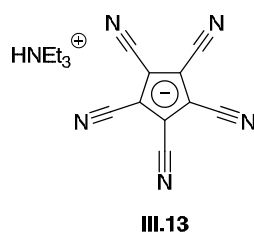
Since **III.12** is air-sensitive, it was stored and weighed in a glove box.

^1H NMR (400 MHz, CDCl_3): $\delta = 7.37\text{-}7.33$ (m, 3H), $7.26\text{-}7.24$ (m, 3H), $7.04\text{-}7.01$ (m, 3H), 3.73 (s, 6H).

^{13}C NMR (150 MHz, CDCl_3): $\delta = 196.3$ (3C), 129.4 (3C), 127.2 (3C), 127.0 (3C), 123.1 (3C), 117.6 (3C), 18.8 (3C).

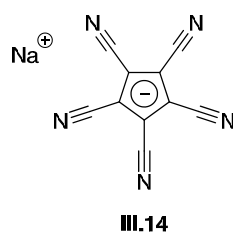
IR (neat): $\tilde{\nu}_{\text{max}} = 2258, 1937, 1893, 1756$.

Triethylammonium pccp (III.13):

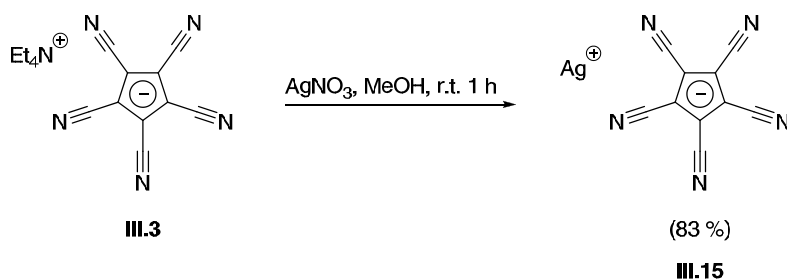


Triethylammonium pccp (**III.13**) was prepared according to the procedure described in Chapter II, Section 3.2, compound II.52.

Sodium pccp (III.14):



Sodium pccp (**III.14**) was prepared according to the procedure described in Chapter II, Section 3.2, compound II.10.

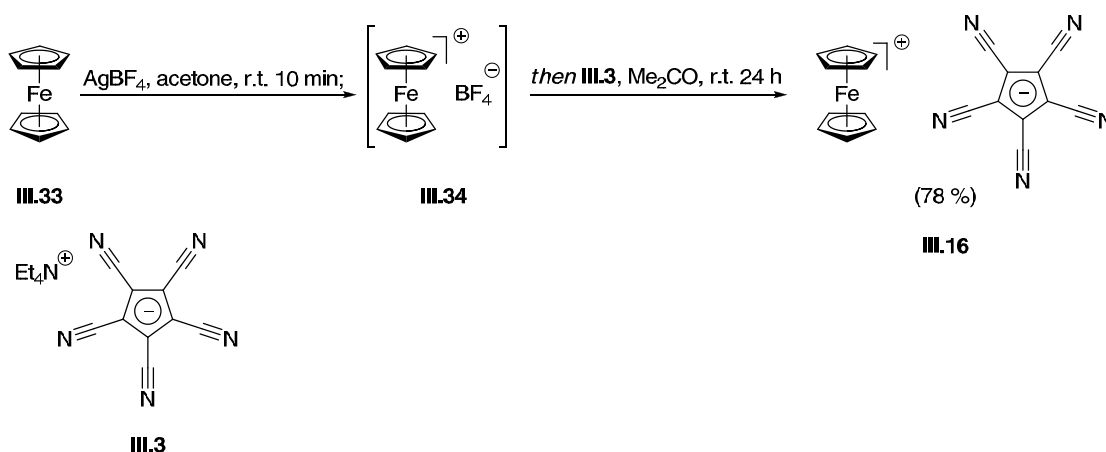
Silver pccp (III.15):^[152]

To a solution of **III.3** (513 mg, 1.60 mmol, 1.00 eq) in methanol (20.0 mL) was added silver nitrate (272 mg, 1.60 mmol, 1.00 eq) in one portion and the mixture was stirred for 1 h at room temperature. The resulting solid was filtered off, washed with methanol (2 x 10.0 mL) and diethyl ether (2 x 10.0 mL) and dried to give **III.15** as a brown colored solid (396 mg, 83 %).

mp: > 400 °C.

¹³C NMR (100 MHz, *d6*-DMSO): $\delta = 123.8$ (5C), 112.9 (5C).

IR (neat): $\tilde{\nu}_{\text{max}} = 2219, 1622, 1485$.

Ferrocenium pccp (III.16):

To a solution of ferrocene (**III.33**, 186 mg, 1.00 mmol, 1.00 eq) in acetone (8.00 mL) was added silver tetrafluoroborate (195 mg, 1.00 mmol, 1.00 eq) and the mixture was stirred for 10 min at room temperature. Then, the suspension was filtered and the resulting blue colored filtrate containing **III.34** was added to a solution of **III.3** (320 mg, 1.00 mmol, 1.00 eq) in acetone (4.00 mL). The resulting deep green colored mixture was stirred for 24 h at room

temperature. **III.16** was isolated from the mixture by allowing the solvent to evaporate over the course of two days until green crystals had formed, which were collected and washed with diethyl ether (2.00 mL). A second crop of product could be obtained by cooling the mother liquor to $-25\text{ }^{\circ}\text{C}$ (combined yield: 293 mg, 78 %).

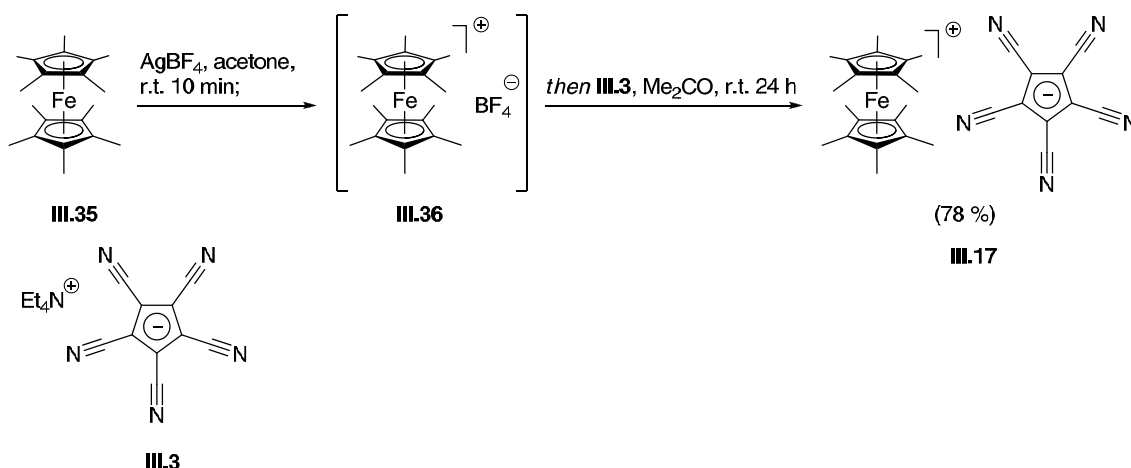
mp: $240\text{ }^{\circ}\text{C}$ (dec.).

^{13}C NMR (100 MHz, d_6 -acetone): Due to the presence of paramagnetic iron(III), no signals were observed.

IR (neat): $\tilde{\nu}_{\text{max}} = 2215, 1469, 1393, 1052$.

UV/VIS: $\lambda_{\text{max}} = 252, 296, 389, 777$.

Decamethylferrocenium pccp (**III.17**):



To a solution of decamethylferrocene (**III.35**, 326 mg, 1.00 mmol, 1.00 eq) in acetone (8.00 mL) was added silver tetrafluoroborate (195 mg, 1.00 mmol, 1.00 eq). The resulting suspension was stirred for 10 min at room temperature and filtered. The blue colored filtrate containing **III.36** was added to a solution of **III.3** (320 mg, 1.00 mmol, 1.00 eq) in acetone (4.00 mL). The resulting green colored mixture was stirred for 24 h at room temperature and then concentrated to a volume of ca. 4 mL. The residual suspension was heated to $60\text{ }^{\circ}\text{C}$, hot filtered and then allowed to cool to room temperature to give **III.17** as green crystals. A second crop of **III.17** was obtained by concentrating the mother liquor (combined yield: 418 mg, 81 %).

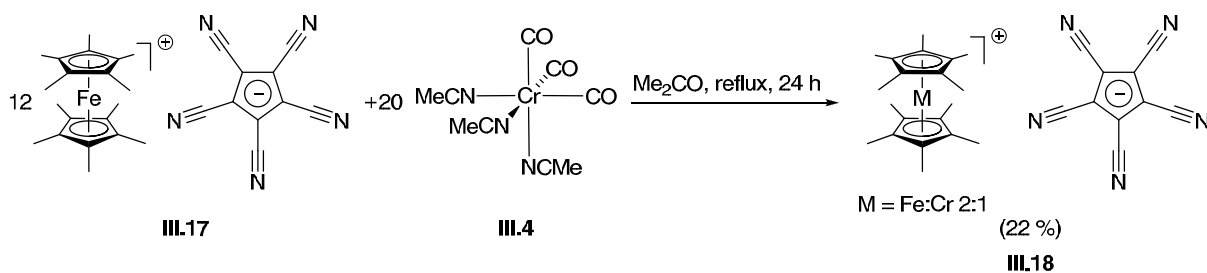
mp: $315\text{ }^{\circ}\text{C}$ (dec.).

^{13}C NMR (100 MHz, *d6*-acetone): 113.5, 102.8 (due to the presence of paramagnetic iron(III), no signals of the ferrocenium cation were observed).

IR (neat): $\tilde{\nu}_{\text{max}} = 2214, 1464, 1389, 1023$.

UV/VIS: $\lambda_{\text{max}} = 346, 390, 782$.

Decamethylmetallocenium ($\text{Fe}_{0.67}\text{Cr}_{0.33}$) pccp (III.18):



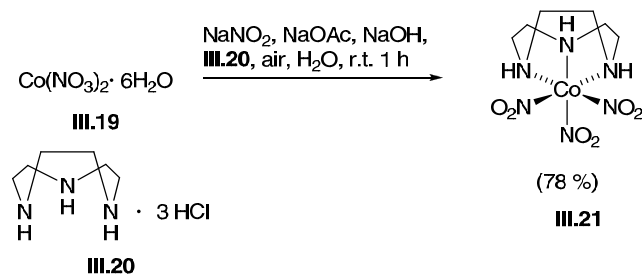
To a mixture of **III.17** (50.0 mg, 968 μmol , 3.00 eq) and **III.4** (41.0 mg, 161 μmol , 5.00 eq) was added degassed acetone (5.00 mL) and the resulting mixture was heated to reflux for 24 h. The mixture was allowed to cool to room temperature, cooled to 5 °C and filtered. Slow evaporation of solvent gave green crystals of **III.18**, which were washed with diethyl ether (1.00 mL) and dried (10.9 mg, 22 %).

mp: 290 °C (dec.).

^{13}C NMR (100 MHz, *d6*-acetone): 113.1, 102.4 (due to the presence of paramagnetic iron(III), no signals of the ferrocenium cation were observed).

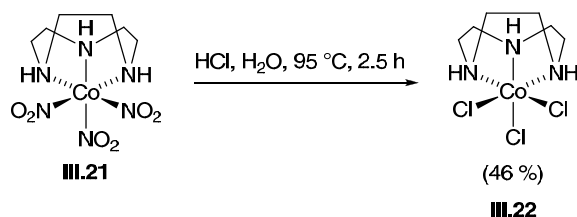
IR (neat): $\tilde{\nu}_{\text{max}} = 2213, 1464, 1390, 1053$.

UV/VIS: $\lambda_{\text{max}} = 304, 348, 401, 784$.

(1,4,7-triazacyclononane)cobalt(III) trinitrite (III.21):^[157]

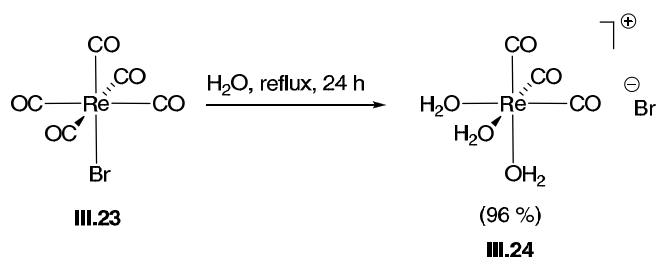
To a mixture of cobalt(II)nitrate hexahydrate (**III.19**, 327 mg, 1.12 mmol, 1.30 eq) and sodium nitrite (341 mg, 4.95 mmol, 5.90 eq) was added a buffer solution made of sodium hydroxide (899 mg, 22.5 mmol, 26.8 eq), acetic acid (2.57 mL, 44.9 mmol, 53.6 eq) and water (22.5 mL). The mixture was stirred and air was bubbled through the resulting solution. A mixture of 1,4,7-triazacyclononane trihydrochloride (**III.20**, 200 mg, 0.830 mmol, 1.00 eq), sodium hydroxide (101 mg, 2.51 mmol, 3.00 eq) and water (2.50 mL) was added dropwise to the reaction mixture. After complete addition, stirring and aeration was continued for 1 h, then the resulting yellow-green precipitate was collected, washed with water (100 mL) and acetone (5.00 mL) and dried *in vacuo* to afford **III.21** as an amorphous powder (211 mg, 78 %).

IR (neat): $\tilde{\nu}_{\text{max}} = 3216$.

(1,4,7-triazacyclononane)cobalt(III) trichloride (III.22):^[157]

A suspension of $[\text{Co}(\text{TACN})(\text{NO}_2)_3]$ (**III.21**, 64.0 mg, 0.179 mmol, 1.00 eq) in an aq. HCl solution (1.00 M, 3.50 mL, 3.57 mmol, 20.0 eq) was heated to 95°C for 2.5 h. The resulting dark violet solution was concentrated to dryness. The blue-green residue was washed with water (3 x 1.00 mL) and acetone (1.00 mL) and dried to give **III.22** as a turquoise solid (24.0 mg, 46 %).

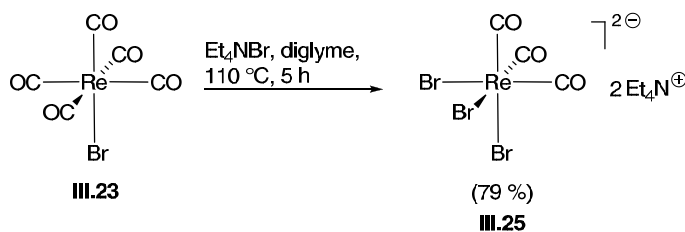
IR (neat): $\tilde{\nu}_{\text{max}} = 3220$.

Tris(aqua)tricarbonylrhenium(I) bromide (III.24):^[158]

A mixture of bromopentacarbonylrhenium bromide (**III.23**, 500 mg, 1.23 mmol, 1.00 eq) and water (5.00 mL) was heated to reflux. After 16 h, the condenser was rinsed with water (1.50 mL and refluxing was continued for another 8 h. Then, the mixture was allowed to cool to room temperature, filtered through a small plug of celite and concentrated to dryness to give **III.24** as a slightly green colored solid (477 mg, 96 %).

mp: 270 °C (dec.).

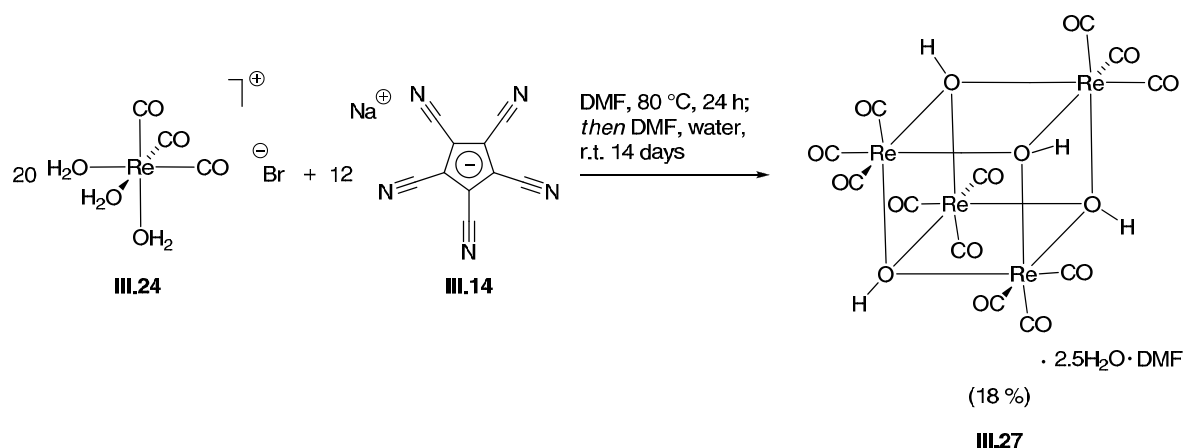
IR (neat): $\tilde{\nu}_{\max} = 2025, 1941$.

Ditetraethylammonium tricarbonylrhenium(I) tribromide (III.25):^[159]

A suspension of rheniumpentacarbonyl bromide (**III.23**, 1.00 g, 2.46 mmol, 1.00 eq) in diglyme (16.0 mL) was heated to 50 °C. A second suspension of tetraethylammonium bromide (1.10 g, 5.26 mmol, 2.14 eq) in diglyme (51.0 mL) was heated to 70 °C and was then cannulated to the first suspension containing **III.23**. The resulting mixture was heated to 110 °C for 5 h and was then allowed to cool to room temperature. The resulting precipitate was filtered off and dried. The crude mixture was purified by suspending in hot ethanol (8.00 mL) and filtration. The residual filter cake was washed with hot ethanol (2 x 5.00 mL) and dried to give **III.25** as a colorless solid (1.50 g, 79 %).

mp: 310 °C (dec.).

IR (neat): $\tilde{\nu}_{\max} = 2000, 1866$.

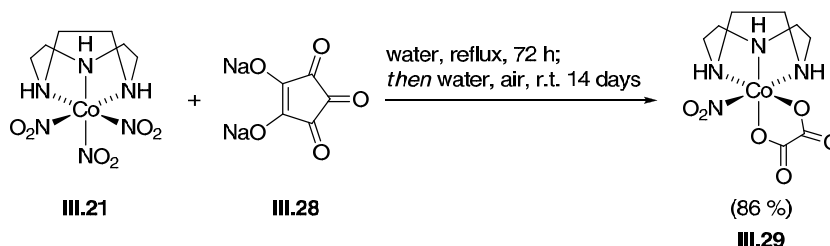
Tetrakis(tricarbonyl- μ 3-hydroxo-rhenium (III.27):

To a solution of sodium pccp (**III.14**, 23.0 mg, 111 μ mol, 3.00 eq) in DMF (3.10 mL) was added tris(aqua)tricarbonylrhenium(I) bromide (**III.24**, 75.0 mg, 0.184 mmol, 5.00 eq). The mixture was heated to 80 $^\circ\text{C}$ for 24 h and was then allowed to cool to room temperature. The reaction mixture was filtered and the filtrate was subjected to water-diffusion for 14 days, upon which time crystals suitable for X-ray crystallography formed, which were collected and dried to afford **III.27** (11.2 mg, 18 %) as a colorless solid.

mp: 290 $^\circ\text{C}$ (dec.).

IR (neat): $\tilde{\nu}_{\text{max}} = 2027, 1921$.

$^1\text{H NMR}$ (300 MHz, d_6 -acetone): 6.50 (s, 4H).

(1,4,7-triazacyclononane)(oxalato)cobalt(III) nitrite (III.29):

A mixture of [(TACN)Co(NO₂)₃] (**III.21**, 36.5 mg, 0.102 mmol, 5.00 eq), disodium croconate (**III.28**, 11.4 mg, 0.061 mmol, 3.00 eq) and water (5.00 mL) was heated to 60 $^\circ\text{C}$ for 72 h. Then, the mixture was allowed to cool to room temperature and the flask was opened to allow for slow evaporation of solvent. After 14 days, crystals suitable for X-ray crystallography had

formed, which were collected and dried to furnish **III.29** as an orange colored crystalline solid (28.3 mg, 86 %).

mp: 210 °C (dec.).

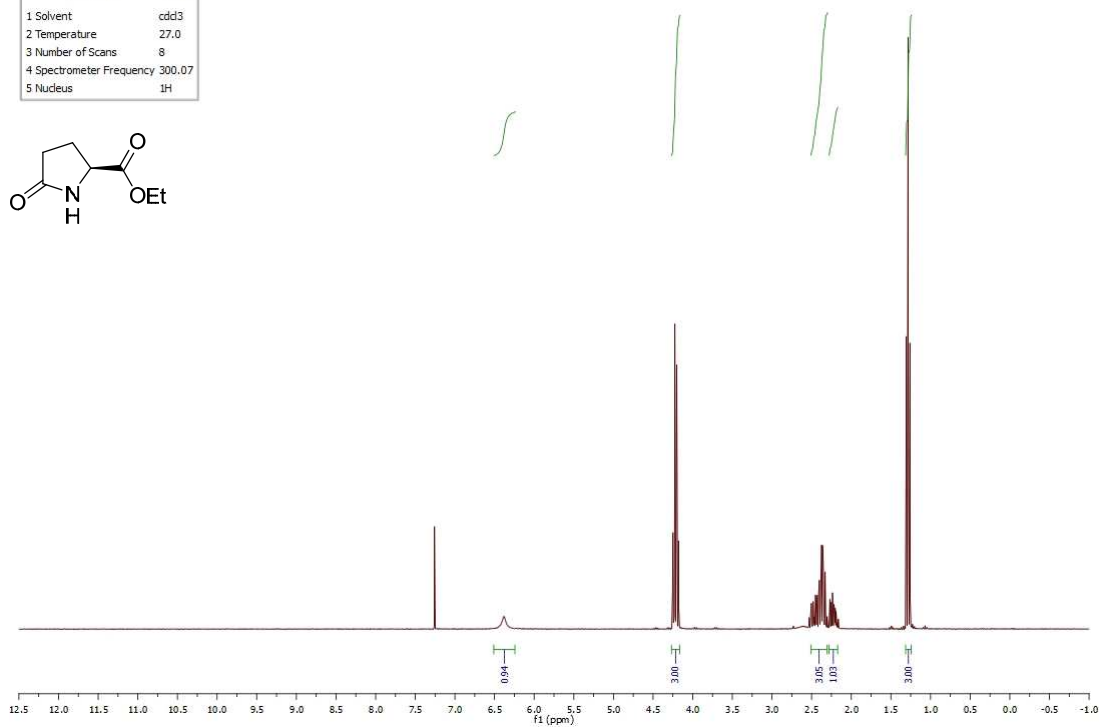
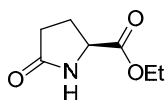
IR (neat): $\tilde{\nu}_{\text{max}} = 3144, 1694, 1661$.

APPENDICES

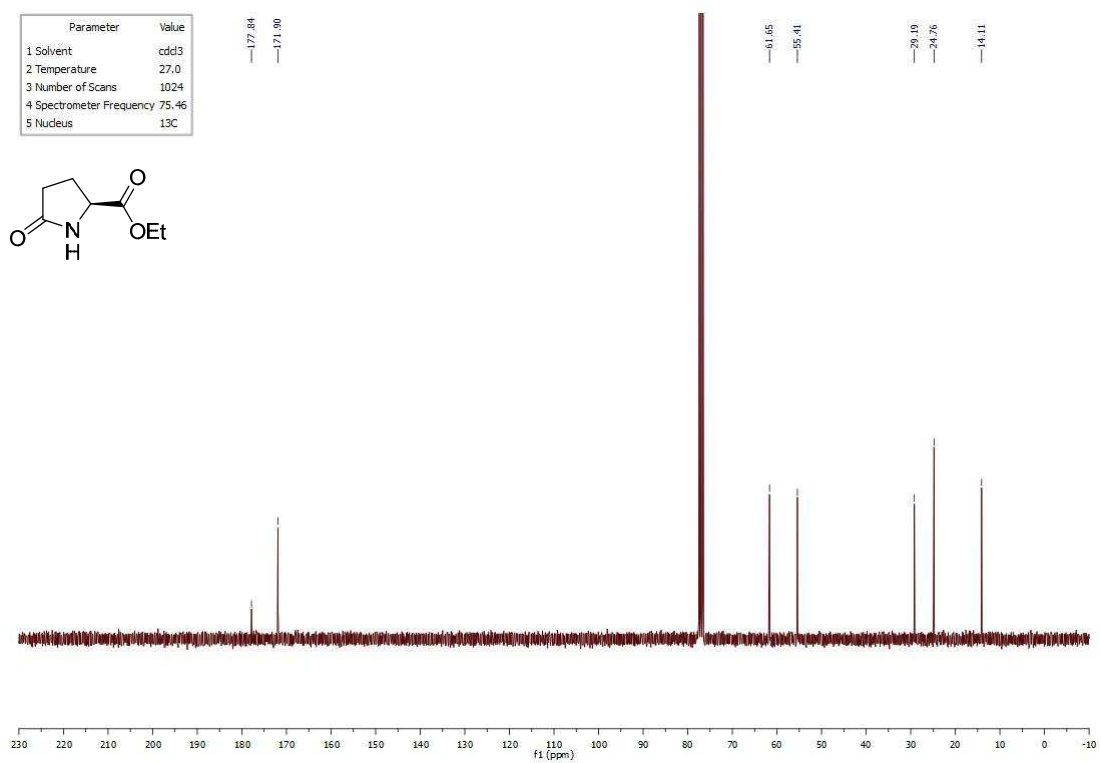
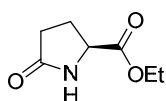
Appendix 1: NMR Spectra of Chapter I

¹H NMR spectrum of **I.338**:

Parameter	Value
1 Solvent	cdd3
2 Temperature	27.0
3 Number of Scans	8
4 Spectrometer Frequency	300.07
5 Nucleus	¹ H

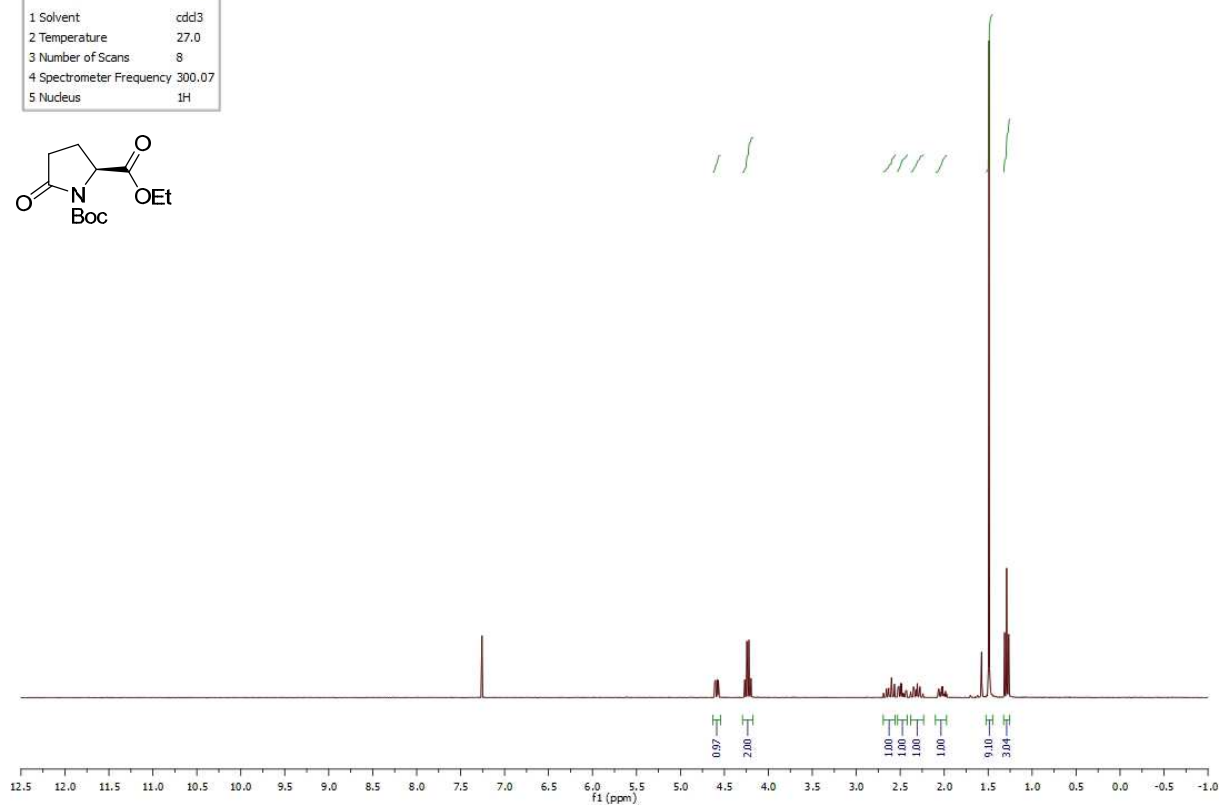
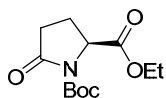
¹³C NMR spectrum of **I.338**:

Parameter	Value
1 Solvent	cdd3
2 Temperature	27.0
3 Number of Scans	1024
4 Spectrometer Frequency	75.46
5 Nucleus	¹³ C

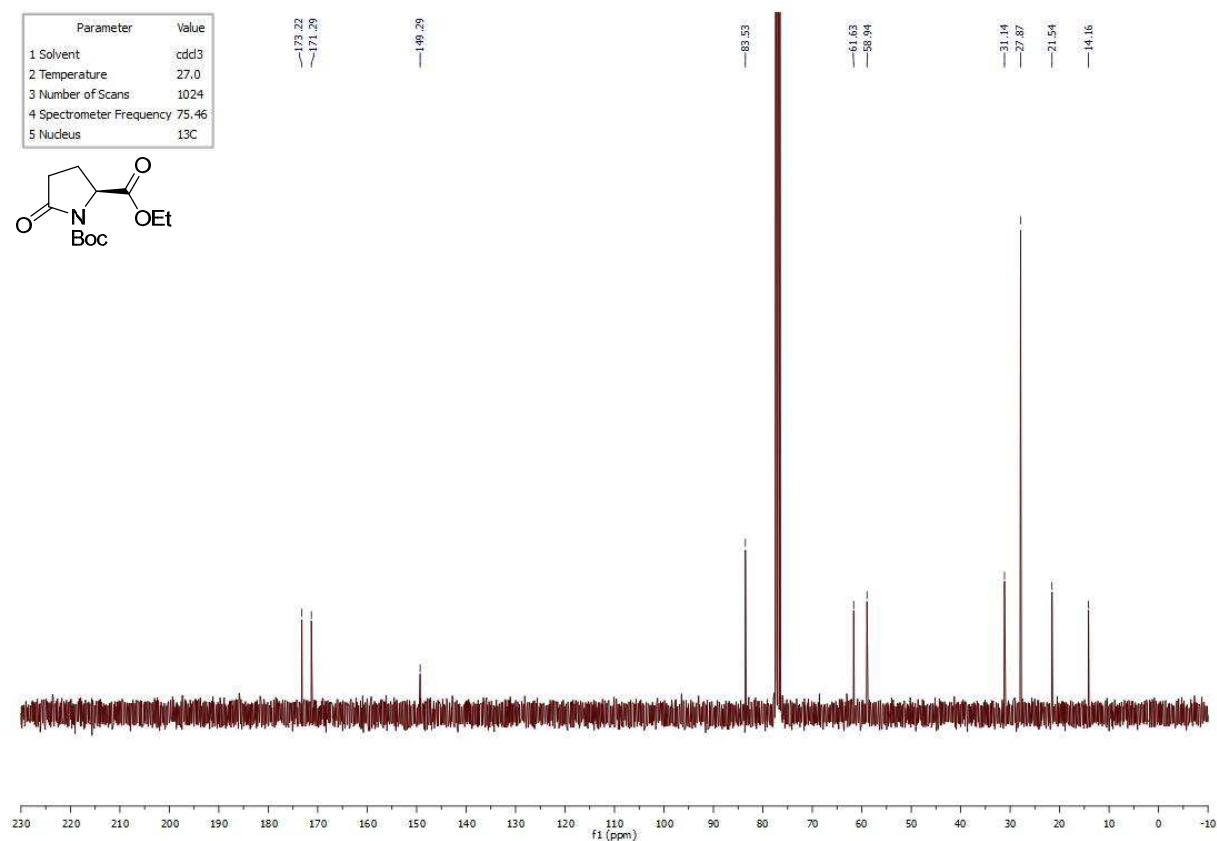
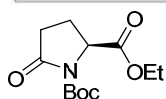


¹H NMR spectrum of **I.257**:

Parameter	Value
1 Solvent	cdcl3
2 Temperature	27.0
3 Number of Scans	8
4 Spectrometer Frequency	300.07
5 Nucleus	¹ H

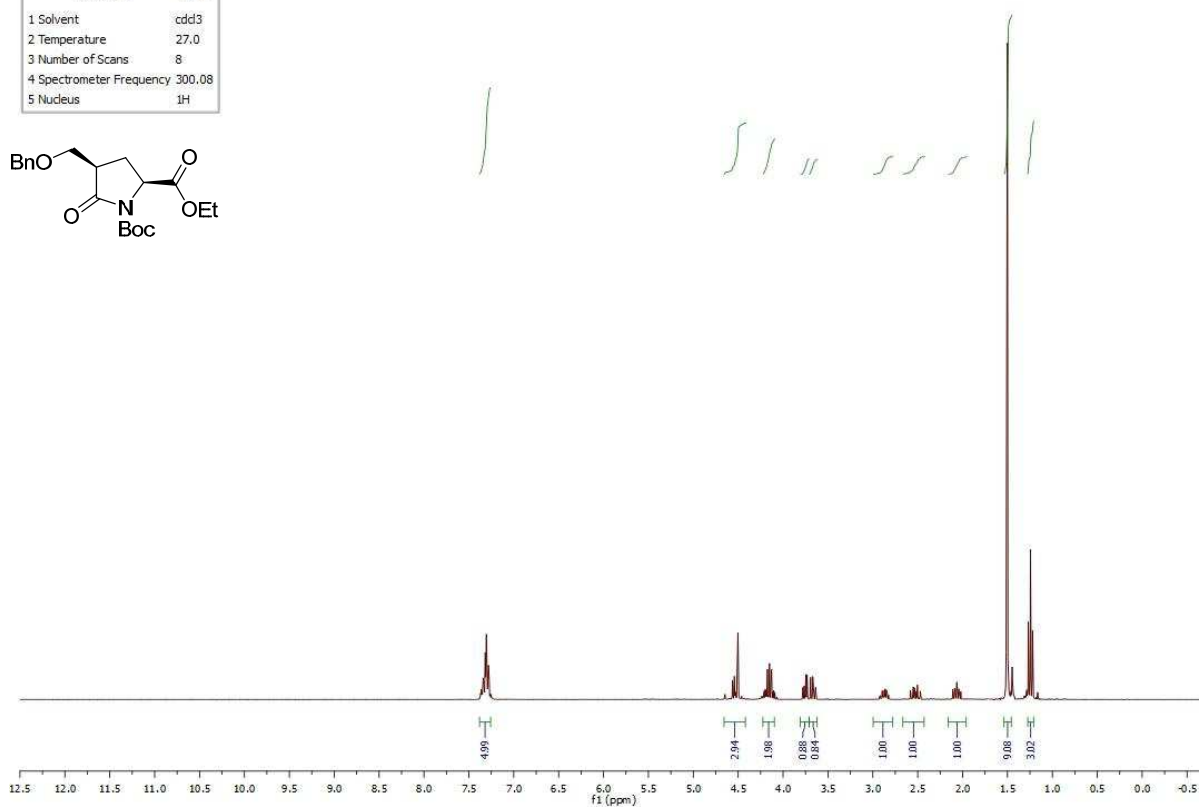
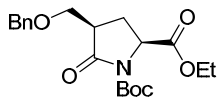
¹³C NMR spectrum of **I.257**:

Parameter	Value
1 Solvent	cdcl3
2 Temperature	27.0
3 Number of Scans	1024
4 Spectrometer Frequency	75.46
5 Nucleus	¹³ C

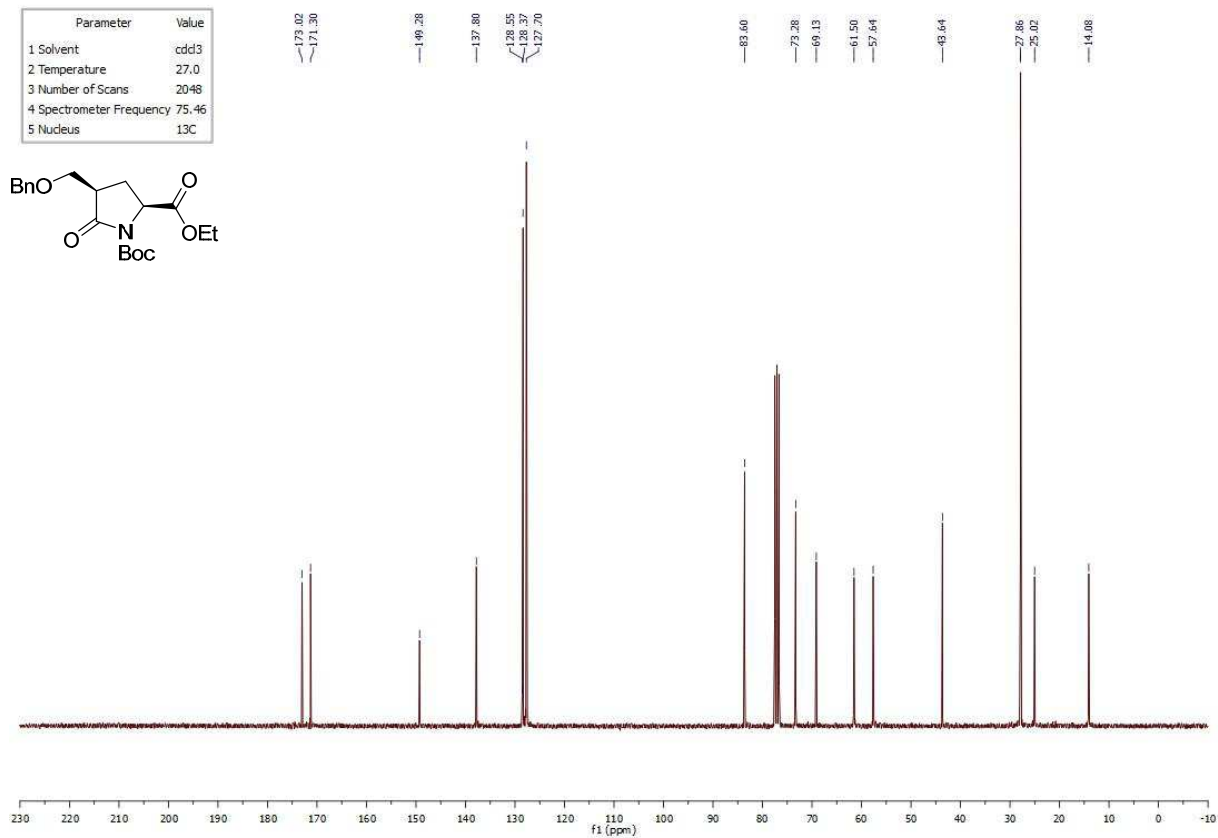
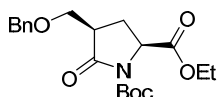


¹H NMR spectrum of **I.250**:

Parameter	Value
1 Solvent	cdd3
2 Temperature	27.0
3 Number of Scans	8
4 Spectrometer Frequency	300.08
5 Nucleus	¹ H

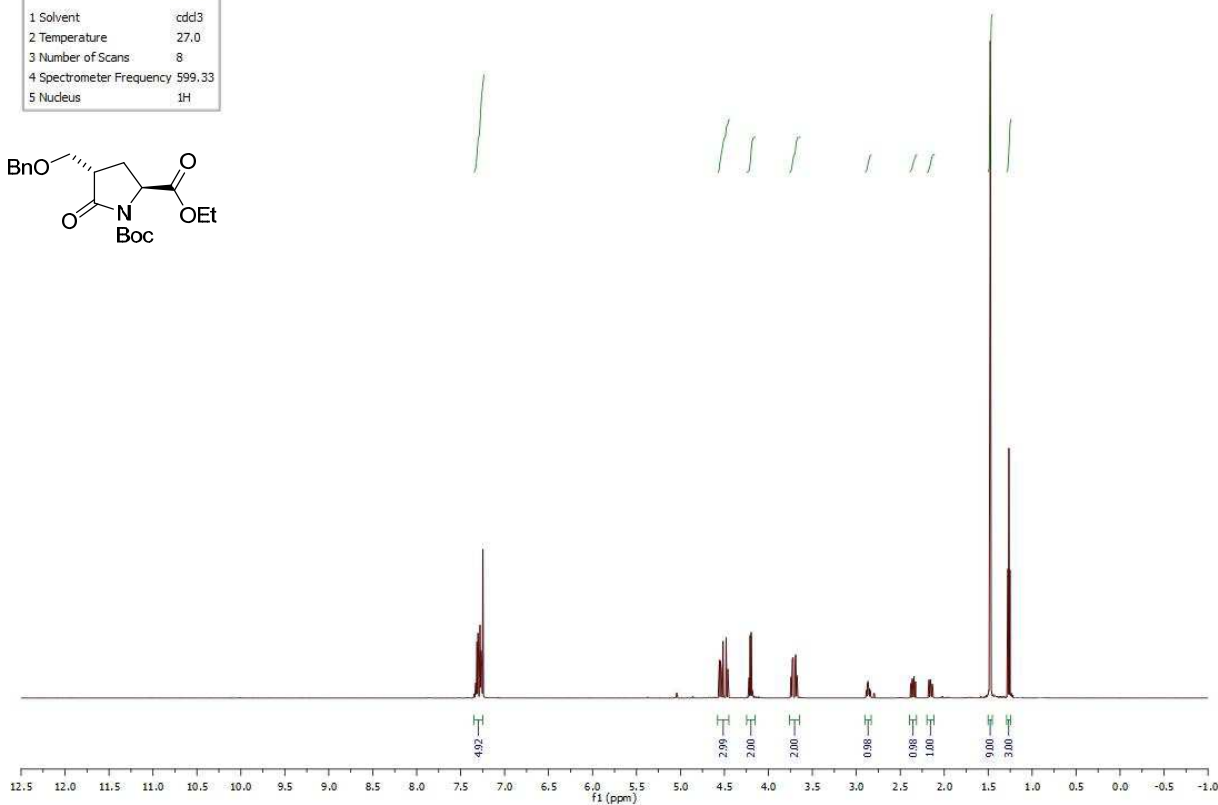
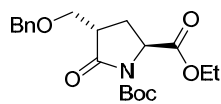
¹³C NMR spectrum of **I.250**:

Parameter	Value
1 Solvent	cdd3
2 Temperature	27.0
3 Number of Scans	2048
4 Spectrometer Frequency	75.46
5 Nucleus	¹³ C



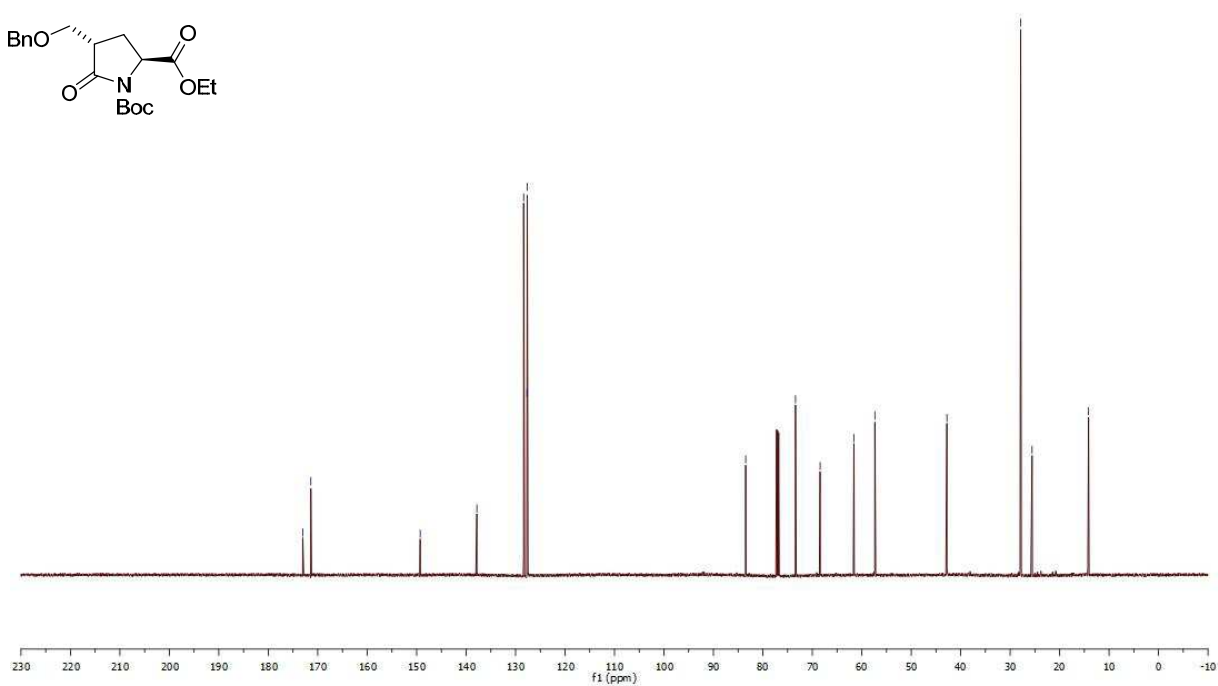
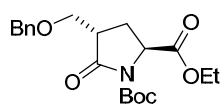
¹H NMR spectrum of **I.261**:

Parameter	Value
1 Solvent	cdcl3
2 Temperature	27,0
3 Number of Scans	8
4 Spectrometer Frequency	599,33
5 Nucleus	1H

¹³C NMR spectrum of **I.261**:

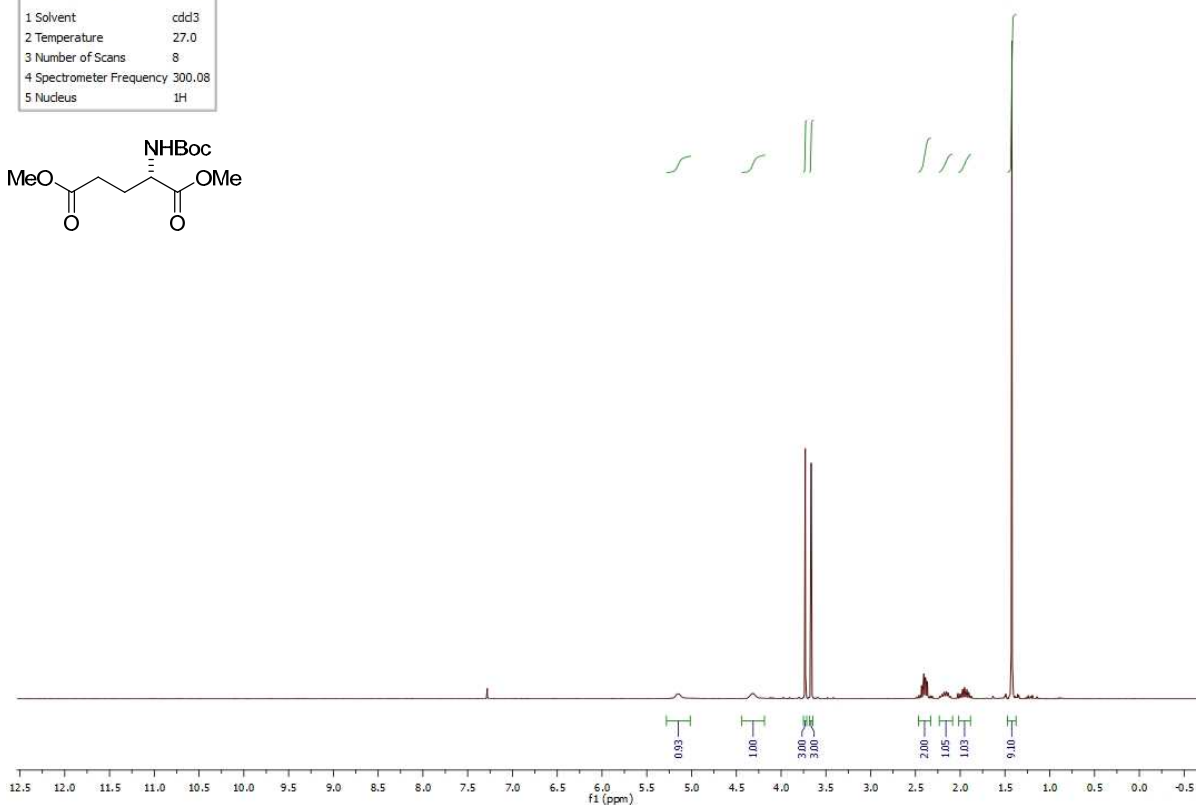
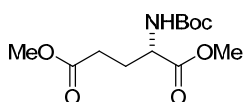
Parameter	Value
1 Solvent	cdcl3
2 Temperature	27,0
3 Number of Scans	2048
4 Spectrometer Frequency	150,72
5 Nucleus	13C

Chemical shift values (ppm): 173.03, 171.39, 149.29, 137.82, 128.37, 127.70, 127.63, 83.47, 73.40, 68.42, 61.58, 57.35, 42.79, 27.87, 25.57, 14.15.

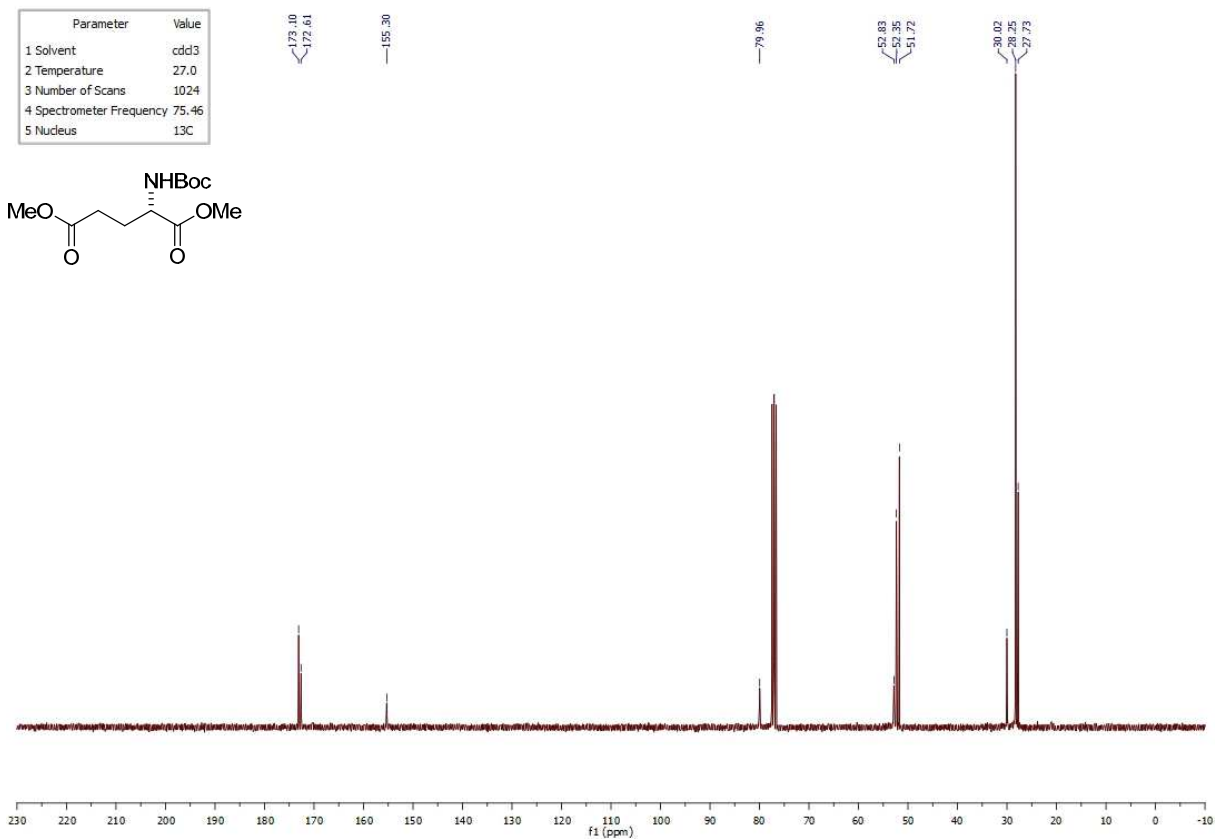
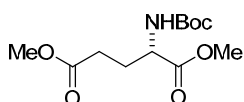


¹H NMR spectrum of **I.258**:

Parameter	Value
1 Solvent	cdd3
2 Temperature	27.0
3 Number of Scans	8
4 Spectrometer Frequency	300.08
5 Nucleus	¹ H

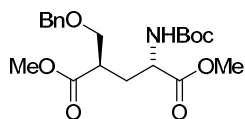
¹³C NMR spectrum of **I.258**:

Parameter	Value
1 Solvent	cdd3
2 Temperature	27.0
3 Number of Scans	1024
4 Spectrometer Frequency	75.46
5 Nucleus	¹³ C

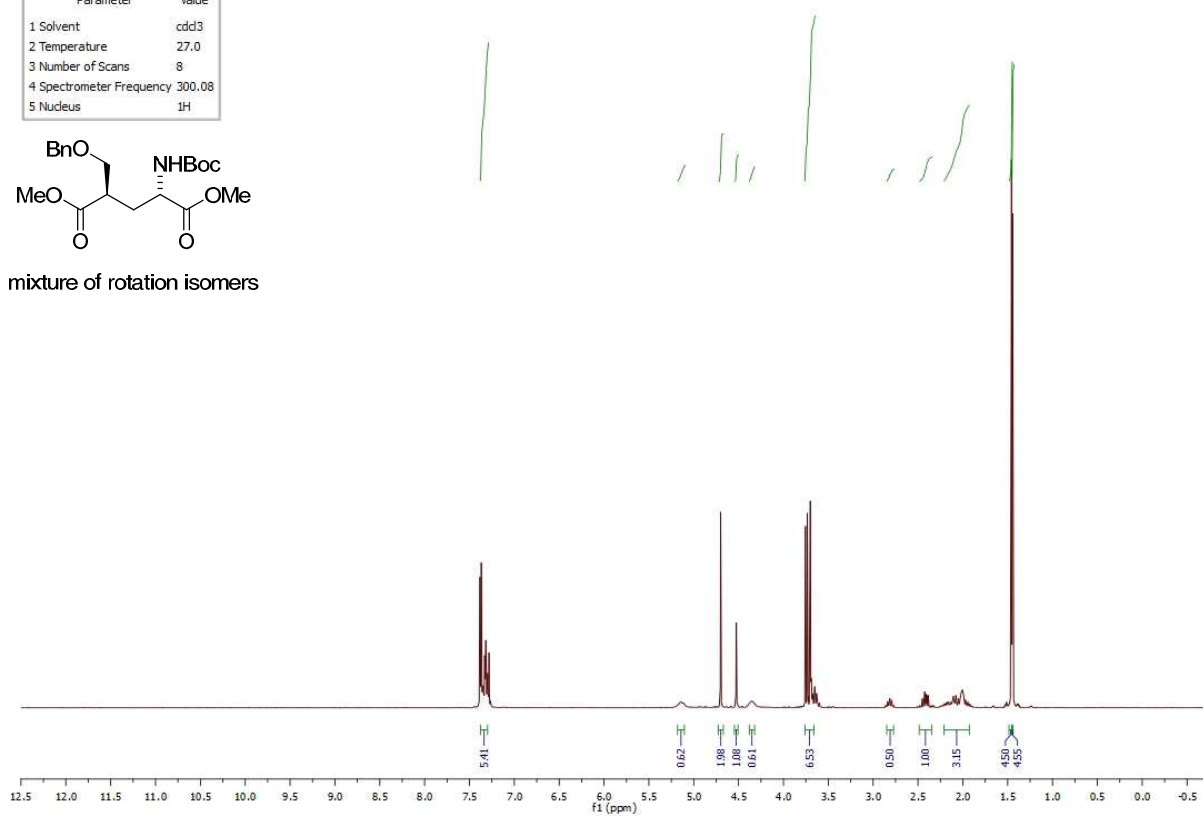


^1H NMR spectrum of **I.259**:

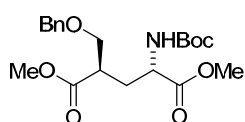
Parameter	Value
1 Solvent	cdcl3
2 Temperature	27.0
3 Number of Scans	8
4 Spectrometer Frequency	300.08
5 Nucleus	^1H



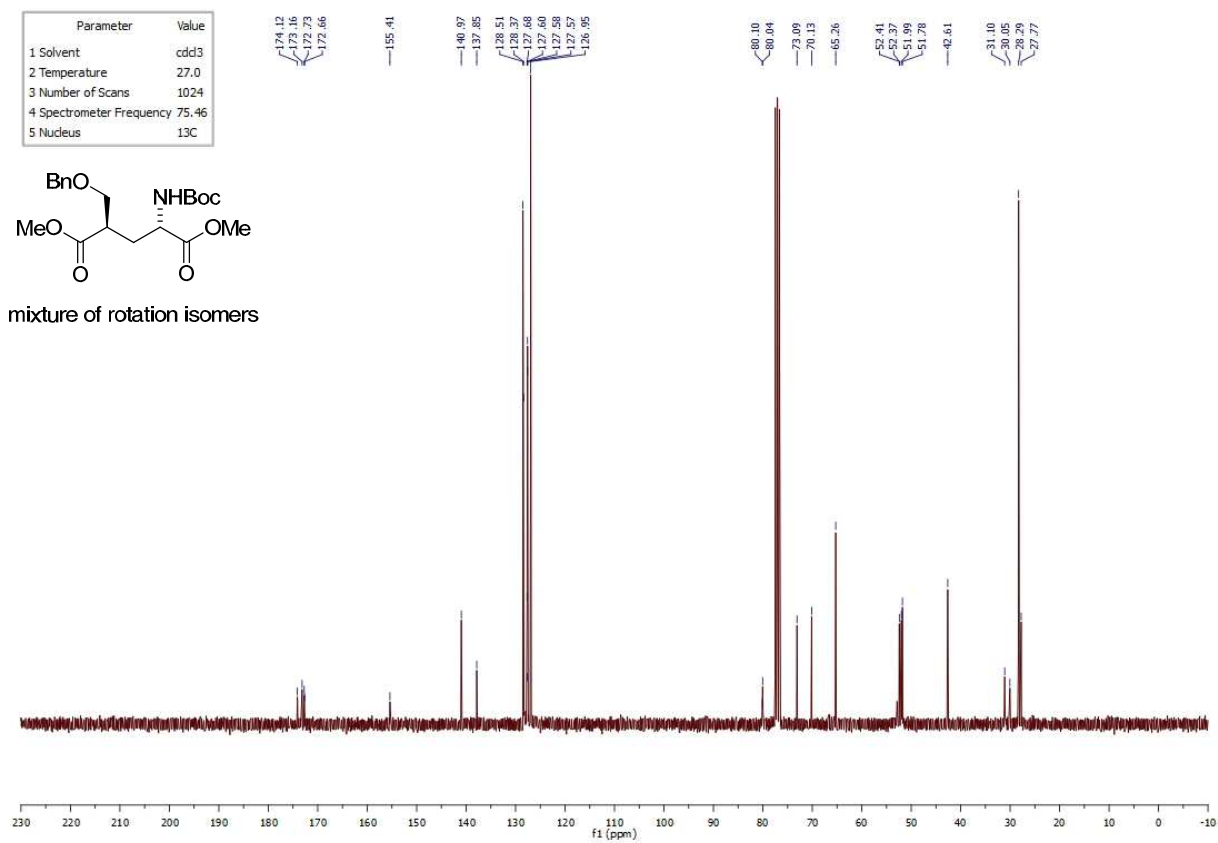
mixture of rotation isomers

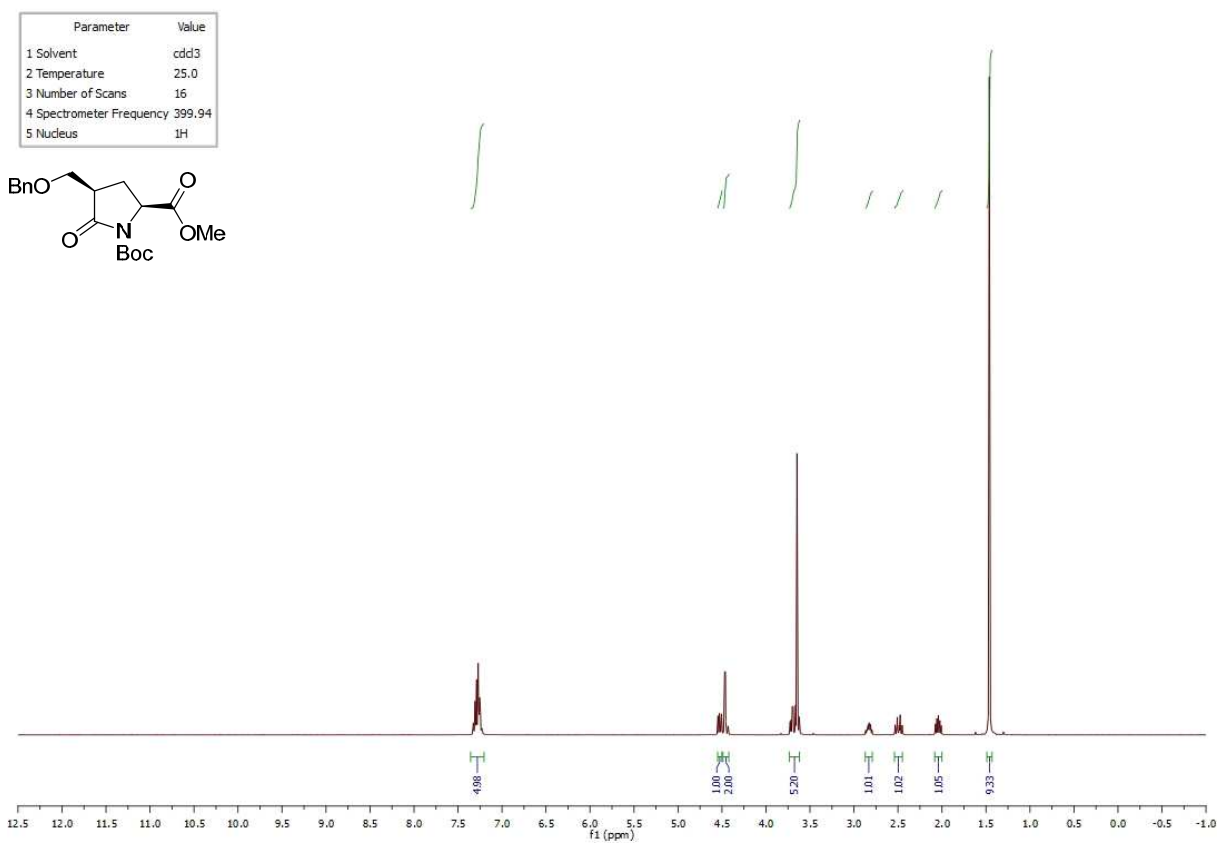
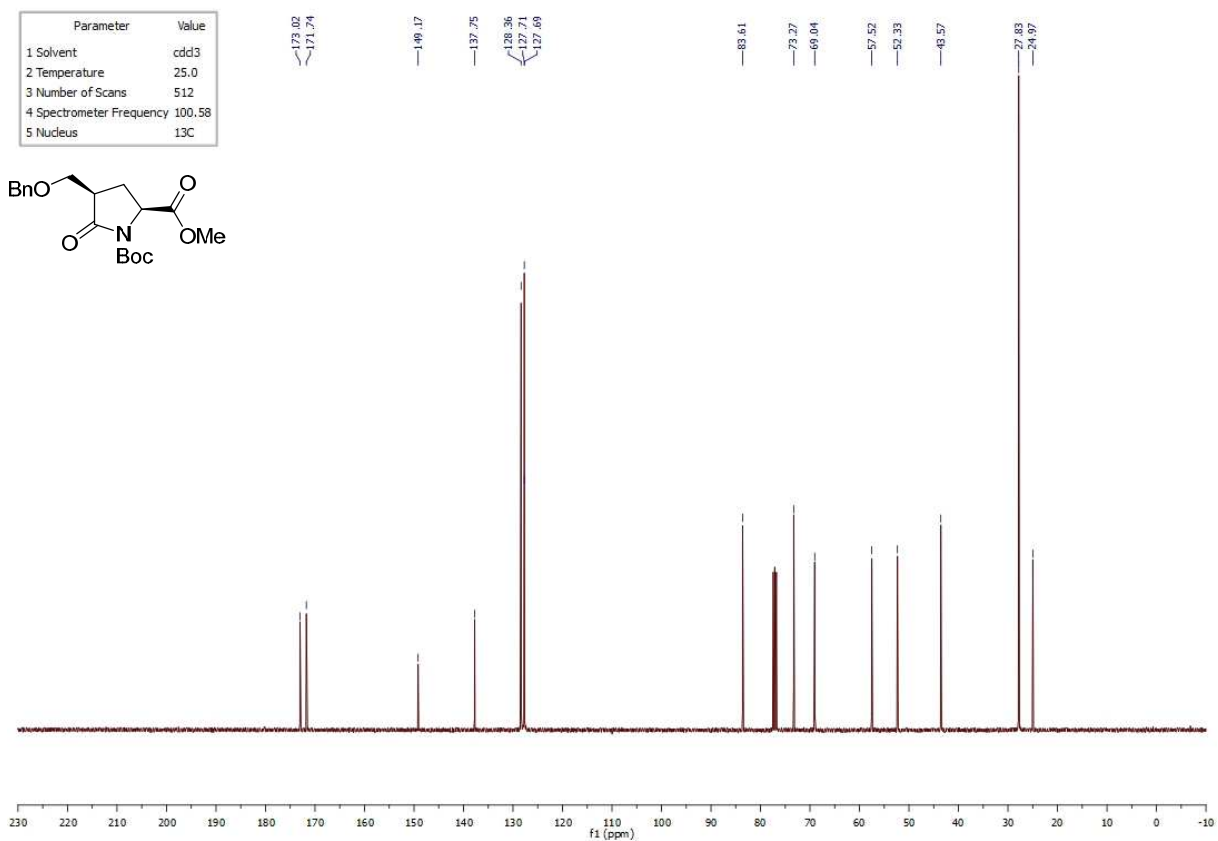
 ^{13}C NMR spectrum of **I.259**:

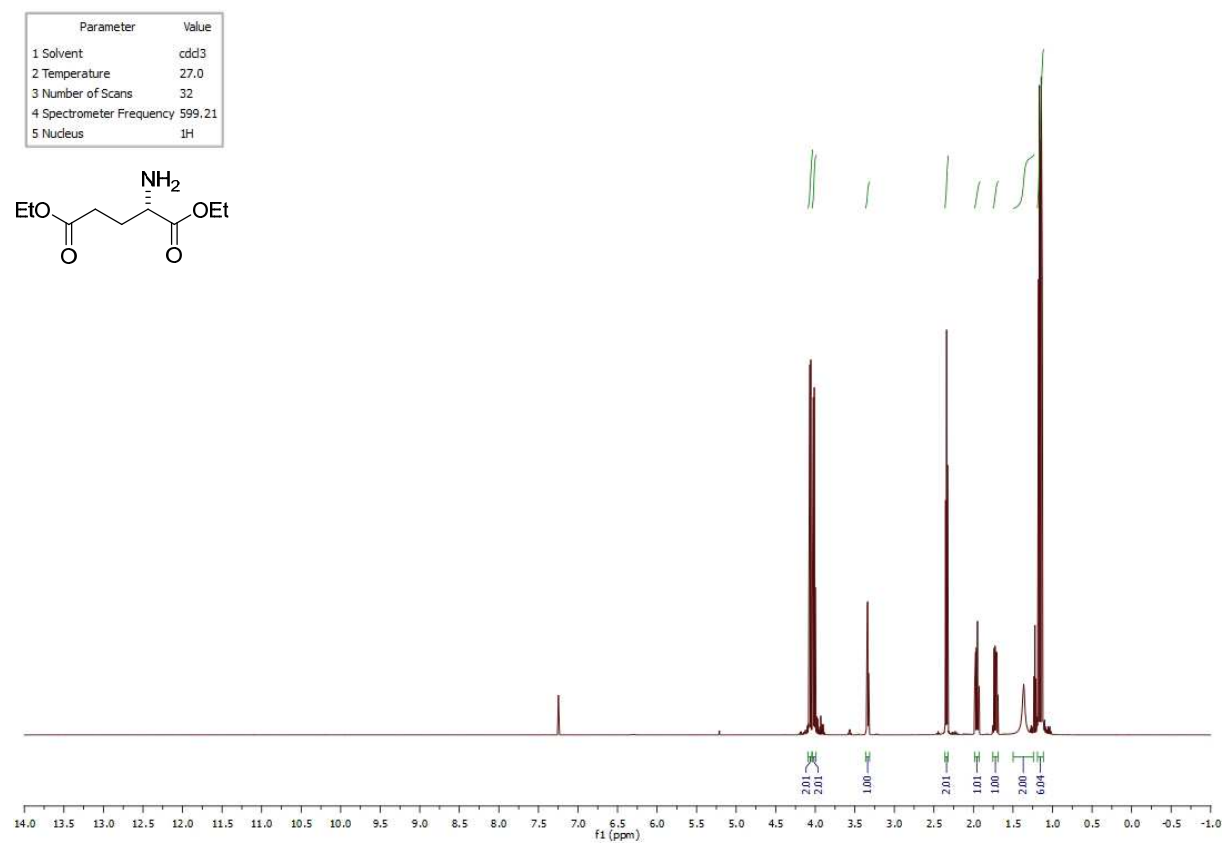
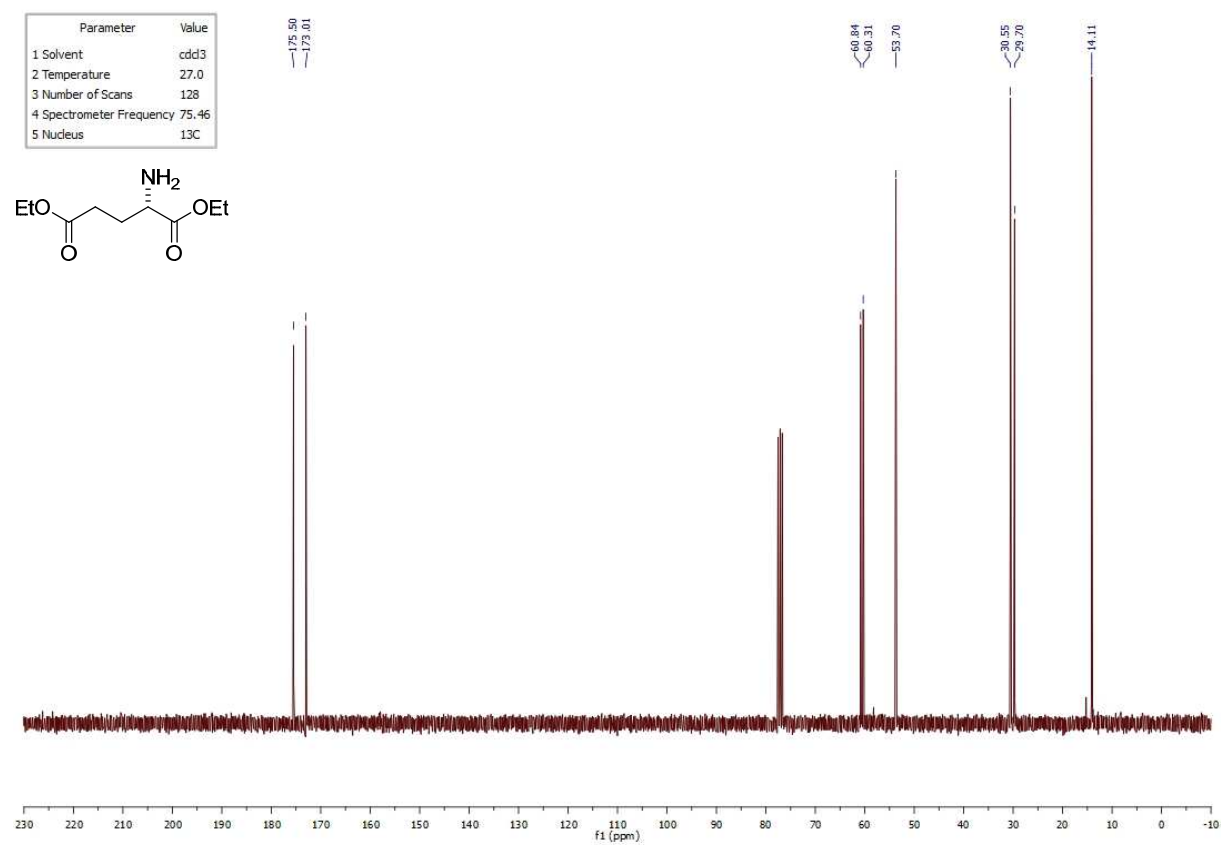
Parameter	Value
1 Solvent	cdcl3
2 Temperature	27.0
3 Number of Scans	1024
4 Spectrometer Frequency	75.46
5 Nucleus	^{13}C



mixture of rotation isomers

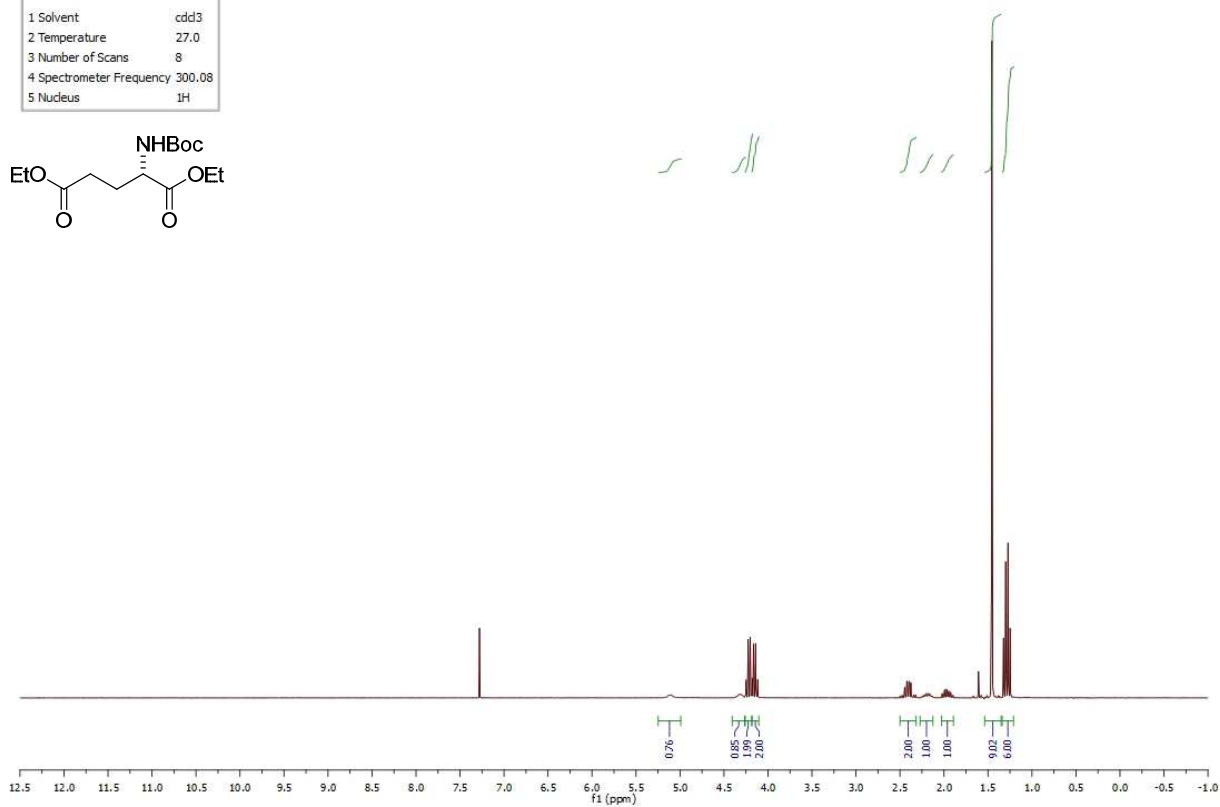
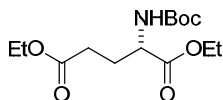


¹H NMR spectrum of **I.341**:¹³C NMR spectrum of **I.341**:

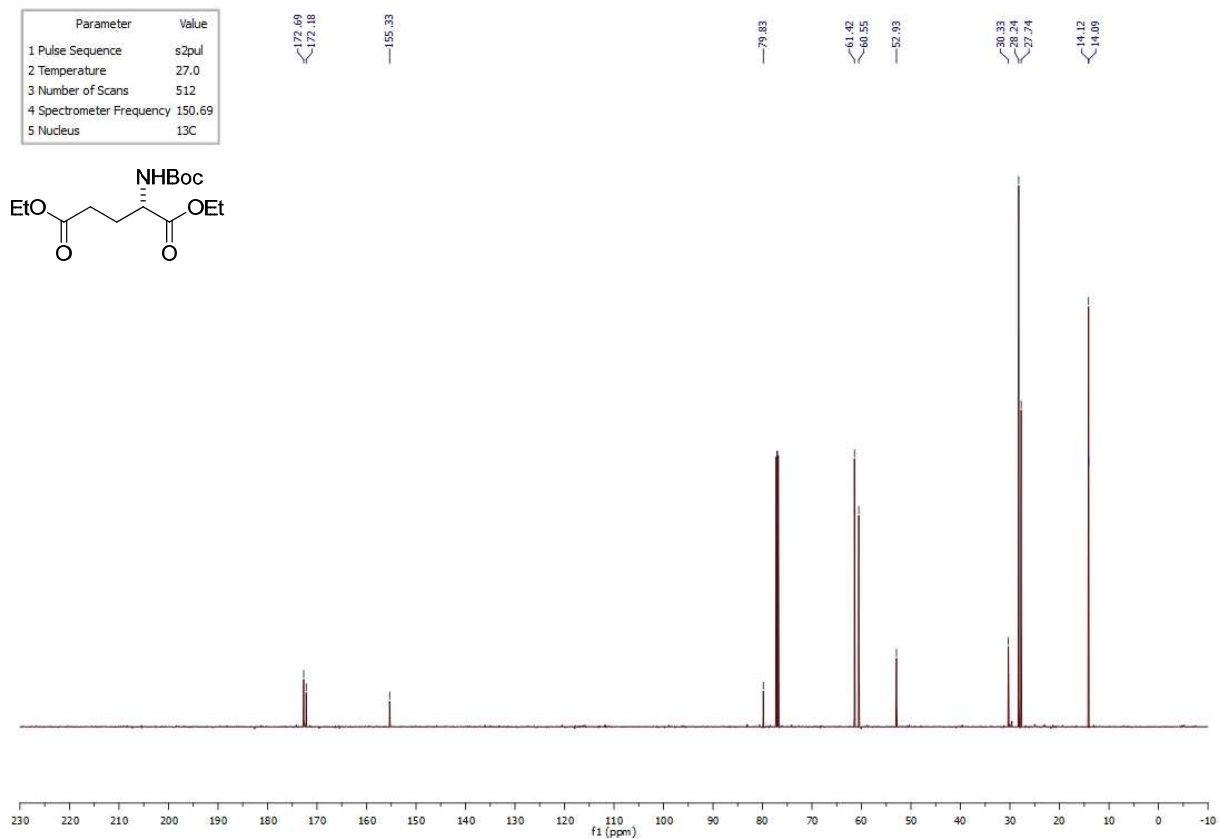
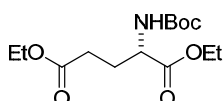
¹H NMR spectrum of **I.263**:¹³C NMR spectrum of **I.263**:

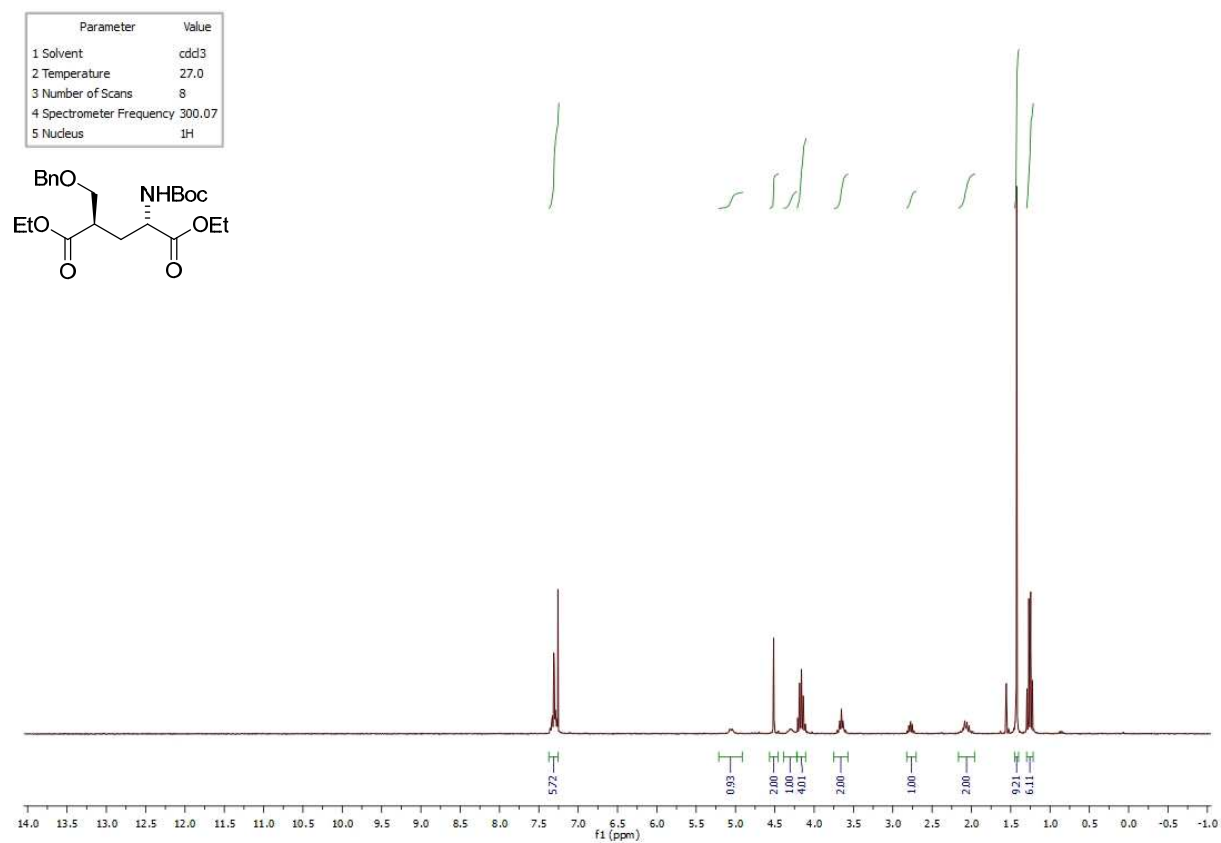
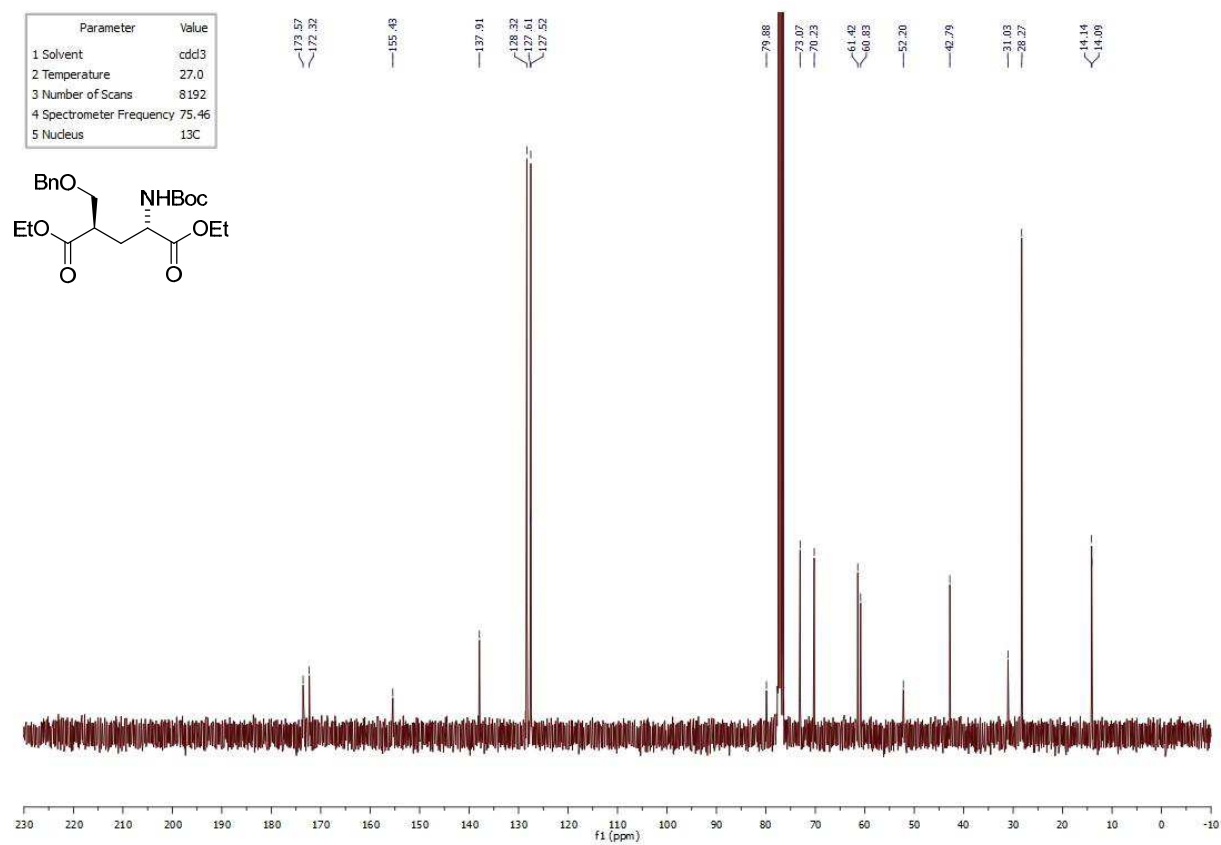
¹H NMR spectrum of **I.264**:

Parameter	Value
1 Solvent	cdd3
2 Temperature	27.0
3 Number of Scans	8
4 Spectrometer Frequency	300.08
5 Nucleus	¹ H

¹³C NMR spectrum of **I.264**:

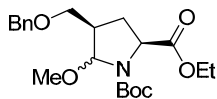
Parameter	Value
1 Pulse Sequence	s2pul
2 Temperature	27.0
3 Number of Scans	512
4 Spectrometer Frequency	150.69
5 Nucleus	¹³ C



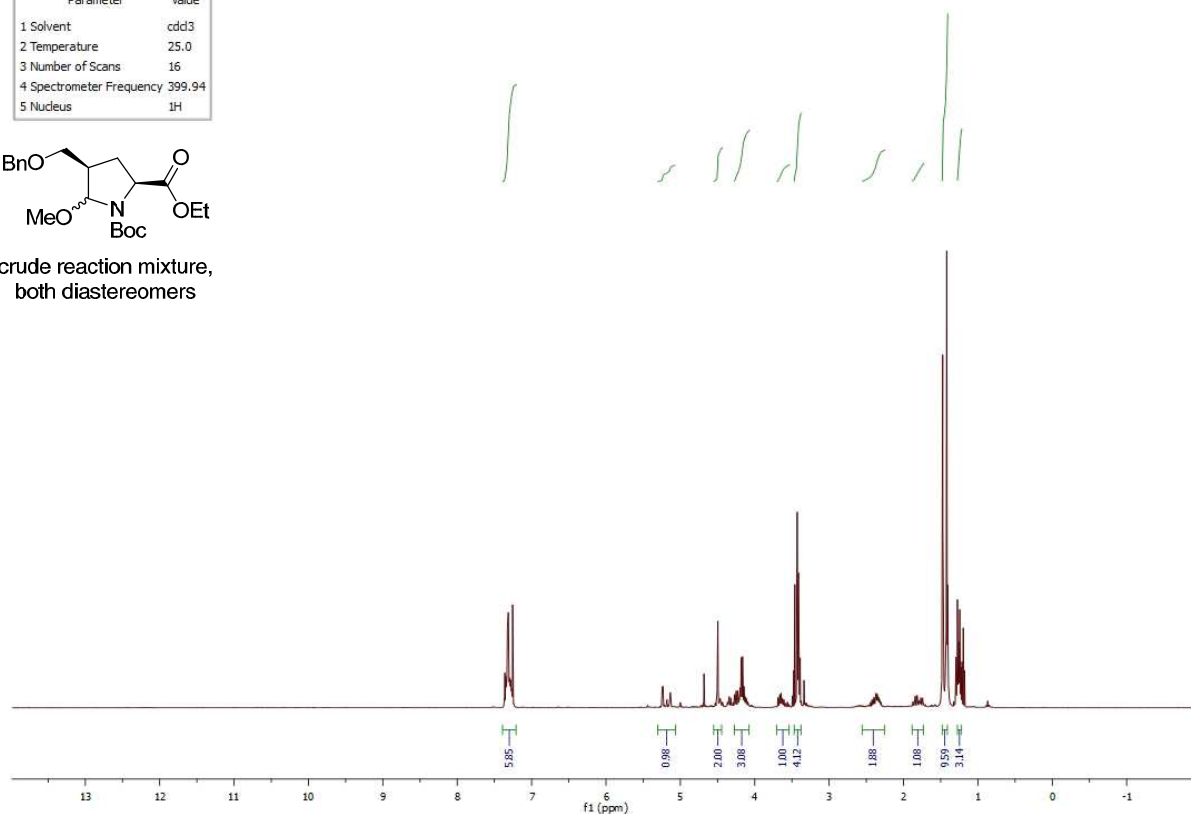
¹H NMR spectrum of **I.265**:¹³C NMR spectrum of **I.265**:

¹H NMR spectrum of **I.266**:

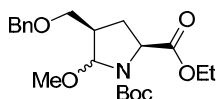
Parameter	Value
1 Solvent	cdd3
2 Temperature	25.0
3 Number of Scans	16
4 Spectrometer Frequency	399.94
5 Nucleus	¹ H



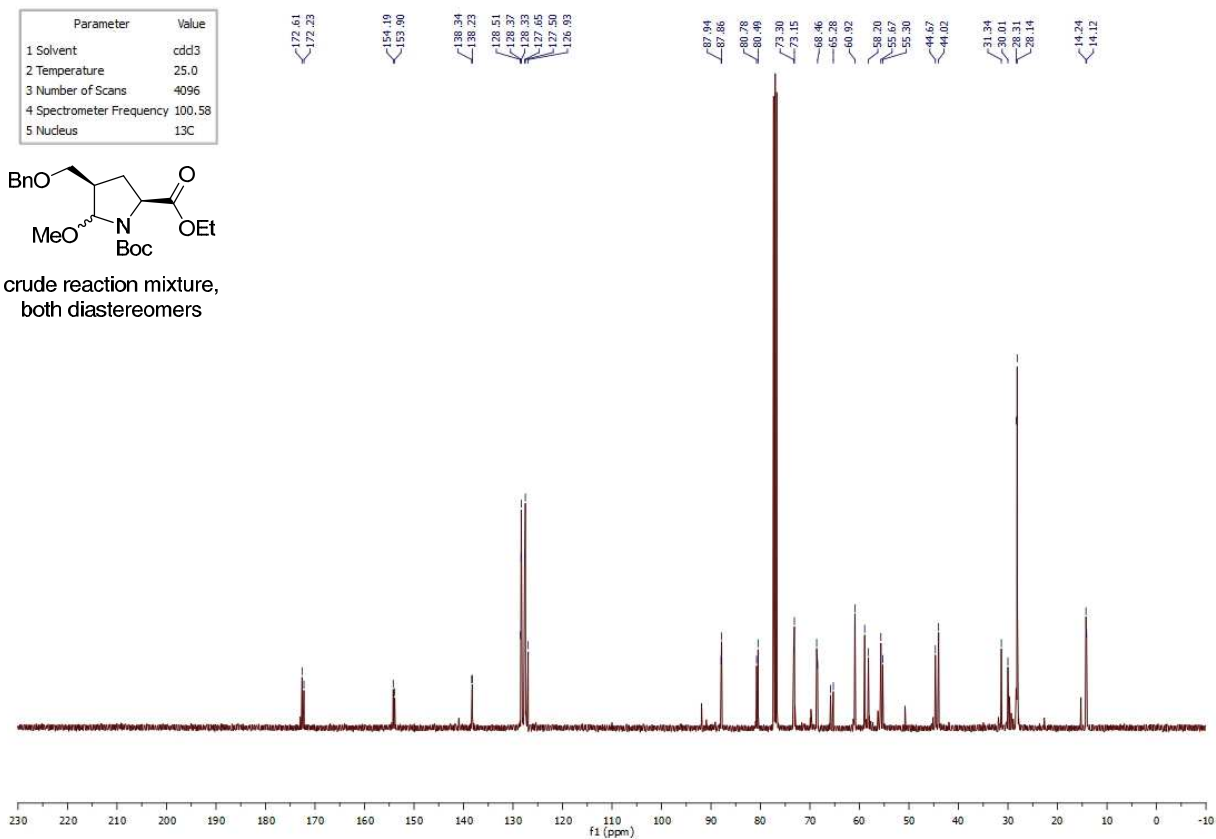
crude reaction mixture,
both diastereomers

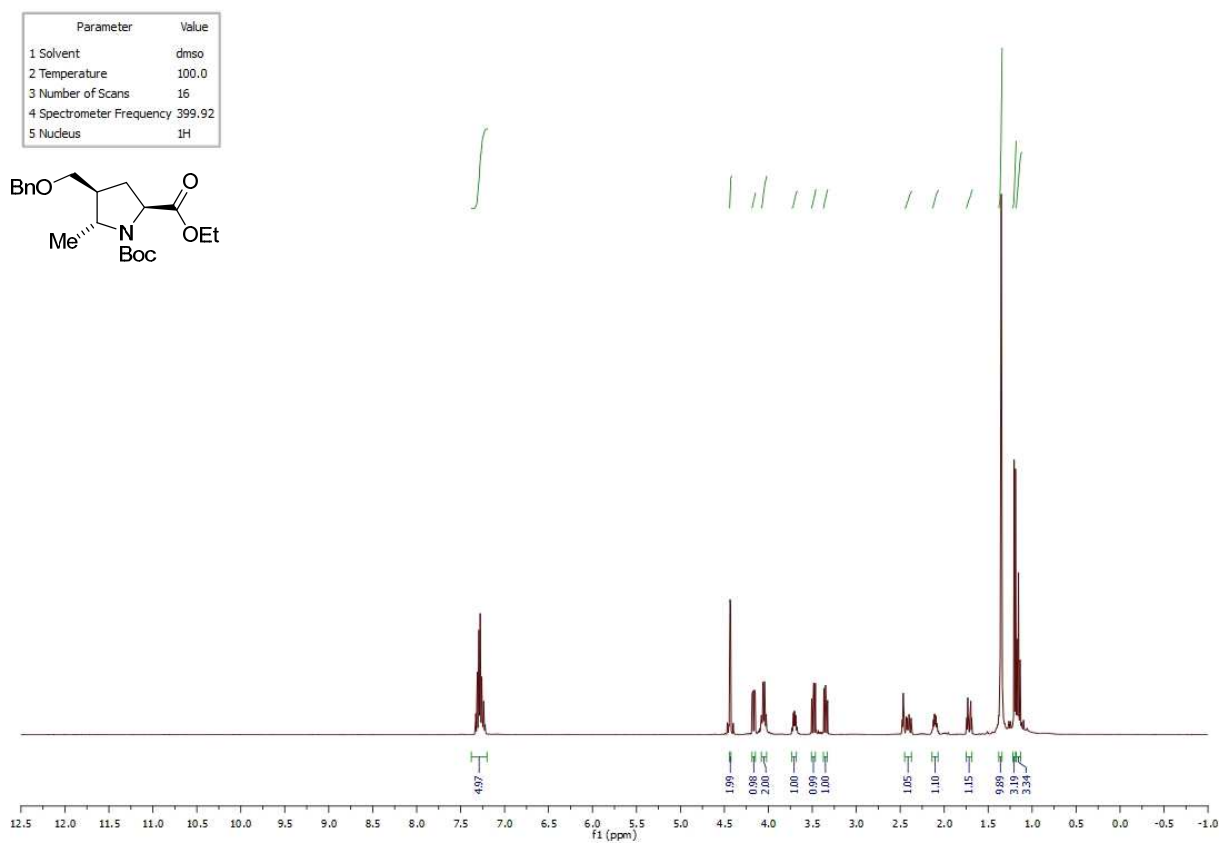
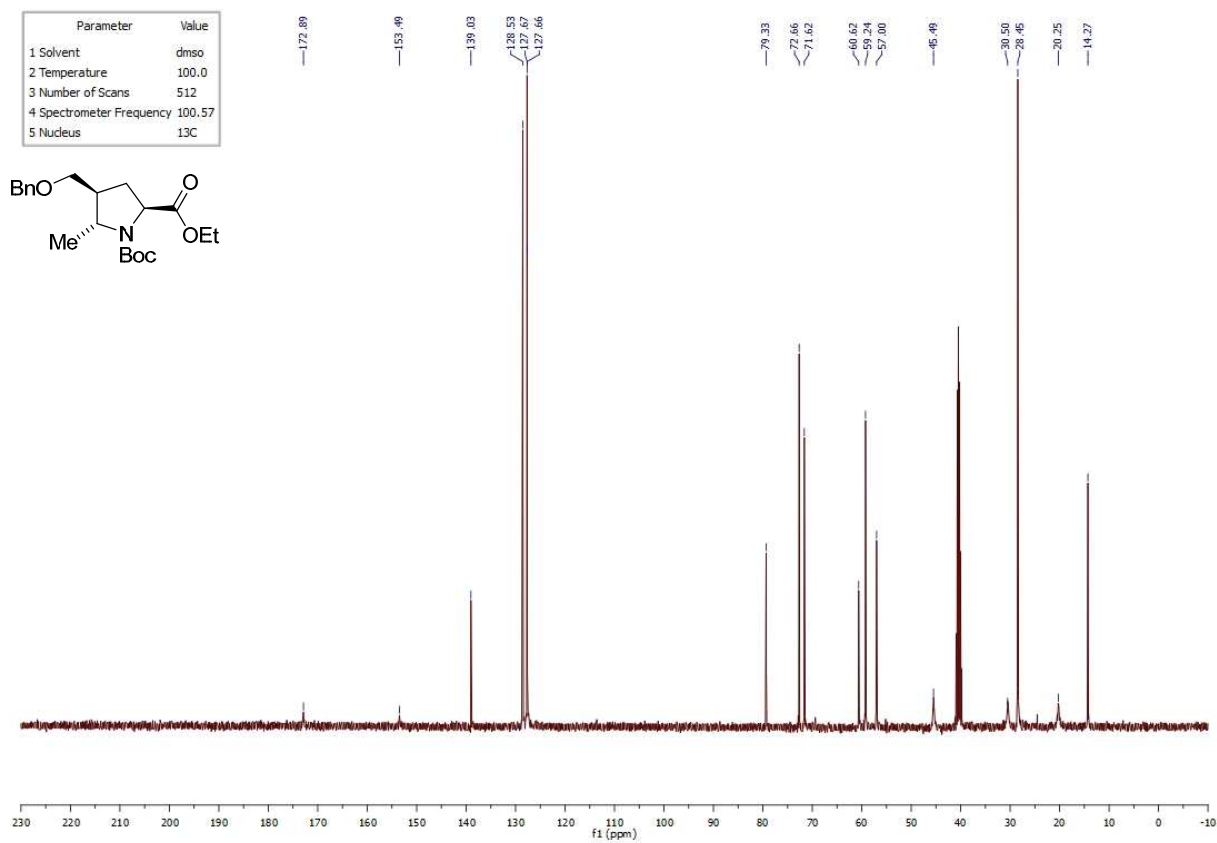
¹³C NMR spectrum of **I.266**:

Parameter	Value
1 Solvent	cdd3
2 Temperature	25.0
3 Number of Scans	4096
4 Spectrometer Frequency	100.58
5 Nucleus	¹³ C



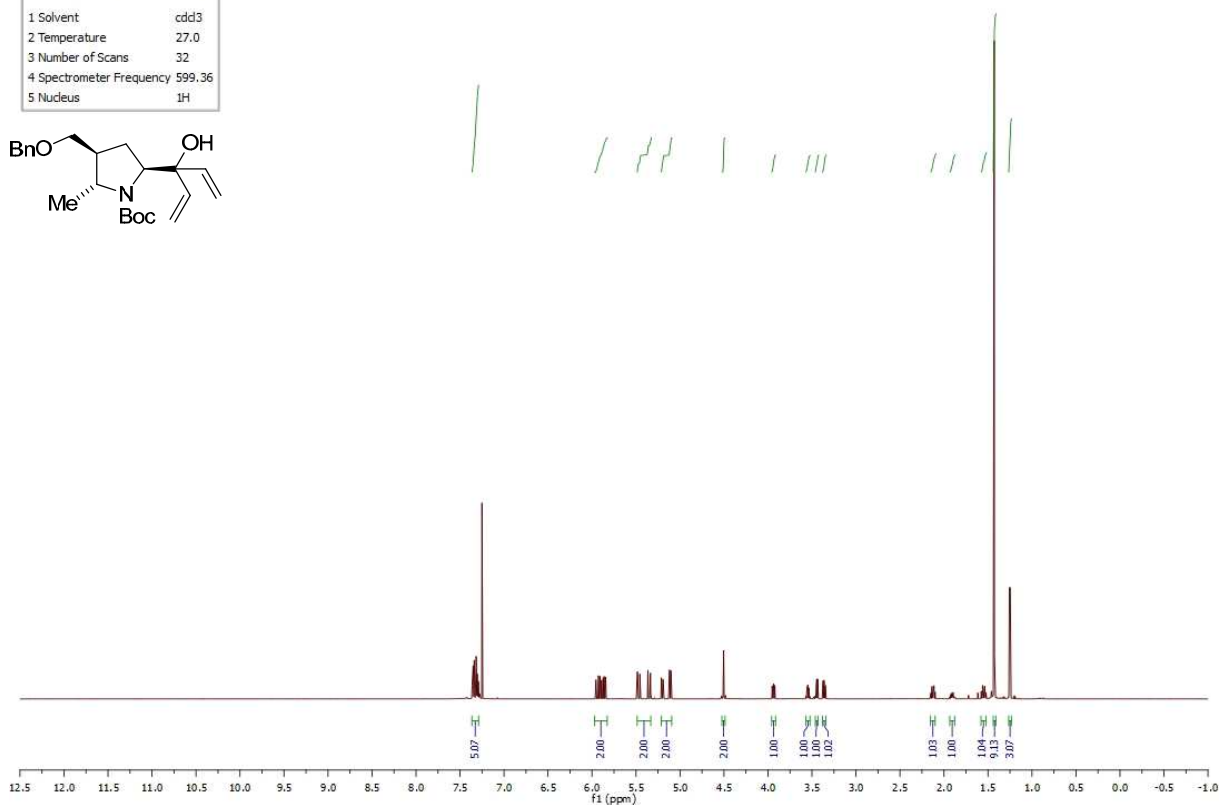
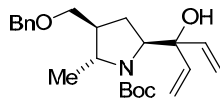
crude reaction mixture,
both diastereomers



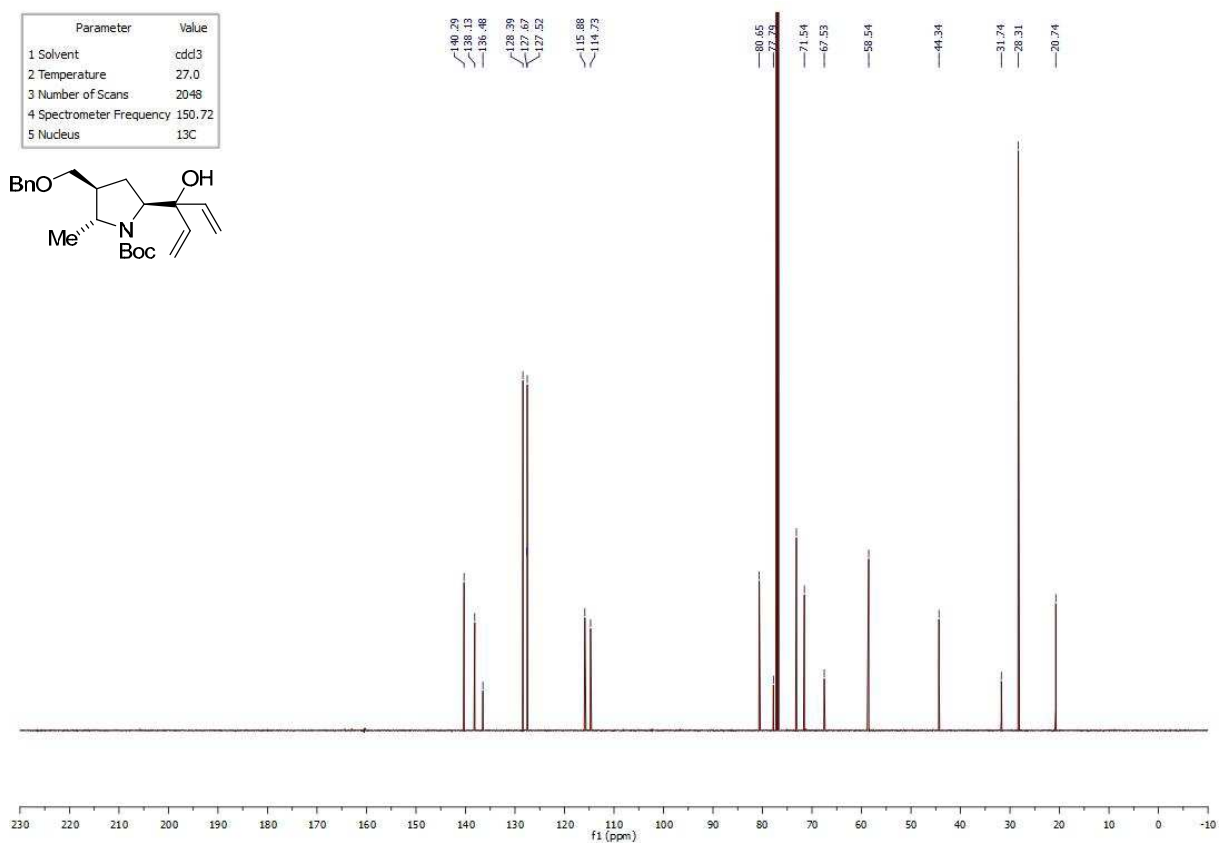
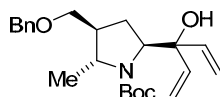
¹H NMR spectrum of **I.249**:¹³C NMR spectrum of **I.249**:

¹H NMR spectrum of **I.273**:

Parameter	Value
1 Solvent	cdd3
2 Temperature	27.0
3 Number of Scans	32
4 Spectrometer Frequency	599.36
5 Nucleus	¹ H

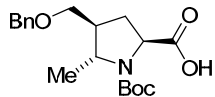
¹³C NMR spectrum of **I.273**:

Parameter	Value
1 Solvent	cdd3
2 Temperature	27.0
3 Number of Scans	2048
4 Spectrometer Frequency	150.72
5 Nucleus	¹³ C

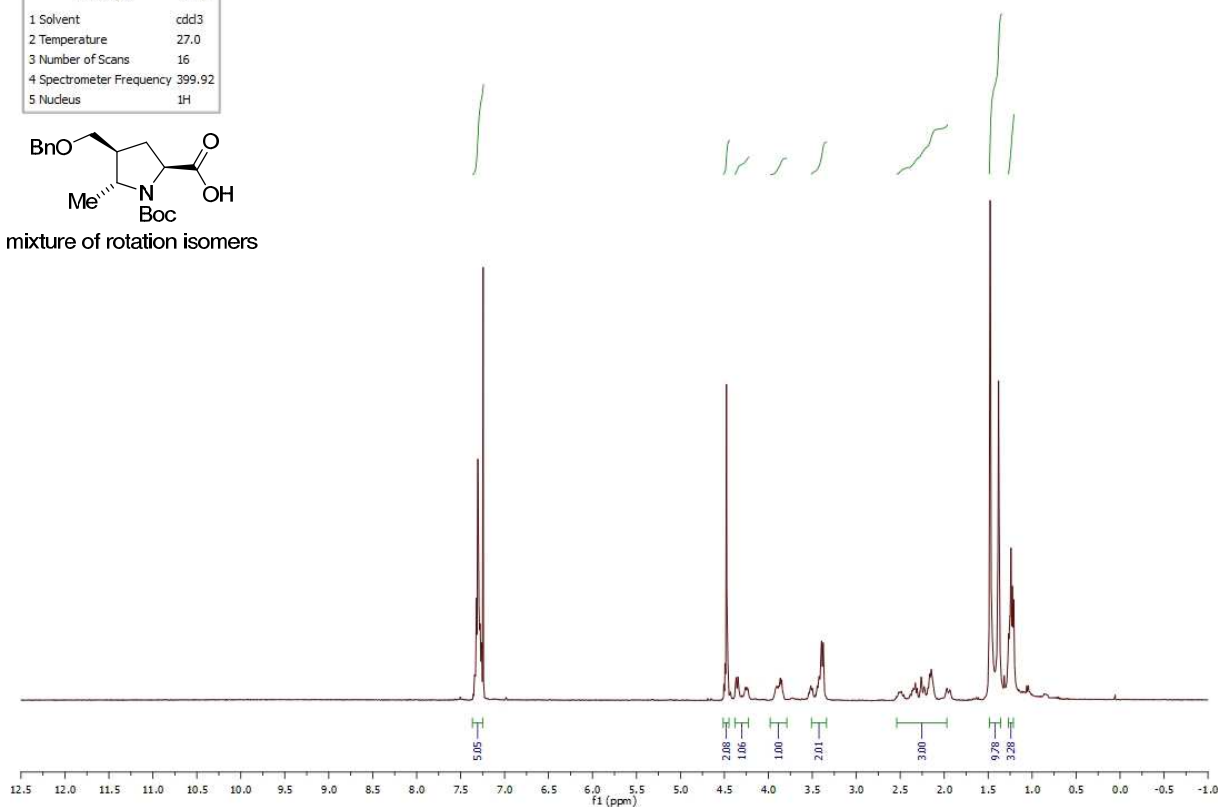


^1H NMR spectrum of **I.271**:

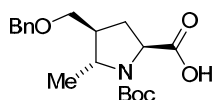
Parameter	Value
1 Solvent	cdd3
2 Temperature	27.0
3 Number of Scans	16
4 Spectrometer Frequency	399.92
5 Nucleus	^1H



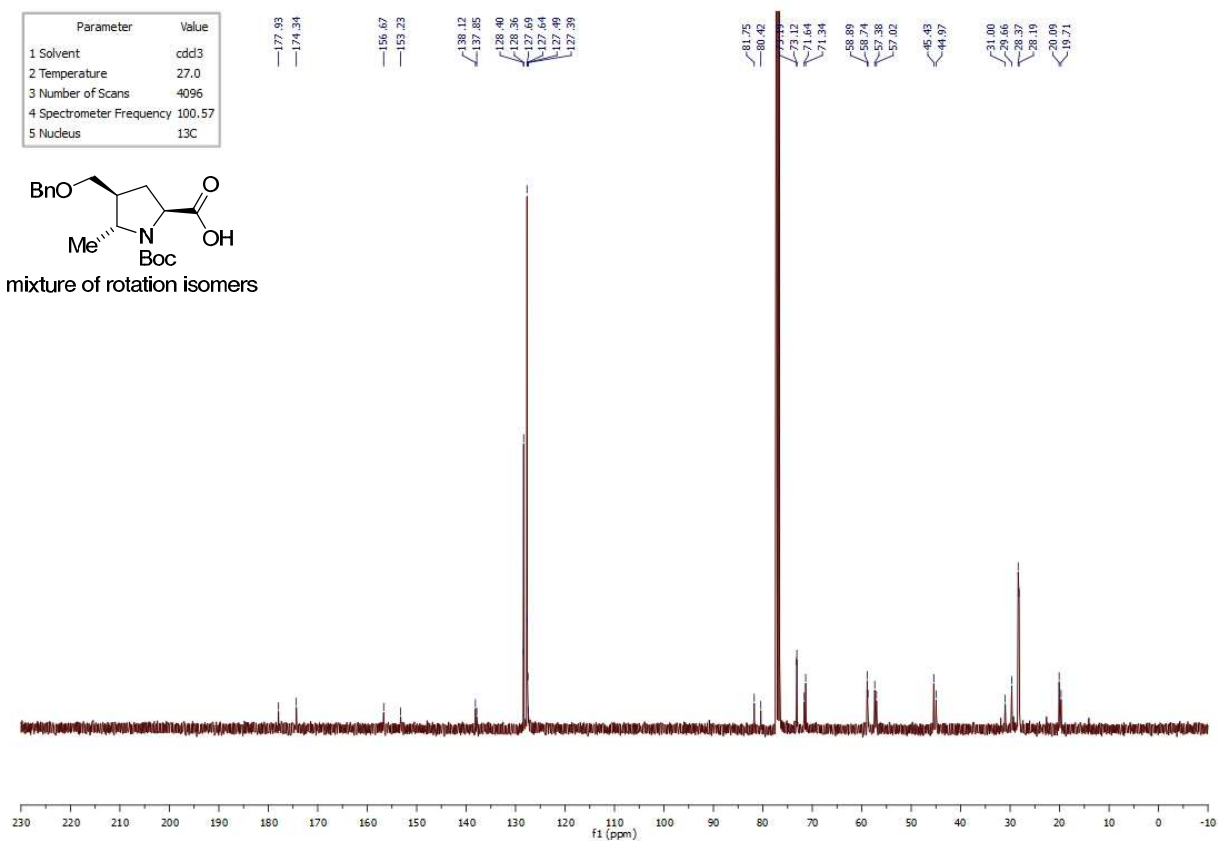
mixture of rotation isomers

 ^{13}C NMR spectrum of **I.271**:

Parameter	Value
1 Solvent	cdd3
2 Temperature	27.0
3 Number of Scans	4096
4 Spectrometer Frequency	100.57
5 Nucleus	^{13}C

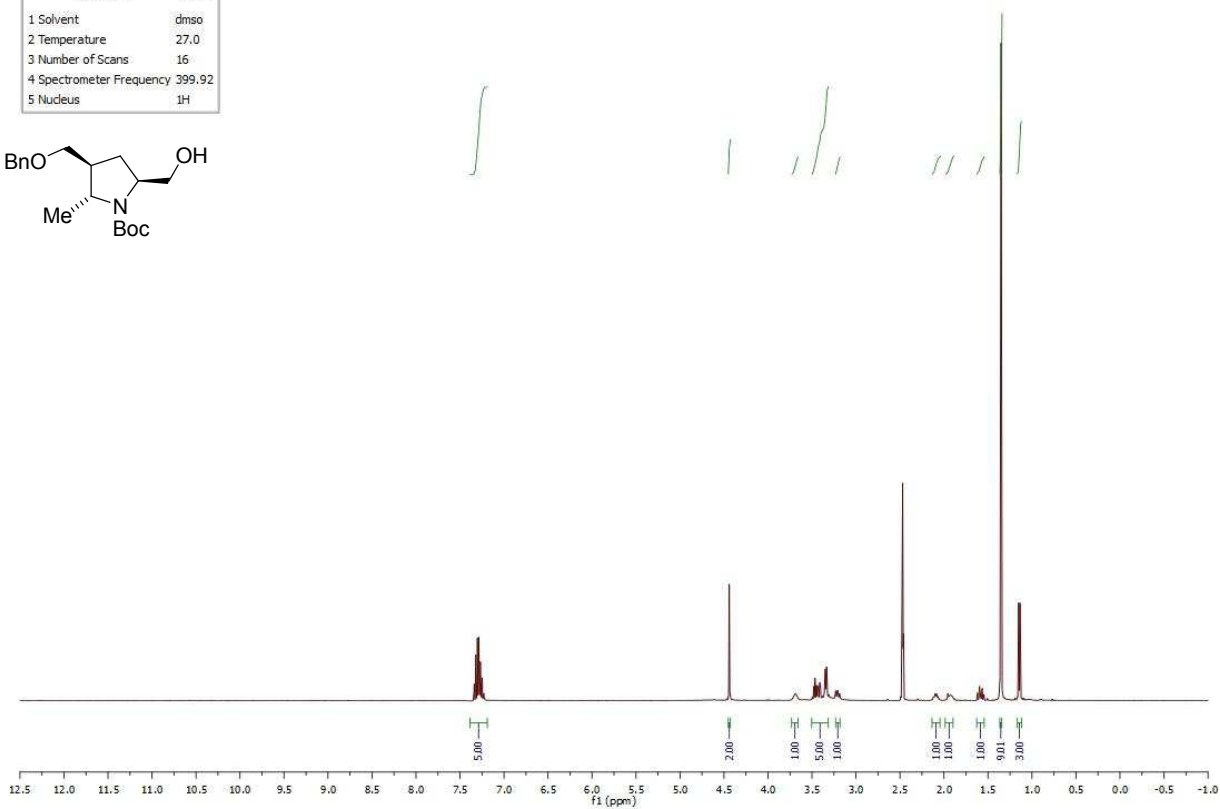
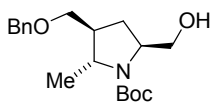


mixture of rotation isomers

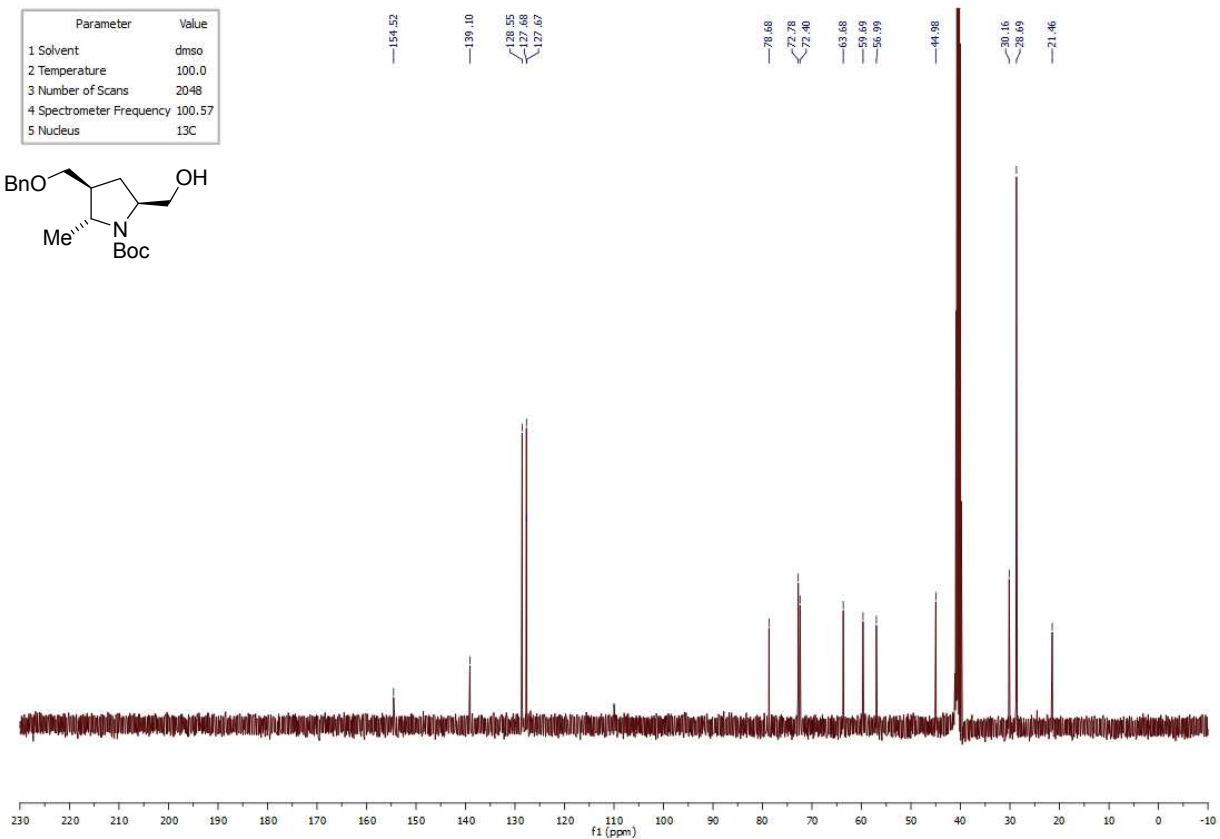
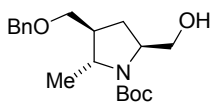


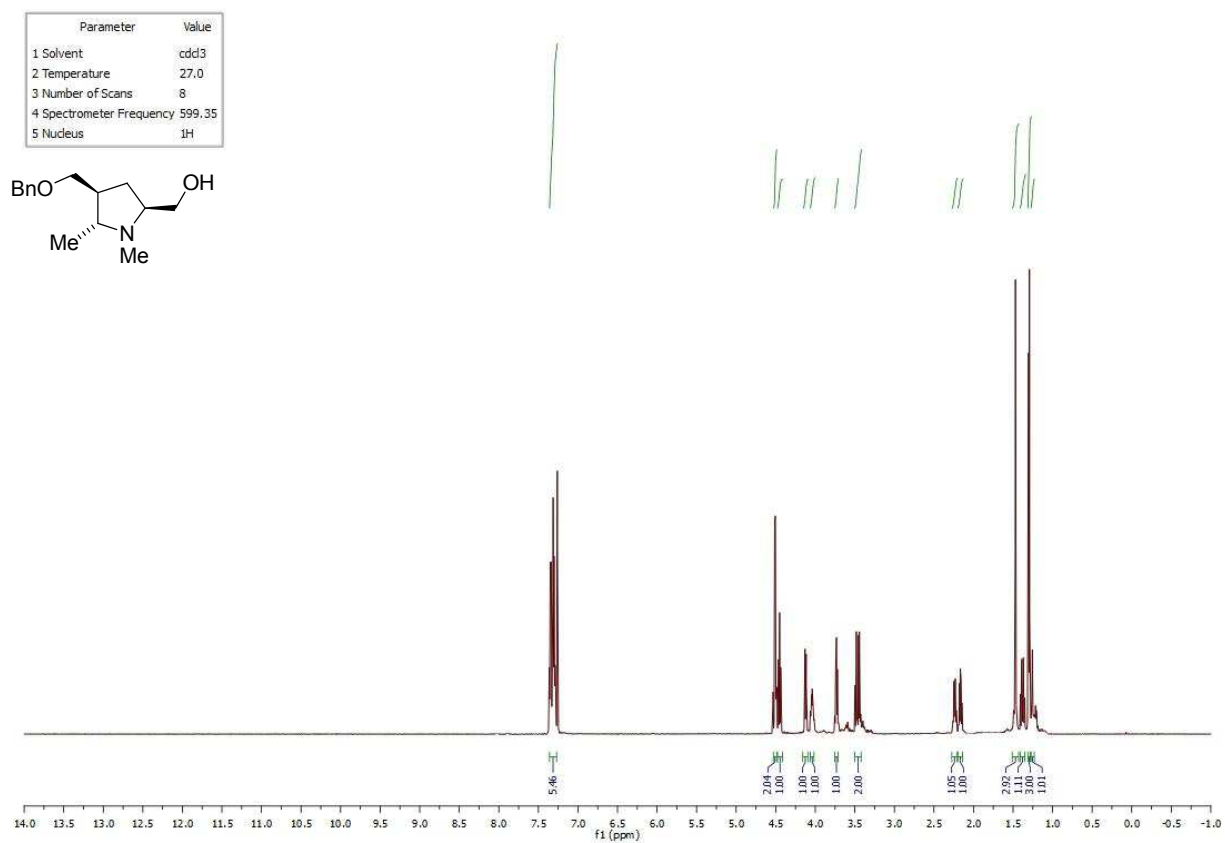
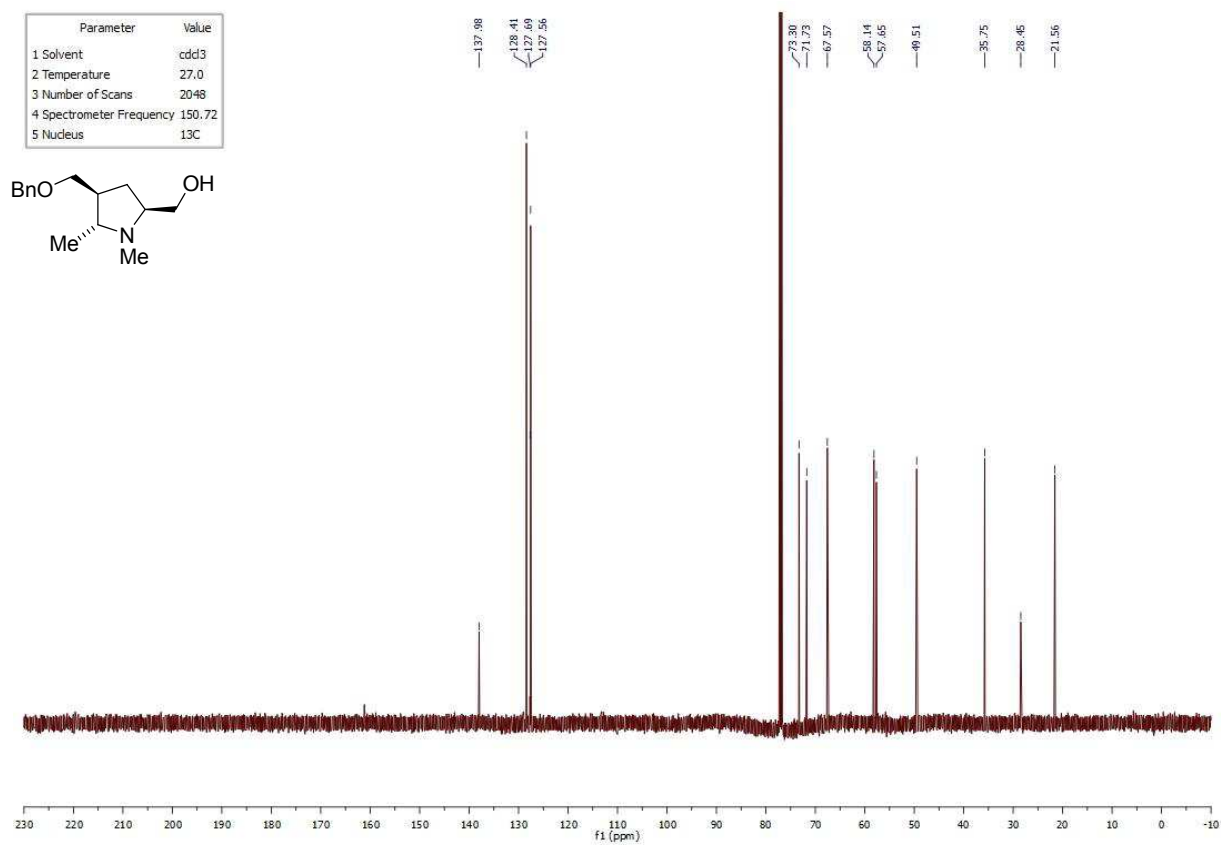
¹H NMR spectrum of **I.272**:

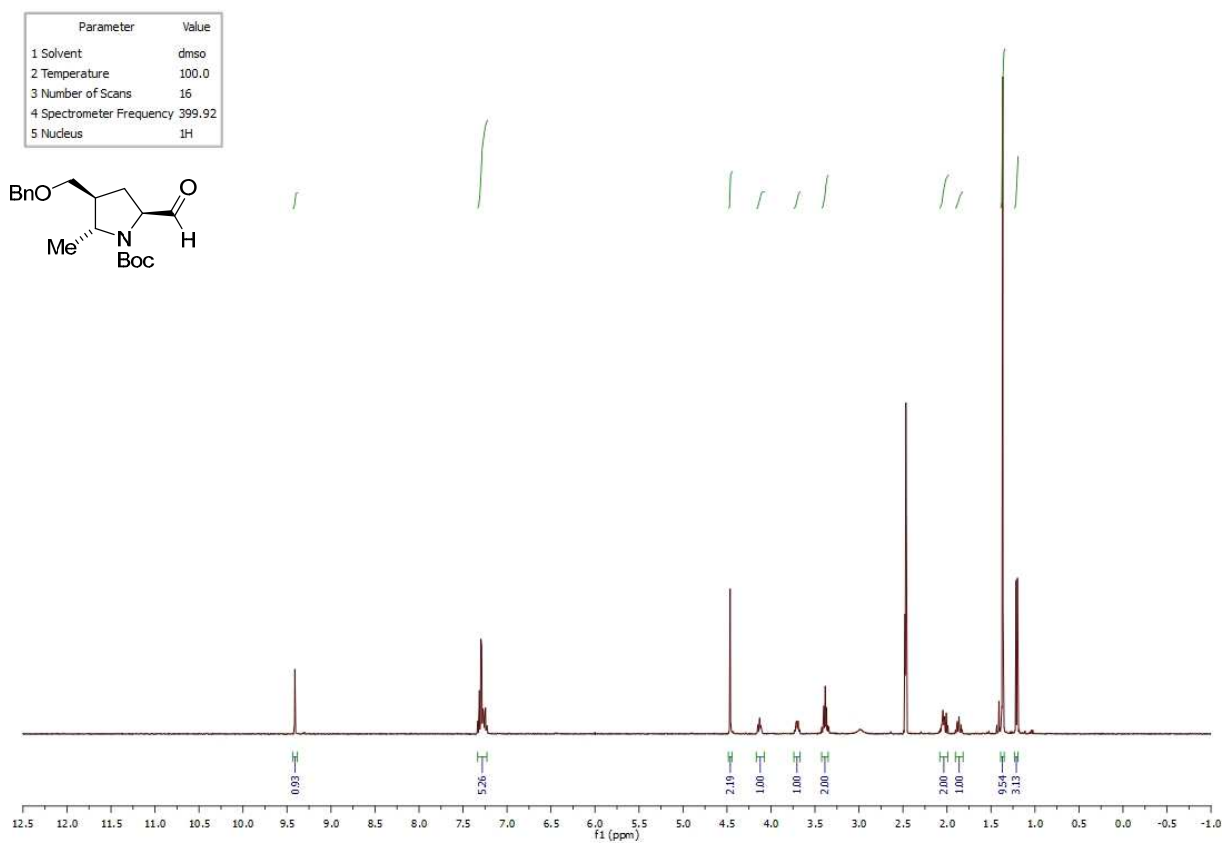
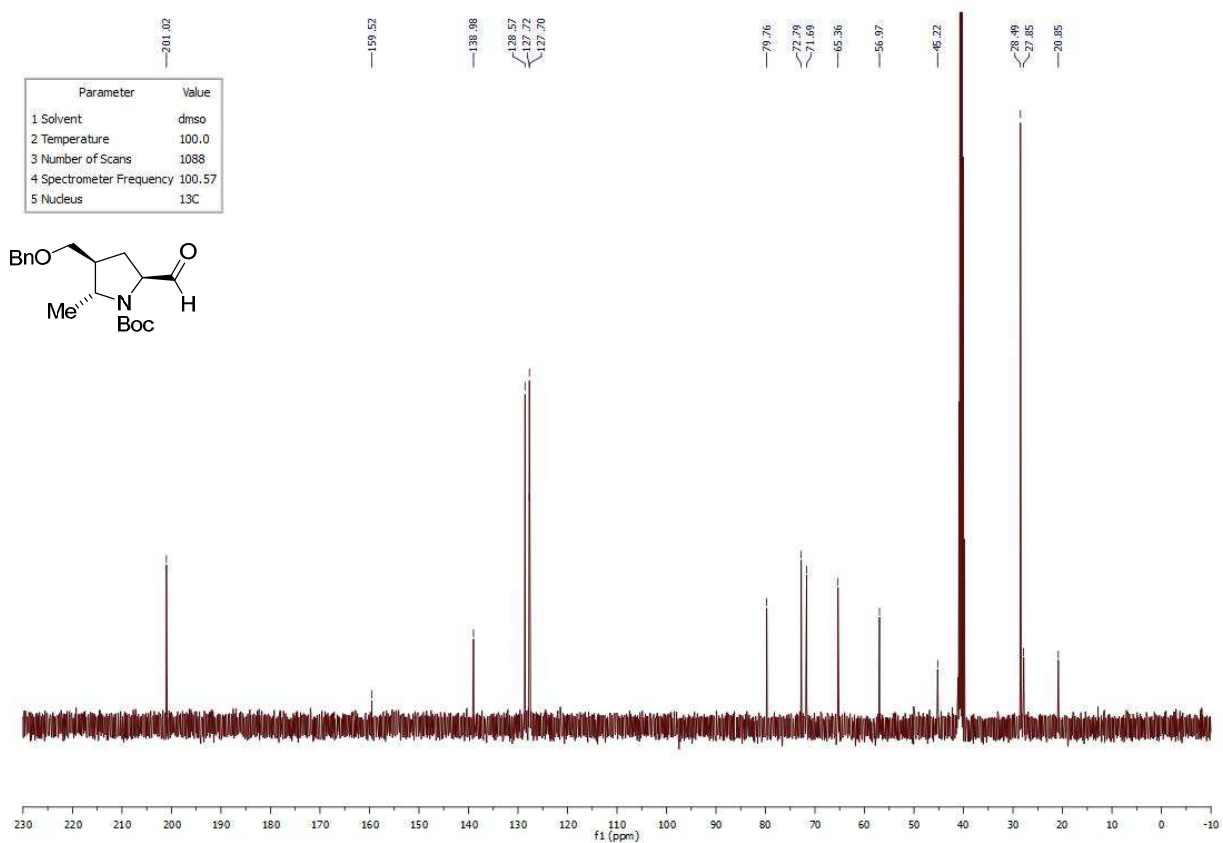
Parameter	Value
1 Solvent	dms0
2 Temperature	27.0
3 Number of Scans	16
4 Spectrometer Frequency	399.92
5 Nucleus	1H

¹³C NMR spectrum of **I.272**:

Parameter	Value
1 Solvent	dms0
2 Temperature	100.0
3 Number of Scans	2048
4 Spectrometer Frequency	100.57
5 Nucleus	13C

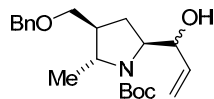


¹H NMR spectrum of **I.274**:¹³C NMR spectrum of **I.274**:

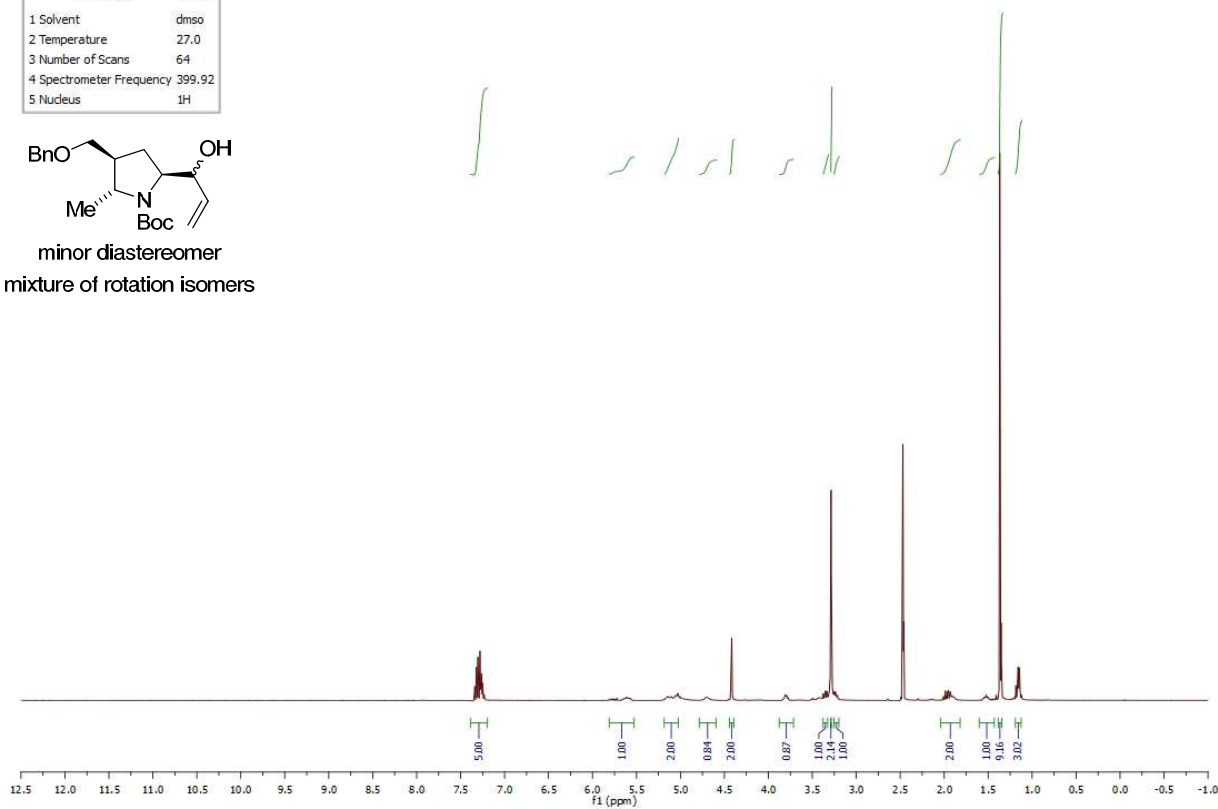
¹H NMR spectrum of **I.275**:¹³C NMR spectrum of **I.275**:

^1H NMR spectrum of **I.269**:

Parameter	Value
1 Solvent	dmsO
2 Temperature	27.0
3 Number of Scans	64
4 Spectrometer Frequency	399.92
5 Nucleus	^1H



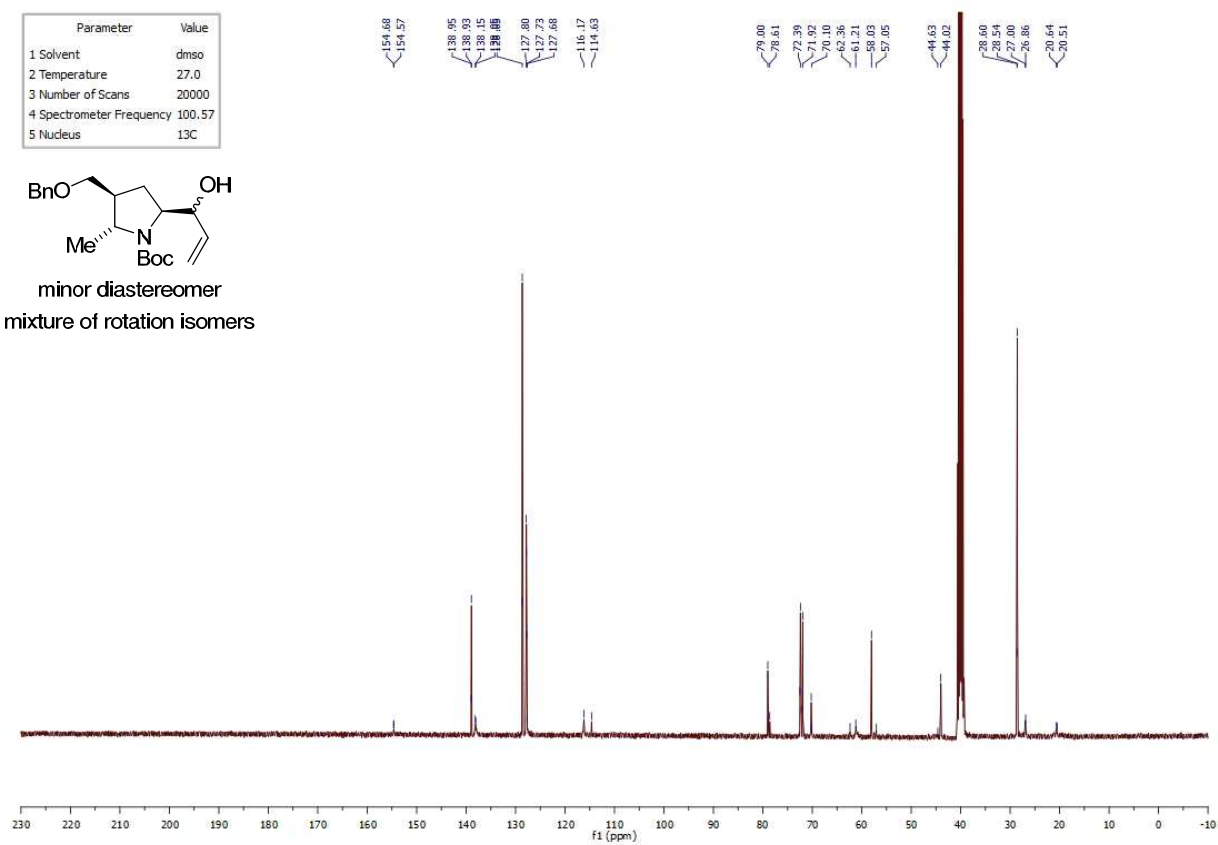
minor diastereomer
mixture of rotation isomers

 ^{13}C NMR spectrum of **I.269**:

Parameter	Value
1 Solvent	dmsO
2 Temperature	27.0
3 Number of Scans	20000
4 Spectrometer Frequency	100.57
5 Nucleus	^{13}C

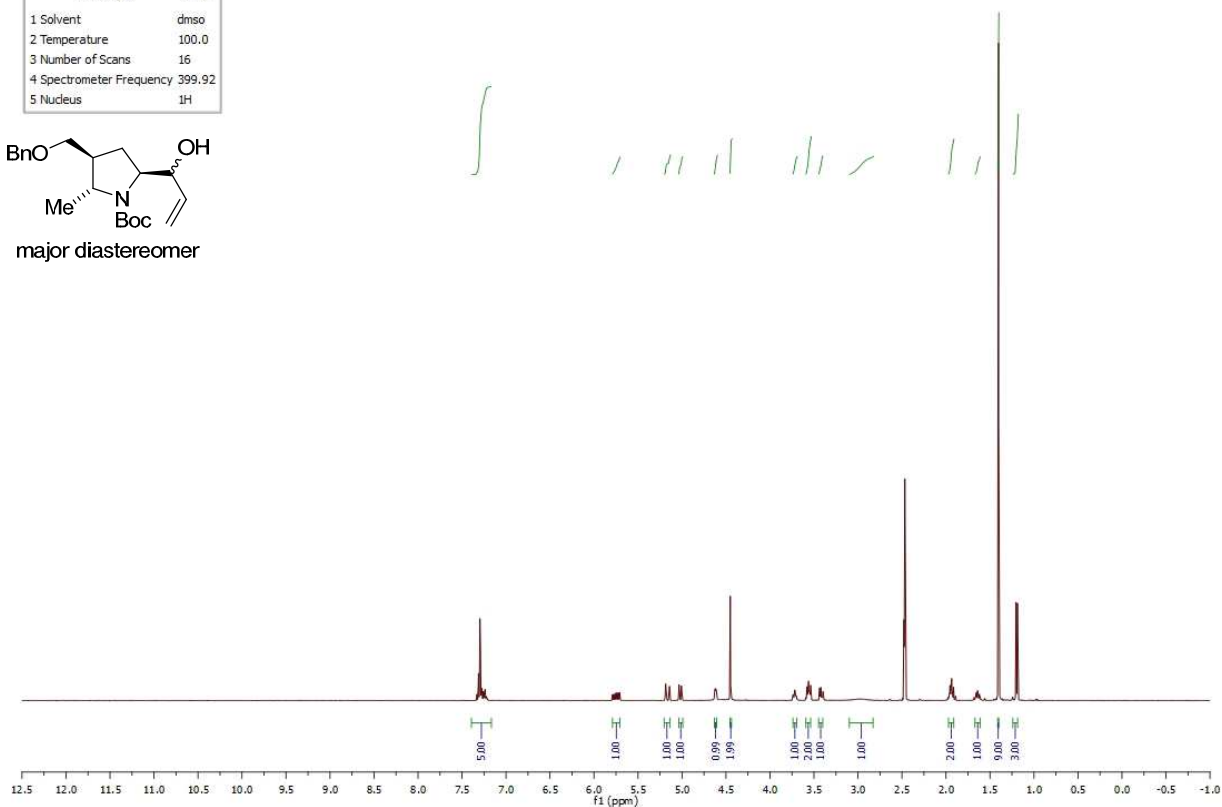
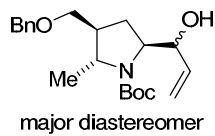


minor diastereomer
mixture of rotation isomers

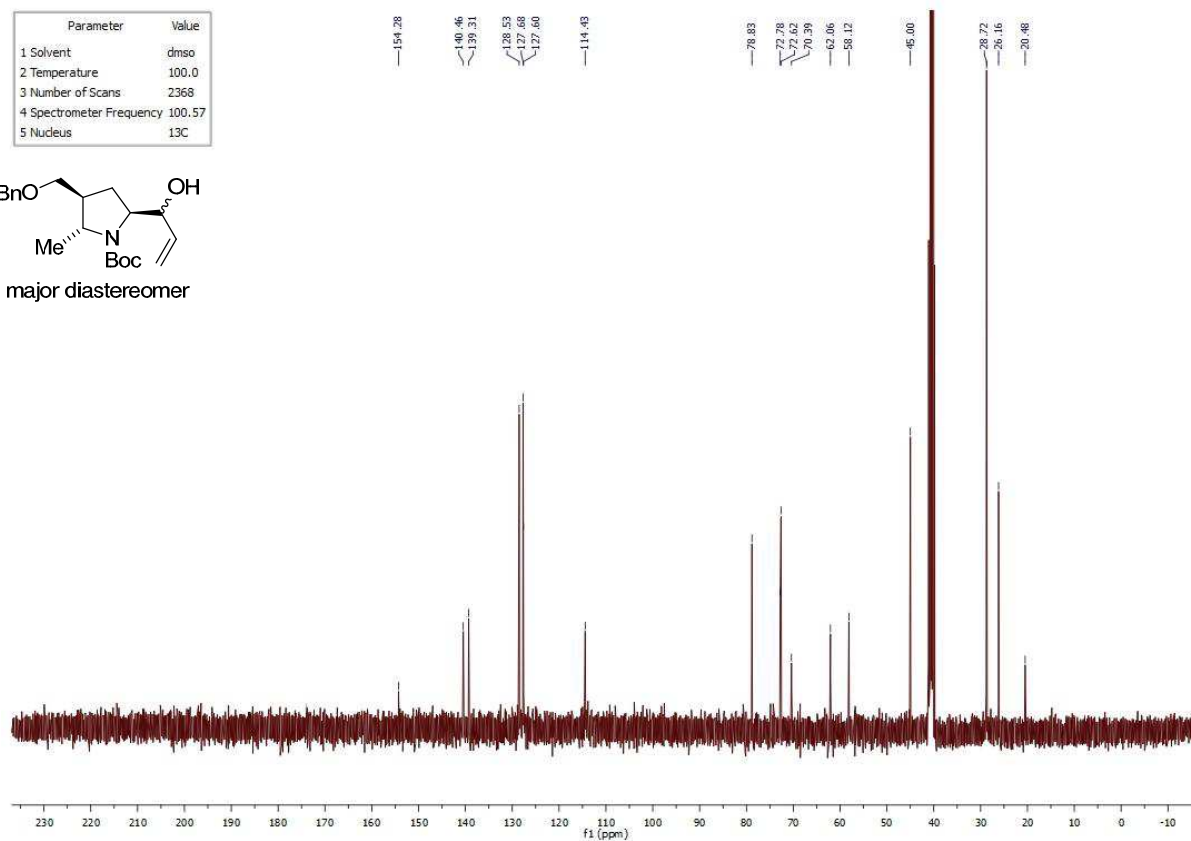
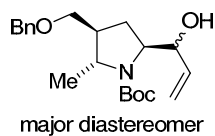


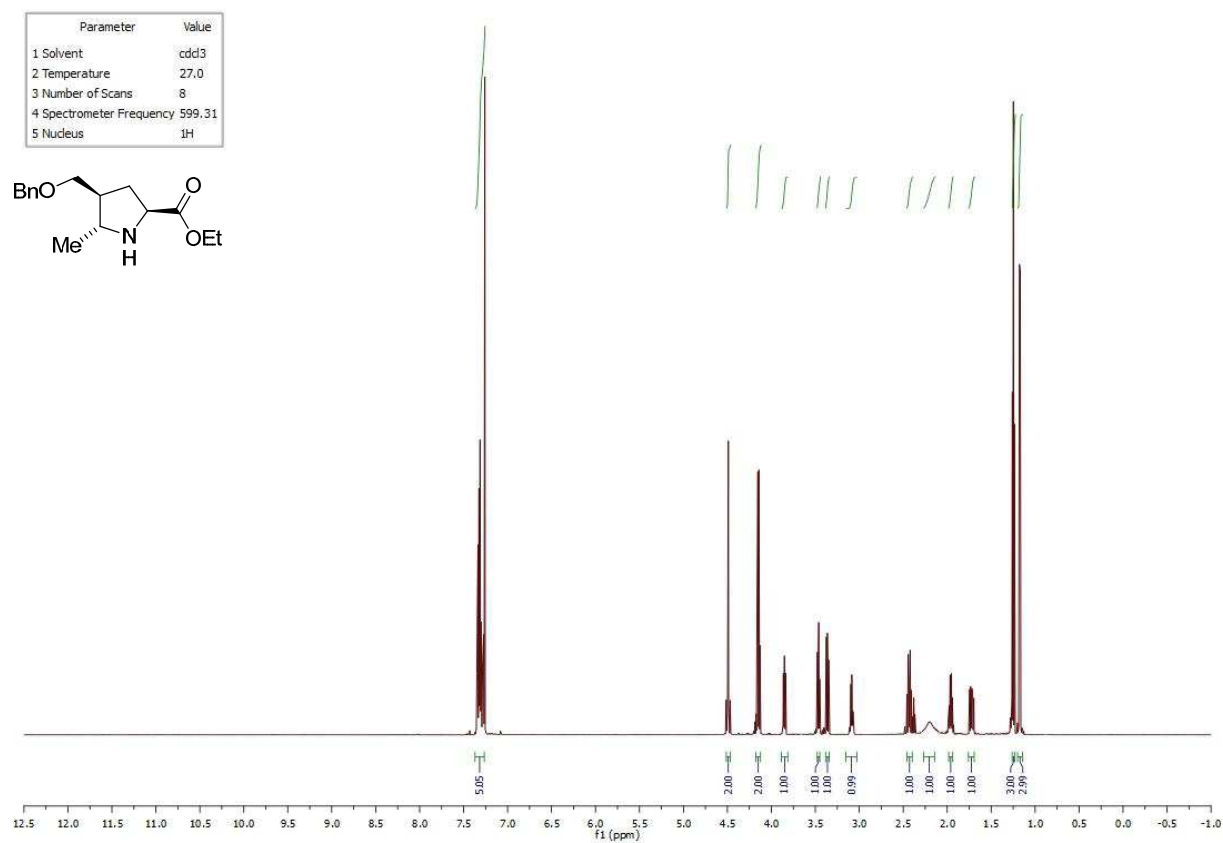
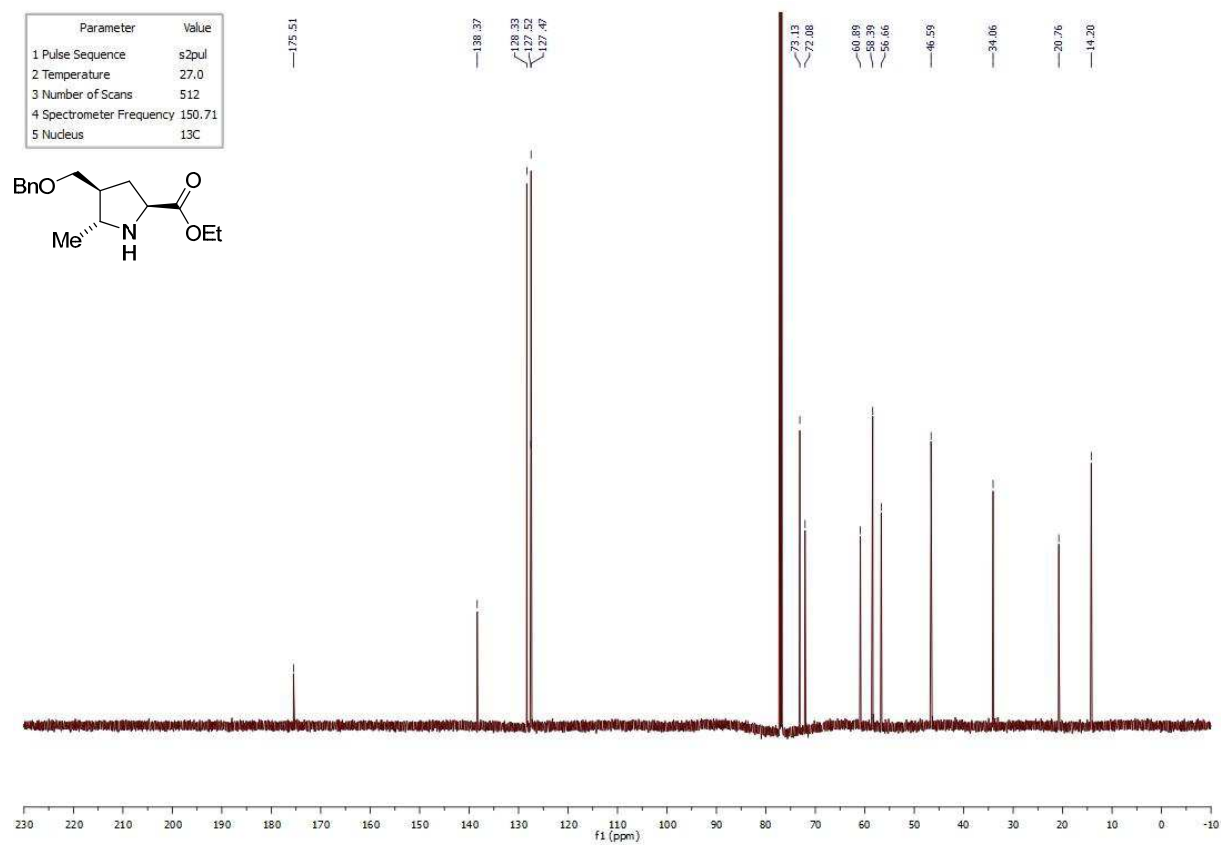
^1H NMR spectrum of **I.269**:

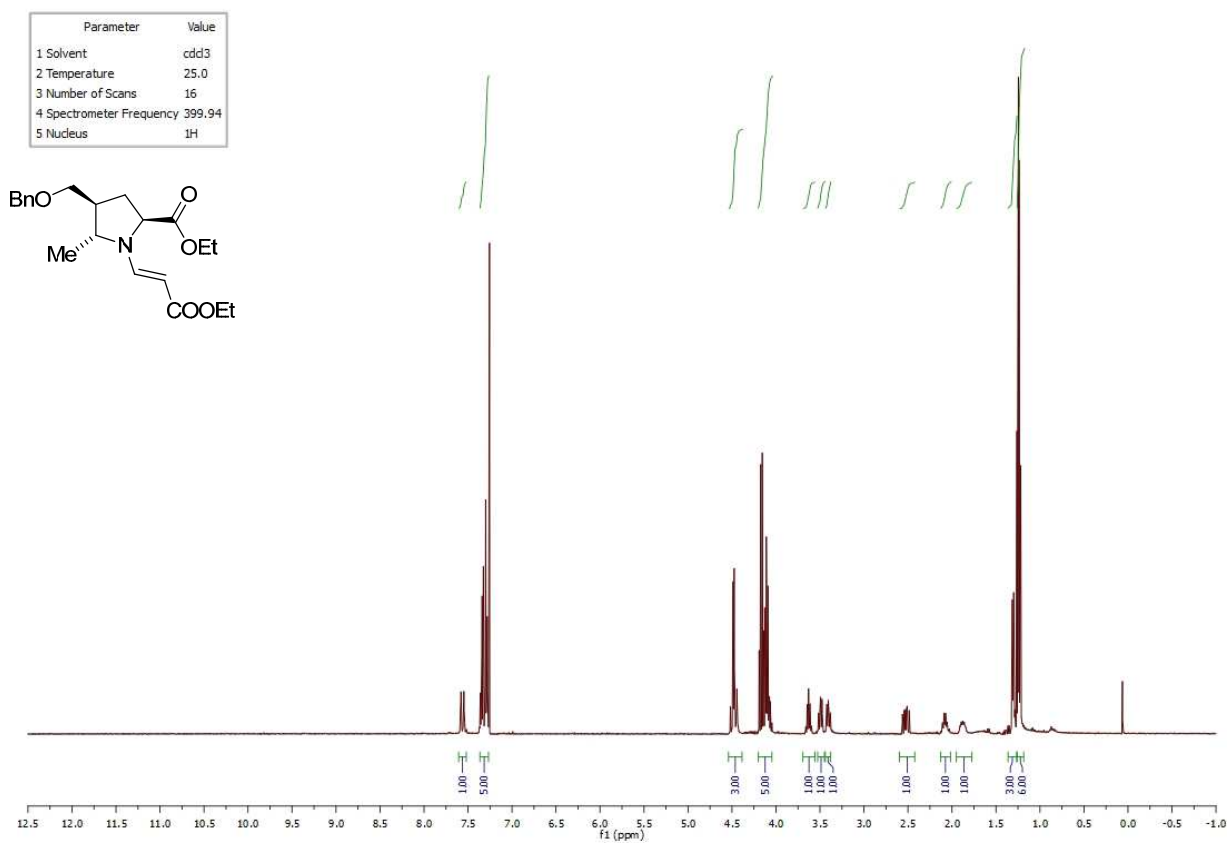
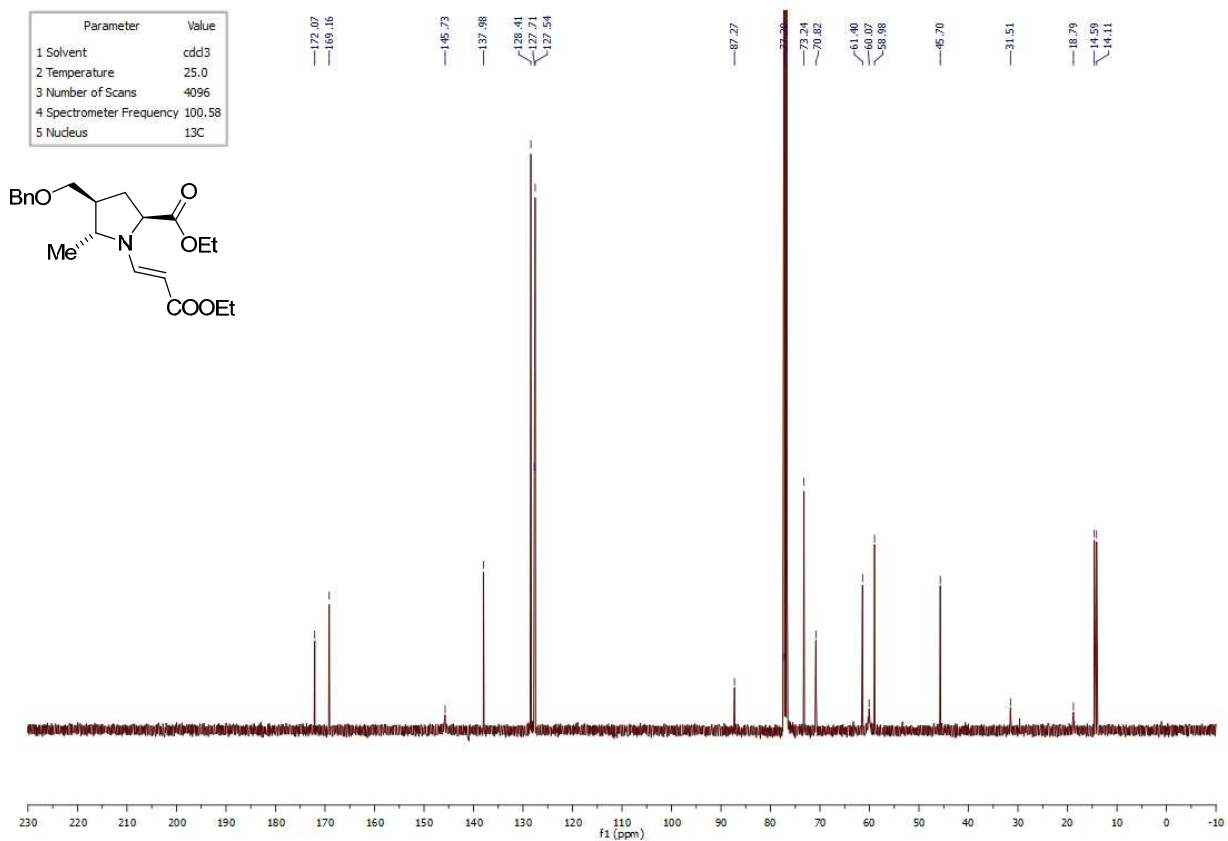
Parameter	Value
1 Solvent	dms0
2 Temperature	100.0
3 Number of Scans	16
4 Spectrometer Frequency	399.92
5 Nucleus	^1H

 ^{13}C NMR spectrum of **I.269**:

Parameter	Value
1 Solvent	dms0
2 Temperature	100.0
3 Number of Scans	2368
4 Spectrometer Frequency	100.57
5 Nucleus	^{13}C

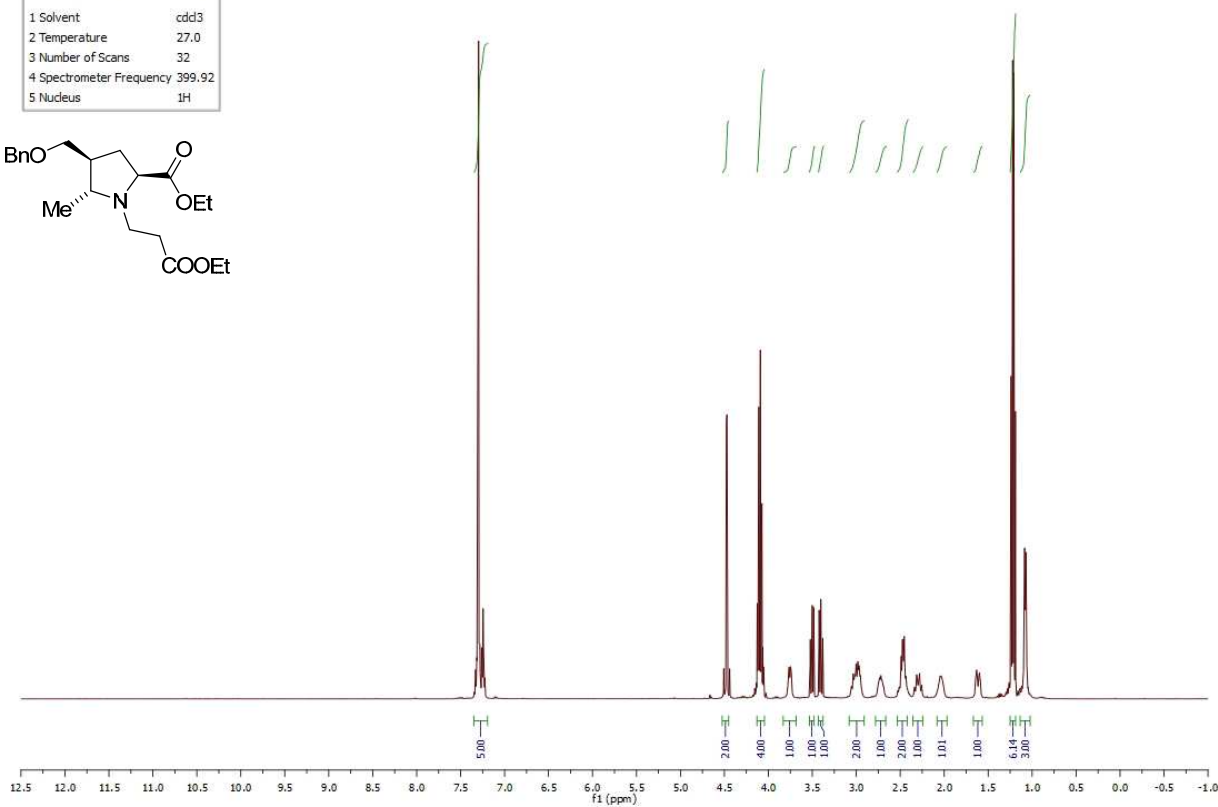
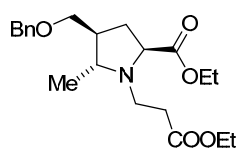


¹H NMR spectrum of **I.277**:¹³C NMR spectrum of **I.277**:

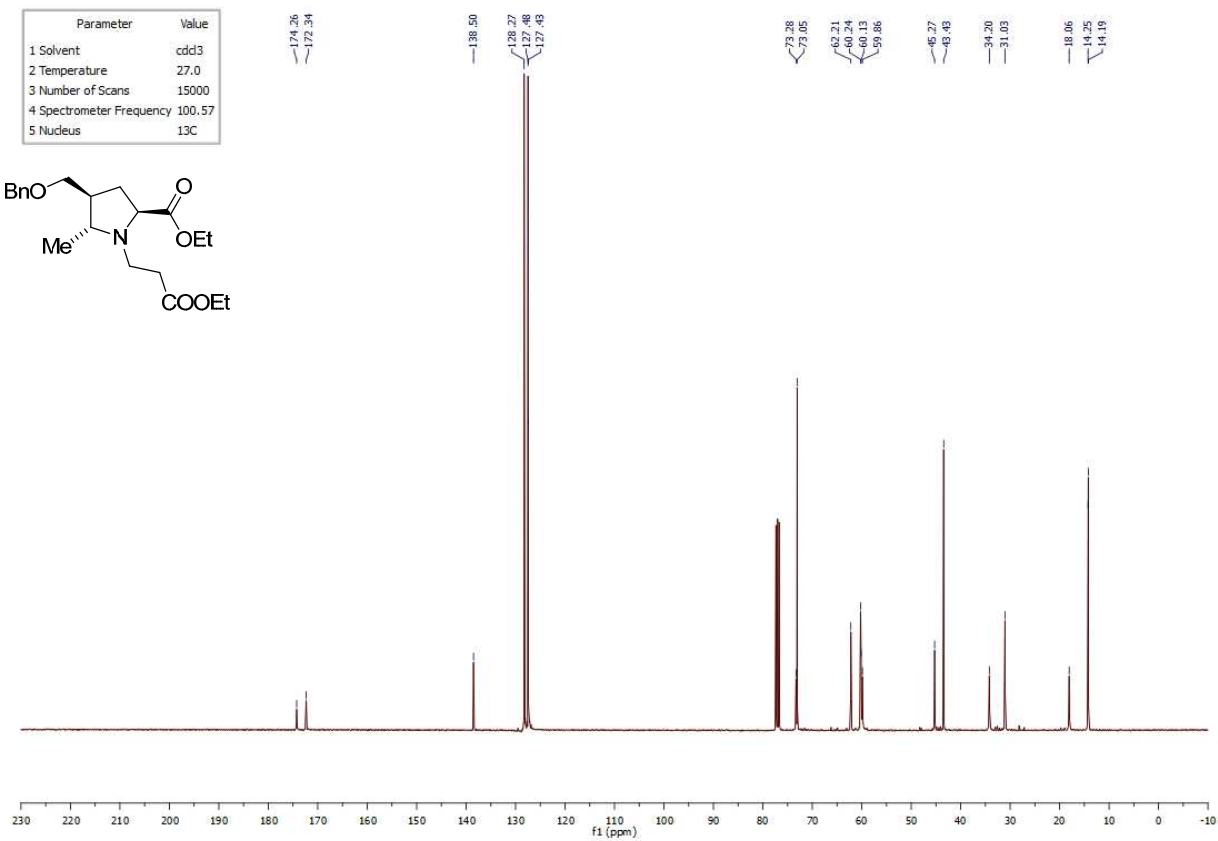
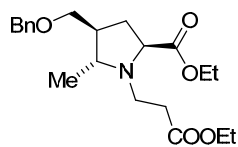
^1H NMR spectrum of **I.269**: ^{13}C NMR spectrum of **I.269**:

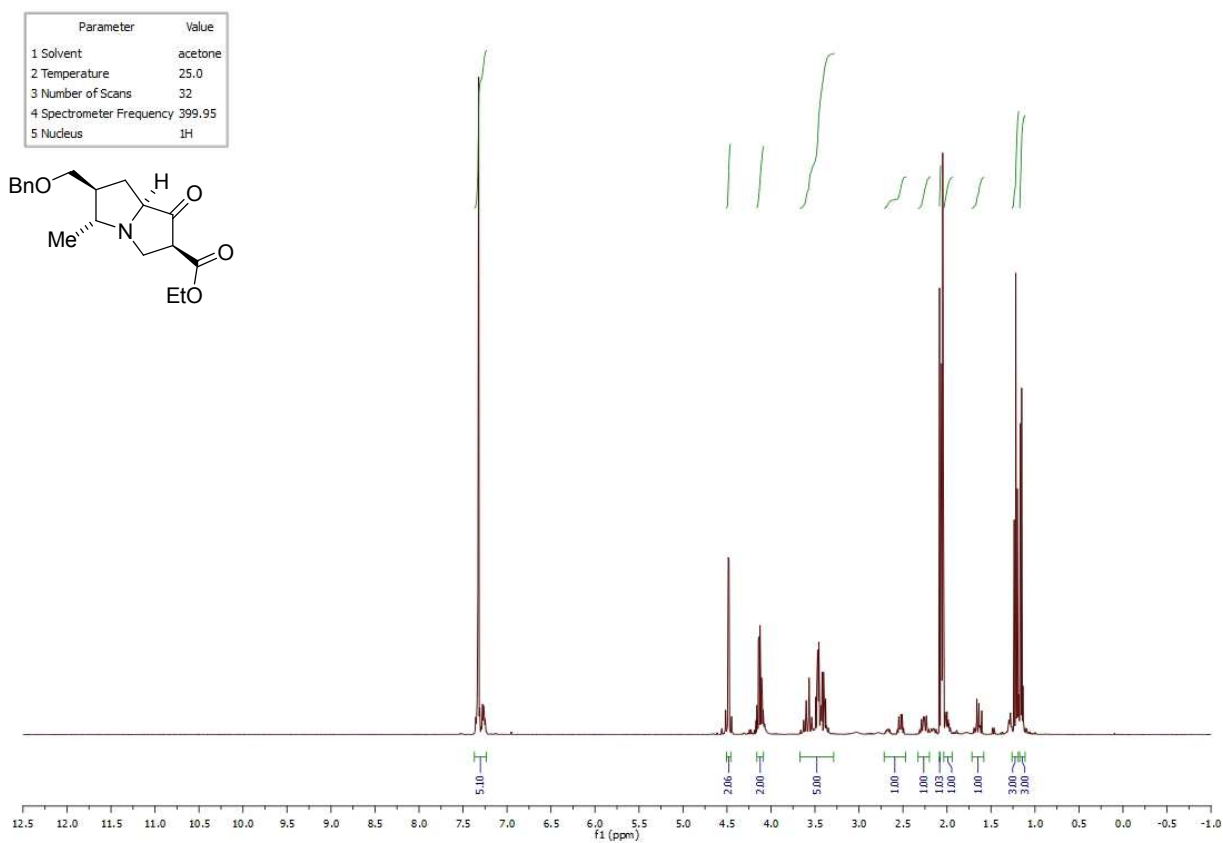
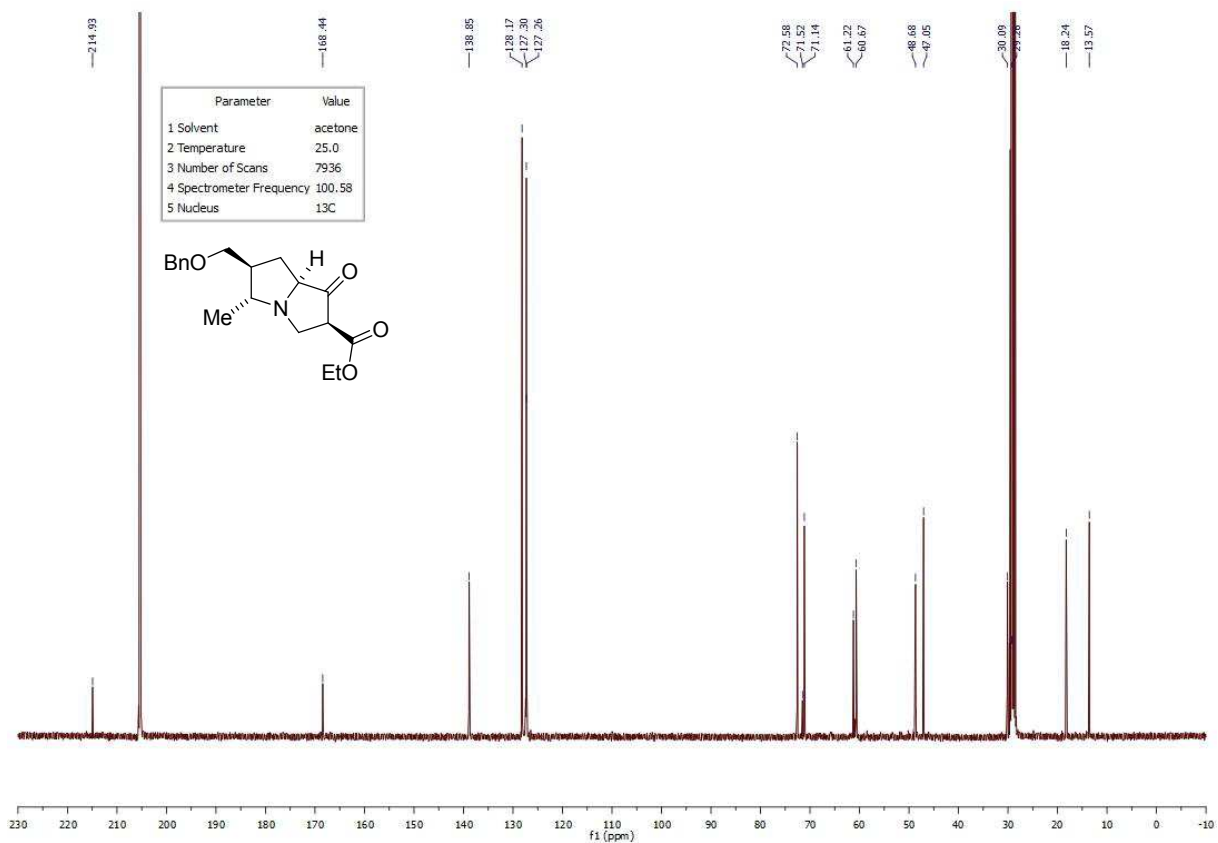
^1H NMR spectrum of **I.247**:

Parameter	Value
1 Solvent	cdd3
2 Temperature	27.0
3 Number of Scans	32
4 Spectrometer Frequency	399.92
5 Nucleus	^1H

 ^{13}C NMR spectrum of **I.247**:

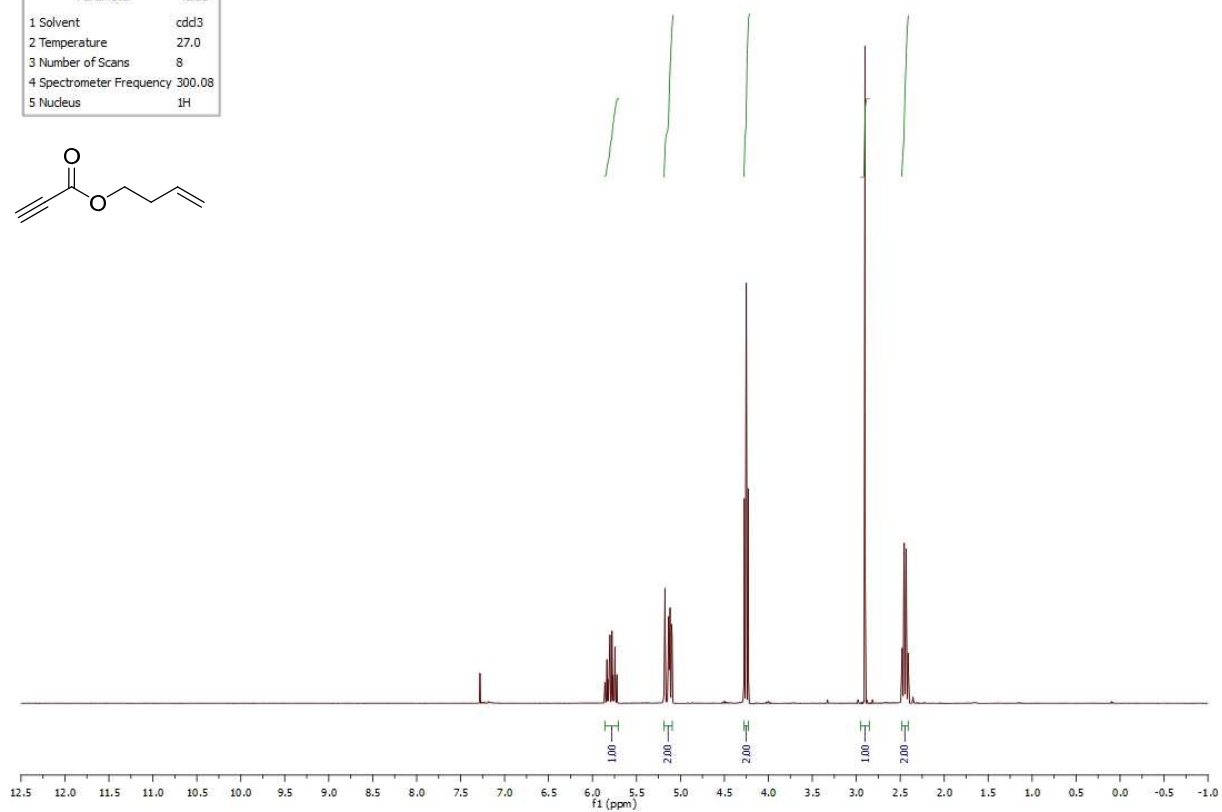
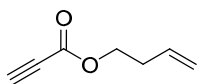
Parameter	Value
1 Solvent	cdd3
2 Temperature	27.0
3 Number of Scans	15000
4 Spectrometer Frequency	100.57
5 Nucleus	^{13}C



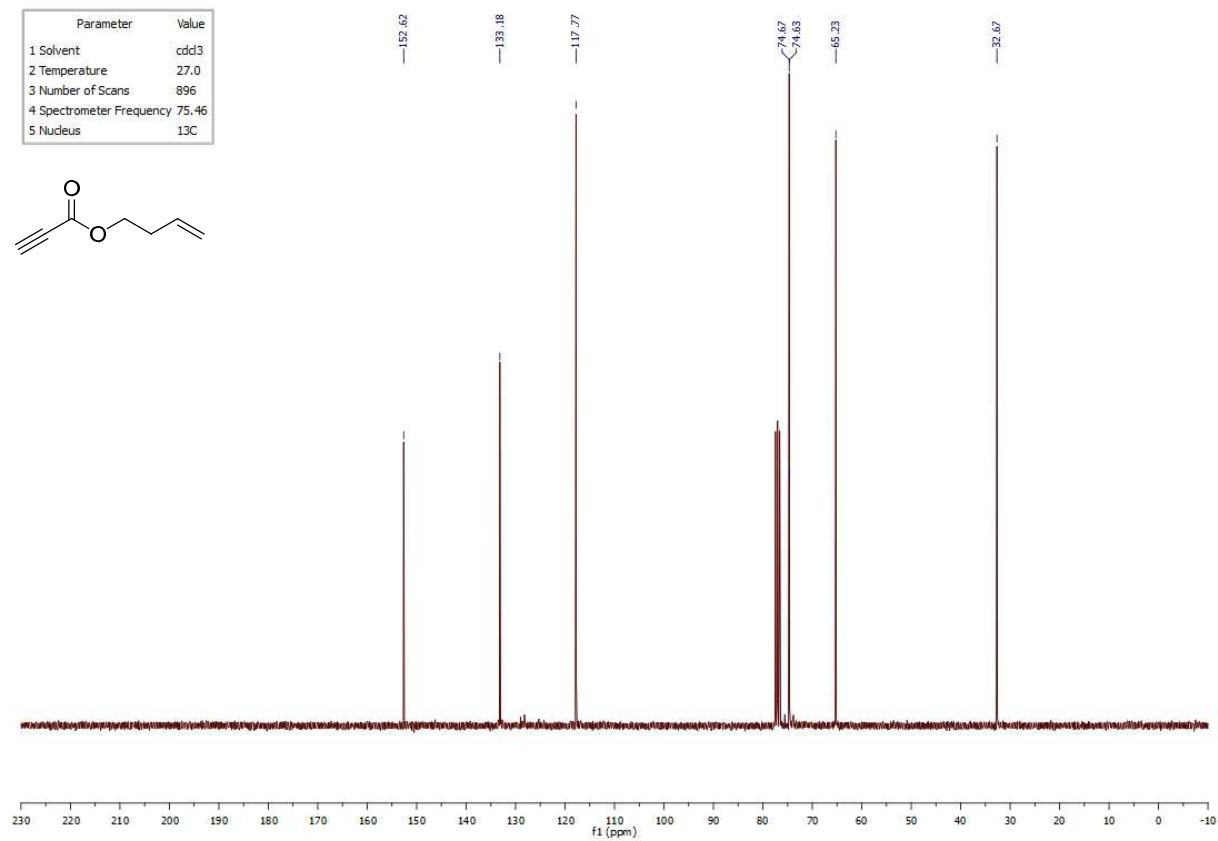
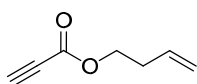
¹H NMR spectrum of **I.245**:¹³C NMR spectrum of **I.245**:

¹H NMR spectrum of **I.254**:

Parameter	Value
1 Solvent	cdcl3
2 Temperature	27.0
3 Number of Scans	8
4 Spectrometer Frequency	300.08
5 Nucleus	¹ H

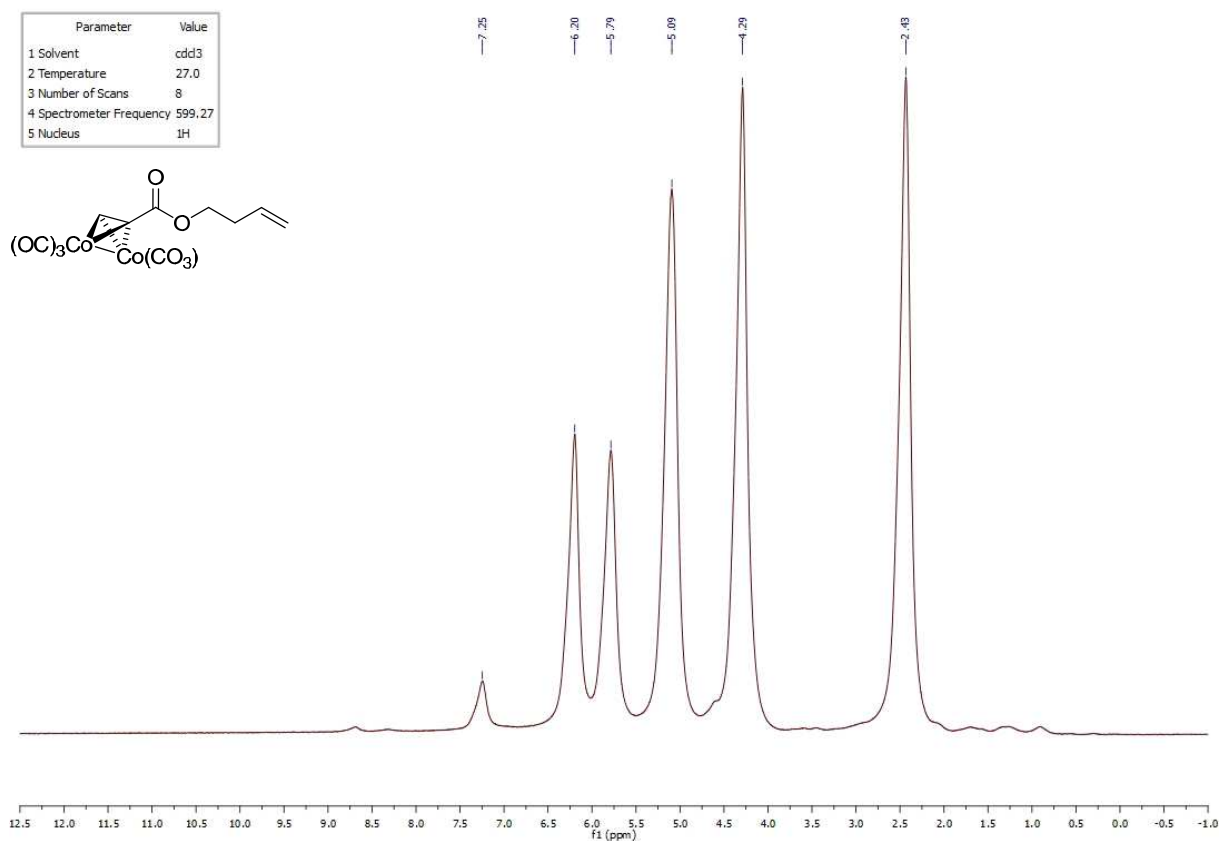
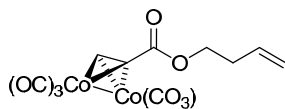
¹³C NMR spectrum of **I.254**:

Parameter	Value
1 Solvent	cdcl3
2 Temperature	27.0
3 Number of Scans	896
4 Spectrometer Frequency	75.46
5 Nucleus	¹³ C

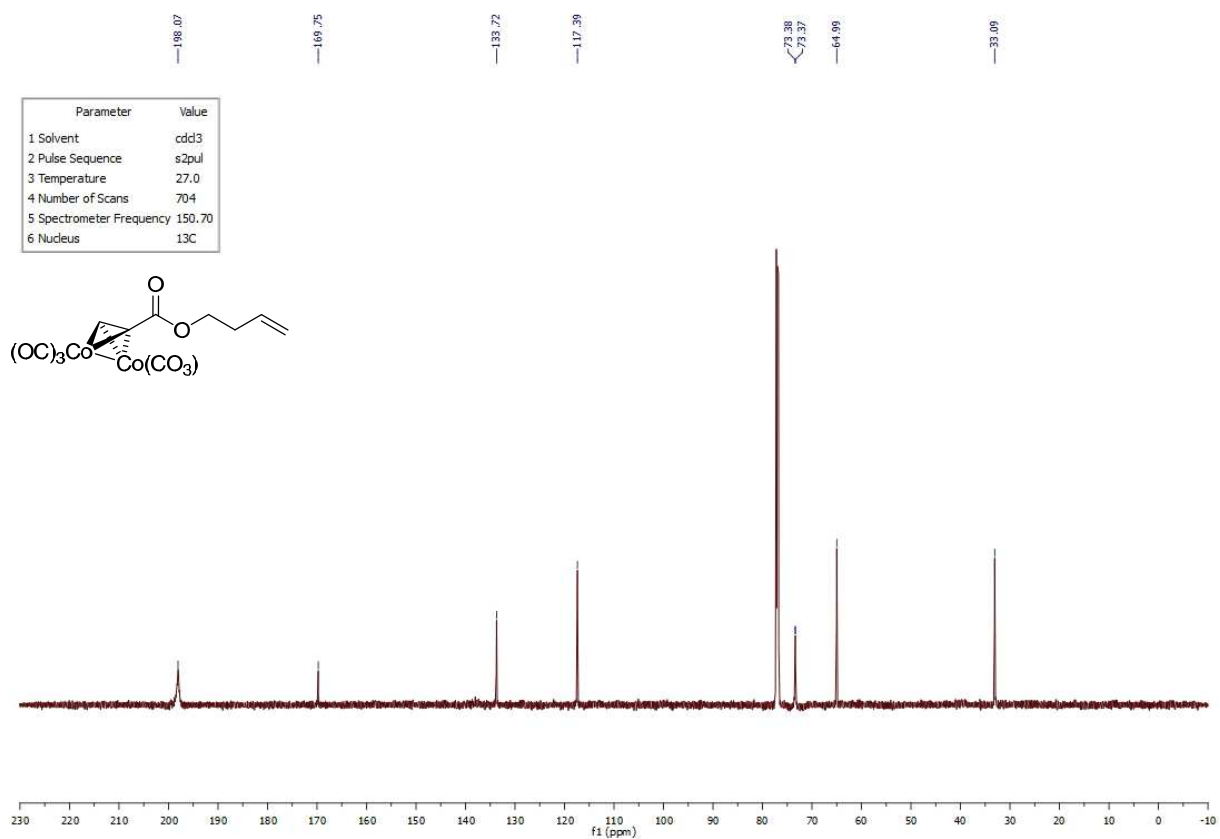
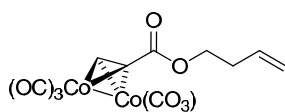


¹H NMR spectrum of **I.282**:

Parameter	Value
1 Solvent	cdd3
2 Temperature	27.0
3 Number of Scans	8
4 Spectrometer Frequency	599.27
5 Nucleus	¹ H

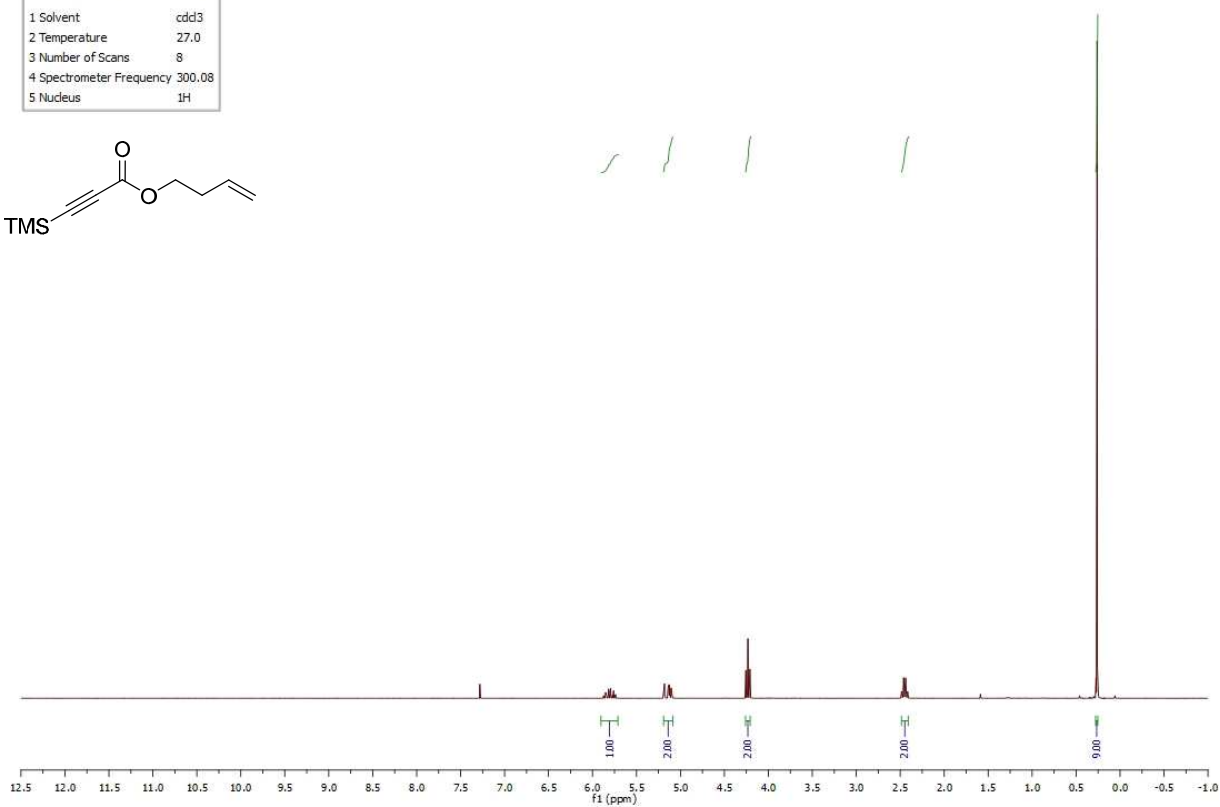
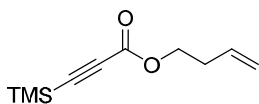
¹³C NMR spectrum of **I.282**:

Parameter	Value
1 Solvent	cdd3
2 Pulse Sequence	s2pul
3 Temperature	27.0
4 Number of Scans	704
5 Spectrometer Frequency	150.70
6 Nucleus	¹³ C

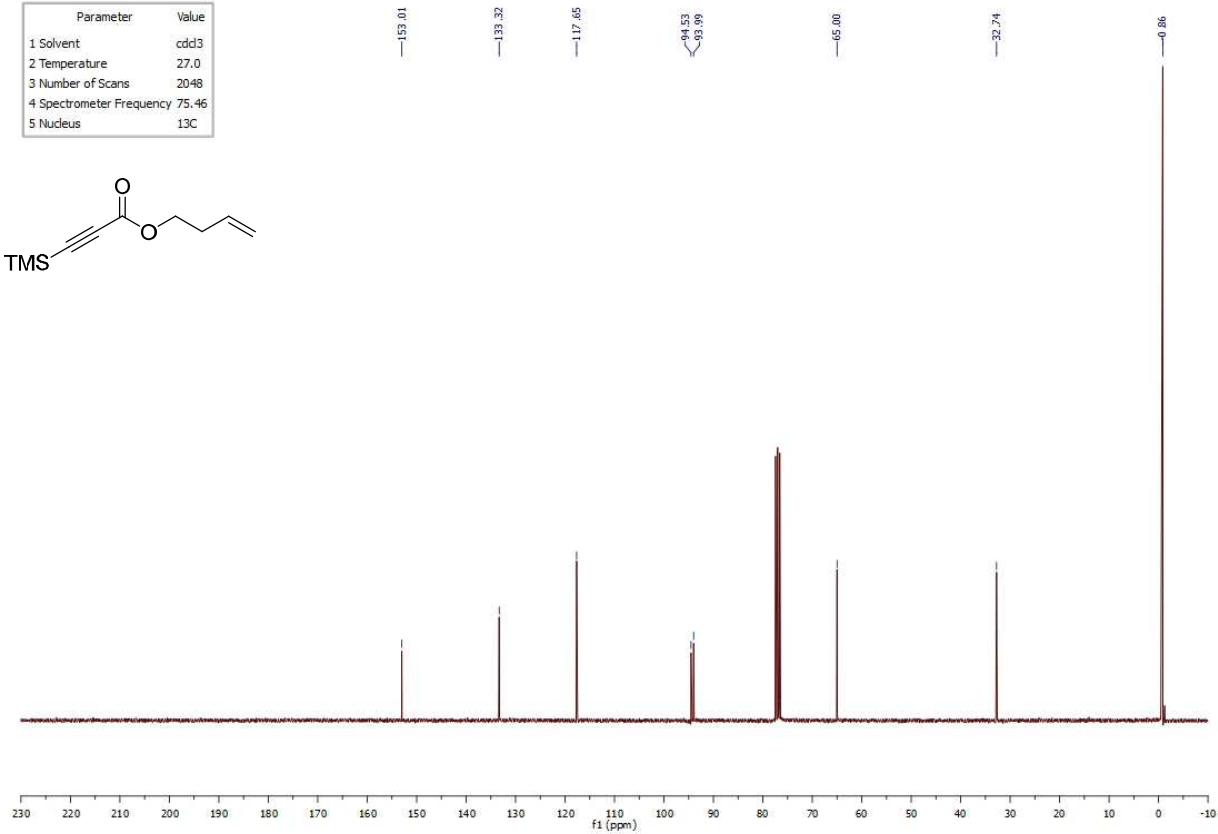
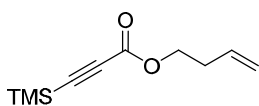


¹H NMR spectrum of **I.284**:

Parameter	Value
1 Solvent	cdcl3
2 Temperature	27.0
3 Number of Scans	8
4 Spectrometer Frequency	300.08
5 Nucleus	¹ H

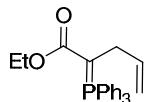
¹³C NMR spectrum of **I.284**:

Parameter	Value
1 Solvent	cdcl3
2 Temperature	27.0
3 Number of Scans	2048
4 Spectrometer Frequency	75.46
5 Nucleus	¹³ C

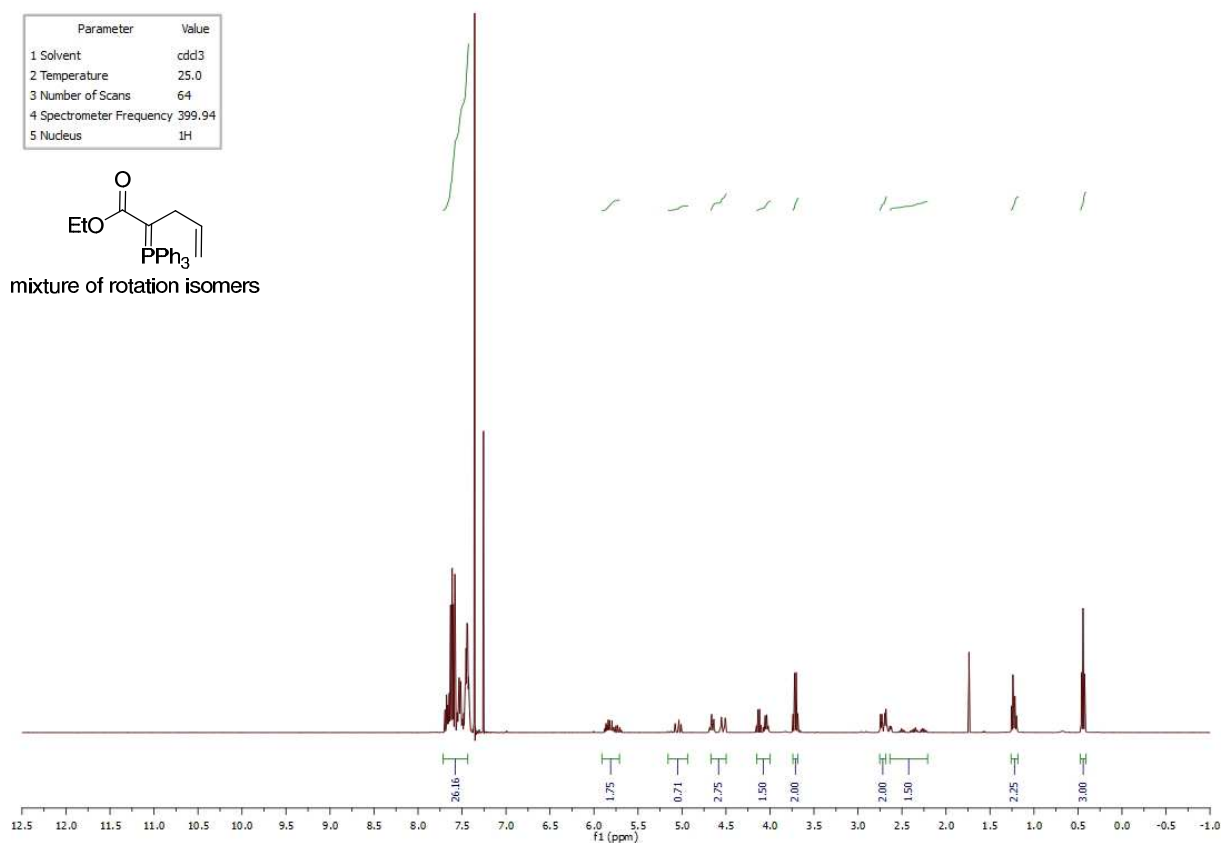


^1H NMR spectrum of **I.289**:

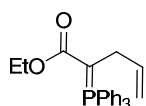
Parameter	Value
1 Solvent	cdd3
2 Temperature	25.0
3 Number of Scans	64
4 Spectrometer Frequency	399.94
5 Nucleus	^1H



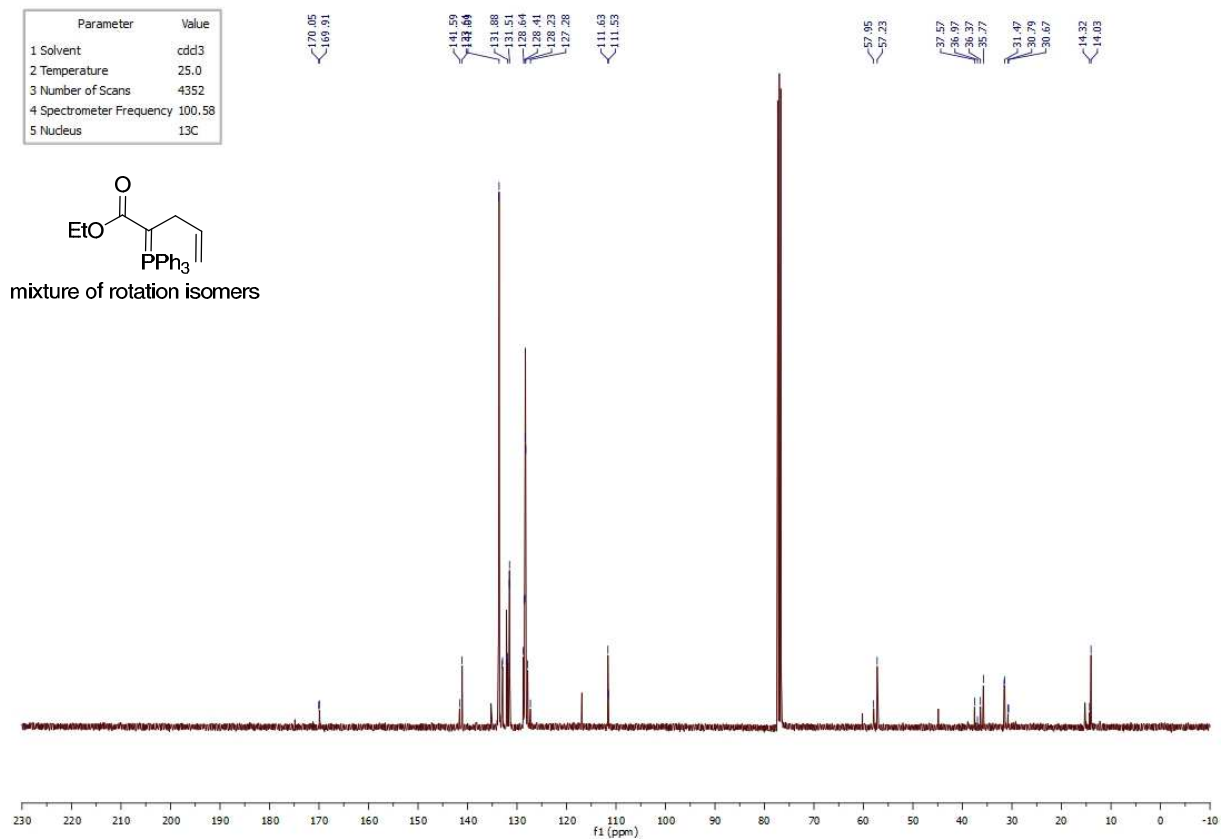
mixture of rotation isomers

 ^{13}C NMR spectrum of **I.289**:

Parameter	Value
1 Solvent	cdd3
2 Temperature	25.0
3 Number of Scans	4352
4 Spectrometer Frequency	100.58
5 Nucleus	^{13}C

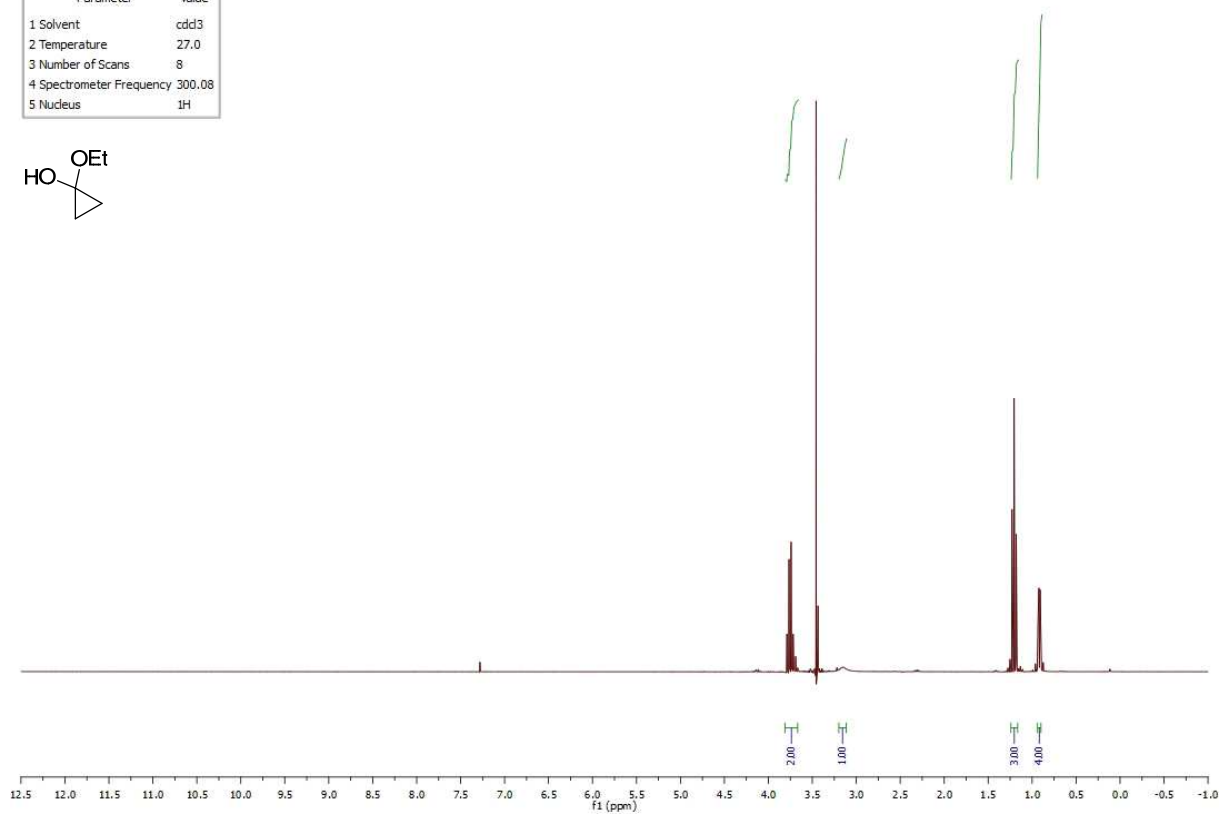


mixture of rotation isomers

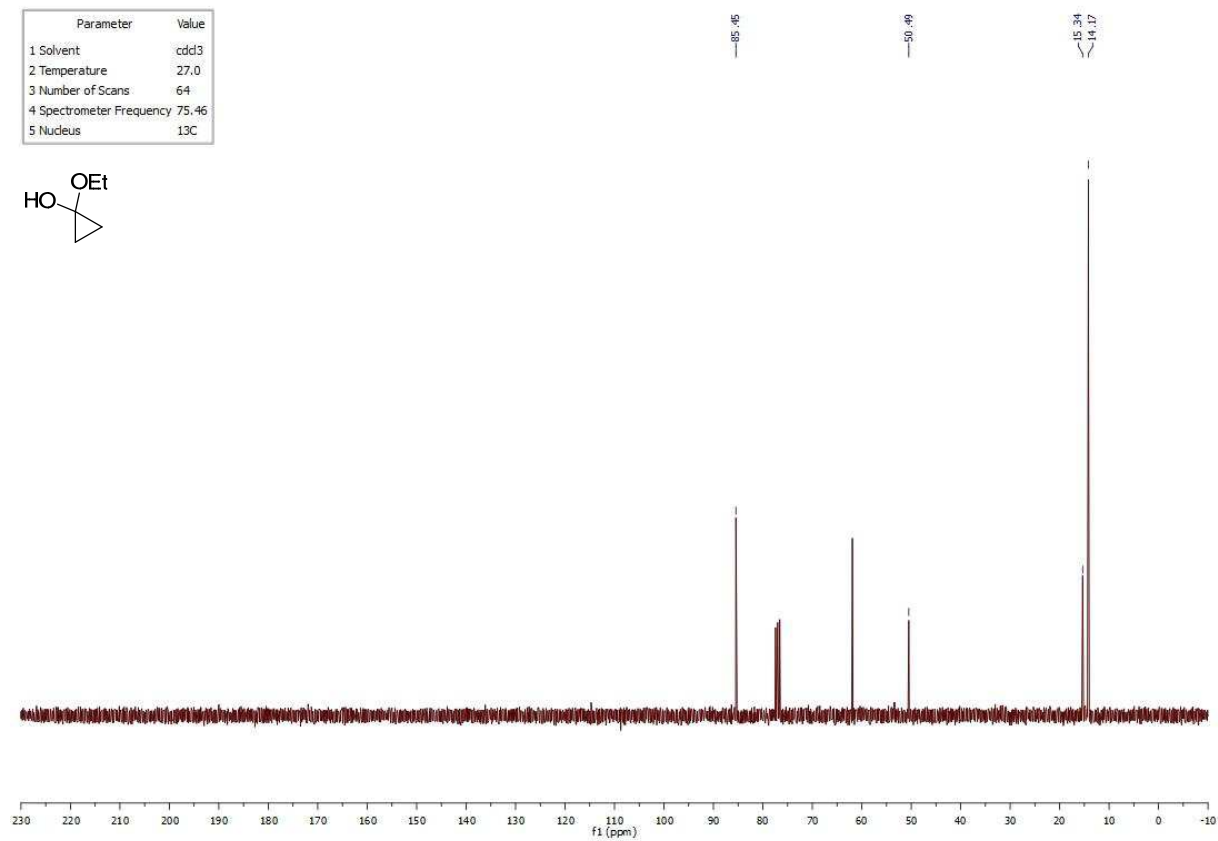


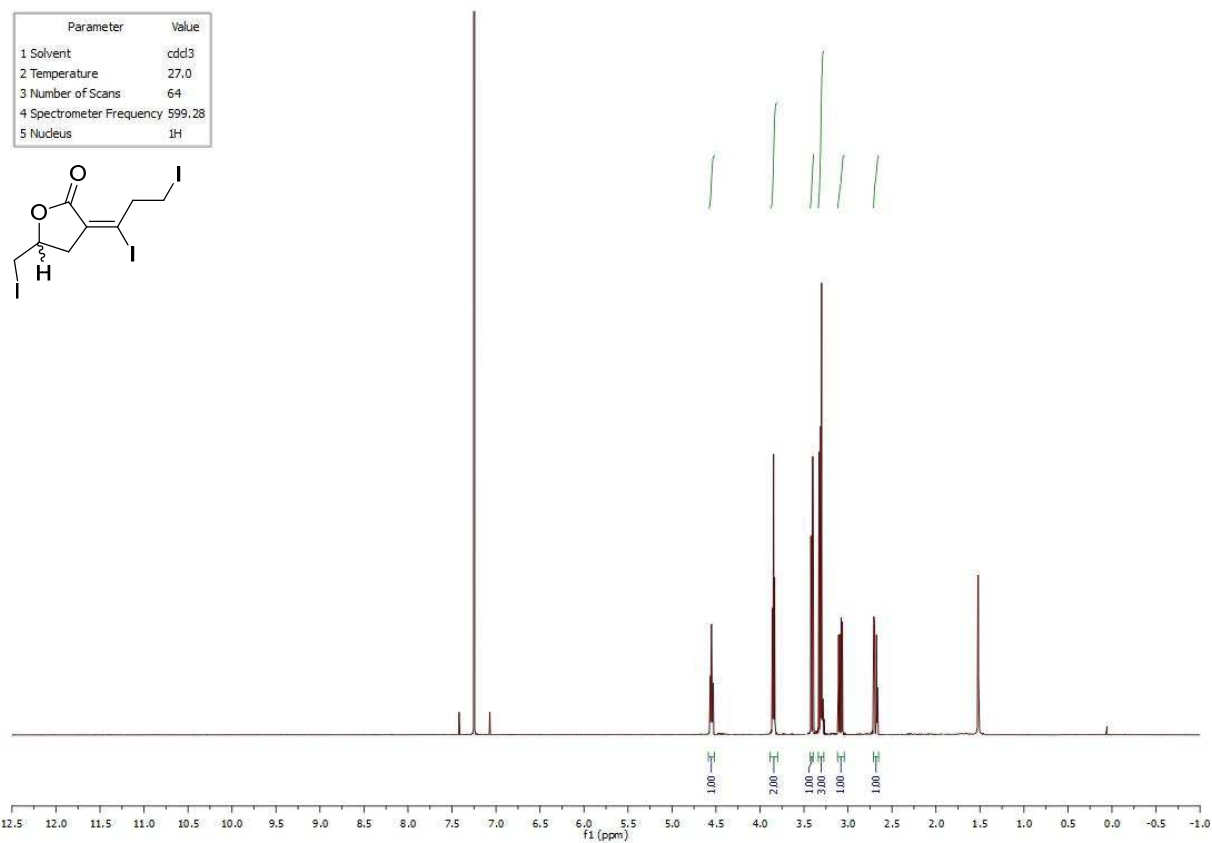
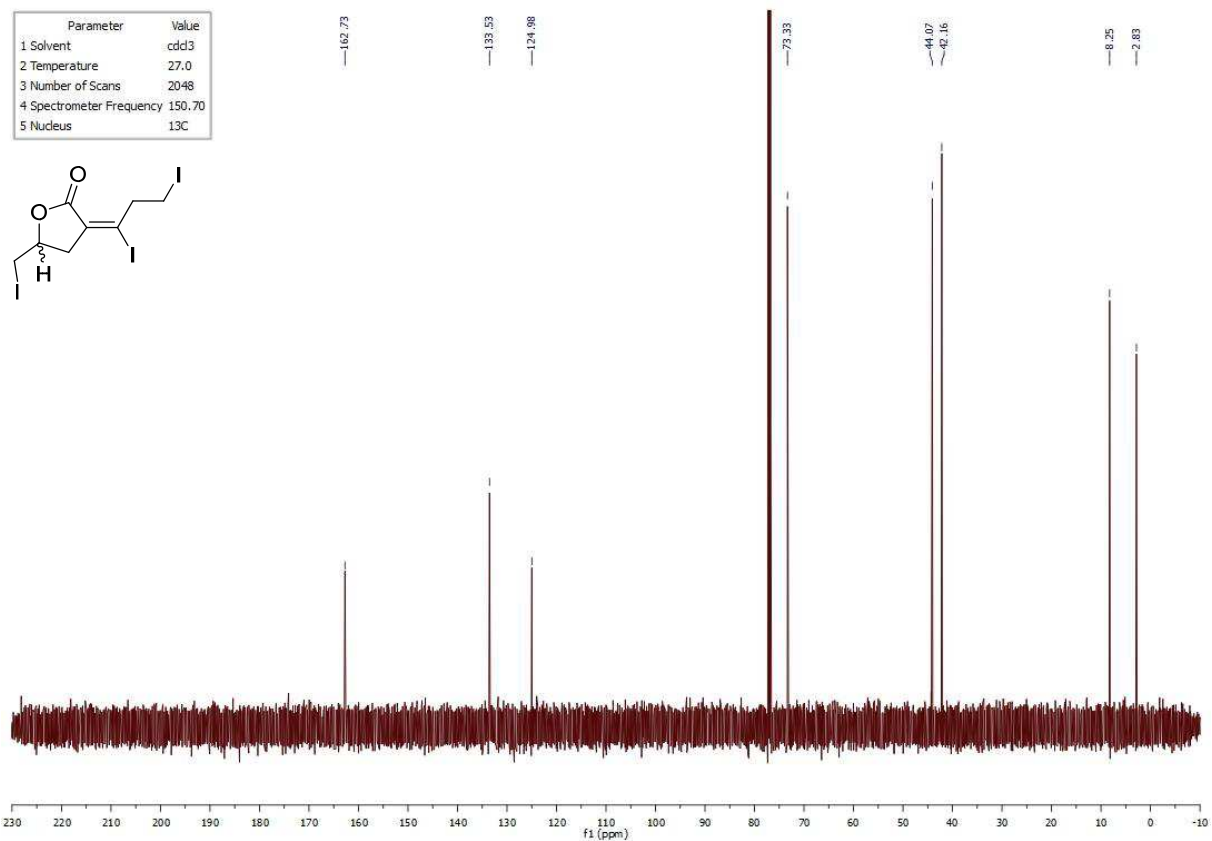
¹H NMR spectrum of **I.290**:

Parameter	Value
1 Solvent	cdcl3
2 Temperature	27.0
3 Number of Scans	8
4 Spectrometer Frequency	300.08
5 Nucleus	¹ H

¹³C NMR spectrum of **I.290**:

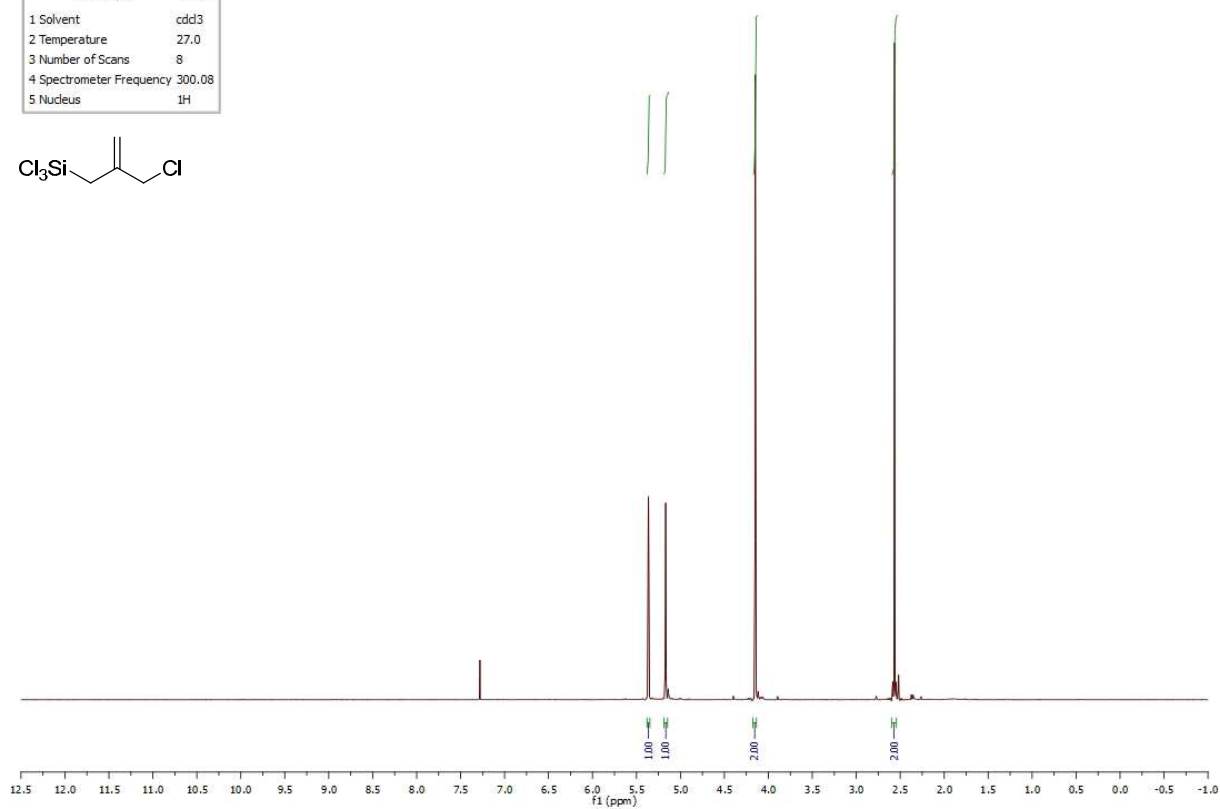
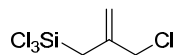
Parameter	Value
1 Solvent	cdcl3
2 Temperature	27.0
3 Number of Scans	64
4 Spectrometer Frequency	75.46
5 Nucleus	¹³ C



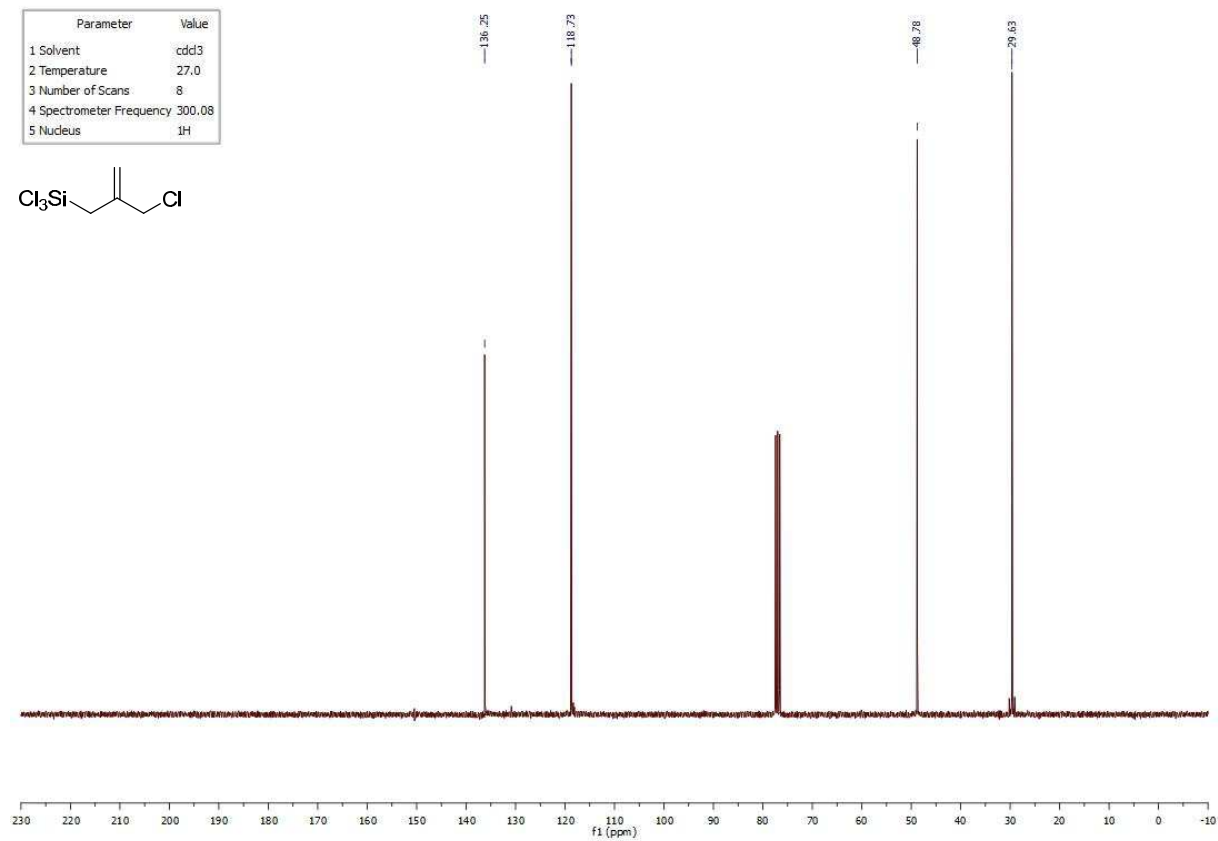
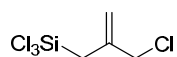
¹H NMR spectrum of **I.291**:¹³C NMR spectrum of **I.291**:

¹H NMR spectrum of **I.300**:

Parameter	Value
1 Solvent	cdcl3
2 Temperature	27.0
3 Number of Scans	8
4 Spectrometer Frequency	300.08
5 Nucleus	¹ H

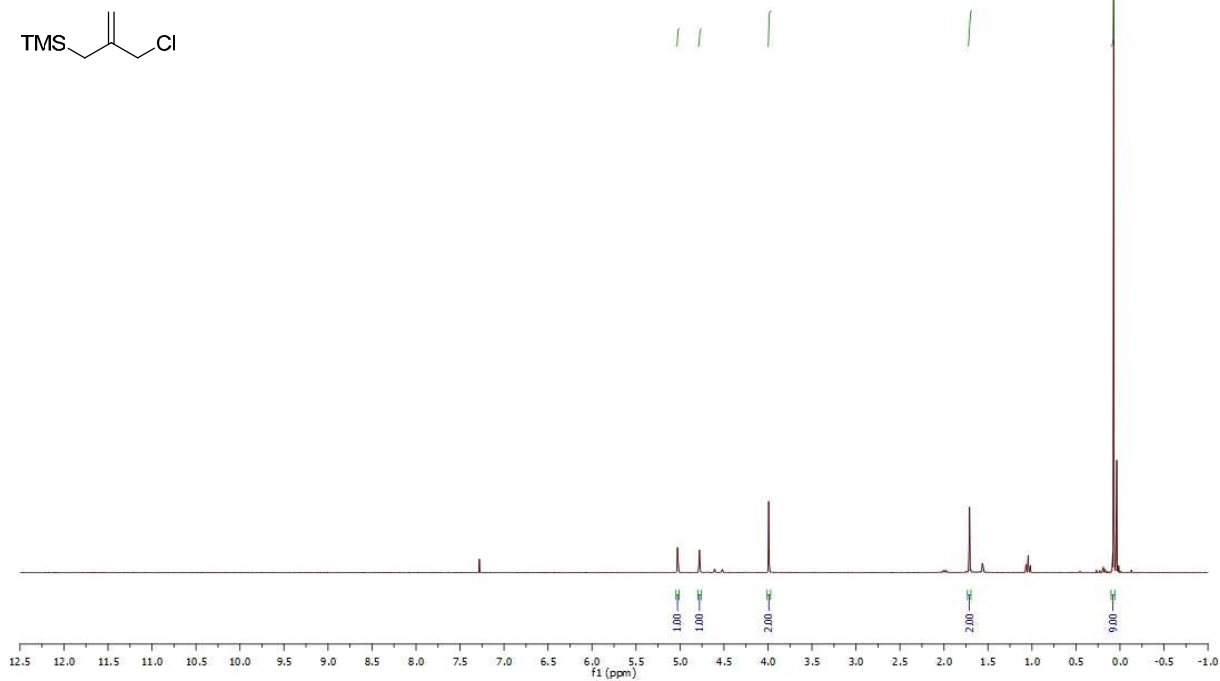
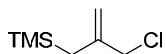
¹³C NMR spectrum of **I.300**:

Parameter	Value
1 Solvent	cdcl3
2 Temperature	27.0
3 Number of Scans	8
4 Spectrometer Frequency	300.08
5 Nucleus	¹³ C

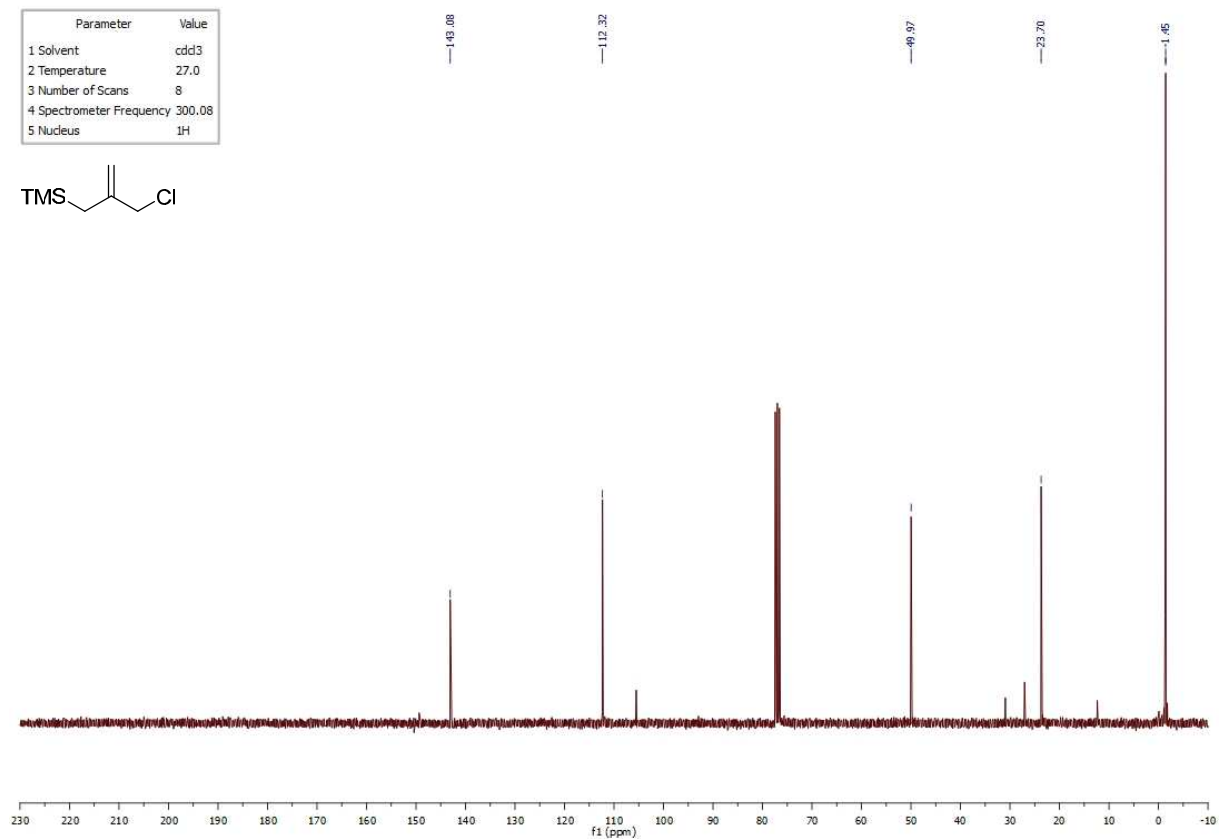
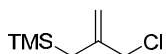


¹H NMR spectrum of **I.301**:

Parameter	Value
1 Solvent	cdd3
2 Temperature	27.0
3 Number of Scans	8
4 Spectrometer Frequency	300.08
5 Nucleus	¹ H

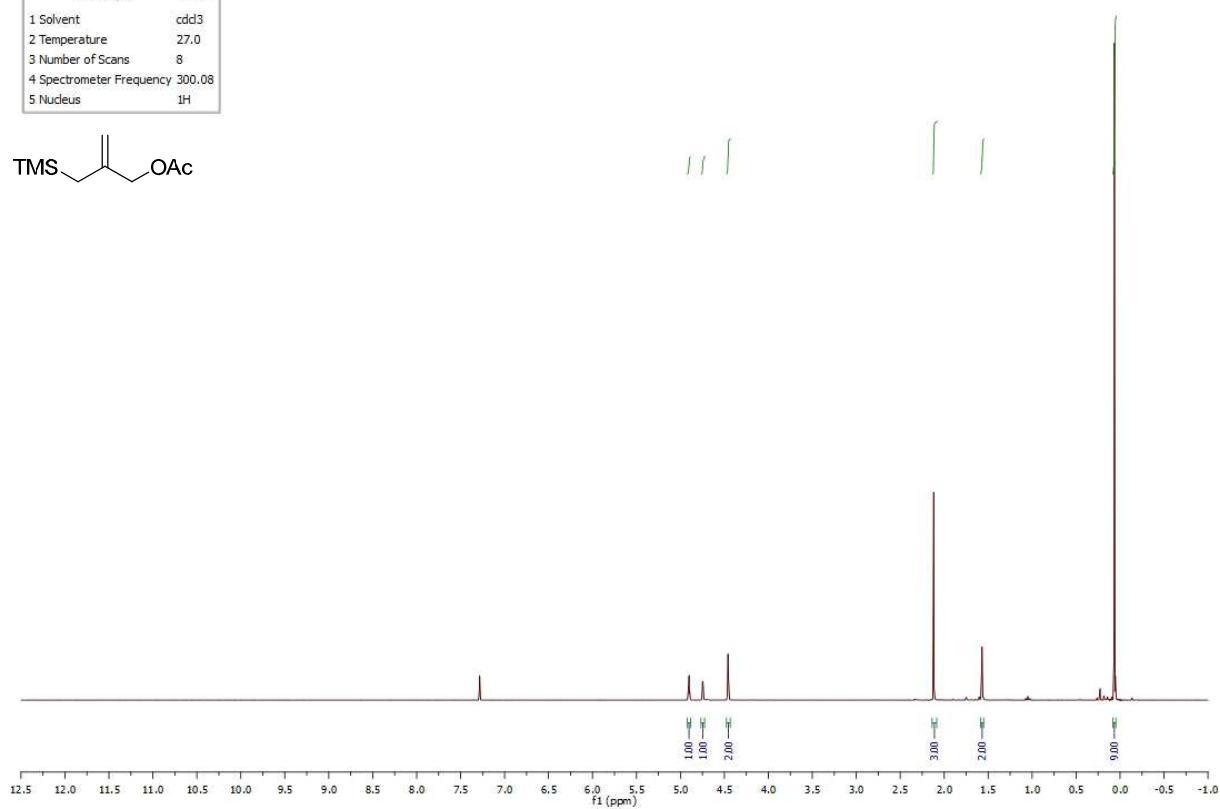
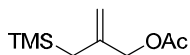
¹³C NMR spectrum of **I.301**:

Parameter	Value
1 Solvent	cdd3
2 Temperature	27.0
3 Number of Scans	8
4 Spectrometer Frequency	300.08
5 Nucleus	¹³ C

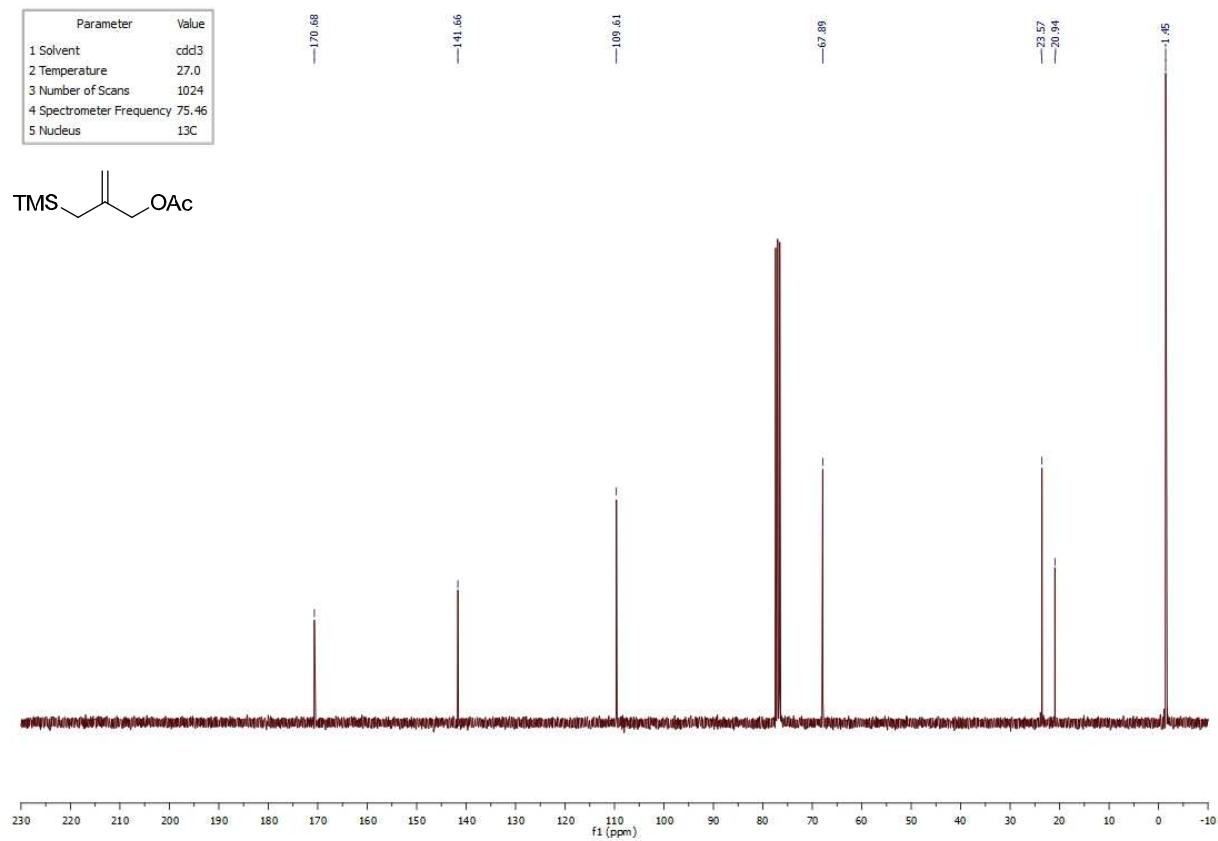
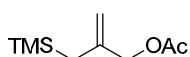


¹H NMR spectrum of **I.255**:

Parameter	Value
1 Solvent	cdcl3
2 Temperature	27.0
3 Number of Scans	8
4 Spectrometer Frequency	300.08
5 Nucleus	¹ H

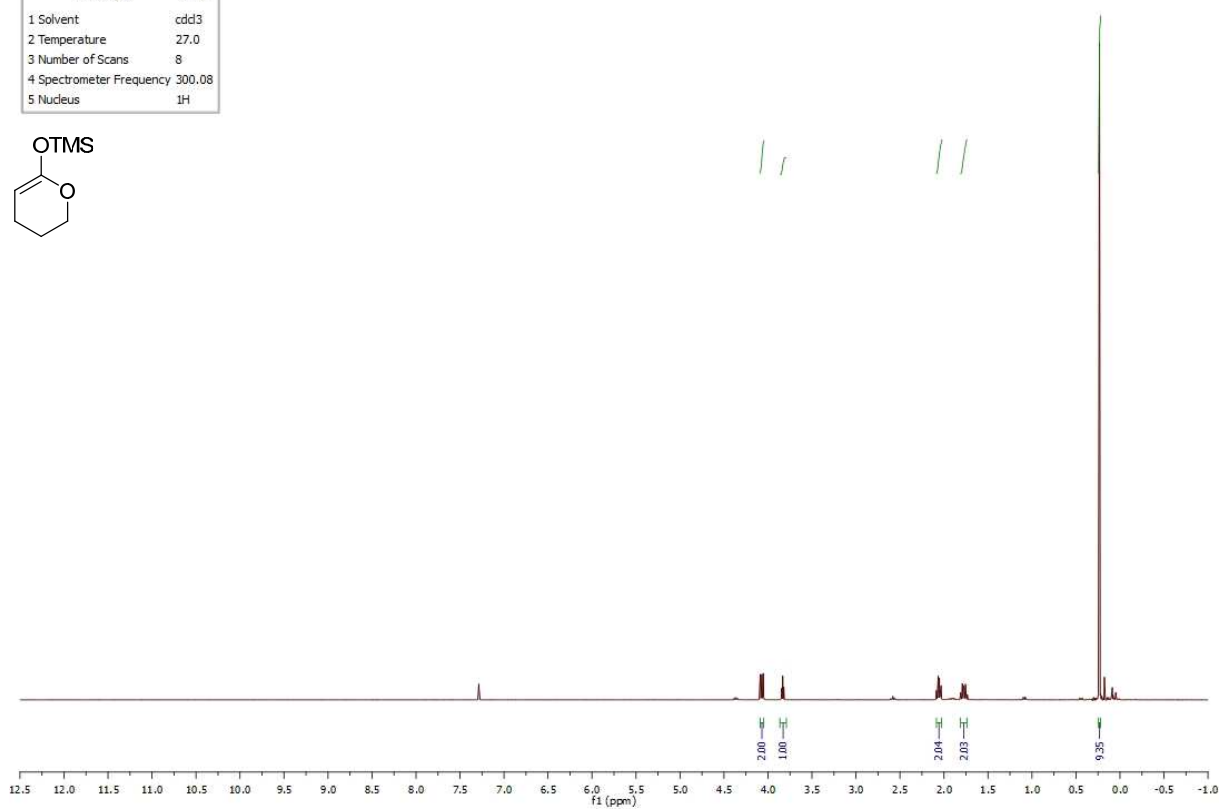
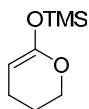
¹³C NMR spectrum of **I.255**:

Parameter	Value
1 Solvent	cdcl3
2 Temperature	27.0
3 Number of Scans	1024
4 Spectrometer Frequency	75.46
5 Nucleus	¹³ C

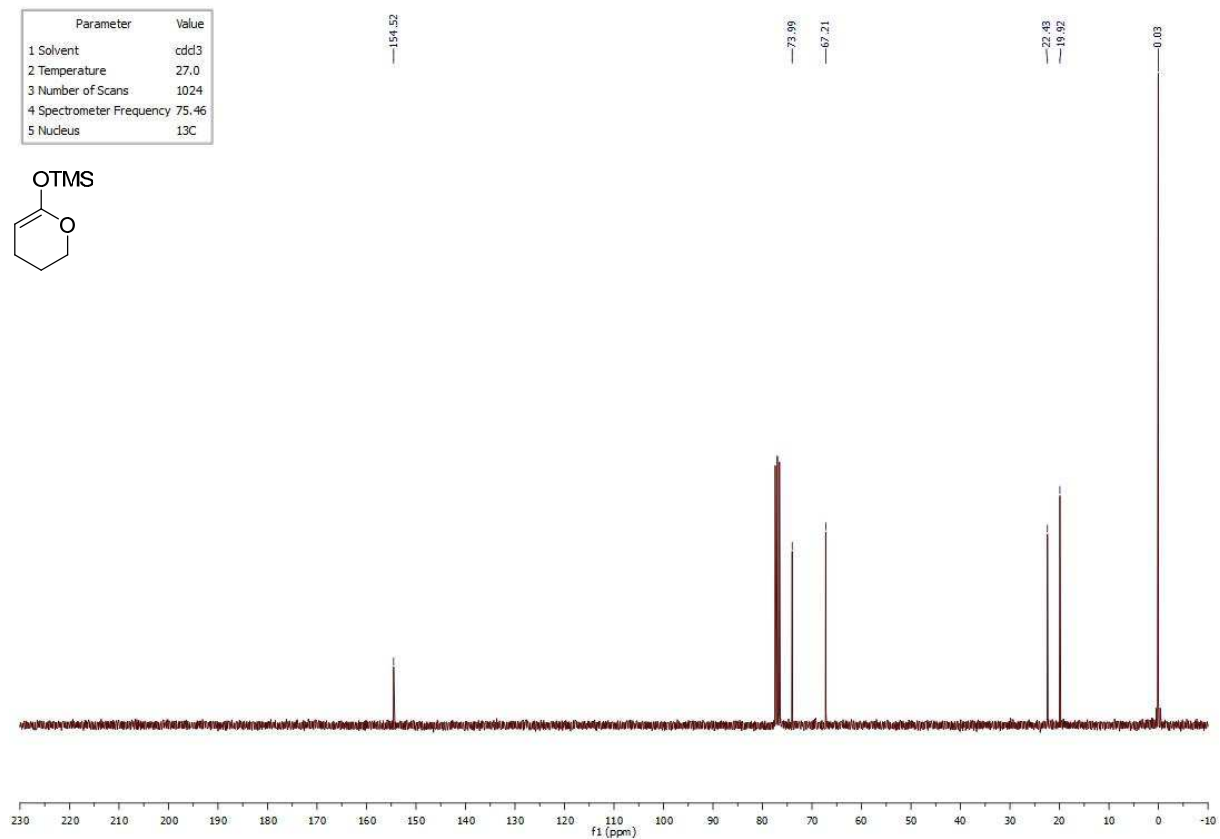
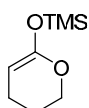


^1H NMR spectrum of **I.303**:

Parameter	Value
1 Solvent	cdd3
2 Temperature	27.0
3 Number of Scans	8
4 Spectrometer Frequency	300.08
5 Nucleus	^1H

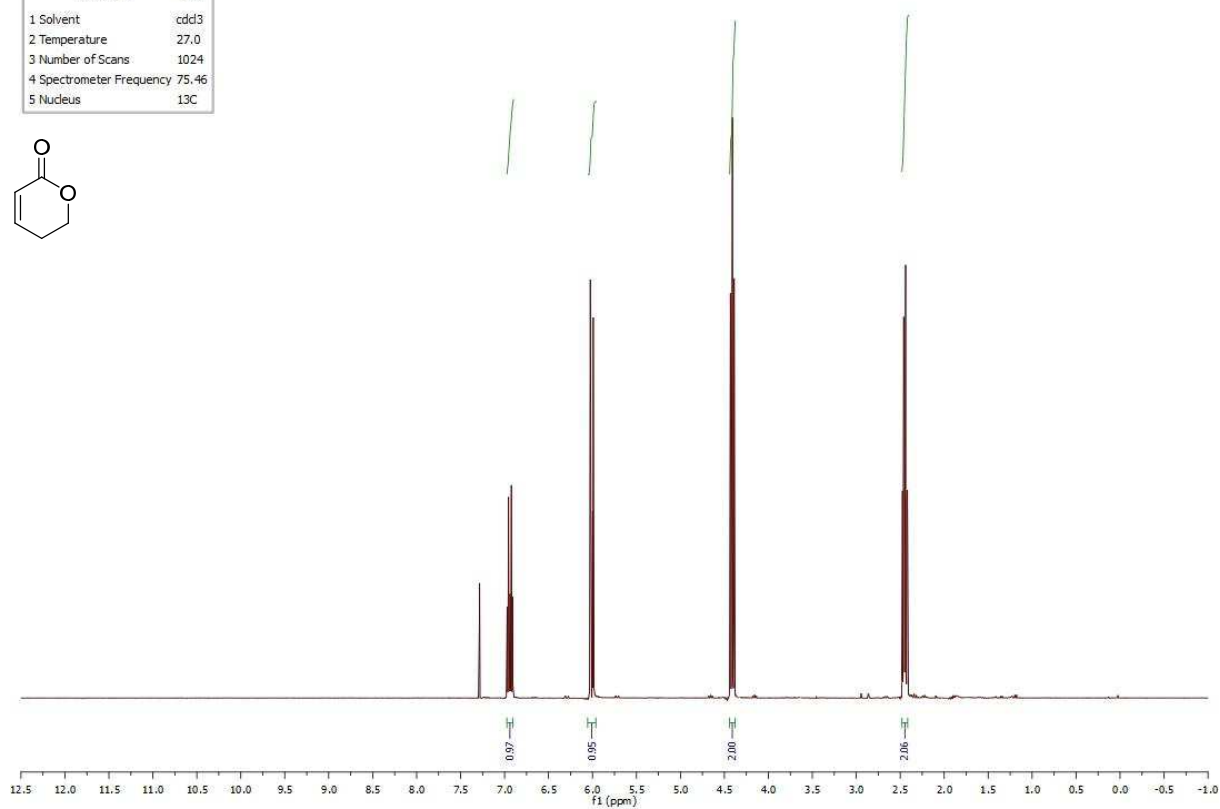
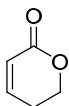
 ^{13}C NMR spectrum of **I.303**:

Parameter	Value
1 Solvent	cdd3
2 Temperature	27.0
3 Number of Scans	1024
4 Spectrometer Frequency	75.46
5 Nucleus	^{13}C

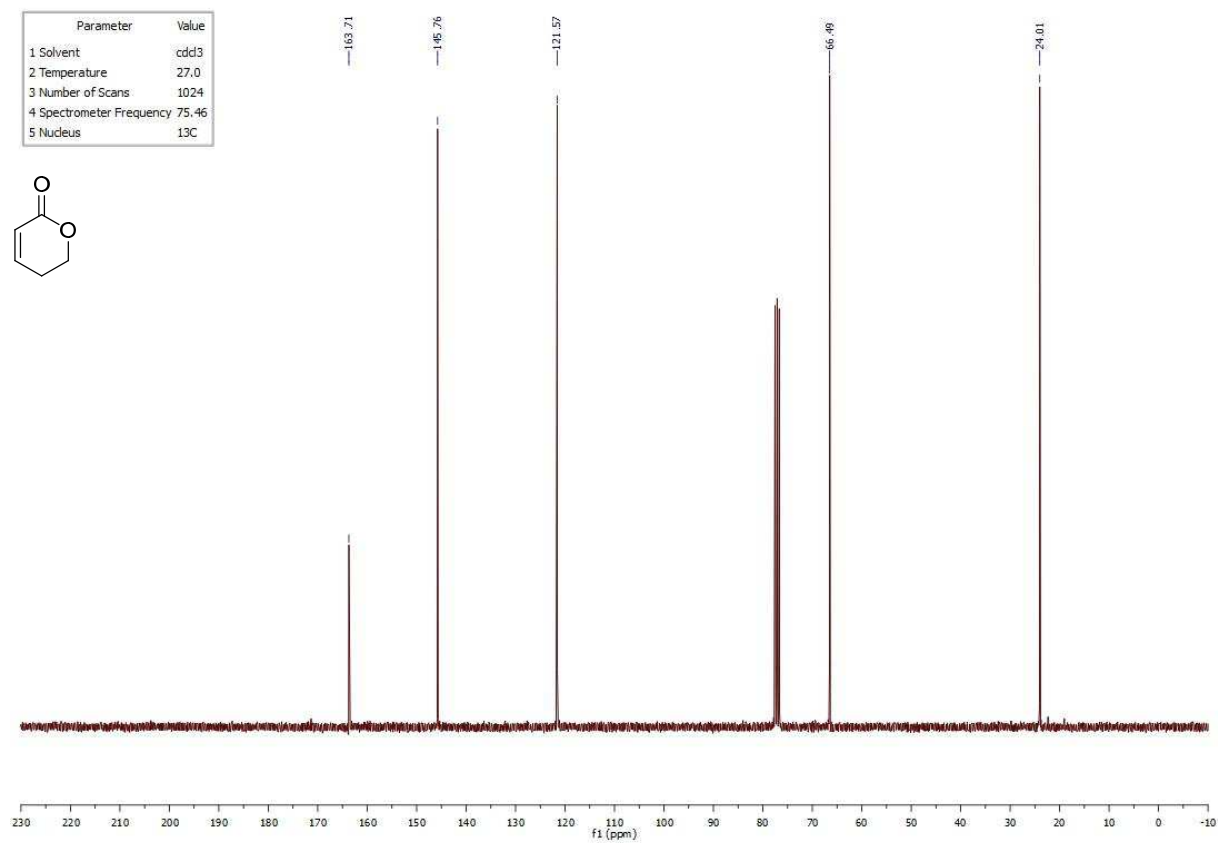
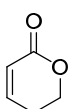


¹H NMR spectrum of **I.256**:

Parameter	Value
1 Solvent	cdcl3
2 Temperature	27,0
3 Number of Scans	1024
4 Spectrometer Frequency	75,46
5 Nucleus	13C

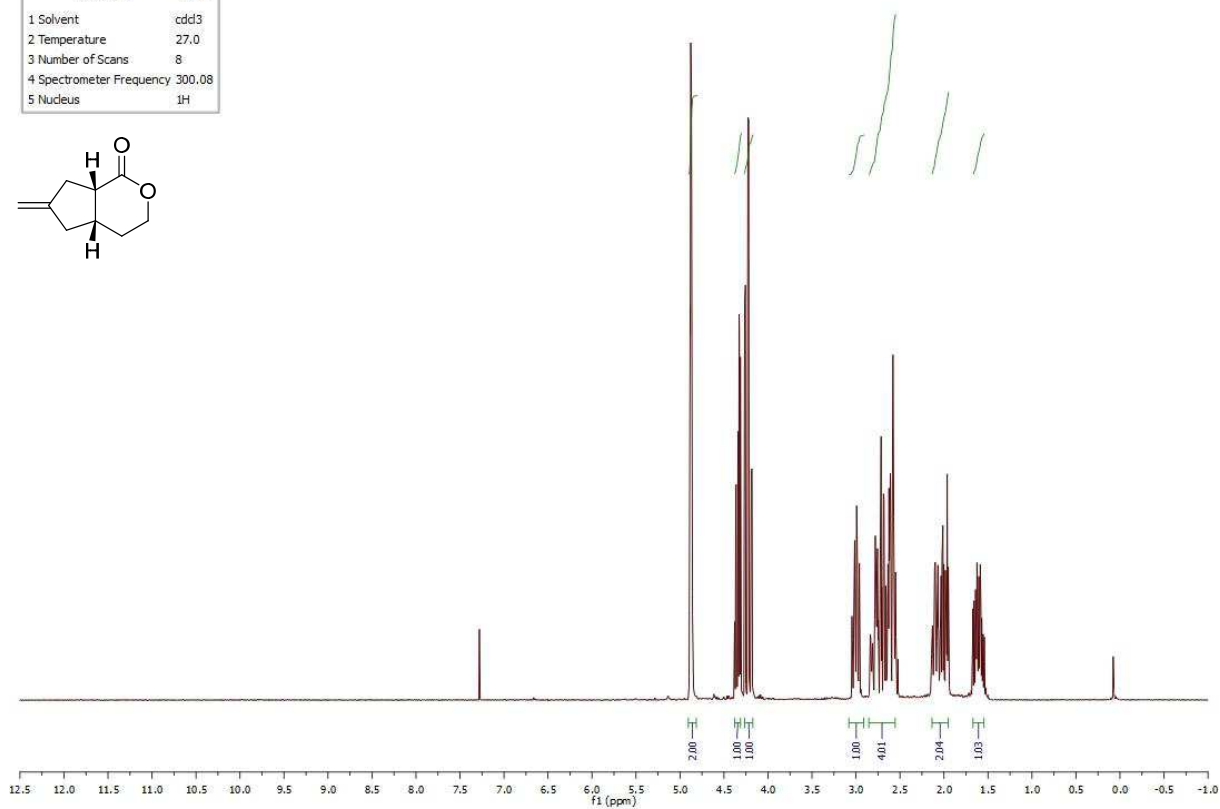
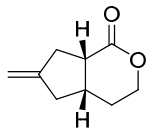
¹³C NMR spectrum of **I.256**:

Parameter	Value
1 Solvent	cdcl3
2 Temperature	27,0
3 Number of Scans	1024
4 Spectrometer Frequency	75,46
5 Nucleus	13C

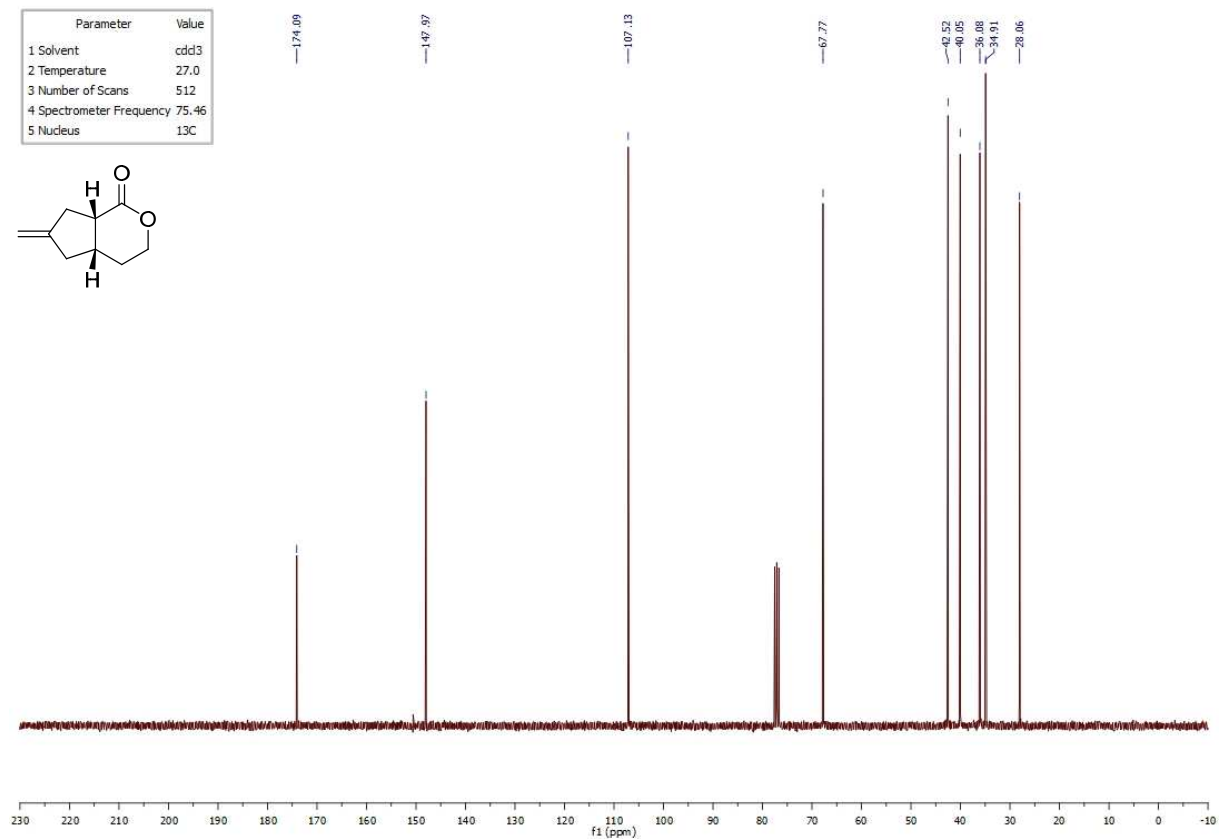
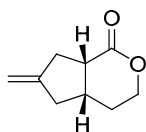


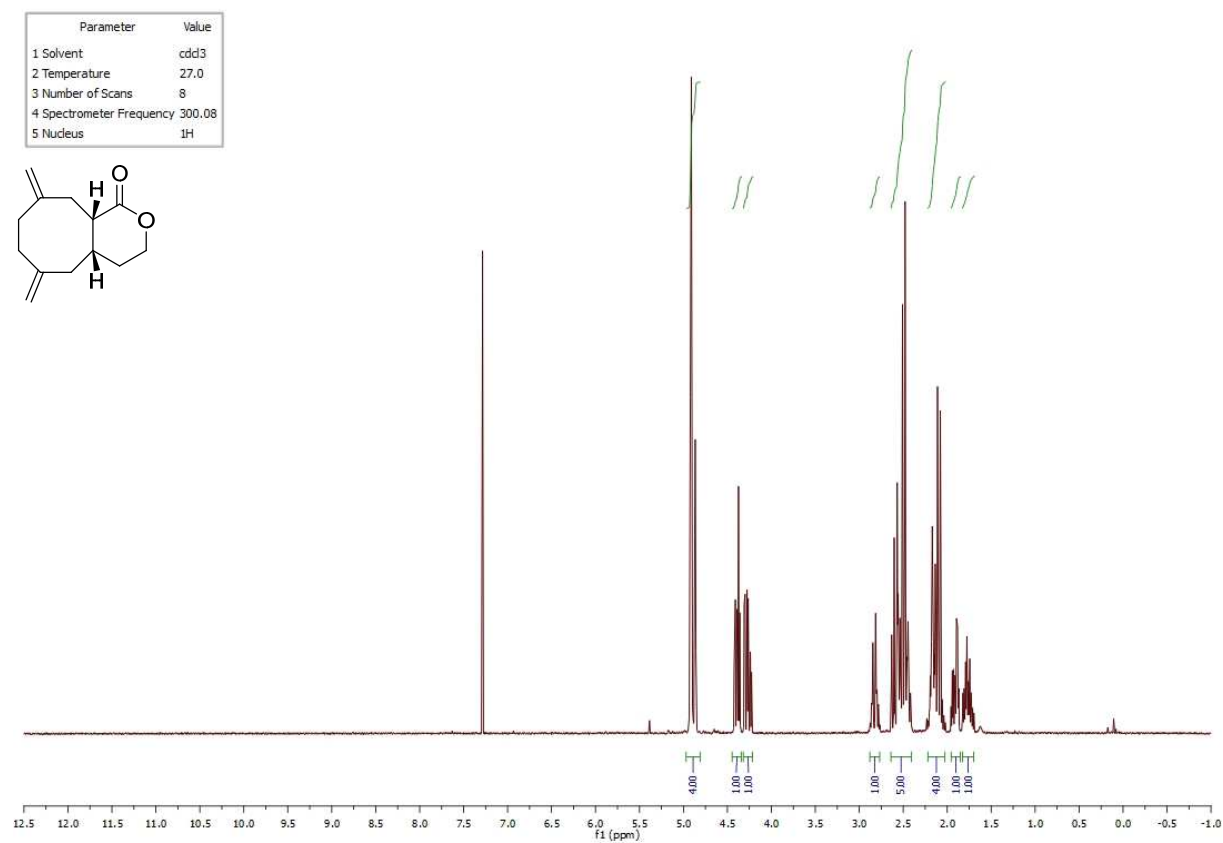
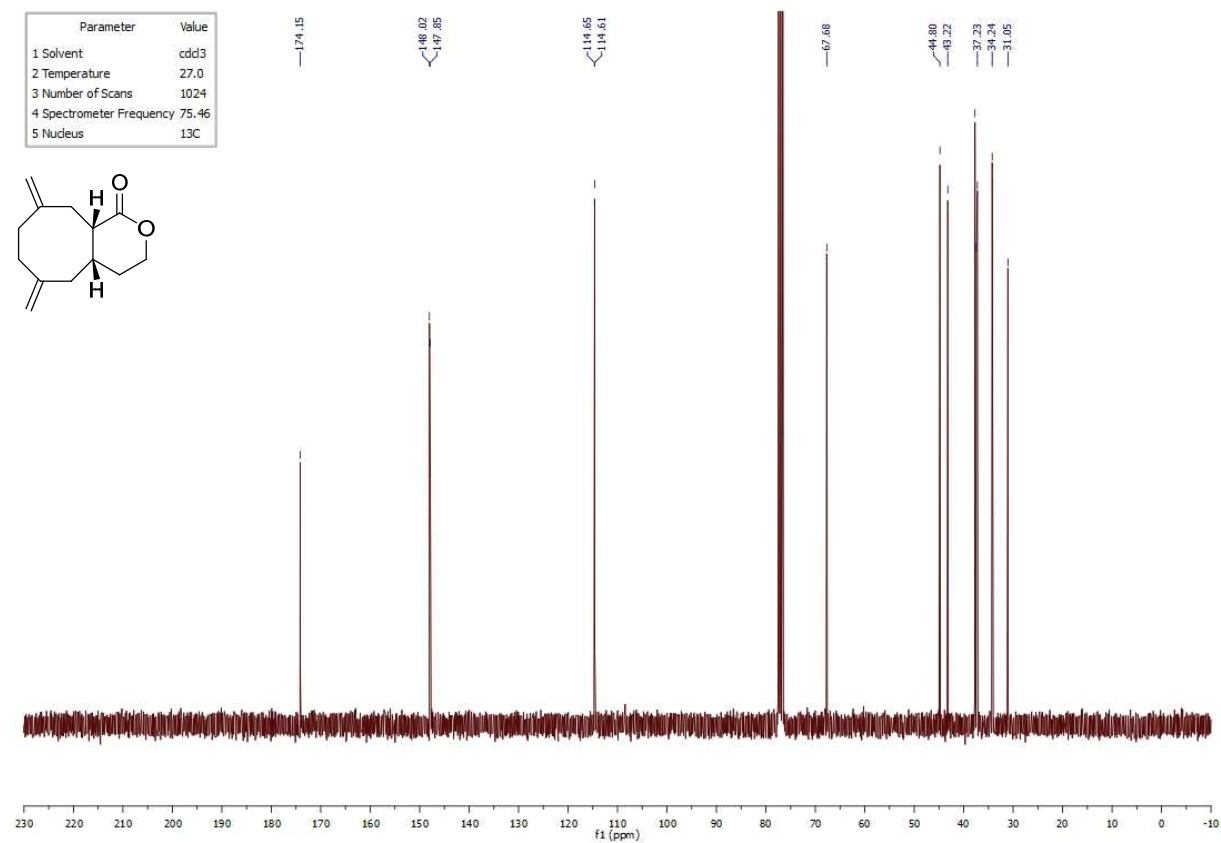
¹H NMR spectrum of **I.298**:

Parameter	Value
1 Solvent	cdd3
2 Temperature	27.0
3 Number of Scans	8
4 Spectrometer Frequency	300.08
5 Nucleus	¹ H

¹³C NMR spectrum of **I.298**:

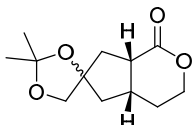
Parameter	Value
1 Solvent	cdd3
2 Temperature	27.0
3 Number of Scans	512
4 Spectrometer Frequency	75.46
5 Nucleus	¹³ C



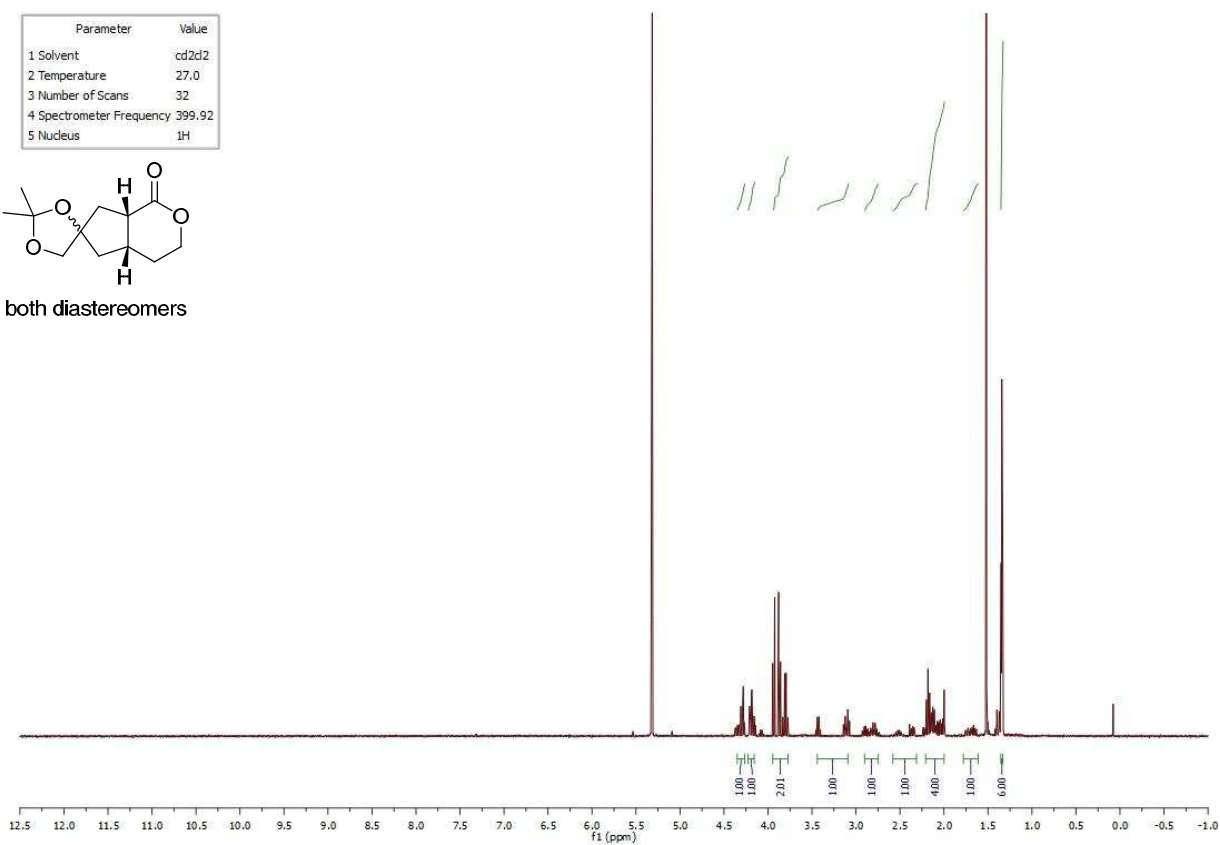
¹H NMR spectrum of **I.305**:¹³C NMR spectrum of **I.305**:

^1H NMR spectrum of **I.322**:

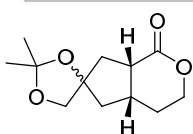
Parameter	Value
1 Solvent	cd2d2
2 Temperature	27.0
3 Number of Scans	32
4 Spectrometer Frequency	399.92
5 Nucleus	^1H



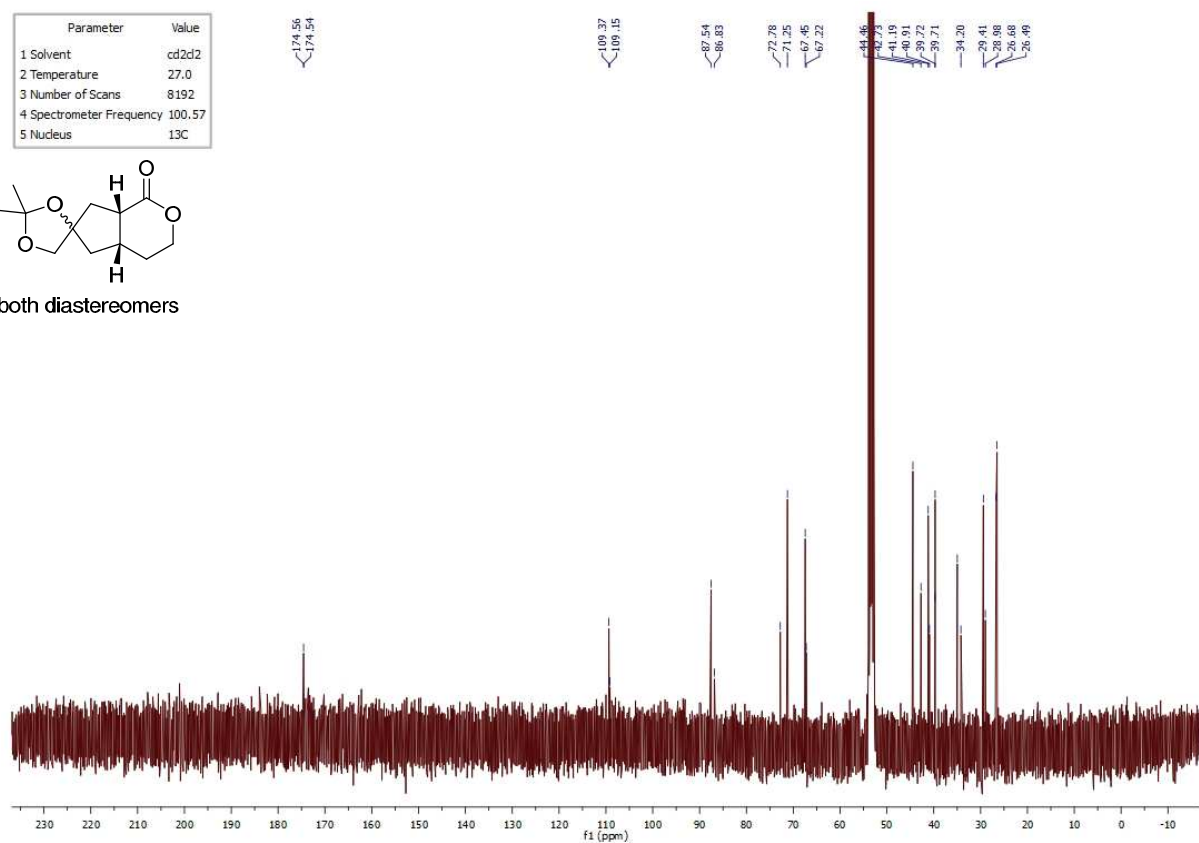
both diastereomers

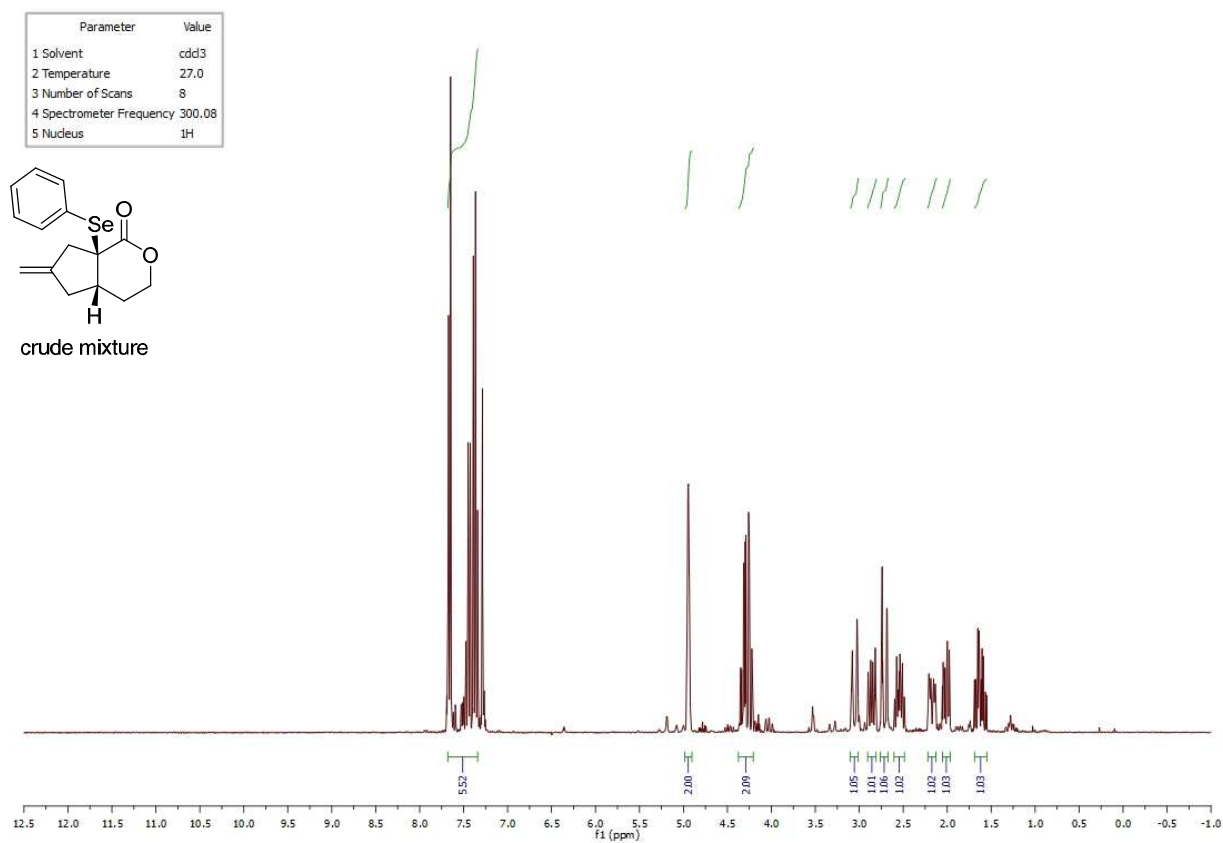
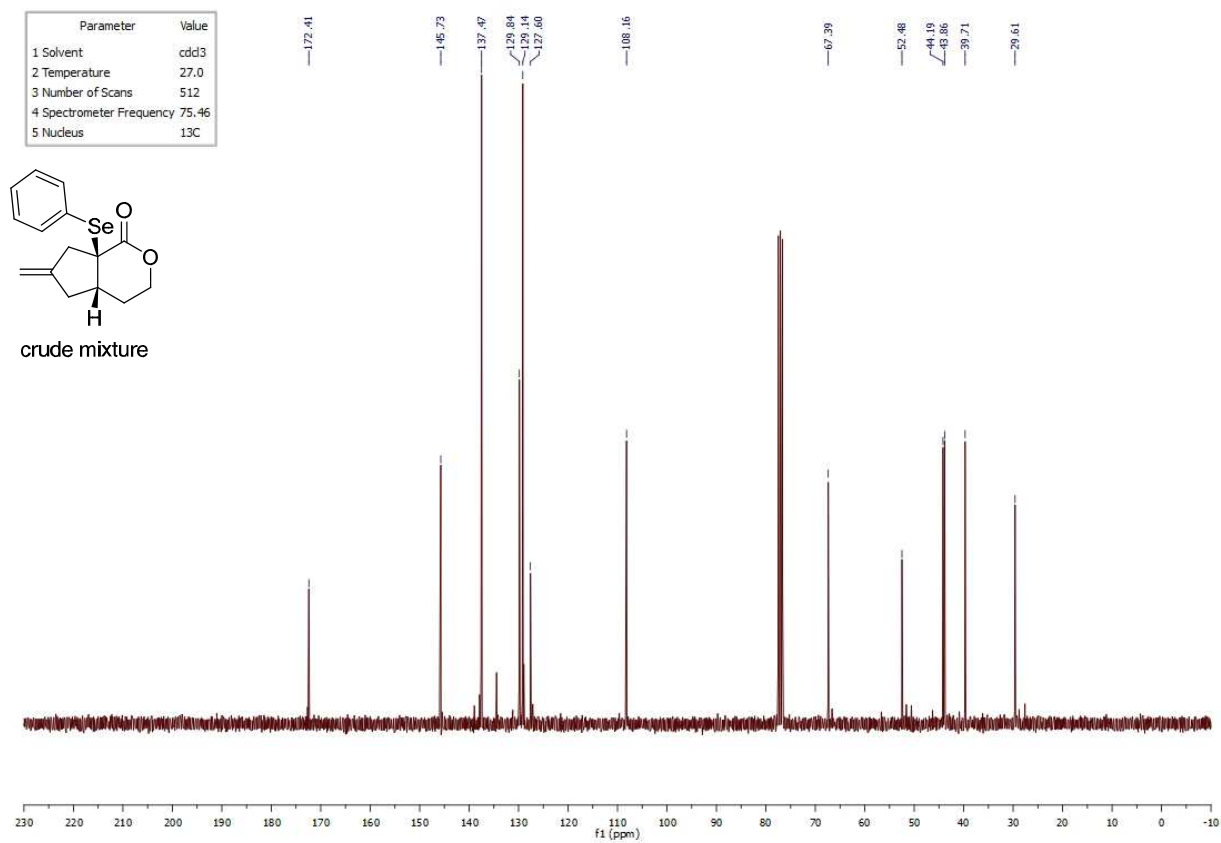
 ^{13}C NMR spectrum of **I.322**:

Parameter	Value
1 Solvent	cd2d2
2 Temperature	27.0
3 Number of Scans	8192
4 Spectrometer Frequency	100.57
5 Nucleus	^{13}C



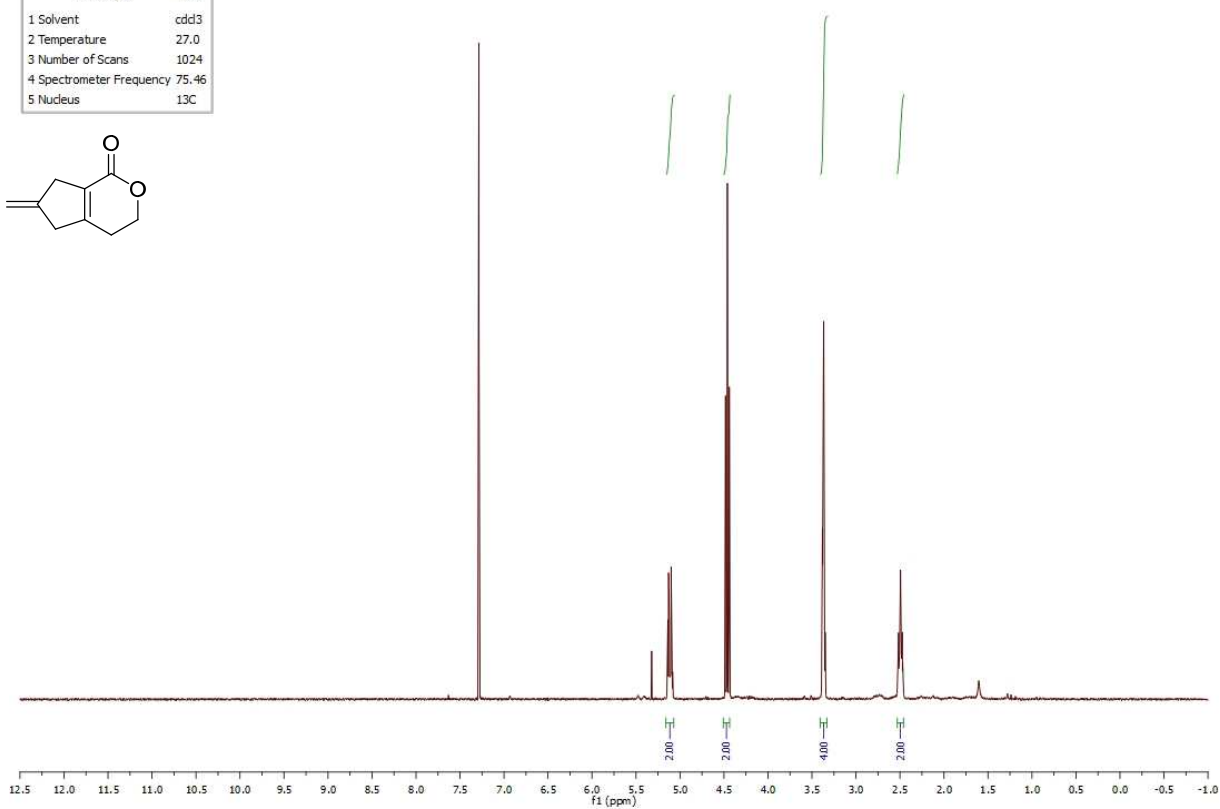
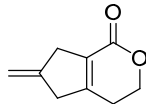
both diastereomers



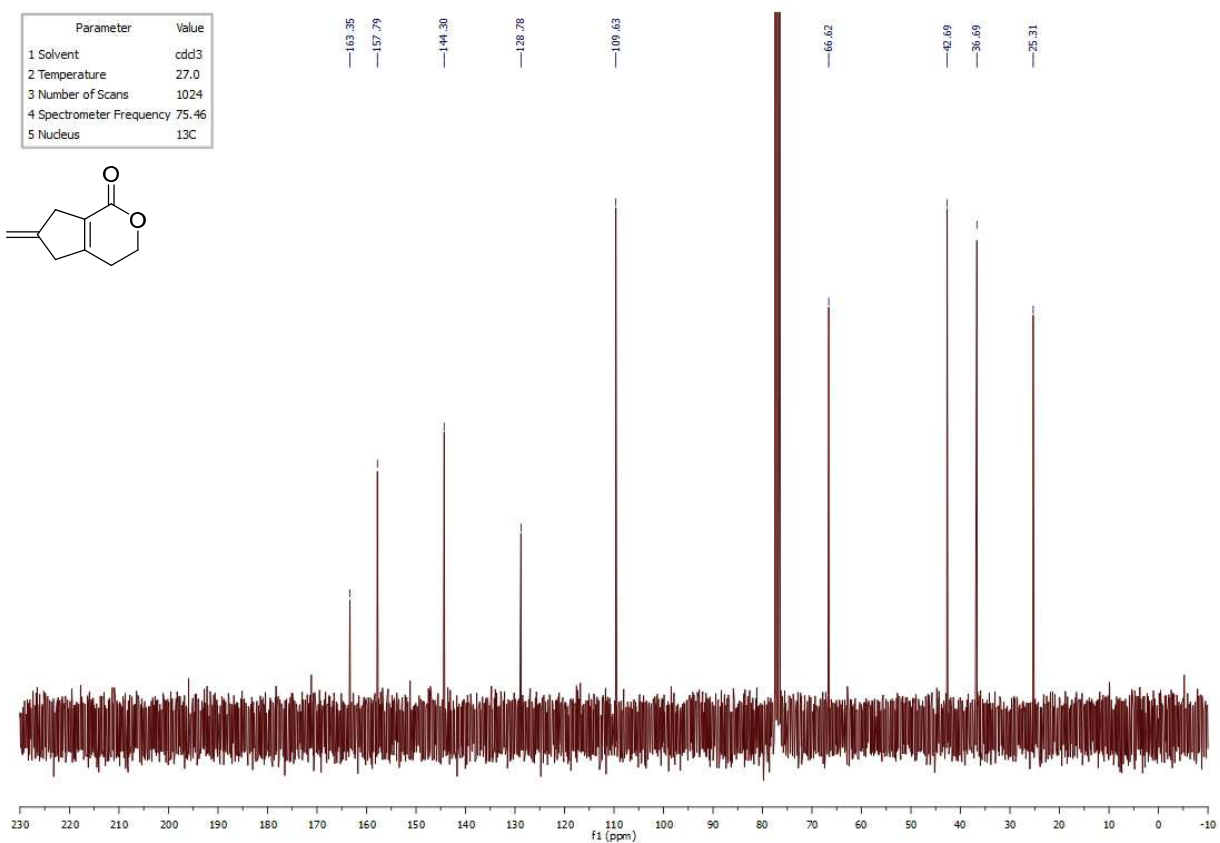
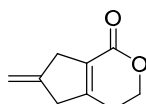
¹H NMR spectrum of **I.314**:¹³C NMR spectrum of **I.314**:

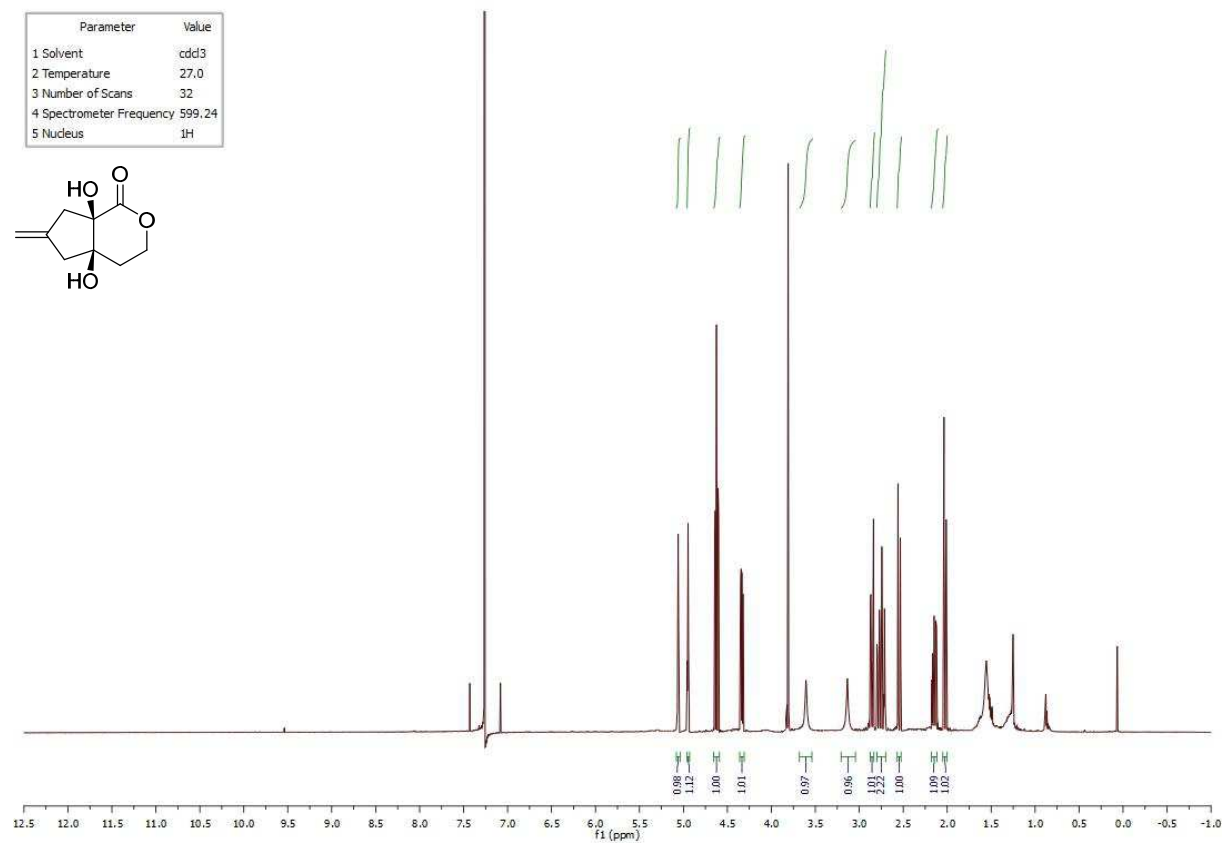
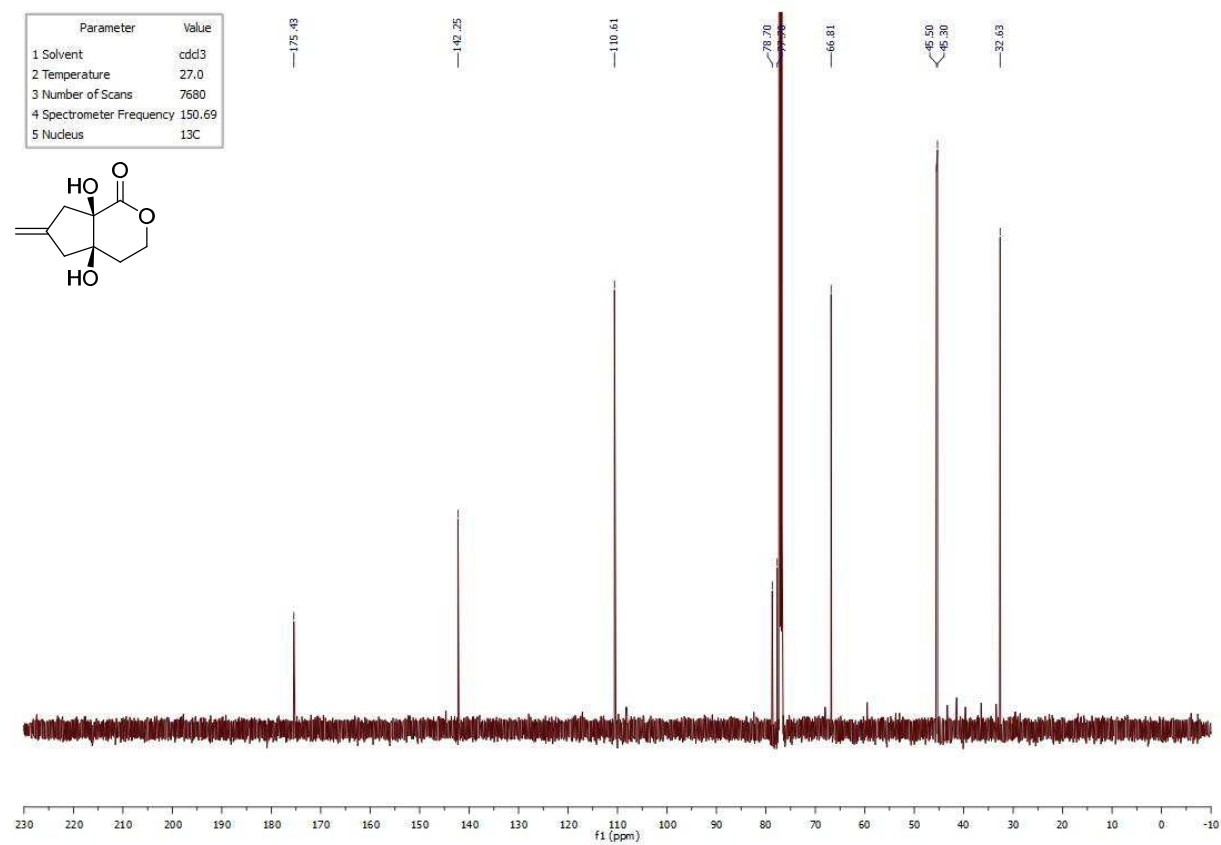
¹H NMR spectrum of **I.315**:

Parameter	Value
1 Solvent	cdd3
2 Temperature	27.0
3 Number of Scans	1024
4 Spectrometer Frequency	75.46
5 Nucleus	¹³ C

¹³C NMR spectrum of **I.315**:

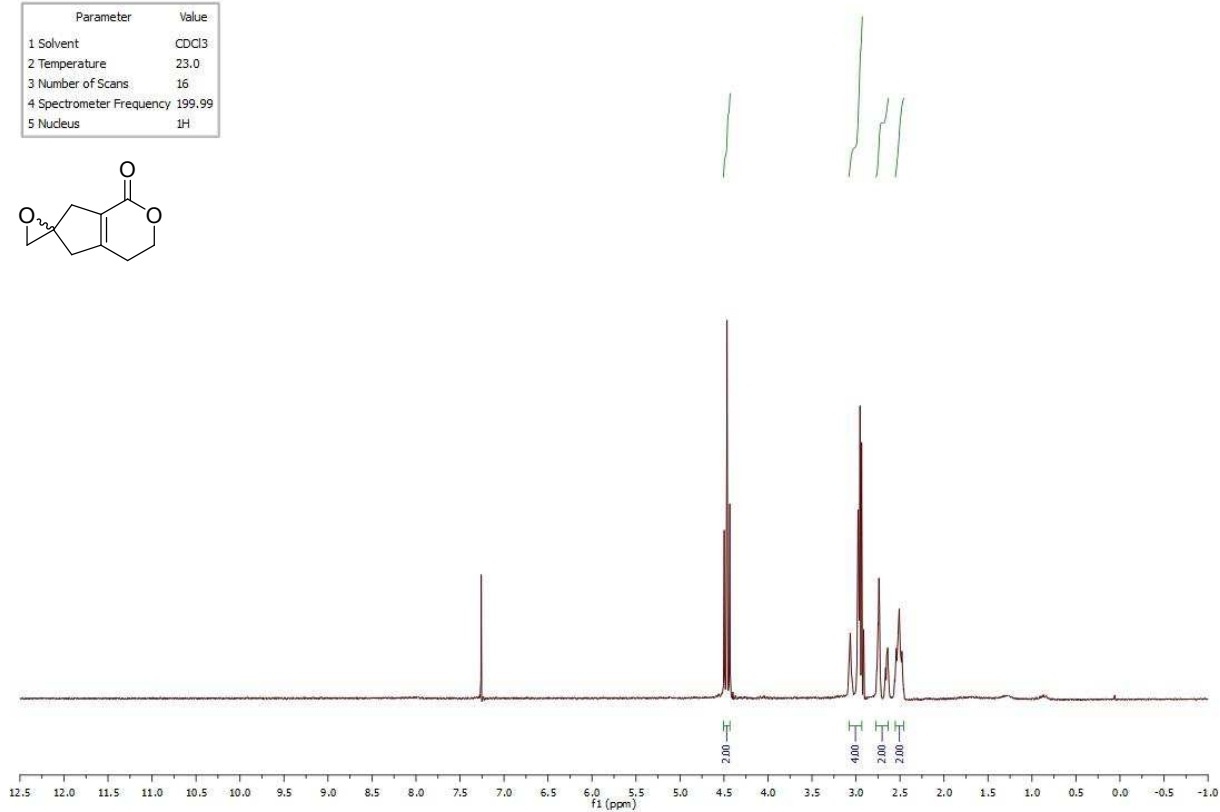
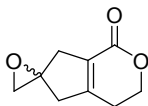
Parameter	Value
1 Solvent	cdd3
2 Temperature	27.0
3 Number of Scans	1024
4 Spectrometer Frequency	75.46
5 Nucleus	¹³ C



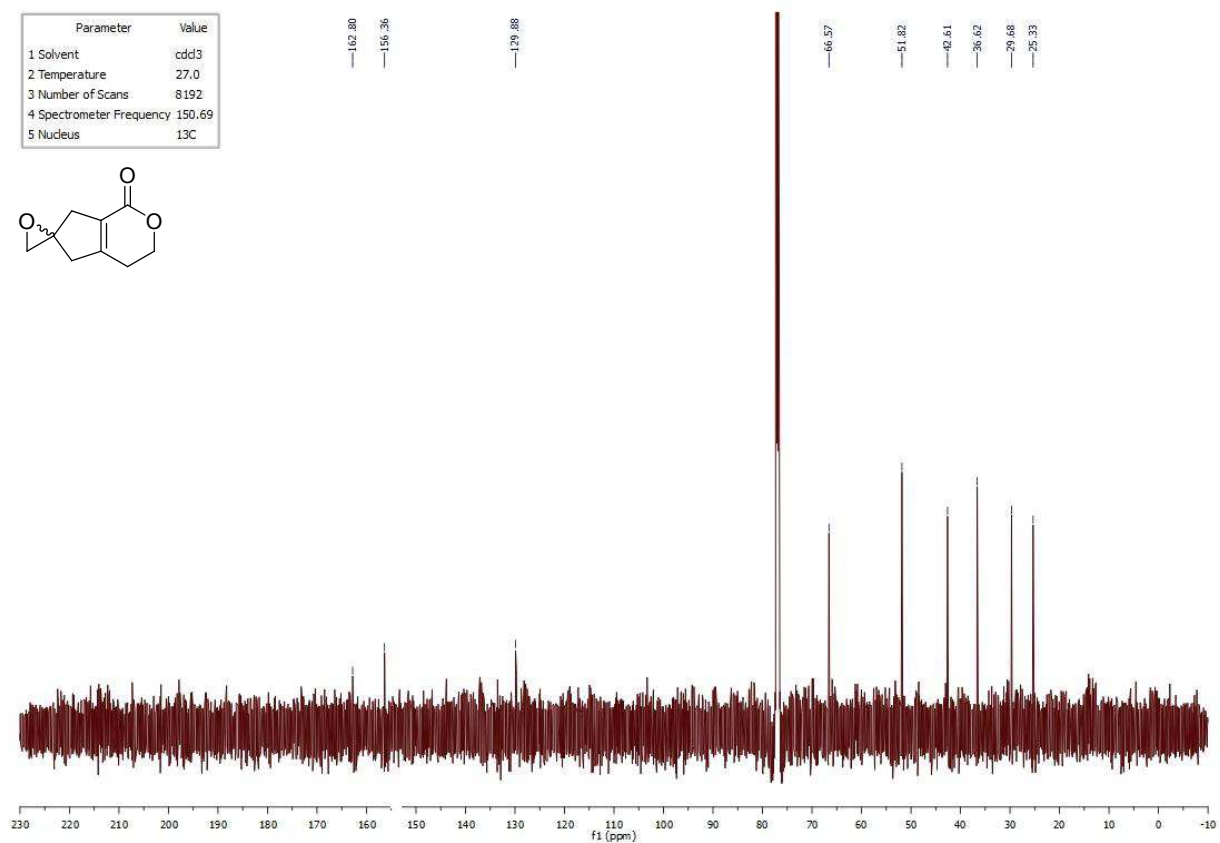
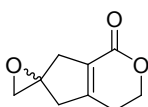
¹H NMR spectrum of **I.318**:¹³C NMR spectrum of **I.318**:

^1H NMR spectrum of **I.317**:

Parameter	Value
1 Solvent	CDCl_3
2 Temperature	23.0
3 Number of Scans	16
4 Spectrometer Frequency	199.99
5 Nucleus	^1H

 ^{13}C NMR spectrum of **I.317**:

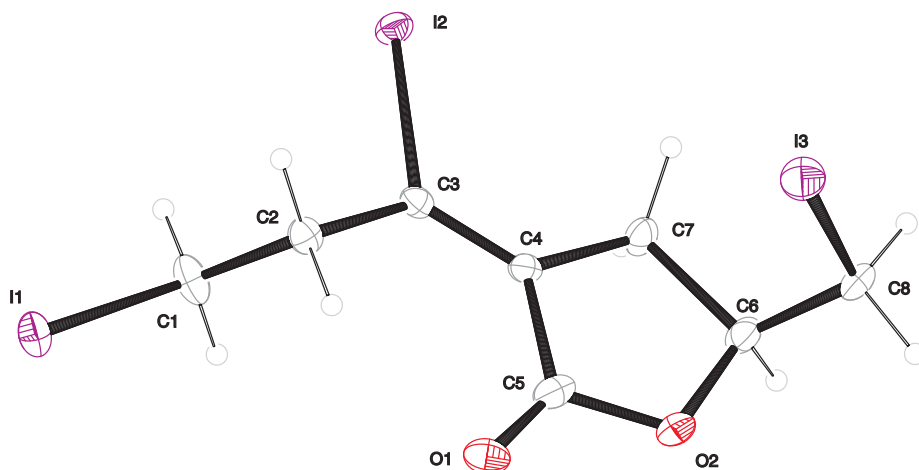
Parameter	Value
1 Solvent	cdcl_3
2 Temperature	27.0
3 Number of Scans	8192
4 Spectrometer Frequency	150.69
5 Nucleus	^{13}C



Appendix 2: Crystallographic Data of Chapter I

The X-ray analysis was carried out by Dr. Peter Mayer in the analytics department in the Ludwig-Maximilians-Universität, München. The data collection was performed on an *Oxford Diffraction Xcalibur* diffractometer at $-100\text{ }^{\circ}\text{C}$ using $\text{MoK}\alpha$ -radiation ($\lambda = 0.71073\text{ \AA}$, graphite monochromator). The CrysAlisPro software (version number 1.171.33.41)^[163] was applied for the integration, scaling and multi-scan absorption correction of the data. The structures were solved by direct methods with SIR97^[164] and refined by least-squares methods against F^2 with SHELXL-97.^[165]

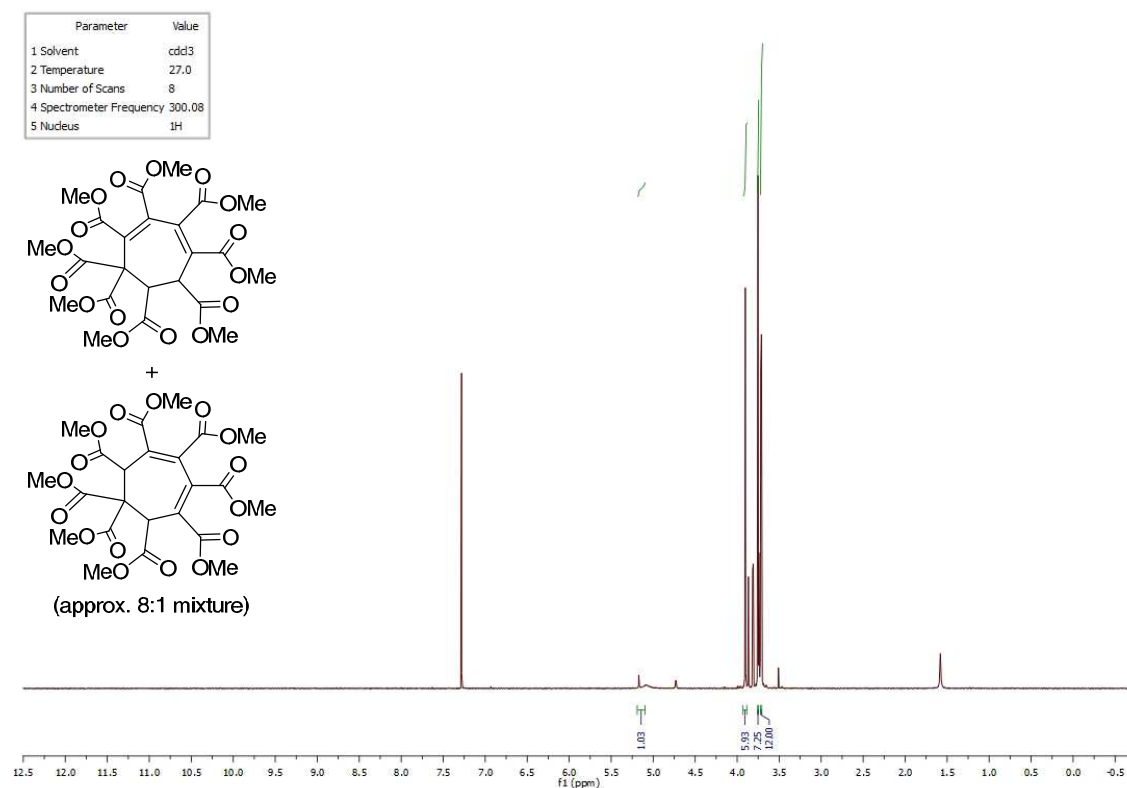
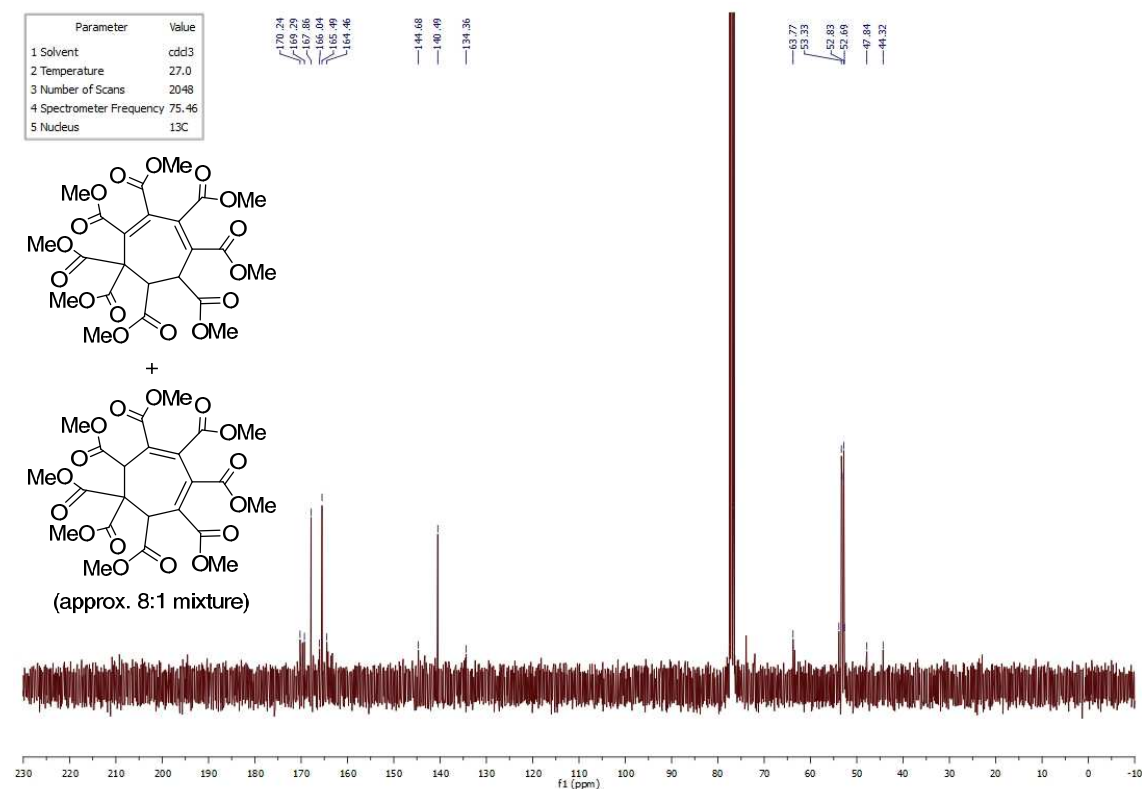
Single-Crystal X-ray Analysis for compound I.291



Compound	I.291
net formula	$\text{C}_8\text{H}_9\text{I}_3\text{O}_2$
$M_r/\text{g mol}^{-1}$	517.869
crystal size/mm	$0.19 \times 0.14 \times 0.09$
T/K	173(2)
radiation	$\text{MoK}\alpha$
diffractometer	'Oxford XCalibur'
crystal system	orthorhombic
space group	<i>Pbca</i>
$a/\text{\AA}$	5.8979(3)

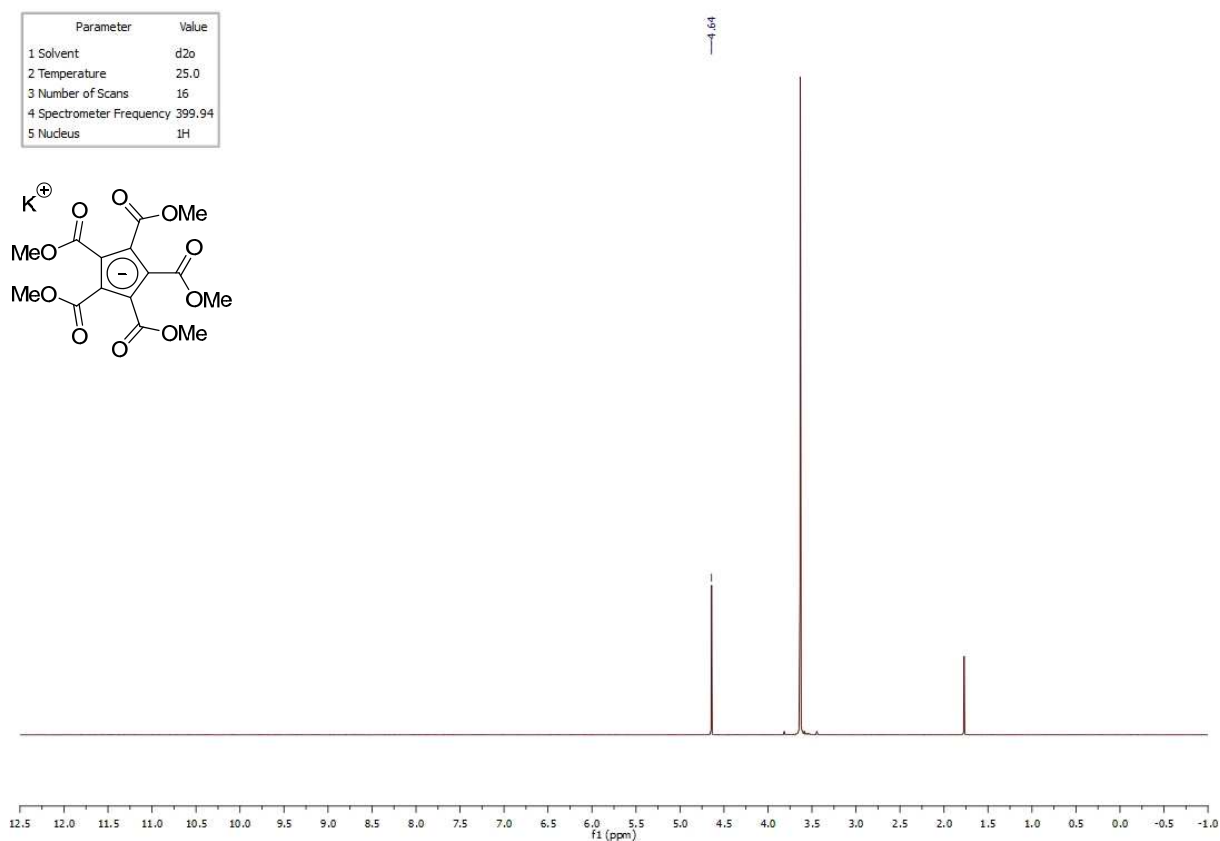
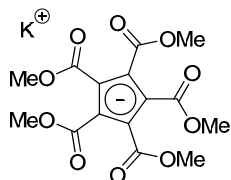
$b/\text{\AA}$	13.0985(6)
$c/\text{\AA}$	31.4580(15)
$\alpha/^\circ$	90
$\beta/^\circ$	90
$\gamma/^\circ$	90
$V/\text{\AA}^3$	2430.2(2)
Z	8
calc. density/ g cm^{-3}	2.8309(2)
μ/mm^{-1}	7.687
absorption correction	'multi-scan'
transmission factor range	0.79863–1.00000
refls. measured	9218
R_{int}	0.0334
mean $\sigma(I)/I$	0.0352
θ range	4.26–26.35
observed refls.	1876
x, y (weighting scheme)	0.0254, 0
hydrogen refinement	constr
refls in refinement	2460
parameters	118
restraints	0
$R(F_{\text{obs}})$	0.0270
$R_w(F^2)$	0.0562
S	0.978
shift/error $_{\text{max}}$	0.003
max electron density/ e \AA^{-3}	0.902
min electron density/ e \AA^{-3}	-0.694

Appendix 3: NMR Spectra and IR Spectra of Chapter II

¹H NMR spectrum of **II.20/II.21**:¹³C NMR spectrum of **II.20/II.21**:

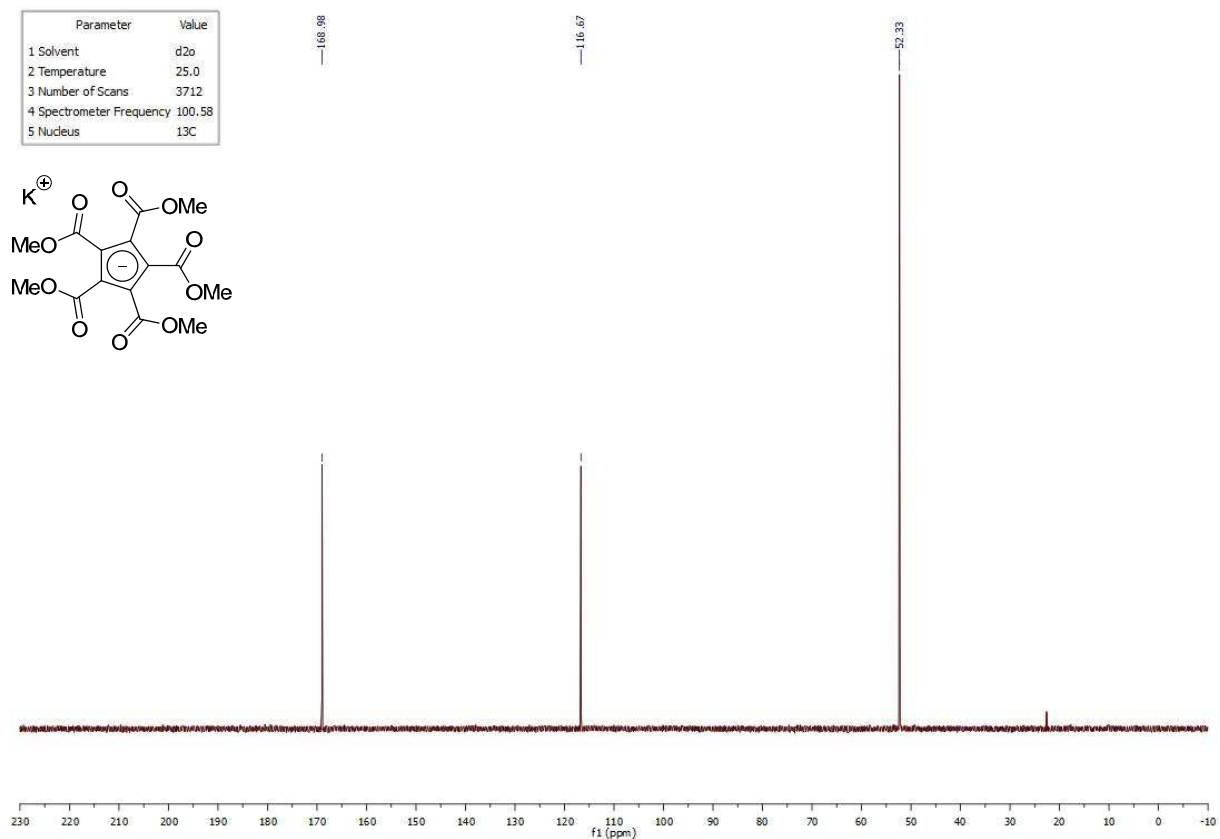
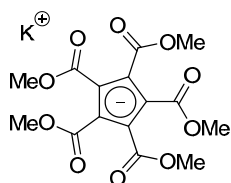
^1H NMR spectrum of **II.22**:

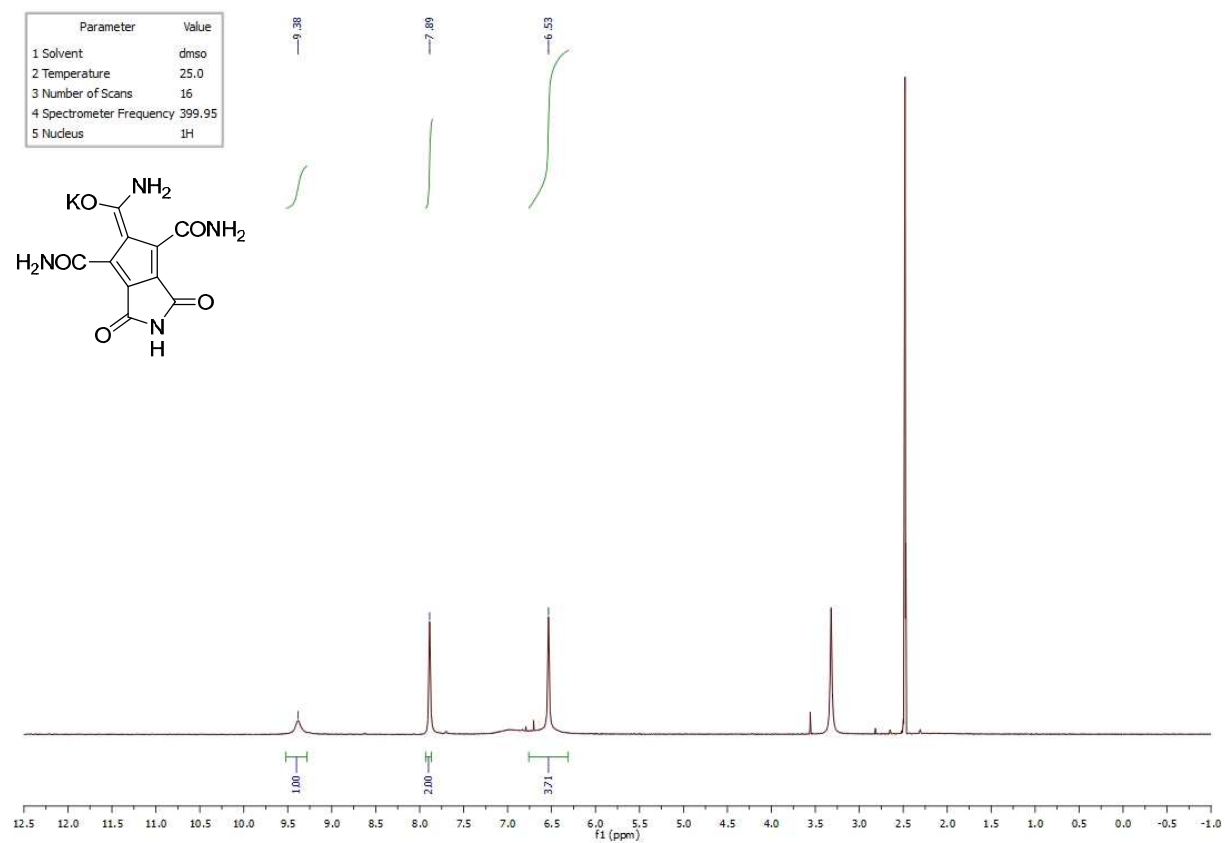
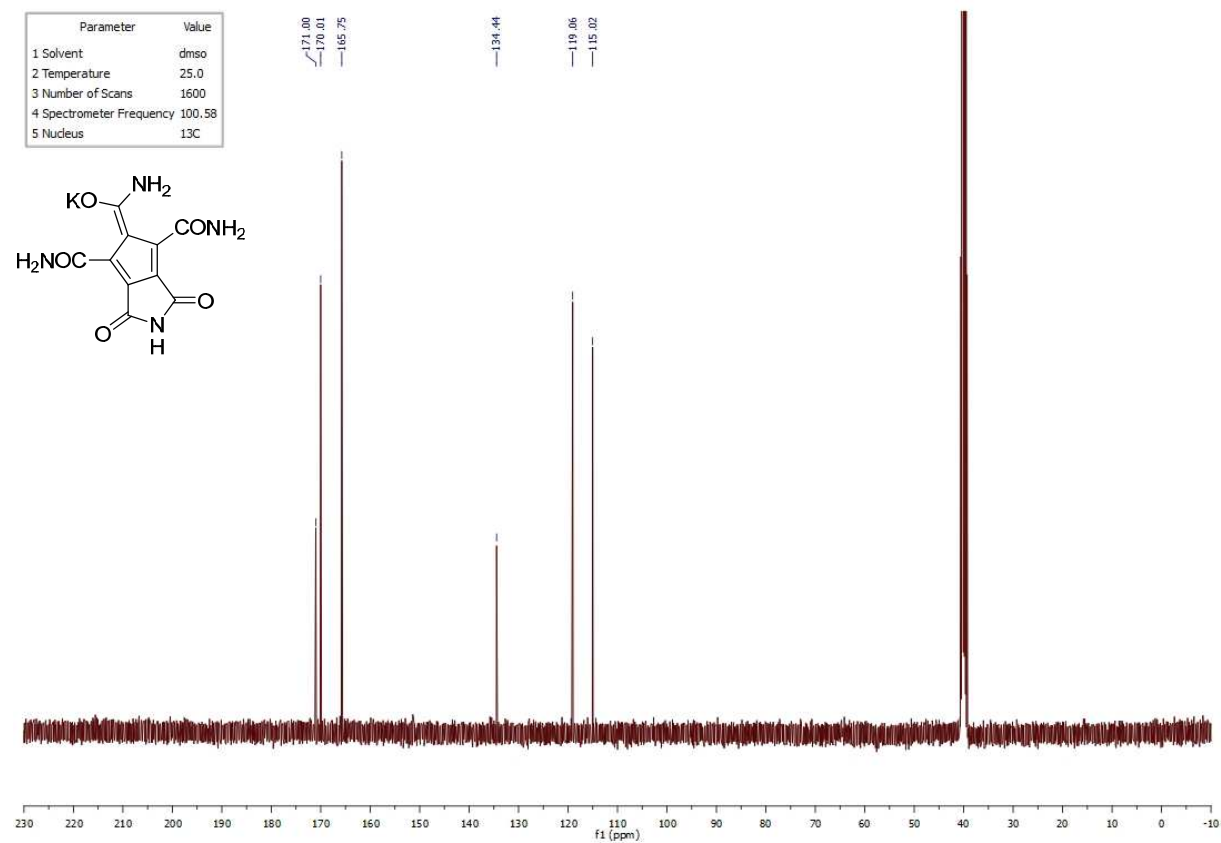
Parameter	Value
1 Solvent	d2o
2 Temperature	25.0
3 Number of Scans	16
4 Spectrometer Frequency	399.94
5 Nucleus	^1H

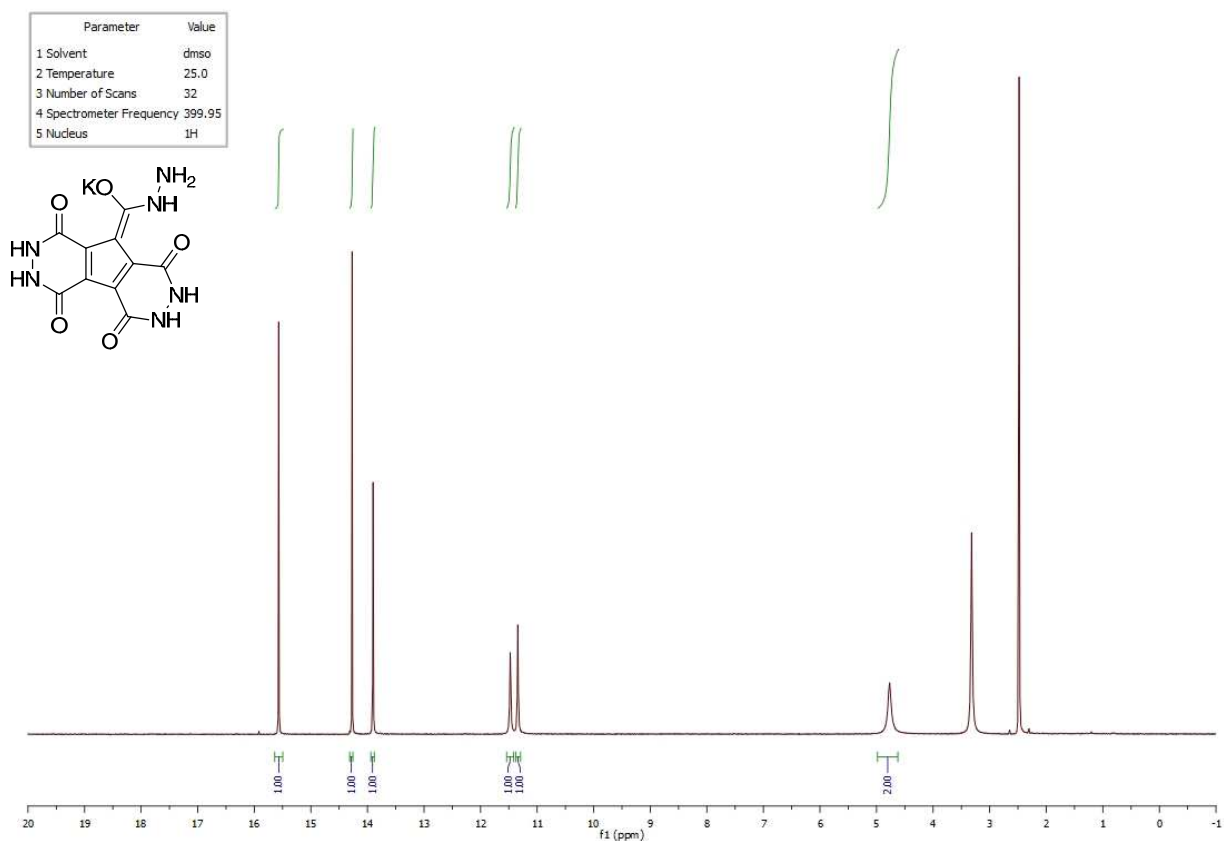
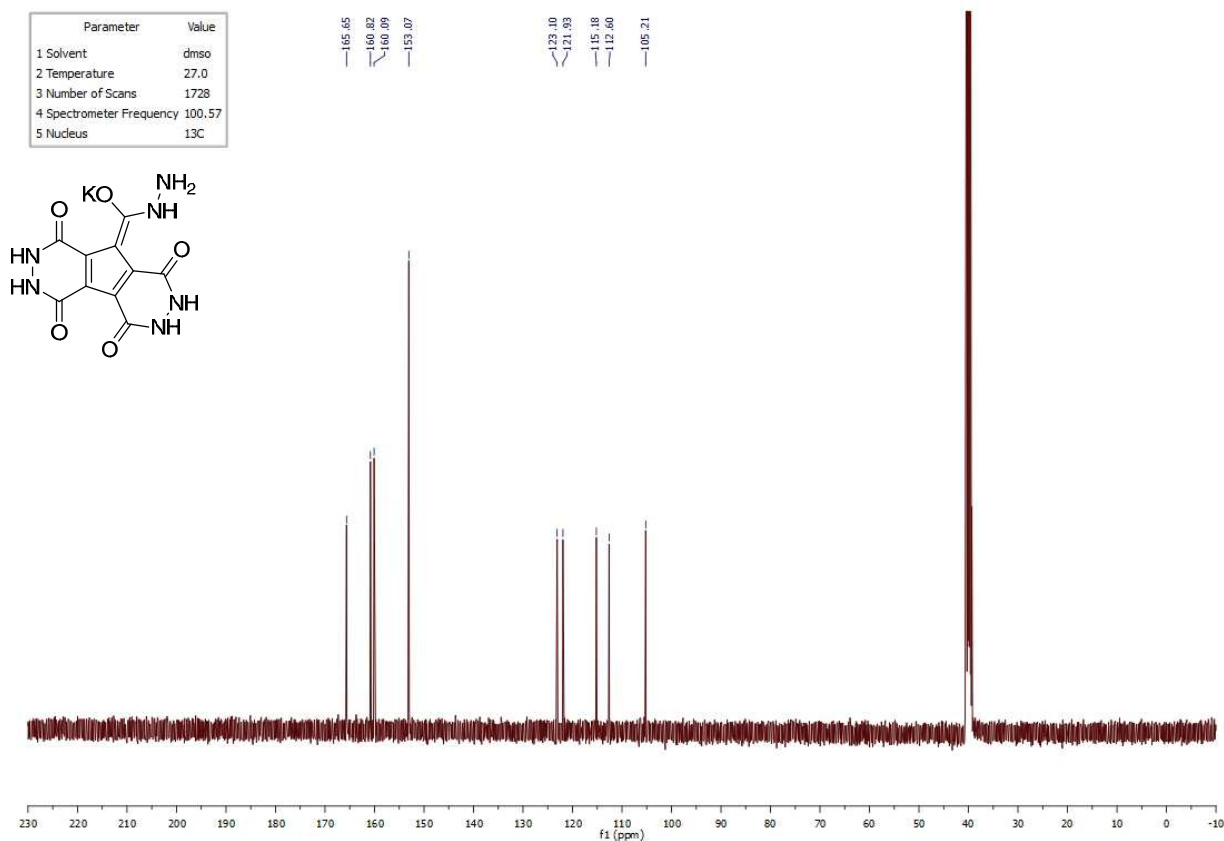


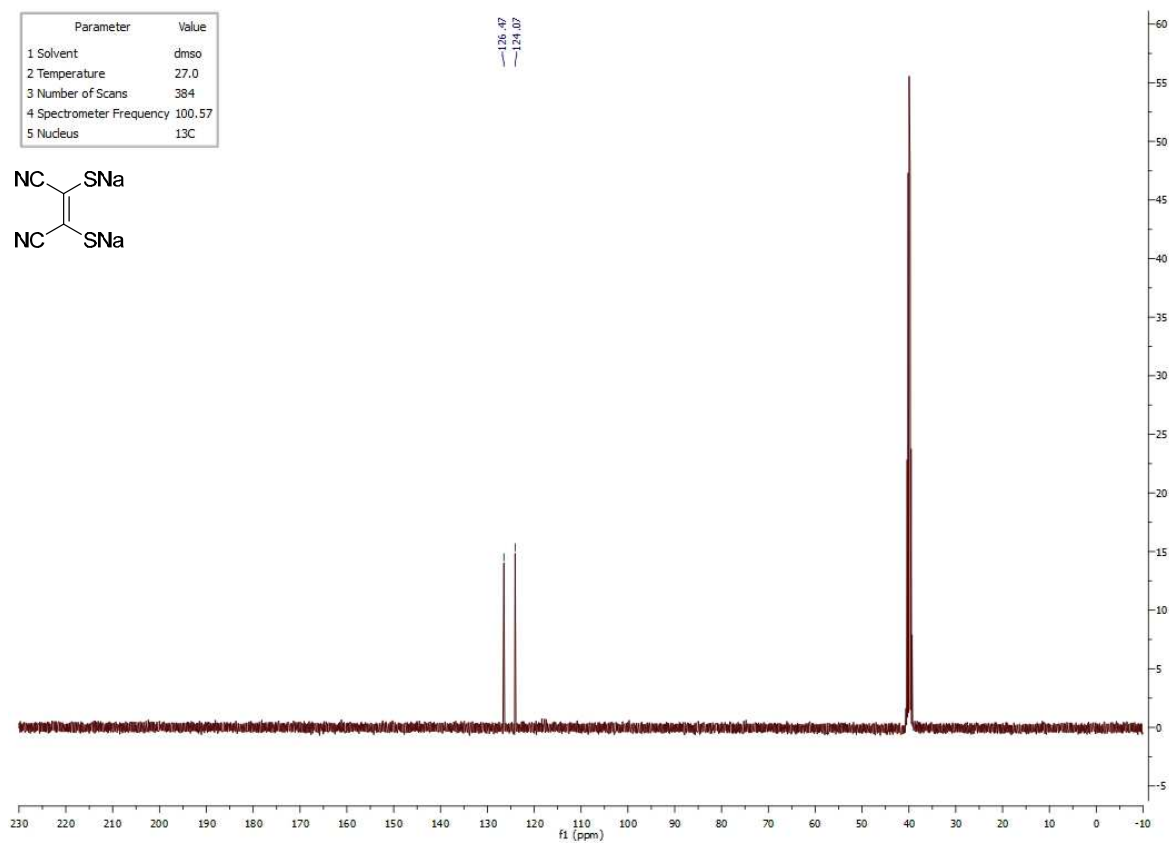
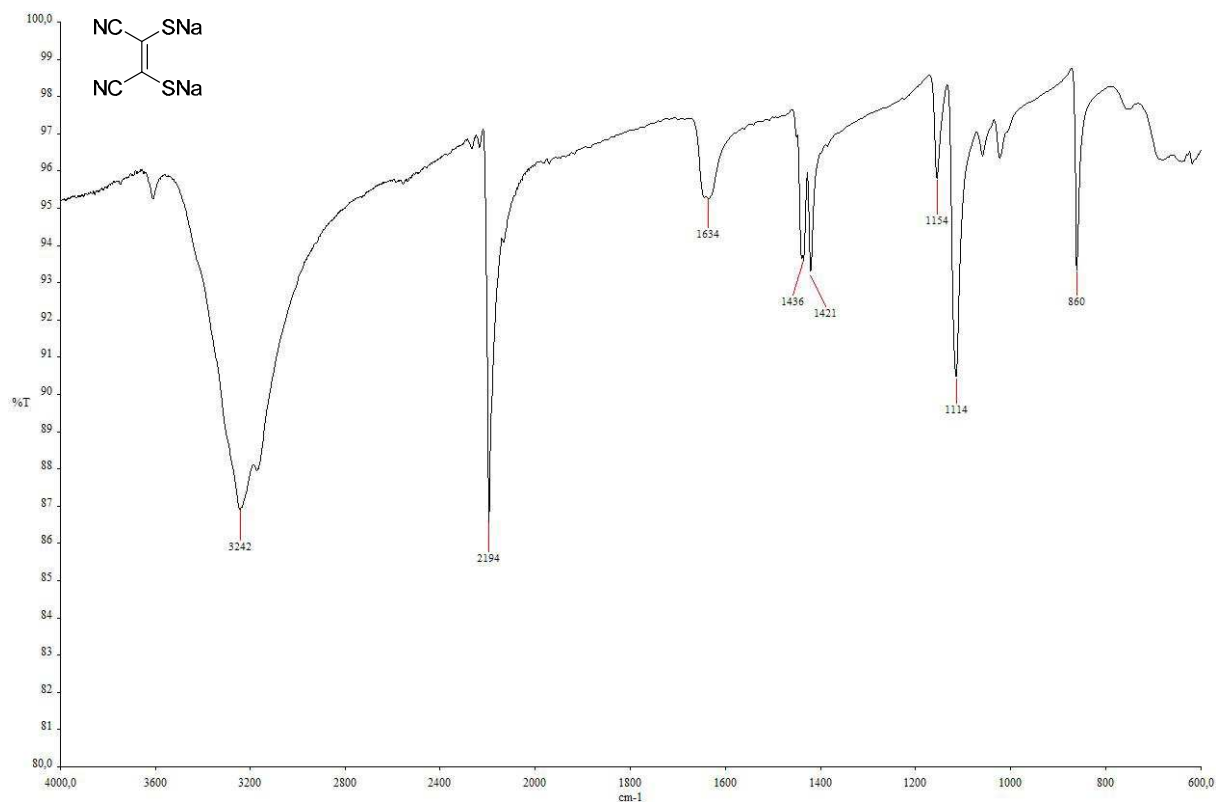
^{13}C NMR spectrum of **II.22**:

Parameter	Value
1 Solvent	d2o
2 Temperature	25.0
3 Number of Scans	3712
4 Spectrometer Frequency	100.58
5 Nucleus	^{13}C

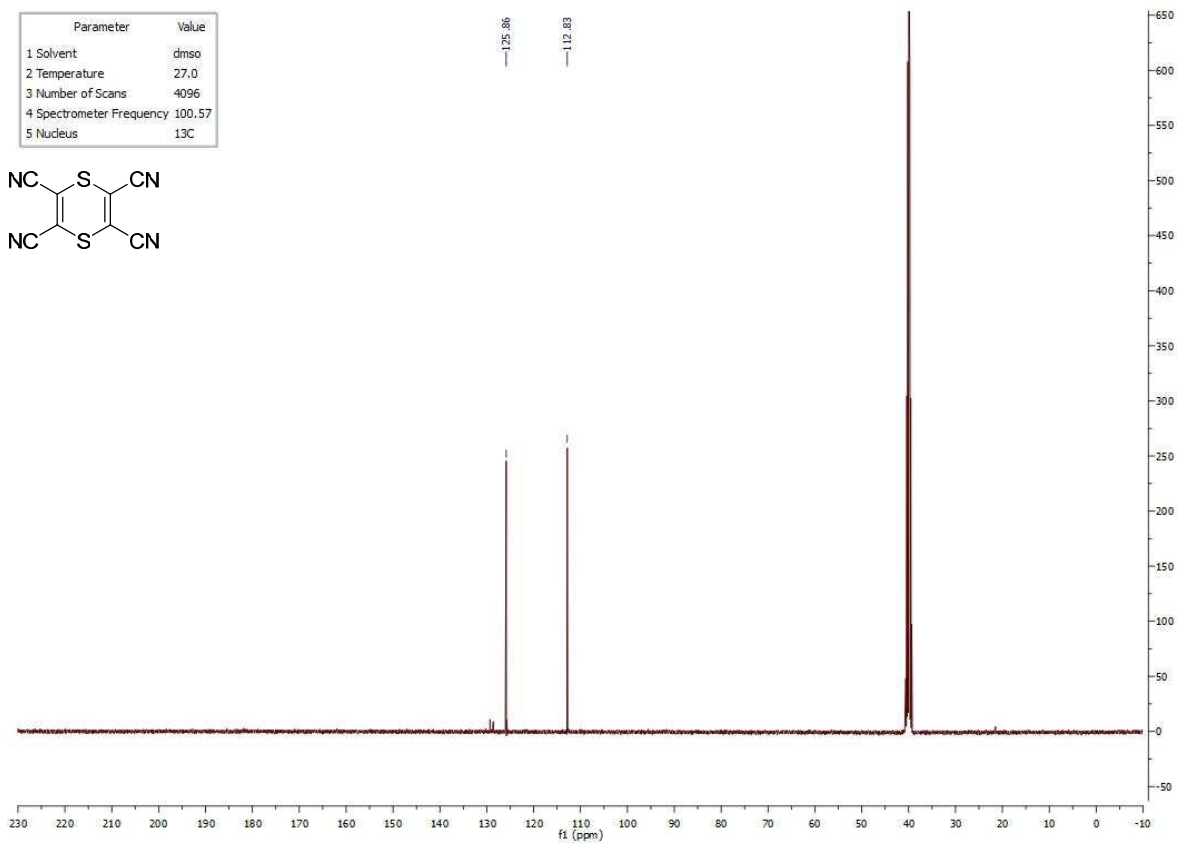


¹H NMR spectrum of **II.30**:¹³C NMR spectrum of **II.30**:

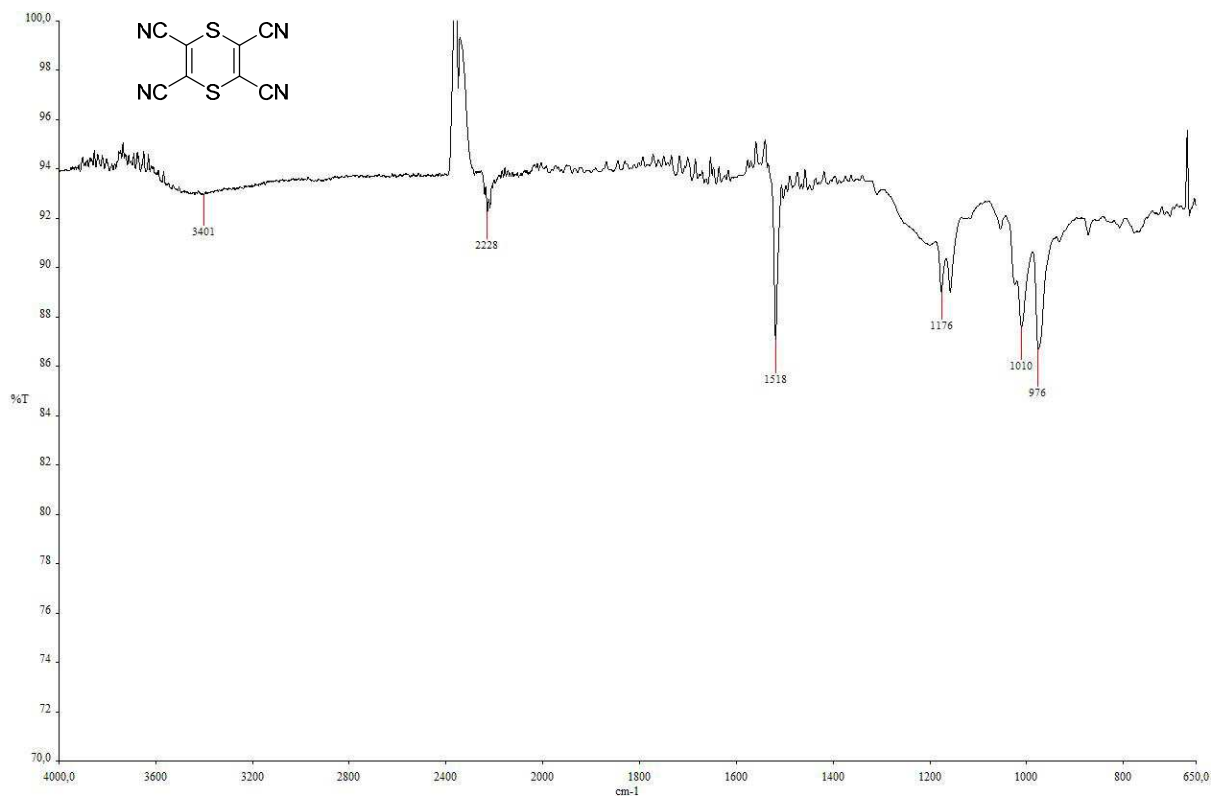
^1H NMR spectrum of **II.31**: ^{13}C NMR spectrum of **II.31**:

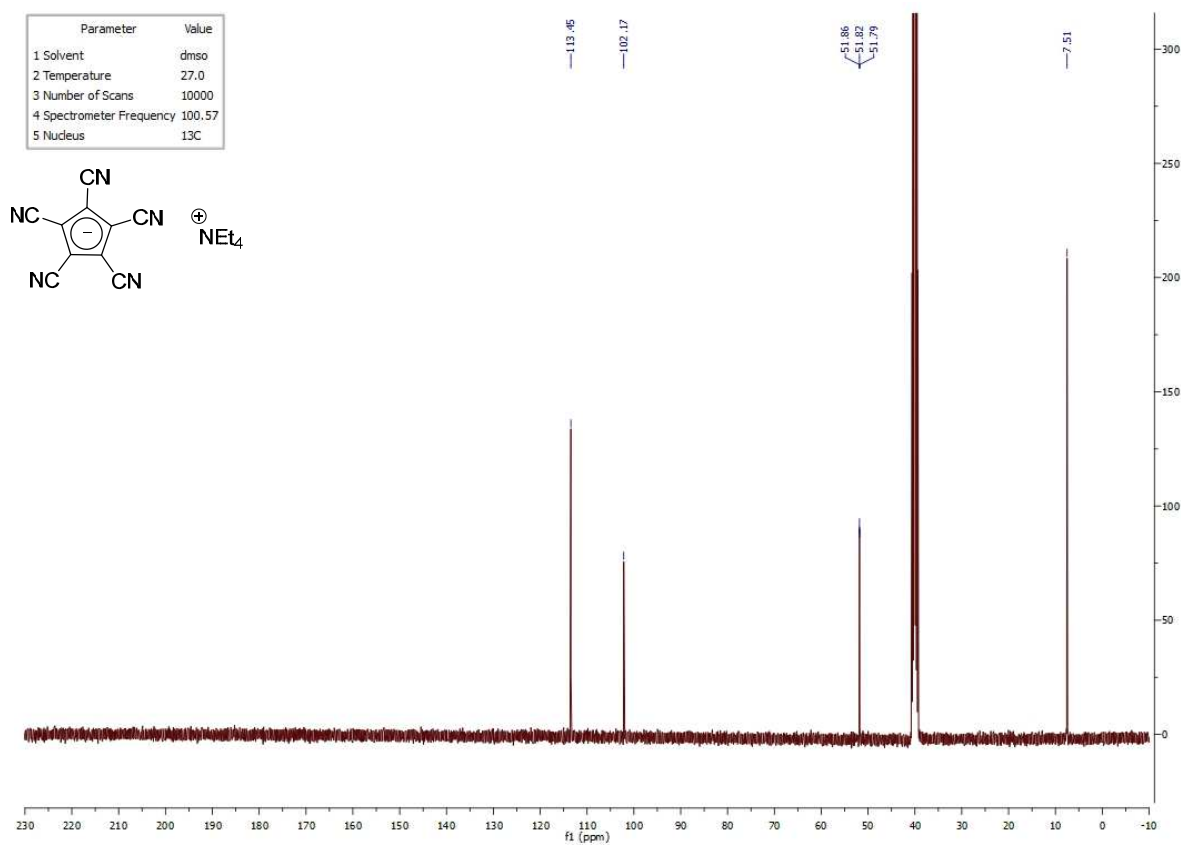
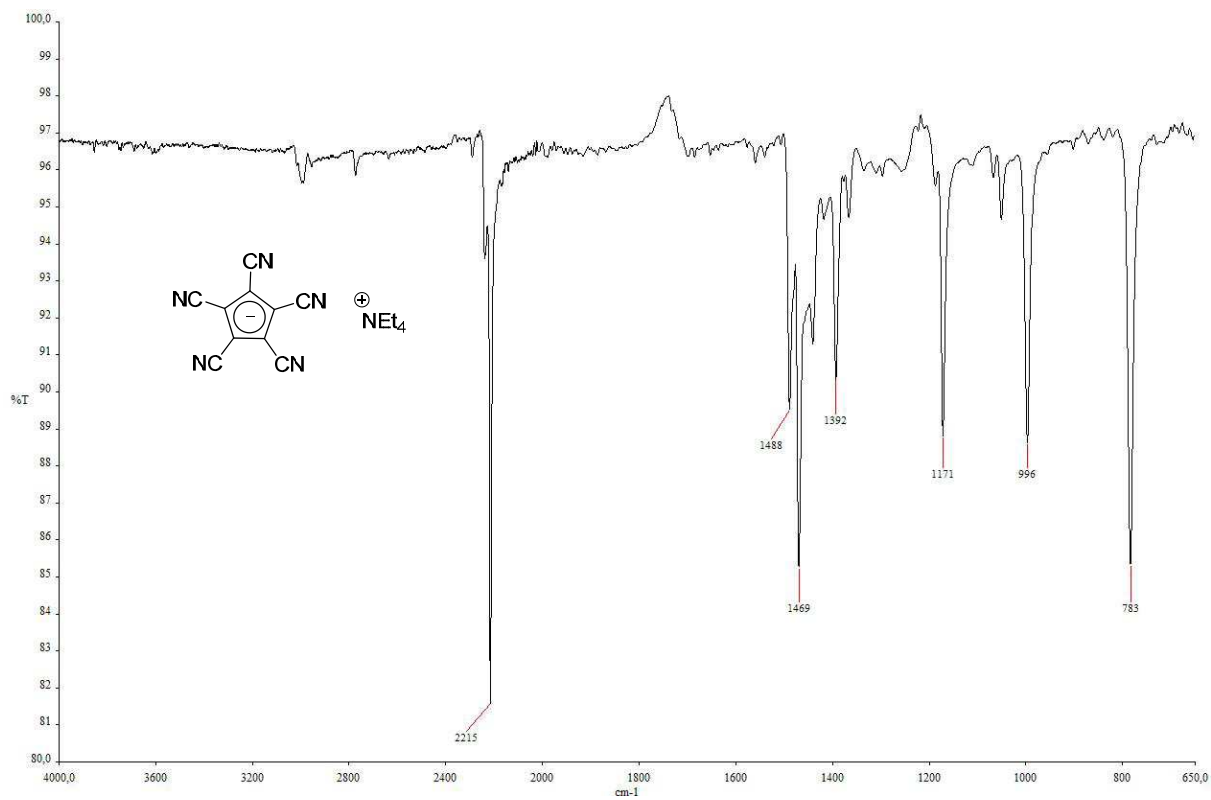
^{13}C NMR spectrum of **II.34**:IR spectrum of **II.34**:

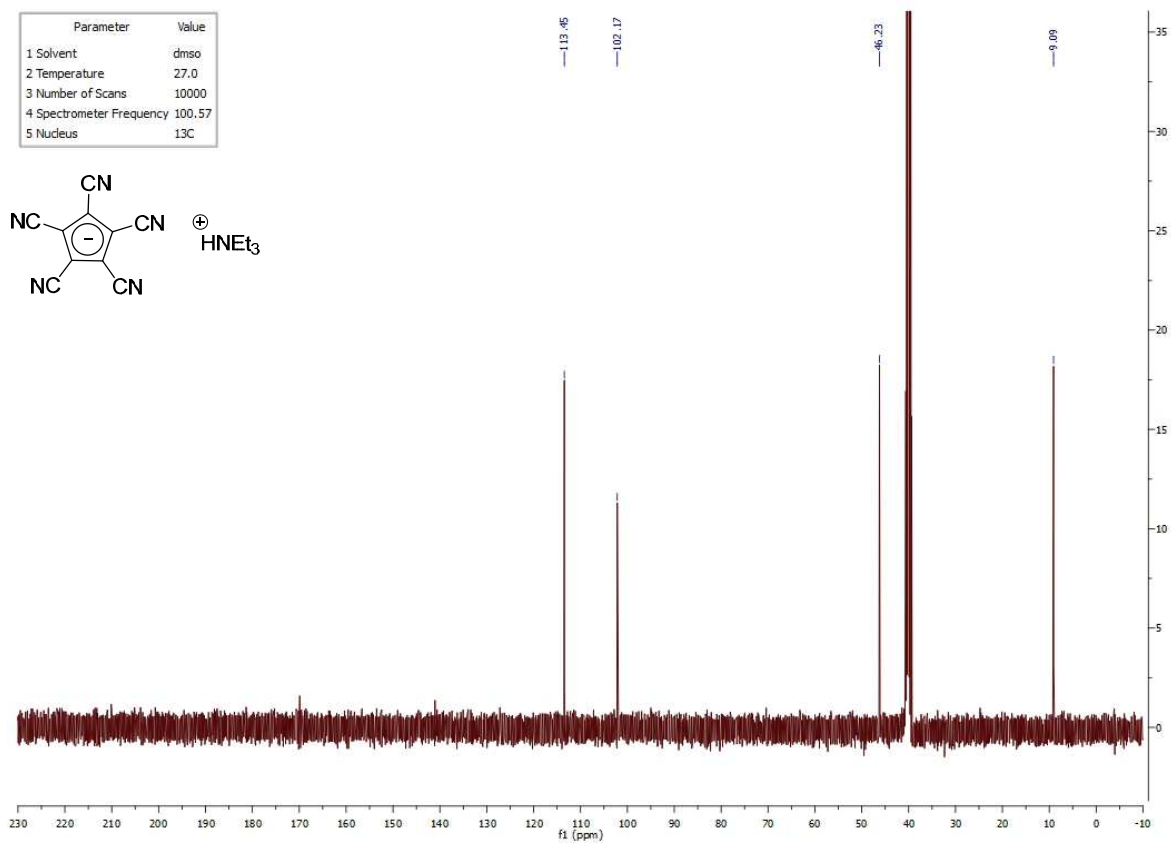
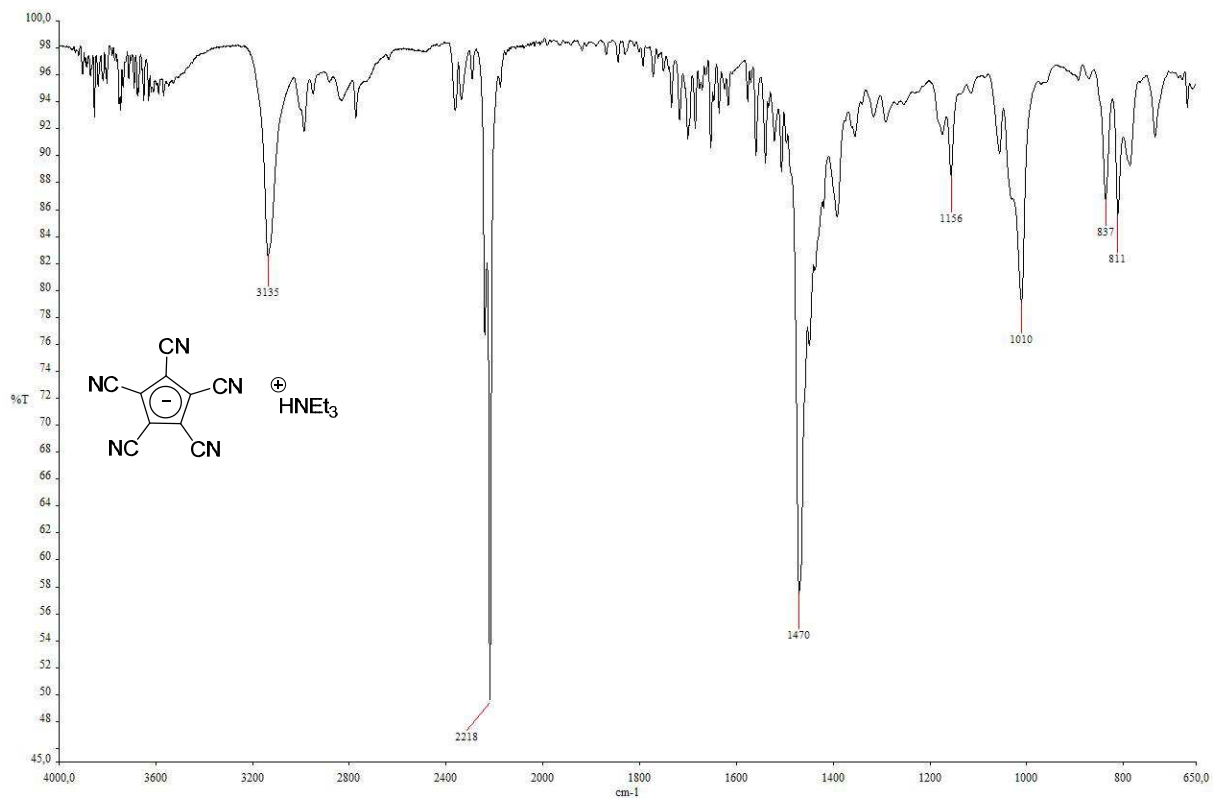
^{13}C NMR spectrum of **II.35**:

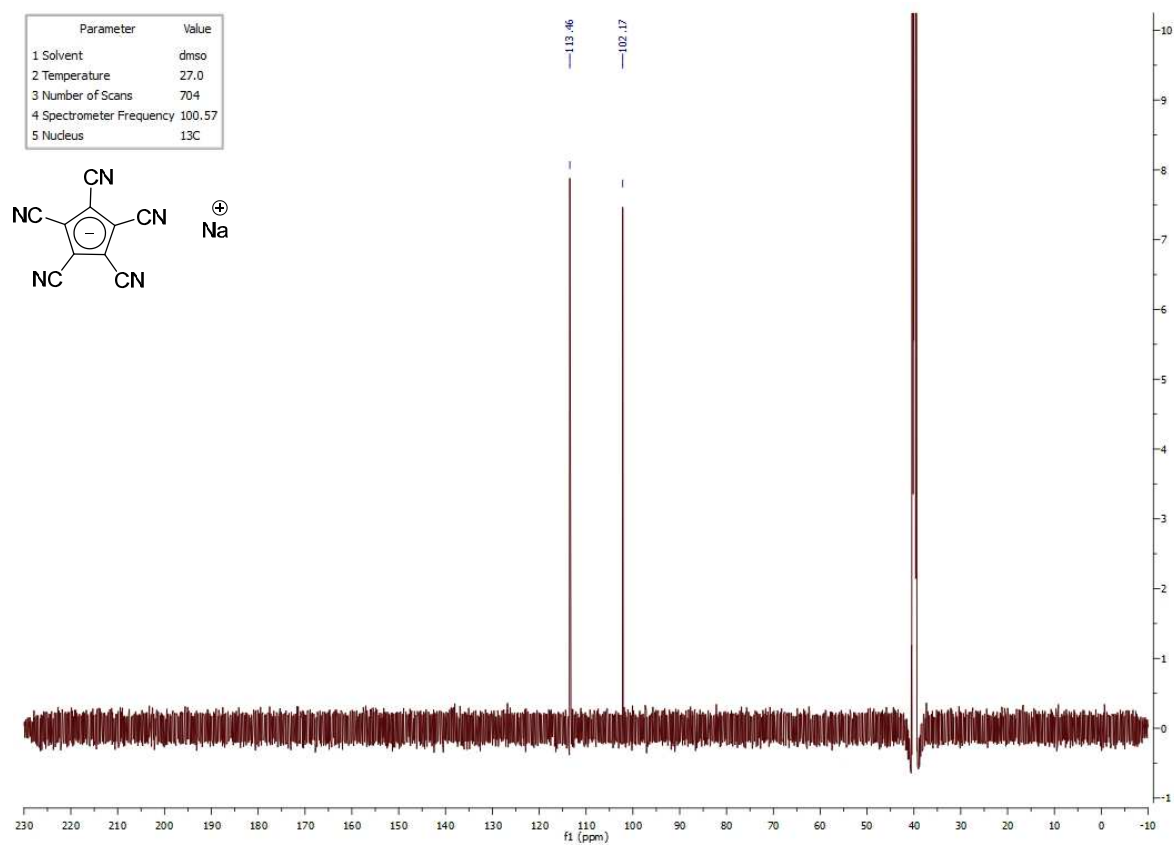
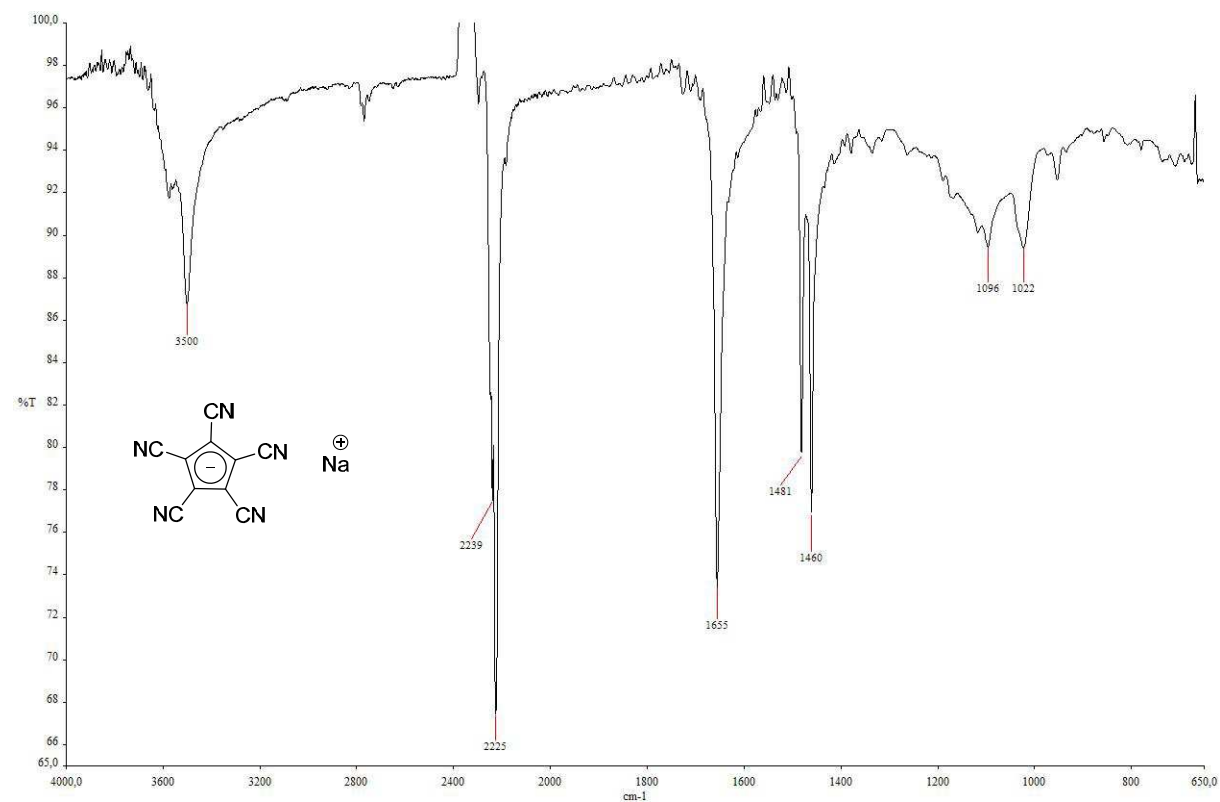


IR spectrum of **II.35**:



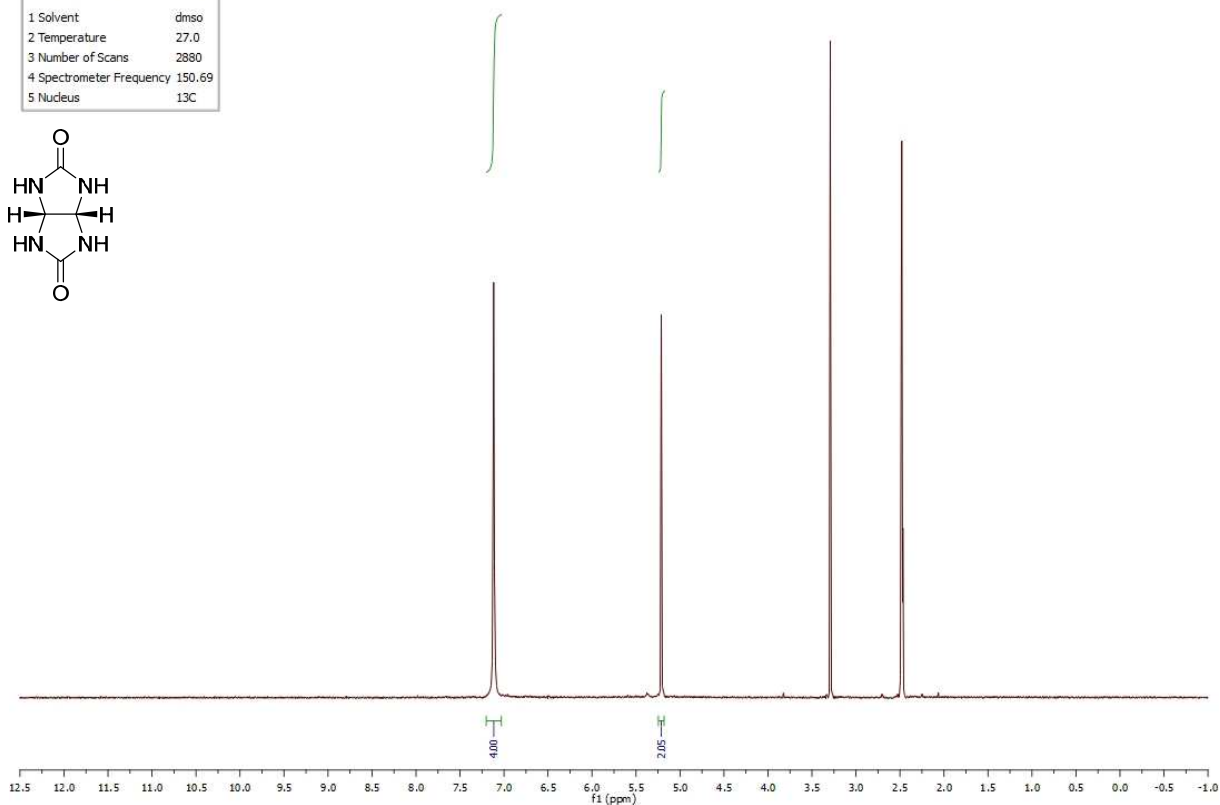
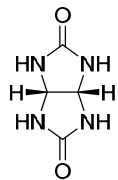
^{13}C NMR spectrum of **II.37**:IR spectrum of **II.37**:

^{13}C NMR spectrum of **II.52**:IR spectrum of **II.52**:

^{13}C NMR spectrum of **II.10**:IR spectrum of **II.10**:

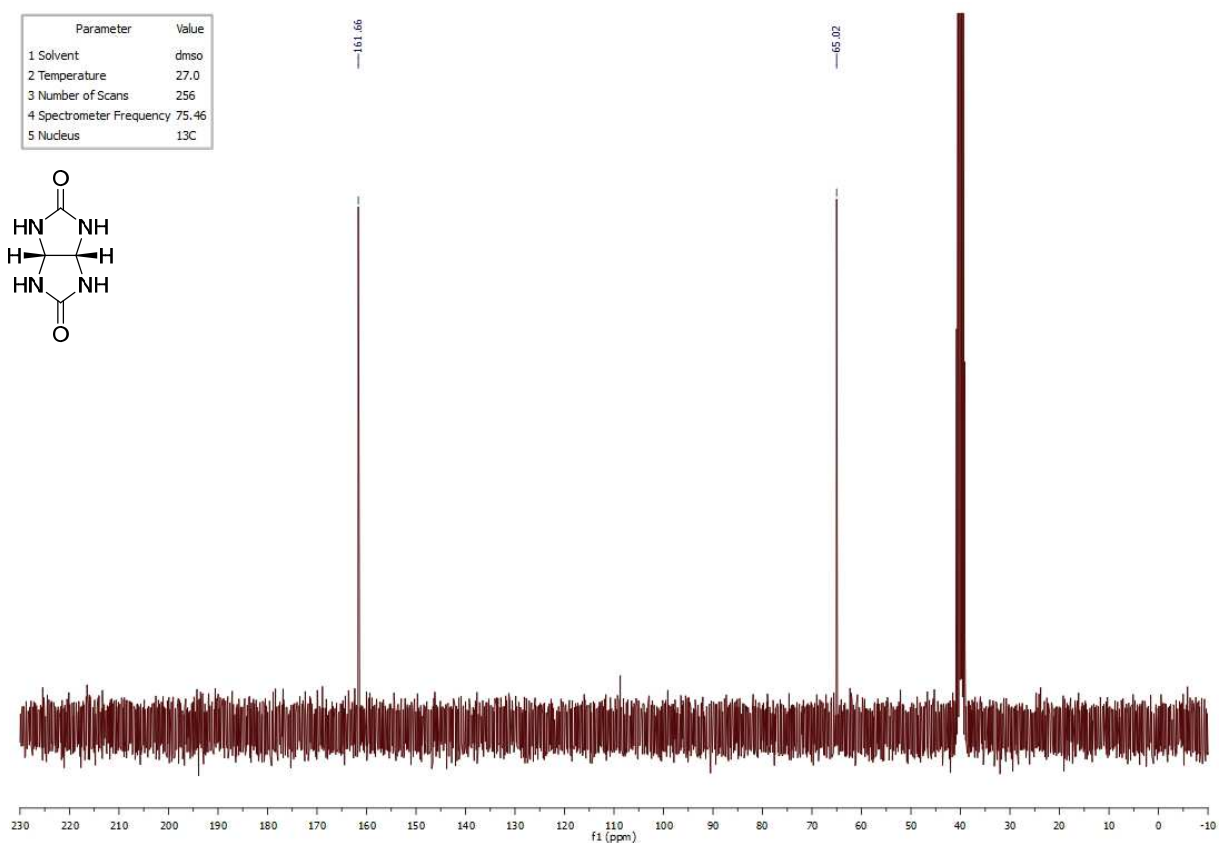
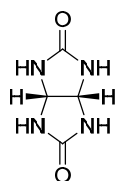
^1H NMR spectrum of **II.55**:

Parameter	Value
1 Solvent	dmsd
2 Temperature	27.0
3 Number of Scans	2880
4 Spectrometer Frequency	150.69
5 Nucleus	^{13}C



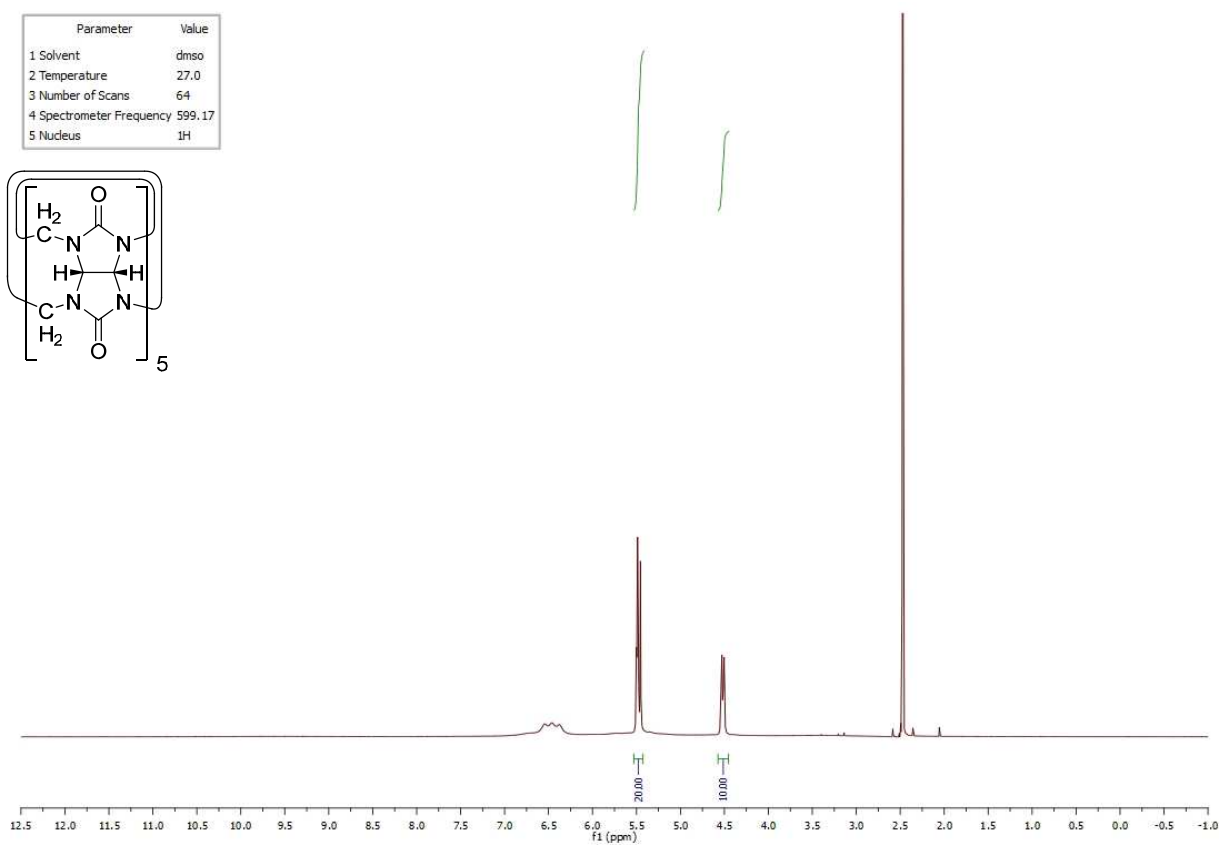
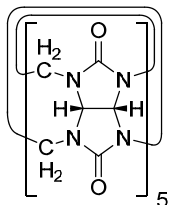
^{13}C NMR spectrum of **II.55**:

Parameter	Value
1 Solvent	dmsd
2 Temperature	27.0
3 Number of Scans	256
4 Spectrometer Frequency	75.46
5 Nucleus	^{13}C

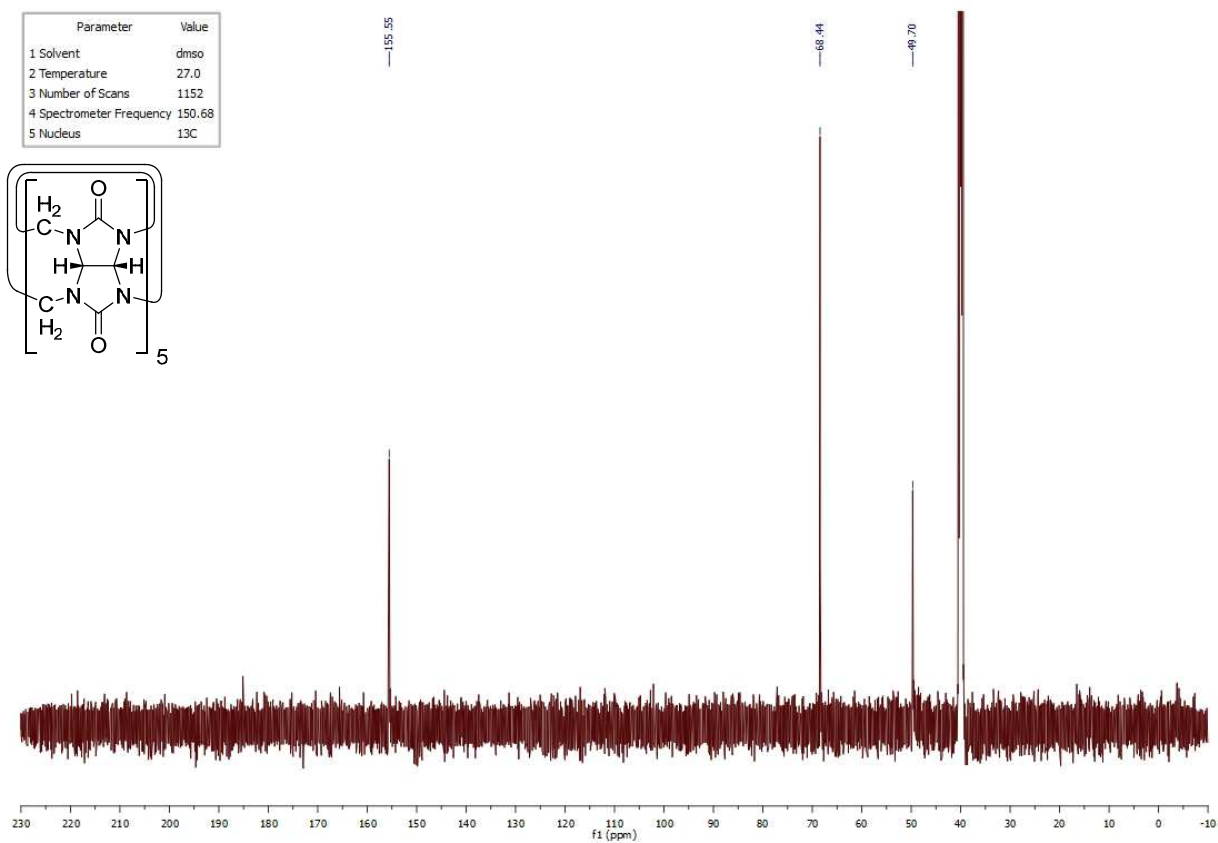
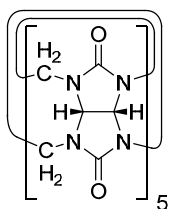


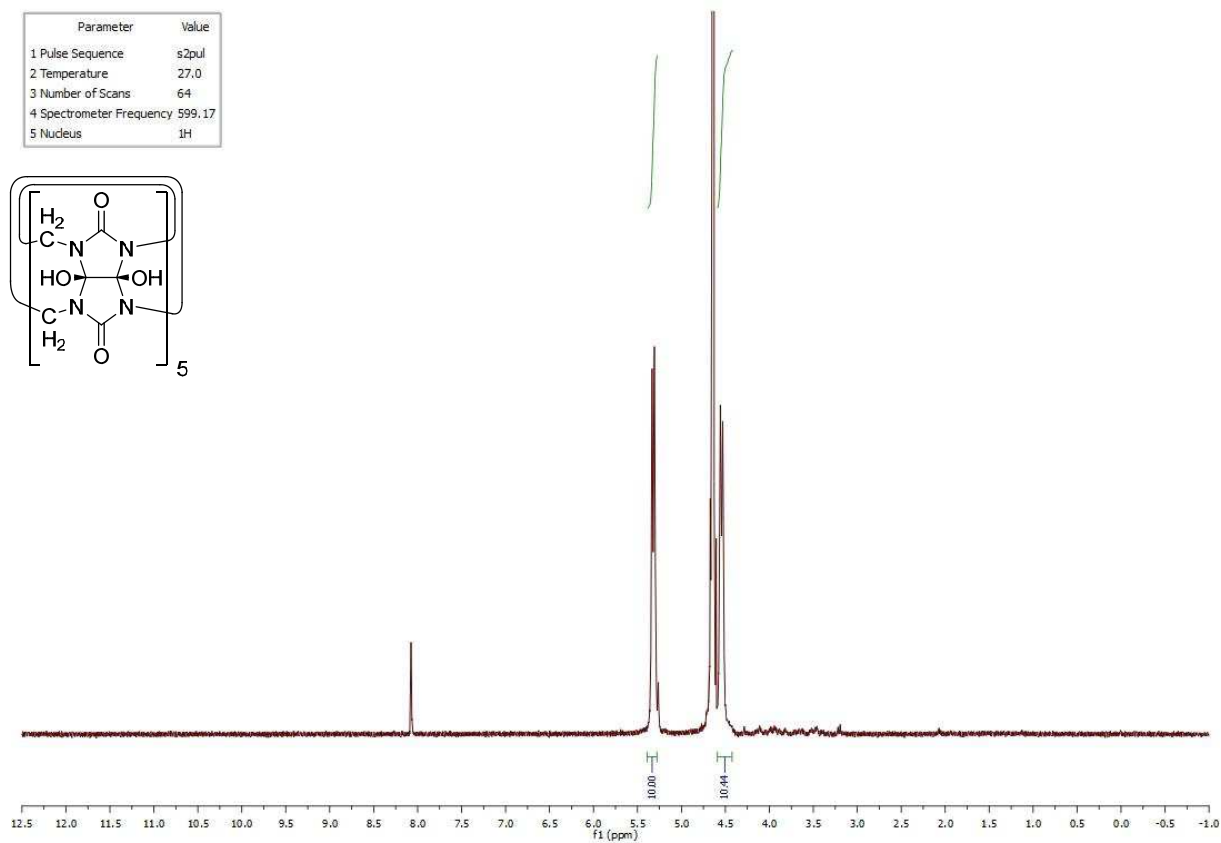
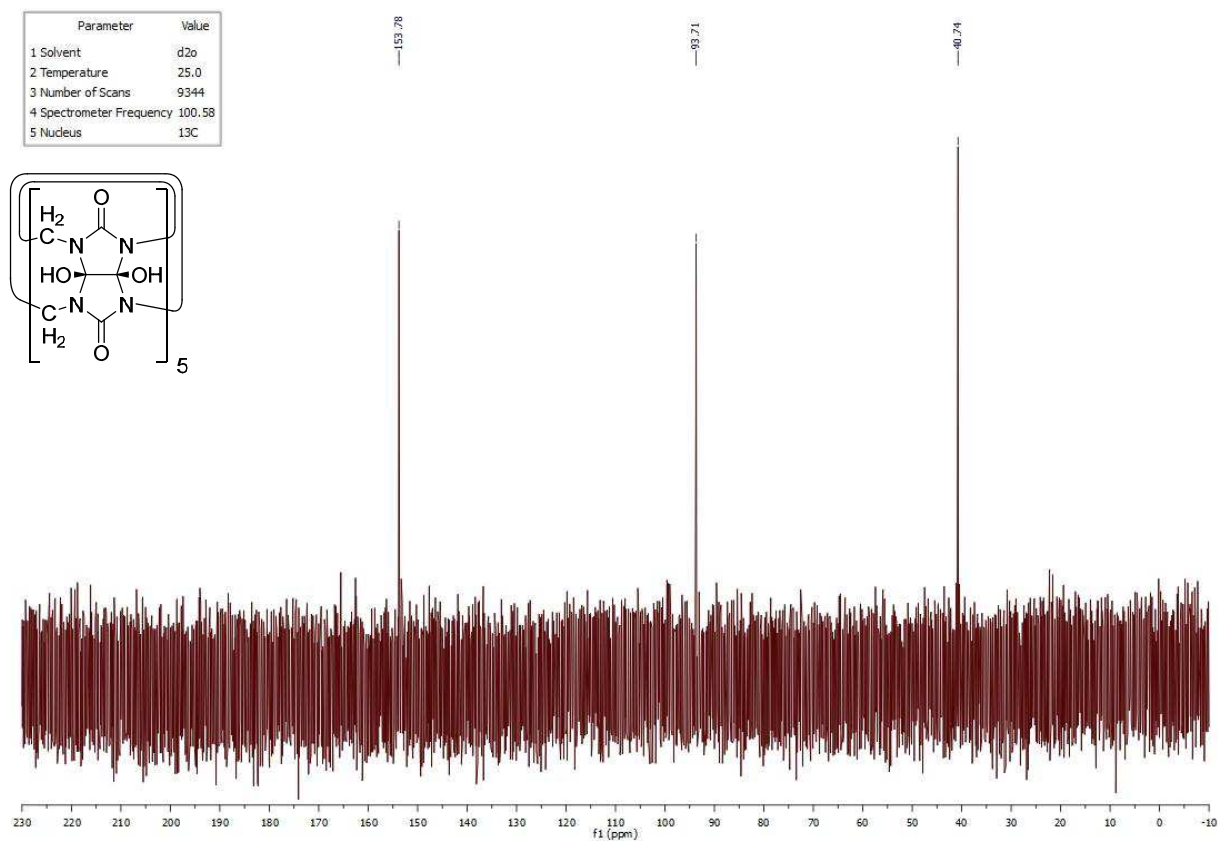
^1H NMR spectrum of **II.11**:

Parameter	Value
1 Solvent	dmsd
2 Temperature	27.0
3 Number of Scans	64
4 Spectrometer Frequency	599.17
5 Nucleus	^1H

 ^{13}C NMR spectrum of **II.11**:

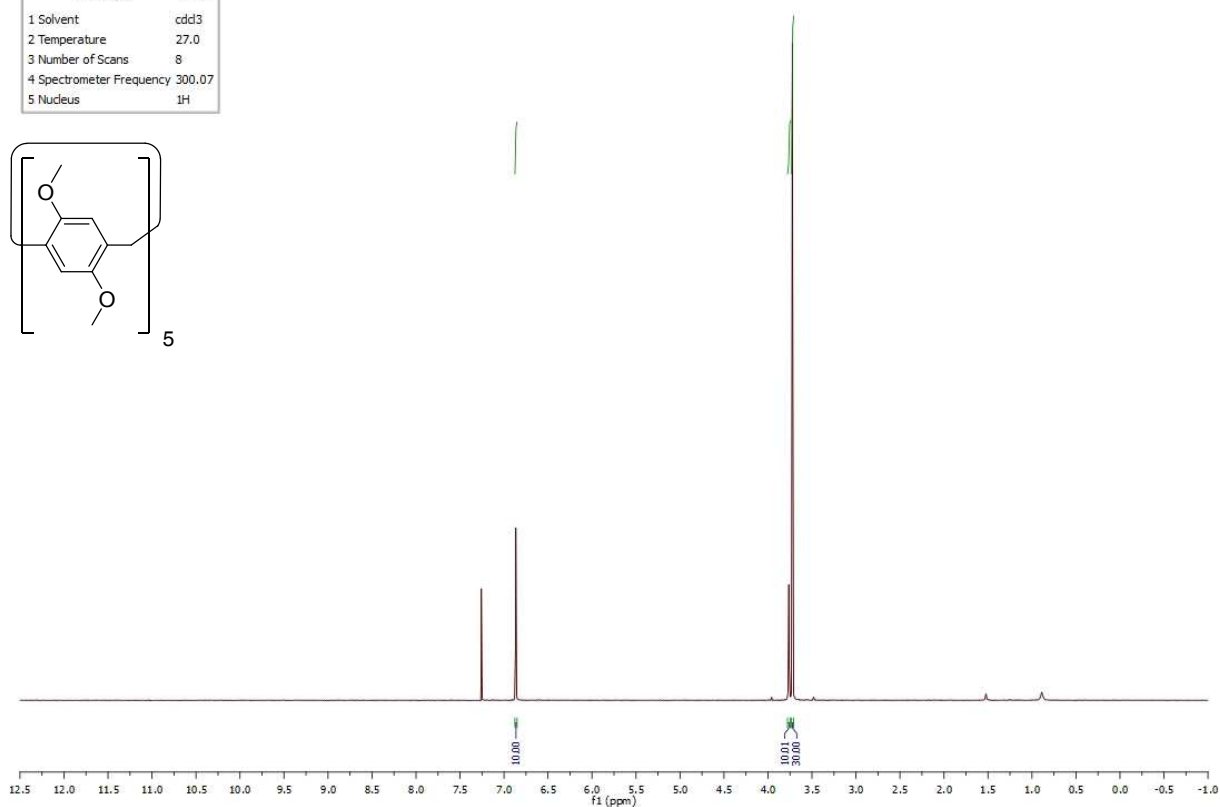
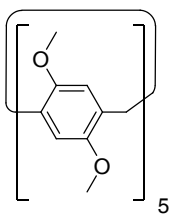
Parameter	Value
1 Solvent	dmsd
2 Temperature	27.0
3 Number of Scans	1152
4 Spectrometer Frequency	150.68
5 Nucleus	^{13}C



^1H NMR spectrum of **II.12**: ^{13}C NMR spectrum of **II.12**:

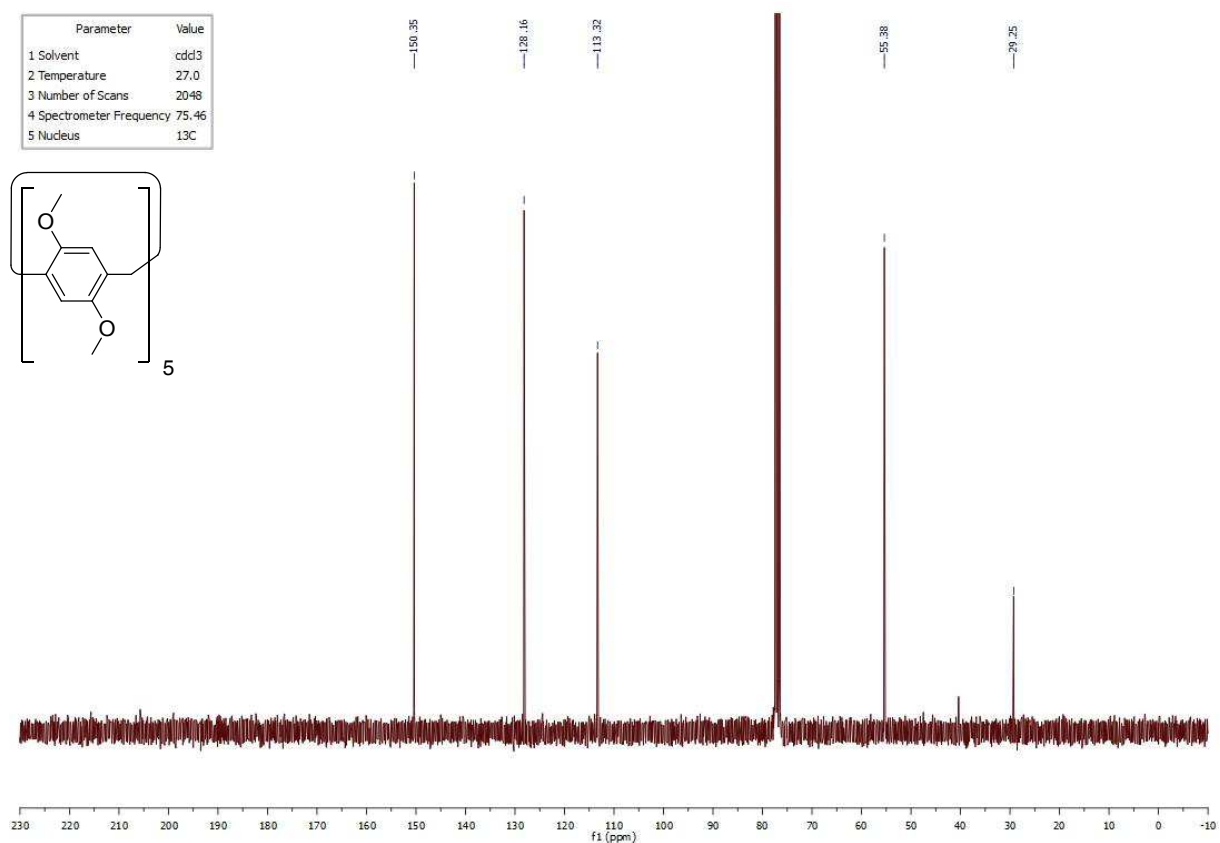
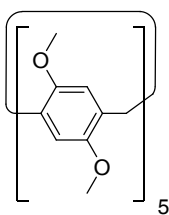
^1H NMR spectrum of **II.59**:

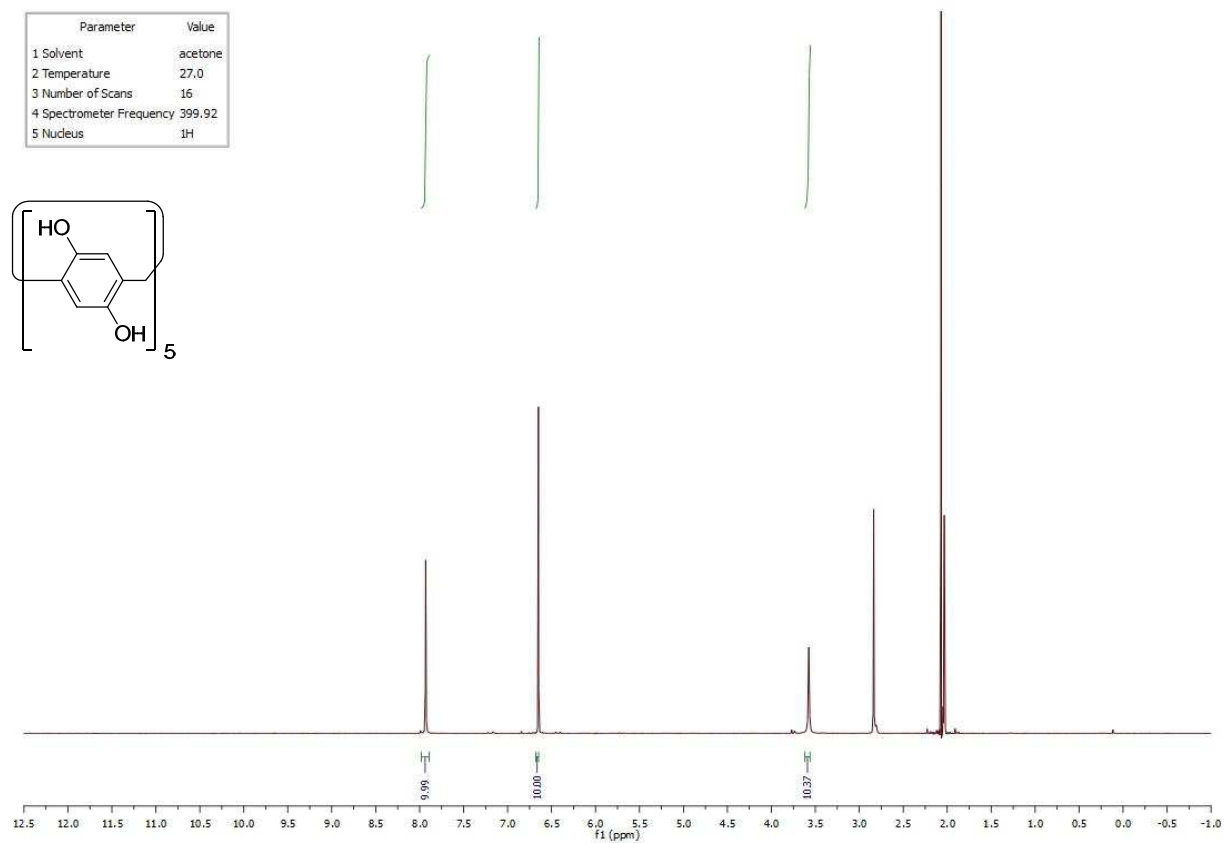
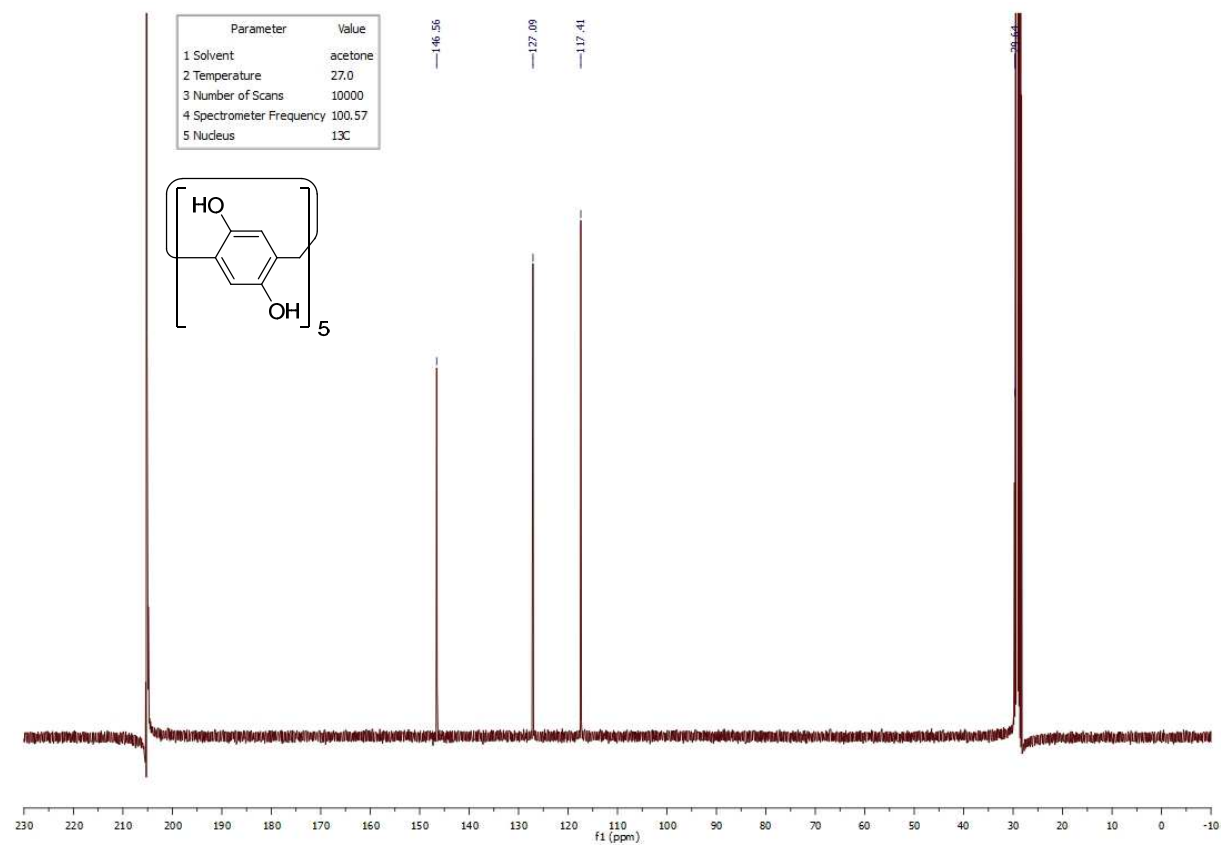
Parameter	Value
1 Solvent	cdd3
2 Temperature	27.0
3 Number of Scans	8
4 Spectrometer Frequency	300.07
5 Nucleus	^1H



^{13}C NMR spectrum of **II.59**:

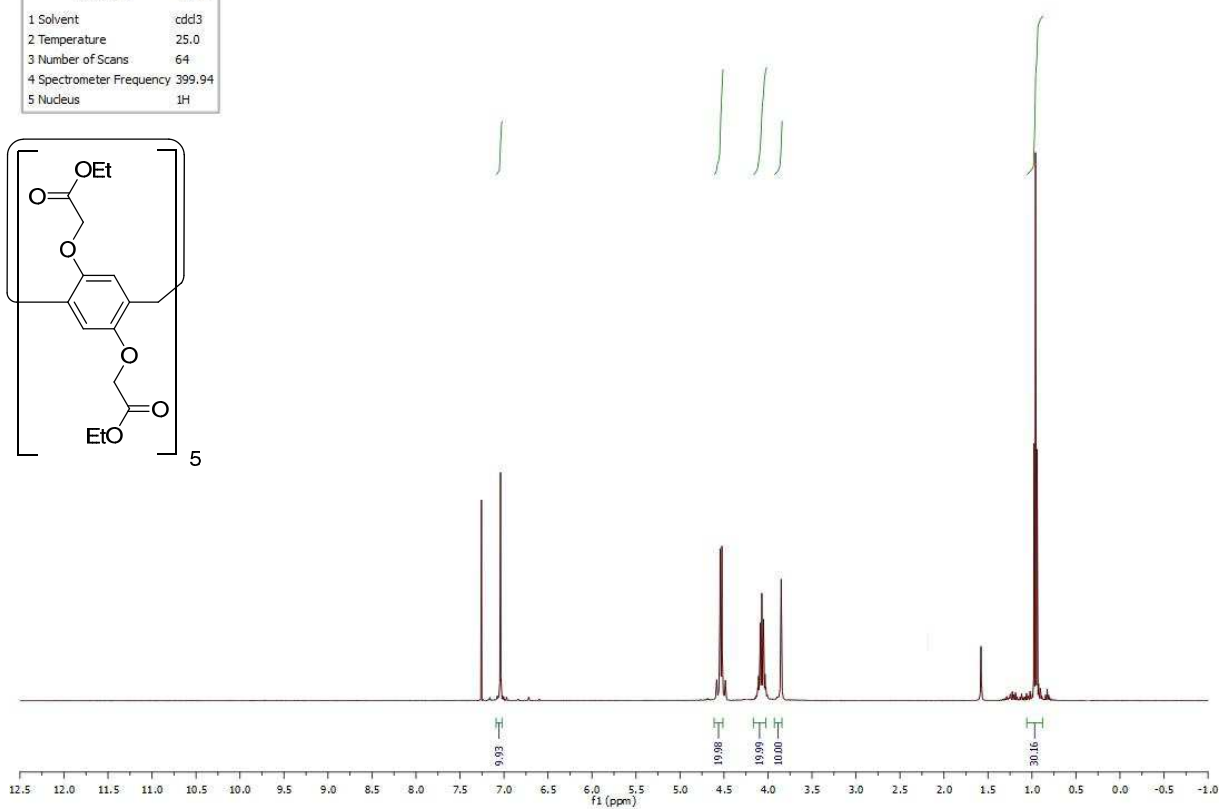
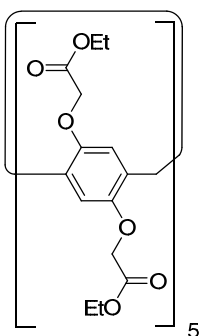
Parameter	Value
1 Solvent	cdd3
2 Temperature	27.0
3 Number of Scans	2048
4 Spectrometer Frequency	75.46
5 Nucleus	^{13}C



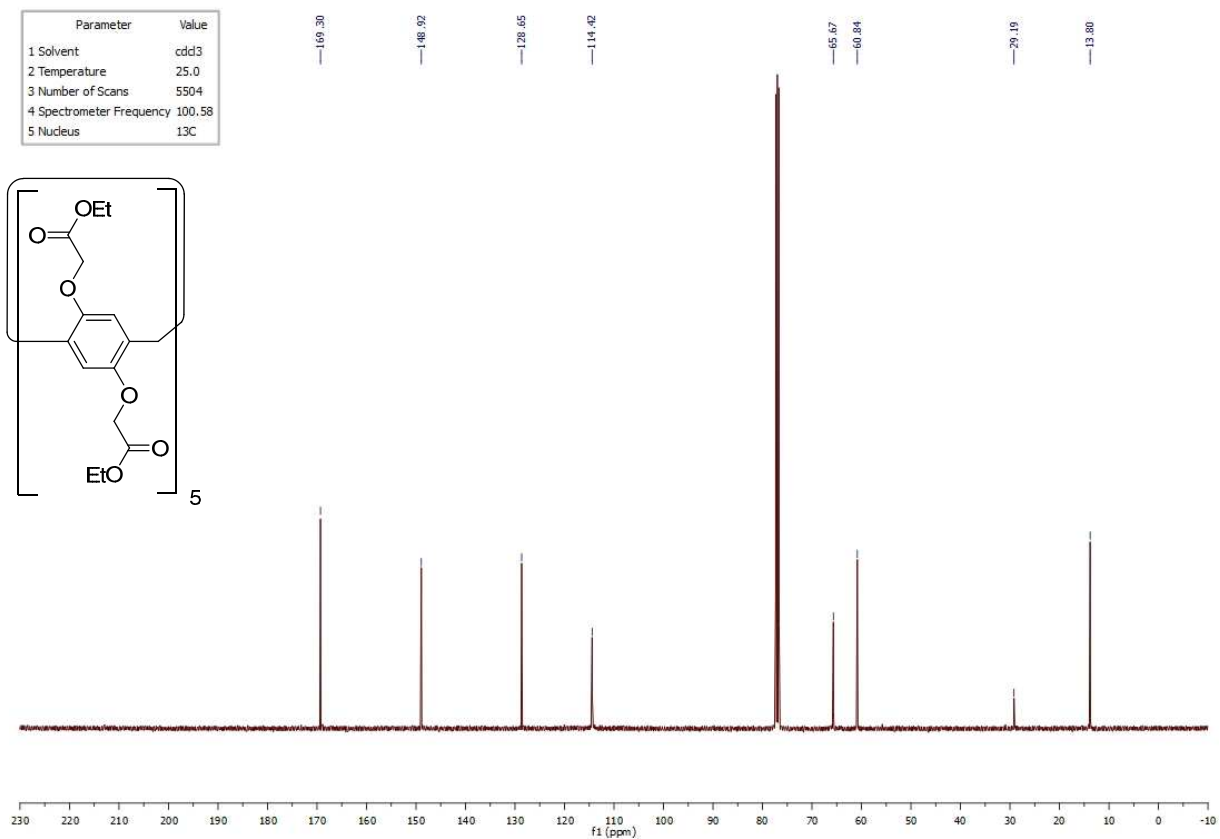
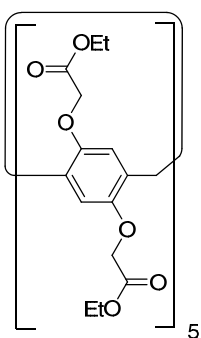
^1H NMR spectrum of **II.13**: ^{13}C NMR spectrum of **II.13**:

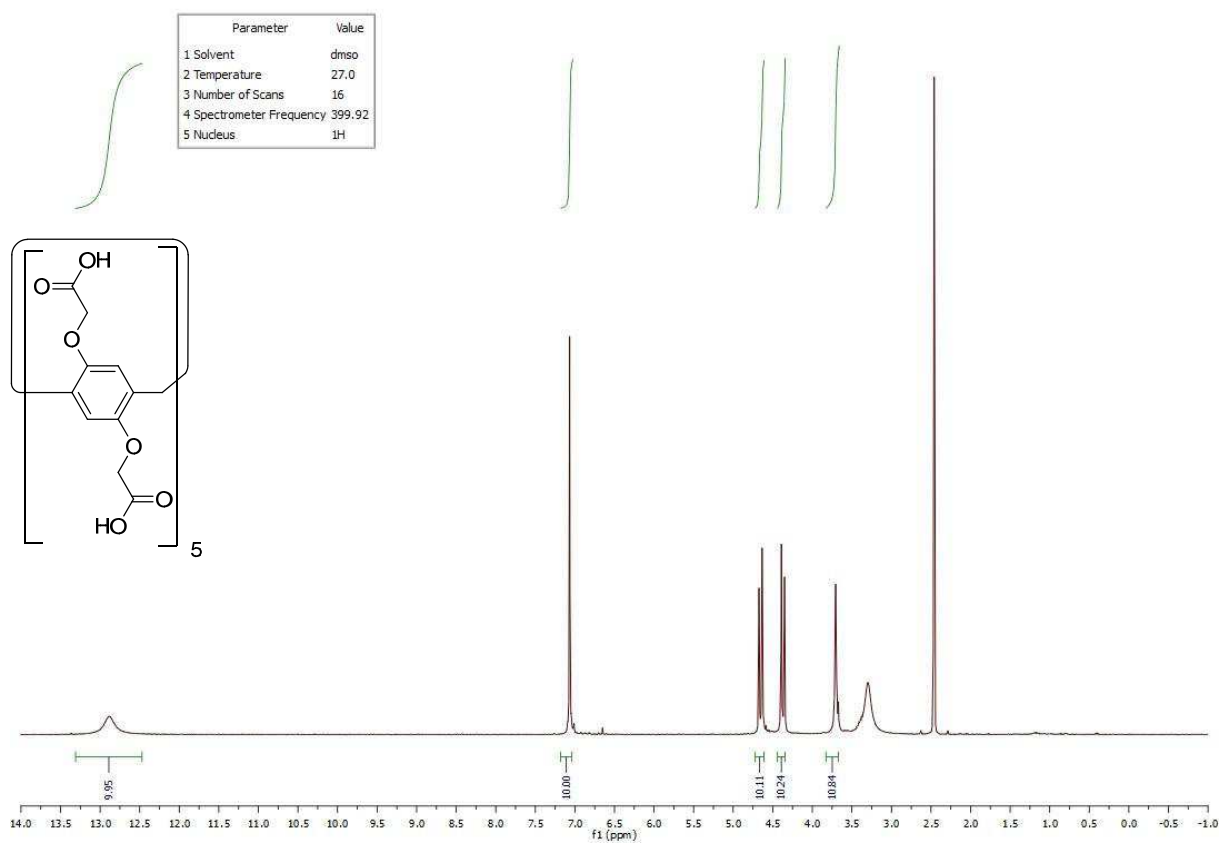
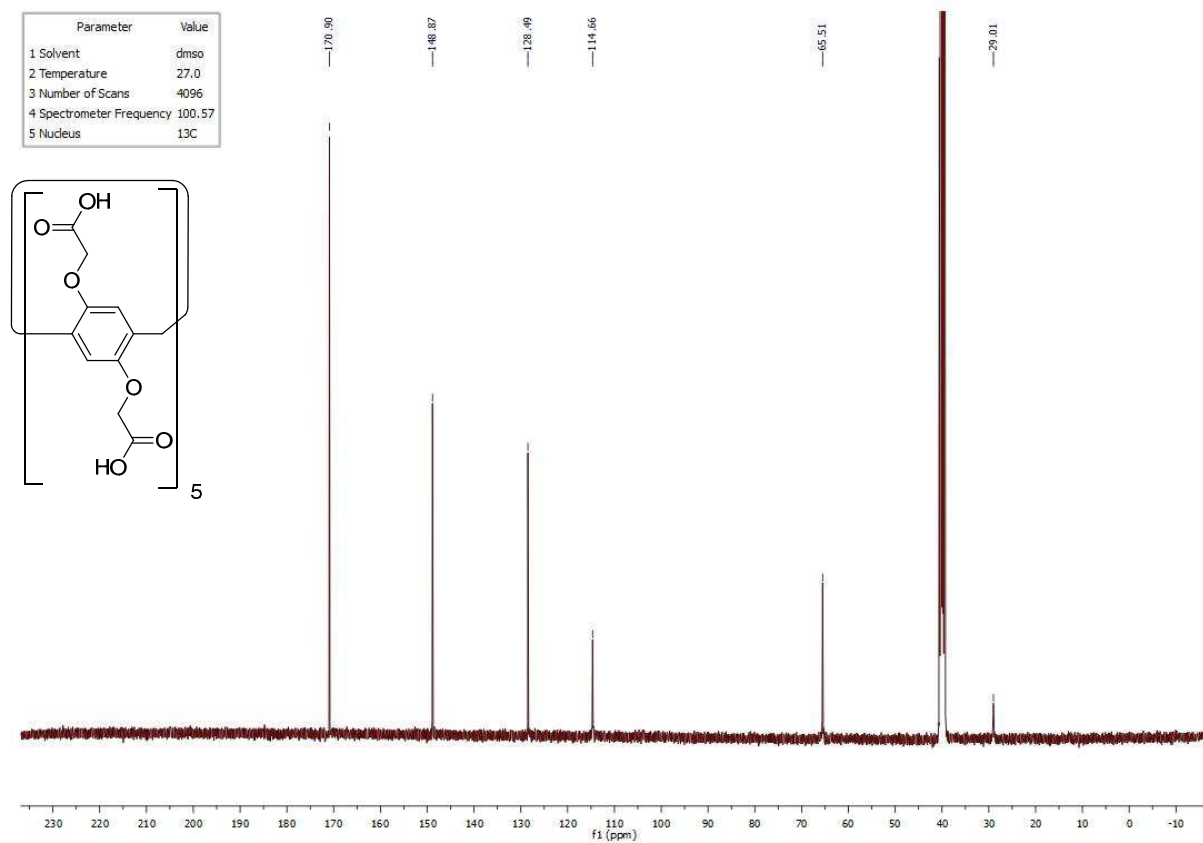
¹H NMR spectrum of **II.14**:

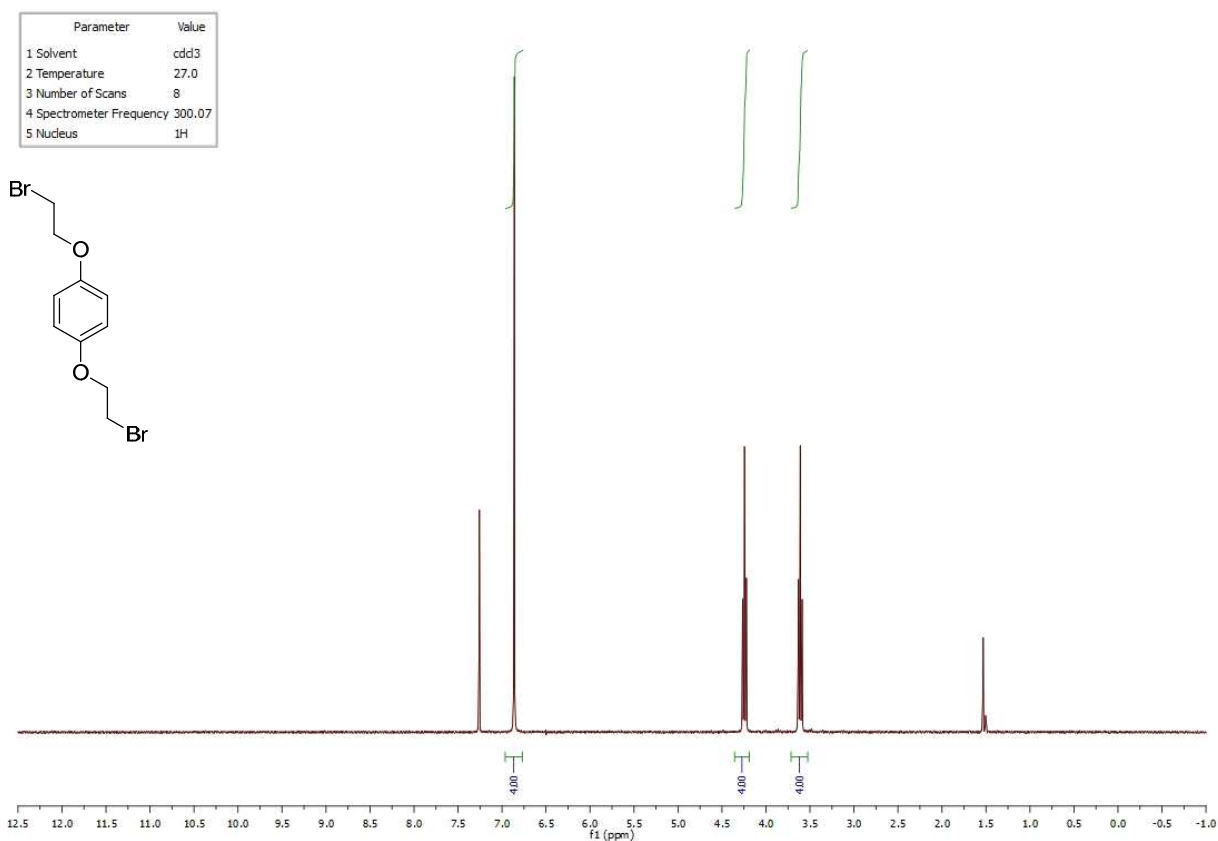
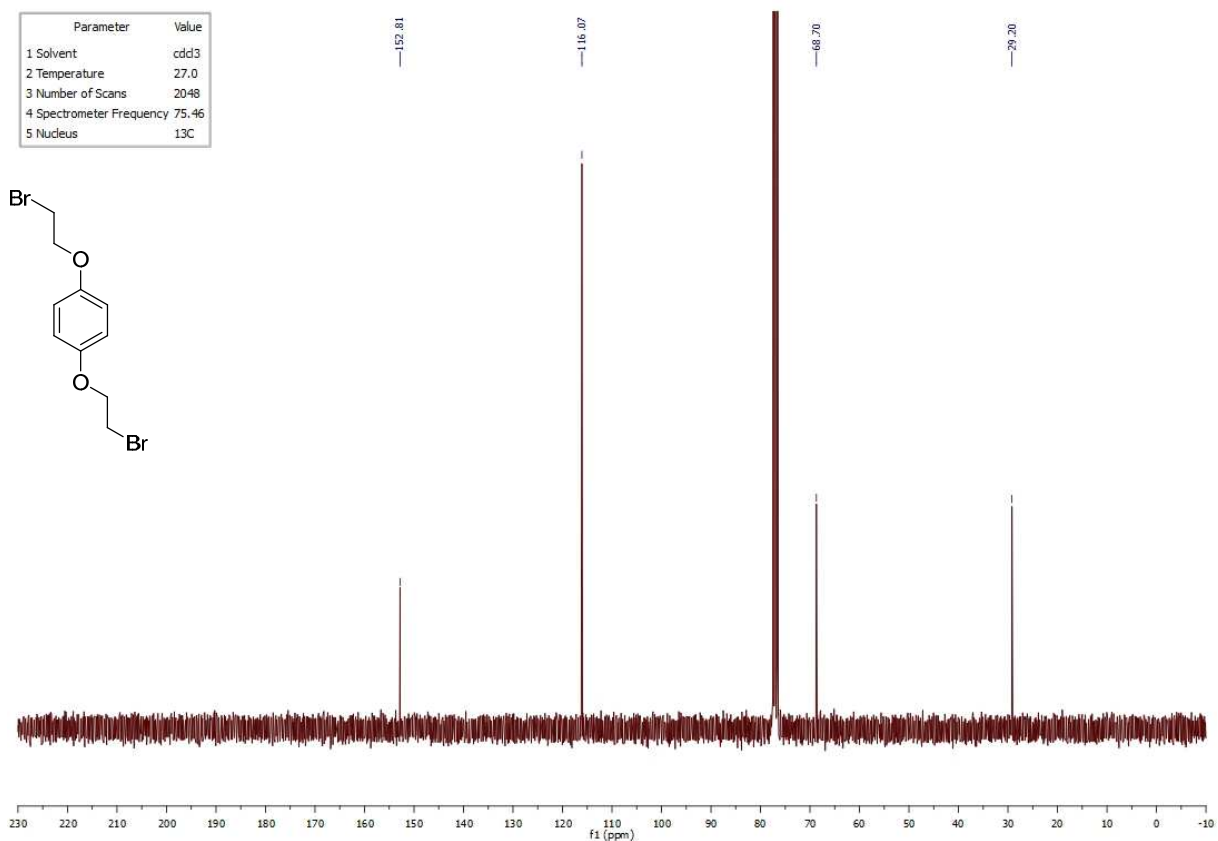
Parameter	Value
1 Solvent	cdd3
2 Temperature	25.0
3 Number of Scans	64
4 Spectrometer Frequency	399,94
5 Nucleus	¹ H

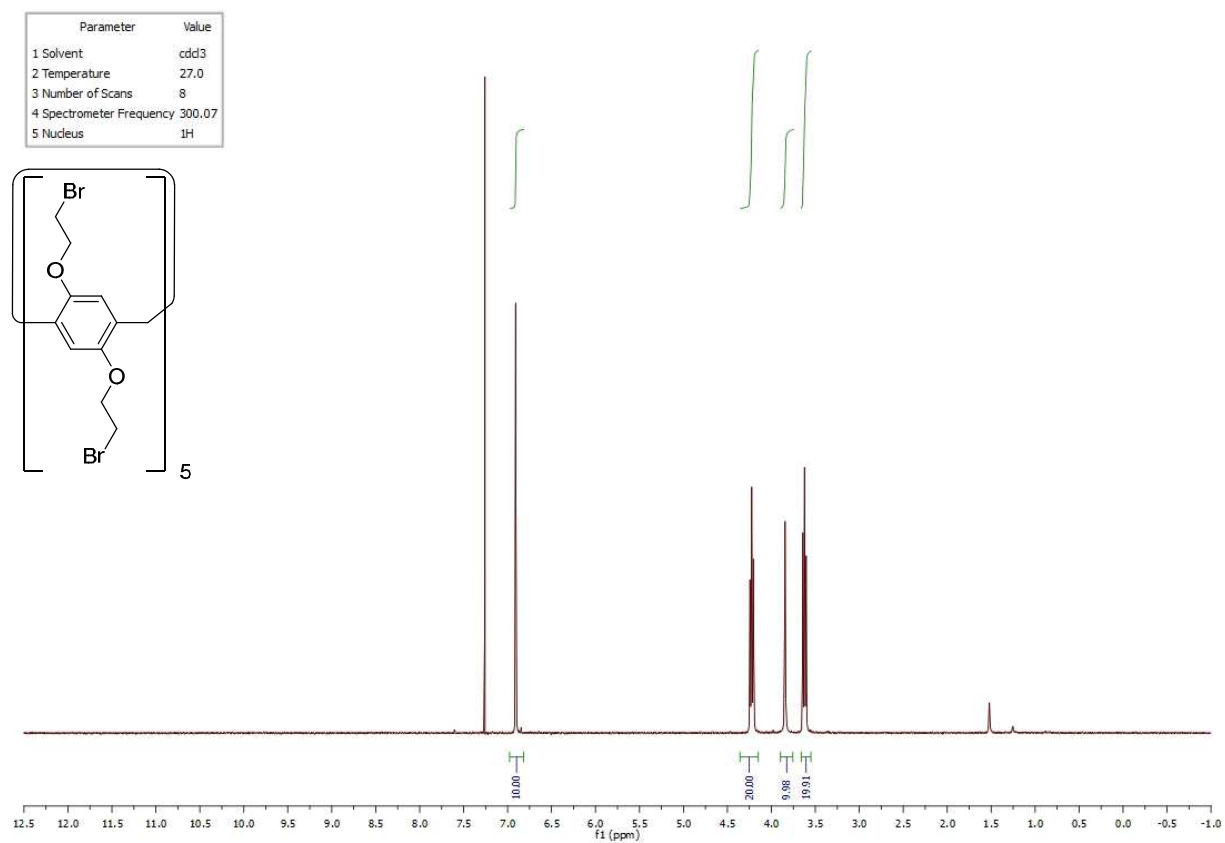
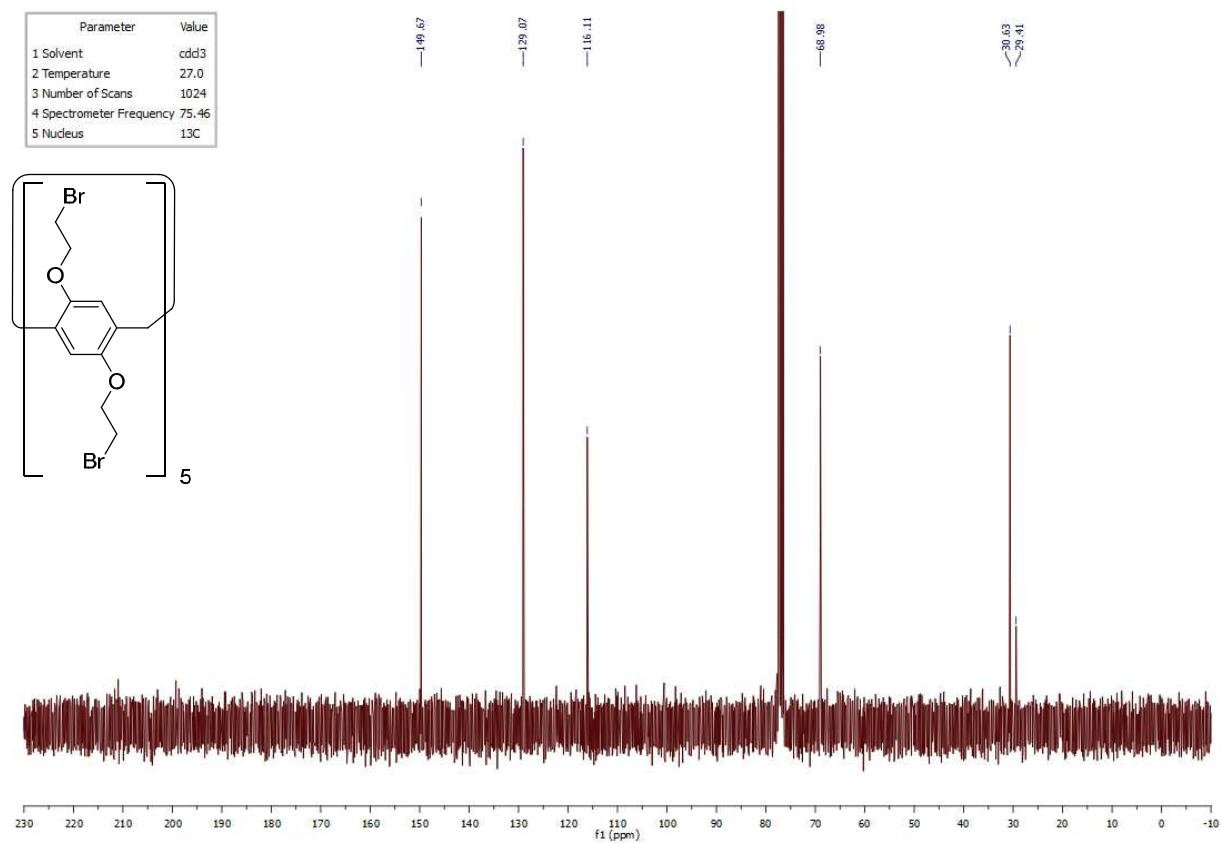
¹³C NMR spectrum of **II.14**:

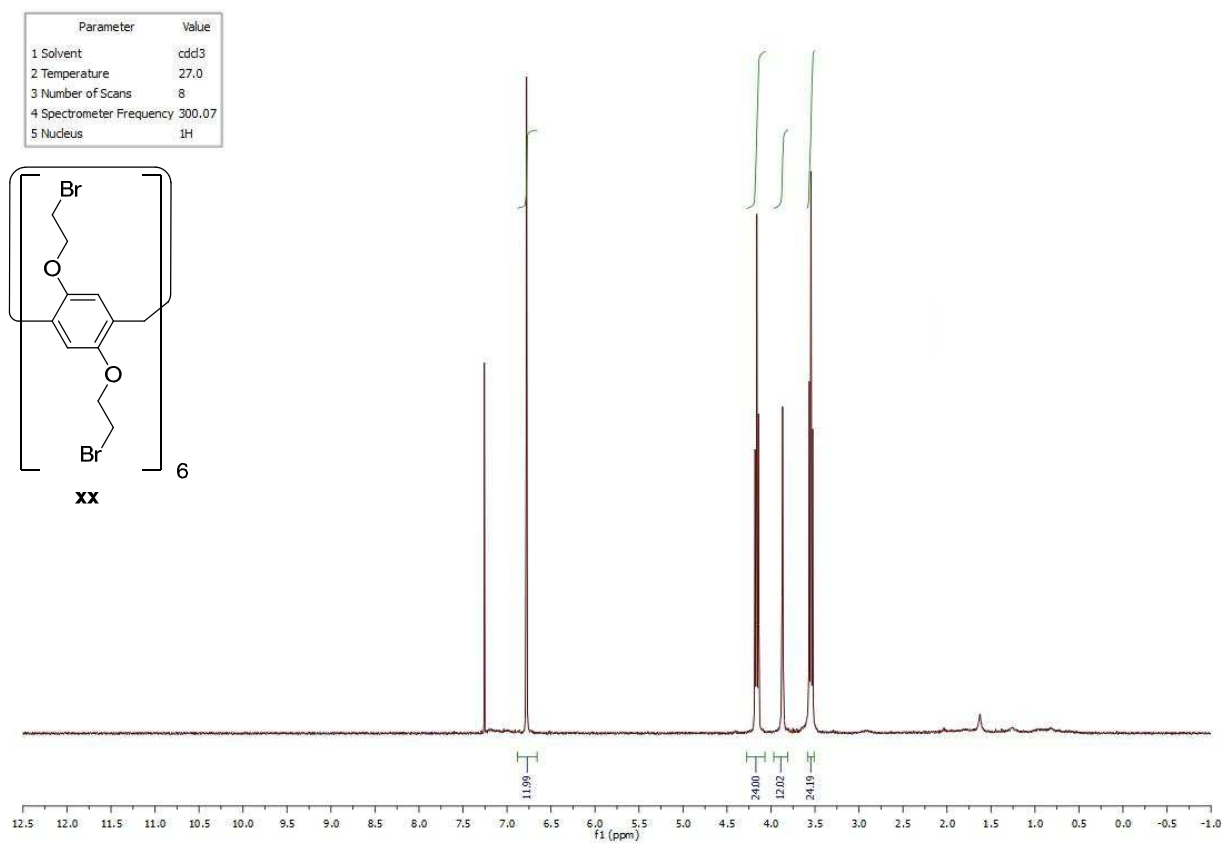
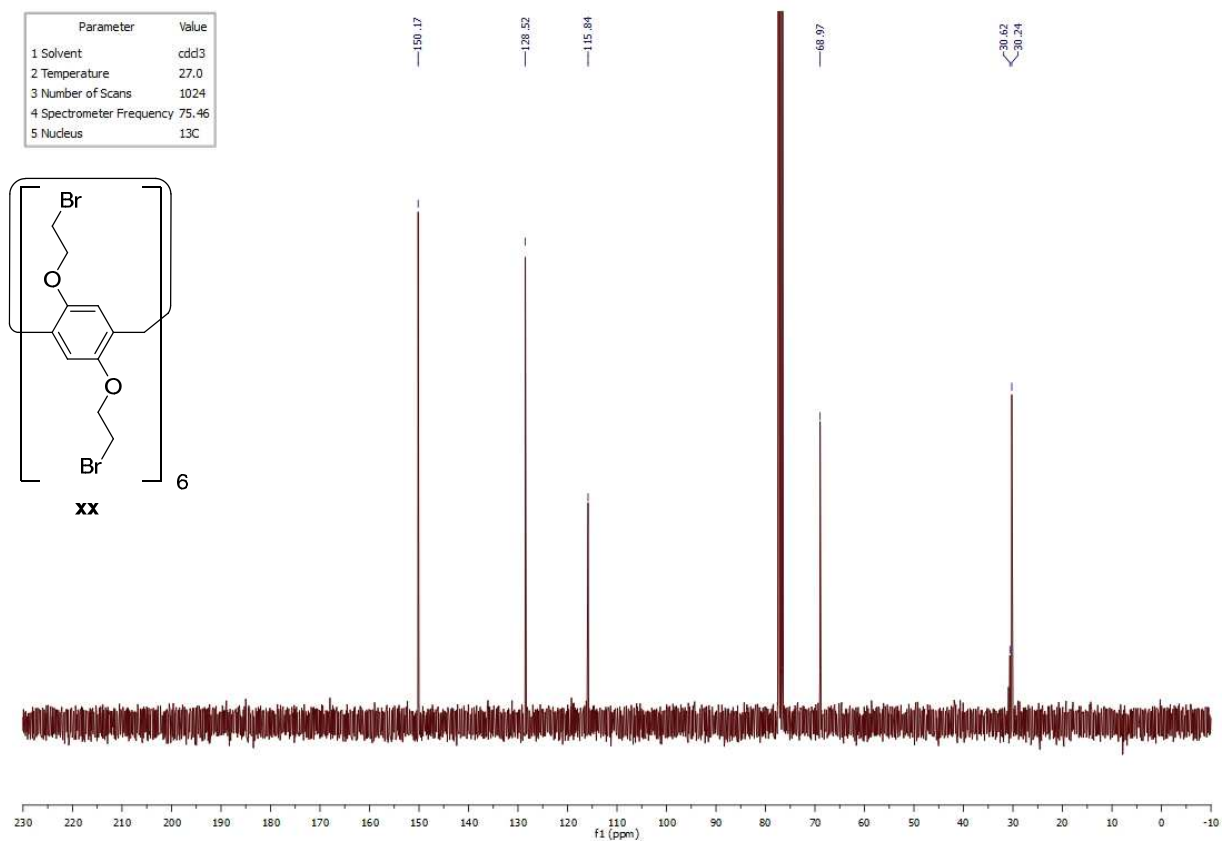
Parameter	Value
1 Solvent	cdd3
2 Temperature	25.0
3 Number of Scans	5504
4 Spectrometer Frequency	100,58
5 Nucleus	¹³ C

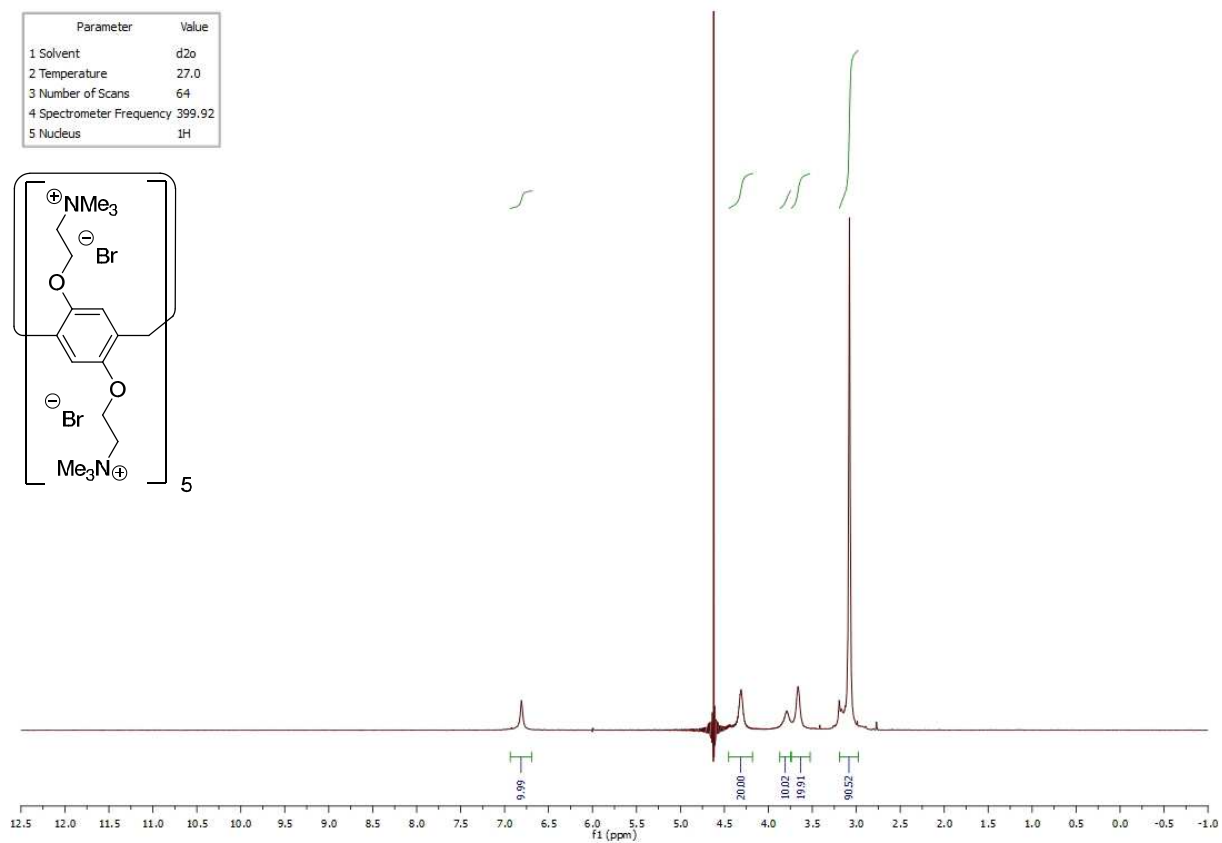
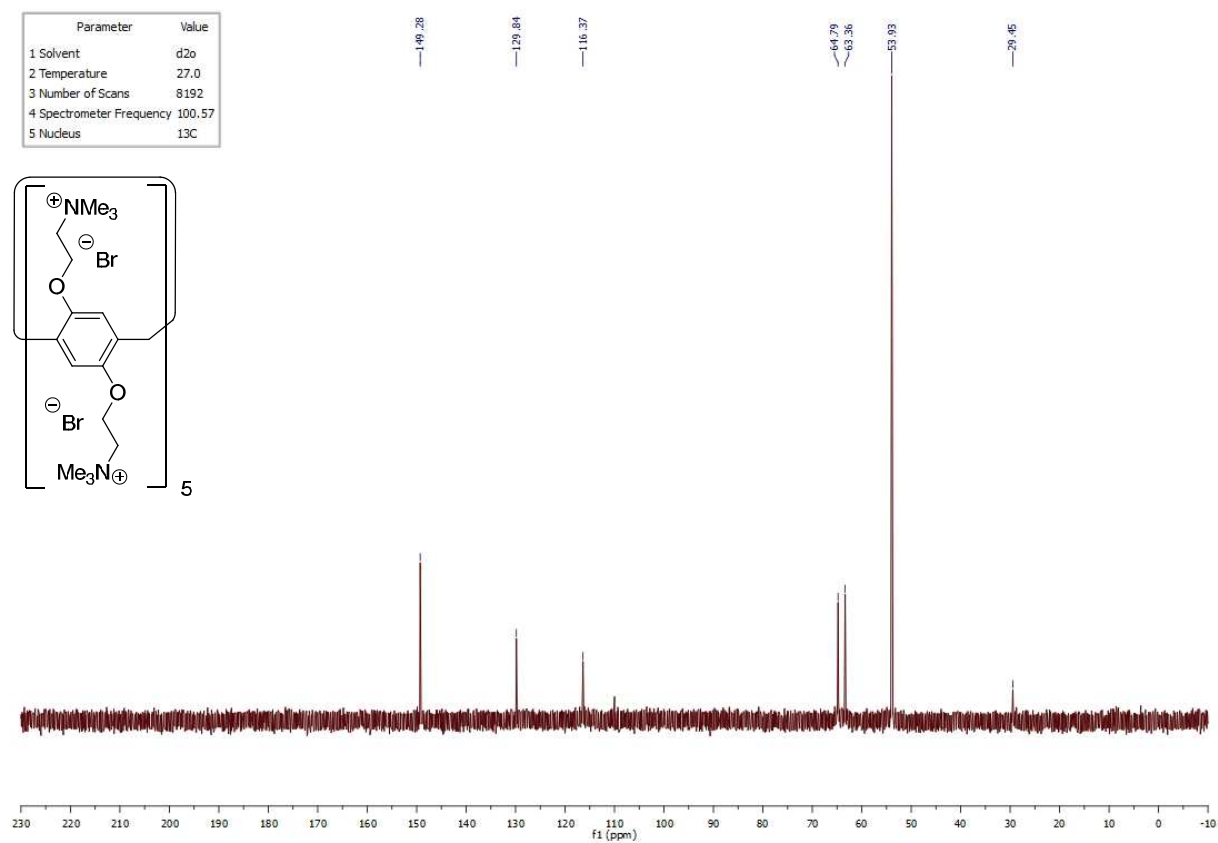


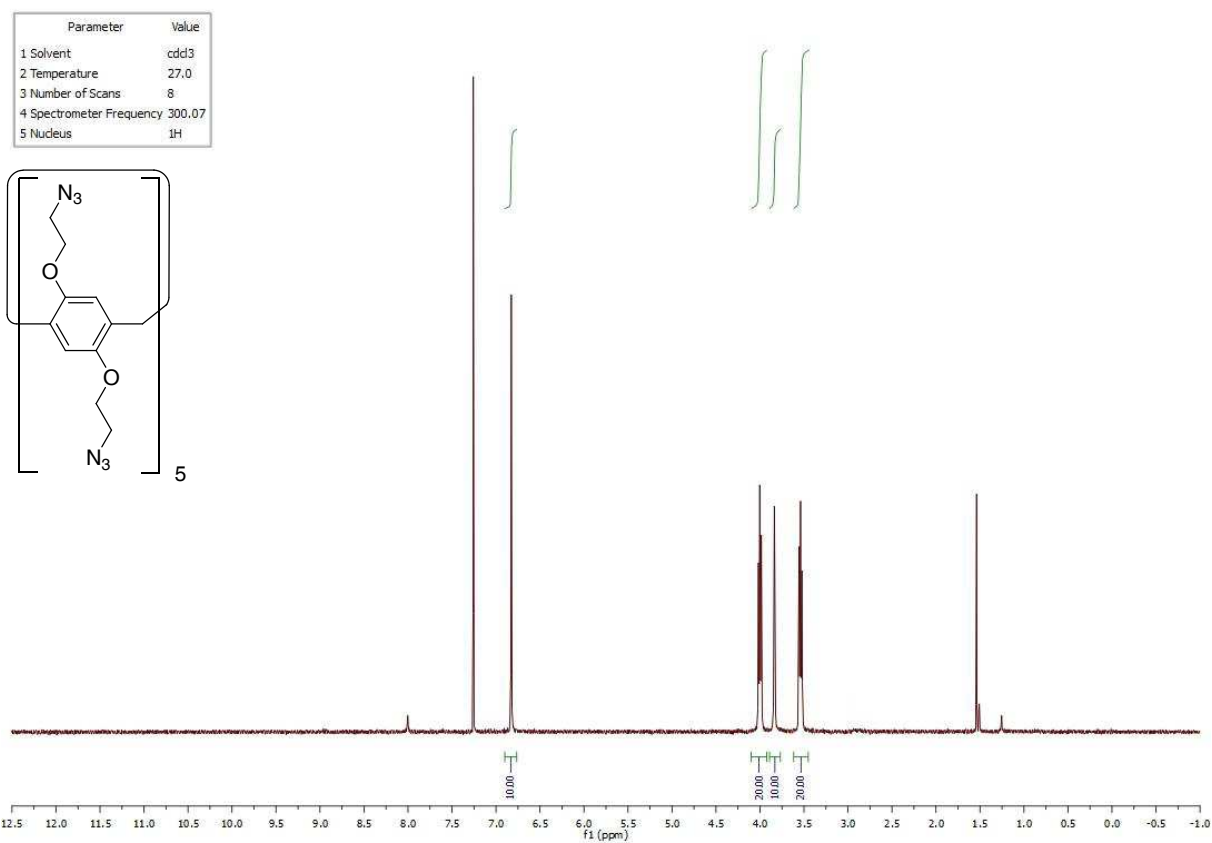
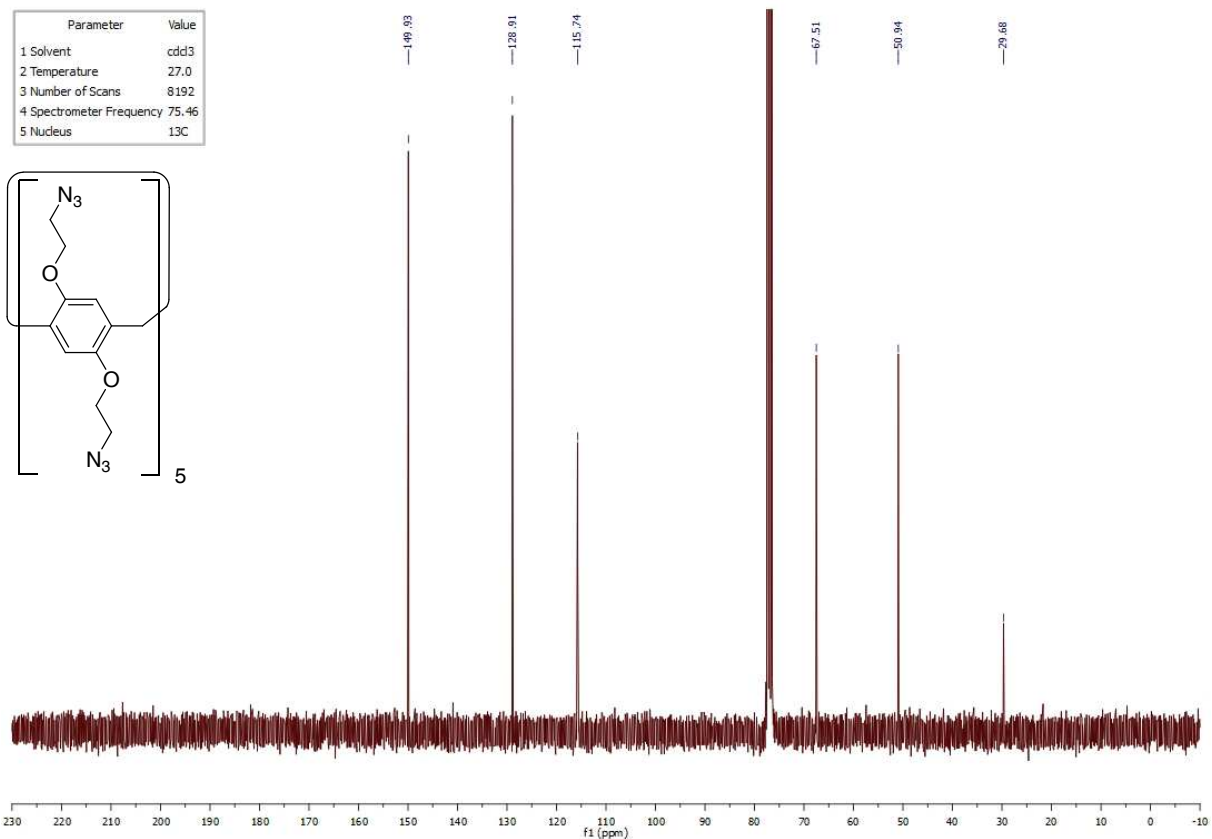
¹H NMR spectrum of **II.15**:¹³C NMR spectrum of **II.15**:

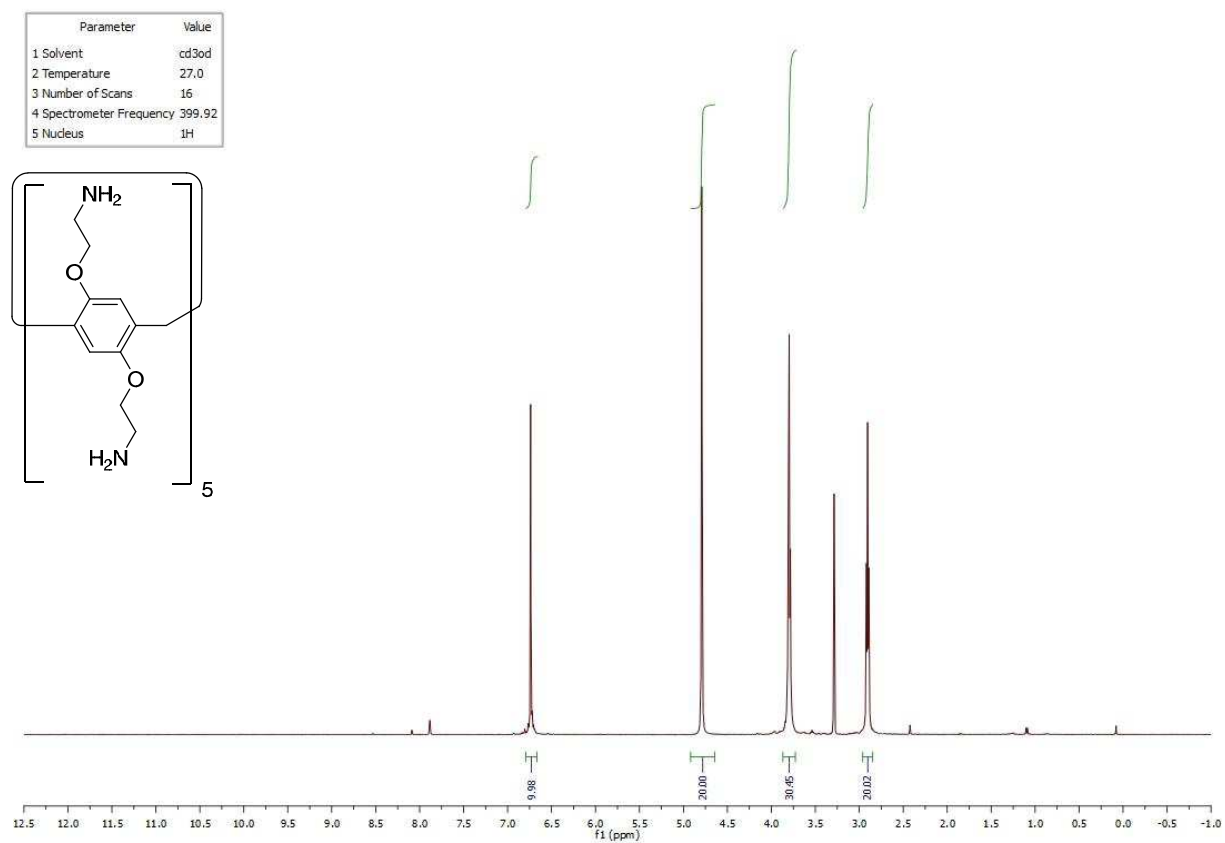
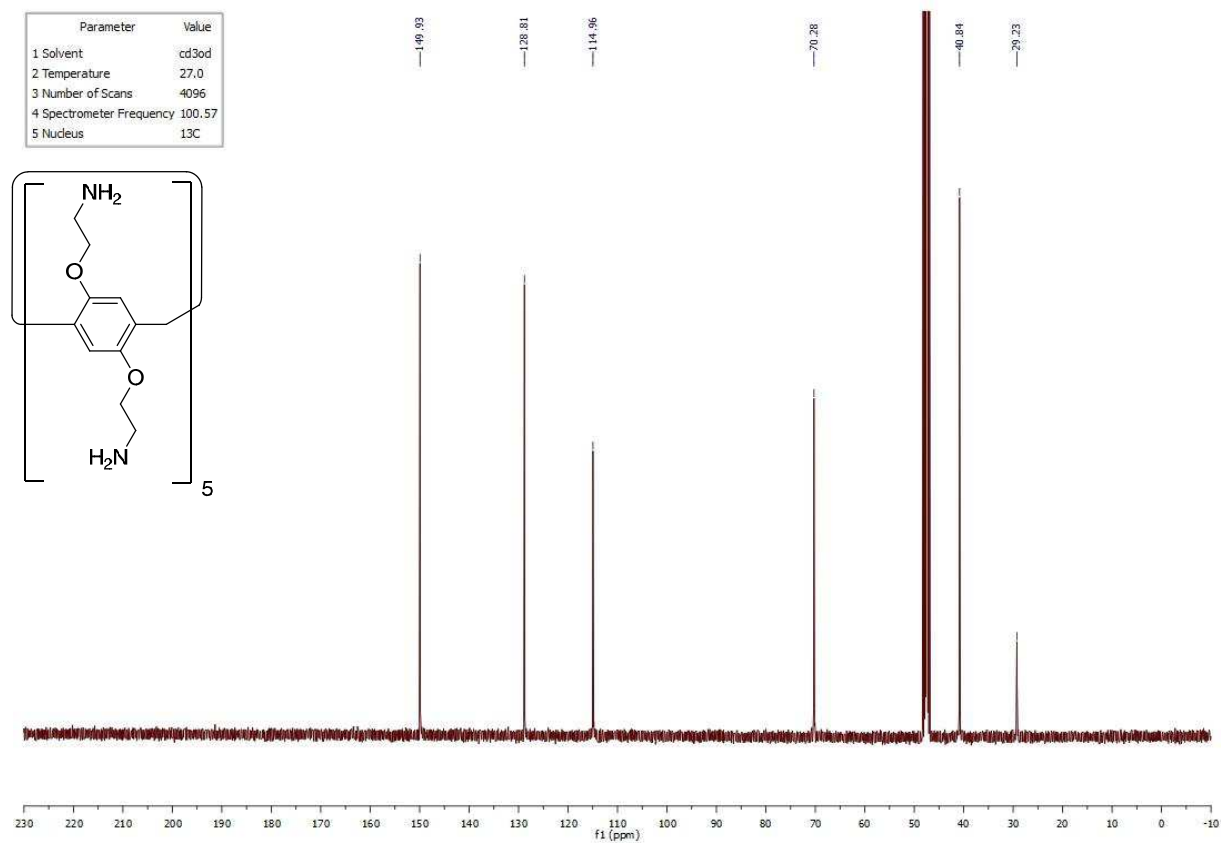
^1H NMR spectrum of **II.62**: ^{13}C NMR spectrum of **II.62**:

^1H NMR spectrum of **II.63**: ^{13}C NMR spectrum of **II.63**:

^1H NMR spectrum of **II.64**: ^{13}C NMR spectrum of **II.64**:

¹H NMR spectrum of **II.17**:¹³C NMR spectrum of **II.17**:

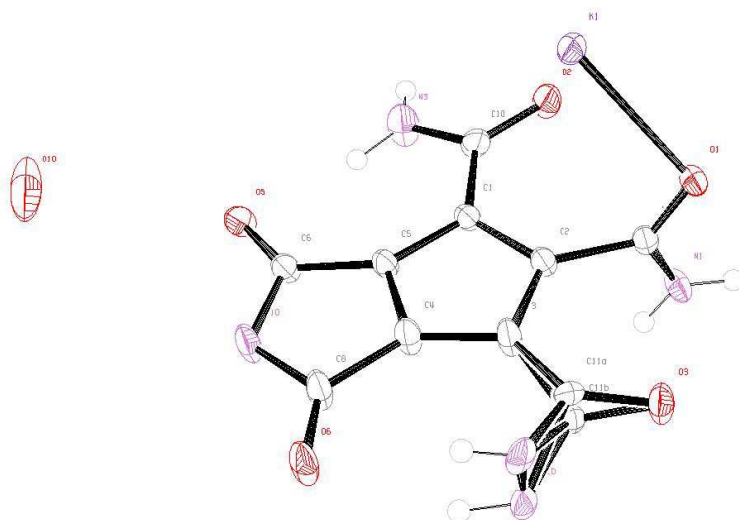
¹H NMR spectrum of **II.65**:¹³C NMR spectrum of **II.65**:

^1H NMR spectrum of **II.16**: ^{13}C NMR spectrum of **II.16**:

Appendix 4: Crystallographic Data of Chapter II

The X-ray analysis was carried out by Dr. Peter Mayer in the analytics department and Prof. Dr. Karaghiosoff in the Ludwig-Maximilians-Universität, München. The data collection was performed on an *Oxford Diffraction Xcalibur* or *KappaCCD* diffractometers at $-100\text{ }^{\circ}\text{C}$ using $\text{MoK}\alpha$ -radiation ($\lambda = 0.71073\text{ \AA}$, graphite monochromator). The *CrysAlisPro* software (version number 1.171.33.41)^[163] was applied for the integration, scaling and multi-scan absorption correction of the data. The structures were solved by direct methods with *SIR97*^[164] and refined by least-squares methods against F^2 with *SHELXL-97*.^[165]

Single-Crystal X-ray Analysis for compound II.30



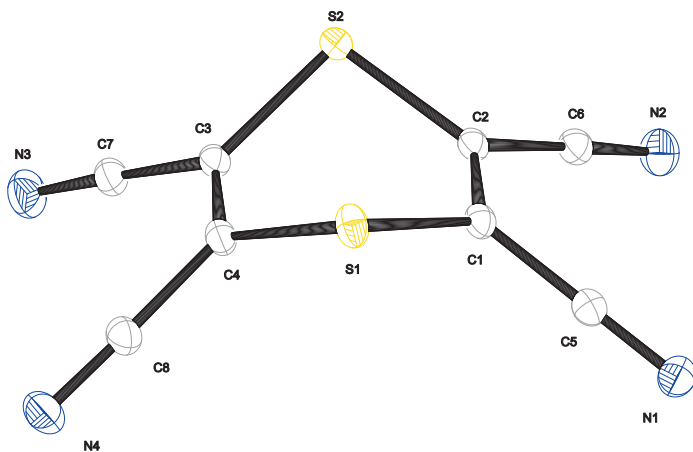
Compound	II.30
net formula	$\text{C}_{10}\text{H}_9\text{KN}_4\text{O}_6$
$M_r/\text{g mol}^{-1}$	320.31
crystal size/mm	$0.88 \times 2.19 \times 0.15$
T/K	173(2)
radiation	$\text{MoK}\alpha$
diffractometer	'KappaCCD'
crystal system	triclinic
space group	$P(-1)$
$a/\text{\AA}$	7.3745(5)

APPENDICES

$b/\text{\AA}$	8.4899(6)
$c/\text{\AA}$	9.5893(6)
$\alpha/^\circ$	96.261(5)
$\beta/^\circ$	91.385(5)
$\gamma/^\circ$	93.897(5)
$V/\text{\AA}^3$	595.11(7)
Z	2
calc. density/g cm ⁻³	1.788
μ/mm^{-1}	0.485
absorption correction	'multi-scan'
refls. measured	8916
R_{int}	0.0279
mean $\sigma(I)/I$	0.0264
θ range	4.19– 26.00
observed refls.	1937
hydrogen refinement	mixed
refls in refinement	2328
parameters	253
restraints	0
$R(F_{\text{obs}})$	0.0333
$R_w(F^2)$	0.0928
S	1.085
shift/error _{max}	0.000
max electron density/e \AA^{-3}	0.349
min electron density/e \AA^{-3}	-0.530

Single-Crystal X-ray Analysis for compound II.35

There are 0.5 toluene per formula unit; toluene is disordered and is not shown in the following figure.



Compound	II.35
net formula	$C_{11.50}H_4N_4S_2$
$M_r/g\ mol^{-1}$	262.314
crystal size/mm	$0.29 \times 0.22 \times 0.18$
T/K	173(2)
radiation	MoK α
diffractometer	'KappaCCD'
crystal system	monoclinic
space group	$C2/c$
$a/\text{\AA}$	26.1954(4)
$b/\text{\AA}$	7.07390(10)
$c/\text{\AA}$	16.3214(2)
$\alpha/^\circ$	90
$\beta/^\circ$	128.1483(8)
$\gamma/^\circ$	90
$V/\text{\AA}^3$	2378.44(6)
Z	8
calc. density/ $g\ cm^{-3}$	1.46512(4)
μ/mm^{-1}	0.430
absorption correction	none
refls. measured	9587

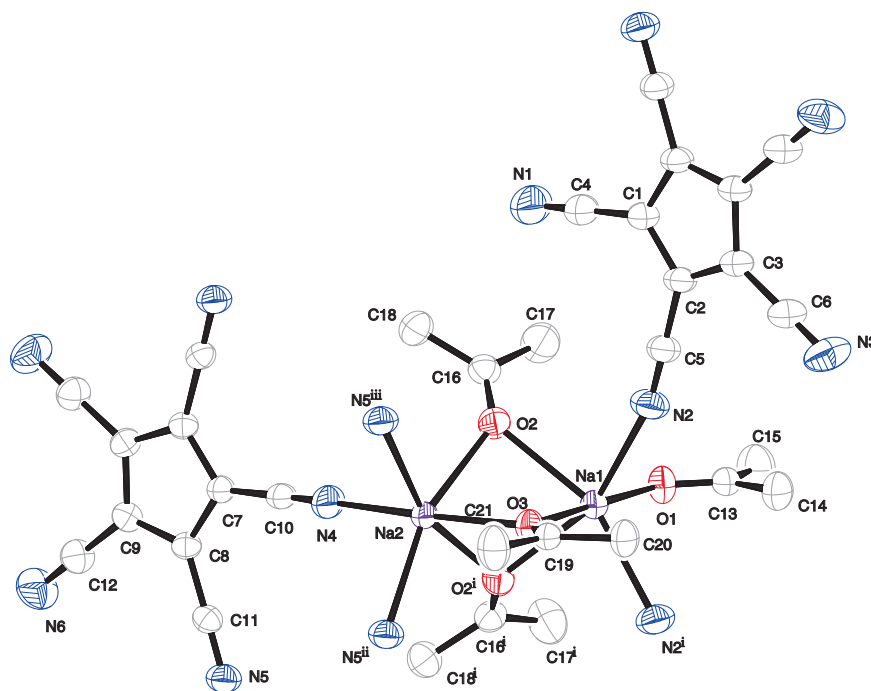
APPENDICES

R_{int}	0.0156
mean $\sigma(I)/I$	0.0156
θ range	3.14–27.49
observed refls.	2478
x, y (weighting scheme)	0.0600, 2.1778
hydrogen refinement	undef
refls in refinement	2726
parameters	163
restraints	0
$R(F_{\text{obs}})$	0.0340
$R_w(F^2)$	0.1048
S	1.073
shift/error _{max}	0.001
max electron density/e \AA^{-3}	0.451
min electron density/e \AA^{-3}	–0.290

The hydrogen atoms of the disordered toluene molecule have not been considered in the refinement.

Single-Crystal X-ray Analysis for compound II.10

The symmetry-generating $C_{10}N_5$ units as well as hydrogen atoms have been omitted for clarity with the exception of the respective coordinating N -atoms. Unlabeled atoms in $C_{10}N_5$ units are symmetry-generating.



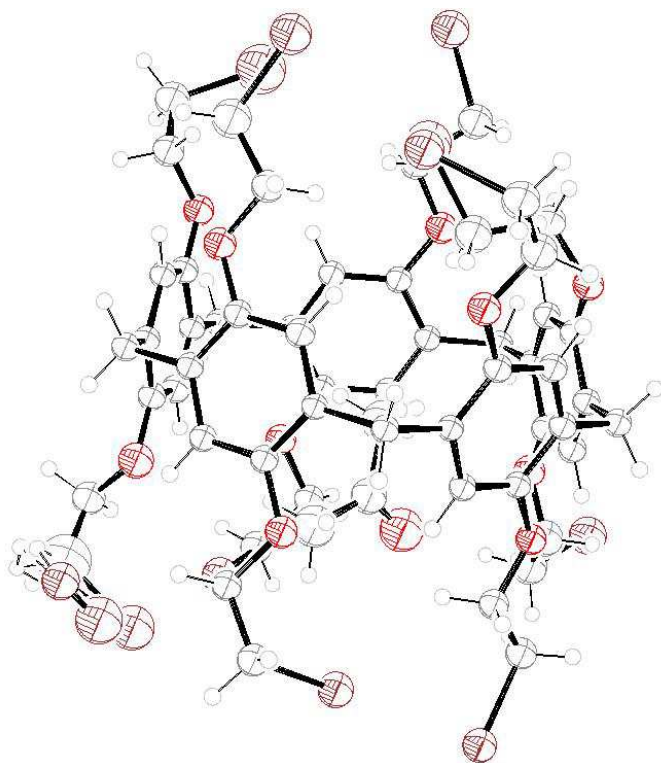
Compound	II.10
net formula	$C_{16}H_{12}N_5NaO_2$
$M_r/g\ mol^{-1}$	329.289
crystal size/mm	$0.40 \times 0.30 \times 0.19$
T/K	173(2)
radiation	MoK α
diffractometer	'Oxford Xcalibur'
crystal system	monoclinic
space group	$C2/m$
$a/\text{\AA}$	19.4091(14)
$b/\text{\AA}$	11.2357(8)
$c/\text{\AA}$	16.6773(14)
$\alpha/^\circ$	90
$\beta/^\circ$	93.812(6)

APPENDICES

$\gamma/^\circ$	90
$V/\text{\AA}^3$	3628.9(5)
Z	8
calc. density/g cm ⁻³	1.20544(17)
μ/mm^{-1}	0.104
absorption correction	'multi-scan'
transmission factor range	0.74635–1.00000
refls. measured	10091
R_{int}	0.0344
mean $\sigma(I)/I$	0.0365
θ range	4.27–26.40
observed refls.	3028
x, y (weighting scheme)	0.0598, 0.6438
hydrogen refinement	constr
refls in refinement	3873
parameters	247
restraints	0
$R(F_{\text{obs}})$	0.0409
$R_w(F^2)$	0.1196
S	1.038
shift/error _{max}	0.001
max electron density/e \AA^{-3}	0.211
min electron density/e \AA^{-3}	-0.238

Symmetry code: i = $x, -y, z$; ii = $0.5-x, 0.5-y, 1-z$; iii = $0.5-x, -1-y, z$.

Single-Crystal X-ray Analysis for compound II.63



Compound	II.63
net formula	$C_{58}H_{66}Br_{10}O_{11}$
$M_r/g\ mol^{-1}$	1738.178
crystal size/mm	$0.21 \times 0.04 \times 0.02$
T/K	200(2)
radiation	MoK α
diffractometer	'KappaCCD'
crystal system	monoclinic
space group	$P2_1/c$
$a/\text{\AA}$	21.4170(5)
$b/\text{\AA}$	12.4879(2)
$c/\text{\AA}$	25.0458(6)
$\alpha/^\circ$	90
$\beta/^\circ$	105.0069(9)
$\gamma/^\circ$	90
$V/\text{\AA}^3$	6470.1(2)
Z	4

APPENDICES

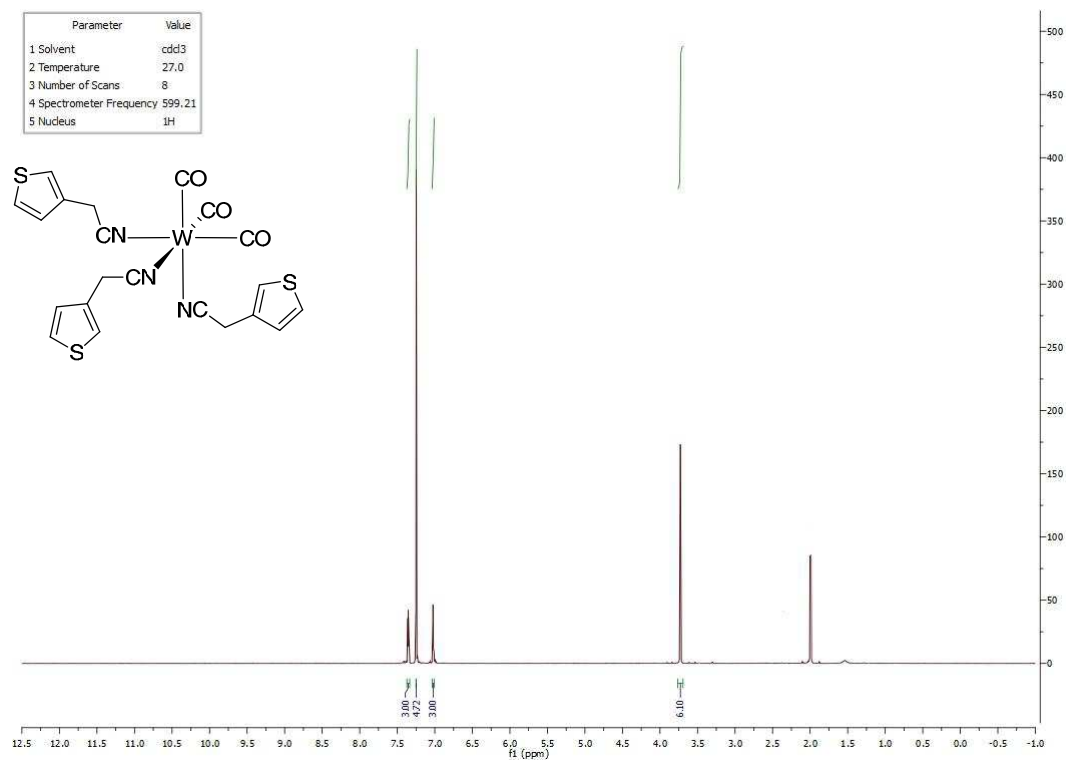
calc. density/g cm ⁻³	1.78443(6)
μ/mm ⁻¹	6.248
absorption correction	multi-scan
transmission factor range	0.5960–0.7303
refls. measured	75308
R_{int}	0.0896
mean $\sigma(I)/I$	0.0618
θ range	3.22–25.36
observed refls.	7736
x, y (weighting scheme)	0.0540, 26.7326
hydrogen refinement	constr
refls in refinement	11800
parameters	729
restraints	1
$R(F_{\text{obs}})$	0.0552
$R_w(F^2)$	0.1411
S	1.018
shift/error _{max}	0.002
max electron density/e Å ⁻³	3.208
min electron density/e Å ⁻³	-1.388

Bromide is disordered over three sites, split model applied, sof ratio: 0.35442 : 0.45264 : 0.19294.

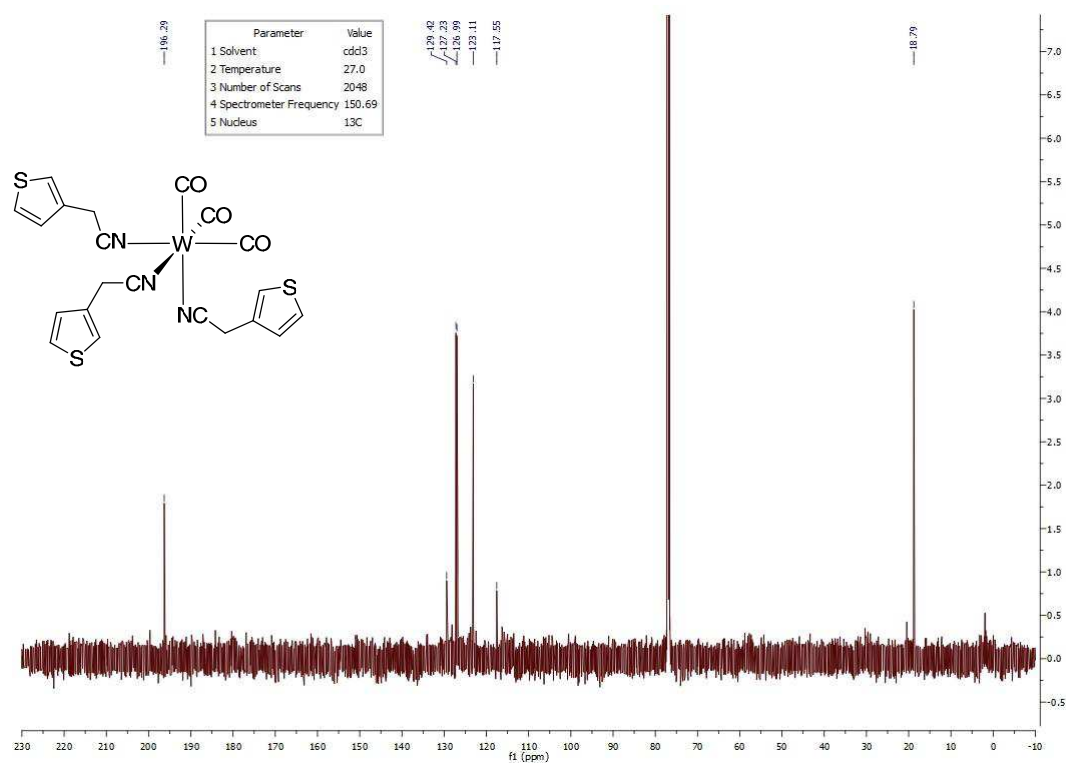
Solution of the structures of compounds **II.11**, **II.15**, **II.22**, and **II.17** requires further refinement, which is carried out by Dr. Peter Mayer in the analytics department in the Ludwig-Maximilians-Universität München. Illustrations of these compounds shown in Chapter II are based on preliminary data, as also mentioned under the respective Figures.

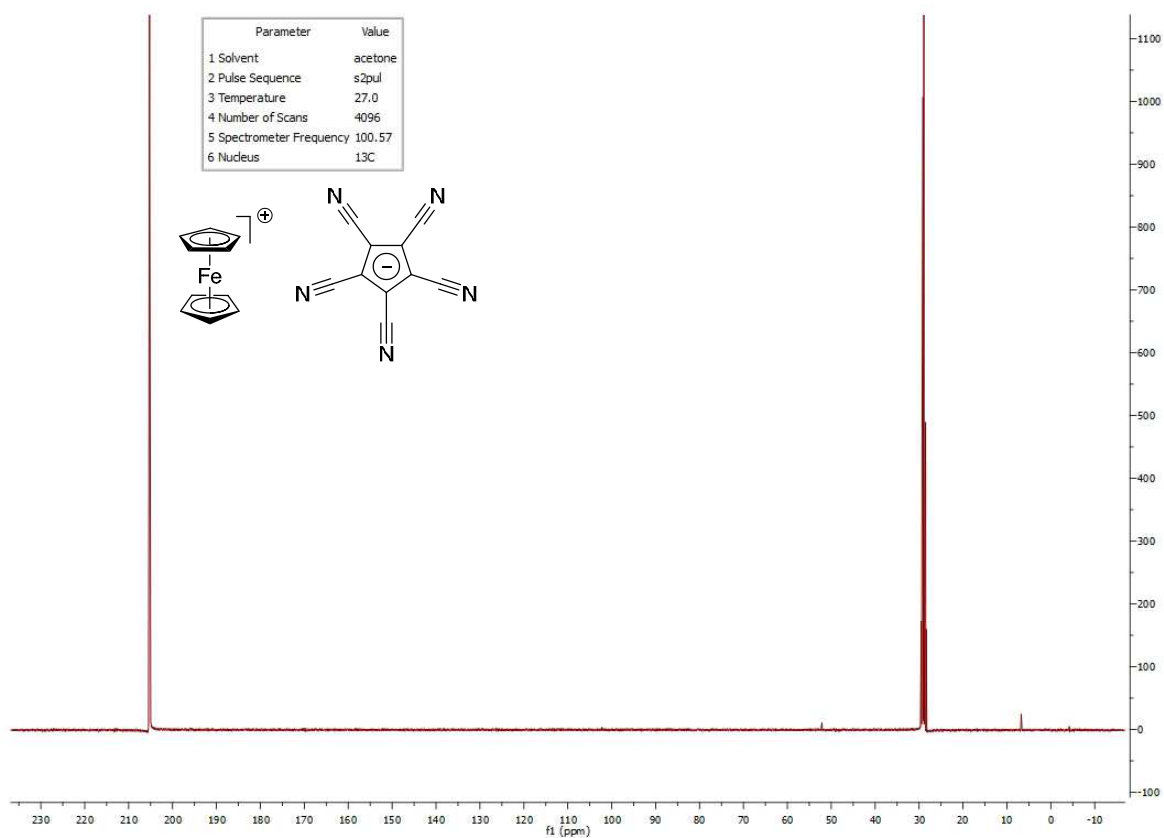
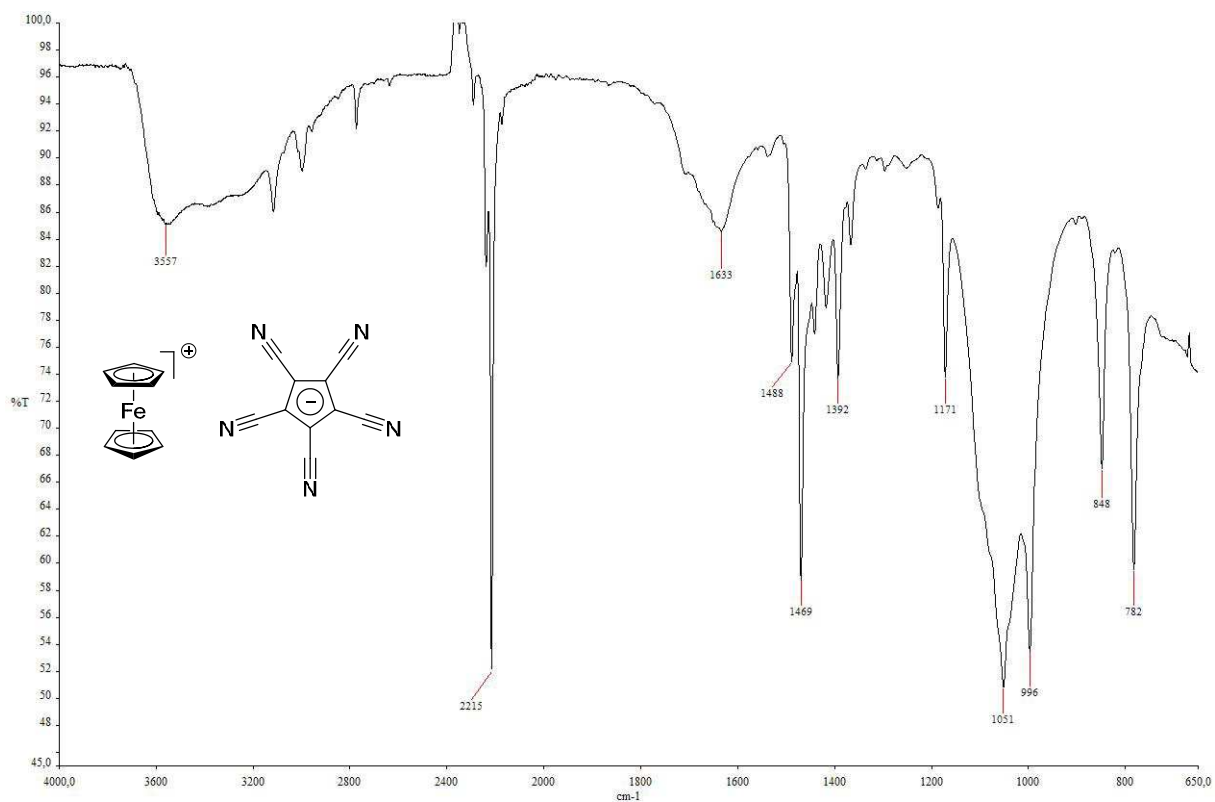
Appendix 5: NMR and IR Spectra of Chapter III, Magnetic Properties of III.17

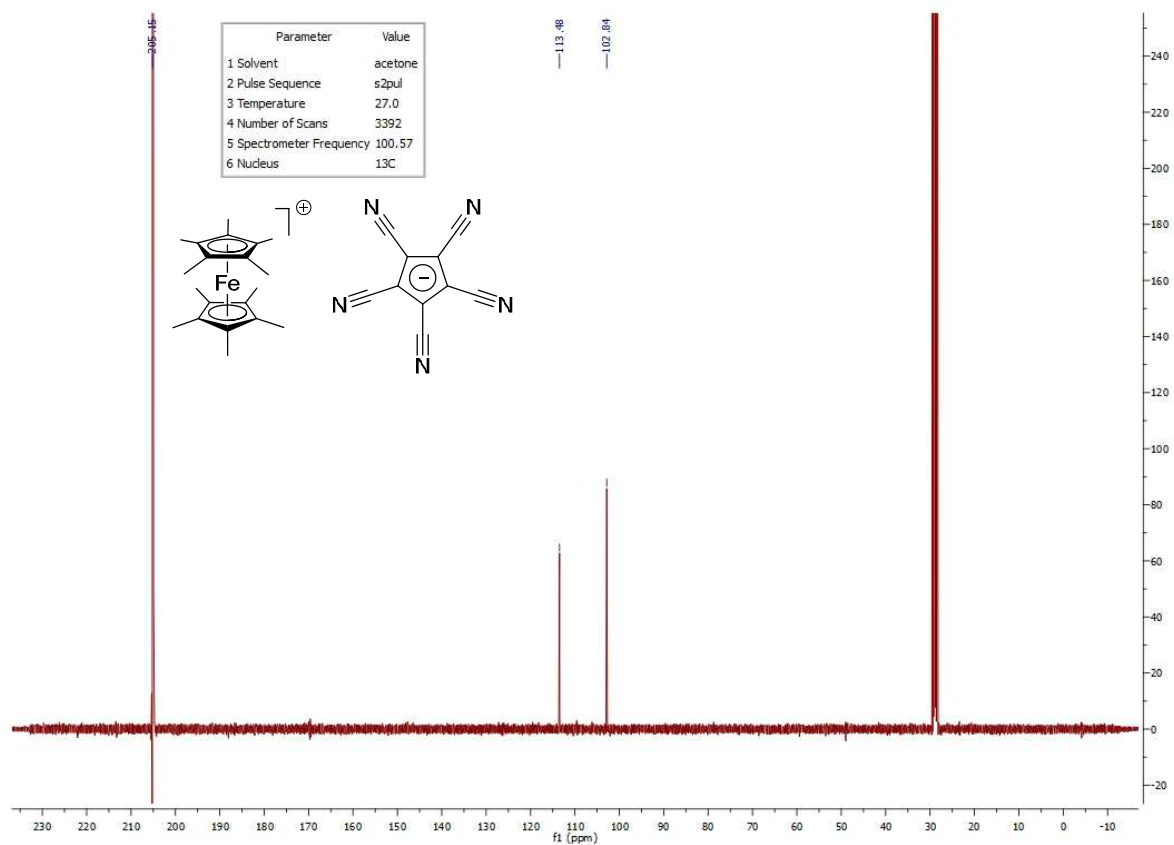
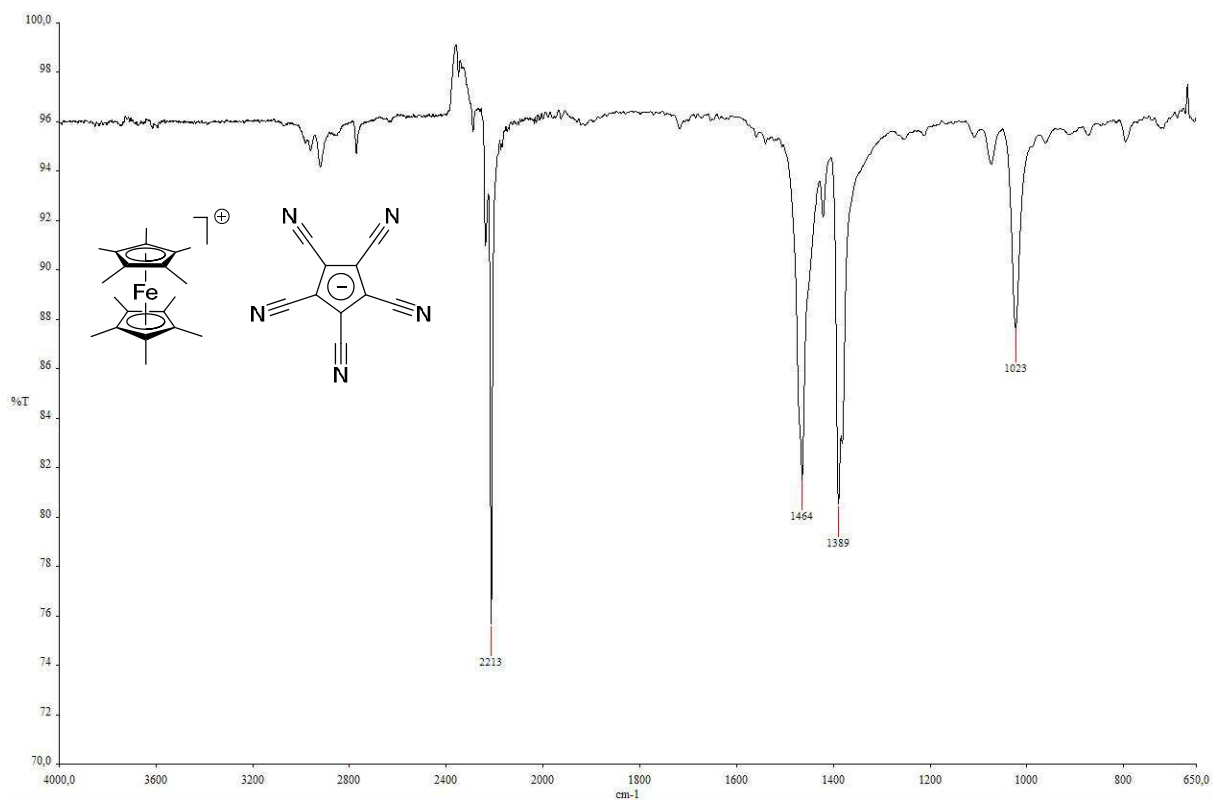
^1H NMR spectrum of III.12:

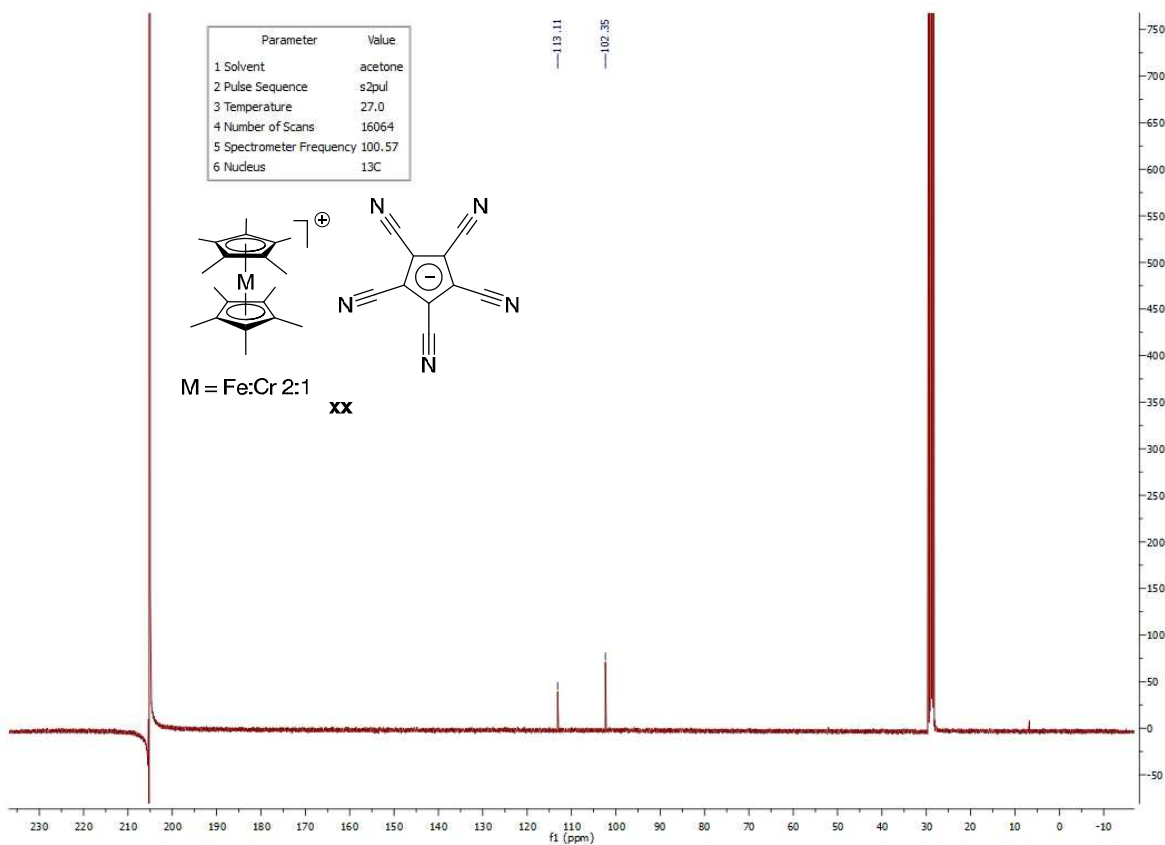
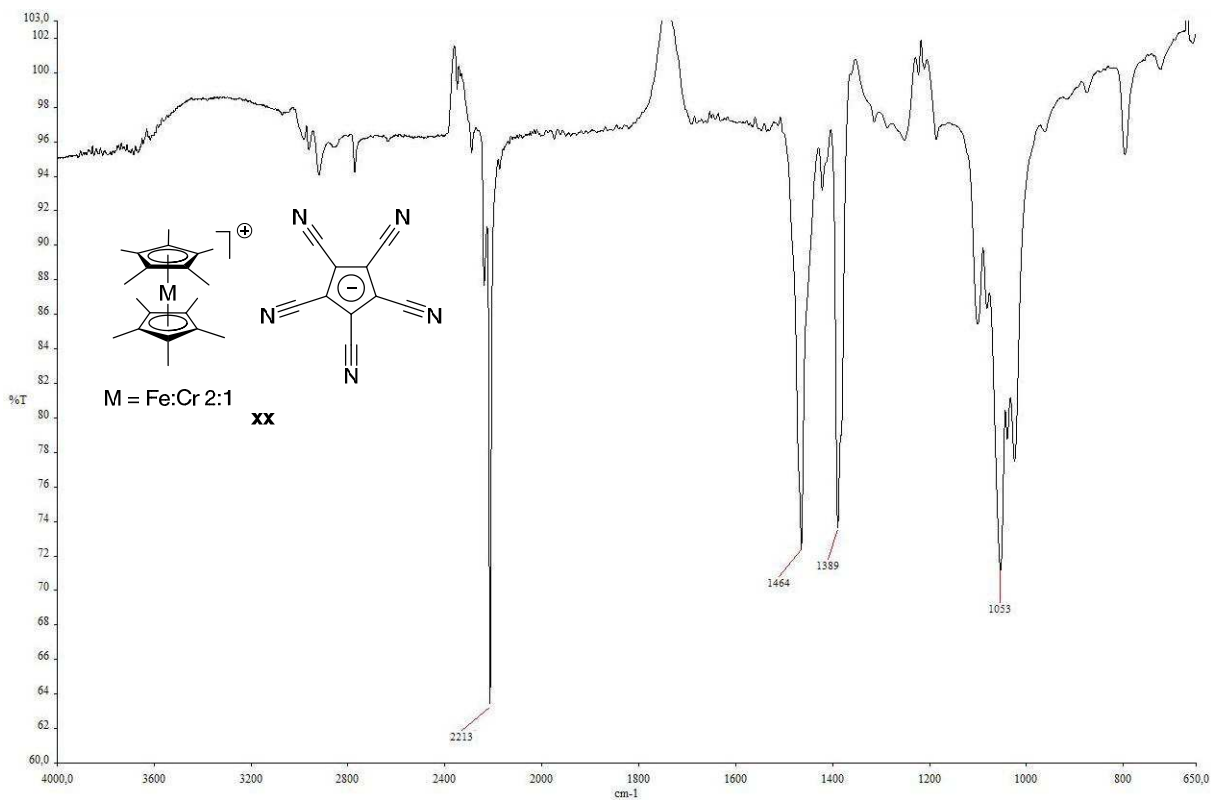


^{13}C NMR spectrum of III.12:



^{13}C NMR spectrum of **III.16**:IR spectrum **III.16**:

¹³C NMR spectrum of **III.17**:IR spectrum of DMferrocenium pccp (**III.17**):

^{13}C NMR spectrum **III.18**:IR spectrum of **III.18**:

Magnetic properties of compound III.17

The magnetic characterizations of **III.17** was performed on a *MPMS-XL5* SQUID magnetometer made by *Quantum Design Inc.*^[166] by Rainer Frankovsky (group of Prof. Dr. D. Johrendt, Ludwig-Maximilians-Universität München) at the laboratories of Prof. Dr. T. Fässler (TU Munich). The magnetometer was controlled and data were collected with the MPMS MultiVu software^[167]. For the measurement, 14 mg of substance were put into a gelatine capsule, which was fixed in a straw as sample holder. The generated data file was processed with the fully automatic SQUID processor software^[168] and corrections were made for diamagnetic contributions of the sample holder and the diamagnetic increments of the ions, which can be found in^[169].

Compound **III.17** is paramagnetic between 1.8 K and 380 K. The inverse susceptibility was fitted with the extended Curie-Weiss law (1.8 K – 380 K)^[169] to obtain an effective moment of $2.65 \mu_B$ per formula unit (Figure App.5a) and which is in good agreement with the listed value of $2.5 \mu_B$ for Fe^{3+} with low spin configuration^[169].

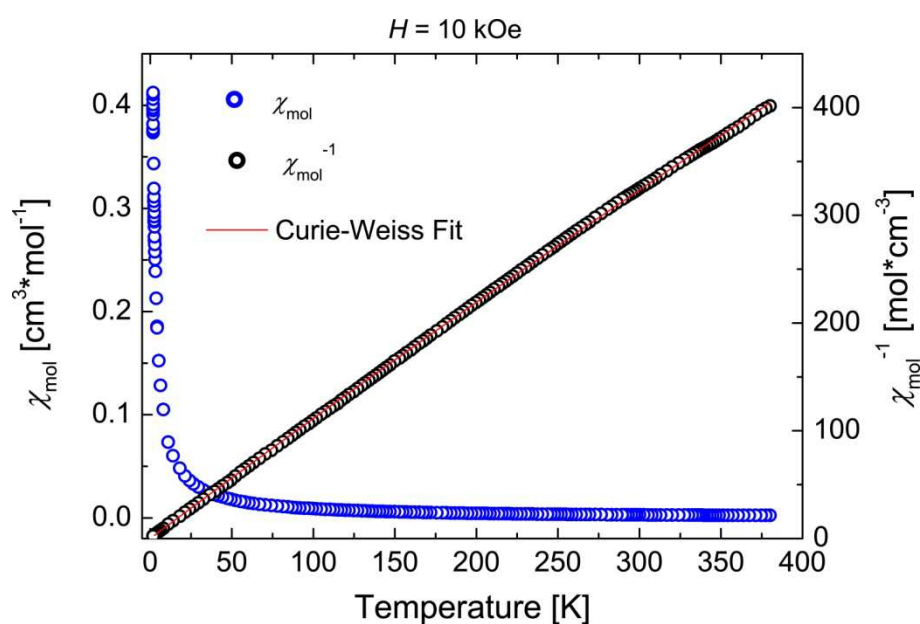
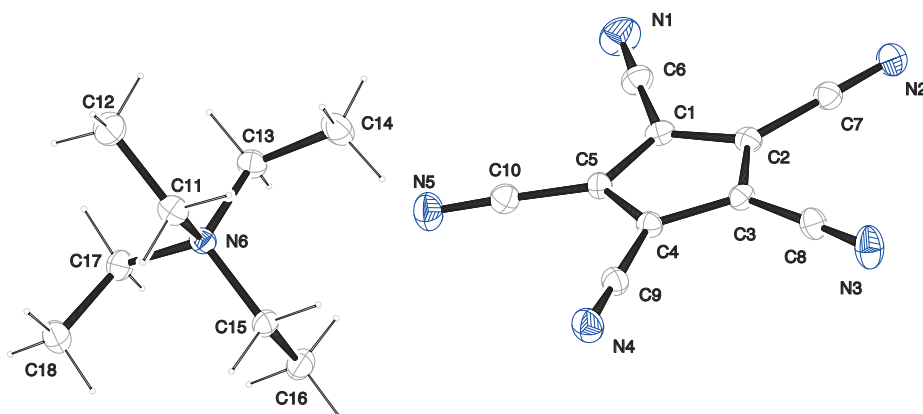


Figure App.5a: Magnetic susceptibility (blue) vs. temperature and inverse susceptibility (black) fitted with the extended Curie-Weiss law (red) of **III.17**.

Appendix 6: Crystallographic Data of Chapter III

The X-ray analysis was carried out by Dr. Peter Mayer in the analytics department in the Ludwig-Maximilians-Universität, München. The data collection was performed on an *Oxford Diffraction Xcalibur* or *KappaCCD* or *Bruker D8Quest* diffractometers at $-100\text{ }^{\circ}\text{C}$ using $\text{MoK}\alpha$ -radiation ($\lambda = 0.71073\text{ \AA}$, graphite monochromator). The CrysAlisPro software (version number 1.171.33.41)^[163] was applied for the integration, scaling and multi-scan absorption correction of the data. The structures were solved by direct methods with SIR97^[164] and refined by least-squares methods against F^2 with SHELXL-97.^[165]

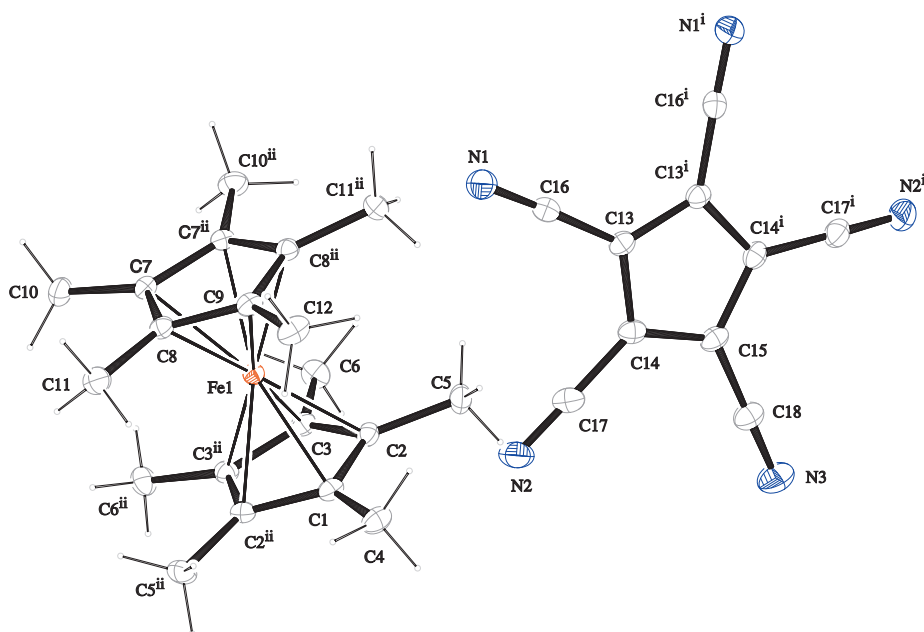
Single-Crystal X-ray Analysis for compound III.3



Compound	III.3 (<i>Cc</i> isomorph)	III.3 (<i>Pc</i> isomorph)
net formula	$\text{C}_{18}\text{H}_{20}\text{N}_6$	$\text{C}_{18}\text{H}_{20}\text{N}_6$
$M_r/\text{g mol}^{-1}$	320.392	320.392
crystal size/mm	$0.23 \times 0.08 \times 0.04$	$0.27 \times 0.15 \times 0.08$
T/K	173(2)	173(2)
radiation	$\text{MoK}\alpha$	$\text{MoK}\alpha$
diffractometer	'KappaCCD'	'Oxford Xcalibur'
crystal system	monoclinic	monoclinic
space group	<i>Cc</i>	<i>Pc</i>
$a/\text{\AA}$	13.8374(6)	12.3823(17)
$b/\text{\AA}$	20.8710(8)	20.721(3)
$c/\text{\AA}$	6.9984(3)	7.1748(12)
$\alpha/^\circ$	90	90

$\beta/^\circ$	117.991(2)	102.583(16)
$\gamma/^\circ$	90	90
$V/\text{\AA}^3$	1784.71(13)	1796.6(5)
Z	4	4
calc. density/ g cm^{-3}	1.19242(9)	1.1845(3)
μ/mm^{-1}	0.076	0.075
absorption correction	none	'multi-scan'
refls. measured	5869	9394
R_{int}	0.0396	0.0753
mean $\sigma(I)/I$	0.0303	0.0685
θ range	3.37–25.33	4.16–25.34
observed refls.	1453	2789
x, y (weighting scheme)	0.0482, 0.3533	0.0340, 0
hydrogen refinement	constr	constr
Flack parameter	0(3)	–1(3)
refls in refinement	1628	3290
parameters	221	441
restraints	2	2
$R(F_{\text{obs}})$	0.0341	0.0450
$R_w(F^2)$	0.0852	0.1042
S	1.036	1.051
shift/error $_{\text{max}}$	0.001	0.001
max electron density/ e \AA^{-3}	0.121	0.145
min electron density/ e \AA^{-3}	–0.163	–0.173
Flack parameter meaningless,	1470 Friedel pairs merged,	2734 Friedel pairs merged.

Single-Crystal X-ray Analysis for compound III.17

**Compound****III.17**

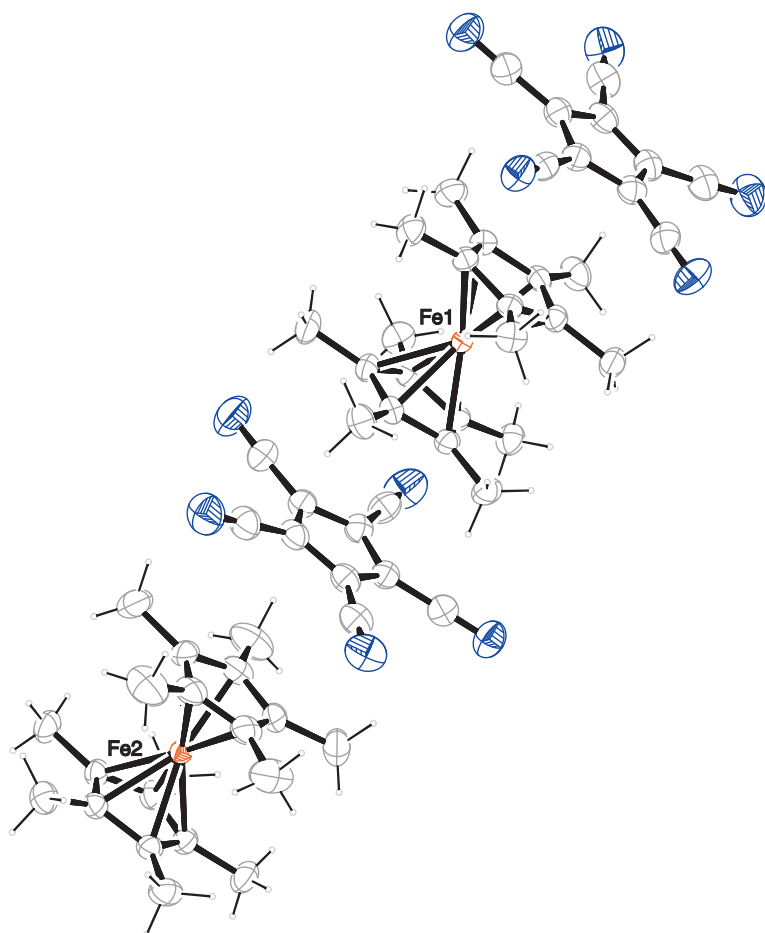
net formula	$C_{30}H_{30}FeN_5$
$M_r/g\ mol^{-1}$	516.438
crystal size/mm	$0.13 \times 0.08 \times 0.07$
T/K	173(2)
radiation	MoK α
diffractometer	'KappaCCD'
crystal system	orthorhombic
space group	$Cmc2_1$
$a/\text{\AA}$	14.5774(4)
$b/\text{\AA}$	13.1067(4)
$c/\text{\AA}$	13.7993(5)
$\alpha/^\circ$	90
$\beta/^\circ$	90
$\gamma/^\circ$	90
$V/\text{\AA}^3$	2636.52(14)
Z	4
calc. density/ $g\ cm^{-3}$	1.30108(7)
μ/mm^{-1}	0.600
absorption correction	none

refls. measured	10568
R_{int}	0.0333
mean $\sigma(I)/I$	0.0315
θ range	3.44–27.49
observed refls.	2850
x, y (weighting scheme)	0.0313, 0.7778
hydrogen refinement	constr
Flack parameter	–0.015(14)
refls in refinement	3110
parameters	181
restraints	1
$R(F_{\text{obs}})$	0.0285
$R_w(F^2)$	0.0651
S	1.067
shift/error _{max}	0.001
max electron density/e \AA^{-3}	0.409
min electron density/e \AA^{-3}	–0.212

1488 Friedel pairs measured.

Symmetry code: i = $-x, y, x$; ii = $1-x, y, z$

Single-Crystal X-ray Analysis for compound III.18

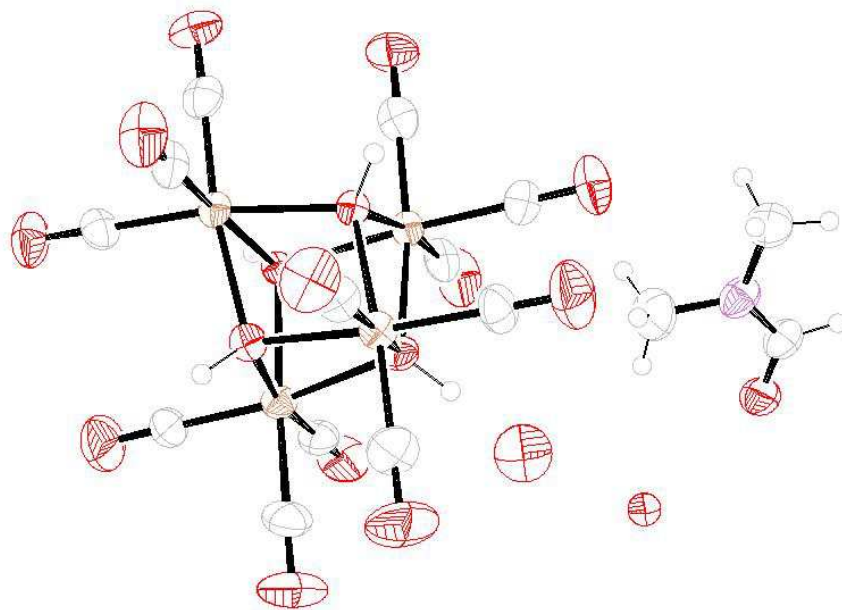


Compound	III.18
net formula	$C_{30}H_{30}Cr_{0.33}Fe_{0.67}N_5$
$M_r/g\ mol^{-1}$	515.168
crystal size/mm	$0.17 \times 0.09 \times 0.07$
T/K	173(2)
radiation	MoK α
diffractometer	'KappaCCD'
crystal system	monoclinic
space group	$P2_1/c$
$a/\text{\AA}$	17.9099(4)
$b/\text{\AA}$	16.9951(3)
$c/\text{\AA}$	18.4217(3)
$\alpha/^\circ$	90
$\beta/^\circ$	108.0576(12)

$\gamma/^\circ$	90
$V/\text{\AA}^3$	5331.02(17)
Z	8
calc. density/ g cm^{-3}	1.28376(4)
μ/mm^{-1}	0.548
absorption correction	none
refls. measured	34214
R_{int}	0.0499
mean $\sigma(I)/I$	0.0419
θ range	3.16–25.34
observed refls.	7155
x, y (weighting scheme)	0.0349, 2.8816
hydrogen refinement	constr
refls in refinement	9706
parameters	671
restraints	0
$R(F_{\text{obs}})$	0.0394
$R_w(F^2)$	0.0952
S	1.028
shift/error $_{\text{max}}$	0.001
max electron density/ e \AA^{-3}	0.297
min electron density/ e \AA^{-3}	-0.226

Fe/Cr-disorder: both Fe sites are occupied by Cr as well, sof ratio Fe/Cr = 2/1.

Single-Crystal X-ray Analysis for compound III.27



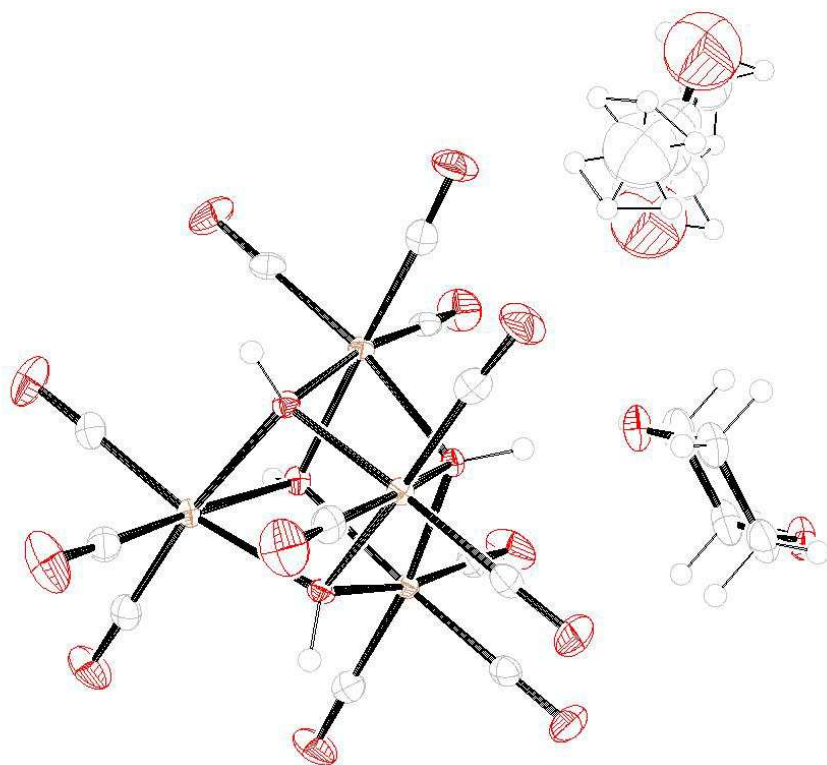
Compound	III.27·DMF·3H ₂ O
net formula	C ₁₈ H ₂₃ N ₂ O _{20.5} Re ₄
M_r /g mol ⁻¹	1340.204
crystal size/mm	0.186 × 0.175 × 0.151
T /K	200(2)
radiation	'Mo K α
diffractometer	'Bruker D8Quest'
crystal system	trigonal
space group	$P3_221$
a /Å	17.2248(2)
b /Å	17.2248(2)
c /Å	13.3495(4)
α /°	90
β /°	90
γ /°	120
V /Å ³	3430.08(12)
Z	3
calc. density/g cm ⁻³	1.94645(7)
μ /mm ⁻¹	10.611
absorption correction	multi-scan

transmission factor range	0.2124–0.3378
refls. measured	80723
R_{int}	0.0338
mean $\sigma(I)/I$	0.0151
θ range	2.36–27.61
observed refls.	5045
x , y (weighting scheme)	0.0366, 11.5936
hydrogen refinement	mixed
Flack parameter	–0.050(17)
refls in refinement	5278
parameters	205
restraints	0
$R(F_{\text{obs}})$	0.0268
$R_w(F^2)$	0.0746
S	1.211
shift/error _{max}	0.001
max electron density/e \AA^{-3}	1.348
min electron density/e \AA^{-3}	–0.735

Water hydrogens are not included, all other H : constr.

Symmetry code $i = y, x, -z$.

Single-Crystal X-ray Analysis for compound III.27



Compound	III.27·dioxane·acetone
net formula	$C_{23}H_{26}O_{21}Re_4$
$M_r/g\ mol^{-1}$	1383.268
crystal size/mm	$0.25 \times 0.22 \times 0.20$
T/K	173(2)
radiation	MoK α
diffractometer	'Oxford Xcalibur'
crystal system	tetragonal
space group	$P4_22_12$
$a/\text{\AA}$	14.7154(2)
$b/\text{\AA}$	14.7154(2)
$c/\text{\AA}$	15.0385(4)
$\alpha/^\circ$	90
$\beta/^\circ$	90
$\gamma/^\circ$	90
$V/\text{\AA}^3$	3256.48(11)
Z	4
calc. density/ $g\ cm^{-3}$	2.82146(10)

μ/mm^{-1}	14.907
absorption correction	'multi-scan'
transmission factor range	0.55301–1.00000
refls. measured	30274
R_{int}	0.0382
mean $\sigma(I)/I$	0.0241
θ range	4.11–30.50
observed refls.	4722
x, y (weighting scheme)	0.0194, 5.7767
hydrogen refinement	constr
Flack parameter	0.499(15)
refls in refinement	4959
parameters	213
restraints	1
$R(F_{\text{obs}})$	0.0213
$R_w(F^2)$	0.0499
S	1.120
shift/error _{max}	0.002
max electron density/e \AA^{-3}	0.971
min electron density/e \AA^{-3}	-1.880

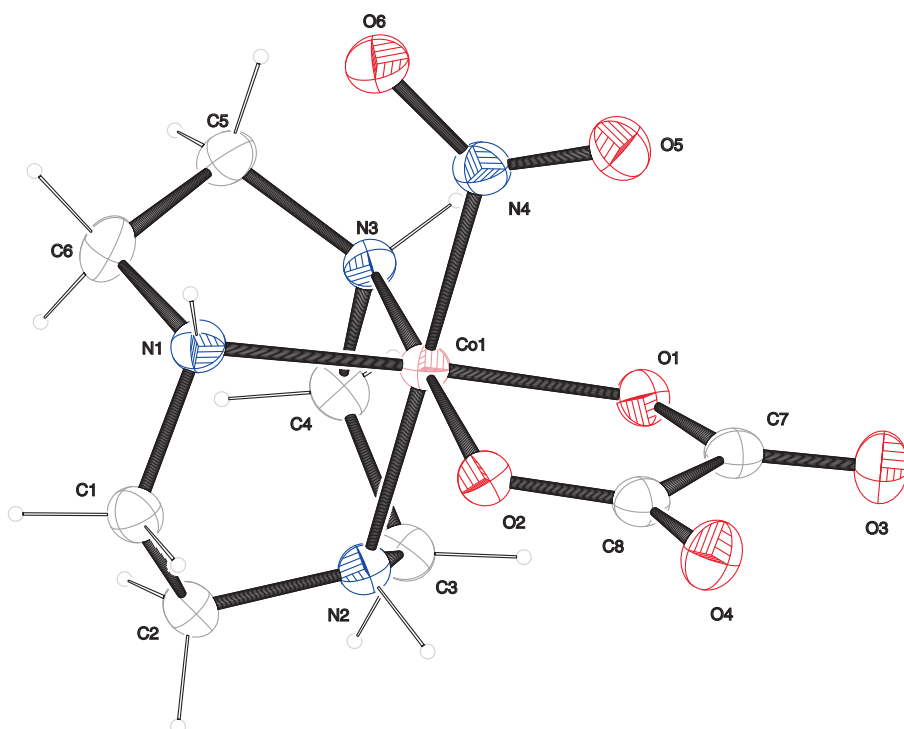
Acetone disordered, split model applied, sof fixed to 0.5.

Refined as racemic twin.

Symmetry code: $i = 1-y, 1-x, -z$.

Disordered acetone not depicted in figure.

Single-Crystal X-ray Analysis for compound III.29



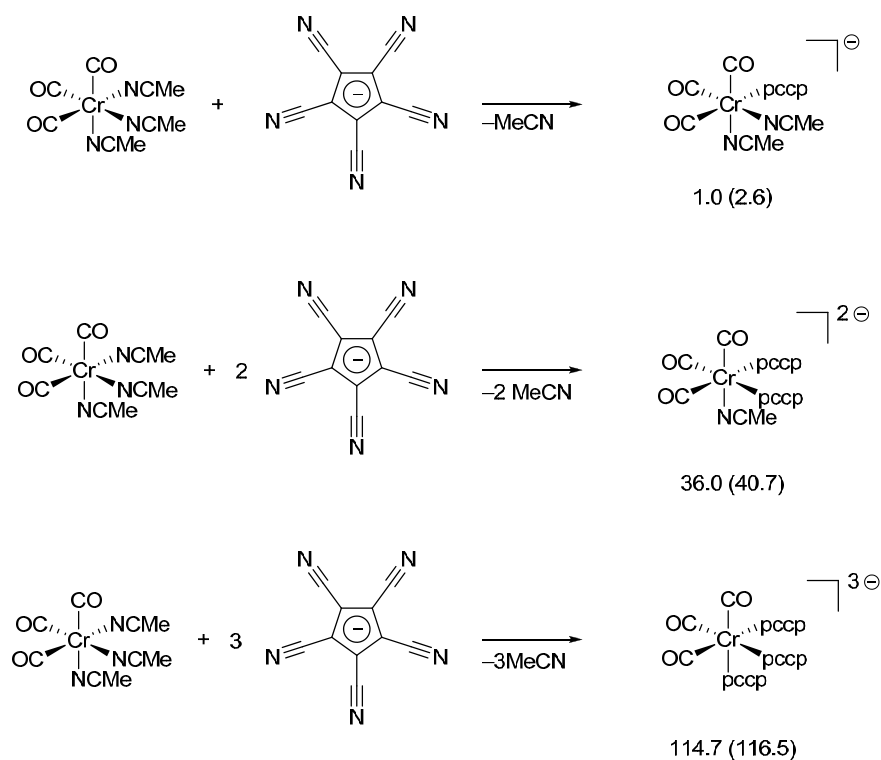
Compound	III.29
net formula	$C_8H_{15}CoN_4O_6$
$M_r/g\ mol^{-1}$	322.161
crystal size/mm	$0.15 \times 0.07 \times 0.02$
T/K	173(2)
radiation	MoK α
diffractometer	'KappaCCD'
crystal system	orthorhombic
space group	<i>Pbca</i>
$a/\text{\AA}$	13.1338(5)
$b/\text{\AA}$	10.5900(3)
$c/\text{\AA}$	16.6901(6)
$\alpha/^\circ$	90
$\beta/^\circ$	90
$\gamma/^\circ$	90
$V/\text{\AA}^3$	2321.38(14)
Z	8
calc. density/ $g\ cm^{-3}$	1.84362(11)

μ/mm^{-1}	1.511
absorption correction	none
refls. measured	13451
R_{int}	0.0608
mean $\sigma(I)/I$	0.0327
θ range	3.47–25.36
observed refls.	1688
x, y (weighting scheme)	0.0399, 1.2695
hydrogen refinement	constr
refls in refinement	2120
parameters	172
restraints	0
$R(F_{\text{obs}})$	0.0310
$R_w(F^2)$	0.0803
S	1.054
shift/error _{max}	0.001
max electron density/e \AA^{-3}	0.441
min electron density/e \AA^{-3}	-0.328

Solution of the structures of compound **III.6** requires further refinement, which is carried out by Dr. Peter Mayer in the analytics department in the Ludwig-Maximilians-Universität München. The illustration of **III.6** shown in Chapter III, Section 3.2.1, Figure III.12 is based on preliminary data, as also mentioned under the respective Figure.

Appendix 7: Computational Details

All calculations were performed by Dr. Elena Herrero-Gómez with Gaussian03.^[170] The method was B3LYP.^[171] The inner electrons of Cr were described by an effective core potential (SDD),^[172] and the associated double- ζ basis set was used for the outer electrons. The 6-31G(d) basis set was used for H, C, N.^[173] The starting complex structure was taken from available X-ray structures.^[153] Optimizations of the ligands and anionic complexes were performed. The nature of the stationary points as local minima was confirmed through frequency calculations. No solvation effects were considered in these calculations (Scheme App.7a).



Scheme App.7a: SCF Energies and Free Energies (in brackets) in kcal·mol⁻¹

Cartesian Coordinates (in Å) and Absolute Energies (in a.u.)

Cartesian coordinates of C3_AcCN (E = -825.334125110 a.u.)

Center Number	Atomic Number	Atomic Type	Coordinates (Angstroms)		
			X	Y	Z
1	6	0	0.973218	1.179828	1.612754
2	7	0	-0.626547	1.526326	-0.659442

3	8	0	1.577687	1.925306	2.275265
4	6	0	0.603614	-1.422540	1.600513
5	7	0	-1.025677	-1.288275	-0.674301
6	8	0	0.974544	-2.313460	2.255268
7	6	0	-0.999036	2.420559	-1.298818
8	7	0	1.612743	-0.226540	-0.721779
9	8	0	-2.397481	0.324268	2.347612
10	6	0	-1.643085	-2.024921	-1.324939
11	6	0	2.548030	-0.356256	-1.396748
12	6	0	-1.466010	0.196950	1.657492
13	24	0	0.013826	-0.006264	0.559311
14	6	0	-1.475245	3.568985	-2.062026
15	1	0	-1.703272	3.280446	-3.093604
16	1	0	-2.383789	3.975995	-1.605012
17	1	0	-0.713703	4.356092	-2.080144
18	6	0	3.750784	-0.523893	-2.205101
19	1	0	3.491658	-0.667299	-3.259469
20	1	0	4.391948	0.360170	-2.120356
21	1	0	4.317116	-1.397109	-1.863505
22	6	0	-2.425639	-2.978606	-2.103539
23	1	0	-3.468573	-2.976042	-1.768604
24	1	0	-2.400771	-2.722037	-3.167945
25	1	0	-2.023862	-3.990001	-1.978871

 Cartesian coordinates of AcCN (E = -132.754924908 a.u.)

Center Number	Atomic Number	Atomic Type	Coordinates (Angstroms)		
			X	Y	Z
1	7	0	-1.440859	0.000842	-0.001490
2	6	0	-0.280454	-0.001984	0.003541
3	6	0	1.180943	0.000412	-0.000725
4	1	0	1.565401	-0.226419	0.998722
5	1	0	1.559875	-0.751922	-0.699710
6	1	0	1.557805	0.981881	-0.305480

 Cartesian coordinates of C5_unit(E = -654.845730687 a.u.)

Center Number	Atomic Number	Atomic Type	Coordinates (Angstroms)		
			X	Y	Z
1	6	0	0.083319	1.204672	-0.000293
2	7	0	0.260492	3.781214	0.006349
3	6	0	-1.119728	0.451172	-0.000804

APPENDICES

4	7	0	-3.515658	1.415579	-0.005051
5	6	0	-0.774958	-0.925943	-0.000179
6	7	0	-2.435103	-2.904336	0.005002
7	6	0	0.641165	-1.023472	0.000272
8	7	0	2.012325	-3.212128	-0.001864
9	6	0	1.171510	0.293064	-0.000041
10	7	0	3.676975	0.920090	-0.003303
11	6	0	0.180480	2.618173	-0.000311
12	6	0	-2.434234	0.980211	-0.001723
13	6	0	-1.685788	-2.011258	-0.000613
14	6	0	1.393296	-2.224268	0.001941
15	6	0	2.546068	0.637159	0.000430

Cartesian coordinates of Crplex 1(E = -1347.42339992 a.u.)

Center Number	Atomic Number	Atomic Type	Coordinates (Angstroms)		
			X	Y	Z
1	6	0	2.776791	-0.363932	-2.136672
2	7	0	2.259895	1.715359	-0.306276
3	8	0	2.893931	-0.387614	-3.297722
4	6	0	2.847925	-2.163217	-0.226063
5	7	0	2.359738	-0.235655	1.749955
6	8	0	3.016740	-3.317340	-0.183891
7	6	0	1.978049	2.839440	-0.345097
8	8	0	5.603331	0.067097	-0.037176
9	6	0	2.168344	-0.210593	2.894109
10	6	0	4.447092	-0.083173	-0.133777
11	24	0	2.621809	-0.326617	-0.289762
12	6	0	1.585668	4.242293	-0.414801
13	1	0	2.071303	4.816426	0.381760
14	1	0	1.877574	4.667810	-1.381130
15	1	0	0.497180	4.312714	-0.303257
16	6	0	1.939360	-0.198765	4.334335
17	1	0	2.831496	0.156636	4.861577
18	1	0	1.100671	0.460644	4.582410
19	1	0	1.703299	-1.207940	4.689356
20	6	0	-2.001984	-0.263818	-0.218526
21	7	0	0.563714	-0.449311	-0.347524
22	6	0	-2.700261	0.973875	-0.124787
23	7	0	-1.598503	3.306491	-0.074374
24	6	0	-4.088660	0.691517	-0.047469

25	7	0	-5.973268	2.445672	0.154863
26	6	0	-4.250949	-0.717546	-0.092146
27	7	0	-6.500746	-1.981686	0.014951
28	6	0	-2.963997	-1.308288	-0.196782
29	7	0	-2.470520	-3.841211	-0.295523
30	6	0	-0.599955	-0.397743	-0.297621
31	6	0	-2.103259	2.255447	-0.100162
32	6	0	-5.125648	1.650940	0.062053
33	6	0	-5.484840	-1.412775	-0.034911
34	6	0	-2.690198	-2.697367	-0.254791

 Cartesian coordinates of Crplex2 (E = -1869.45832005 a.u.)

Center Number	Atomic Number	Atomic Type	Coordinates (Angstroms)		
			X	Y	Z
1	6	0	-1.289829	3.798115	0.597631
2	7	0	-0.001548	1.685174	2.023517
3	8	0	-2.088997	4.600495	0.891947
4	6	0	0.004089	3.191821	-1.607381
5	8	0	0.006294	3.621569	-2.692649
6	6	0	-0.003124	1.084838	3.014551
7	8	0	2.105874	4.586520	0.889864
8	6	0	1.301251	3.789040	0.597075
9	24	0	0.001304	2.559282	0.132407
10	6	0	-0.005368	0.289974	4.236635
11	1	0	0.887412	-0.345540	4.249817
12	1	0	0.000273	0.943317	5.116096
13	1	0	-0.905342	-0.335148	4.253296
14	6	0	-3.405738	-0.532165	-0.360335
15	7	0	-1.455622	1.149375	-0.251923
16	6	0	-3.871777	-1.277183	0.760242
17	7	0	-2.906652	-1.190413	3.152552
18	6	0	-4.973255	-2.067402	0.338656
19	7	0	-6.352304	-3.671430	1.820445
20	6	0	-5.191125	-1.812572	-1.040465
21	7	0	-7.039510	-2.881868	-2.493478
22	6	0	-4.224625	-0.865373	-1.472881
23	7	0	-4.051536	0.073753	-3.872256
24	6	0	-2.331832	0.384400	-0.335876
25	6	0	-3.339195	-1.229922	2.070331
26	6	0	-5.728070	-2.948362	1.151553

APPENDICES

27	6	0	-6.202943	-2.398414	-1.840701
28	6	0	-4.118173	-0.344773	-2.786354
29	6	0	3.402221	-0.538796	-0.355842
30	7	0	1.449303	1.139717	-0.250669
31	6	0	3.861711	-1.291006	0.762610
32	7	0	2.879603	-1.220973	3.148559
33	6	0	4.967437	-2.076397	0.343147
34	7	0	6.339187	-3.688270	1.823189
35	6	0	5.194121	-1.811776	-1.032709
36	7	0	7.054108	-2.867957	-2.480513
37	6	0	4.229194	-0.862970	-1.465109
38	7	0	4.071119	0.092601	-3.859015
39	6	0	2.326762	0.375896	-0.332214
40	6	0	3.319918	-1.253409	2.069242
41	6	0	5.718210	-2.961668	1.155091
42	6	0	6.212298	-2.390443	-1.830109
43	6	0	4.130838	-0.333459	-2.775643

Cartesian coordinates of Crplex3 (E = -2391.42383805 a.u.)

Center Number	Atomic Number	Atomic Type	Coordinates (Angstroms)		
			X	Y	Z
1	6	0	1.168200	0.938403	3.258396
2	8	0	1.896348	1.505535	3.975086
3	6	0	0.248087	-1.492788	3.251474
4	8	0	0.376728	-2.410796	3.963016
5	8	0	-2.247520	0.862539	3.986726
6	6	0	-1.394730	0.520190	3.264810
7	24	0	0.004231	-0.007630	2.174424
8	6	0	3.790648	-1.190643	-0.231479
9	7	0	1.591979	-0.552683	0.957236
10	6	0	4.345319	-0.592078	-1.396649
11	7	0	3.353209	1.330880	-2.805990
12	6	0	5.588978	-1.221146	-1.667816
13	7	0	7.208009	-0.675820	-3.604986
14	6	0	5.807562	-2.209638	-0.671640
15	7	0	7.878695	-3.744011	-0.505658
16	6	0	4.698929	-2.191661	0.215461
17	7	0	4.484565	-3.731318	2.277486
18	6	0	2.572339	-0.839668	0.394624
19	6	0	3.783907	0.460877	-2.160829

20	6	0	6.470243	-0.917696	-2.734222
21	6	0	6.940213	-3.054527	-0.578319
22	6	0	4.559208	-3.028855	1.349831
23	6	0	-2.946357	-2.684998	-0.202790
24	7	0	-1.273827	-1.106353	0.965507
25	6	0	-4.310898	-2.853284	0.166286
26	7	0	-5.614529	-1.647924	2.041416
27	6	0	-4.876677	-3.846890	-0.675770
28	7	0	-7.305980	-4.720987	-0.599244
29	6	0	-3.865438	-4.295518	-1.566485
30	7	0	-4.170304	-6.118179	-3.370984
31	6	0	-2.674540	-3.579499	-1.275038
32	7	0	-0.430752	-3.932791	-2.503378
33	6	0	-2.022788	-1.808881	0.412759
34	6	0	-5.007893	-2.177124	1.197945
35	6	0	-6.210394	-4.320970	-0.631943
36	6	0	-4.025383	-5.292224	-2.559904
37	6	0	-1.436379	-3.757193	-1.940739
38	6	0	-0.847783	3.877978	-0.215416
39	7	0	-0.315998	1.648106	0.967486
40	6	0	-0.372649	5.155375	0.196000
41	7	0	1.189590	5.712229	2.175334
42	6	0	-0.924665	6.132800	-0.673658
43	7	0	-0.543462	8.684454	-0.550633
44	6	0	-1.741723	5.464040	-1.623622
45	7	0	-3.083914	6.615517	-3.506154
46	6	0	-1.694853	4.073354	-1.341415
47	7	0	-2.988140	2.277581	-2.672201
48	6	0	-0.551376	2.643975	0.408191
49	6	0	0.488126	5.437995	1.285202
50	6	0	-0.710942	7.530977	-0.604138
51	6	0	-2.478655	6.087569	-2.660020
52	6	0	-2.394295	3.074084	-2.062666

Appendix 8: Screening Tables

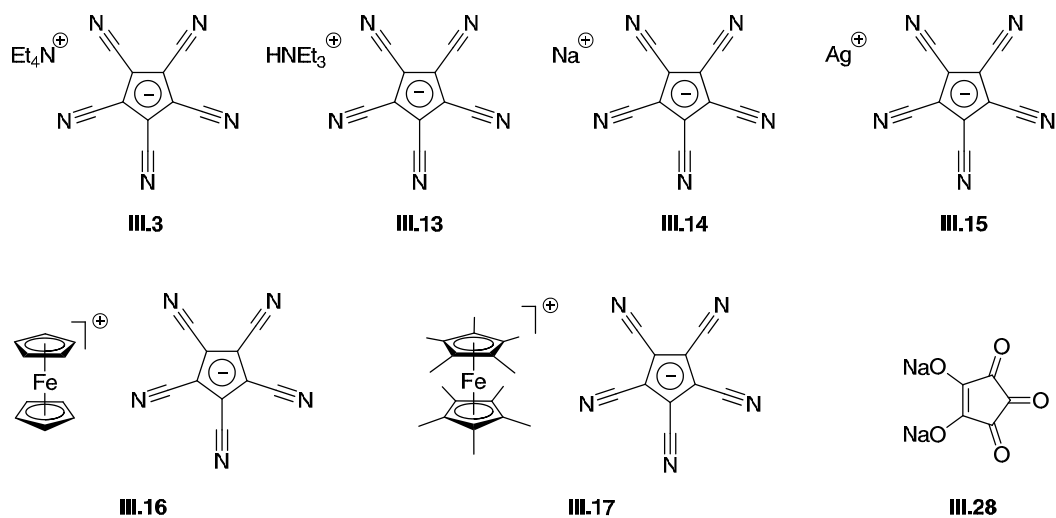
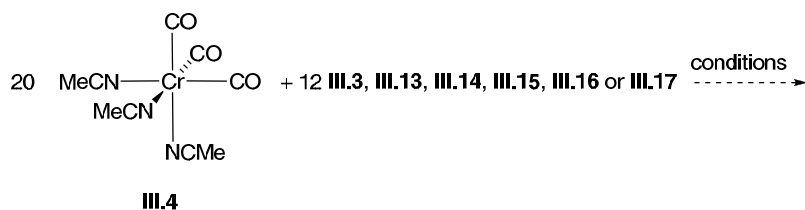


Figure App.8a: Chemical structure of pccp salts and of disodium croconate

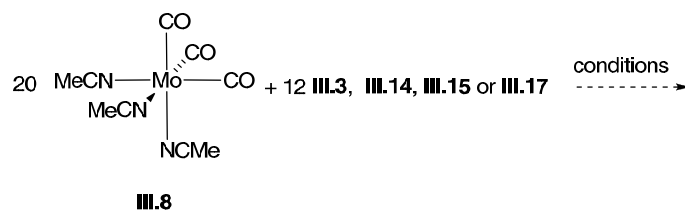


Entry	Pccp salt	Additive	Solvent	Temperature	Time	Observation
1	Et ₄ N, III.3	-	MeCN	reflux	16 h	starting material
2	Et ₄ N, III.3	-	MeCN	r.t.	6 d	starting material ^[a]
3	Et ₄ N, III.3	-	MeCN	reflux	6 d	complex mixture
4	Et ₄ N, III.3	-	toluene	reflux	48 h	starting material
5	Et ₄ N, III.3	-	THF	reflux	48 h	complex mixture
6	Et ₄ N, III.3	-	DMSO	100 °C	48 h	complex mixture
7	Et ₄ N, III.3	-	DME	reflux	48 h	complex mixture
8	Et ₄ N, III.3	-	diglyme	reflux	48 h	complex mixture
9	Et ₄ N, III.3	-	acetone	reflux	48 h	complex mixture
10	Et ₄ N, III.3	C ₆₀ (III.6)	<i>o</i> -C ₆ H ₄ Cl ₂	reflux	96 h	starting material ^[b]
11	Et ₄ N, III.3	C ₆₀ (III.6)	acetone	reflux	48 h	complex mixture
12	HNEt ₃ , III.13	-	MeCN	reflux	16 h	starting material
13	HNEt ₃ , III.13	-	MeCN	reflux	6 d	complex mixture

14	Ag, III.15	-	MeCN ^[c]	reflux	16 h	complex mixture
15	Ag, III.15	-	MeCN ^[c]	reflux	6 d	complex mixture
16	Ag, III.15	-	MeCN ^[c]	r.t.	6 d	starting material
17	Ag, III.15	-	DMSO ^[c]	120 °C	48 h	complex mixture
18	Ag, III.15	C ₆₀ (III.6)	<i>o</i> -C ₆ H ₄ Cl ₂	reflux	72 h	complex mixture
19	Na, III.14	-	MeCN	reflux	16 h	starting material
20	Na, III.14	-	MeCN	reflux	6 d	complex mixture
21	Na, III.14	-	MeCN	r.t.	6 d	starting material
22	Na, III.14	-	toluene	reflux	48 h	starting material
23	Na, III.14	-	THF	reflux	48 h	complex mixture
24	Na, III.14	-	DME	reflux	48 h	complex mixture
25	Na, III.14	-	diglyme	reflux	48 h	complex mixture
26	Na, III.14	C ₆₀ (III.6)	<i>o</i> -C ₆ H ₄ Cl ₂	reflux	72 h	starting material
27	cp ₂ Fe, III.16	-	MeCN	reflux	16 h	complex mixture ^[d]
28	cp ₂ Fe, III.16	-	MeCN	r.t.	6 d	complex mixture ^[d]
29	cp ₂ Fe, III.16	-	THF	50 °C	16 h	complex mixture ^[d]
30	cp ₂ Fe, III.16	-	DMF	r.t.	16 h	complex mixture ^[d]
31	cp ₂ Fe, III.16	C ₆₀ (III.6)	<i>o</i> -C ₆ H ₄ Cl ₂	80 °C	16 h	complex mixture ^[d]
32	cp* ₂ Fe, III.17	-	MeCN	reflux	16 h	complex mixture ^[e]
33	cp* ₂ Fe, III.17	-	MeCN	r.t.	6 d	complex mixture ^[e]
34	cp* ₂ Fe, III.17	-	acetone	reflux	24 h	complex mixture ^[e,f]
35	cp* ₂ Fe, III.17	C ₆₀ (III.6)	<i>o</i> -C ₆ H ₄ Cl ₂	r.t.	16 h	complex mixture ^[e]
36	cp* ₂ Fe, III.17	C ₆₀ (III.6)	benzene	reflux	16 h	complex mixture ^[e]

[a] Upon recrystallization, crystalline material of **III.3** was obtained (*Cc*-cell, Chapter III, Section 3.2.1, Figure III.13) [b] crystal structure of C₆₀·*o*-C₆H₄Cl₂ was obtained upon recrystallization (Chapter III, Section 3.2.1, Figure III.12); [c] reaction was performed as a suspension due to low solubility of **III.15**; [d] ferrocene (**III.33**) was formed during the reaction, which could be separated by filtration and was the only reaction product that could be characterized; [e] decamethylferrocene (**III.35**) was formed during the reaction, which could be separated by filtration and was the only reaction product that could be characterized; [f] crystal structure of decamethylmetallocenium (Fe_{0.67}Cr_{0.33}) pccp (**III.18**) was obtained upon recrystallization (Chapter III, Section 3.2.1, Figure III.17)

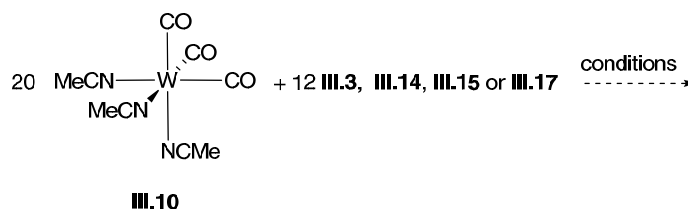
Table App.8a: Conditions and observations for self-assembly of **III.4** with pccp salts.



Entry	Pccp salt	Additive	Solvent	Temperature	Time	Observation
1	Et ₄ N, III.3	-	MeCN	reflux	96 h	complex mixture
2	Et ₄ N, III.3	-	DME	reflux	24 h	complex mixture
3	Et ₄ N, III.3	-	diglyme	reflux	48 h	complex mixture
4	Et ₄ N, III.3	C ₆₀ (III.6)	<i>o</i> -C ₆ H ₄ Cl ₂	reflux	96 h	starting material
5	Ag, III.15	-	MeCN ^[a]	reflux	16 h	complex mixture
6	Na, III.14	-	MeCN	reflux	72 h	starting material
7	Na, III.14	-	MeCN	reflux	6 d	complex mixture
8	Na, III.14	-	MeCN	r.t.	6 d	starting material
9	Na, III.14	-	DME	reflux	48 h	complex mixture
10	cp* ₂ Fe, III.17	-	MeCN	reflux	16 h	complex mixture

[a] Reaction was performed as a suspension due to low solubility of **III.15**.

Table App.8b: Conditions and observations for self-assembly of **III.7** with pccp salts.

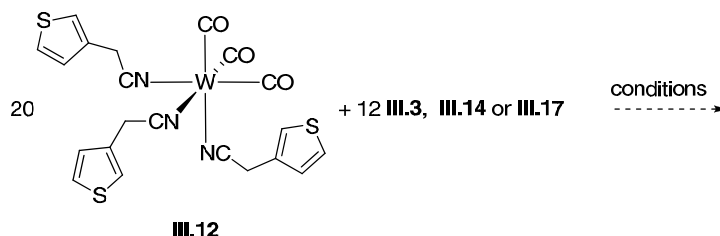


Entry	Pccp salt	Additive	Solvent	Temperature	Time	Observation
1	Et ₄ N, III.3	-	MeCN	reflux	6 d	complex mixture
2	Et ₄ N, III.3	-	DME	reflux	96 h	complex mixture
3	Et ₄ N, III.3	-	MeCN	microwave, 80 °C	2 h	complex mixture ^[a]
4	Et ₄ N, III.3	C ₆₀ (III.6)	<i>o</i> -C ₆ H ₄ Cl ₂	reflux	96 h	starting material
5	Ag, III.15	-	MeCN ^[b]	reflux	16 h	complex mixture
6	Na, III.14	-	MeCN	reflux	16 h	complex mixture
7	Na, III.14	-	MeCN	reflux	6 d	complex mixture
8	Na, III.14	-	DME	r.t.	6 d	complex mixture
9	Na, III.14	-	diglyme	reflux	48 h	complex mixture
10	Na, III.14	-	dioxane	reflux	24 h	complex mixture

11 cp^*_2Fe , **III.17** - MeCN reflux 16 h complex mixture

[a] Upon recrystallization crystalline material of **III.3** was obtained (Cc-cell, Chapter III, Section 3.2.1, Figure III.13); [b] reaction was performed as a suspension due to low solubility of **III.15**.

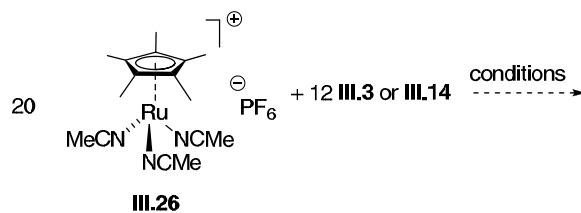
Table App.8c: Conditions and observations for self-assembly of **III.10** with pccp salts.



Entry	Pccp salt	Additive	Solvent	Temperature	Time	Observation
1	Et ₄ N, III.3	-	MeCN	reflux	6 d	complex mixture
2	Et ₄ N, III.3	-	DME	reflux	24 h	complex mixture
3	Et ₄ N, III.3	C ₆₀ (III.6)	<i>o</i> -C ₆ H ₄ Cl ₂	reflux	72 h	starting material ^[a]
4	Na, III.14	-	MeCN	reflux	16 h	complex mixture
5	Na, III.14	-	DME	r.t.	6 d	complex mixture
6	Na, III.14	-	DMSO	80 °C	24 h	complex mixture
7	cp^*_2Fe , III.17	-	MeCN	reflux	16 h	complex mixture

[a] Upon recrystallization crystalline material of **III.3** was obtained (Cc-cell, Chapter III, Section 3.2.1, Figure III.13).

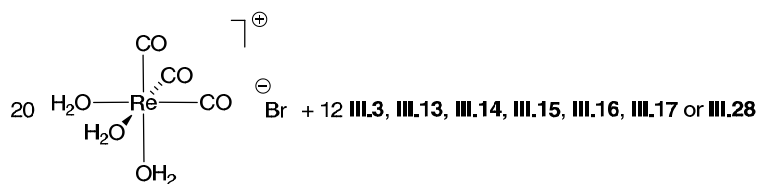
Table App.8d: Conditions and observations for self-assembly of **III.12** with pccp salts.



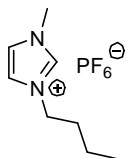
Entry	Pccp salt	Additive	Solvent	Temperature	Time	Observation
1	Et ₄ N, III.3	-	CD ₃ CN	r.t.	18 h	starting material
2	Et ₄ N, III.3	-	CD ₂ Cl ₂ ^[a]	r.t.	18 h	complex mixture
3	Et ₄ N, III.3	-	<i>d</i> ₆ -acetone	r.t.	18 h	starting material
4	Et ₄ N, III.3	-	H ₂ O/EtOH	reflux	1 h	complex mixture
5	Et ₄ N, III.3	-	THF	reflux	1 h	complex mixture
6	Et ₄ N, III.3	C ₆₀ (III.6)	<i>o</i> -C ₆ H ₄ Cl ₂	80 °C	24 h	complex mixture
7	Na, III.14	-	MeCN	reflux	16 h	complex mixture

[a] Reaction was performed as a suspension due to low solubility of **III.3**.

Table App.8e: Conditions and observations for self-assembly of **III.26** with pccp salts.



additive, solvent, r.t. 18 h,
then vapor diffusion of a non-
 solvent into the reaction
 mixture over a period of time
 ----->

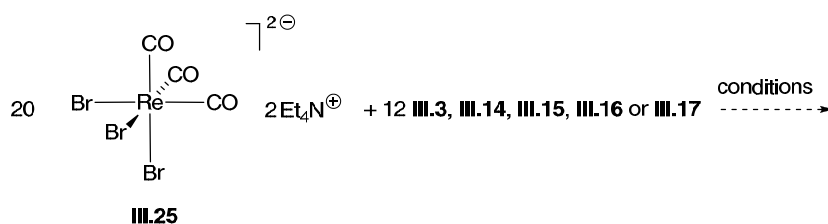
III.24**III.37**

Entry	Pccp salt	Additive	Solvent	Non-solvent	Time	Observation
1	Et ₄ N, III.3	-	H ₂ O, THF	Et ₂ O	2 d	starting material
2	Et ₄ N, III.3	-	H ₂ O, acetone	EtOAc	20 d	starting material
3	Et ₄ N, III.3	-	diglyme	Et ₂ O	4 d	starting material
4	Et ₄ N, III.3	-	diglyme	CHCl ₃	11 d	starting material
5	Et ₄ N, III.3	-	ionic liquid III.37	MeNO ₂ , Et ₂ O	18 d	complex mixture
6	Et ₄ N, III.3	-	ionic liquid III.37	THF	14 d	complex mixture
7	Et ₄ N, III.3	-	ionic liquid III.37	CHCl ₃	12 d	complex mixture
8	Et ₄ N, III.3	-	DMSO	Et ₂ O ^[a]	12 d	starting material ^[b]
9	Et ₄ N, III.3	C ₆₀ (III.6)	<i>o</i> -C ₆ H ₄ Cl ₂ ^[c]	- ^[d]	52 d	starting material
10	HNEt ₃ , III.13	-	H ₂ O, acetone	Et ₂ O	3 d	starting material
11	Na, III.15	-	H ₂ O, acetone ^[e]	Et ₂ O	3 d	complex mixture
12	Na, III.15	-	H ₂ O, acetone ^[e]	CHCl ₃	5 d	complex mixture
13	Na, III.15	-	MeCN	Et ₂ O	2 d	complex mixture
14	Na, III.15	-	MeCN	CHCl ₃	4 d	complex mixture
15	Na, III.15	-	MeCN	- ^[d]	5 d	complex mixture
16	Na, III.15	-	DMSO	Et ₂ O	4 d	complex mixture
17	Na, III.15	-	DMSO	EtOAc	18 d	complex mixture
18	Na, III.15	-	DMSO	MTBE	4 d	complex mixture
19	Na, III.15	-	DMSO	CH ₂ Cl ₂	4 d	complex mixture
20	Na, III.15	-	DMSO	CHCl ₃	4 d	complex mixture
21	Na, III.15	-	DMSO	H ₂ O	14 d	complex mixture
22	Na, III.15	-	DMSO	EtOH	21 d	complex mixture
23	Na, III.15	-	dioxane, H ₂ O	acetone	21 d	formation of III.27 ^[f]
24	Na, III.15	-	DMF	Et ₂ O	5 d	complex mixture
25	Na, III.15	-	DMF	EtOAc	5 d	complex mixture
26	Na, III.15	-	DMF	MTBE	5 d	complex mixture
27	Na, III.15	-	DMF	CH ₂ Cl ₂	16 d	complex mixture

28	Na, III.15	-	DMF	CHCl ₃	8 d	complex mixture
29	Na, III.15	-	DMF	benzene	8 d	complex mixture
30	Na, III.15	-	DMF	H ₂ O	20 d	formation of III.27 ^[g]
31	Na, III.15	-	DMF	EtOH	8 d	complex mixture
32	Na, III.15	-	MeNO ₂	Et ₂ O	3 d	complex mixture
33	Na, III.15	-	MeNO ₂	CH ₂ Cl ₂	3 d	complex mixture
34	Na, III.15	-	MeNO ₂	- ^[d]	25 d	complex mixture
35	Ag, III.14	-	H ₂ O ^[h]	-	-	starting material
36	Ag, III.14	-	DMSO ^[h]	-	-	starting material
37	Ag, III.14	-	DMF ^[h]	-	-	starting material
38	cp ₂ Fe, III.16	-	acetone	- ^[d]	6 d	starting material
39	cp ₂ Fe, III.16	C ₆₀ (III.6)	acetone	- ^[d]	8 d	starting material
40	cp ₂ Fe, III.16	-	MeCN	- ^[d]	5 d	complex mixture
41	cp ₂ Fe, III.16	-	DMF	Et ₂ O	5 d	complex mixture
42	cp* ₂ Fe, III.17	-	MeCN	- ^[d]	10 d	complex mixture
43	cp* ₂ Fe, III.17	-	acetone	- ^[d]	10 d	complex mixture
44	cp* ₂ Fe, III.17	C ₆₀ (III.6)	acetone	- ^[d]	10 d	complex mixture
45	cp* ₂ Fe, III.17	-	DMF	Et ₂ O	3 d	complex mixture
46	cp* ₂ Fe, III.17	-	DMSO	Et ₂ O	3 d	complex mixture
47	cp* ₂ Fe, III.17	-	MeNO ₂	Et ₂ O	3 d	complex mixture
48	III.28	-	H ₂ O	- ^[d]	24 d	complex mixture
49	III.28	-	H ₂ O	acetone	12 d	complex mixture

[a] Initially, a biphasic system of Et₂O over DMSO was obtained; solvents diffusion was then triggered by addition of 2 drops of THF to the ether layer [b] crystalline material of **III.3** was obtained (Cc-cell, Chapter III, Section 3.2.1, Figure III.13); [c] Reaction was performed as a suspension due to low solubility of **III.14**; [d] sample was filtered and solvent was allowed to evaporate; [e] mixture was heated to 60 °C until a homogenous solution was obtained (30 min); [f] **III.27**·dioxane·acetone was obtained as a crystalline solid (for crystal structure see Chapter III, Section 3.2.1, Figure III.19); [g] **III.27**·DMF·3H₂O was obtained as a crystalline solid (for crystal structure see Chapter III, Section 3.2.1, Figure III.18); [h] Reaction was performed as a suspension due to low solubility of **III.14**.

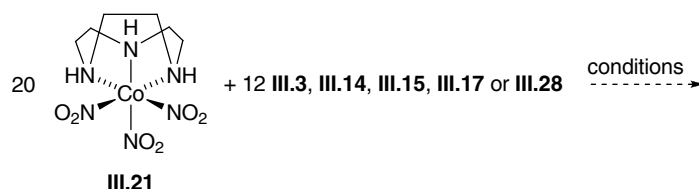
Table App.8f. Conditions and observations for self-assembly of **III.24** with pccp salts and **III.28**.



Entry	Pccp salt	Additive	Solvent	Temperature	Time	Observation
1	Et ₄ N, III.3	-	MeCN	reflux	48 h	starting material
2	Et ₄ N, III.3	-	acetone	reflux	48 h	starting material ^[a]
3	Et ₄ N, III.3	-	DMSO	100 °C	48 h	starting material
4	Et ₄ N, III.3	NaPF ₆	MeCN	reflux	48 h	starting material
5	Na, III.15	-	MeCN	reflux	48 h	formation of III.3 ^[b]
6	Na, III.15	-	acetone	reflux	48 h	formation of III.3 ^[b]
7	Na, III.15	-	DMSO	100 °C	48 h	formation of III.3
8	Na, III.15	NaPF ₆	MeCN	reflux	48 h	formation of III.3
9	Ag, III.14	-	H ₂ O ^[c]	reflux	48 h	complex mixture
10	Ag, III.14	-	DMSO ^[c]	100 °C	48 h	complex mixture
11	Ag, III.14	-	DMF ^[c]	100 °C	48 h	complex mixture
12	cp ₂ Fe, III.16	-	MeCN	reflux	48 h	formation of III.3
13	cp ₂ Fe, III.16	-	acetone	reflux	48 h	formation of III.3
14	cp ₂ Fe, III.16	-	DMSO	100 °C	48 h	complex mixture
15	cp* ₂ Fe, III.17	-	MeCN	reflux	48 h	formation of III.3
16	cp* ₂ Fe, III.17	-	acetone	reflux	48 h	formation of III.3 ^[b]
17	cp* ₂ Fe, III.17	-	DMSO	100 °C	48 h	complex mixture

[a] crystalline material of **III.3** was obtained (*Pc*-cell, Chapter III, Section 3.2.1, Figure III.14); [b] crystalline material of **III.3** was obtained (*Cc*-cell, Chapter III, Section 3.2.1, Figure III.13); [c] Reaction was performed as a suspension due to low solubility of **III.14**.

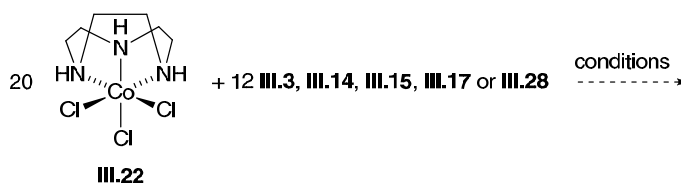
Table App.8g: Conditions and observations for self-assembly of **III.25** with pccp salts.



Entry	Pccp salt	Additive	Solvent	Temperature	Time	Observation
1	Et ₄ N, III.3	-	DMSO	100 °C	72 h	complex mixture
2	Et ₄ N, III.3	-	H ₂ O, acetone	reflux	72 h	complex mixture
3	Ag, III.14	-	DMSO	100 °C	72 h	complex mixture
4	Na, III.15	-	DMSO	100 °C	72 h	complex mixture
5	cp* ₂ Fe, III.17	-	DMSO	100 °C	72 h	complex mixture
6	III.28	-	H ₂ O	reflux	72 h	formation of III.29 ^[a]

[a] upon slow evaporation of solvent on air, crystalline material of **III.29** was obtained after 14 days (for crystal structure see Chapter III, Section 3.2.1, Figure III.20).

Table App.8h: Conditions and observations for self-assembly of **III.21** with pccp salts and **III.28**.



Entry	Pccp salt	Additive	Solvent	Temperature	Time	Observation
1	Et ₄ N, III.3	-	DMSO ^[a]	100 °C	72 h	complex mixture
2	Et ₄ N, III.3	-	H ₂ O, acetone ^[a]	reflux	72 h	complex mixture
3	Ag, III.14	-	DMSO ^[a]	100 °C	72 h	complex mixture
4	Na, III.15	-	DMSO ^[a]	100 °C	72 h	complex mixture
5	cp* ₂ Fe, III.17	-	DMSO ^[a]	100 °C	72 h	complex mixture
6	III.28	-	H ₂ O ^[a]	reflux	72 h	complex mixture

[a] Reaction was performed as a suspension due to low solubility of **III.22**.

Table App.8i: Conditions and observations for self-assembly of **III.22** with pccp salts and **III.28**.

REFERENCES

- [1] R. M. Wilson, S. J. Danishefsky, *J. Org. Chem.* **2006**, *71*, 8329–8351.
- [2] *Durchschnittliche weitere Lebenserwartung nach Altersstufen ab 1871-81 bis 2009-11*, Arbeitsschriften des Statistischen Bundesamtes, **2012**.
- [3] J. Kobayashi, H. Morita, *The Alkaloids, Vol. 60*, Cordell, G. A., Ed.; Academic Press, San Diego, **2003**.
- [4] C. H. Heathcock, *Angew. Chem.* **1992**, *104*, 675–691.
- [5] a) H. Morita, J. Kobayashi, *Tetrahedron* **2002**, *58*, 6637–6641; b) J. Kobayashi, S. Ueno, H. Morita, *J. Org. Chem.* **2002**, *67*, 6546–6549.
- [6] S. Mu, X. Yang, Y. Di, H. He, Y. Wang, Y. Wang, L. Li, X. Hao, *Chem. Biodiv.* **2007**, *4*, 129–138.
- [7] S. Saito, H. Yahata, T. Kubota, Y. Obara, N. Nakahata, J. Kobayashi, *Tetrahedron* **2008**, *64*, 1901–1908.
- [8] S. Yagi, *Kyoto Igaku Zasshi* **1909**, *6*, 208–222.
- [9] J. Kobayashi, T. Kubota, *Natural Product Reports* **2009**, *26*, 936–962 and references therein.
- [10] a) Y. Zhang, H. He, L. Guo, S. Li, Y. Di, X. Hao, *Z. Naturforsch.* **2012**, *67b*, 407–410; b) C. Tan, Y. Wang, Y. Di, H. He, S. Mu, S. Li, Y. Zhang, X. Hao, *Tetrahedron Lett.* **2012**, *53*, 2588–2591.
- [11] S. Mu, J. Wang, X. Yang, H. He, C. Li, Y. Di, Y. Wang, Y. Zhang, X. Fang, L. Huang, X. Hao, *J. Nat. Prod.* **2008**, *71*, 564–569.
- [12] T. He, Y. Zhou, Y. Wang, S. Mu, X. Hao, *Helv. Chim. Acta* **2011**, *94*, 1019–1023.
- [13] T. Kubota, Y. Matsuno, H. Morita, T. Shinzato, M. Sekiguchi, J. Kobayashi, *Tetrahedron* **2006**, *62*, 4743–4748.
- [14] H. Morita, N. Yoshida, J. Kobayashi, *Tetrahedron* **2000**, *56*, 2641–2646.
- [15] C. Lia, Y. Dia, J. Guo, Q. Zhang, X. Fang, X. Hao, *Z. Naturforsch.* **2010**, *65b*, 1406–1408.
- [16] C. Zhang, S. Yang, J. Yue, *J. Nat. Prod.* **2008**, *71*, 1663–1668.
- [17] H. Morita, N. Yoshida, J. Kobayashi, *J. Org. Chem.* **1999**, *64*, 7208–7212.
- [18] T. Yang, Y. Di, H. He, Q. Zhang, Y. Zhang, X. Hao, *Helv. Chim. Acta* **2011**, *94*, 397–403.
- [19] C. Zhang, C. Fan, S. Dong, H. Liu, W. Zhou, Y. Wu, J. Yue, *Org. Lett.* **2011**, *13*, 2440–2443.
- [20] H. Morita, N. Ishioka, H. Takatsu, T. Shinzato, Y. Obara, N. Nakahata, J. Kobayashi, *Org. Lett.* **2005**, *7*, 459–462.
- [21] N. Kong, H. He, Y. Wang, S. Mu, Y. Di, X. Hao, *J. Nat. Prod.* **2007**, *70*, 1348–1351.
- [22] H. Takatsu, H. Morita, Y. Shen, J. Kobayashi, *Tetrahedron* **2004**, *60*, 6279–6284.
- [23] X. Chen, Z. Zhan, J. Yue, *Chem. Biodiv.* **2004**, *1*, 1513–1518.
- [24] Y. Di, H. He, Y. Wang, L. Li, Y. Lu, J. Gong, X. Fang, N. Kong, S. Li, H. Zhu, X. Hao, *Org. Lett.* **2007**, *9*, 1355–1358.
- [25] S. Saito, T. Kubota, J. Kobayashi, *Tetrahedron Lett.* **2007**, *48*, 3809–3812.

- [26] C. Li, Y. Di, S. Mu, H. He, Q. Zhang, X. Fang, Y. Zhang, S.-L. Li, Y. Lu, Y. Gong, X. Hao, *J. Nat. Prod.* **2008**, *71*, 1202–1206.
- [27] S. Saito, T. Kubota, J. Kobayashi, *Tetrahedron Lett.* **2007**, *48*, 5693–5695.
- [28] K. T. Suzuki, S. Okuda, H. Niwa, M. Toda, Y. Hirata, S. Yamamura, *Tetrahedron Lett.* **1973**, *14*, 799–802.
- [29] C. H. Heathcock, S. Piettre, J. C. Kath, *Pure Appl. Chem.* **1990**, *62*, 1911–1920.
- [30] S. Piettre, C. H. Heathcock, *Science* **1990**, *248*, 1532–1534.
- [31] H. Niwa, Y. Hirata, K. T. Suzuki, S. Yamamura, *Tetrahedron Lett.* **1973**, *14*, 2129–2132.
- [32] a) C. H. Heathcock, S. Piettre, R. B. Ruggeri, J. A. Ragan, J. C. Kath, *J. Org. Chem.* **1992**, *57*, 2554–2566; b) C. H. Heathcock, D. Joe, *J. Org. Chem.* **1995**, *60*, 1131–1142; c) C. H. Heathcock, *Proc. Natl. Acad. Sci.* **1996**, *93*, 14323–14327.
- [33] R. B. Ruggeri, C. H. Heathcock, *Pure Appl. Chem.* **1989**, 289–292.
- [34] J. Orban, J. V. Turner, *Tetrahedron Lett.* **1983**, *24*, 2697–2700.
- [35] S. Nishiyama, Y. Ikeda, S. Yamamura, *Bull. Chem. Soc. Jpn.* **1986**, *59*, 875–878.
- [36] H. Irikawa, N. Sakabe, S. Yamamura, Y. Hirata, *Tetrahedron* **1968**, *24*, 5691–5700.
- [37] a) C. H. Heathcock, S. K. Davidsen, S. Mills, M. A. Sanner, *J. Am. Chem. Soc.* **1986**, *108*, 5650–5651; b) C. H. Heathcock, S. K. Davidsen, S. G. Mills, M. A. Sanner, *J. Org. Chem.* **1992**, *57*, 2531–2544.
- [38] a) R. B. Ruggeri, C. H. Heathcock, *J. Org. Chem.* **1987**, *52*, 5745–5746; b) R. B. Ruggeri, K. F. McClure, C. H. Heathcock, *J. Am. Chem. Soc.* **1989**, *111*, 1530–1531.
- [39] a) R. B. Ruggeri, M. M. Hansen, C. H. Heathcock, *J. Am. Chem. Soc.* **1988**, *110*, 8734–8736; b) C. H. Heathcock, M. M. Hansen, R. B. Ruggeri, J. C. Kath, *J. Org. Chem.* **1992**, *57*, 2544–2553.
- [40] R. B. Ruggeri, C. H. Heathcock, *J. Org. Chem.* **1990**, *55*, 3714–3715.
- [41] C. H. Heathcock, R. B. Ruggeri, K. F. McClure, *J. Org. Chem.* **1992**, *57*, 2585–2594.
- [42] a) J. A. Stafford, C. H. Heathcock, *J. Org. Chem.* **1990**, *55*, 5433–5434; b) C. H. Heathcock, J. A. Stafford, *J. Org. Chem.* **1992**, *57*, 2566–2574.
- [43] C. H. Heathcock, J. A. Stafford, D. L. Clark, *J. Org. Chem.* **1992**, *57*, 2575–2585.
- [44] C. H. Heathcock, J. C. Kath, R. B. Ruggeri, *J. Org. Chem.* **1995**, *60*, 1120–1130.
- [45] a) S. E. Denmark, R. Y. Baiazitov, *J. Org. Chem.* **2005**, *71*, 593–605; b) S. E. Denmark, R. Y. Baiazitov, *Org. Lett.* **2005**, *7*, 5617–5620.
- [46] a) S. E. Denmark, R. Y. Baiazitov, S. T. Nguyen, *Tetrahedron* **2009**, *65*, 6535–6548; b) S. E. Denmark, S. T. Nguyen, R. Y. Baiazitov, *Heterocycles* **2008**, *76*, 143–154.
- [47] S. E. Schaus, B. D. Brandes, J. F. Larrow, M. Tokunaga, K. B. Hansen, A. E. Gould, M. E. Furrow, E. N. Jacobsen, *J. Am. Chem. Soc.* **2002**, *124*, 1307–1315.
- [48] a) A. Cordero-Vargas, X. Urbaneja, J. Bonjoch, *Synlett* **2007**, *15*, 2379–2382; b) D. Solé, X. Urbaneja, J. Bonjoch, *Org. Lett.* **2005**, *7*, 5461–5464.
- [49] K. Tanabe, A. Fujie, N. Ohmori, Y. Hiraga, S. Kojima, K. Ohkata, *Bull. Chem. Soc. Jpn.* **2007**, *80*, 1597–1604.
- [50] T. B. Dunn, J. M. Ellis, C. C. Kofink, J. R. Manning, L. E. Overman, *Org. Lett.* **2009**, *11*, 5658–5661.

REFERENCES

- [51] K. A. Ahrendt, C. J. Borths, D. W. C. MacMillan, *J. Am. Chem. Soc.* **2000**, *122*, 4243–4244.
- [52] K. Biswas, O. Prieto, P. J. Goldsmith, S. Woodward, *Angew. Chem. Int. Ed.* **2005**, *44*, 2232–2234.
- [53] S. Ikeda, M. Shibuya, N. Kanoh, Y. Iwabuchi, *Org. Lett.* **2009**, *11*, 1833–1836.
- [54] M. E. Weiss, E. M. Carreira, *Angew. Chem. Int. Ed.* **2011**, *50*, 11501–11505.
- [55] I. Coldham, L. Watson, H. Adams, N. G. Martin, *J. Org. Chem.* **2011**, *76*, 2360–2366.
- [56] I. Coldham, A. J. M. Burrell, H. I. n. D. S. Guerrand, N. Oram, *Org. Lett.* **2011**, *13*, 1267–1269.
- [57] C. Xu, Z. Liu, H. Wang, B. Zhang, Z. Xiang, X. Hao, D. Z. Wang, *Org. Lett.* **2011**, *13*, 1812–1815.
- [58] C. Xu, L. Wang, X. Hao, D. Z. Wang, *J. Org. Chem.* **2012**, *77*, 6307–6313.
- [59] O. Corminboeuf, L. E. Overman, L. D. Pennington, *J. Am. Chem. Soc.* **2003**, *125*, 6650–6652.
- [60] G. Bélanger, J. Boudreault, F. Lévesque, *Org. Lett.* **2011**, *13*, 6204–6207.
- [61] F. Sladojevich, I. N. Michaelides, D. Benjamin, J. W. Ward, D. J. Dixon, *Org. Lett.* **2011**, *13*, 5132–5135.
- [62] B. Darses, I. N. Michaelides, F. Sladojevich, J. W. Ward, P. R. Rzepa, D. J. Dixon, *Org. Lett.* **2012**, *14*, 1684–1687.
- [63] C. Tan, Y. Di, Y. Wang, Y. Wang, S. Mu, S. Gao, Y. Zhang, N. Kong, H. He, J. Zhang, X. Fang, C. Li, Y. Lu, X. Hao, *Tetrahedron Lett.* **2008**, *49*, 3376–3379.
- [64] *Daphniphyllum oldhamii*, version from 13.04.2013, http://www.efloras.org/florataxon.aspx?flora_id=2&taxon_id=242316885, **13.04.2013**.
- [65] W. Zhang, Y. Guo, K. Krohn, *Chem. Eur. J.* **2006**, *12*, 5122–5127.
- [66] J. Kobayashi, Y. Inaba, M. Shiro, N. Yoshida, H. Morita, *J. Am. Chem. Soc.* **2001**, *123*, 11402–11408.
- [67] a) D. Polo-Cerón, S. Gómez-Ruiz, S. Prashara, M. Fajardo, A. Antiñolo, A. Otero, *Collect. Czech. Chem. Commun.* **2007**, *72*, 747–763; b) M. Fischer, P. Bönzli, B. Stofer, M. Neuenschwander, *Helv. Chim. Acta* **1999**, *82*, 1509–1520.
- [68] a) K. C. Nicolaou, Z. Yang, J. J. Liu, H. Ueno, P. G. Nantermet, R. K. Guy, C. F. Claiborne, J. Renaud, E. A. Couladouros, K. Paulvannan, E. J. Sorensen, *Nature* **1994**, *367*, 630–634; b) K. C. Nicolaou, J. J. Liu, Z. Yang, H. Ueno, E. J. Sorensen, C. F. Claiborne, R. K. Guy, C. K. Hwang, M. Nakada, P. G. Nantermet, *J. Am. Chem. Soc.* **1995**, *117*, 634–644; c) K. C. Nicolaou, Z. Yang, J. J. Liu, P. G. Nantermet, C. F. Claiborne, J. Renaud, R. K. Guy, K. Shibayama, *J. Am. Chem. Soc.* **1995**, *117*, 645–652.
- [69] C. Christine, K. Ikhiri, A. Ahond, A. A. Mourabit, C. Poupat, P. Potier, *Tetrahedron* **2000**, *56*, 1837–1850.
- [70] T. Kondo, T. Nekado, I. Sugimoto, K. Ochi, S. Takai, A. Kinoshita, A. Hatayama, S. Yamamoto, K. Kawabata, H. Nakai, M. Toda, *Biorg. Med. Chem.* **2008**, *16*, 190–208.
- [71] a) X. Huang, H. Zhou, W. Chen, *J. Org. Chem.* **2004**, *69*, 839–842; b) X. Huang, H. Zhou, *Org. Lett.* **2002**, *4*, 4419–4422.

- [72] B. M. Trost, D. M. T. Chan, *J. Am. Chem. Soc.* **1979**, *101*, 6429–6432.
- [73] a) B. M. Trost, R. I. Higuchi, *J. Am. Chem. Soc.* **1996**, *118*, 10094–10105; b) D. F. Taber, K. J. Frankowski, *J. Org. Chem.* **2005**, *70*, 6417–6421.
- [74] R. B. Silverman, M. A. Levy, *J. Org. Chem.* **1980**, *45*, 815–818.
- [75] R. Jain, *Org. Prep. Proced. Int.* **2001**, *33*, 405–409.
- [76] S. Hanessian, R. Margarita, *Tetrahedron Lett.* **1998**, *39*, 5887–5890.
- [77] G. Kokotos, J. M. Padrón, T. Martín, W. A. Gibbons, V. S. Martín, *J. Org. Chem.* **1998**, *63*, 3741–3744.
- [78] J. D. McKerrow, J. M. A. Al-Rawi, P. Brooks, *Synth. Commun.* **2010**, *40*, 1161–1179.
- [79] S. Conde, P. López-Serrano, M. Fierros, M. I. Biezma, A. Martínez, M. I. Rodríguez-Franco, *Tetrahedron* **1997**, *53*, 11745–11752.
- [80] W. Pfister, Bachelor Thesis, *Stereoselective functionalisation of L-glutamic acid: Synthetic studies towards the total synthesis of oldhamine A*, Ludwig-Maximilians-Universität München, **2011**.
- [81] a) J. Cabral, P. Laszlo, L. Mahé, M. T. Montaufier, S. L. Randriamahefa, *Tetrahedron Lett.* **1989**, *30*, 3969–3972; b) R. Varala, M. M. Alam, S. R. Adapa, *Synlett* **2003**, *2003*, 720–722.
- [82] A. T. Khan, T. Parvin, S. Gazi, L. H. Choudhury, *Tetrahedron Lett.* **2007**, *48*, 3805–3808.
- [83] a) S. Cossu, O. De Lucchi, R. Durr, *Synth. Commun.* **1996**, *26*, 4597–4601; b) Y. I. Élnatanov, R. G. Kostyanovskii, *B. Acad. Sci. USSR Ch+* **1988**, *37*, 302–311.
- [84] I. Höhlelein, Bachelor Thesis, *Synthesis of Functionalized Pyrrolizidines as Intermediates in the Total Synthesis of the Daphniphyllum Alkaloid Oldhamine A*, Ludwig-Maximilians-Universität München, **2010**.
- [85] a) M. E. Krafft, R. H. Romero, I. L. Scott, *J. Org. Chem.* **1992**, *57*, 5277–5278; b) N. Jeong, Y. K. Chung, B. Y. Lee, S. H. Lee, S.-E. Yoo, *Synlett* **1991**, *1991*, 204–206; c) M. E. Krafft, L. V. R. Boñaga, C. Hiroswawa, *J. Org. Chem.* **2001**, *66*, 3004–3020; d) T. Sugihara, M. Yamada, H. Ban, M. Yamaguchi, C. Kaneko, *Angew. Chem. Int. Ed.* **1997**, *36*, 2801–2804; e) M. C. Patel, T. Livinghouse, B. L. Pagenkopf, *Org. Synth.* **2003**, *80*, 93–103; f) I. U. Khand, G. R. Knox, P. L. Pauson, W. E. Watts, M. I. Foreman, *J. Chem. Soc., Perkin Trans. 1* **1973**, *0*, 977–981.
- [86] P. L. Pauson, *Tetrahedron* **1985**, *41*, 5855–5860.
- [87] M. D. Chordia, N. S. Narasimhan, *J. Chem. Soc., Perkin Trans. 1* **1991**, *0*, 371–376.
- [88] a) N. F. Osborne, *J. Chem. Soc., Perkin Trans. 1* **1982**, *0*, 1435–1439; b) J. Salaun, *J. Org. Chem.* **1976**, *41*, 1237–1240.
- [89] B. M. Trost, M. Buch, M. L. Miller, *J. Org. Chem.* **1988**, *53*, 4887–4888.
- [90] G. M. Rubottom, J. M. Gruber, R. Marrero, H. D. Juve, C. W. Kim, *J. Org. Chem.* **1983**, *48*, 4940–4944.
- [91] a) J. Tsuji, K. Takahashi, I. Minami, I. Shimizu, *Tetrahedron Lett.* **1984**, *25*, 4783–4786; b) I. Minami, K. Takahashi, I. Shimizu, T. Kimura, J. Tsuji, *Tetrahedron* **1986**, *42*, 2971–2977.
- [92] B. M. Trost, D. M. T. Chan, *J. Am. Chem. Soc.* **1983**, *105*, 2315–2325.

- [93] P. Jüstel, Bachelor Thesis, *Synthesis of functionalized bicyclic Lactones as Intermediates in the Total Synthesis Program towards the Daphniphyllum Alkaloid Oldhamine A*, Ludwig-Maximilians-Universität München, **2012**.
- [94] W. C. Still, M. Kahn, A. Mitra, *J. Org. Chem.* **1978**, *43*, 2923–2925.
- [95] G. R. Fulmer, A. J. M. Miller, N. H. Sherden, H. E. Gottlieb, A. Nudelman, B. M. Stoltz, J. E. Bercaw, K. I. Goldberg, *Organometallics* **2010**, *29*, 2176–2179.
- [96] a) D. B. Dess, J. C. Martin, *J. Org. Chem.* **1983**, *48*, 4155–4156; b) A. Schröckeneder, D. Stichnoth, P. Mayer, D. Trauner, *Beilstein J. Org. Chem.* **2012**, *8*, 1523–1527.
- [97] B. Hille, *Ion Channels of Excitable Membranes (3rd ed.)*, Sinauer Associates, Inc., Sunderland, **2001**.
- [98] M. E. Fraser, M. Fujinaga, M. M. Cherney, A. R. Melton-Celsa, E. M. Twiddy, A. D. O'Brien, M. N. G. James, *J. Biol. Chem.* **2004**, *279*, 27511–27517.
- [99] N. Unwin, *J. Mol. Biol.* **2005**, *346*, 967–989.
- [100] V. Vasquez, E. Perozo, *Nature* **2009**, *461*, 47–49.
- [101] R. J. C. Hilf, R. Dutzler, *Nature* **2008**, *452*, 375–379.
- [102] T. Fehrentz, M. Schönberger, D. Trauner, *Angew. Chem. Int. Ed.* **2011**, *50*, 12156–12182.
- [103] E. R. Kandel, J. Schwartz, T. Jessell, *Principles of Neural Science, 4 ed.*, Elsevier, Dordrecht, **2000**.
- [104] M. Stein, S. J. Middendorp, V. Carta, E. Pejo, D. E. Raines, S. A. Forman, E. Sigel, D. Trauner, *Angew. Chem. Int. Ed.* **2012**, *51*, 10500–10504.
- [105] D. Lemoine, R. Jiang, A. Taly, T. Chataigneau, A. Specht, T. Grutter, *Chem. Rev.* **2012**, *112*, 6285–6318.
- [106] N. R. Carlson, *Foundations of Physiological Psychology*, Simon & Schuster, Needham Heights, Massachusetts, **1990**.
- [107] David Randall, Warren Burggren, K. French, *Eckert Animal Physiology, Fifth Edition edition*, W. H. Freeman, **2001**.
- [108] J. N. C. Kew, C. H. Davies, *Ion Channels - From Structure to Function*, Oxford University Press, Oxford New York, **2010**.
- [109] V. Campagna-Slater, D. F. Weaver, *J. Mol. Graphics Modell.* **2007**, *25*, 721–730.
- [110] *GABA_A receptor*, version from 08.04.2013
http://en.wikipedia.org/wiki/GABAA_receptor, **09.04.2013**.
- [111] R. Spurny, J. Ramerstorfer, K. Price, M. Brams, M. Ernst, H. Nury, M. Verheij, P. Legrand, D. Bertrand, S. Bertrand, D. A. Dougherty, I. J. P. de Esch, P.-J. Corringer, W. Sieghart, S. C. R. Lummis, C. Ulens, *Proc. Natl. Acad. Sci.* **2012**, *109*, E3028–E3034.
- [112] P. F. G. Boullay, *Bulletin de Pharmacie* **1812**, *4*, 1–34.
- [113] G. A. R. Johnston, *Pharmacol. Ther.* **1996**, *69*, 173–198.
- [114] A. R. Korshoej, M. M. Holm, K. Jensen, J. D. C. Lambert, *Brit. J. Pharmacol.* **2010**, *159*, 636–649.
- [115] B. E. Erkkila, A. V. Sedelnikova, D. S. Weiss, *Biophys. J.* **2008**, *94*, 4299–4306.
- [116] A. Sedelnikova, B. E. Erkkila, H. Harris, S. O. Zakharkin, D. S. Weiss, *J. Physiol.* **2006**, *577*, 569–577.
- [117] R. E. Hibbs, E. Gouaux, *Nature* **2011**, *474*, 54–60.

- [118] a) Gerber, *Molecular Design*, version from 01.03.2013 www.moloc.ch, **10.03.2013**; b) P. Gerber, K. Müller, *J. Comput. Aided Mol. Des.* **1995**, *9*, 251–268.
- [119] E. L. Goff, R. B. LaCount, *J. Org. Chem.* **1964**, *29*, 423–427.
- [120] R. C. Cookson, J. B. Henstock, J. Hudec, B. R. D. Whitear, *J. Chem. Soc. C* **1967**, *0*, 1986–1993.
- [121] G. Bähr, G. Schleitzer, *Chem. Ber.* **1955**, *88*, 1771–1777.
- [122] G. Bähr, G. Schleitzer, *Chem. Ber.* **1957**, *90*, 438–443.
- [123] H. E. Simmons, R. D. Vest, D. C. Blomstrom, J. R. Roland, T. L. Cairns, *J. Am. Chem. Soc.* **1962**, *84*, 4746–4756.
- [124] H. E. Simmons, R. D. Vest, S. A. Vladuchick, O. W. Webster, *J. Org. Chem.* **1980**, *45*, 5113–5121.
- [125] H. Yu, G. Srdanov, K. Hasharoni, F. Wudl, *Tetrahedron* **1997**, *53*, 15593–15602.
- [126] R. J. Less, M. McPartlin, J. M. Rawson, P. T. Wood, D. S. Wright, *Chem. Eur. J.* **2010**, *16*, 13723–13728.
- [127] F. Slezak, A. Hirsch, I. Rosen, *J. Org. Chem.* **1960**, *25*, 660–661.
- [128] a) J. Kim, I. Jung, S. Kim, E. Lee, J. Kang, S. Sakamoto, K. Yamaguchi, K. Kim, *J. Am. Chem. Soc.* **2000**, *122*, 540–541; b) J. Kim, I. Jung, S. Kim, E. Lee, J. Kang, S. Sakamoto, K. Yamaguchi, K. Kim, *Vol. US6365734 B1*, Pohang University of Science and Technology Foundation (Pohang, KR) US, **2002**.
- [129] S. Y. Jon, N. Selvapalam, D. H. Oh, J. Kang, S. Kim, Y. J. Jeon, J. W. Lee, K. Kim, *J. Am. Chem. Soc.* **2003**, *125*, 10186–10187.
- [130] D. Bardelang, K. A. Udachin, D. M. Leek, J. C. Margeson, G. Chan, C. I. Ratcliffe, J. A. Ripmeester, *Cryst. Growth Des.* **2011**, *11*, 5598–5614.
- [131] J.-X. Liu, Y.-F. Hu, R.-L. Lin, W.-Q. Sun, X.-H. Liu, W.-R. Yao, *J. Coord. Chem.* **2010**, *63*, 1369–1378.
- [132] A. Wego, K. Jansen, H. Buschmann, E. Schollmeyer, D. Döpp, *J. Incl. Phenom. Macro.* **2002**, *43*, 201–205.
- [133] a) T. Ogoshi, T. Aoki, K. Kitajima, S. Fujinami, T. Yamagishi, Y. Nakamoto, *J. Org. Chem.* **2010**, *76*, 328–331; b) T. Ogoshi, S. Kanai, S. Fujinami, T. Yamagishi, Y. Nakamoto, *J. Am. Chem. Soc.* **2008**, *130*, 5022–5023.
- [134] T. Ogoshi, M. Hashizume, T.-a. Yamagishi, Y. Nakamoto, *Chem. Commun.* **2010**, *46*, 3708–3710.
- [135] Y. Ma, X. Ji, F. Xiang, X. Chi, C. Han, J. He, Z. Abliz, W. Chen, F. Huang, *Chem. Commun.* **2011**, *47*, 12340–12342.
- [136] X.-B. Hu, L. Chen, W. Si, Y. Yu, J.-L. Hou, *Chem. Commun.* **2011**, *47*, 4694–4696.
- [137] V. Havel, J. Svec, M. Wimmerova, M. Dusek, M. Pojarova, V. Sindelar, *Org. Lett.* **2011**, *13*, 4000–4003.
- [138] S. T. Schneebeli, C. Cheng, K. J. Hartlieb, N. L. Strutt, A. A. Sarjeant, C. L. Stern, J. F. Stoddart, *Chem. Eur. J.* **2013**, *19*, 3860–3868.
- [139] P. Werth, *De Divina Proportione oder Über die fünf Platonischen Körper*, **2005**.
- [140] K. Critchlow, *Time stands still: New light on megalithic science*, St. Martin's Press; Second edition, **1982**

- [141] *The Sacrament of the Last Supper*, version from 17.03.2013, http://en.wikipedia.org/wiki/The_Sacrament_of_the_Last_Supper, **01.04.2013**.
- [142] A. Koyré, *The Astronomical Revolution: Copernicus--Kepler--Borelli*, Dover Publications, **1992**.
- [143] W. F. Ochoa, A. Chatterji, T. Lin, J. E. Johnson, *Chem. Biol.* **2006**, *13*, 771–778.
- [144] R. Chakrabarty, P. S. Mukherjee, P. J. Stang, *Chem. Rev.* **2011**, *111*, 6810–6918.
- [145] S. Leininger, B. Olenyuk, P. J. Stang, *Chem. Rev.* **2000**, *100*, 853–908.
- [146] B. J. Holliday, C. A. Mirkin, *Angew. Chem. Int. Ed.* **2001**, *40*, 2022–2043.
- [147] D. J. Tranchemontagne, Z. Ni, M. O'Keeffe, O. M. Yaghi, *Angew. Chem. Int. Ed.* **2008**, *47*, 5136–5147.
- [148] B. Olenyuk, M. D. Levin, J. A. Whiteford, J. E. Shield, P. J. Stang, *J. Am. Chem. Soc.* **1999**, *121*, 10434–10435.
- [149] J. Bacsá, R. J. Less, H. E. Skelton, Z. Soracevic, A. Steiner, T. C. Wilson, P. T. Wood, D. S. Wright, *Angew. Chem. Int. Ed.* **2011**, *50*, 8279–8282.
- [150] S. Pasquale, S. Sattin, E. C. Escudero-Adán, M. Martínez-Belmonte, J. de Mendoza, *Nat. Commun.* **2012**, *3*, 785–792.
- [151] P. J. Stang, B. Olenyuk, *Acc. Chem. Res.* **1997**, *30*, 502–518.
- [152] C. da Silva, M. Bergamo, R. Černý, A. F. Williams, *Helv. Chim. Acta* **2009**, *92*, 2480–2487.
- [153] F. Liu, Y. Sheu, J. She, Y. Chang, F. E. Hong, G. Lee, S. Peng, *J. Organomet. Chem.* **2004**, *689*, 544–551.
- [154] K. DuBay, D. Trauner, *unpublished results*.
- [155] F. Edelmann, P. Behrens, S. Behrens, U. Behrens, *J. Organomet. Chem.* **1986**, *310*, 333–355.
- [156] P. K. Baker, M. G. B. Drew, M. M. Meehan, *Inorg. Chem. Commun.* **1999**, *2*, 442–444.
- [157] M. S. Okamoto, E. K. Barefield, *Inorg. Chim. Acta* **1976**, *17*, 91–96.
- [158] a) N. Lazarova, S. James, J. Babich, J. Zubieta, *Inorg. Chem. Commun.* **2004**, *7*, 1023–1026; b) B. Salignac, P. V. Grundler, S. Cayemittes, U. Frey, R. Scopelliti, A. E. Merbach, R. Hedinger, K. Hegetschweiler, R. Alberto, U. Prinz, G. Raabe, U. Kölle, S. Hall, *Inorg. Chem.* **2003**, *42*, 3516–3526.
- [159] a) R. Alberto, A. Egli, U. Abram, K. Hegetschweiler, V. Gramlich, P. A. Schubiger, *J. Chem. Soc., Dalton Trans.* **1994**, *0*, 2815–2820; b) M. Hinrichs, F. R. Hofbauer, P. Klüfers, M. Suhanji, *Inorg. Chem.* **2006**, *45*, 6688–6693.
- [160] a) M. Herberhold, G. Süß, *Angew. Chem.* **1975**, *87*, 710; b) M. Herberhold, G. Süß, *Angew. Chem. Int. Ed.* **1975**, *14*, 700.
- [161] C. Richardson, C. A. Reed, *Chem. Commun.* **2004**, *0*, 706–707.
- [162] a) R. J. Less, T. C. Wilson, M. McPartlin, P. T. Wood, D. S. Wright, *Chem. Commun.* **2011**, *47*, 10007–10009; b) R. J. Less, B. Guan, N. M. Muresan, M. McPartlin, E. Reisner, T. C. Wilson, D. S. Wright, *Dalton Trans.* **2012**, *41*, 5919–5924.
- [163] CrysAlisPro, Oxford Diffraction Ltd. Version 1.171.33.41, **06.05.2009**.

- [164] A. Altomare, M. C. Burla, M. Camalli, G. L. Cascarano, C. Giacovazzo, A. Guagliardi, A. G. G. Moliterni, G. Polidori, R. Spagna, *J. Appl. Crystallogr.* **1999**, *32*, 115–119.
- [165] G. Sheldrick, *Acta Cryst. Sect. A* **2008**, *64*, 112–122.
- [166] a) M. Mc Elfresh, *Fundamentals of Magnetism and Magnetic Measurements featuring Quantum Design's Magnetic Property Measurement System*, Quantum Design & Purdue University, **1994**; b) *Magnetic Property Measurement System MPMS XL, Hardware Reference Manual*, Quantum Design, San Diego, **2005**.
- [167] *MPMS MultiVU*, 1.56 Build 72 ed., Quantum Design Inc., San Diego, **2005**.
- [168] M. Tegel, *SQUID Processor* ed., 0.2 (Mac/Windows), Ludwig-Maximilians-Universität, München, **2010**.
- [169] H. Lueken, *Magnetochemie*, Teubner Verlag, Stuttgart, Leipzig, **1999**.
- [170] J. M. Frisch, G. W. Trucks, H. B. Schlegel, G. E. Scuseria, M. A. Robb, J. R. Cheeseman, J. A. M. Jr., T. Vreven, K. N. Kudin, J. C. Burant, J. M. Millam, S. S. Iyengar, J. Tomasi, V. Barone, B. Mennucci, M. Cossi, G. Scalmani, N. Rega, G. A. Petersson, H. Nakatsuji, M. Hada, M. Ehara, K. Toyota, R. Fukuda, J. Hasegawa, M. Ishida, T. Nakajima, Y. Honda, O. Kitao, H. Nakai, M. Klene, X. Li, J. E. Knox, H. P. Hratchian, J. B. Cross, V. Bakken, C. Adamo, J. Jaramillo, R. Gomperts, R. E. Stratmann, O. Yazyev, A. J. Austin, R. Cammi, C. Pomelli, J. W. Ochterski, P. Y. Ayala, K. Morokuma, G. A. Voth, P. Salvador, J. J. Dannenberg, V. G. Z. S. Dapprich, A. D. Daniels, M. C. Strain, O. Farkas, D. K. Malick, A. D. Rabuck, K. Raghavachari, J. B. Foresman, J. V. Ortiz, Q. Cui, A. G. Baboul, S. Clifford, J. Cioslowski, B. B. Stefanov, G. Liu, A. Liashenko, P. Piskorz, I. Komaromi, R. L. Martin, D. J. Fox, T. Keith, M. A. Al-Laham, C. Y. Peng, A. Nanayakkara, M. Challacombe, P. M. W. Gill, B. Johnson, W. Chen, M. W. Wong, C. Gonzalez, J. A. Pople, *Gaussian 03, Revision C.02*, Gaussian, Inc., Wallingford, CT, **2004**.
- [171] a) C. Lee, W. Yang, R. G. Parr, *Phys. Rev. B* **1988**, *37*, 785–789; b) P. J. Stephens, F. J. Devlin, C. F. Chabalowski, M. J. Frisch, *J. Phys. Chem.* **1994**, *98*, 11623–11627.
- [172] a) P. J. Hay, W. R. Wadt, *J. Chem. Phys.* **1985**, *82*, 299–310; b) W. R. Wadt, P. J. Hay, *J. Chem. Phys.* **1985**, *82*, 284–298.
- [173] M. M. Francl, W. J. Pietro, W. J. Hehre, J. S. Binkley, M. S. Gordon, D. J. DeFrees, J. A. Pople, *J. Chem. Phys.* **1982**, *77*, 3654–3665.

PERSÖNLICHE DATEN

Name: Michael Pangerl
Geburtsdatum: 21.10.1984
Geburtsort: Gräfelfing
Nationalität: Deutsch

SCHULAUSBILDUNG UND AKADEMISCHER WERDEGANG

Ludwig-Maximilians-Universität, München, Department für Chemie und Pharmazie

11/2009 – heute Erstellung der vorliegenden Doktorarbeit unter Leitung von Prof. Dr. Trauner
Forschungsbereich: Totalsynthese bioaktiver Naturstoffe, Design potentieller Ionenkanalblocker und *self-assembly* hochsymmetrischer Moleküle

02/2008 – 10/2009 Master of Science, Chemie
Schwerpunkte: Organische Chemie, Anorganische Chemie

09/2004 – 02/2008 Bachelor of Science, Chemie und Biochemie
Schwerpunkte: Organische Chemie, Biochemie

Max-Born-Gymnasium, Germering

09/1995 – 05/2004 Abitur

AUSZEICHNUNGEN

10/2012 1. Posterpreis beim "Second International Symposium of the Collaborative Research Center 765" in Berlin
Thema: Multivalency in Chemistry and Biochemistry

12/2010 Auszeichnung für exzellente Forschung, Dr. Klaus Römer Stiftung
Preiskategorie: Masterarbeit

SPRACHKENNTNISSE

Deutsch Muttersprache
Englisch Verhandlungssicher
Französisch Grundkenntnisse

PUBLIKATIONEN

- 1) M. Pangerl, V. Carta, R. Baur, E. Sigel, D. Trauner, A symmetry-based approach towards new ion channel blockers, manuscript in preparation.
- 2) M. Pangerl, I. Höhle, D. Trauner, Towards the total synthesis of (-)-oldhamine A, *manuscript in preparation*.
- 3) M. Pangerl, D. Trauner, Pentacyanocyclopentadienide salts with fivefold symmetric counter ion, *manuscript in preparation*.
- 4) M. Pangerl, C. C. Hughes, D. Trauner, Total synthesis of newbouldine via reductive N-N bond formation, *Tetrahedron*, **2010**, 66, 6626-6631.
- 5) M. Rotter, M. Pangerl, M. Tegel, D. Johrendt, Superconductivity and crystal structures of $(\text{Ba}_{1-x}\text{K}_x)\text{Fe}_2\text{As}_2$ ($x=0-1$), *Angew. Chem. Int. Ed.* **2008**, 47, 7949-7952.